DEPARTMENT OF CIVIL & STRUCTURAL ENGINEERING

UNIVERSITY OF SHEFFIELD

VIBRATION SERVICEABILITY OF LONG-SPAN CAST IN-SITU CONCRETE FLOORS

by

Aleksandar Pavic

A thesis submitted for the Degree of Doctor of Philosophy in Engineering
at the University of Sheffield

July 1999

" All generalisations are dangerous, including this one."

Alexandre Dumas

Abstract

This thesis describes an investigation into the vibration serviceability of long-span and slender in-situ concrete floors, which are typically post-tensioned. The motivation for the research is the present trend towards increased slenderness of post-tensioned floors supporting open-plan high-quality offices where vibration serviceability may easily become the governing design criterion. The vibration serviceability issue in post-tensioned floors is now also recognised by the UK Concrete Society which proposed, for the first time, guidelines for performing a vibration serviceability check when designing office floors. The guidelines were published in Concrete Society Technical Report 43 (CSTR43) in 1994 and its publication prompted the initialisation of this research project. There were two reasons for this. Firstly, problems were reported with the reliability and practical application of these guidelines, and, secondly, the guidelines were not experimentally verified which is unusual for any design provision related to vibration serviceability.

In order to improve understanding of the dynamic performance of a rather specific group of office floors which are long-span and made of cast in-situ concrete, a combined experimental and analytical approach has been adopted. A state-of-the-art facility comprising hardware and software suitable for field modal testing and dynamic response measurements of prototype floor structures was commissioned as a part of this research. The facility is built up around the instrumented sledge hammer, which served as the main excitation source in modal testing, and multi-degree-of-freedom vibration parameter estimation procedures utilising measured floor frequency response functions.

The main testing programme consisted of modal testing of four prototype floor structures of varying complexity weighing between 13 and 1000 tonnes. All four slab structures were slender and made of in-situ concrete. These tests were complemented by measurements of the floors' acceleration responses to a single person walking excitation tuned to create as large as realistically possible responses. The modal testing experimental data (measured natural frequencies, mode shapes and modal damping ratios) were used to validate numerical finite element (FE) models representing each floor structure. To do this, advanced FE model correlation and manual updating procedures were employed. Results of these exercises highlighted a number of important issues related to the dynamic behaviour of the concrete floors investigated.

Firstly, the bending stiffness of in-situ concrete columns and walls contributed significantly to overall floor bending stiffness and must be considered. Secondly, higher modes of vibration which are close to the fundamental frequency appear in concrete floors, and should not be neglected as they can be easily excited by walking leading to dynamic responses greater than those associated with the fundamental mode. Thirdly, the width of band beams contributes significantly to the lateral stiffness of post-tensioned floors, which, in turn, may be very beneficial for their vibration serviceability.

The validated numerical FE models were then used to check the performance of three representative walking excitation models available in the literature. It was shown that, in general, all three models overestimated the measured response to the 3rd harmonic of the walking excitation, which is particularly important for low-frequency office floors. Only one of the models did so in a way which is not overly conservative. This model is recommended for use in vibration serviceability assessment of post-tensioned floors.

Finally, gross oversimplification of these important issues is identified as the principal reason for the failure of the current CSTR43 vibration serviceability guidelines to predict reliably vibration response of a wide range of post-tensioned in-situ cast concrete floors.

Acknowledgements

The work described in this thesis was carried out in the Department of Civil and Structural Engineering at the University of Sheffield between October 1993 and December 1995, while the author was working as a full-time postgraduate research student, and between January 1996 and July 1999, while the author worked part-time on the project as a staff-candidate employed as a full-time Lecturer in Structural Engineering in the Department.

The author is indebted to his supervisor, Professor Peter Waldron, for his trust, valuable advice and encouragement throughout the course of this project. His energy, enthusiasm, commitment, and patience were a constant inspiration in coping with this project.

Thanks are also expressed to Drs Roger Crouch, James Brownjohn and Martin Williams for their understanding and unequivocal support over the past years. The author is particularly grateful to Messrs Robert Caverson, Mihail Petkovski, Paul Reynolds and Michael Hartley for their help in conducting the field tests. Mr Kevin Bennett of Freyssinet Ltd and Mr Ian Feltham of Ove Arup R & D were always very supportive of this research and helped the author to gain access to valuable information and to the prototype floors tested in London and Birmingham.

My gratitude must also be expressed to the numerous friends and colleagues who have provided so much help and support during various stages of this project. These include Glenn and Kenko Hook, Andy and Ruth Vann, Giovanni Raimondi, Joseph Giacomin, and my former colleagues at the Faculty of Civil Engineering, University of Belgrade, Yugoslavia.

The financial assistance of the University of Sheffield, the CVCP's Overseas Research Student Award number ORS/9336018 and of the 1995 DETR Partners in Technology research grant number CI 39/3/393(cc0952) is also gratefully acknowledged.

Finally, and certainly most importantly, everything would be absolutely impossible without Suzana.

Memorandum

The accompanying thesis entitled "Vibration Serviceability of Long-Span Cast In-Situ Concrete Floors" is submitted for the degree of Doctor of Philosophy in the Faculty of Engineering at the University of Sheffield. The thesis is based entirely on the independent work carried out by the author in the University of Sheffield between October 1993 and December 1995 (as full-time student candidate), and January 1996 and July 1999 (as part-time staff candidate) under the supervision of Professor Peter Waldron. All the work and ideas recorded are original except where acknowledged in the text or by reference. The work contained in the thesis has not previously been submitted for a degree or diploma at this, or any other, University or Examining Body.

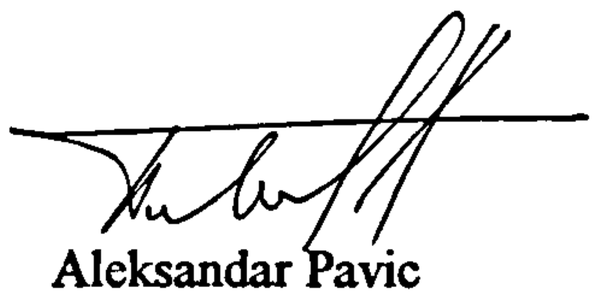

Aleksandar Pavic
July 1999

Contents

List of Figures

List of Tables

List of Abbreviations

A - Accelerometer
AC - Alternating Current
ACI - American Concrete Institute
ACSE – American Society of Civil Engineers
AISCE - American Institute of Steel Construction Engineering
APS – Acoustic Power Systems
APDL – ANSYS Parametric Design Language
ARRB - Australian Road Research Board
ASD - Auto-Spectral Density
ASME - American Society of Mechanical Engineers
Auto-MAC - Auto Modal Assurance Criterion.
BCA - British Cement Association.
BRS - Building Research Station
BSI - British Standards Institution
CCC – Centre for Cement and Concrete
CEB - Comité Euro-International du Betón
COMAC - Co-Ordinate Modal Assurance Criterion
CSTR – Concrete Society Technical Report
CSA - Canadian Standards Association
DC - Direct Current
DDS – Dynamic Data Solutions n.v.
DI – Diagnostic Instruments
DFT - Discrete Fourier Transform
DOF – Degree of Freedom
DOE – Department of Environment
DOT – Department of Transport
DSP – Digital Signal Processing
DTA - Dynamic Testing Agency
EMPA - Swiss Federal Laboratories for Materials Testing and Research
EU – European Union
FE - Finite Element
FEM - Finite Element Method
FFT - Fast Fourier Transform
FIP - Fédération Internationale de la Précontrainte
FRF – Frequency Response Function
HMSO - Her Majesty's Stationery Office
HSC - High-Strength Concrete
IABSE – International Association for Bridge and Structural Engineering
ICATS - Imperial College Analysis, Testing and Software, London, UK.
ICE - Institution of Civil Engineers
IMAC – International Modal Analysis Conference
IRF - Impulse Response Function
ISO - International Standardisation Organisation
ISVR - Institute of Sound and Vibration Research, The University of Southampton, UK.
LBTF - Large Building Testing Facility
LVDT - Linear Variable Differential Transformer
MAC - Modal Assurance Criterion
MDOF - Multiple (or Multi) Degree of Freedom
MIF - Mode Indicator Function
MSSD - Mean Square Spectral Density
NAFEMS - National Agency for Finite Element Methods and Standards.
NRCC - National Research Council of Canada

PC - Personal Computer
PCI - Precast/Prestressed Concrete Institute
PSC – Prestressed Concrete
PSD - Power-Spectral Density
PT - Post-Tensioned
PTI - Post-Tensioning Institute
PVT - PiezoVelocity Transducer™
QA - Quality Assurance; Quality Assured
RC – Reinforced Concrete
RILEM - Reunion Internationale des Laboratoires d'Essais et de researches sur les Matériaux et les constructions (Union of Testing and Research Laboratories for Materials and Structures)
RMS - Root-Mean-Square
RRL - Road Research Laboratory
SAE- Society of Automotive Engineers
SCI - Steel Construction Institute
SDOF - Single Degree of Freedom
SEM - Society for Experimental Mechanics
SESA - Society for Experimental Stress Analysis
SECED - Society for Earthquake and Civil Engineering Dynamics
SIMO - Single Input Multiple Output
SISO – Single Input Single Output
SJI - Steel Joist Institute
SLS - Serviceability Limit State(s)
spm - Steps per minute
TM - Trade Mark
TP - Test Point (on an established structural test grid).
TRADA - Timber Research and Development Association
TRRL – Transport and Road Research Laboratory
ULS - Ultimate Limit State(s)
VDV - Vibration Dose Value
WM - Walking Model
WP – Walking Path

Notation

Matrix Symbols

[ ]	Matrix.
{ }	Column vector.
( )	Single element of matrix or vector
[\ ]	Diagonal matrix
[ ]^T	Transpose of a matrix
{ }^{T}	Transpose of a vector
{0}	Zero vector.
[C]	Damping matrix.
[D]	Damping matrix.
[H(ω)]	FRF matrix.
[K]	Stiffness matrix.
$[K]_E$	Effective stiffness matrix.
$[K]_G$	Geometric stiffness matrix.
[M]	Mass matrix.
$\{\bar{X}\}$	Vector of time-independent displacement amplitudes.
$[\omega_r]$	Diagonal matrix of natural frequencies.
$[k_r]$	Diagonal matrix of modal stiffnesses.
$[m_r]$	Diagonal matrix of modal masses.
(ψ_{jr})	The j^{th} element of the r^{th} mode shape (or eigenvector).
$\{\psi\}_r$	The r^{th} mode shape (or eigenvector).
$[\Psi]$	Mode shape (or eigenvector, or modal) matrix.
(ϕ_{jr})	The j^{th} element of mass-normalised the r^{th} mode shape (or eigenvector).
$[\Phi]$	Mass-normalised mode shape/eigenvector matrix.

Alphabet Notation

a_0	Peak acceleration of an equivalent SDOF system; peak acceleration of a SDOF system at the start of exponential decay used to measure damping of a SDOF system.
$a_{max.allowed}$	Maximum measurable acceleration by the accelerometer.
a_n	Peak acceleration of a SDOF system after n cycles of exponentially decaying vibrations.
$a_{RMS,10w}$	RMS accelerations, weighted and averaged over 10s.
a_{RMS}	RMS accelerations.
$a(t)=\ddot{x}(t)$	Acceleration time history.
$a_w(t)$	Weighted acceleration time history.
$_A$	'$_A$' as subscript stands for 'analytical'.
A_0	Initial displacement amplitude.
$A(\omega)$	Accelerance (acceleration/force) FRF.
$A_{jk}(\omega)$	Accelerance FRF between coordinates 'j' and 'k' (acceleration at coordinate 'j' caused by excitation at coordinate 'k'). This type of FRF is also known as 'inertance'.
$_rA_{jk}$	Modal constant/residue corresponding to coordinates 'j' and 'k' of the r^{th} mode of vibration
$a_w(t)$	Frequency weighted acceleration time history
c_r	Modal (or effective) viscous damping of r^{th} mode; proportional damping.
C_r	Floor response coefficient corresponding to the r-direction
E	Modulus of elasticity.
E_c	Static modulus of elasticity for concrete
$E_{c,dyn}$	Dynamic modulus of elasticity for concrete
F	Direct Fourier transform
F^{-1}	Inverse Fourier transform
f	Frequency; floor natural frequency.
f_0	Lowest allowable floor natural frequency.
f_h	Frequency of the h^{th} harmonic of the Ohlsson's M2 periodic walking excitation model.
f_r	Natural frequency of the r^{th} mode of vibration.
f_s	Pacing rate.
$F_{max.assumed}$	Maximum force applied to the calibration mass.
$F_p(t)$	Time-varying vertical force caused by a single person walking.
F_{RMS}	Amplitude of a sinusoidal force which causes the same RMS (resonant) accelerations as the walking excitation force ASD.
$f(t)$	Time-varying force excitation; system input.
$f_j(t)$	The j^{th} time varying force excitation.

$f_I(t)$	Time-varying inertia force
$f_D(t)$	Time-varying damping force.
$f_E(t)$	Time-varying elastic force.
$F(\omega)$	Input spectrum. Force (or excitation) spectrum; Fourier transform of the system input.
G	Weight of a person walking.
g	Acceleration due to gravity ($g = 9.81 m/s^2$)
$h(t)$	Impulse response function
$H(\omega)$	Frequency response function; receptance.
$H_{jk}(\omega)$ or $H(j,k)$	Individual element of FRF matrix between coordinates 'j' and 'k' (response at coordinate 'j' due to excitation at coordinate 'k').
$H^{(i)}{}_{jk}(\omega)$ or $H(i)(j,k)$	The i^{th} measurement of $H_{jk}(\omega)$.
$\lvert H_{j,sum}(\omega) \rvert$	Sum of the moduli of all FRFs in the j^{th} row or column of the FRF matrix.
I	Impulse of the triangular hell-drop forcing function,
$Im^2(H_{j,sum}(\omega))$	Sum of the squared imaginary parts of all FRFs in the j^{th} row or column of the FRF matrix,
I_x	Second moment of area per unit width of an orthotropic plate in the x-direction.
I_y	Second moment of area per unit width of an orthotropic plate in the y-direction.
i	$\sqrt{-1}$.
k_r	Modal (or effective) stiffness of r^{th} mode.
K	Factor depending on the permissible acceleration limits.
m_r	Modal (or effective) mass of r^{th} mode.
m	Mass of the equivalent SDOF system representing a real-life concrete floor structure; calibration mass.
m_{min}	Minimum calibration mass required.
n	Number of cycles.
n_a	Number of mode shape half-waves in the x-direction.
n_b	Number of mode shape half-waves in the y-direction.
n_x	Number of floor spans in the x-direction.
n_y	Number of floor spans in the y-direction.
P_h	Amplitude of the h^{th} harmonic of the periodic walking excitation model.
$P_r(t)$	The r^{th} modal force.
$q(t)$	Time-varying generalised coordinate.
$\dot{q}(t)$	First derivative of time-varying generalised coordinate.
$\ddot{q}(t)$	Second derivative of time-varying generalised coordinate.
$q_r(t)$	The r^{th} time-varying generalised coordinate.
$\dot{q}_r(t)$	First derivative of the r^{th} time-varying generalised coordinate.
$\ddot{q}_r(t)$	Second derivative of the r^{th} time-varying generalised coordinate.

$q_{r,transient}(t)$	Transient part of the r^{th} time-varying generalised coordinate.
$q_{r,forced}(t)$	Forced part of the r^{th} time-varying generalised coordinate.
R	Vibration response rating; floor response factor.
$R_{aa}(\tau)$	Acceleration auto-correlation function
$R_{ff}(\tau)$	Force auto-correlation function
R_{total}	Total floor response factor
R_x	Floor response factor in the x-direction
R_y	Floor response factor in the y-direction
$S_{aa}(\omega)$	Acceleration ASD.
$S_{ff}(\omega)$	Force ASD.
t	Time variable.
t_1	Vibration start time.
t_2	Vibration end time.
T	Duration of vibration; vibration exposure duration.
T_{acq}	Data acquisition time.
TC	Exponential widow constant.
T_s	Time required to make a single step.
V	Ultrasonic pulse velocity.
V_{input}	Input voltage.
V_{output}	Output voltage.
W	Total floor weight supported by a beam.
$w_{exp}(t)$	Exponential time window.
x	'$_x$' as subscript stands for 'experimental'.
$x(t)$	Time-varying response; time-varying displacement; time-varying system output.
$\dot{x}(t)$	Time-varying velocity.
$\ddot{x}(t) = a(t)$	Time-varying acceleration.
$X(\omega)$	Output (or response) spectrum; displacement spectrum; Fourier transform of the system output.
$\ddot{x}_h(t)$	Acceleration response of a SDOF system to the h^{th} excitation harmonic.
$\ddot{x}_{h,peak}$	Peak acceleration response of a SDOF system to the h^{th} excitation harmonic.
$x_i(t)$	Linear system time-varying input; displacement of the i^{th} DOF
$x_o(t)$	Linear system time-varying output.
$x_s(t)$	Transducer support motion.
$\dot{x}_s(t)$	First derivative of transducer support motion.
$\ddot{x}_s(t)$	Second derivative of transducer support motion.
$x_r(t)$	Relative motion of transducer's seismic mass.
$\dot{x}_r(t)$	First derivative of relative motion of transducer's seismic mass.

$\ddot{x}_{RMS}$	RMS acceleration
$Y_{jk}(\omega)$	Mobility (velocity/force) FRF between coordinates 'j' and 'k' (velocity at coordinate 'j' caused by excitation at coordinate 'k').

Greek Letters

$\alpha_{jk}(\omega)$	Receptance (displacement/force) FRF between coordinates 'j' and 'k' (response at coordinate 'j' caused by excitation at coordinate 'k'). This type of FRF is also known as 'dynamic compliance'.
η	Structural damping loss factor.
η_r	Structural damping loss factor of the r^{th} mode.
ρ_c	Density of concrete.
λ_r	Rayleigh quotient for the r^{th} mode of vibration; CSTR43 effective aspect ratio in the r-direction.
φ	Physical magnitude representing vibrations;
φ_2	Phase angle corresponding to the 2^{nd} harmonic of walking.
φ_3	Phase angle corresponding to the 3^{rd} harmonic of walking.
φ_h	Phase angle of the h^{th} harmonic of periodic walking excitation
ω	Frequency of vibration (in rad/s); frequency.
ω_{ot}	Natural frequency of a seismic vibration transducer.
$\omega_r = 2\pi f_r$	Natural frequency of the r^{th} mode.
$\omega_{rd} = \omega_r\sqrt{1-\zeta_r^2}$	Damped natural frequency in the r^{th} mode of vibration.
ν_c	Poisson ratio of concrete.
ζ	Damping ratio; viscous damping ratio for the first mode of vibration.
ζ_r	Viscous damping ratio of the r^{th} mode.
$\zeta_{r,windowed}$	Viscous damping ratio of the r^{th} mode estimated from exponentially 'windowed' FRFs.

1 Introduction

A floor is an integral part of practically every modern industrial, commercial or residential building. As expectations of building users, who are in everyday contact with the floors, rise, so the performance of floor structures in day-to-day service is becoming increasingly important. The research reported in this thesis is concerned with the vibration performance of slender long-span concrete floors in buildings. Its rationale is described in this chapter.

1.1 The Emergence of the Research Problem

Modern suspended concrete floor structures are becoming increasingly bold in conception and slender in cross section. To achieve this, in the UK relatively new construction techniques, such as post-tensioning of in-situ concrete floors and new quality construction materials, such as cast in-situ high-strength concrete, are gaining popularity. Typical applications where post-tensioned floors in particular are becoming competitive are: offices, car parks, shopping centres, hospitals, apartments and industrial buildings (Concrete Society, 1994).

Generally speaking, human induced footfall loading has proved to be the major source of floor vibration disturbance as it happens frequently and, in practice, cannot be isolated (Murray, 1975; Ohlsson, 1988b; Hanagan & Murray, 1997). Therefore, excessive floor vibrations due to human induced loading have been characterised as "probably the most persistent floor serviceability problem encountered by designers" (Murray, 1988). Consequently, floor vibration serviceability is becoming a major design and research challenge. In addition to the design trend towards increased floor slenderness, the following factors have also contributed to the emergence of the research problem:

- Trend towards reduced floor damping;
- Awareness of the potential of vibration serviceability problems occurring in the development of slender floors in relatively quiet occupancies, such as offices, and the lack of reliable information as to how to tackle it in the design stage;
- Lack of research interest in the past leading to unverified performance of various walking excitation models used in numerical vibration response analysis of long-span concrete floors.

These four general factors will be briefly outlined.

1.1.1 Increased Floor Slenderness

The thickness of cast in-situ post-tensioned concrete slabs may be 30% less than that of slabs containing normal unstressed reinforcement (Lin & Burns, 1982). However, although such slabs still have sufficient strength, this reduced floor depth leads to a drastic reduction in stiffness and mass which could give rise to structural serviceability problems, such as unacceptable levels of floor deflection, vibration or cracking.

Concrete cracking and excessive static deflection in a post-tensioned slab can be overcome to a large extent by the careful choice of the amount and location of the prestress. No amount of prestressing, however, will improve significantly the floor dynamic behaviour. This is governed largely by slab stiffness, mass and damping on which different levels of prestressing do not have a significant influence (Caverson et al., 1994). Therefore, although beneficial with respect to the other serviceability design requirements, by allowing greater floor slenderness, prestressing can actually be detrimental to concrete floor vibration serviceability (Pavic et al., 1994; Maguire & Wyatt, 1999).

Cast in-situ concrete slabs made of high-strength concrete may fail for the same reason. Their increased strength in principle permits an increased slenderness which may result in lively structures.

1.1.2 Reduced Floor Damping

In addition to increased slenderness and longer floor spans, building owners and developers are increasingly specifying uninterrupted open-space environments. Little or no permanent partitioning of floors is desirable in new office or commercial building developments in order to provide its occupants with maximum flexibility. When compared with partitioned layouts, the damping in unpartitioned floors is commonly considered to be lower (ISO, 1992). Bolton (1994) states that the introduction of large open-plan offices "might harm" and is "bad practice" with regard to floor vibration serviceability. However, the trend towards such practice continues, and this fact may further impair the vibration performance of slender concrete floors.

1.1.3 Industrial Awareness of the Problem

Floors generate the second most frequent source of complaints from building users; second only to roofs (Gerber, 1991).

Floor performance which is sufficiently poor to cause users to complain may incur loss of confidence, costly remedial measures and/or litigation (Ellingwood, 1996). Building developers in general and concrete floor designers in particular should therefore be very concerned about anything that may undermine the performance of floors.

Perceptible vibrations annoying the floor occupants, disfunctional equipment sensitive to vibrations and localised damage are manifestations of the lack of the floor vibration serviceability (Hughes, 1971). In the past, a number of composite and timber floors were found to be too lively under normal everyday dynamic excitations, although they were strong enough and did not deflect excessively. Following complaints by their users, the floors were tested and failed the vibration serviceability design criterion (Murray, 1981; Bachmann et al., 1991a; 1995a). Although not uniquely formulated, this criterion has emerged as a general design requirement in practically all modern building codes based on limit state design principles.

Unlike composite and timber floors, monolithic cast in-situ concrete floors used widely in office construction have an excellent track record with regard to their past vibration performance (Ohlsson, 1988a; Khan & Williams, 1995). In other words, complaints about their vibration behaviour are rare, in fact, almost non-existent. Therefore, the focus of researchers in the past was mainly on the more lively composite and timber floors.

Vibration serviceability problems were first observed to occur in greater extent in steel joist-concrete composite floors in the 1950s and 1960s. This was a consequence of the move to greater slenderness and larger open-space areas. A similar push towards new technology with prestressed post-tensioned floors could result in similar problems of excessive liveliness.

At the moment, designers of post-tensioned floors in the UK are aware of the potential problem if longer spans are required. This fact has been confirmed through private correspondence with leading UK designers and developers of post-tensioned concrete floors. These include the UK division of PSC Freyssinet (Bennett, 1995), Bunyan Meyer & Partners (Khan, 1994; Pearman, 1997), and Gifford & Partners (Stevenson, 1995). However, although some design guidelines exist (Concrete Society, 1994), these design authorities have also confirmed that checking and/or assessing the vibration serviceability of post-tensioned floors is, at the moment, far from being a routine design procedure.

The UK Concrete Society tried to address this issue in their recently published Technical Report 43 (Concrete Society, 1994). Technical Report 43 is the third and the latest edition of a Concrete Society handbook which describes the state-of-the-art in the design of post-tensioned floors. The handbook has been used since the late-1970s throughout the world. The previous editions were Technical Report 17 (Concrete Society, 1979) and Technical Report 25 (Concrete Society, 1984). The 1994 edition contains, for the first time, procedures for checking the vibration serviceability of long-span post-tensioned floors supporting office environments. Unfortunately, some initial trials (Caverson, 1992; Williams & Waldron, 1994) and the feedback which the writer received from industry (Bennett, 1995; Khan, 1994; Pearman, 1997) indicate that the vibration serviceability provisions in this design handbook are producing erratic results and, frequently, over-conservative designs. Strong indications exist that such, seemingly defective, design guidelines could seriously undermine the market competitiveness of long-span cast in-situ post-tensioned floors. At the moment, however, it is not clear what *exactly* causes such poor performance of the guidelines for checking the vibration serviceability proposed by the Concrete Society (1994). Without this piece of information it is difficult to improve them.

1.1.4 Lack of Research

In 1988, when vibration serviceability due to the above mentioned design trends was becoming an issue for a much wider range of floors, including concrete floors, the following three general research tasks requiring further work were identified (Galambos, 1988):

1. to quantify rationally human response to vibrating floors as expressed by the emotions of annoyance and fear,
2. to define rationally the excitation input from human activity on the floor which causes vibration, and
3. to define effectively the structural dynamic model of a real floor in service including determination of more reliable damping.

Very little research has been conducted to date into the development of reliable dynamic modelling techniques for monolithic cast in-situ floors, appropriate for checking their vibration serviceability under low-level excitation. When developing such modelling guidelines, research into the vibration serviceability of other floor types established the common practice of coupling experimental and analytical investigations. The former being dynamic testing of full-scale floors and the latter being the mathematical modelling of the tested structures. Nevertheless, it is interesting to note here that the current vibration serviceability design guidelines featured in the mentioned Technical Report 43 are not based on any experimental work on full-scale post-tensioned floors, as has been confirmed by one of its authors (Feltham, 1995).

There are two types of loading which usually need considering when analysing the dynamic performance of long-span floors under human induced excitation. The first is normal walking and the second includes various rhythmic exercise and dance activities (Ji & Ellis, 1994).

The research reported in this thesis will be focused on vibration serviceability of long-span floors accommodating relatively 'quiet' occupancies such as offices. For these occupancies, the dynamic loading induced by walking has proved to be the most critical, as vibrations caused by normal walking are frequent and may become annoying to other floor users (Ohlsson, 1988b; Wyatt, 1989; Eriksson, 1994). Therefore, normal walking is usually related only to a vibration serviceability problem. Bachmann et al. (1991a; 1995a) classified floors under such dynamic loading as the "floors with walking people". This was done in order to differentiate this class of floors from those supporting places of assembly under crowd loading, groups of people involved in joint exercises and dance-type activities.

Although a number of mathematical models exist for the simulation of very complex walking excitation, there is a general lack of scientifically reliable information as to the performance of these models. This is particularly true in the case of numerical modelling of in-situ cast concrete floors where the structural response calculations need verification with experimentally obtained data on real structures.

1.2 Proposed Solution and Scope

In order to improve understanding of the dynamic performance of cast in-situ long-span concrete floors, a combined experimental and analytical approach will be adopted in this thesis. An excellent overview of the general philosophy on which this research strategy is based has been given by Meyer (1987).

1.2.1 Experimental Testing of Full-Scale Floor Structures

The principal way forward in order to improve understanding of the dynamic performance of as-built concrete floors is to gather and analyse experimental data from field tests performed on full-scale structures. There are two main reasons for conducting such experiments. The first is to measure realistic dynamic responses of as-built floor structures to various patterns of walking excitation. The second is to determine the as-built key dynamic properties of such floors. These are the natural frequencies, mode shapes and modal damping ratios. They will be determined by transferring and employing the state-of-the-art modal testing technology and procedures as used in more advanced structural dynamic testing employed in the mechanical and aerospace engineering disciplines.

Quality assured modal testing and response measurements performed on each full-scale structure will render sets of reliable experimental data which can then be used for comparison with and improvement of the analytical modelling.

1.2.2 Analytical Modelling

The full-scale floor structures tested will be mathematically modelled mainly using finite element (FE) analyses of varying complexity. The FE models will be used to determine the natural frequencies and mode shapes, as well as structural dynamic responses to various patterns of walking. In other words, FE modelling will be used to produce the measured parameters analytically and enable correlation of the two sets of data.

1.2.3 Correlation Between Experiments and Analytical Modelling

The aim of correlating results from experiments and relatively sophisticated FE analyses is to produce clues as to the vibration behaviour of the floors tested. Firstly, to determine the ways to model their mass, stiffness and damping characteristics with more confidence. This approach will produce 'manually' updated FE models having the key dynamic properties as close as possible to the relevant measured properties of the real structure.

Secondly, the response measurements coupled with the response calculations using the updated FE models will be used to evaluate some of the existing procedures for modelling walking across the floors. In addition, using the state-of-the-art vibration assessment procedures outlined in the rapidly changing national and international vibration assessment standards, the vibration serviceability of the tested floors will be appraised. The assessment results, produced from both measurements and FE simulations, will be compared in order to determine their degree of correlation and to make conclusions about the appropriateness of the various modelling techniques used.

1.2.4 Critical Appraisal of Vibration Serviceability Guidelines Recommended by the Concrete Society

The modelling techniques recommended by the Concrete Society (1994) Technical Report 43 (CSTR43) will be carefully scrutinised. The dynamic properties and the vibration serviceability of the test structures will be assessed following the simplified, but not verified, guidelines given in CSTR43. The aim of this exercise is to compare these calculations with the experimental results and with the results of advanced FE modelling in order to determine possible deficiencies and suggest improvements.

The proposed strategy, combining experimental and analytical work, is graphically outlined in Figure 1.1.

1.3 Thesis Outline

The research work reported in this thesis is presented in nine chapters. As already seen, Chapter 1 contains an introduction to the general problem. The pertinent background reviews and the literature surveyed are outlined in Chapter 2. The presented background to the problem is used to pinpoint precisely the gaps in knowledge worth investigating in this research. As the proposed solution of the research problem relies on analytical modelling, experimental full-scale testing and correlation of analytically and experimentally obtained results, the most relevant aspects of the modelling assumptions and procedures adopted are outlined in Chapter 3. Due to the fact that no experimental facilities suitable for this research existed in the institution prior to this research, Chapter 4 describes the involved process of their commissioning and setting up. Chapter 5 deals with the usage of these facilities and execution of field testing performed on four prototype floors, including the initial experimental data analysis. These experimental results were used in Chapter 6 for various trial and error parametric studies aimed at learning how to improve analytical models of the tested floors. Such updated models served as a test-bed for numerical simulations of the walking excitation, which are also presented in Chapter 6. A discussion of the research and its findings is given in Chapter 7, whereas Chapter 8 contains a summary of its conclusions and recommendations for future work.

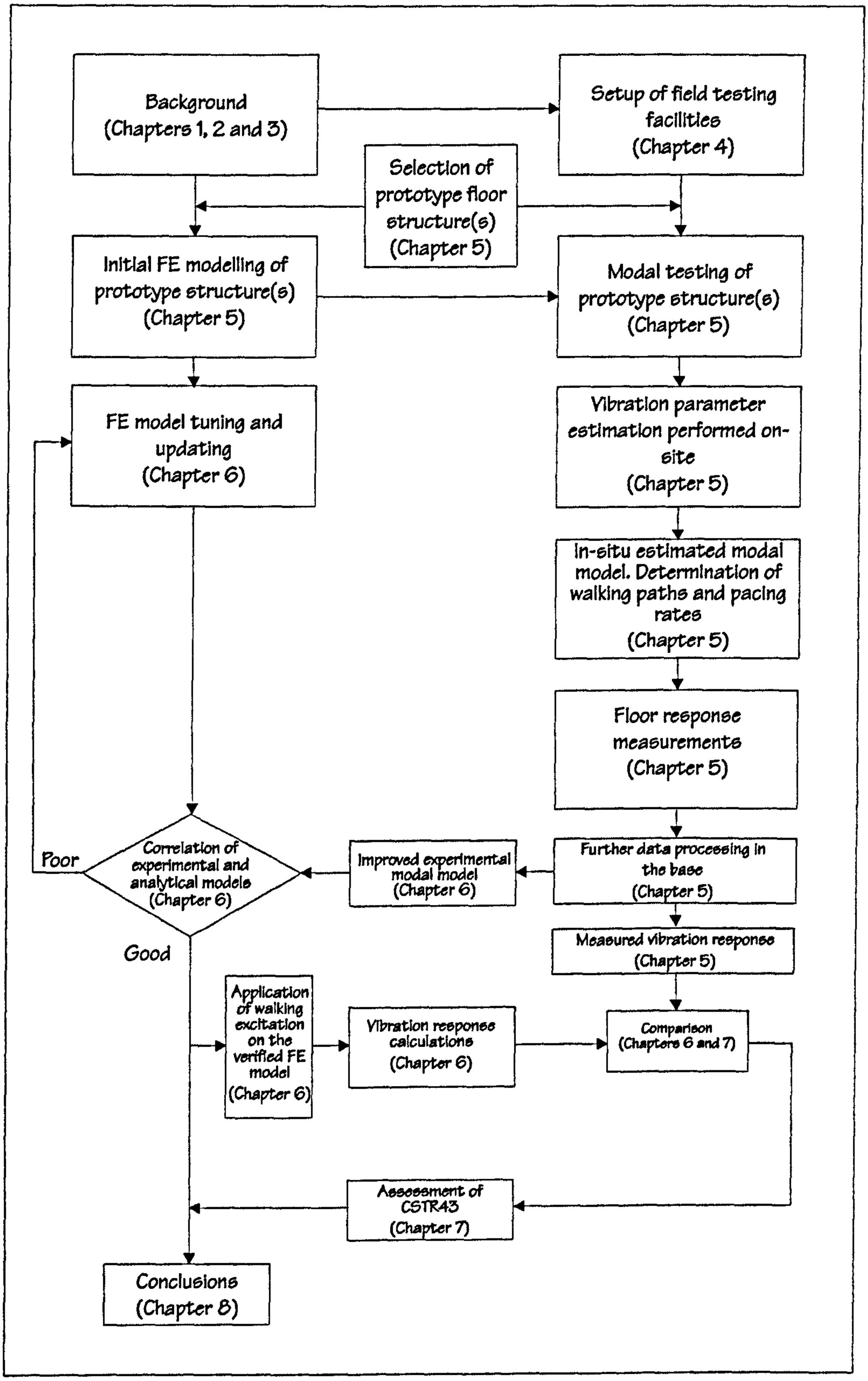

Figure 1.1: Proposed research flow chart.

2 Background and Literature Reviews

There are two general types of floors in buildings: (1) suspended floors, which are supported by other building elements such as beams, columns or walls, and (2) ground floors, also known as slabs on grade, made of concrete and whose surface is supported directly by the ground. Suspended floors are normally considered to be a constitutive part of a building structure, frequently termed the building frame. Excitation induced by walking which causes vibration serviceability problems is in principle an issue only in the case of suspended floors in which annoying vertical vibrations can be developed through bending.

2.1 Design of Post-Tensioned Concrete Floors

From a construction point of view, suspended floors are usually made entirely of concrete or of a combination of concrete and other construction materials such as steel or timber. Cast in-situ concrete floors typically consist of elements made entirely of concrete poured onto formwork on site together with the rest of the supporting building frame. Such floors are also known as cast in-place or, simply, in-situ concrete floors.

On the other hand, composite floors are made of pre-manufactured concrete, steel or timber elements acting compositely with the concrete slab (or 'topping') which forms the floor surface. Such forms of construction are typically supported by a system of beams and a building frame which is made of concrete, steel or timber. Floors made entirely of steel, timber or other non-concrete materials do exist, but they are not widely utilised in modern building developments.

Concrete floors, therefore, can be divided into two large sub-groups: (1) in-situ floors; and (2) composite floors. In-situ concrete floors as defined above are typically either reinforced or prestressed post-tensioned (PT). If composite floors are made entirely of concrete, precast elements are typically utilised. Such elements can be either classically reinforced or prestressed. The focus of this research work is on vibration performance of in-situ concrete floors, particularly long-span PT floors. Vibration behaviour of long-span floors made of in-situ high-strength concrete (HSC) with normal unstressed reinforcement will also be investigated, but to a much lesser extent.

A prerequisite for successful dynamic analysis of PT floors is, naturally, a clear understanding of the principles of their design under static load. Compared with the other flooring systems, design of PT floors is not routinely carried out in typical UK design offices. Only a handful of specialised UK consultants and contractors have the capability of designing PT floors. However, this, almost half-a-century old technology is extensively used overseas.

A detailed description of the basic design principles, materials, equipment and construction methods for post-tensioned floors are given by Khan and Williams (1995) and other more or less specialised texts on prestressed concrete design (Lin & Burns, 1982; Nilson, 1987; Gilbert & Mickleborough, 1990; Fintel, 1985; Hurst, 1988; Gerber, 1991; Stevenson, 1994; Concrete Society, 1979, 1984, 1994; FIP, 1980; PTI, 1977, 1990; VSL International, 1972; Ritz et al., 1985; Matthew & Bennett, 1990; Goodchild, 1995; Zahn & Ganz, 1992). Most of these references have already been summarised by the writer (Pavic, 1993) and the same exercise will not be repeated here.

The references consulted clearly indicate that modern design practice considers vibration serviceability as just one of several key design requirements which suspended concrete floors have to satisfy. These design requirements are based on philosophy of limit state design formulated in order to satisfy the principal aims in civil engineering structural design.

2.1.1 Limit State Design

Firstly, and most importantly, a structure has to be safe. Secondly, the safe structure must be functional, that is it is able to perform satisfactorily from day-to-day throughout its life span. If a structure becomes unsafe or is safe but fails to perform in service, then it reaches one or more of these limit states. The principal idea behind the limit state design method is to adopt a probabilistic approach and keep the structure from reaching the limit states with a certain pre-determined level of confidence (Kong & Evans, 1987; Gilbert & Mickleborough, 1990).

2.1.2 Limit States of Concrete Structures

Methods for the application of the limit state design philosophy, adopted by modern concrete design codes, vary slightly from country to country. All of them, nevertheless, define two main categories of limit states: ultimate and serviceability.

Ultimate limit states (ULS) are reached when a concrete structure or element collapses due to any reason such as loss of equilibrium of the whole structure, instability, rupture or transformation of a structure into a mechanism.

The new ASCE Standard 7-95 (ASCE, 1995) defines the serviceability limit states (SLS) as:

> "...conditions in which the functions of a building or other structure are impaired because of local damage, deterioration or deformation of building components or because of occupant discomfort".

Occupant discomfort is mainly caused by vibration motion of a building as a whole or of individual building floors. Whereas wind typically excites (tall) building vibrations, the occupant activities are the main source of floor vibrations (Ellingwood, 1996).

Reaching any of the ultimate limit states is highly undesirable as it may have catastrophic consequences leading to loss of life. Naturally, much research effort in the past has been devoted to these limit states (Ellingwood et al., 1986) in order to provide the engineering community with reliable design procedures which produce safe structures. However, a good design must also not be over-conservative as it will not be considered economically viable. It should, therefore, be stressed that, apart from safety and serviceability, economy plays a major role in successful contemporary concrete design.

Interestingly, Deak and Holicky (1993) recently reported that an "overwhelming majority of structural defects observed today are classified as serviceability, rather than safety problems". This was explained to some extent by MacGregor (1988) who blames the inability of engineers to formulate reliable models for dealing effectively with serviceability problems in design. The reason for this is that it is much more difficult to define SLS failure than ULS failure. This is because binary 'pass' or 'fail' criteria, typical for ULS analyses, may not be easily definable for their SLS counterparts. If minor structural damage or equipment malfunction is the criteria against which the selected SLS (deflection, vibration, etc.) is going to be evaluated, then such failure is relatively easy to define mathematically. However, if an SLS failure is to be detected by a subjective human response (feeling vibrations, fear of sagging or cracking, etc.), then the acceptable limits are, to use MacGregor's expression, much more "fuzzy". This is because of the great variability in perception of different human observers. Together with the generally lower amount of research effort put into SLS problems (compared to ULS problems), this prompted MacGregor to conclude that:

> "The calculation models available in serviceability limit states are much poorer than the strength calculation models. As a result, the treatment of serviceability in design is at a much less sophisticated level than the treatment of structural safety."

Irwin (1978), Ellingwood and Tallin (1984), Ellingwood et al. (1986), Ellingwood (1989) and Eriksson (1994) reached similar conclusions and stated the probable reasons for the general lack of interest in serviceability issues. In addition to the reasons already mentioned, basic experimental data on as-built performance was identified as being more available to practitioners than researchers.

Not surprisingly, since the construction of PT floors started in the USA in the 1950s, the bulk of the research work into their behaviour has been focused on the investigation of ultimate limit states such as flexure and shear. Comparatively fewer investigations have been carried out on the floor serviceability problems such as deflections and cracking. Almost no published research, of the systematic kind and amount performed for other limit states, existed into vibration serviceability of PT concrete floors prior to the commencement of the work on this doctoral thesis in September 1993.

2.1.3 Typical Design Procedure

Whereas strength considerations typically govern the design of reinforced concrete structures, serviceability tends to be the governing design criterion in the practical design of typical prestressed concrete structures.

Khan and Williams published an excellent textbook (Khan & Williams, 1995), the first of its kind, describing the state-of-the-art in the design and construction of PT concrete floors. They offered an algorithm, shown in Figure 2.1, of the steps which are typically performed when designing a PT floor in practice. Whereas the control of cracking is indirectly incorporated in the check of initial and final concrete stresses, and the check of deflections is explicitly shown, the algorithm does not offer a stage in the design when a vibration serviceability check(s) should be performed. Although the textbook contains a discussion of the vibration serviceability problem, clearly indicating that the authors did not neglect it, this omission illustrates that the whole issue is, somehow, a 'grey area' which practitioners still hesitate to include in everyday design (Williams, 1997). The writer's personal experience gained while working as a consultant on floor vibration serviceability problems for two major UK developers of concrete floors, PSC Freyssinet Ltd (Bracknell) and SCC Ltd (Sheffield), also underpins this view (Bennett, 1995; Waldron & Pavic, 1995, Petkovski et al., 1997; Pavic & Reynolds, 1997; 1999).

Ideally, the vibration serviceability check should be done immediately after the floor occupants and usage, as well as its spans, cross sections, material properties, and loads are determined (shaded box in Figure 2.1). These parameters, in principle, provide enough information for checking the vibration serviceability. Hence, it is prudent to perform this check as soon as possible in order to reduce any waste in design time should the floor be found to be deficient. Any such deficiency may require significant structural changes and a repetition of the design.

Nevertheless, the crucial problem in the design stage of in-situ PT concrete floors is how to create a reliable model to perform such vibration serviceability checks. These floors have some unique structural properties which are difficult to model following the procedures which have been established through combined experimental and analytical research of other types of floors, such as composite steel-concrete or timber floors.

2.1.4 Structural Properties of Post-Tensioned Floors

PT floors are not always fully cast in-situ. They may also be constructed as a hybrid of in-situ and precast concrete elements (Stevenson, 1994; Goodchild, 1995). The principal interest of this thesis is in monolithic long-span concrete floors made entirely of in-situ concrete cast integrally with the rest of the building frame. Therefore, the term 'post-tensioned (PT) floor' is used here to denote such a form of construction which can be built employing a variety of construction methods and structural forms (Khan & Williams, 1995).

2.1.4.1 STRUCTURAL FORMS OF POST-TENSIONED FLOORS

PT floors are typically constructed as:

- One-way spanning ribbed slabs (Figure 2.2);
- Banded beam and slab construction (Figure 2.3);
- Flat slabs (Figures 2.4 and 2.5).

It is worthwhile mentioning that the term flat slab means that there are no downstanding beams protruding from its soffit - such floors are beamless. However, this does not necessarily mean that the slab is always solid because coffered (or waffle) slabs having ribs running in two directions could also be considered as a sub-group of flat slabs (Figure 2.5). A flat plate is a term, frequently used in North America, which is reserved for the solid flat slabs supported directly by columns (Libby, 1990), as shown in Figure 2.4a. Alternatively, column heads or drop panels may be introduced in solid flat slabs (Figure 2.4b and c) in order to increase their punching shear resistance.

2.1.4.2 STIFFNESS AND MASS DISTRIBUTION IN POST-TENSIONED FLOORS

Figures 2.3, 2.4 and 2.5 show some typical configurations of PT floors, such as solid flat slabs or banded beam and slab construction, which normally do not exist in other flooring systems, such as timber and composite steel-concrete floors.

For example, in composite steel-concrete floors, relatively deep and stiff joists and/or girder beams supporting the rest of the floor are clearly identifiable. Flat slabs do not have any such beams, whilst band beams in slab and beam PT construction are usually wide and shallow.

The usual classification of floors into one- and two-way acting systems, based on the static load paths and governed by stiffness distribution, requires further consideration in the case of PT concrete floors. In PT floors, the distribution of static design load depends not only on the geometry (i.e. stiffness) of the floor, but also on the distribution of prestressing and the amount of the design load that it balances. For example, a typical two-way acting flat plate having tendons which balance the design load in only one direction (Figure 2.6b) will become a one-way floor system for the balanced portion of the static load. This is one of the key concepts in the design of PT floors described by Nilson (1987) in considerable detail. However, although one-way acting for static loading, such flat slab or banded beam-and-slab systems may develop two-way action under low-level dynamic loading (Caverson, 1992; Pavic et al., 1994; Khan & Williams, 1995).

If design loads are not excessive, the prestressing tendons may be passed through the slab thickness without any need to introduce downstanding beams. This is how an integral 'invisible' beam is formed in a solid flat slab. If beams are required, then they may typically be wide and shallow as mainly the prestressing, and not the concrete beam bending stiffness, balances a large proportion of the design load and counteracts deflection (Khan & Williams, 1995).

The non-existence of beams, or the presence of wide, shallow and relatively flexible band beams, which nicely blend with the rest of the slab soffit, makes it difficult to determine the mass and stiffness distribution in post-tensioned floors using simplified beam-like models (Williams & Waldron, 1994). Such modelling procedures are typically employed when checking the vibration serviceability of, say, composite steel-concrete floors. In such floors, the concrete slab and the supporting lines made of stiff steel beams are clearly identifiable allowing more confidence in the structural rationalisation using linear beam elements to simulate the assumed one-way action of the whole floor system.

2.1.4.3 MONOLITHIC BEHAVIOUR

PT floor panels (BSI, 1985), which are cast in-place, are expected to act monolithically with the remaining panels and other elements of the building frame. There are several reasons for this. Firstly, they are in-situ structures where, by the very nature of the construction method, the elements which are cast together also act together after the concrete hardens. Secondly, the standard design details associated with the unstressed secondary reinforcement and connections (overlapping, anchoring, etc.) in cast in-place concrete buildings encourages this joint action. Thirdly, prestressing tendons, bonded or unbonded, typically run continuously along several floor spans further ensuring continuity. Finally, there is a design requirement to pass at least two tendons through the supporting columns, primarily in order to enhance the shear resistance of the floor (Concrete Society, 1994). The resulting column-slab connection could, actually, be so strong that Khan and Williams (1995) state that:

> "The moments in a floor may also be affected by the imposition of live load on the floors above and below, but this is normally ignored [in the design for static loads]."

However, the dynamic model aimed at checking the vibration SLS of in-situ PT concrete floors, which is recommended by the Concrete Society (1994), utilises pin-supports allowing free rotation (Feltham, 1995). The roots of such a modelling assumption are in ULS design calculations where such simplifications proved to be perfectly justifiable when structural elements are under a high level of loading (Eriksson, 1994). However, the amount of error introduced by such a modelling assumption and its consequences as to the design assessment of floor vibration serviceability are not exactly known, although some early indications exist that they might be severe (Williams & Waldron, 1994).

On the other hand, composite floors made of pre-manufactured concrete elements are naturally 'disjointed' from the rest of the building frame. Considerable attention must be paid to the connections between the precast elements and the subsequent load bearing elements in a building frame in order to achieve the desired level of joint action.

It is interesting to mention here that rather unfortunate but unique 'dynamic testing' of a number of full-scale concrete buildings utilising precast and in-situ PT concrete floors took place during the Northridge earthquake, USA in 1994. Compared with the in-situ cast counterparts, the precast structures performed rather poorly, the main problem being the lack of continuity between the horizontal and vertical load bearing

elements in many collapsed precast structures (Freyssinet International, 1994). Therefore, it is prudent to make a clear distinction between in-situ and various types of precast composite concrete floors as possibly different levels of the structural monolithisation may affect many aspects of structural behaviour, including vibration performance.

2.1.4.4 ADVANTAGES AND DISADVANTAGES OF PT FLOORS

The main advantage of utilising post-tensioning in in-situ concrete slabs is the reduction in thickness which leads to smaller column and foundation sizes. In practice, PT floors can accommodate 50% greater spans then their classically reinforced counterparts of similar thickness (Figure 2.7).

Stevenson (1994), however, gave a list of popular misconceptions about PT floors mostly related to the utilisation of 'dangerous' unbonded tendons. Industry tends to perceive these misconceptions as disadvantages of PT floors.

Regarding the pros and cons of PT floors as structural systems, in 1979 Mays reviewed and compared the then existing internationally adopted procedures for the design of in-situ PT floors in buildings. The numerous benefits of the structural system were outlined and it was explained that seemingly over-conservative shear design was the principal reason for the unpopularity of the system in the UK.

Mays also mentioned two additional possible deficiencies of long-span in-situ concrete floors. The first was the shortening of long PT slabs due to prestressing, creep and shrinkage. The second was the existence of a limit, which was not stated, to which the thickness of the floor could be reduced before the floor became "springy and disconcerting to walk on" clearly expressing concern about the floor vibration serviceability. Whereas the problem of shortening could be remedied by careful detailing and the use of expansion and construction joints, Mays offered no clue as to how to tackle the possible vibration serviceability issue.

2.2 State-of-the-Art Assessment of Vibration Serviceability

Vibration is an omnipresent form of dynamic motion in which the structure oscillates about an equilibrium position (Meirovitch, 1986). Such motions arise from the interaction between time varying structural disturbances, such as forces or imposed displacements, and inertial properties of the structure (ISO, 1992). Vibrations are a constitutive part of the environment and are unavoidable. In principle, everything vibrates all the time. The problem with vibrations occurs when they become excessive causing annoyance, malfunction of sensitive equipment, damage or structural failure. The human annoyance factor is, however, the most frequent vibration serviceability problem. For example, vibration is regarded as one of the seven main sources of environmental pollution in Japan (Abe et al., 1994).

Although the problem of human vibration is, reportedly, very difficult to deal with, design decisions have to be made in contemporary design practice where the vibration SLS has to be considered. An outline of a general state-of-the-art procedure based on the latest international ISO 10137 (ISO, 1992) and British standards BS 6841 (BSI, 1987a) and BS 6472 (BSI, 1992) will be presented here.

Following the ISO 10137 procedures, the first step towards the assessment of vibration serviceability of floors is to identify and characterise the following three key factors:

1. the vibration source,
2. the transmission path, and
3. the receiver.

2.2.1 Vibration Source

The sources of floor vibration generate dynamic actions which may vary both in time and in space. They can be divided into two groups: (1) inside (or internal), and (2) outside (or external).

Typical examples of internal floor vibration sources, originating in the building, are:

- Human excitation, such as walking, running, jumping and stomping;
- Machinery, such as elevators, lift trucks, punches and presses;
- Various construction activities within the building.

ISO 10137 defines two general classes of vibration serviceability problems depending on the vibration source. Class A problems are much more complex as they involve vibration sources which vary both in space and in time. Class B problems are caused by stationary vibration excitation which changes only in time. Excitation of floors induced by the walking of its occupants is an example of a Class A problem, whereas excitation from mounted machinery is a Class B problem. As regards the Class A problems, ISO 10137 states that:

> "The complexity of these problems is one reason why many of them have been treated by empirical methods, or by extensive use of measurements on similar existing structures."

2.2.2 Transmission Path

The transmission path is a medium which passes on excitation from the vibration source to the receiver. Structural components transmitting vibrations could be foundations, columns, walls and floors, whereas non-structural paths may be access floors, removable partitions, cladding, etc. Physical properties of the transmission path, such as stiffness, mass or damping, modify the vibration excitation at the source into a structural response 'felt' at the position of the receiver.

2.2.3 Receiver

ISO 10137 defines the receiver as "the object or person for which the vibration effects are to be assessed". The persons are, obviously, the human occupants of the building whereas the objects can be either vibrating structural or non-structural elements (windows, walls, beams, slabs, etc.) or contents of the building such as instruments or machinery. An amount of vibration passed to the receiver should be evaluated in accordance to certain established criteria. This evaluation is the core problem of the vibration serviceability assessment.

As to the floors, two types of vibration serviceability assessment exist: (1) the evaluation by calculation during the floor design stage, and (2) the evaluation by vibration measurement of already built full-scale floor structures (ISO, 1992; Griffin, 1996). In both cases, the state-of-the-art assessment approach, based on a proper characterisation of the vibration source, transmission path and receiver, is required. The difference between the calculation and the measurement based assessments comes, naturally, from the way that the response at the receiver is obtained. In the case of the former, it is obtained by mathematical modelling of the structure and performing its (analytical) vibration response calculations for the given vibration excitation. In the case of the latter, the response is obtained by measurements on a real-life floor structure under the specified excitation.

Although this rationalisation of the vibration serviceability problem into the characterisation of the vibration source, transmission path and receiver may seem simple, it is, actually, a very difficult task requiring a thorough understanding of the floor vibration phenomenon. For example, it is common for humans to act as both the floor vibration exciters and receivers (Wyatt, 1989). If this is the case, as it is here, then a considerable amount of background knowledge is required in order to understand the appropriate vibration serviceability criteria and to apply the latest national and international vibration evaluation standards. Those standards are far from being perfect (Bolton, 1994; Eriksson, 1994), but Griffin (1996) justifies this by saying:

> "The shaking of the human body - a complex, active, intelligent, dynamic structure - should not be expected to have a single, simple or easily predictable consequence."

In 1988, Galambos characterised the knowledge of floor vibration serviceability as "only the beginning of what should be known". In addition, only two years ago Ellingwood (1996) assessed treatment of the floor vibration serviceability (together with other serviceability requirements) in the wider engineering community in the USA as having "a significant degree of ambivalence" and as "controversial". The main problem being whether or not to treat the vibration serviceability requirements as mandatory in the building standards and codes of practice. The relevant ASCE Committee 7 was, according to Ellingwood (1996), deeply divided over this issue. As a result, the limited floor vibration serviceability provisions given for the first time by the ASCE (1995) are non-mandatory. Similar provision exists in ISO 10137 (1992), the four Annexes of which contain the most valuable practical information as to the problem of vibration serviceability. The Annexes are still "for information only".

However, this does not mean that vibration serviceability is considered by the ASCE as unimportant. For example, the only consensus the ASCE Committee 7 managed to reach was that compliance with the serviceability requirements directly affects the building cost and is, therefore, very important for the client. This is the main reason why the ASCE (1995) serviceability requirements are given, but are non-mandatory. Consequently, the research community should provide designers with appropriate procedures to deal with all serviceability limit states, including floor vibrations (Ellingwood, 1996).

To conclude, the main idea of the state-of-the-art procedures which are mentioned so far and are, in general, accepted worldwide, is to provide the common framework not only for future designs but also for research (ISO, 1992). Future research work should, nevertheless, draw on the numerous past investigations pertinent to the vibration serviceability of building floors which are presented in the following section.

2.3 Vibration of Floors: Literature Review

The principal aim of the review is to outline the key features of the floor vibration serviceability problem and determine areas where lack of knowledge exists and which it would be prudent to focus on and pursue in this thesis.

2.3.1 Early Works

Most of the knowledge about vibration performance of suspended floors in buildings has been gained during this century. However, evidence that floor vibrations were an issue even in the last century exists. Allen and Rainer (1975) and Sabins (1979) quoted the following statement made in 1828 by Thomas Tredgold, a famous carpenter and one of the fifty founders of the ICE:

> "Girders should always, for long bearings, be made as deep as they can be got; an inch or two taken from the height of a room is of little consequences compared with a ceiling disfigured with cracks, besides the inconvenience of not being able to move on the floor without shaking everything in the room."

Hyde and Lintern reported in 1929 that there had been a considerable concern about the damage to roads and buildings due to external vibrations caused by the growing transportation systems. According to them, the problem was not new as H. R. A. Mallock had experimentally investigated in 1901 vibrations caused by the Central London Railway. Prompted by numerous complaints, Mallock investigated the effects of vibration from passing trains on houses near Hyde Park. This work is one of the earliest pieces of evidence of research on human sensitivity to vibrations in buildings (Steffens, 1965). Mallock considered floor (presumably peak) accelerations of 5% g to be a nuisance whereas five time lesser accelerations could be considered as "noticeable" to the floor users. He also maintained that different people will have different personal

sensitivity to the same floor vibrations. This was one of the first attempts to understand the variability in subjective annoyance to vibrations (Dupius & Zerlett, 1986).

Working almost 30 years later on a similar problem, Hyde and Lintern dismissed the use of Mallock's equipment for measuring vibrations as unsuitable and obsolete so they designed their own. The requirements which the new mechanical vibration measuring instrumentation had to satisfy were: (1) portability, (2) a low natural frequency of the main transducer, (3) an easily reproducible graphical recording, (4) adequate mechanical scaling, (5) long data recording times, and (6) high sensitivity. Interestingly enough, 70 years later, almost the same requirements can be put forward when commissioning a modern digital data acquisition system suitable for field measurements and the assessment of vibration serviceability in buildings, as will be shown in Chapter 4 of this thesis.

Hyde and Lintern measured maximum floor accelerations of 2% g. For the relatively short duration of measurements such acceleration levels were said not to constitute "nuisance". However, it was concluded that "a persistent vibration of this nature would be decidedly uncomfortable to persons in buildings", indicating an awareness of the effects of vibration exposure duration on human response.

Since the 1930s the number of papers related to various aspects of human vibration has been growing rapidly, particularly because of the fast development of transportation where problems due to higher level of vibration imposed on humans are more pronounced. As the problem of such vibrations is generally different to the problem of low-level vibrations in buildings, there was a need in this project to classify the vast literature available to date in order to handle it effectively.

2.3.2 Classification of the Published Literature

Research into vibration serviceability of concrete floors is interdisciplinary as it encompasses broad scientific areas such as signal analysis, human vibration, (bio)mechanics of walking, concrete structural engineering, experimental and analytical structural dynamics, etc. There is a lot of published literature covering one or more of these aspects. However, if focused on low-level vibrations of long-span floors supporting relatively quiet occupancies, which is the subject of this thesis, the range of pertinent literature can be reduced considerably. The literature surveyed may conveniently be divided into the following groups:

Group 1: Literature mainly covering determination and modelling of dynamic forces caused by walking (vibration source characterisation). Apart from office floors, such excitation is important when analysing various more specialised pedestrian structures such as footbridges and stairs.

Group 2: Literature covering research into dynamic properties of floors as structural systems (vibration path characterisation) without considering in detail the vibration source or its receiver's response.

Group 3: Literature covering the area of the receiver's response to vibrations without considering in detail the vibration source or its path (vibration receiver characterisation). Typically, the role of the receiver is taken either by humans (Griffin, 1996) or sensitive equipment (Ungar & White, 1979; Shioya & Maebayashi, 1988), the former being much more publicised than the latter. Publications into general human response to vibrations are pertinent to many areas such as defence, transportation, health and safety. For example, the review by Griffin alone (1996) contains more than one thousand references on human vibration. However, very many of these are not relevant to the problem of low-level floor vibrations in quiet building occupancies. Compared to other applications, human response to building vibrations is under-represented in this group.

Group 4: Literature covering vibration performance of floors in relatively quiet environments where all three key factors, the vibration source, path and receiver, are considered together. This integrated (or 'packaged') approach can frequently be encountered when dealing with vibration serviceability of any type of floors in buildings (Wyatt, 1989; Eriksson, 1996). Consequently, the majority of papers which specifically cover floor vibration serviceability belongs to this group.

Group 5: Literature covering vibration performance of a wider range of structures, mainly under dynamic loads induced by groups of people. These publications typically deal with footbridges (Leonard, 1996; Smith 1969; Blanchard et al.. 1977; Campbell et al., 1979; Wheeler, 1980; 1982; Tilly et al., 1984), grandstands, gymnasia, dance floors (Allen et al., 1985; Rainer & Swallow, 1986; Allen 1990a; 1990b) and other types of structures where, generally, greater levels of vibration occur.

Group 6: State-of-the-art reviews or proceedings of specialised conferences published from time to time, where literature from all the above mentioned groups is included (Steffens, 1952; 1965; 1974; BRS, 1955; Galambos et al., 1973; BRE, 1983; Bachmann et al., 1991a; 1995a; NRCC, 1988; IABSE, 1993).

The literature classified as Group 4, where all the key elements of low-level, but possibly annoying, floor vibrations are considered, is the most relevant to the investigation reported in this thesis. Vibration serviceability of lighter timber and composite steel-concrete floors is particularly well elaborated in this group. However, more relevant for this investigation are heavier low-frequency floors made of concrete (Wyatt, 1989; Eriksson, 1994). Only a handful of papers, mainly published in the course of this research work, treat the vibration serviceability of cast in-situ reinforced and PT concrete floors.

2.3.3 Walking Excitation

One of the first papers dealing with the forces caused by human walking was published by Harper (1962). The research described was not related to vibrations of floors but to the abrasion and slipperiness of floor surfaces. For these, the exact level of vertical and horizontal forces transmitted from a foot to the floor surface is of crucial importance. The reported force vs. time measurements involved several human subjects. All of the traces clearly resemble the characteristic 'two peak' forcing pattern (Figures 2.8 and 2.9) observed by many researchers afterwards (Bachmann et al., 1991a; 1995a). These time-varying force fluctuations are caused by inertial forces developed through the acceleration and deceleration of a human body which rises and falls during walking. As a relatively small single force plate was used, only time-varying forces from a single footstep were recorded. This was the main deficiency of these and other similar measurements (Ohlsson, 1982; Bishop et al., 1995) as no continuous walking excitation including both feet and their interaction was registered. Nevertheless, Harper characterised walking footprint time signatures as "broadly similar for all subjects" indicating that some sort of generalisation of the walking forcing function could be possible for the whole human population.

This was supported by Leonard (1966) and Smith (1969) who investigated vibration serviceability of footbridges and reported that the walking excitation appears to be periodic with frequencies between 1.5 Hz and 2.3 Hz. However, in the late 1960s, the characterisation of such periodic excitation and its implementation into dynamic calculations of footbridge vibration responses was (still) quite difficult. This was the reason for Smith to comment:

> "There is no method known to the author for calculating the dynamic response of a simply supported beam arising from loads applied by a person walking across."

Galbraith and Barton (1970) were involved in the development of an intruder detection system which would be based on earth micro-tremors caused by walking or running of an intruder. Forces induced by such activities were measured. It was found that walking and running produce markedly different forces where those corresponding to running were shorter in duration and greater in magnitude. Also, in running, periods when both feet were off the ground were clearly observable between the forcing peaks. On the other hand, in periods of normal walking forces induced by left and right leg overlapped which means that both legs were periodically on the ground (Figure 2.8). In addition to the type of movement (walking or running), the paper reported that the weight of a walker plays a significant role in determining the magnitude, but has less effect on the actual shape of the force fluctuation. Finally, the type of footwear and traversing surface were found to have little effect on the forces applied by human movements.

Blanchard et al. (1977) used results from measurements of the periodic forcing function induced by walking to establish a procedure for checking vibration serviceability of footbridges adopted in the current UK standard which describes loads for highway bridges (BSI, 1978). By treating the walking forcing function (Figure 2.8) as periodic, and decomposing it into Fourier series components, it was found that the peak of the fundamental harmonic corresponds to a quarter of the weight of the walker. Blanchard et al. proposed only

the fundamental harmonic to play the role of the complete time-varying excitation due to walking. A similar method was used by Matsumoto et al. (1978) who found that the pacing rates are normally distributed around two paces per second. It should be mentioned that the modelling procedure based on a fundamental harmonic only was dismissed by Ellingwood (1989) as inadequate when checking the vibration serviceability of floors. Ellingwood maintained that a more detailed representation which would include the heel impact and toe lift-off (i.e. higher harmonics) is required in the case of floors.

Wheeler (1980; 1982) also investigated pedestrian-induced vibrations in footbridges. After compiling the work of others, he gave an excellent description of the excitation caused by six different modes of human movements: (1) slow walk, (2) normal walk, (3) brisk walk, (4) fast walk, (5) slow jog, and (6) running. These forcing functions are shown in Figure 2.9. The speed of walking was determined to be between 0.75 m/s (slow walk) to 1.75 m/s (fast walk).

2.3.3.1 IMPERFECTNESS OF HUMAN-INDUCED EXCITATION

Tilly et al. (1984) also investigated walking excitation in conjunction with the vibration serviceability of footbridges. It was reported that 95% of people walk normally with a pacing rate of 1.5 to 2.5 steps per second. Also, it was suggested that, being periodic and non-sinusoidal, walking forcing functions have higher harmonics in addition to the fundamental. Frequencies of these are integer multiplies of the fundamental walking frequency (1.5-2.5 Hz) and, in principle, have the potential to excite the fundamental or other vibration resonances in footbridges. However, it was also found that humans are not as perfect exciters as, say, machines, able to maintain the pacing frequency which excites the footbridge resonance spot-on. This is especially so in the case of lightly damped structures. In such structures, due to the narrowness of peaks around resonances in the FRF modulus function, and due to large response amplification at resonance, only a slight off-resonance (or near-resonance) excitation may result in a tremendous reduction in the response. This important aspect was clearly confirmed by Matsumoto et al. (1978) and, to some extent, by Tuan and Saul (1985; Saul & Tuan, 1986). Tuan and Saul reported that movements of an individual or a group of people could not be precisely duplicated in repeated experiments even when a timing device was used.

Rainer et al. (1988b) also reached a similar conclusion about the imperfectness of the periodic excitation induced by walking humans on footbridges. The sinusoidal steady-state SDOF response models of a footbridge, which are based on walking harmonics exciting the first mode resonance, are shown to be conservative. Such analytical models produced peak accelerations which were almost twice higher than the measured peak accelerations even though the pacing rate was deliberately timed in the footbridge experiments to excite the resonance.

Ellis and Ji published in 1994 two linked papers proposing modelling of human induced dance-type loads. The first paper (Ji & Ellis, 1994) maintains that dance-type loads, as somewhat impulsive and periodic, may have many significant Fourier harmonics above the 3rd harmonic, which is usually considered as the highest

important loading harmonic for walking excitations. The sequel to the first paper (Ellis & Ji, 1994) attempts to verify experimentally that even the 6th harmonic of jumping can excite structural resonance (at approximately 14.4 Hz). The experimentally measured peak accelerations were about 20% g, which was 3 times lower than the predicted peak accelerations assuming that the exact resonance of a SDOF dynamic model has been achieved. Difficulties were reported for a single human subject to adjust the jumping frequency so precisely that exact resonance is achieved in a simply supported beam having a low damping ratio of only 0.35%. Despite this, the authors concluded that higher harmonics of dance-type loads can excite "resonance", although, a term 'near-resonance' instead of 'resonance' would have been, perhaps, more appropriate.

2.3.3.2 RECENT ADVANCES IN DEFINING EXCITATION DUE TO WALKING

Recognising that vibration serviceability is increasingly the governing design criterion for floors, Eriksson (1996) proposed that it should be the owner's responsibility to specify dynamic service actions for which the floor should be designed. In order to facilitate such a decision, the following list of so called service action classes is given:

- Class A1: Light domestic type activity;
- Class A2: Intermittent pedestrian traffic (e.g. office corridors);
- Class A3: Public pedestrian traffic and light machine installation;
- Class A4: Crowded open space or mall areas without vehicle traffic;
- Class A5: Open space areas with vehicle traffic and pedestrians;
- Class A6: Medium machine installations and vehicle traffic;
- Class A7: Dance halls and gymnasia;
- Class A8: Assembly areas for concerts or sports events;
- Class A9: Heavy machine installations and vehicle traffic.

This list is similar to the one produced by Bachmann et al. (1991a, 1995a), and, obviously, Class A2 excitations can be identified as pertinent to the research work presented in this thesis. The proposed excitation corresponding to this class is "a single person walking assumed to tread in place". Eriksson also suggested a "return period" for walking excitation, i.e. how often a single person can be expected to traverse a floor and cause vibrations. In the case of offices it may be assumed to be anything between 60-3600 s. Excitation in other classes is typically very much different to Class A2 emphasising that it is extremely important to have a clear idea about the function of the floor prior to embarking on its vibration serviceability assessment. This stresses the role of the client and/or owner who should have the main influence when deciding about the required level of the building performance (i.e. serviceability) in conjunction with the increased cost when better performance is required (ASCE, 1995; Ellingwood, 1996).

Rainer and Pernica (1986), and Pernica (1990) reported measurements of continuous time-varying vertical forces from a number of subsequent footsteps while walking and running. The forces were measured indirectly using a mid-support reaction of a two-span continuous steel truss. The amplitudes of the fundamental and higher harmonics of walking were found to vary considerably depending on the pacing rates and the length of the stride. Also, it was found that the third harmonic of walking (around 6 Hz), which is particularly important for the low frequency floors (Wyatt, 1989), has an amplitude which is approximately only 10% of the weight of the walker and is four times lower than the amplitude of the first harmonic.

Bachmann et al. (1991b; 1995b) also considered the walking forcing function as periodic and, as such, a time-domain force model based on Fourier series was proposed. The amplitudes of such Fourier components are either taken from or are in broad agreement with the published work of others (Tilly et al., 1984; Rainer & Pernica, 1986; Rainer et al., 1988b; Pernica, 1990).

Eriksson and Ohlsson (1988) and Eriksson (1993) maintain that the time-domain floor dynamic response calculations, such as those suggested by Rainer and Pernica (1986), Pernica (1990) and Bachmann et al. (1991b; 1995b), are difficult to perform in practice if several people and several excitation harmonics are to be considered at once. Therefore, a new method was proposed for calculating the floor response in the frequency domain. Such a method is appropriate when assessing the vibration serviceability of low-frequency and relatively heavy concrete floors having closely spaced natural frequencies lower than 8 Hz. The crucial assumption in this case is that walking excitation can be presented in the frequency domain utilising auto-spectral density (ASD) representation of the time-domain forcing signal. The force ASD (McConnell, 1995) and the floor accelerance FRFs (Ewins, 1995) are then used to calculate the floor RMS acceleration responses which are necessary for floor vibration serviceability assessment. However, the authors of this, seemingly very powerful method, suggested further experimental verification of its performance.

This frequency-domain approach became very popular in the 1990s as Mouring and Ellingwood (1993; 1994) proposed such an approach for modelling crowd induced excitation on floors accommodating a large number of people, such as those in shopping malls. In this case an assumption is made that the structure responds only in the first mode of vibration which is restrictive in the case of floors having closely spaced modes of vibration.

The theoretical background to these frequency-domain procedures is outlined in standard textbooks (Newland, 1993; McConnell, 1995) and will not be repeated here. However, the frequency domain approaches and a selection of other practically usable models for numerical simulation of the floor excitation due to single person walking are presented in more detail in Chapter 3 which deals with the analytical modelling procedures adopted in this thesis.

2.3.3.3 HUMAN-STRUCTURE INTERACTION AND CROWD DYNAMIC LOADING

Another interesting aspect of human actions on structures is the problem of human-structure interaction. The key issue here is whether and to what extent the very presence of humans change the structural dynamic properties and the amount of vibration received. Ji and Ellis (1995) indicated that when humans are moving then they are acting only as dynamic forces with little influence on the structural dynamic properties. On the other hand, stationary people have ability to change structural mass, stiffness and/or damping, and should be modelled as a spring-mass-damper system attached to the main structure. Furthermore, Ellis and Ji (1997) expanded on this and specified that human-structure interaction needs considering only when the human mass is relatively substantial (not stated exactly how much) compared to the mass of the supporting structure. These situations typically occur in floor and other structures under crowd loading or in relatively light floor structures where even a single person may change substantially their dynamic properties (Rainer & Pernica, 1981; Fochi & Gupta, 1987). Consequently, human-structure interaction appears to be unimportant when assessing the vibration serviceability of heavier office floors made entirely of concrete for which crowd loading is not normally considered (Eriksson, 1994).

As crowd loading is not directly related to this research it suffices to say only that, in the engineering community, such loading has attracted a considerable amount of attention over the past decade. The reason is that it may become both a safety and serviceability issue when designing places of human assembly (Tuan & Saul, 1985; Saul & Tuan, 1986; Ebrahimpour & Sack, 1988; Ji & Ellis, 1993; Ebrahimpour & Fitts, 1996; Ebrahimpour & Sack, 1996; Ebrahimpour et al., 1996; Reid et al., 1997). Crowd loading may also be important in the case of footbridges and Pimentel (1997) reviewed this aspect in detail.

2.3.4 Dynamics of Concrete Floors

Apart from classical textbooks on statics and dynamics of plate systems (Szilard, 1974), a number of papers specifically cover dynamic characteristics of building floors made of concrete. They are typically related to subjects other than problems of human induced and perceived vibrations, such as the isolation of vibrating machinery.

Burkhardt (1961) proposed a nomogram based procedure for analytical modelling and design checking of floors under resonance excitation from heavy machinery which they support. In this approach the whole floor structure had to be somehow rationalised into a drastically simplified single-span beam which was either simply supported, had fixed ends, or was a propped cantilever. Such dynamic modelling was common in the early 1960s, as the available design tools did not allow any more complex (and accurate) design modelling to be employed.

Petyt and Mirza (1972) used FE modelling and performed a parametric study of natural frequencies and mode shapes of column-supported floor slabs (i.e. flat plates). Their work was inspired by the increasing need from the construction industry where solid flat slabs made of concrete were becoming popular. In the

case of a single floor panel, which was pin-supported at all four corners, the first five natural frequencies, experimentally measured using a small model in a laboratory, were compared with their analytically calculated counterparts. An excellent comparison was obtained justifying the use of the FE technique. However, Petyt and Mirza, commented:

> "... in building construction, if the slab and columns are cast in situ, the joint may be regarded as rigid. Even in the construction of prefabricated panel systems, certain bending rigidity may be introduced if the joints are welded or when additional reinforcement is used and gaps are filled in situ."

In conjunction with this, it was demonstrated that bending stiffness of the in-situ columns may play a significant role in determining the slab natural frequencies which is one of the key dynamic parameters of any floor structure under dynamic loading. Petyt and Mirza have also shown that, as a matter of principle, nodal lines of modes of vibration should not be assumed to run along the 'stiffer' column lines in the case of flat slabs.

The importance of accurate modelling when checking the vibration performance of floors was also demonstrated by Heins and Yoo (1975). They concluded that a properly restrained equivalent grillage was a much better mathematical representation of the floor structure than a single beam-like element(s), typically advocated in the codes of practice.

Fahy and Westcott (1978), and White and Liasjø (1982) made, at that time rare, in-situ measurements of point mobility FRFs using a portable shaker on a number of precast and cast in-situ concrete floors. The measurements were taken under severe time limitations imposed by less than enthusiastic owners and users of the test structures. An analysis of the limited experimental data produced large variations in damping measurements which forced the authors of the latter paper (White & Liasjø, 1982) to conclude that it is very difficult to accurately measure damping in existing building structures. The writer speculates that one of the reasons for this could be a damping estimation procedure based on a SDOF model which was applied on (seemingly) very noisy FRF data having closely spaced modes of vibration. Abe et al. (1990) explained that the floor bending orthotropy, which exists in many forms of concrete slabs, creates closely spaced modes of vibration.

Caetano and Cunha (1993) presented a very advanced method for estimating the vibration properties (natural frequencies, mode shapes and modal damping ratios) of a relatively small (6.6 msquare, weighting approximately 15t) but full-scale reinforced concrete roof slab having closely spaced modes of vibration. This powerful method, adopted from the more advanced mechanical and aero-space engineering disciplines, is based on state-of-the-art modal testing technology (Ewins, 1995; Maia et al., 1997) and it consists of:

1. FRF measurements using a manually operated instrumented sledge-hammer,
2. MDOF vibration parameter estimation using the measured FRFs,
3. FE modelling prior to the full-scale testing, and
4. FE model correlation with the experimental data gathered after modal testing.

An excellent correlation was achieved between the first eight measured and calculated modes of vibration. However, to achieve this, a full 3D FE model had to be developed. Unfortunately, due to the limited scope of the paper, no information was given as to how successful such floor modelling had been with regard to, say, response calculations due to human induced dynamic loading.

2.3.5 Human Response to Vibrations in Buildings

Studies into human response to whole body vibrations (ISO, 1985; Griffin, 1996), which led to the introduction of the existing state-of-the-art vibration assessment procedures, were either laboratory or field based (Irwin, 1978). Although laboratory based research is frequently reported in the literature, field investigations are valued more as they tend to represent more accurately the possibly strong influence of the real-life environments on the human perception of vibrations (Irwin, 1978). However, field investigations are much more difficult to perform in practice and this appears to be the main reason for the general lack of such data.

2.3.5.1 Early Research into Human Perception of Vibrations

One of the first laboratory studies into human vibration was carried out by Reiher and Meister. In 1931 they published a paper (unavailable to the writer) entitled "The Sensitiveness of the Human Body to Vibrations" in which they investigated the effects of sinusoidal whole-body vibrations. This research, which, according to the secondary sources, had a great impact on the scientific community, recommended bounds for "imperceptible", "just perceptible", "clearly perceptible", "annoying", "unpleasant" and "painful" vibrations as a function of harmonic displacements and frequency (Figure 2.10).

Inspired by the great inconsistency in the available data on human response to vibrations, in 1944 Postlethwaite presented an overview of the research work that had been carried out to date. He interpreted the then existing research data and determined a vibration perception threshold ('feel'-'no feel') of only $0.01 ft/s^2$ (0.03% g) for frequencies lower than 10 Hz. This (probably sinusoidal peak acceleration) value was much lower than the values reported as "noticeable" (1% g) by Mallock at the beginning of the century, who did not explain what noticeable exactly meant (Hyde & Linterm, 1929). Obviously, the weakness of Reiher and Meister's and other approaches based on similar subjective ratings of vibration is that it is not clear what precisely the vibration quantifiers, such as "annoying" or "unpleasant", mean and what is the difference between them. The problem of semantics in human vibration research was becoming apparent, as numerous authors would later observe (Guignard, 1971; Jones & Saunders, 1972; Galambos et al., 1973; Rasmunsen, 1982). However, Postlethwaite's vibration threshold was experimentally confirmed by Dieckmann (1958) who determined it at $4 cm/s^2$ (0.4% g). Dieckmann also established the existence of a lumped-parameter model of a human body of the kind shown in Figure 2.11, but much simpler.

Wright & Green (1959) detected a trend towards the proliferation of various vibration perception scales which were applicable only to specific situations. Although numerous human vibrations studies and state-of-the-art reviews existed at the time when Wright and Green compiled their report, they found them "incomplete and often misleading" lacking interdisciplinarity because "most shortcomings in reviews have been due to limited interests related to specific fields of application". With regard to civil engineering applications, such as vibration of bridges or floors in buildings, this means that little guidance existed as to how to apply the numerous vibration rating scales when assessing the performance of real-life structures at the design stage or after they were built.

In the same year, Guignard and Irving (1959) recognised that whole-body human vibrations can be caused not only by steady-state sinusoidal and periodic, but also by transient non-periodic disturbances. Although transient vibration is frequently happening in real-life situations, it was stated that the research community in the late 1950s "generally favoured" simpler sinusoidal excitation when investigating human response to vibrations.

2.3.5.2 PERCEPTION OF LOW-LEVEL VIBRATIONS

Waller (1969), pointed out that the occupants of high-quality buildings were much more worried about the very presence of low-level floor vibrations due to walking than about their actual level once they were perceived. For such premises a reduction of perceptible to imperceptible vibration levels was defined as the principal aim for the anti-vibration design of the floor. But, when building vibrations were expected and considered as normal, the duration to exposure starts playing an important role and should be reduced as much as possible.

Guignard (1971) wrote a review paper on human perception of low-level whole-body vibrations specifically aimed at building applications. He expressed a dissatisfaction with the fragmented research work in the area lacking co-ordination in spite of the fact that it dealt with such a complex scientific problem. This view was supported by Jones and Saunders (1972). Guignard was also very reserved towards the application of findings established, from whole-body vibration investigations using relatively intensive "pure" sinusoidal excitations in laboratory conditions to the field assessment of building vibrations. Also, the importance of vibration perception thresholds in buildings was acknowledged. For frequencies less than 30 Hz the peak acceleration marking the boundary between 'feel' and 'no feel' was determined to be as low as 1 cm/s^2 (0.1% g).

Wiss and Parmelee (1974) established an empirical formula linking the floor vibration response rating R, the initial displacement amplitude A_0 [in] of the exponentially decaying sinusoidal vibration, having frequency f [Hz], and damping ratio ζ:

$$R = 5.08\left[\frac{fA_0}{\zeta^{0.217}}\right]^{0.265} \qquad \text{Equation 2.1}$$

where five floor vibration ratings varied from $R=1$ (imperceptible) to $R=5$ (severe).

The formula is the product of a thorough investigation into the effects of carefully engineered damped transient vibrations induced on a human subject by the shaker on which the subject was standing. The shaker excitation signals were simulating floor vibrations under one footfall impact. The design of the research clearly aimed to overcome the criticism of similar previous investigations, with regard to the type of signals used and the environment in which the human subjects were tested.

It was found that there was a tendency for test subjects to rate more favourably transient vibrations which decreased quickly. This is in agreement with Nelson's (1974) findings. However, Aswad and Chen (1993) commented that raising the damping ratio ζ to the power of only $0.217\times0.265=0.058$ de-emphasises the importance of damping. Also, only individual transients were used which does not reflect realistically a train of transient responses due to a series of footfalls induced while walking across a floor. Finally, it should be mentioned that Wiss and Parmelee explicitly stressed that the formula they developed was applicable only to the excitation signals which they used during the investigation. In other words, its application to real walking or heel-drop induced vibrations is not warranted.

Cowley (1976) outlined chronologically a historical development of ISO 2631 ("Guide for Evaluation of Human Exposure to Whole-Body Vibration") between 1964 and 1974, the latter year being when the first official version of the international standard was published. Although the original brief was for the guide to cover the effects of "vibration exposure for industrial situations, transport vehicles and residential situations", the last aspect received very little attention in the 1974 edition.

Irwin's work (1978) remedied this to some extent as it served as the basis for the revised version of ISO 2631 published in 1985 (Wyatt, 1989; Wyatt & Dier, 1989). The paper generally covers the aspects of human response to motions of large structures such as buildings, off-shore platforms and bridges. As the main reason for people to be particularly sensitive to low-level vibrations in large static objects, Irwin singles out the lack of expectation. Users of large objects of infrastructure simply do not expect them to move and, if the movement is perceived, then annoyance may arise. This is, probably, the reason for Wyatt (1989) to point out that human reactions to low-level vibrations in buildings are more psychological than physiological phenomena.

Although Irwin (1978) does not specifically consider the vibration of floors, the baseline curve for general whole-body vertical vibrations and its weighting factors were given. The factors depend on the time of the day (or night), the type of the building usage (residential, office, workshop, etc.) and the type of vibration (continuous, intermittent or impulsive). It is worthwhile mentioning that intermittent vibrations are specified to occur when:

> "...a level of motion is built up and held up for a number of cycles followed by a transient decline and similar repetition, although the whole duration of vibration may be only a few seconds."

Considering this definition, it appears that the floor vibrations caused by occasional walking should be classified as intermittent and the weighting of the base curves applicable to this type of vibration should be used (Allen & Murray, 1993).

Irwin presented the vertical vibration 'base curve' in terms of RMS accelerations corresponding to discrete frequencies only. In the case of vibrations occurring at several frequencies simultaneously, it was suggested that "they should be evaluated and assessed separately". Although not precisely defined, this probably means that a one-third octave rating (Griffin, 1996) procedure is applicable. Nevertheless, Griffin (1996) and the current relevant British Standards BS 6841 (BSI, 1987a), and BS 6472 (BSI, 1992) favour the 'weighting' instead of the 'rating' approach when applying the vibration limits and assessing the effects of the multi-frequency composed vibrations. In any case, it is suggested that the limits are applicable only if there is no noise or sound associated with the vibrations. The presence of acoustic effects may significantly reduce the acceptable vibration magnitudes.

An additional explanation as to as to how to use (the 1980 draft of) ISO 2631 (1985) when assessing vibrations in buildings is given by Griffin (1982). Particularly informative is a comment on the applicability of the lowest RMS acceleration limits in the base curve set at 0.05 m/s^2 (0.5% g) for frequencies between 4 and 8 Hz. Griffin characterised this acceleration limit as "at about the same level as the threshold of human perception of vibrations". However, it was maintained that there was a degree of uncertainty regarding this limit as there had been a lack of reliable research into vibration perception thresholds.

Furthermore, Charlier (1986) explained that, although acceptable vibrations in buildings should be below or only slightly above the perception thresholds, the evaluation of this threshold by experiments proved to be quite difficult resulting in different numerical values which indicated the same 'feel' or 'no-feel' boundary. Only four years ago Eriksson (1994) confirmed that there was severe lack of reliable data which would convert the descriptive requirements for vibration "comfortable" environments into physical values suitable for engineering calculations. Although, as already mentioned, certain guidelines exist (ISO, 1992; BSI, 1992), with regard to the perception of low-level floor vibrations, Eriksson maintains that these still require considerable development.

An example of such a development is investigations conducted by Griffin (1982), and Parsons and Griffin (1988). They found that in the frequency range from 2 Hz to 100 Hz an RMS acceleration of 0.1% g was an average perception threshold for complex multi-frequency vertical vibrations. This value is twice the threshold level proposed in BS 6472 (BSI, 1992) as the base curve for frequency weighted accelerations applicable to most sensitive environments. Also, it was suggested that an RMS acceleration of only 0.2% g might not be acceptable if it occurs in residential buildings. These threshold values compare favourably with the peak acceleration of 34 mm/s^2 (0.34% g) reported by Pretlove and Rainer (1991; 1995) to be "just perceptible". This latest peak acceleration value has been obtained by compiling data from various sources. Eriksson (1994) did a similar compilation of available data on RMS accelerations for offices and determined that acceptable acceleration levels are 0.02-0.06 m/s^2 RMS (0.2-0.6% g), depending on the type of office ("special", "general" or "busy").

2.3.6 Parameters and Procedures Used in Modern Vibration Serviceability Assessment

When assessing whole-body vibration, modern codes of practice typically require its effects to be evaluated. The guidelines generally offer five groups of such effects: (1) degraded comfort, (2) interference with activities, (3) impaired health, (4) occurrence of motion sickness, and (5) perception of low-magnitude vibration (Griffin, 1996). A clear distinction between the environments to which these vibration effects relate is essential. Degraded comfort, interference with activities, impaired health and motion sickness are effects of whole-body vibration typically occurring in transportation, mechanical or industrial systems where vibration severity is generally greater. For example, the overall level of acceptable car vibrations, which does not impair the car riding comfort whatsoever, almost certainly is not going to be acceptable for vibrations of floors in a quiet office. This is because typical car vibrations are prolonged and way above the vibration perception thresholds. Nevertheless, Griffin (1996) warned that the word "perception" has sometimes been used too broadly in literature to describe a "degree of discomfort" and not a "threshold between feeling and no feeling". Therefore, it is prudent to know the context in which "perceptible" vibrations were obtained.

2.3.6.1 Acceptability of Low-Magnitude Floor Vibrations

Perceptible non-stop whole-body vibrations in buildings accompanied by complaints from the building occupants are commonly considered as unacceptable. Consequently, the absence of vibrations above the whole-body vibration perception thresholds for "most of the time" is acceptable (Griffin, 1996). Von Gierke and Brammer (1996), clarified this by saying:

> "Experience has shown that the criterion of acceptability for continuous, or intermittent, building vibration lies at, or only slightly above, the threshold of perception for most living spaces."

The modern vibration assessment guidelines, therefore, tend to acknowledge the relatively recent research findings. They accept that perception thresholds are likely to govern the acceptability of floors as regards their vibration performance. Nevertheless, floor vibration could be acceptable for levels of vibrations higher than the perception threshold. Perceptible vibrations which are acceptable, therefore, cover a band of human responses which vary from the vibration perception thresholds to certain upper vibration sensation limits. Many, mostly environmental, factors influence these sensation limits in a way which is extremely difficult to predict (ISO, 1992; Bolton, 1994; Eriksson, 1994; Griffin, 1996).

The duration of exposure to vibration has been determined to be a very important factor. Extensive research (Griffin, 1996) established a simple, formula based, model for assessing the effect of duration on vibration sensation and, consequently, vibration acceptability. According to Griffin, there is currently a consensus in the scientific community that prolonged exposure to vibrations increases discomfort. This is expressed using the following power law describing the constant level of sensation:

$$\varphi^n T = \text{const.} \qquad \text{Equation 2.2}$$

where, φ is the physical magnitude representing the vibrations, say accelerations, and T is the vibration exposure duration. For whole-body vibrations the value of n is usually 2 or 4. If the value is, say, 4, this means in practice that magnitudes of φ which are halved (but still perceptible), may be experienced 16 times longer for the equivalent overall sensation as the reference acceleration time-history. The greater value of n also emphasises the importance of transient vibrations having large magnitudes φ during short exposure times T (compared to prolonged steady-state vibrations with relatively smaller magnitudes). The general time dependence shown in Equation 2.2 serves as the basis for formulating vibration limits related to certain vibration criteria.

2.3.6.2 VIBRATION CRITERIA AND VIBRATION LIMITS

The human body is an incredibly complex and sensitive receiver which is self adapting and more or less susceptible to almost any type and level of motion, such as periodic, random or transient vibrations, which normally occur in nature. In addition, humans are characterised by huge inter- and intra-subject differences between their responses to 'nominally' the same vibrations. Inter-subject variability means that different people will react differently to the same whole-body vibration excitation. Intra-subject variability happens within the same person who may react differently to the same excitation under different circumstances. Age, fitness, prior training, type of activity, body posture, attitude and motivation are just some of the numerous causes for the inter- and intra-subject variabilities.

All this means that there may be a considerable uncertainty when assessing the effects of vibrations and, generally, a probabilistic approach is prudent. Hence, modern vibration assessment procedures define two terms: the vibration criterion and the corresponding vibration limit (Griffin, 1996). The vibration criterion is basically a statement which aims to describe certain vibration effects, for example 'perception of low-magnitude vibration'. A vibration limit tends to be a number, describing a certain physical (or non-physical) quantity obtained from the vibration time-domain signature. The limit is experimentally determined in such a way that, when vibrations reach it, there is a more or less quantifiable probability that the corresponding vibration criterion is also reached. Due to the enormous complexity (and importance) of the whole-body vibration problem, vast research efforts have been and still are being made in order to define vibration criteria and limits for various circumstances.

2.3.6.3 QUANTIFICATION OF WHOLE BODY VIBRATIONS

In order to quantify whole-body vibration and its effects, a relevant dynamic motion descriptor has to be chosen. Displacement, velocity, acceleration or 'jerk' (first derivative of acceleration) could be selected. Typically, accelerations are selected due to the ease of instrumentation (Griffin, 1996). In addition, body posture, type of vibration (periodic, random, or transient) and its frequency content, magnitudes and duration have to be known. The body posture may be defined using a coordinate system as shown in Figure 2.12

(ISO, 1985). A frequency analysis of an acceleration time history, measured or calculated over a certain period of time, provides all necessary information to describe the whole body vibration.

Griffin (1996) demonstrates in considerable detail how research data collected and reported worldwide confirm that human response to vibrations, although fairly unpredictable, follows certain patterns. For the given type, frequency, magnitude and duration of excitation curves, such as the one shown in Figure 2.13, can be plotted. These curves are termed equal comfort contours. They usually show the change of the RMS of accelerations, which cause the same sensation, as a function of the frequency content of the vibrations. The accelerations are obtained (either measured or calculated) on the vibrating surface at the point of its contact with the body (Rasmunsen, 1982).

The general shape of the equal comfort contours used for vibration serviceability assessment corresponds to the curve shown in Figure 2.13b, although Wright and Green (1959) claim that the lines are never so "straight". The graph shows that the human response tends to remain constant in clearly identifiable frequency bands if accelerations (bands 1 and 3), velocities (band 4), displacements (band 5), or 'jerk' (band 2) remain constant for varying frequencies. Equal comfort contours, where acceleration is plotted as a function of frequency (Figure 2.13b), tend to have troughs around 4-8 Hz. This indicates higher human sensitivity to accelerations in this frequency region. The explanation of this phenomenon is simple if a human body is considered as a linear dynamic system made of masses, springs and damping dashpots as shown in Figure 2.11 (Smith et al., 1996). The linearity assumption seemingly holds for very low amplitudes of vibration which is the case for vibrations in buildings (Von Gierke & Brammer, 1996). Acceleration, having a frequency content between 4 and 8 Hz, acts as the whole-body 'base' excitation causing resonances of some internal organs which are easily sensed by a normal healthy human. Apart from these 'internal' resonances, tactile receptors under the skin of the soles of the feet, the palms of the hands and the finger tips play a major role in sensing the lowest levels of vibration, that are used in determining the vibration perception thresholds (Smith, 1969).

As human sensitivity to vibrations is frequency dependent, the method of frequency weighting is nowadays employed to account for this. The weighting leaves vibration levels where the contour is low (say, between 4 and 8 Hz) unchanged and attenuates the levels at frequencies to which humans are more 'resistant'. In this way, vibration response is 'normalised' to the same sensation level no matter what the excitation frequency is. Supported by a considerable review of available research findings, Griffin (1996) maintains that there is now sufficient evidence to underpin the view that the weighting is always applicable no matter if the vibration is periodic, random, or transient. The principle of frequency weighting for assessing the perception of vertical vibrations is shown in Figure 2.14. Such weighted (typically acceleration) time-histories can then be used to determine a single value (or parameter) which characterises the vibration. Fifteen years ago, Rasmunsen (1982) listed as many as 14 parameters which could be compared with the given vibration limit in order to determine the vibration effect. Today, there are two parameters which are typically used in modern codes of practice, such as BS 6472 (BSI, 1992) or ISO 10137 (ISO, 1992), for assessing the amount

of vibration and its effects. These are the RMS acceleration, and the recently established vibration dose value (VDV).

Vibrations in buildings are seldom simple sinusoids. Often, the vibration time signatures are modulated, transient or random, and they contain a range of frequencies, where a more or less narrow range of frequencies exists. After being weighted, the most common method for mapping such vibrations into a single numerical ('effective') value to be compared with the vibration limit is to calculate the RMS of the weighted acceleration time-history $a_w(t)$ using the following formula:

$$\text{RMS acceleration} = \left[\frac{\int_{t_1}^{t_2} a_w^2(t)dt}{t_2 - t_1}\right]^{1/2} \qquad \text{Equation 2.3}$$

RMS acceleration is used as it is a measure of the total vibration causing distress to the human body. Greater RMS accelerations correspond to higher vibration magnitudes causing more annoyance. However, an assessment of the human distress using the RMS relationship is appropriate for, as Griffin defines them, "well behaved" vibrations which are steady-state long-lasting periodic or stationary random. If the vibrations are short lived transients, then the RMS acceleration no longer appears to be a reliable effective value (Griffin, 1996).

A method, which addresses this problem and is gaining acceptance internationally, is the previously mentioned vibration dose value (VDV) method. This method is suitable for assessing all types of vibratory motion (periodic, random and transient). The VDV is a cumulative measure of the vibration transmitted to a human receiver during a certain period of interest $T = t_2 - t_1$, and is calculated as:

$$\text{VDV} = \left[\int_{t_1}^{t_2} a_w^4(t)dt\right]^{1/4} \qquad \text{Equation 2.4}$$

Although the VDV is, allegedly, a more reliable parameter which correlates relatively well with human sensation of all types of vibration, as shown in numerous relatively recent experimental studies (Griffin, 1996), it does not have a physical meaning. Whereas units for RMS accelerations are ms^{-2} the VDV units are $ms^{-1.75}$.

2.3.6.4 STANDARDS FOR VIBRATION EVALUATION

The VDV was developed during the early 1980s. Reportedly more reliable than the RMS acceleration, it easily found its way into the relevant vibration evaluation guidelines used in the UK such as BS 6841 (BSI, 1987a) and BS 6472 (BSI, 1992).

Compared to its 1984 predecessor, BS 6472 from 1992 offers a more detailed account of the VDV approach reflecting what is written in BS 6841 (BSI, 1987a). BS 6841 is aimed at evaluating the whole-body vibrations in transportation, mechanical and industrial systems where higher levels of vibration need to be considered. However, it can be used to assess the perceptibility of low-magnitude vibrations which are important in floor vibration serviceability considerations (Griffin, 1996).

Although the application of the VDV method has been introduced in BS 6472 (BSI, 1984) and developed considerably further in BS 6841 (BSI, 1987a), ISO 2631-2 published in 1989 still mentions the VDV in its Annex B under the title "Evaluation Methods under Development". However, the latest ISO 2631-1, recently published in summer 1997, more firmly adopts the VDV concept.

The applicability of the VDV concept in the assessment of building floor vibrations caused by walking has also been recently discussed by Eriksson (1994). He gave an extensive overview of the vibration standards and clarified procedures suitable for the vibration assessment of long-span floors having relatively low natural frequencies. As to the assessment procedures based on RMS acceleration, the lack of information in the codes of practice about the required averaging time $T = t_2 - t_1$ (Equation 2.3) has been singled out as the biggest problem. Whereas Rasmunsen (1982) stated that a 1 s and 60 s RMS averaging (or integration) period was commonly used in general human vibration studies, Eriksson proposes 10 s as more appropriate for the calculation of floor RMS accelerations, denoted as $a_{RMS,10w}$. Eriksson argues for all the valuable experimental data from future full-scale measurements to be processed and reported using the same parameter every time. This is suggested in order for the wider engineering community to obtain some sort of 'common denominator' describing floor vibration performance always in the same way. Such a commonly used parameter does not currently exist in the research literature on floor vibration due to the lack of a general strategy when reporting measurement data, making the interpretation of the past investigations difficult if not impossible.

2.3.6.5 Other Considerations Related to Human Perception of Low-Level Vibration

Farah (1979) used lumped parameter models of humans, such as the one shown in Figure 2.11, to measure the "absorbed power" of vibration by the human body in order to assess the vibration serviceability of floors. He supported this advanced approach by stating that similar human models were extensively used in aero-space, aircraft and automobile industries, whereas they were lacking in the civil structural engineering sector. There is little evidence to suggest that this approach has been widely accepted although Ellis and Ji (1997) very recently suggested that this might be the way forward.

Amongst the many previously mentioned factors, vibration perception also depends on whether the human body is stationary or moving while experiencing the vibration. Wyatt (1989) points out that, due to rising and falling while walking, a human body can experience accelerations as high as 3 m/s^2 (30% g). This is perfectly acceptable even though it is several hundred times greater than the vibration perception threshold. This is because the nervous system of humans is capable of associating such high accelerations with walking

in progress and simply disregards them (Wyatt, 1989). As a consequence, very small vibrations of the structure, across which the walking is performed, pass unnoticed by walkers as their vibration perception thresholds are automatically adjusted to a much higher level. This is the reason why equal contour criteria applicable to stationary people are not applicable to those who are moving.

2.3.7 Integrated Approaches to Lightweight and Composite Steel-Concrete Floors

Over the last 40 years numerous attempts have been made to link the three key features of floor vibration serviceability and to develop an integrated procedure (a 'package') for assessing the floor performance. Typically, these procedures tried to map the ULS philosophy to the vibration SLS assessment rendering a simple design formula with a 'pass' or 'fail' answer. These procedures were usually validated to a greater or lesser extent through experience gained by applying them on one of the three main floor types:

1. lightweight timber or steel-framed floors with timber decking,
2. composite steel-concrete or precast concrete floors, and
3. cast in-situ floors made entirely of concrete.

2.3.7.1 VIBRATION SERVICEABILITY OF LIGHTWEIGHT FLOORS

Polensek (1970) surveyed sources of vibration acting on lightweight residential floors. A single person walking was determined to be the most frequent source of vibration which causes a high degree of objection. It is interesting to note that Atherton et al. (1976) established that the repetitive static-like deflections due to the sheer weight of the walker proved to be more annoying to the observers than the rapidly decaying transient vibrations due to mechanical impact.

Noting that "building vibrations are a controversial matter", Ohlsson (1982), in his doctoral thesis, gave a very detailed, educated and realistic state-of-the-art review of floor vibration performance due to human induced loading. He divided the floor vibration serviceability problem into two categories:

- Springiness, where the person causing vibrations feels them as well i.e. simultaneously acts as the vibration source and receiver;
- Footfall induced vibrations, where the floor vibration source and receiver are different persons.

Ohlsson also divided floors into lightweight and heavy floors. Heavy floors are defined as those where the presence of a human does not alter (significantly) modal masses, natural frequencies, and modal damping ratios. Floors having a modal mass of more than 1000 kg in all modes of interest are classified as heavy floors. The modal mass is calculated using unity normalised mode shapes. In such floors, typically comprising a concrete slab, springiness, caused mainly by local deflection due to the weight of the walker, is not an issue (Ohlsson, 1982).

Written 15 years ago, Ohlsson's work is still a very useful reference for the vibration serviceability of lightweight timber floors which were its main subject. However, it is prudent to list some of the problems which the writer identified in Ohlsson's research:

- Although more representative of a real-life situation, the field tests on full-scale floors were described as significantly more difficult to conduct, thus resulting in less reliable experimental data collected (when compared with laboratory tests).
- Damping estimation from the measured FRFs proved to be unreliable. This is probably due to the fact that only SDOF estimation procedures hard wired into the spectrum analyser were employed on the FRF data characterised by the high modal density.
- It appears that no analytical modelling had been performed prior to the testing. This led to 'educated guesses' as to the position of measurement points and sometimes to spatial aliasing (NAFEMS, 1992; Friswell & Mottershead, 1995), where mode shapes corresponding to the modes of interest could not be resolved.
- All data analysis was, seemingly, performed after the testing and flaws in the measurements were identified when it was too late to repeat them.

In spite of a considerable amount of past research effort aimed at a better understanding of the vibration serviceability performance of lightweight floors, this problem is still being analysed in an ever increasing number of recent publications. As the dynamic performance of lightweight timber or steel-timber floors is specific due to the floor springiness and the effects of humans on their dynamic properties, a variety of parameters is proposed in the literature to formulate criteria for the assessment of their vibration serviceability. Pham and Yang (1993) listed three prominent ones: static deflection under a pre-specified point force, frequency weighted RMS transient accelerations due to footfall impacts, and the initial peak velocity due to an idealised force impulse. These criteria are of varying reliability, but all of them were developed from a combined experimental and analytical procedure. Typically, a number of full-scale structures were investigated and their experimentally determined performance compared with the prediction using more or less sophisticated analytical modelling techniques (Onysko, 1988a; 1988b; Smith & Chui, 1988a; 1988b; Hveem, 1990, Smith & Hu, 1993, Pham & Stark, 1993, Nash; 1993, Bainbridge & Mettem, 1997; Kraus & Murray, 1997).

2.3.7.2 VIBRATION SERVICEABILITY OF COMPOSITE STEEL-CONCRETE FLOORS

In 1958, prompted by "occasional" vibration problems, the American Steel Joist Institute commissioned a research team led by Professor Kenneth Lenzen at the University of Kansas, USA. The team studied the vibration behaviour of composite steel joist-concrete slabs. This was the beginning of more than two decades of research work for Professor Lenzen's group which is described in a number of papers and reports (Lenzen, 1962; 1966; 1972; Ohmart & Lenzen 1968; Lenzen & Murray, 1969; Lenzen et al., 1971; Murray, 1975; Galambos, 1988). These will be summarised here.

- Lenzen (1962) determined that walking vibrations are transient in nature and as such require special vibration rating scales. Beneficial effects of damping on the floor vibration performance were noted.
- Lenzen (1966) proposed a modified Reiher-Meister scale for the assessment of floor transient vibrations. A heel-drop impact has been introduced as a 'standard'.
- Ohmart and Lenzen (1968) established an analytical model of a heel-drop excitation in the form of a triangular pulse. Such excitation should be applied to simplified SDOF floor dynamic models in order to calculate their initial peak response and assess it in accordance with the modified Reiher-Meister scale. An increase in thickness of the floor concrete slab was determined to be the most efficient method for reducing the peak responses due to heel-drop and improving the overall floor vibration performance.
- Lenzen and Murray (1969) used the impact excitation and amplitude decay method to measure damping on 20 full-scale steel-concrete floors. The estimated damping ratios varied between 3.8% and 15.9%, the average value being 7.9%. These, and other similarly obtained damping values were dismissed later as unreliable by Wyatt (1985), Ohlsson (1988a) and Eriksson (1994), due to inappropriate measurement techniques. Similar problems with damping measurements can be seen in the papers by Lenzen et al. (1971), Lenzen (1972) and Murray (1975).

In the mid-1970s researchers from Canada were working on new floor vibration serviceability guidelines in the Canadian steel design code published in 1974 (CSA Standard S16.1-1974 "Steel Structures for Buildings - Limit States Design"). The guidelines are based on Lenzen's heel-drop methodology.

D. L. Allen (1974a; 1974b) published a private communication with his namesake D. E. Allen of the NRCC Division of Building Research who investigated results of field vibration tests performed by others on a total of 34 floors. D. E. Allen came up with the threshold of annoyance criteria as a function of acceleration and floor damping. Interestingly, the procedure outlined for assessing the floor vibration serviceability at the design stage was based on a heel-drop test and a SDOF model of a single T beam, which had already been dismissed as over-conservative by Lenzen and Murray (1969).

D. L. Allen and Swallow (1975) stressed the importance of the higher modes of floor vibration which frequently exist in composite steel-concrete floors. The two authors noted that the higher modes of vibration were "always present" creating "multiple frequencies" which made any damping estimation from heel-drop measurements very difficult. Despite this, 12 years later Pernica (1987) again used the heel-drop excitation to measure damping from various non-structural elements (de-mountable full-height partitioning walls, ceilings, carpets and tiling) in contact with a composite floor with closely spaced modes of vibration. Some curious results were produced which Pernica could not explain.

With regard to the treatment of non-structural elements it is interesting to mention the opinion of Ohlsson (1988b) who recognised that non-structural components such as false floors or temporary partitions may have a significant positive impact on the vibration properties of floors. However, Ohlsson also maintained that an assessment of the vibration serviceability of floors should not depend upon such elements which may or may not be existent as the floor usage changes. Instead, a reliable vibration serviceability design method

should rely upon the effects of the "well defined quantities, such as the floor [modal] mass, that are possible both to calculate and to measure".

D. L. Allen and Swallow (1975) also reported that an error up to 100% regularly occurred between the measured and analytically calculated peak acceleration amplitudes induced by a heel-drop. The analytical models again made use of simplified SDOF systems representing complex three-dimensional floor structures.

Allen and Rainer (1975; 1976) described in detail the development of the interim recommendations which appeared as Appendix G in the 1974 Canadian steel design code already mentioned. It was explained that the code considers two types of floor vibration: continuous vibration and walking induced vibration. The criteria proposed for floor evaluation are shown in Figure 2.15.

In this figure, the peak acceleration amplitudes corresponding to floor damping ratios of 3%, 6% and 12% are caused by a heel-drop which could be either measured or calculated. If it is measured, Allen and Rainer suggested the removal, by filtering, of all frequency components higher than the lowest natural frequency. Although to some extent paradoxical, it should be stressed that the acceleration peaks, measured from normal walking, should not be used for assessing walking vibrations using the graphs corresponding to 3%, 6%, and 12% damping in Figure 2.15.

As Hatfield (1992) outlined, the CSA criteria were 'calibrated' to work with acceleration peaks corresponding only to the heel-drop tests, and the actual floor subjective rating ('acceptable' or 'not acceptable') was done when a single person was traversing the same floor. Therefore, if reliability of the CSA scale is to be verified, the subjective assessment of real floor vibrations should be based on the perception of floor vibrations caused by normal walking, and not by heel-drops. The reason for this appears to be that the criteria used in the Canadian code (CSA, 1989) had to be equally applicable to the rating of already built floors as well as in the design of non-existent future floors where only mathematical models could exist. The heel-drop rating of floors was proposed in order to simplify the design checking procedure. The triangular forcing function from a heel-drop is much easier to treat analytically, compared to the modelling of walking where the excitation changes in space and in time.

Although the heel-drop test has remained in the Canadian steel-design code for more than two decades, in as early as 1981, Murray dismissed it as unreliable. Using the assessment procedures based after:

1. modified Reiher and Meister scale (Lenzen, 1966; Murray, 1975),
2. Appendix G of the Canadian steel design code (Allen & Rainer, 1975; 1976),
3. ISO 2631 provisions available in early 1980s, and
4. Wiss and Parmelee's work (1974).

Murray tried to determine analytically the vibration serviceability of five real floors by applying all four procedures to each structure.

The result was disastrous. A total inconsistency was observed as floors analytically assessed as unacceptable were actually rated as absolutely acceptable by their users, and, vice-versa, floors analytically assessed as acccptable failed subjective tests. A similar conclusion was reached by Ellingwood and Tallin (1984) whose private correspondence with numerous practising engineers revealed that floors that failed the heel-drop test in the design stage (but were anyway built) proved to be quite acceptable after they were constructed.

Expressing grave concern about this situation and denouncing practically all methods available in the early 1980s for vibration serviceability assessment of composite steel-concrete floors, including his own (Murray, 1975), Murray (1981) proposed a new simple design criterion. In order to be acceptable, a floor had to have damping ratio ζ which satisfied the following empirical condition:

$$\zeta \geq 35A_0 f + 2.5 \qquad \text{Equation 2.5}$$

where: A_0 [in] is the initial amplitude from a heel-drop impact and f [Hz] is the first natural frequency of the floor. However, the damping ratio ζ [%] was to be measured from amplitude decays after a heel-drop, disregarding the numerous problems with such measurements already reported (D. L. Allen & Swallow, 1975). Also, it remained unclear if A_0 was to be established from filtered or unfiltered response measurements when assessing an existing floor structure.

After a few years of receiving feedback from industry about the performance of his formula (Equation 2.5), Murray (1985; 1991) stressed that the formula had proved itself but is applicable only to steel-concrete composite floors where the concrete slab is cast in situ. Also, he warned that the assumptions which are considered as conservative in ULS calculations for static loading, are typically not conservative in vibration serviceability assessments using Equation 2.5. For example, neglecting composite action is conservative in ULS analysis, but it reduces the natural frequency f and the product $A_0 f$, making less demand on the required damping ratio ζ. Also, it is 'safe' to assume the full design load in strength calculations, but this assumption increases the floor mass and reduces natural frequency f, again making less demand on the required damping.

Murray's criterion in Equation 2.5 was established from a statistical analysis of the lowest natural frequencies, peak displacement amplitudes due to heel-drops and damping ratios measured on more than 90 composite steel-concrete floors. This simple one-formula criterion is therefore empirical. However, Whale (1983) expressed reservations towards the ability of similar simplified mathematical models to represent real-life floor dynamic behaviour and called for more work on the improvement of such models. Regarding modelling, Chadha and Allen (1972) stated that simplifications of the boundary conditions of steel-concrete composite floors into either pinned or fully fixed may introduce "potentially large errors". In addition, Wilson and Heidebrecht (1976) called for more experimental work on full-scale composite steel-concrete floor structures in order to improve their modelling, particularly regarding the assumption of damping values.

Wyatt and Dier (1989) introduced a concept of low-frequency and high-frequency floors into the official SCI guidelines (Wyatt, 1989) for checking the vibration SLS of composite steel-concrete floors. This frequency

division is important in order to establish a proper walking loading and floor response calculation model. The core of the method assumes that walking excitation has, not only strong low-frequency components, but also impulsive (i.e. higher-frequency) components as well (Ohlsson, 1988a). These impulses correspond to heel strikes (Figure 2.16). Therefore, if the floor is low-frequency having a first mode of vibration which is less than approximately 7 Hz, the low-frequency loading components may create a strong "resonant" vibration response. On the other hand, higher frequency floors are more responsive to the impulsive components of walking. In this case, the floor response is a string of damped responses to impulse-like excitation which tend to die out between two heel strikes, depending on the natural frequency and amount of damping.

Apart from this division into low- and high-frequency floors other main features of the Wyatt's method for assessing the vibration serviceability of composite steel-concrete floors are as follows:

- The scales for assessing floor vibration response due to walking are taken from the British standard BS 6472 (BSI, 1984). Interestingly, this was done despite Wyatt's claims that BS 6472 is more appropriate for assessing the effects of externally generated vibrations.
- Simplified SDOF floor models were used to calculate peak accelerations corresponding to a steady state (low-frequency floors) or transient case (high-frequency floors). Although walking excitations were characterised as "closely periodic", the conservative steady-state case was assumed where low-frequency floor resonance is excited exactly by an appropriate harmonic of walking disregarding the possibility of its imperfectness. The peak accelerations for both steady-state and transient cases were converted into the corresponding RMS accelerations as required in BS 6472 (BSI, 1984). However, this might be particularly conservative in the case of high-frequency floors where the initial peak acceleration reduces significantly during vibration which beneficial short duration is not taken into account.
- The floor natural frequency is considered to be the key parameter governing its classification (low- or high-frequency). However, it appears that models for its calculation are mainly based on grossly simplified 2D beams which may have several spans and are either pin- or fixed-end supported.
- Wyatt and Dier (1989) concede that more accurate frequency and response calculations are possible by using computer packages mainly based on the FE method. However, they effectively discouraged such an exercise due to "basic uncertainties" in the FE modelling of the of composite floors in terms of their continuity, support conditions and the amount of composite action in the steel-concrete cross-sections.
- In order to justify the proposed method, Wyatt (1989) presented a back analysis of 14 floors in already existing buildings in which a subjective vibration serviceability rating had proven to be satisfactory. The back-analysis also showed that all floors had satisfactory vibration performance. Consequently, Wyatt's method seems to perform much better than the four methods previously mentioned, which had failed a similar test set by Murray (1981). However, it also appears that no experimental vibration measurements on the 14 full-scale floors were made (Zaman & Boswell, 1996c) in order to compare the actual level of floor vibrations due to a single person walking with the predicted values. Only subjective ratings were available. Without this verification, the method, assessed by Wyatt himself as "conservative" might prove to be actually over-conservative, which is clearly not satisfactory.

Osborne and Ellis (1990) indirectly confirmed the last concern by comparing the result of Wyatt's method with the subjective rating of the floor vibration determined from experiments on a full-scale structure. The full-scale floor was dynamically tested and the lowest natural frequency of approximately 5.5 Hz accompanied by a very low modal damping ratio of only $\zeta = 1\%$ were determined. Despite this, the floor vibrations due to walking were rated as acceptable by its occupants. However, the SCI method for low-frequency floors with $\zeta = 1\%$ damping would have rated this floor as unacceptable for an office environment. This observation is particularly important as Osborne and Ellis (1990) stated that damping values as low as 1% of critical damping may be expected in composite steel-concrete floors although such values are several times lower than those reported in the literature in 1960s and 1970s. In order to simplify the calculations, the floor peak acceleration response is assumed by Wyatt (1989) to be inversely proportional to damping for low-frequency floors. Consequently, the use of lower and seemingly more realistic damping values may have detrimental effects on the vibration performance of the composite floors checked in accordance with the current SCI guide during design.

Following Hatfield's (1992) detailed review of the available methods for assessing the vibration serviceability of composite steel-concrete floors, Allen and Murray (1993; Murray & Allen, 1993) made a similar, but more critical, overview of the design procedures for such structures under walking excitation. These included composite steel-concrete floors and footbridges. Wyatt's (1989) concept of low- and high-frequency structures has been accepted, but different frequency boundaries were introduced as follows:

- For structures where $f_1 \leq 9\,\text{Hz}$, the continuous vibration responses due to resonance caused by low-frequency walking harmonics govern the design
- For structures where $9\,\text{Hz} \leq f_1 \leq 18\,\text{Hz}$, the impulsive responses due to heel-strikes while walking govern the design
- For structures where $f_1 \geq 18\,\text{Hz}$, the static deflection due to the weight of the walker (1 kN vertical point force) governs the design.

Obviously, Allen and Murray consider the 4^{th} harmonic of walking to be as capable as the first three harmonics of exciting floor resonance. Rainer et al. (1988b) maintained this view as well. Hence, the increase of the low-frequency cut-off from 7 Hz (Wyatt, 1989) to 9 Hz. There is, however, little experimental research published to support this analytical modelling feature.

In the case of low-frequency floors the paper aims to replace the heavily criticised heel-drop testing (CSA, 1989) by a procedure developed in accordance with ISO 10137 (ISO, 1992) but with a number of simplifications. Neglecting the imperfectness of walking excitation, floor resonance under one of the first four walking harmonics is assumed. Similar to Wyatt's (1989) approach, a beam-like SDOF floor model is recommended once again to calculate the acceleration peak response which should then be compared with the assumed/given vibration limits. From a condition of having peak accelerations lower than the ISO 10137 limits, Allen and Murray (1993) developed the following formula for the calculation of the lowest allowable floor natural frequency f_o [Hz]:

$$f_o \geq 2.86 \ln\left(\frac{K}{\zeta W}\right) \qquad \text{Equation 2.6}$$

where: K [kN] is a factor depending on the permissible acceleration limits which, in the case of offices, may be taken to be $K = 54kN$, W is "the total weight supported by the beam", and ζ is the viscous damping ratio for the first mode of vibration.

The key parameter in this expression is the floor (modal) mass participating in the first mode of vibration (expressed in terms of W), and the two authors called for additional research work which would help to estimate it more accurately. Uncertain modelling of key floor elements (support conditions, continuity, lateral stiffness, etc.) was singled out as the biggest problem in the accurate estimation of the floor modal properties.

Although Allen and Murray (1993) developed their new proposal (Equation 2.6) from simplified SDOF modelling, Murray, interestingly, started advocating computer analysis based on more realistic and complex MDOF models formulated through an FE method (Morley & Murray, 1993). Such models can account for all of the excited modes of vibration when checking floor vibration serviceability under walking excitation. A justification for this recommendation, which also indicates a shift in attitude toward more advanced (and accurate) floor modelling, was the increased availability and affordability of commercially available powerful FE computer packages in the 1990s. Therefore, Morley and Murray started considering dynamic FE analysis as a "practical computational method", a term which was in the past reserved only for simple hand calculations based on simplified SDOF modelling. The need for such methods of more advanced analysis was recently proved by Ellis et al. (1993). Their tests on three full-scale composite steel-concrete floors showed that the dominant modes of vibration caused by walking may be the 2nd or even the 3rd mode, provided that they are closely spaced to the fundamental mode.

Nevertheless, Zaman and Boswell (1996c), have recently focused on the ability of relatively simplified modelling to predict only the first mode of floor vibration. They measured frequencies of only the fundamental modes of vibration of three full-scale composite steel-concrete floors in the Large Building Testing Facility (LBTF) based in Cardington, UK. The frequencies were compared with the results of dynamic FE analyses of the floors. The analyses were, however, performed by representing the whole floor by a single panel bound by four columns. The four columns were modelled as pin-supports and it was concluded that such relatively simple modelling is capable of predicting the fundamental floor natural frequency quite accurately. No attempts were made to calculate the floor responses. It should be mentioned that considerable difficulties were experienced while extracting damping from experimental measurements performed on one of the floors which clearly had closely spaced modes of vibration, as indicated by a beating effect visible in heel-drop acceleration time signatures.

Zaman & Boswell (1996d) also reviewed modern vibration serviceability criteria for composite steel-concrete floors. The four criteria considered were those proposed by Allan and Murray (1993), Murray (1981), Wyatt (1989) and the CSA (1989). Experimental results collected on six full-scale floors were based

on peak accelerations measured after a heel-drop. During the measurements very high peak accelerations reaching 9.2% g were reported and three out of six already built floors were rated as unacceptable according to the CSA (1989) scale. It was concluded that the four criteria "do not always lead to consistent results". However, it appears that no filtering of the acceleration signals has been performed prior to assessing the reported peak accelerations. As the way forward, and in order to avoid dealing with the floor damping, which is traditionally an uncertain parameter, Zaman and Boswell suggested eliminating the problem of floor resonance due to walking simply by shifting its natural frequency above 9 Hz, the low-frequency limit proposed by Allen & Murray (1993). A simple FE model representing just one panel of a floor (Zaman & Boswell, 1996c), may be used to reliably achieve such a frequency tuning design goal and reduce the floor vibrations.

Active control is another very advanced method for reducing floor vibrations. The method, utilising an electrodynamic shaker and a control feedback circuit, was recently piloted on a small laboratory based floor (Hanagan et al., 1996; Hanagan & Murray, 1997). Vibrations caused by normal walking were very successfully reduced by almost 10 times. However, extremely high cost, maintenance and reliability issues prevent wider use of active control at the moment.

2.3.8 Integrated Approaches to Vibration Serviceability of Composite and In-Situ Concrete Floors

A decade ago, Tilly (1986) reported that concrete was gradually replacing steel in even more demanding applications and concluded that:

> "Engineering development of concrete structures has reached the stage where dynamic behaviour could be critical to design."

However, as early as 1961, Janney and Wiss made an attempt to relate a problematic vibration performance of an existing concrete floor to its excitation due to walking and to rate its measured vibration levels. A precast concrete floor had been experiencing "noticeable vibration" produced by walking across it when it was not loaded. When the same floor was loaded, the vibrations ceased to be noticeable. Although Janney and Wiss used the inappropriate original Reiher and Meister scale to rate the problematic vibrations as "annoying", this is one of the first attempts known to the writer to deal with the vibration serviceability of floors made entirely of concrete. It also illustrates the positive effect of the increased mass on the floor vibration performance, which was confirmed later by Rainer et al. (1988a).

In the 1970s the renowned ACI Committee 435 prepared and disseminated two reports related to SLS of deflections and vibrations in concrete structures: (1) the SP-43 publication titled "Deflections of Concrete Structures" in 1974, and the SP-60 publication titled "Vibrations of Concrete Structures" in 1979.

2.3.8.1 ACI SP-60 PUBLICATION, 1979

Sabins (1979) introduced the ACI SP-60 publication as being aimed at helping designers cope with the fairly new challenges over which the American concrete design code ACI 318 had no provisions whatsoever.

Warwaruk (1979) contributed to the publication by presenting a detailed historical development of static deflection requirements in various building codes and their relationship with vibrations. He commented that static deflections or span-to-depth ratios did not appear to be a reliable parameter for controlling vibration serviceability of concrete floors and concluded:

> "More experimentation and study is necessary to clearly delineate the critical parameters and limitations for satisfactory [vibration serviceability] performance."

Allen et al. (1979) were invited to propose in the ACI SP-60 publication the vibration serviceability criteria applicable to both precast and in-situ concrete floors. Introducing the problem when dealing with the latter type of floor construction, they wrote:

> "Because of its relatively large mass and inherent stiffness to short-term load, cast-in-place construction generally is not prone to unsatisfactory vibration for normal human occupancy. The trend toward longer spans, less damping and thinner sections could result in problems if special care is not taken in design."

In the proposal, Allen et al. applied the logic used in composite floors and formulated assessment criteria based upon the heel-drop test (Allen & Rainer, 1975; 1976). It was suggested that the approximate peak accelerations should be calculated from the SDOF model of the floor using the following formula:

$$a_0 \approx 0.9 \cdot \frac{2\pi f I}{m} \qquad \text{Equation 2.7}$$

where a_0 is the peak acceleration of an equivalent SDOF system [m/s^2], f is the floor natural frequency [Hz], I [kg·m/s] is the impulse of the triangular heel-drop forcing function, and m [kg] is the mass of the equivalent SDOF system representing a real-life concrete floor structure.

Also presented were two groups of human response criteria developed by the late 1970s for checking vibration performance of composite steel-concrete floors: (1) for "quiet" occupancies, such as offices, residences and schools, and (2) for "active" occupancies, such as walkways, bridges, car parks, and general working areas. The criteria were clearly stemming from the previously mentioned Canadian steel design code (CSA Standard S16.1-1974 "Steel Structures for Buildings - Limit States Design") which was by then available. Regarding the applicability of the CSA criteria to concrete floors, it is worthwhile mentioning again that Murray (1981) strongly emphasised that subjective vibration serviceability criteria obtained from full-scale testing of composite steel-concrete floors are not applicable to concrete or timber floors as:

> "...other systems may cause completely different psychological responses because of long-time conditioning or expected feel."

The two key parameters required for the calculation of a_0 are the natural frequency f and the SDOF mass m (Equation 2.7). As has previously been seen, in the case of composite steel-concrete floors, a wealth of combined experimental and analytical research, extending over two decades in the 1960s and 1970s, existed to support recommendations as to what to do in order to establish as reliable as possible values of f and m when designing a floor. It appears that nothing similarly comprehensive existed in the case of in-situ concrete floors, so Allen et al. (1979) tried to produce experimental evidence by testing three full-scale concrete floors which were cast in-place together with the columns.

Following the established routine for composite steel-concrete floors, the floor was represented as an SDOF model. Peak accelerations obtained using these models were compared with the measured responses due to heel-drops from which the frequencies corresponding to higher modes of vibration were filtered out. The authors admitted that the modelling of the in-situ floors proved to be difficult. Firstly, it appears that by assuming pin-supports and neglecting the floor continuity over several panels, the calculated natural frequencies were underestimated and an error of the order of about 50% occurred. Secondly, when determining the modal mass m, it was assumed that it corresponds to the tributary area established from static considerations of the in-situ T beam. No evidence to support these assumptions either experimentally or analytically was produced. In addition, Allen et al. suggested further modelling simplifications as to the floor boundary conditions which were ultimately aimed at using a simply supported beam to represent the continous concrete floor structure.

The authors obviously had a difficult task to develop a procedure suitable for hand calculations, for checking the vibration serviceability of a floor type about which little was known. It appears that certain unwarranted assumptions and recommendations were made and an oversimplified procedure, based more on engineering intuition than on hard scientific evidence, was created. Large discrepancies between experiments and measurements indicate that the direct mapping of the heel-drop procedure, which was underperforming even when applied to composite steel-concrete floors for which it was developed, is not likely to be a suitable solution for in-situ concrete floors. In the case of in-situ concrete floors such an oversimplification may be desirable by practitioners, but could lead to an unreliable checking procedure. This view has been further underpinned by Pernica and Allen (1982) who could not develop a reliable SDOF model of a concrete floor which would cope successfully with the closely spaced modes of vibration observed in the measurements. The effect of concrete floor continuity over several bays on the SDOF (modal) mass m (Equation 2.7) was left undetermined.

2.3.8.2 Additional Literature on Vibration Serviceability of Concrete Floors Published in the 1980s

Becker (1980) also made use of heel-drop testing, but only in the case of floors having a natural frequency greater than 10 Hz. In the case of floors having a lower natural frequency, the displacement responses to both heel-drops and walking had to be calculated separately and assessed. This method, obviously, made a clear distinction between low- and high-frequency floors and recognised the important differences in their

bchaviour under normal human induced loading. Closed form solutions for SDOF floor models were used, with a significantly simplified continuous walking forcing function represented as a train of triangles.

Huggins and Barber (1982) made an interesting survey by asking 400 Canadian consulting engineers to report problems with floor serviceability including excessive vibrations. Although the strictest confidence was guaranteed, only 70 replies were received. Of those, 17 addressed problems with vibration serviceability of various types of floor construction. One "prestressed solid slab" and one in-situ reinforced concrete slab were reported to have unsatisfactory vibration performance, but no further details were given. It was concluded that a relatively poor response to the important questionnaire was a result of the difficulties to sift through old technical records, and of a reluctance to disclose confidential information which could lead to damage claims.

Although requirements for the floor vibration serviceability frequently appeared in the 1980s in numerous national codes of practice, the concrete design guidelines were giving little practical guidance as to how to perform the design checks. This situation has not been improved even nowadays when, for example, the contemporary British (BSI, 1985) and European (CEB, 1991) concrete design codes require vibration serviceability in buildings, but suggest the designer should seek specialist literature. Mickleborough and Gilbert (1986) gave a practical illustration of this unsatisfactory situation created by the 1986 draft of the Australian concrete structures design code. The new code specified that the concrete structural serviceability should not be negatively affected by vibrations from machinery, vehicular or pedestrian traffic. As no explanation whatsoever was given regarding what effects are considered to be adverse and how the design checks should be performed, Mickleborough and Gilbert commented:

> "... designers in general ignore vibration in most slabs and hope that provided the slab static response to load is acceptable, then its dynamic response will be also."

As has already been mentioned, for longer spans this assumption in unlikely to hold (Warwaruk, 1979). In order to produce at least some vibration analysis tools for the designers of concrete floors, Mickleborough and Gilbert simplified the problem considerably by assuming that concrete floors will have satisfactory vibration serviceability if their natural frequency is greater than 5 Hz. No references were given or scientific evidence produced to confirm that the 5 Hz frequency tuning assumption has ever been verified in the case of in-situ concrete floors under walking excitation. In another attempt to determine the initial thickness of post-tensioned slabs which would satisfy all serviceability requirements, Gilbert (1989) mentioned the importance of the floor vibration serviceability, but did not take it into account when developing a formula for initial floor thickness.

Cantieni and Pretlove (1986a) stressed that the civil engineering sector was used to simplified analytical models when dealing with dynamic problems. Amongst other reasons, this was a result of the lack of experimental work carried out on large-scale as-built civil engineering structures aimed at producing more reliable dynamic models. In addition, the same authors (Cantieni & Pretlove, 1986b) were not aware that any

building loading code was covering dynamic loads pertinent to vibration serviceability problems in the same way that static load was treated.

Bachmann and Ammann (1987) considered human-induced vibrations to be the governing design criterion for floors in office buildings. In order to tackle the vibration serviceability problem at the design stage, simpler frequency tuning and more complex response calculation methods were suggested. Nevertheless, Bachmann and Ammann (1987), and also Rainer et al. (1988a), pointed out that the latter method is more suitable for checking the vibration serviceability of heavier floors in offices. This method is based on the calculation of a vibration response due to walking which could be assumed to be treading in place at the point which would produce greatest response. The practical calculation recommended was to tune the pacing frequency so that one of its harmonics 'hit' the calculated floor resonance. Then the complete periodic excitation or just a single higher harmonic should be assumed to excite the structure and the steady-state response to such excitation can be calculated.

Such responses should then be compared with some pre-selected vibration acceptance criteria. After trying to apply a few criteria from the relevant national and international codes of practice for assessing the vibration serviceability to several case studies, Bachmann & Amman (1987) and Cantieni (1988) concluded that considerable scatter in the floor rating existed. However, BS 6472 (BSI, 1984) was recommended for checking the vibration serviceability of office buildings as it seemed to be the most appropriate. In addition, Bachmann and Ammann also derived their own simple vibration limiting values which were termed "overall acccptance levels". These, in the case of offices, were allowed to go as high as 2% g. This unusually high allowable peak acceleration was assessed to be more practicable than the "more sophisticated" approaches which existed in, say, BS 6472 (BSI, 1984). Three years later, Allen (1990a) recommended a much reduced peak acceleration limit for offices and residences of only up to 0.4-0.7% g, whilst Caverson (1992) determined that the 2% g peak acceleration limit is too relaxed for in-situ concrete floors used in offices.

Finally, amongst 22 case studies presented by Bachmann and Ammann (1987), a vibration serviceability problem caused by gymnastic exercises on a floor placed at the top of a high rise building was particularly interesting as it appears that the floor and the building were made of in-situ concrete. The problem was that vibrations during exercises on this highest floor were felt down through the top quarter of the building. Although the floor was estimated to have a natural frequency at about 10 Hz (presumably assuming some sort of ideal pin-supported or fixed boundary conditions), its very long support columns actually acted as relatively soft vertical springs. As such, they reduced the floor natural frequency to only 4.4 Hz, which is right in the range of the 2nd harmonic of the human-induced excitation. The columns also served as the 'transmitters' of annoying vibrations to the floors below the gym. It was concluded that this phenomenon, also reported by Rosenthal and Itskovitch (1988) and Allen (1990a), "needs further investigation". This is particularly so because Allen (1990a) concluded that concrete columns supporting concrete floors actually increase the flexibility of the floor system thus reducing its natural frequency.

In 1988, the NRCC Institute for Research in Construction organised a symposium on general serviceability of buildings (NRCC, 1988). A large proportion of the papers was devoted to the vibration SLS problem. Of

particular interest amongst them is the work of Bachmann (1988) who presented another case study of an in-situ cast ribbed concrete floor spanning 15m. Although it was stated that slender columns provided "virtually no rotational restraint" to the floor structure, little evidence was given to support that this view has been experimentally or analytically verified.

2.3.8.3 VIBRATION SERVICEABILITY OF COMPOSITE CONCRETE FLOORS

Vibration performance of concrete floors made of either classically reinforced or prestressed precast concrete elements has attracted considerable attention in the 1990s. The main advantages of precast over cast in-situ concrete floors are: absence of formwork and props, shorter construction times, smoother soffit, high mechanical and durability performance, and, particularly important for this investigation, longer spans and lower weight (FIP, 1994).

Aswad and Chen (1993; Chen & Aswad, 1994) analytically investigated vibration performance of precast building floors made of double-T precast beams. The work was based on FE modelling of a number of precast floors in precast concrete buildings. The floors were assumed to be pin-supported although no experimental work has been done to validate this modelling assumption. The FE modelling was, nevertheless, used to calculate and assess the floor vibration response in the time domain. The following three forcing functions were used to simulate normal walking numerically:

1. a single heel-drop in conjunction with the Murray's (1981) rating (Equation 2.5),
2. multiple heel-drops as proposed by Tolaymat (1988a; 1988b), and
3. time domain representation of the single-person walking excitation assumed to be periodic and represented by the first three harmonics having amplitudes of 350N, 140N and 70N, respectively. The calculated acceleration response was compared with the ISO 2631-2 (ISO, 1989) thresholds.

The way Aswad and Chen applied each of the three methods deserves comment. Firstly, Murray's method (Equation 2.5), was used although it was developed for composite steel-concrete and not composite concrete structures. Secondly, Tolaymat's method neglects higher modes of vibration and repeated heel-drops are not a very realistic form of excitation in normal residential or office environments where single person walking should be the governing design consideration. Also, the method was not experimentally verified using data from concrete floors. Finally, when applying the third method, the authors assumed only a single pacing frequency of 2 Hz which produced relevant higher harmonics at 4 Hz and 6 Hz. However, none of these three frequencies were close to any of the calculated natural frequencies of the low-frequency precast floor configurations investigated. Having neither resonant nor near-resonant conditions simulated, calculation of both peak and RMS accelerations showed little dependence on floor damping. This is not surprising and the parametric studies presented of the effect of damping, when such off-resonant human induced excitation is applied, seem to be unnecessary.

2.3.8.4 ERIKSSON'S DOCTORAL THESIS (1994)

Low-frequency composite concrete floors were investigated by Eriksson (1994). Particularly important parts of this impressive work, pertinent to the vibration serviceability of office floors, have already been frequently referred to in this thesis. Therefore, only a critical review of the main features and problems which merit further investigation will be outlined here.

Eriksson experimentally investigated seven full-scale floors, five of which were composite concrete whilst the remaining two were composite steel-concrete construction. Precast concrete elements were employed in all cases. Advanced modal testing technology based on input-output FRF measurements was used to determine modal properties of the floors. However, only four of the tested floors were analytically modelled using FE analysis, based on floor grillage analogy, in order to compare the measured with analytical results. This indicates that analytical modelling was not always a constitutive part of experimental testing. This lack of preparation prior to the tests may have contributed to the complete failure of one of the field tests.

The FRF measurements enabled the existence of closely spaced modes in practically all floors to be determined. It was concluded that higher modes of vibration might easily be excited by normal walking and that their modal damping and mass play a significant role in determining the level of the acceleration response of the floor to such excitation. Nevertheless, only the SODF method was used to determine these two important modal parameters from experimental measurements which lead to their inaccurate estimates.

Although columns were included in some of the grillage FE models developed, their modelling was based on the assumption that they were rigidly connected to the slab but pin-supported at their other ends. However, in some other cases columns were modelled only as pin-supports with no rotational stiffness for no apparent reason. Considering that the author admitted that the agreement between the FE analysis and the modal testing results for almost all precast composite concrete floors had not been "as good as desired", it is clear that there remained a degree of uncertainty as to how to treat columns in analytical models of concrete floors.

2.3.8.5 VIBRATION SERVICEABILITY OF IN-SITU CONCRETE FLOORS

Apart from the Concrete Society (1994) Technical Report 43 already mentioned, there is a limited number of recent publications which have tried to throw more light on dynamic performance of long-span in-situ cast concrete floors, which are investigated in this thesis.

Ouchiyama and Yajima. (1993) loaded until destruction a full-scale concrete slab which was cast in situ and post-tensioned with unbonded tendons. Failure occurred in shear and it appears that columns were developing bending resistance right up to failure. In addition, vibration experiments on another full-scale post-tensioned floor showed that edge beams and non-structural walls substantially increased its fundamental frequency (i.e. the stiffness).

In a series of three papers Zaman and Boswell tried to link field test results with FE modelling of the floors tested. The aim was to develop a method to tackle the vibration serviceability of in-situ PT floors. Firstly,

assuming that only the fundamental mode affects the human perception of vibration, Zaman and Boswell (1995) developed FE models and calibrated them to match only the fundamental frequencies measured on six full-scale floors. The rationale of this approach was to develop a reliable but simple FE modelling method which, by changing its parameters, would ensure that the floor's fundamental frequency exceeded 6 Hz in order to preserve the floor vibration serviceability under walking-induced vibrations. As this frequency tuning approach does not require response calculations, no attempt was made to use 'calibrated' FE models, comprising a limited number of panels, to simulate the actual floor vibration response. In order to tune the fundamental mode of the FE model and keep it as simple as possible, columns were modelled as fixed supports allowing no translation and rotation. In the second paper, Zaman and Boswell (1996a) expanded on this frequency tuning approach by developing a formula, suitable for hand calculations, which was based on static deflections. However, it was concluded that FE modelling provides the most reliable method for estimating the floor fundamental frequency. The third paper (Zaman & Boswell, 1996b) reported fundamental frequencies and peak accelerations to heel-drops measured on 20 already built full-scale PT concrete floors. The floors were rated as "acceptable" or "unacceptable" and the following formula, similar to the Murray's (1981) criterion (Equation 2.5) was developed:

$$\zeta \geq 209 A_0 f - 1 \qquad \text{Equation 2.8}$$

where ζ, A_0 and f are the same parameters having the same units as in Equation 2.5. The graphical representation of this criterion is shown in Figure 2.17 and requires a comment. The figure clearly shows that more than half of 20 floors tested had "unacceptable" vibration performance which is surprising considering traditionally very good past vibration serviceability behaviour of PT floors (Khan & Williams, 1995). Zaman and Boswell (1996b), nevertheless, did not discuss this potentially very worrying observation.

2.3.8.6 Initialisation of the Research Reported in This Thesis

Fast developments in experimental testing and numerical analysis techniques gave a major boost to research into the vibration serviceability of concrete floors in the 1990s. This was mainly through measurements of floor FRFs, more sophisticated vibration parameter estimation and the utilisation of FE modelling.

The basis of the research reported in this thesis was a pilot project initiated at Bristol and Oxford universities in 1991 under the joint supervision of Professor Peter Waldron and Dr Martin Williams. The results of this study were subsequently reported in Caverson's MSc dissertation (1992), and published further by Waldron et al. (1993), Williams et al. (1993), Caverson et al. (1994), Williams and Waldron (1994) and Khan and Williams (1995).

The main aim of this pilot investigation was to gather experimental data on as-built vibration properties and the performance of a range of long-span concrete floors in order to compare them with predictions from simplified analytical models. In total, 13, mainly cast in-situ, PT floors of various configurations were tested in full field conditions. Without going into further details, a critical summary of this pilot study, which is

highly relevant to the investigation reported in this thesis, and in which the writer actively participated, will be outlined here.

During the field investigations two groups of tests were employed. Firstly, an instrumented sledge hammer was used to measure the FRFs corresponding to vertical floor vibrations. These served to extract the structure's modal properties. Secondly, responses due to human excitation such as heel-drop, walking, running and jumping were measured. Results from these two groups of experiments were then used to rate the floors' vibration in accordance with a number of guidelines including the modified Reiher and Meister (Lenzen, 1966), Wiss and Parmalee (1974), Appendix G of the Canadian steel design code (CSA, 1989), ISO 2631-2 (ISO, 1989) and BS 6472 (BSI, 1984).

An attempt was then made to mathematically model the floors investigated, estimate their fundamental frequency and compare the calculated frequencies with the measured results. Simplified analytical modelling was done using the following methods:

1. the equivalent beam method (Allen et al., 1979),
2. the (draft) Concrete Society (1994) method,
3. the equivalent plate method (Williams & Waldron, 1994), and
4. finite element modelling of a limited number of floor bays (Williams et al., 1993).

Three main conclusions were reached. Firstly, all in-situ concrete floors developed a two-way response of a nature which is difficult to estimate using any of the simplified procedures. Secondly, the measured fundamental frequencies were always greater than those calculated using the first two analytical methods. Finally, the application of the various vibration assessment guidelines previously introduced to both measured and calculated results led to inconsistent floor vibration serviceability assessment. The poor performance of all simplified procedures led Williams and Waldron (1994) to conclude:

> "While some improvements may be possible, it is unlikely that hand-calculation methods will ever be useful as more than order-of-magnitude checks. In order to have confidence in the behaviour of slender floors, a more accurate approach is needed. In the future, therefore, it may be necessary to use a computational method such as finite-element analysis as a part of the design approach."

Although the pilot project produced plenty of reliable scientific evidence about the behaviour of long-span concrete floors cast in-situ, the writer has identified, with some hindsight, a number of problems in the study. These are as follows:

- The FRF measurements were made on a relatively limited number of points without using available aids aimed at improving the quality of the measurements. For example, the more sophisticated analytical (FE) modelling could have been used to help the field testing and the selection of suitable measurement points. Also, experimental hardware limitations prevented the use of various signal processing aids, such as exponential windowing, which could have improved the quality of FRF measurements where an instrumented sledge hammer served as the exciter.
- A method based on a SDOF model was used to estimate damping when closely spaced modes of floor vibration occurred, resulting in great scatter and lack of confidence in the measured damping values.

The presence of closely spaced modes of vibration was generally neglected both in the parameter estimation and in response calculations.

- Mode-shapes were manually extracted by visually inspecting the peaks and phase shifts in the measured FRFs. This gives little confidence in the calculated ordinates considering the closely spaced modes of vibration frequently visible in the measured FRFs.
- Heel-drop response measurements were done without filtering out the contribution of the higher modes of vibration which resulted in higher peak acceleration values reported.

Most of these deficiencies were identified during the pilot study and arose as a result of the limited time-scales under which the project operated. Nevertheless, the lessons learned by actively participating in this study helped the writer to formulate a research strategy which would address these and other problems identified through the background reviews presented earlier in order to produce reliable research output.

2.4 Further Considerations and Conclusions

The background reviews have demonstrated that the problem of vibration serviceability of PT floors in office buildings is complex and interdisciplinary in nature. Current state-of-the-art suggests that it is prudent to rationalise it into three key components comprising the characterisation of: (1) the floor vibration sources, (2) the floor structural dynamic properties, and (3) the receiver's response. Of these, the last is, from an engineering point of view, probably the most complex when humans are specified as the vibration receivers.

However, human response to floor vibrations has attracted considerable research in the past. Although fragmented, these research efforts have led to the conclusion that the threshold in perception between 'feel' and 'no feel' of floor vibrations could govern floor vibration serviceability. This is particularly important for relatively quiet environments, such as high-quality offices, because human vibration perception thresholds tend to reduce in such cases. Also, floor vibrations may be perceptible, but, in order to be acceptable, they must be of a very low-level - just above the perception thresholds. Procedures, based on frequency weighting of the floor acceleration responses, now exist to assess the probability of adverse comments regarding such low-level vibration. These procedures are not perfect and they do require further research and development. However, they do exist and are now accepted in the UK (BSI, 1992) and internationally (ISO, 1992; ISO, 1997). Increasingly, they are used in the contemporary design of office floors.

The fact that minute vertical floor vibrations may cause problems in high-quality environments raises the problem of low-level vibrations induced by the floor occupants when walking across it. By its very nature, such excitation is complex and it is difficult to isolate the floor from it. In these circumstances, excitations caused only by a single person walking could be excessive. Therefore, numerous researchers have proposed a single person walking to be the governing loading case when checking the vibration SLS of office floors. Two methods generally exist to do this.

The first is to perform 'frequency tuning' and increase the floor natural frequency above a certain pre-defined level. The second method is to calculate the floor dynamic response to the nearly periodic walking excitation and assess the calculated response in accordance with the existing guidelines. It is important to stress here that it is the floor's actual vibration response, and not its natural frequency, which governs its vibration serviceability in the case of quiet occupancies and low-level vibrations. However, the high-frequency tuning method was popular in the past as analytical calculation of actual floor responses was difficult.

This is particularly important in the case of long-span in-situ concrete floors which, if post-tensioned, are, at the moment, very competitive when used in office developments. In these cases, the majority of the literature surveyed considers the high-frequency tuning method as obsolete as it is likely to produce uneconomical design. Therefore, the calculation of actual responses appears to be to be the way forward. Full FE analyses are nowadays becoming an affordable tool for such exercises.

Unfortunately, for the particular case of in-situ concrete PT floors, this exercise appears to be difficult to perform. Scarce information as to how to numerically model the floor as a dynamic system and its excitation is conflicting. There is a lack of experimental work on this particular type of structure meaning that the implementation of the modelling procedures for vibration SLS checks, which were developed for other construction types of floors, has not been verified.

In the case of in-situ concrete floors, particularly problematic are the modelling of the distribution of floor mass and (lateral) stiffness, floor boundary conditions, and near periodic excitation due to single-person walking.

2.4.1 Mass and Stiffness Distribution

Although there is a trend towards increasing slenderness leading to the general reduction in weight of PT floors, it should be stressed that they still tend to be relatively heavy compared with other types of floor construction. For example, the writer conducted a survey of the self weights of 30 long-span PT floors, for which geometric properties were reported by Fintel and Ghosh (1982), and Matthew and Bennett (1990), and 20 composite steel-concrete floors (Lenzen & Murray, 1969), used in office buildings. The outcome of the survey was that PT floors are on average more than twice as heavy as their composite steel-concrete counterparts, 596 kg/m^2 compared with 257 kg/m^2.

This is particularly important regarding floor vibration behaviour if the effects of continuity and increased floor lateral stiffness, both of which having a potential to engage larger floor area in vibrations, are taken into account. However, increased floor mass and lateral stiffness, and the effects of continuity over several floor panels are frequently neglected in vibration SLS calculations.

2.4.2 Boundary Conditions

Although the in-situ cast concrete columns affect the floor boundary conditions and may have considerable effect on the floor natural frequencies, the current recommendations as to how to model them are conflicting. The range of options offered in the published literature is wide: from treating them as simple pin- to fully fixed-supports. The first option is, however, utilised in practice more frequently due to the simplifications it offers, but it may result in a reduction in natural frequency and unsatisfactory vibration performance when full walking response calculations are performed. On the other hand, the same floor modelled with fully fixed supports may become high-frequency and satisfy the vibration SLS response requirements. This situation is, obviously, not satisfactory from a designer's point of view and requires clarification.

2.4.3 Near Periodic Walking Excitation

It appears that some scientific evidence exists to suggest that a single person tends to produce imperfect, near periodic, excitation while walking across the floor. Also, floor vibration responses due to a single person walking across it tend to be short-lived transients (Bachmann & Ammann, 1987). Nevertheless, when calculating the floor response these two facts are neglected. Instead, a common assumption found in the literature is that pure resonance conditions under walking excitation are achieved in the case of low-frequency floors meaning that steady-state vibration levels are reached. Typically, this is assumed because it is conservative and it simplifies the calculations. However, the framework set by ISO 10137 (ISO, 1992) considers the research developments in the characterisation of all three key floor vibration serviceability parameters (vibration source, path and receiver) as equally important. Therefore, although there is a great scatter and uncertainty about the actual assessment of human response to vibrations, this should not serve as a justification for the lack of accuracy and (over)simplification in the characterisation of the other two key parameters: walking excitation and floor dynamic modelling, as has sometimes been suggested in the literature.

It should be stated here that, whereas conservative simplifications are often desirable in engineering calculations, they must be justifiable. This means that there must be evidence that the simplifications are not overconservative. It appears that such evidence does not exist in the case of the resonance assumed in low-frequency PT floors under footfall loading. As a consequence, the resonance assumption may well prove to be overconservative. There are two possible reasons for this.

Firstly, the time for the resonant vibrations to build-up is neglected. This time could be considerably increased in the case of lower floor modal damping (Clough & Penzien, 1993). Such lower damping of concrete floors has been frequently reported in the 1990s using measurement techniques more reliable than amplitude decay after a heel-drop which is now widely recognised as being unreliable. Considering that walking across a floor is, in essence, a transient phenomenon having a limited duration, it may well be that there is not sufficient time for vibrations to build up to a full resonant response.

Secondly, the likely inability of humans to keep the pacing rate strictly constant at the resonance frequency of a floor with relatively low damping has frequently been neglected. In this case, even if the steady state response is achieved, a small variation in the excitation frequency may lead to a large reduction in the calculated response due to the greater narrowness of the floor frequency response.

With regard to the walking excitation models, there is also a lack of information as to the performance of the recently formulated frequency-domain models used to simulate a single person walking.

2.5 Research Aims

The writer's thesis is that inconsistent and widely varying current practice for modelling boundary conditions, mass, stiffness, damping and walking excitation are the likely reason why procedures developed for checking the vibration SLS of in-situ cast concrete floors perform poorly. This is further compounded by the lack of modal and dynamic response experimental data pertinent to this type of floor. Consequently, the aims of this research are:

1. to link the numerical modelling and full scale modal testing of a number of prototype floors and, if possible, establish more reliable modelling guidelines, based on the FE method, which would be applicable for checking the vibration serviceability of in-situ concrete floors,
2. to investigate vibration behaviour of relatively heavy and low-damped in-situ concrete floors under walking loading in order to rate the performance of some of the current, widely used walking excitation models, and
3. to investigate the background and performance of the procedure for vibration serviceability checking of in-situ cast post-tensioned concrete floors currently recommended by the Concrete Society (1994) in order to pinpoint the likely reasons for its shortcomings.

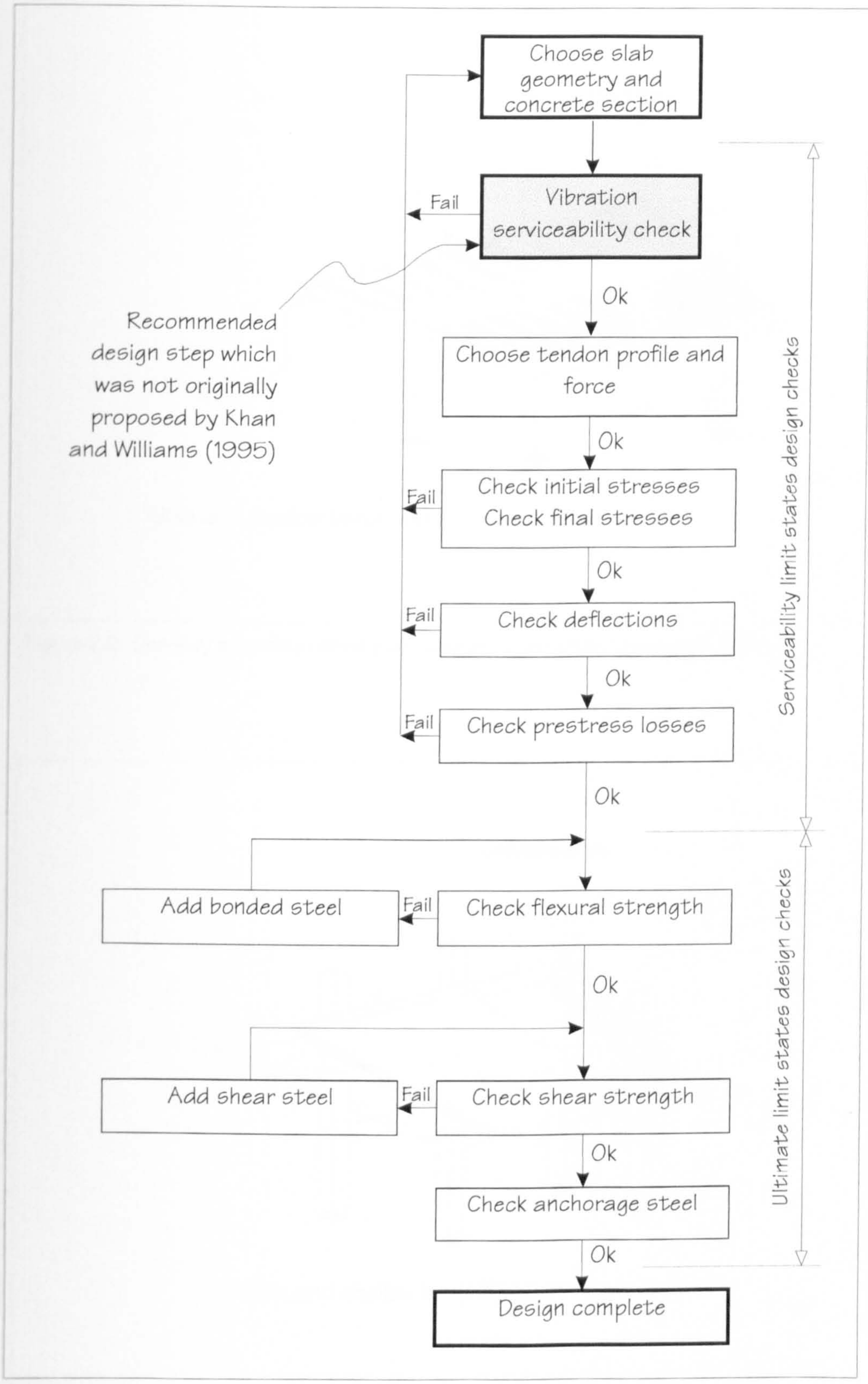

Figure 2.1: The design procedure for PT concrete floors (after Khan and Williams, 1995).

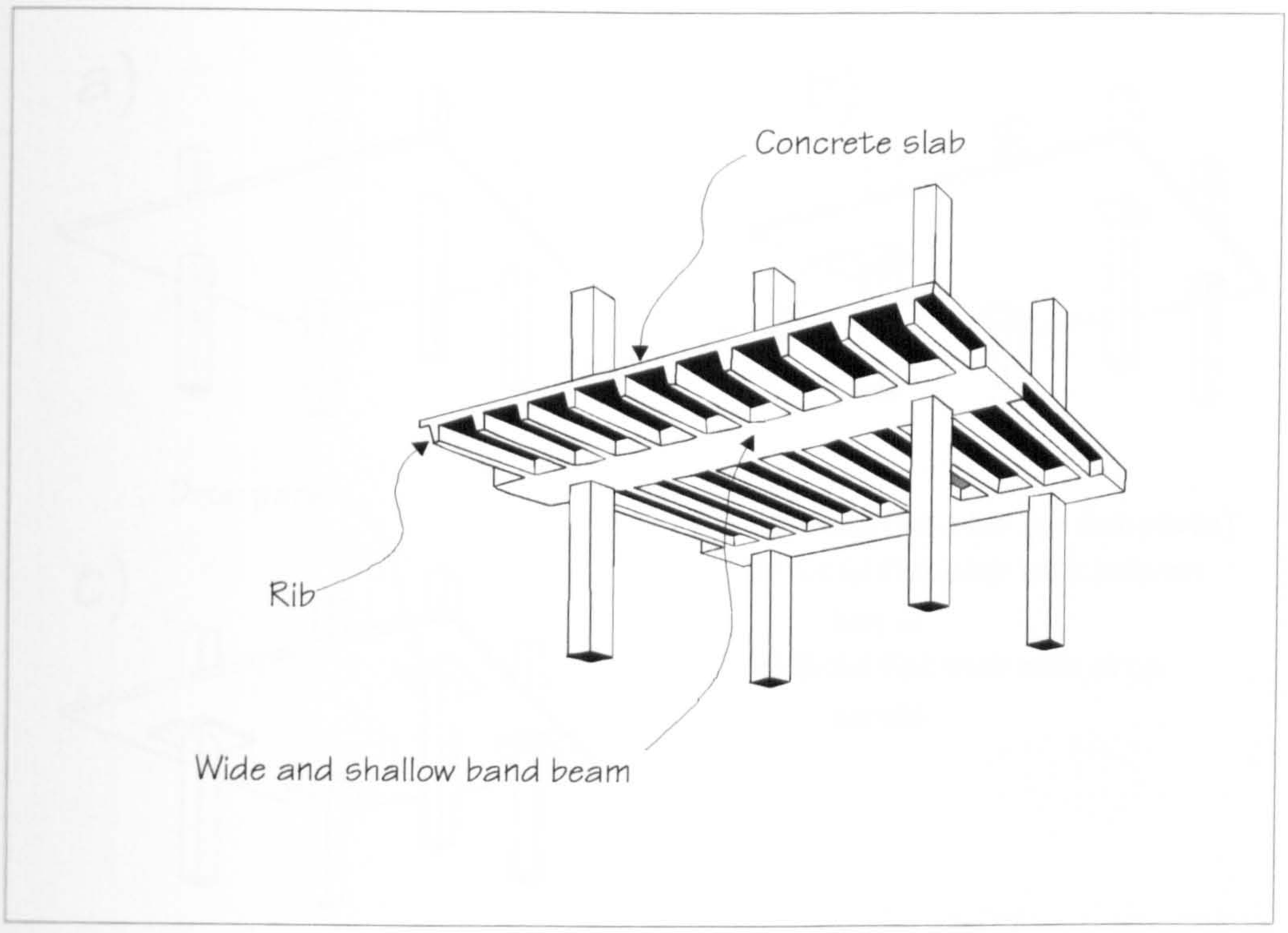

Figure 2.2: One-way spanning ribbed slab construction (after Stevenson, 1994).

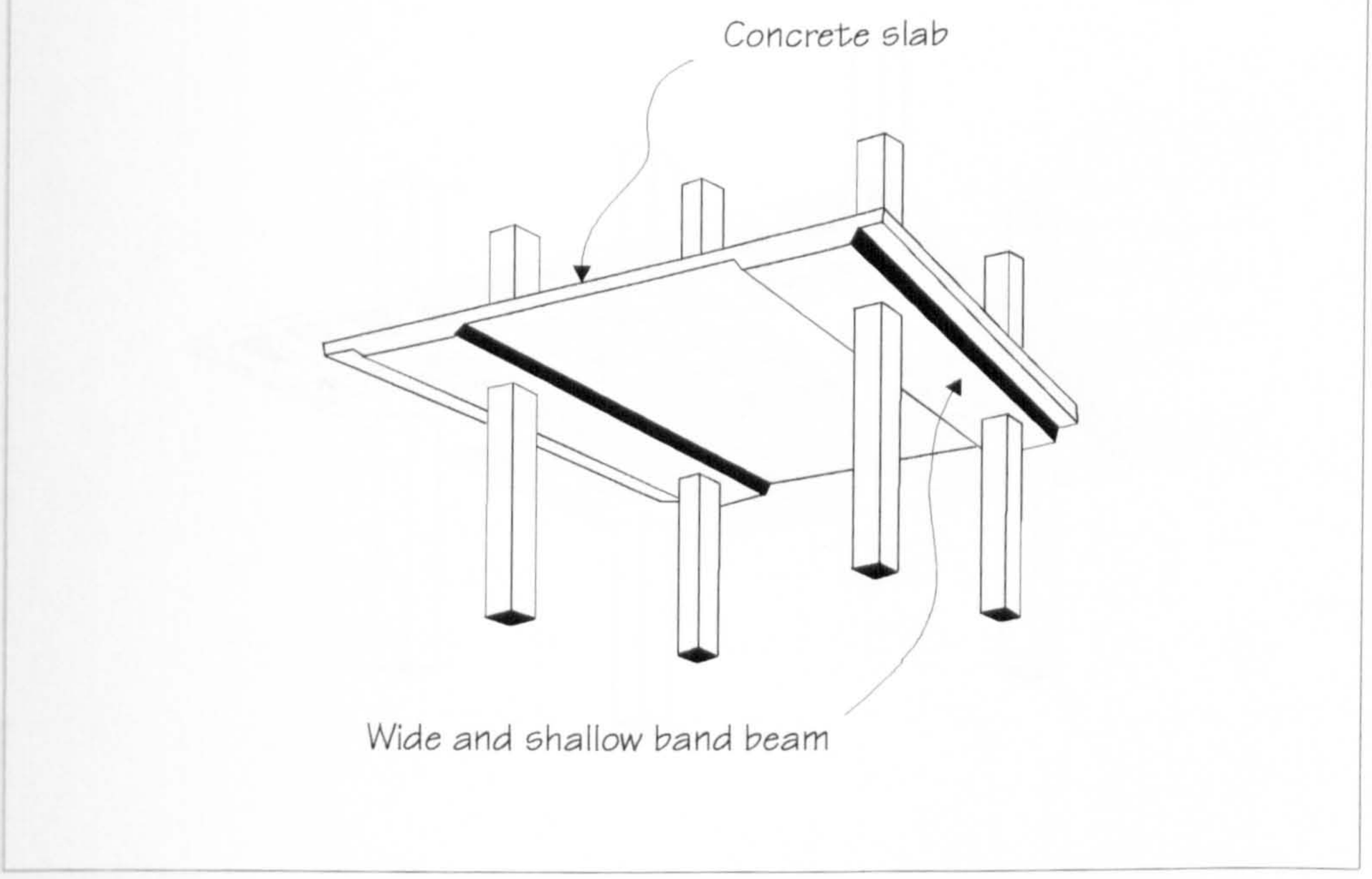

Figure 2.3: Banded beam and slab construction (after Stevenson, 1994).

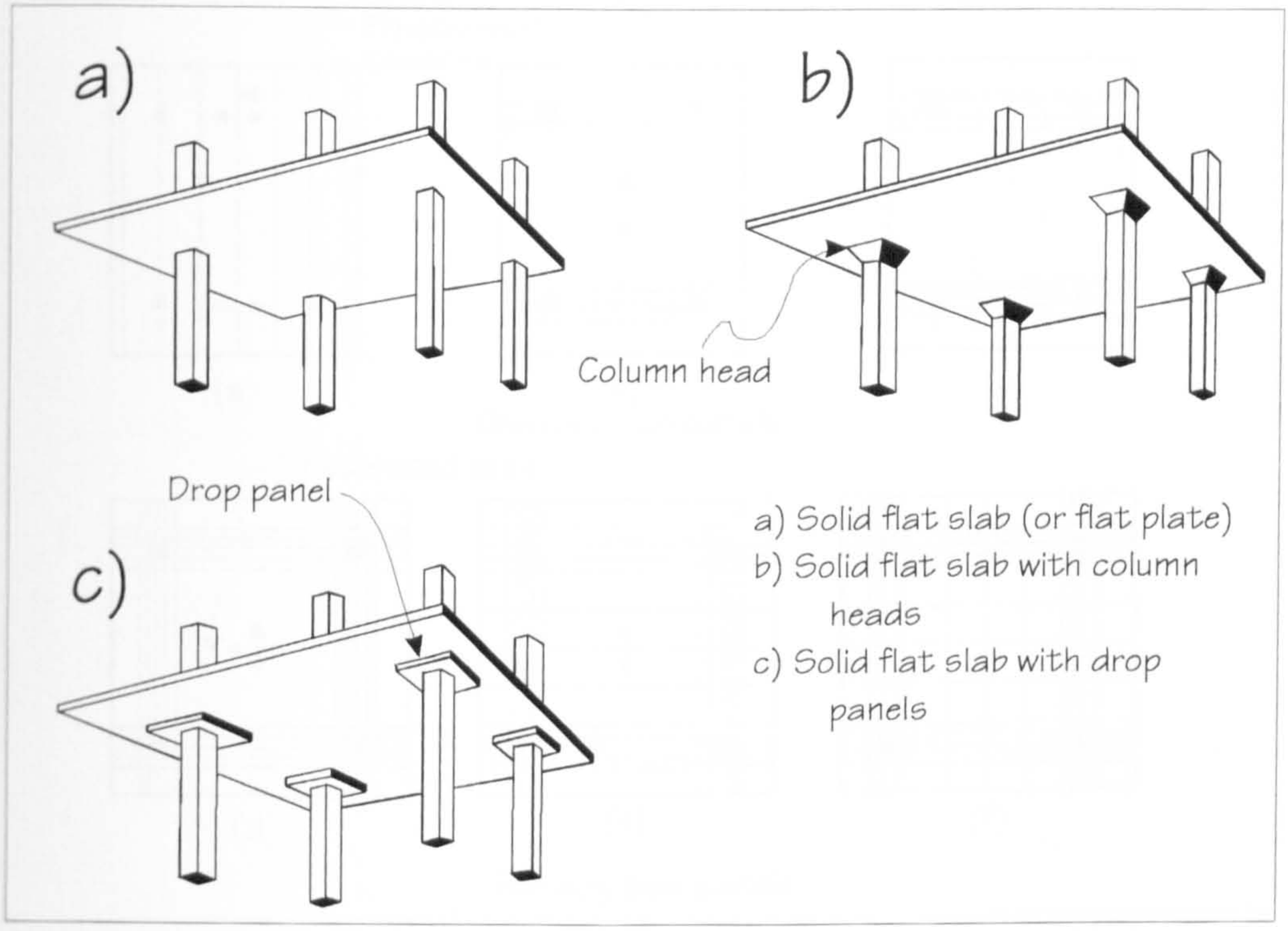

Figure 2.4: Solid flat slab construction (after Stevenson, 1994).

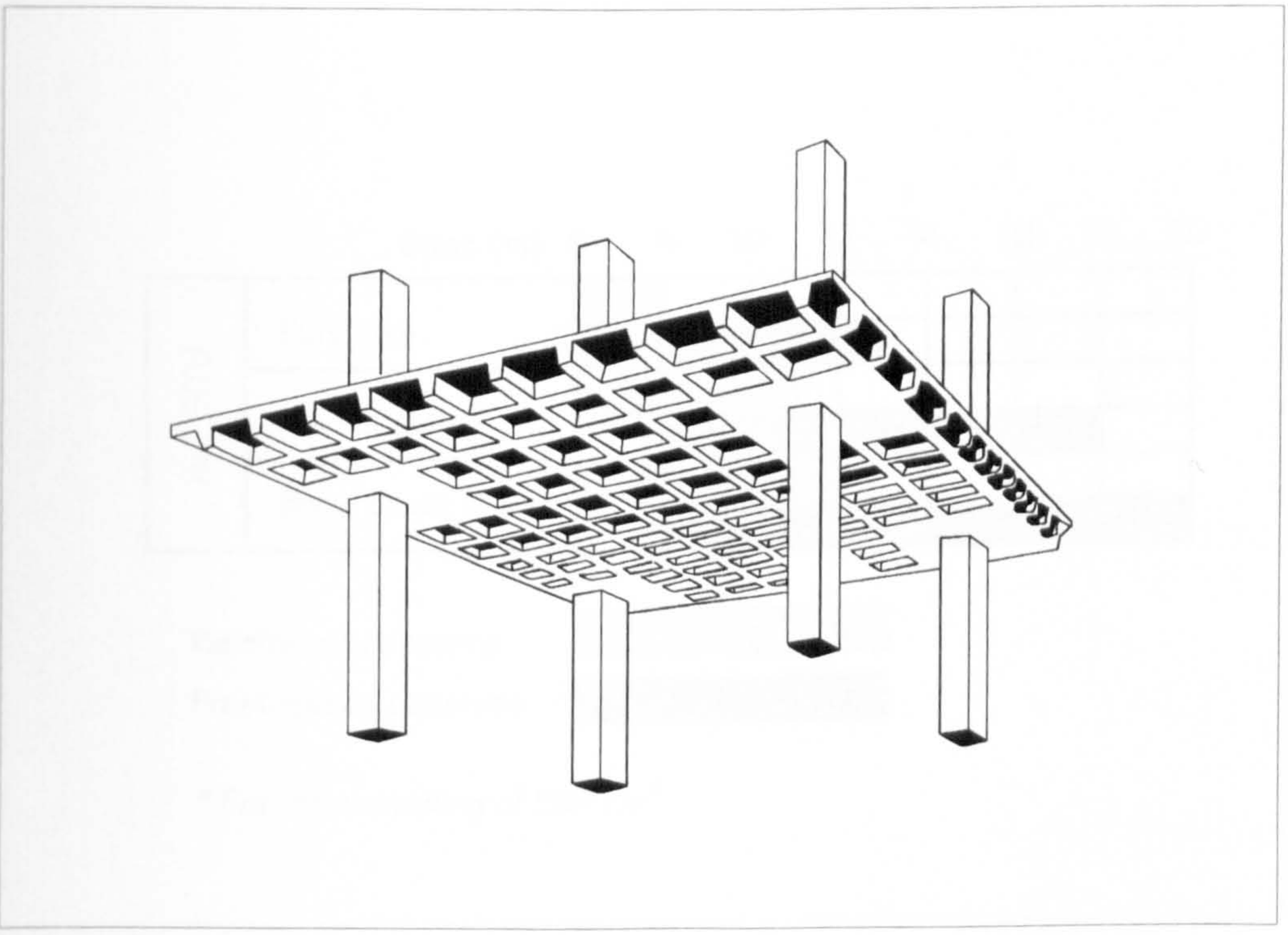

Figure 2.5: Coffered (or waffle) flat slab construction (after Stevenson, 1994).

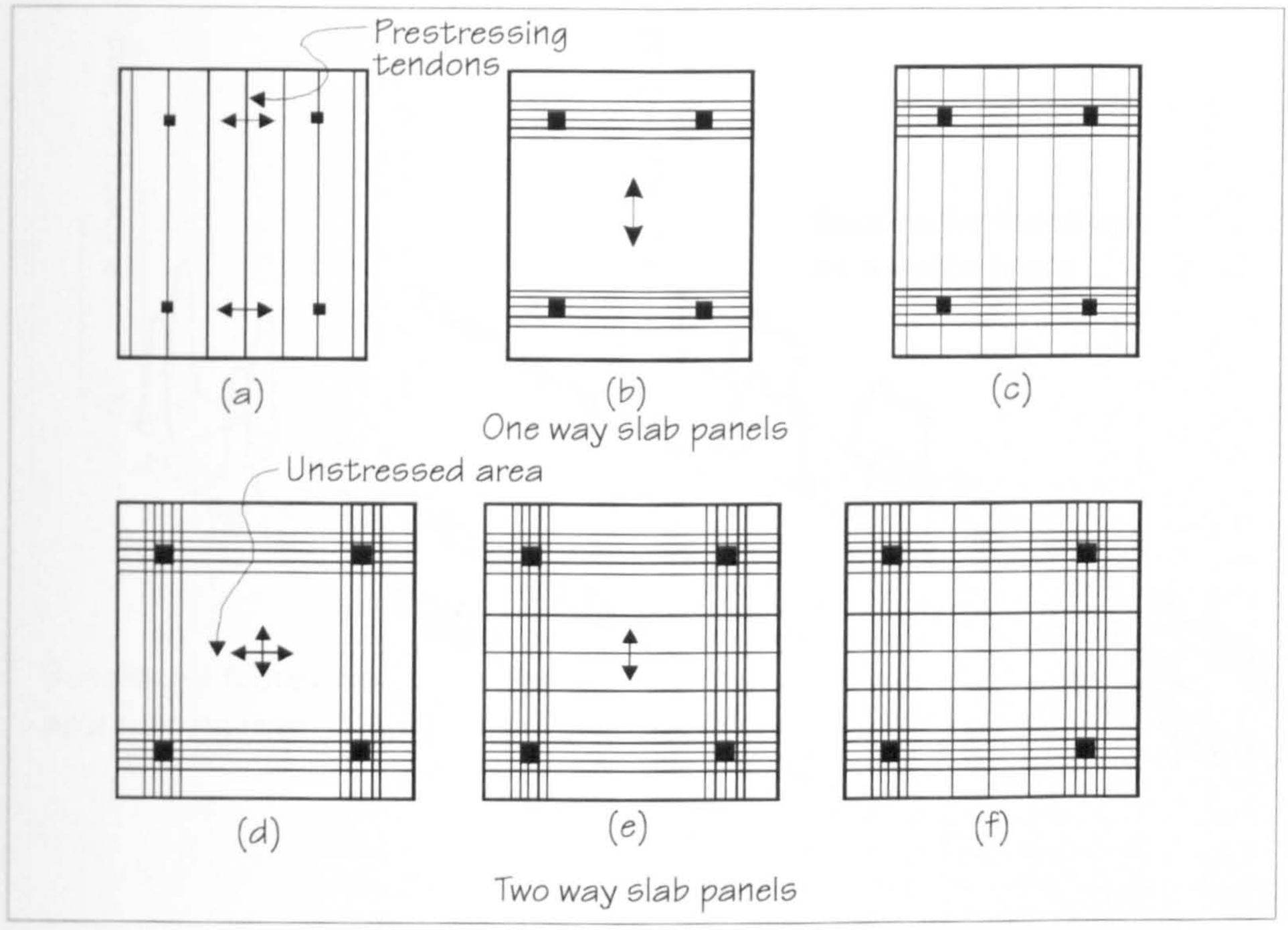

Figure 2.6: Typical prestressed post-tensioned floor panels (after Khan and Williams, 1995).

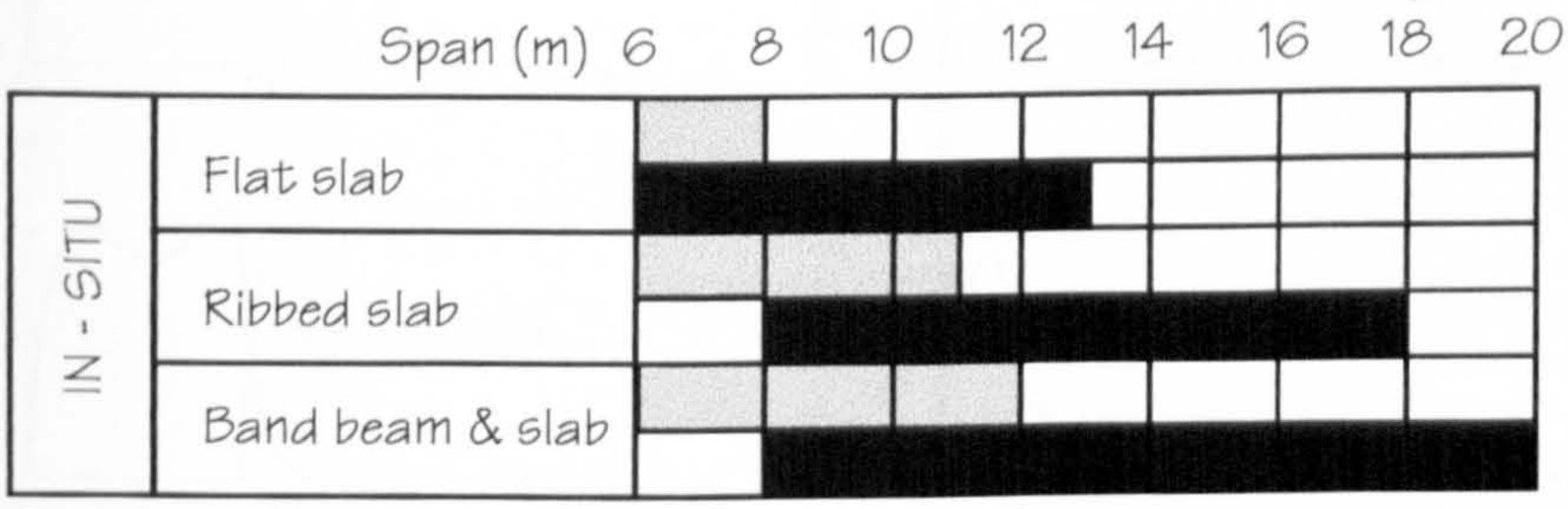

Figure 2.7: Floor spans achievable by in-situ reinforced and prestressed concrete (after Stevenson, 1994).

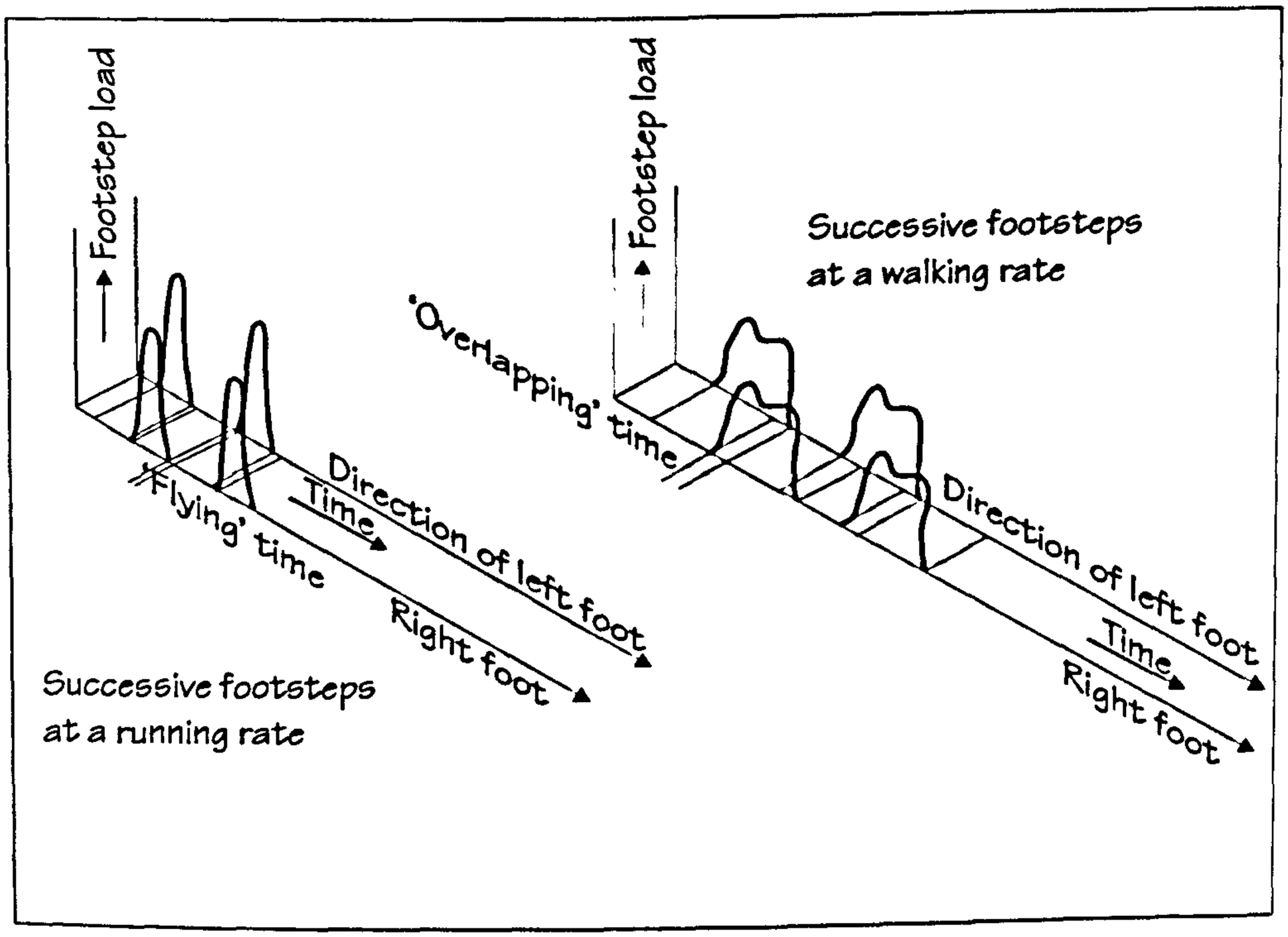

Figure 2.8: Typical forcing patterns for running and walking (after Galbraith and Barton, 1970).

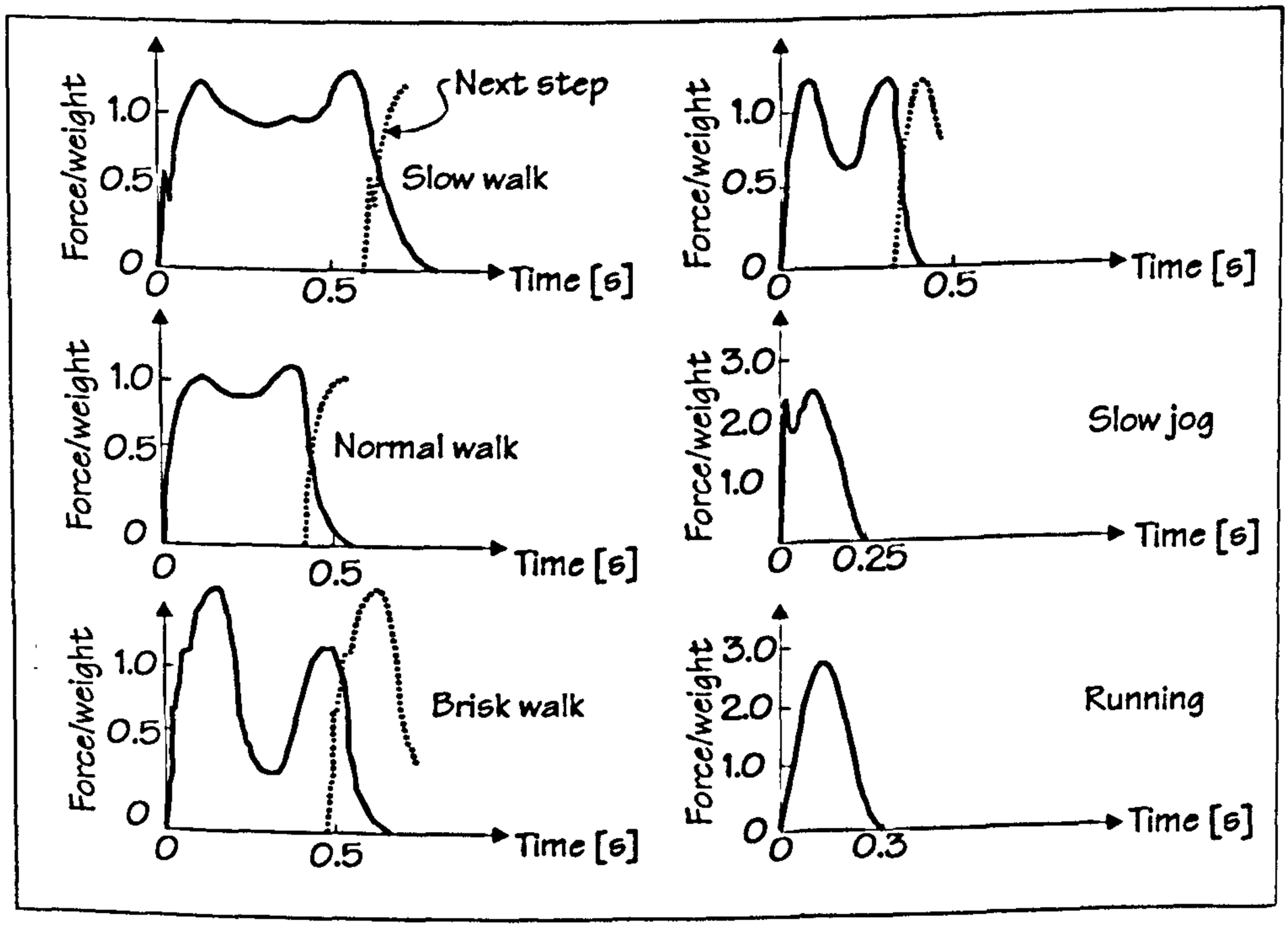

Figure 2.9: Detailed forcing patterns for various modes of walking, jogging and running (after Wheeler, 1982).

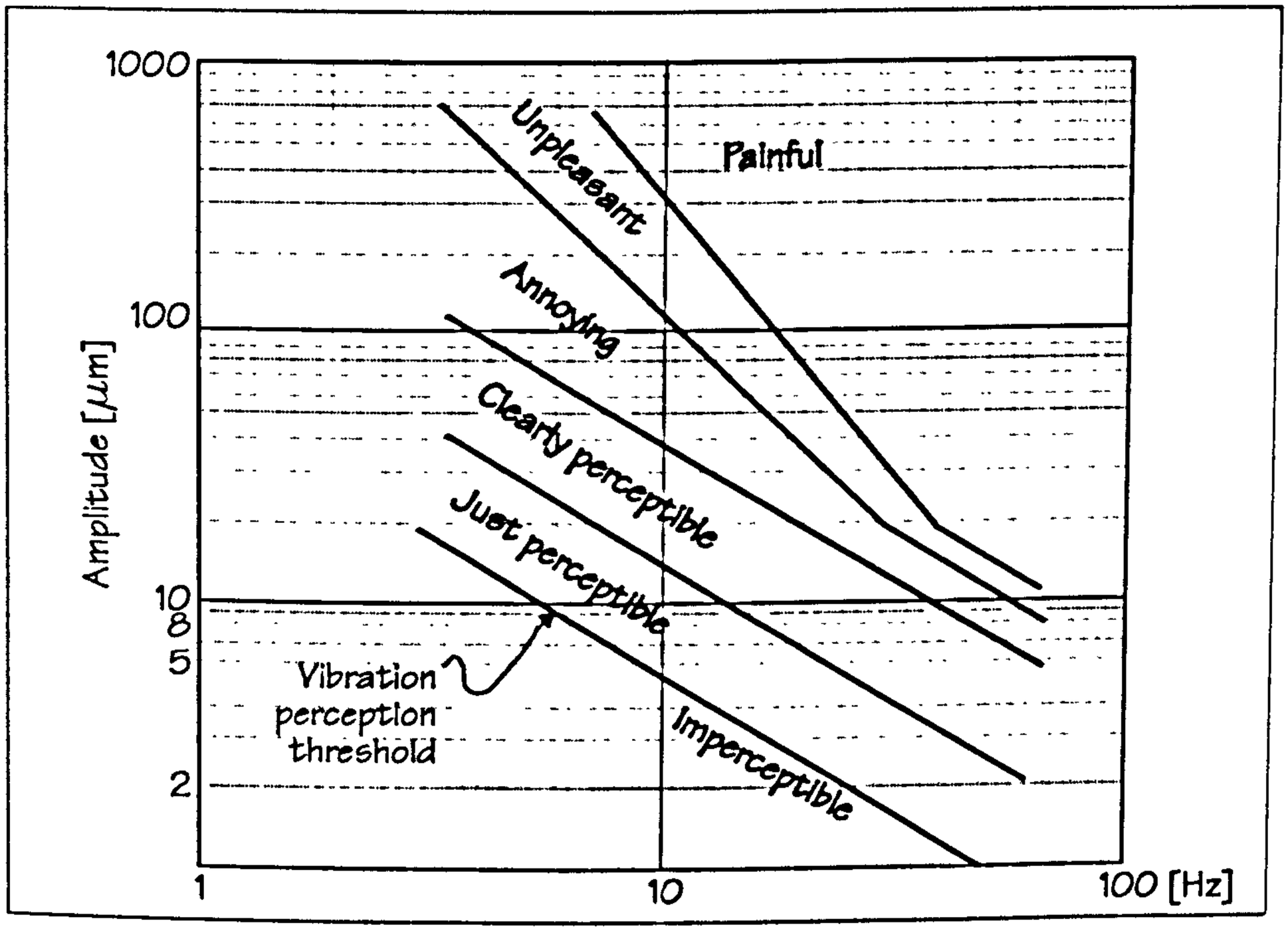

Figure 2.10: The Reiher-Meister (unmodified) scale (after Wright and Green, 1959).

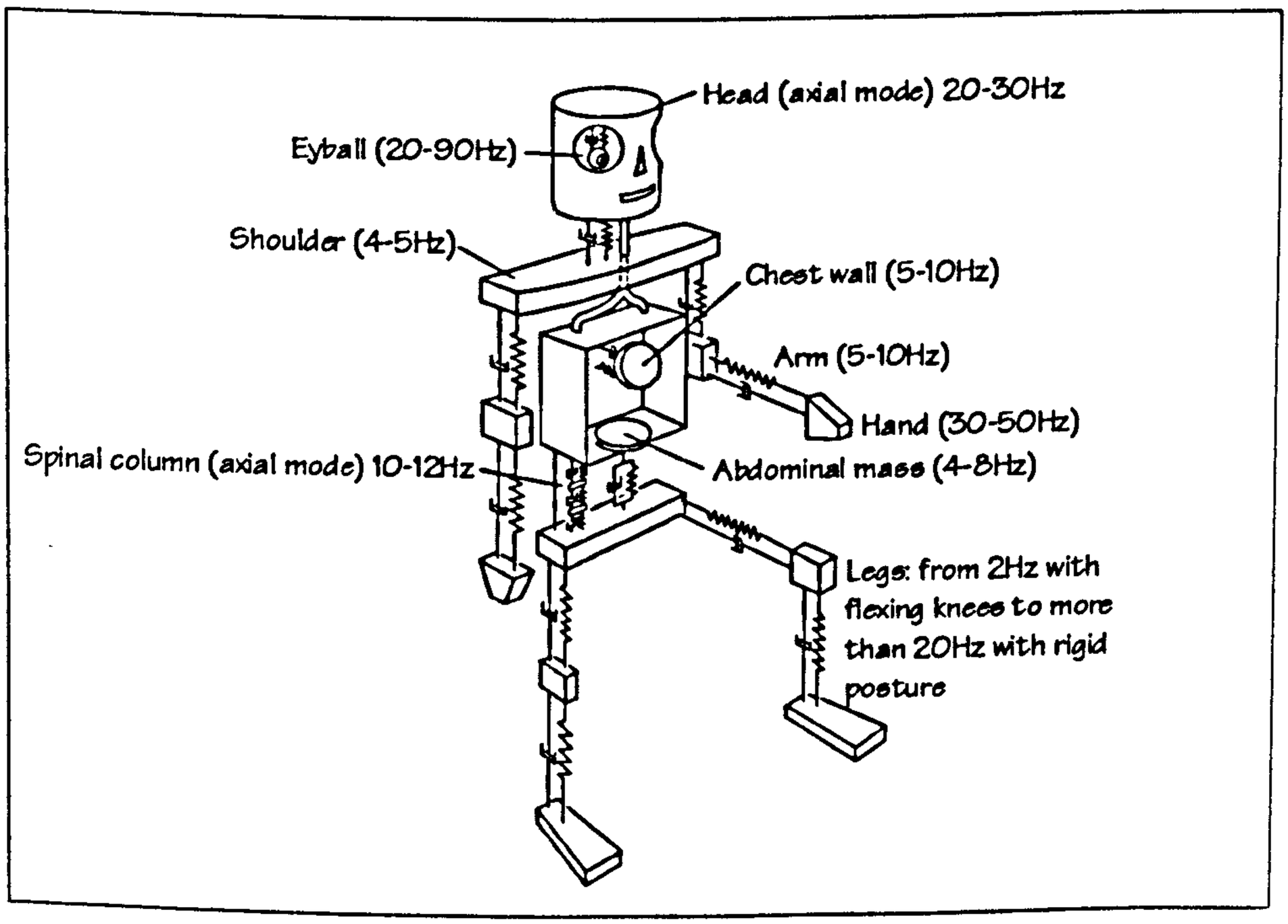

Figure 2.11: Lumped-mass model of human body (after Smith et al, 1996).

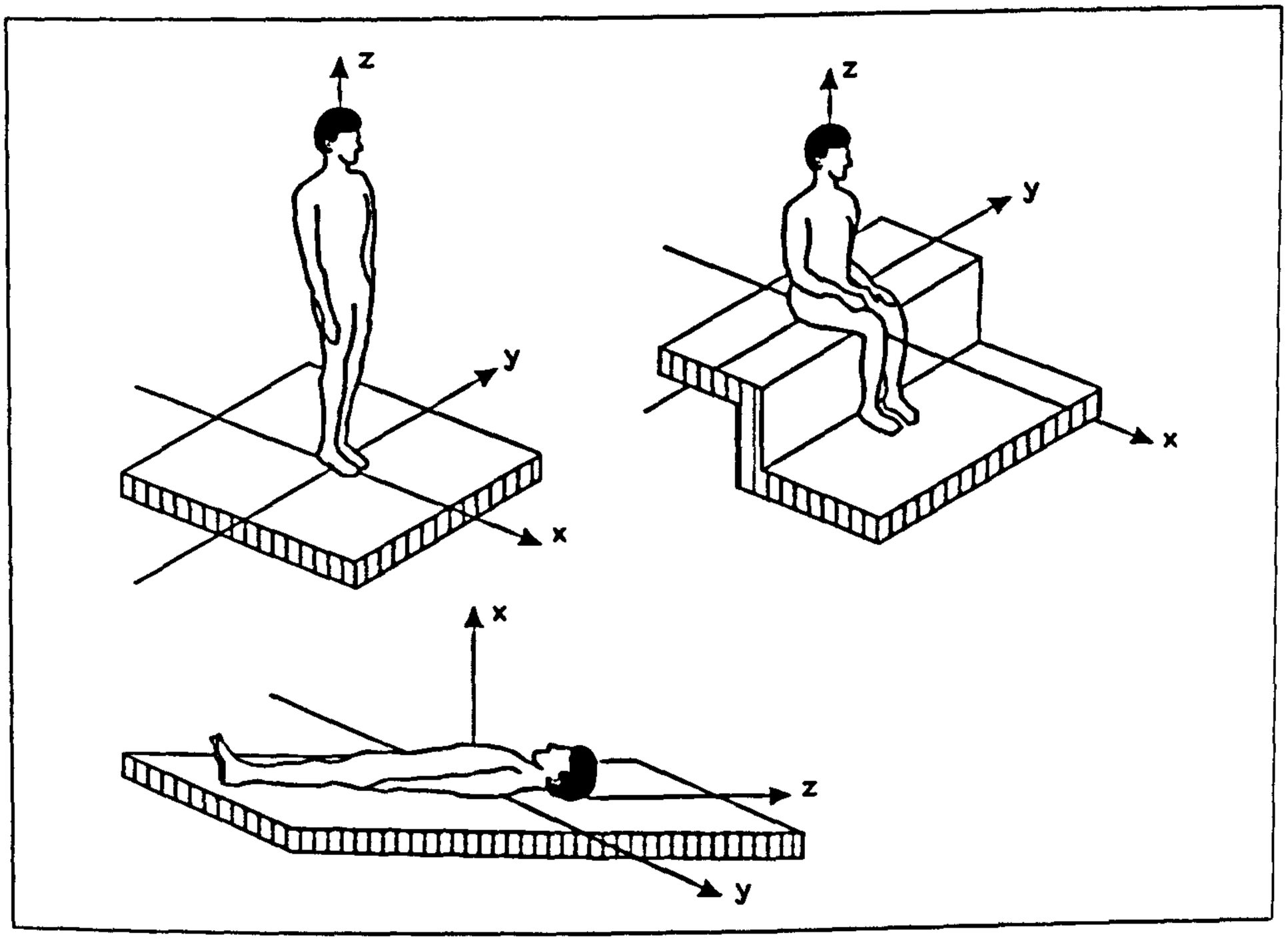

Figure 2.12: Body postures and standardised co-ordinate systems for assessing vibrations (after BSI, 1992).

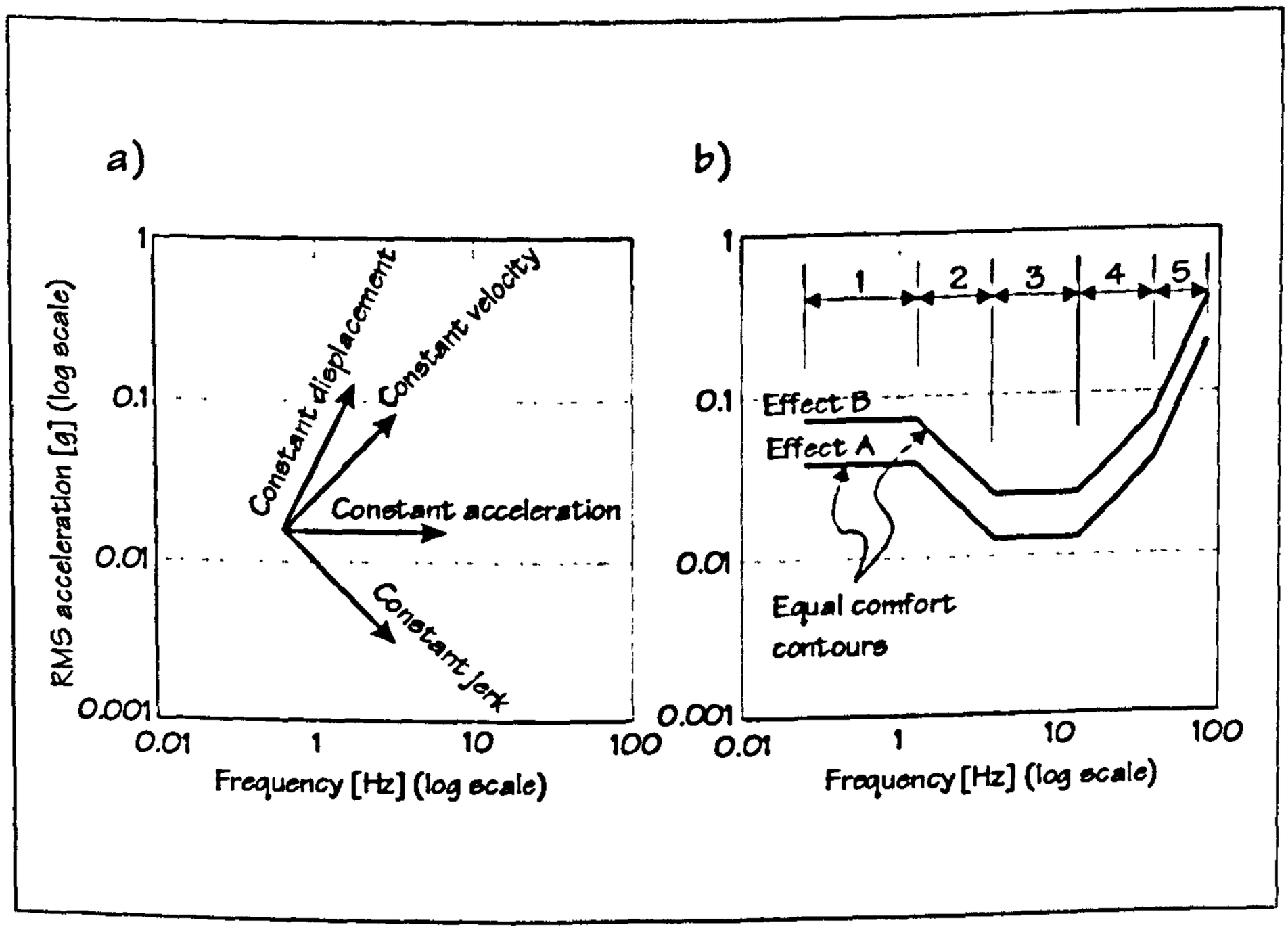

Figure 2.13: The equal contour curves (after Griffin, 1996).

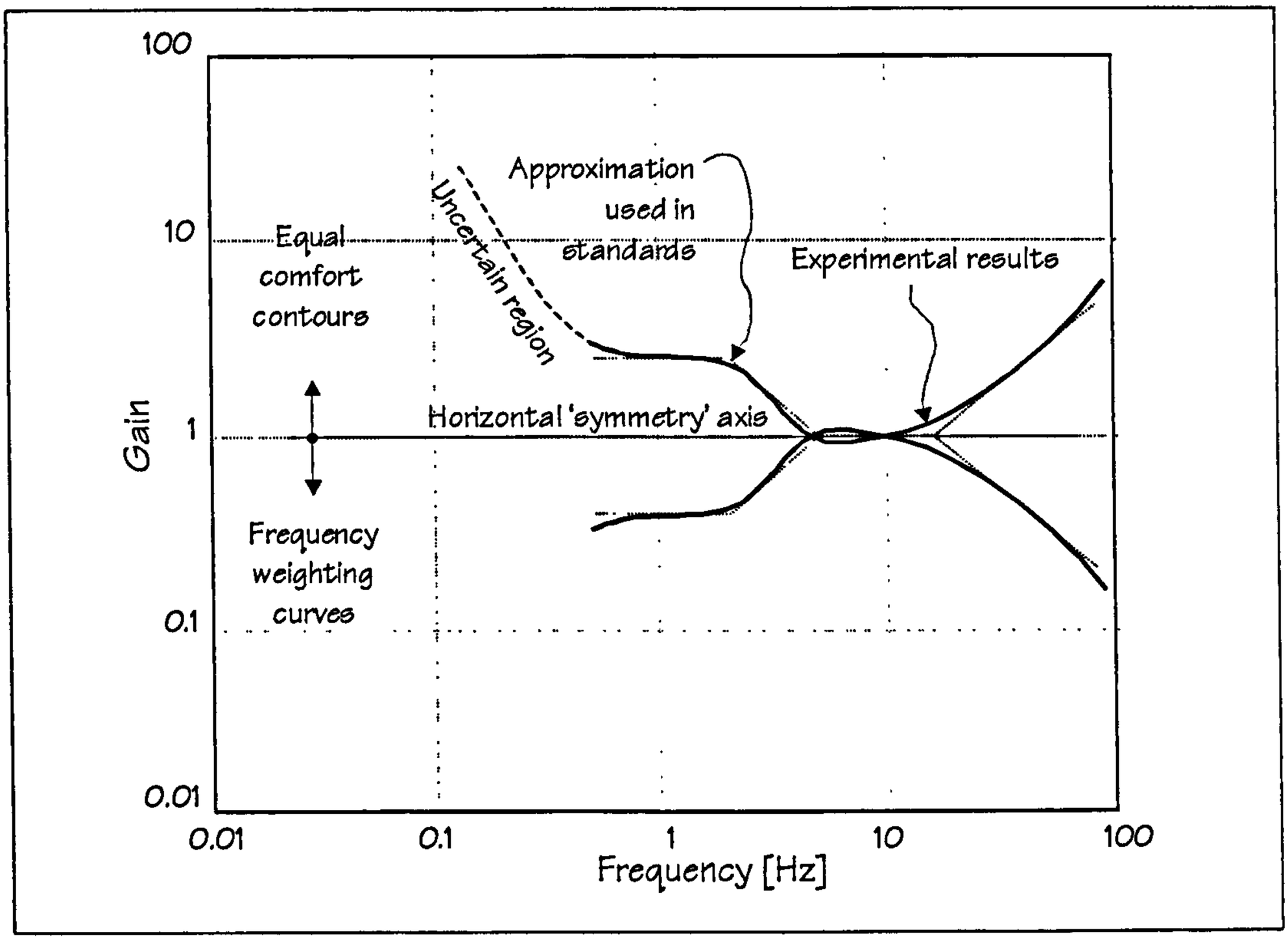

Figure 2.14: Relationship between equal comfort contours and frequency weighting curves (after Griffin, 1996).

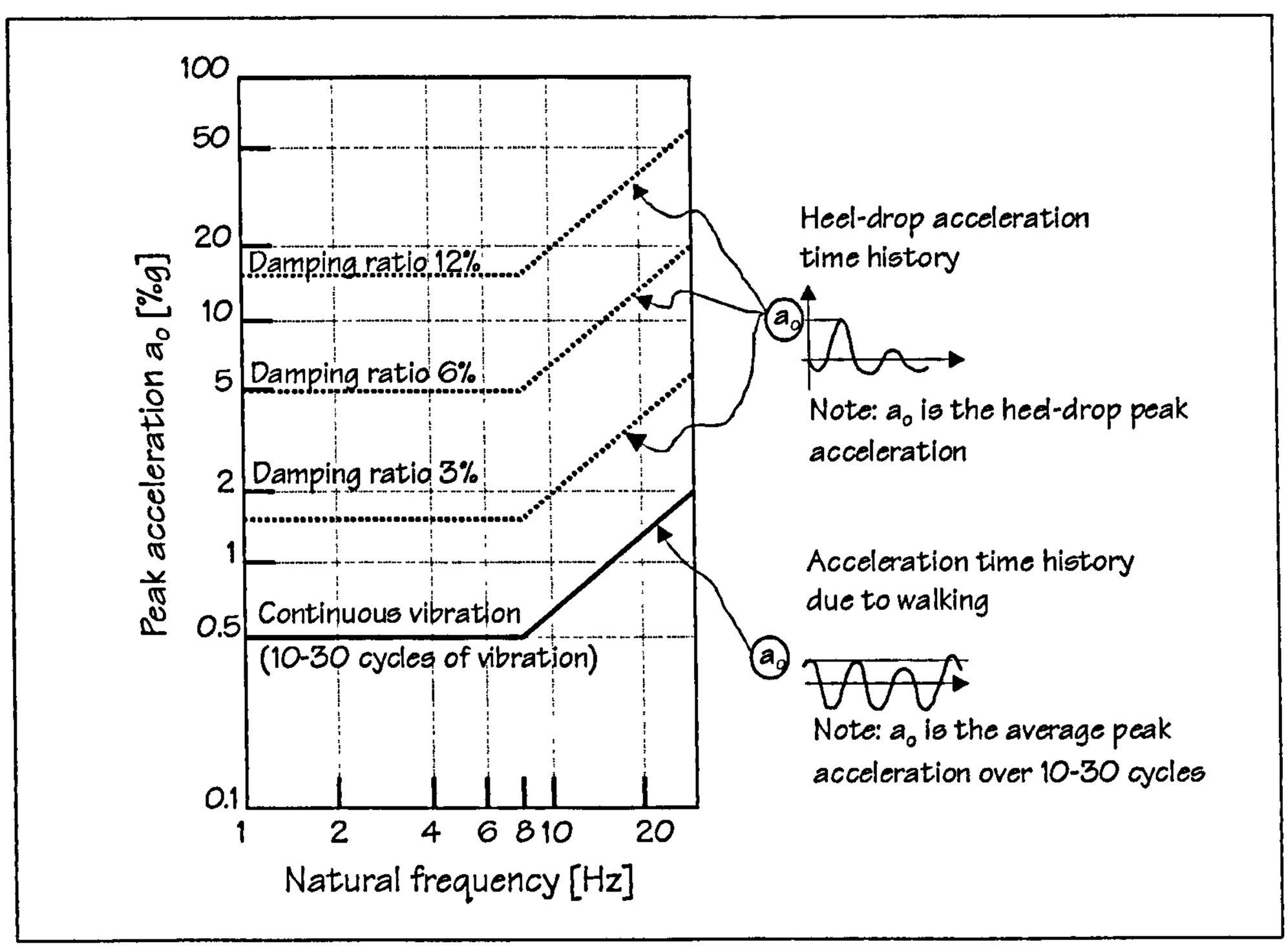

Figure 2.15: The CSA steel design criterion (after CSA, 1989).

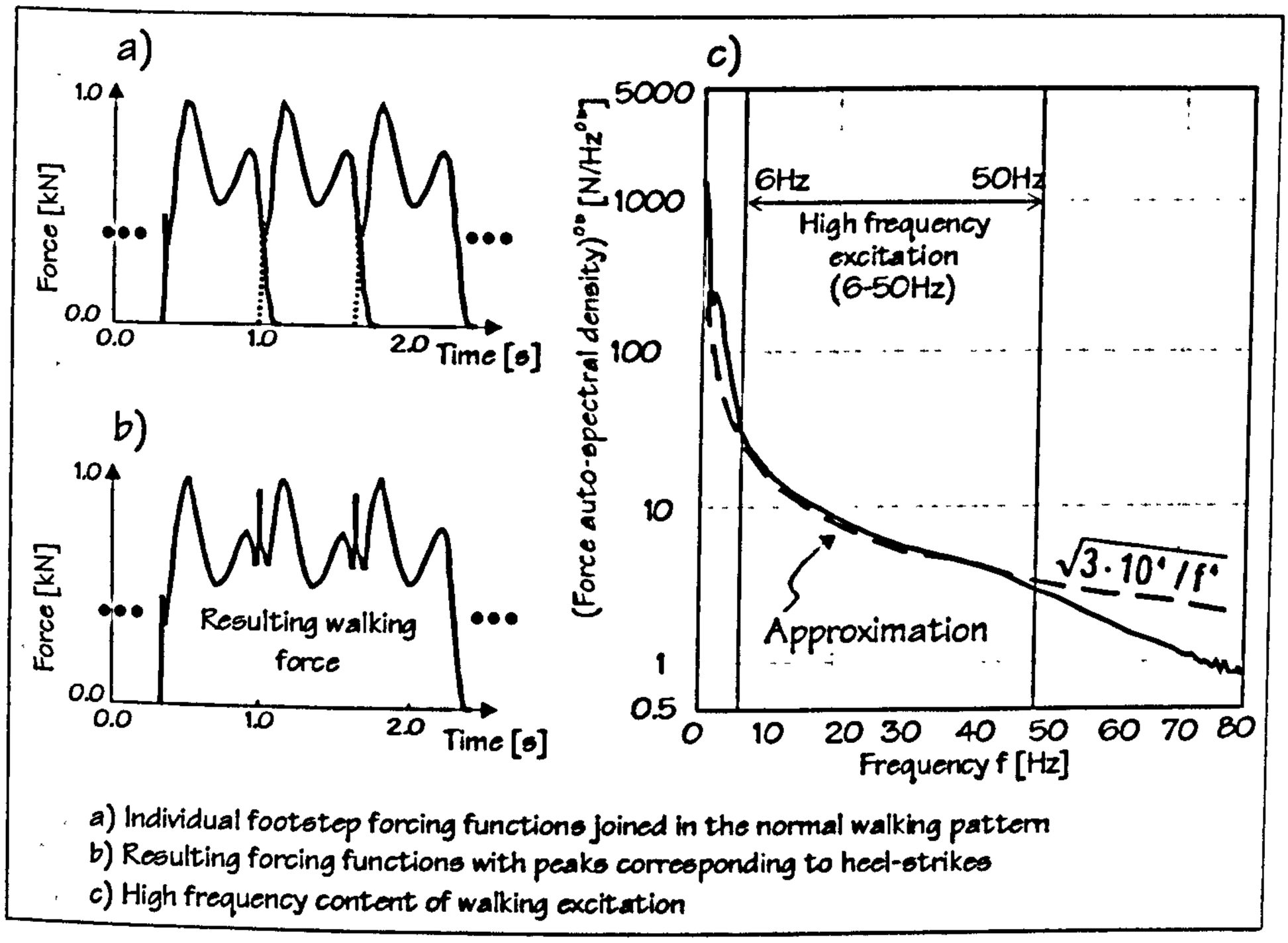

a) Individual footstep forcing functions joined in the normal walking pattern
b) Resulting forcing functions with peaks corresponding to heel-strikes
c) High frequency content of walking excitation

Figure 2.16: Approximation of high-frequency content of walking excitation (after Ohlsson, 1988a).

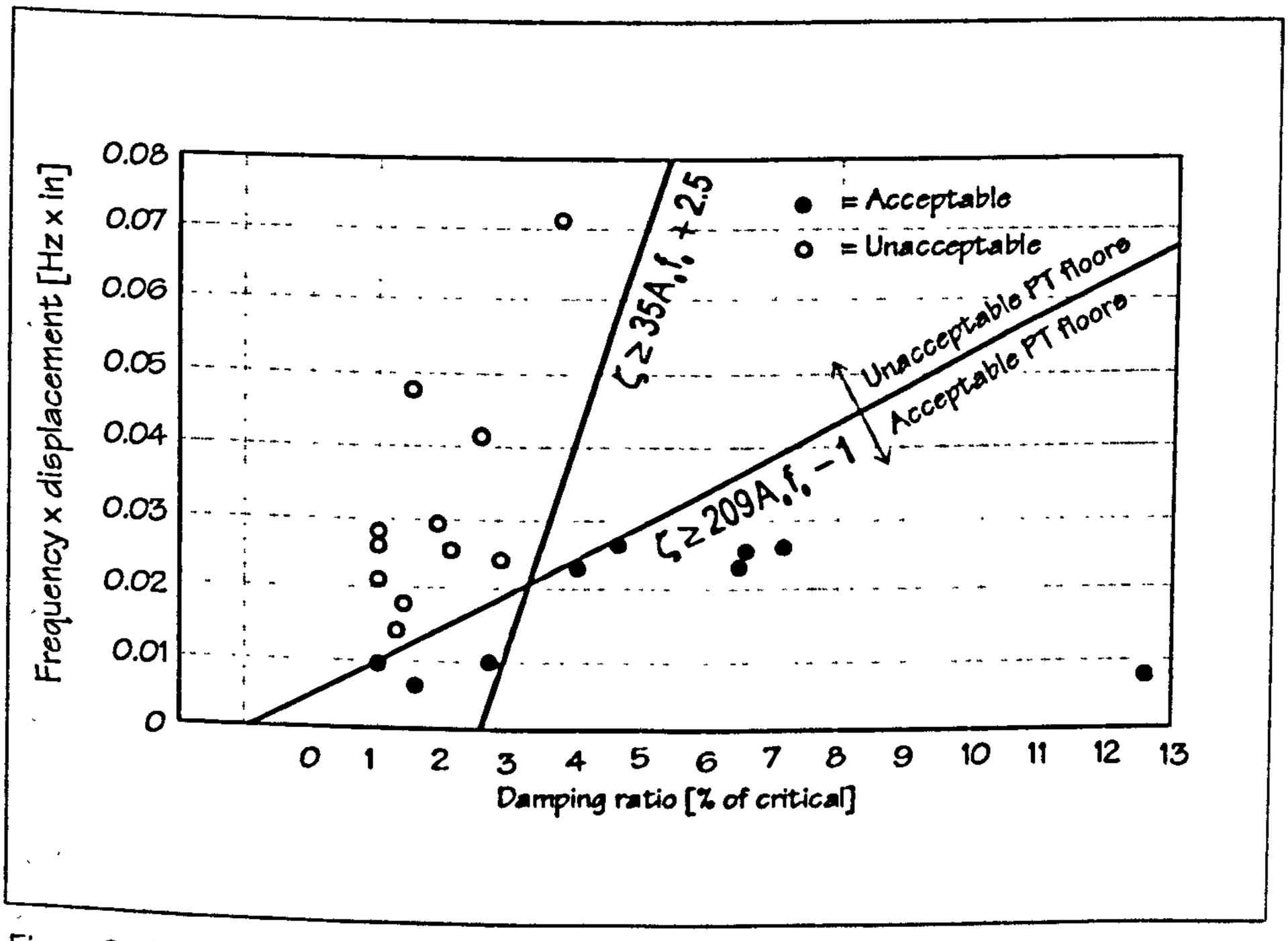

Figure 2.17: Zaman and Boswell's (1996b) proposal based on heel-drop excitation.

3 Analytical Modelling

3.1 Introduction

The main aim of structural analysis is prediction of the structural response to the applied actions. These response predictions are then used to design the structure so that it performs as required. Typically, the response predictions are based on the creation and solution of mathematical models. This is known as mathematical, or analytical, modelling. The aim of the modelling is to produce simulations of real behaviour which are sufficiently accurate but also as simple as possible (Meyer, 1987).

With regard to mathematical modelling in dynamics, a distinction between two groups of problems should firstly be made: wave propagation problems and structural dynamics problems (Cook et al., 1989). Having their lowest natural frequencies of vibration similar to the dominant frequencies of the prescribed excitation, the problem of floor vibration serviceability, as defined in this thesis, can be classified as the latter.

The process of mathematical modelling starts with making certain assumptions. Typically, in civil engineering these assumptions are based on previous experience and intuitive understanding of the expected physical behaviour which is to be modelled. When there is a lack of such knowledge, structural prototype testing is a recommended way forward. Meyer (1987) gave an excellent overview of the role of prototype testing in mathematical modelling, especially when FE modelling is used. This philosophy has been used to develop the link between the experiments and modelling in this research project.

The principles and methods of general structural dynamic analysis are described in detail in many excellent classical textbooks, such as those written by Clough and Penzien (1993) and Meirovitch (1986), and will not be repeated here in great detail. In particular, the FE method, one of the most popular numerical methods for structural dynamic analysis, is nowadays based on a broad scientific consensus. As a consequence, this is a mature technology implemented in much commercially available analysis software. However, it is interesting to note that the practical application of dynamic FE modelling, aimed at predicting dynamic behaviour of real-life structures, is considered as both science and art (Craig, 1981; Meyer, 1987; Clough & Penzien, 1993). This is because the quality of the solution, which is not unique, frequently depends not only on the pure theoretical background but also on the skill, experience and 'feel' of the modeller. Meyer (1987), nevertheless, notes that:

> "The art of modelling has been undervalued [in the research community] as it is often considered as an activity which does not offer anything new."

Partly because of this attitude, the problem of floor vibration serviceability assessment through detailed dynamic response calculations using FE analysis is currently "not carried out routinely" due to a "number of

uncertainties", as observed by Rainer et al. (1995). This is compounded by the fact that dynamic analysis using FE has many options, the selection of which depends on the type of problem in hand (NAFEMS, 1992b). The identified problems in modelling the floor boundary conditions, mass and stiffness distribution and by walking induced excitation make the selection of an appropriate dynamic analysis option difficult.

Therefore, the aim of this chapter is to outline the main FE modelling assumptions and analysis procedures deemed to be appropriate for carrying out dynamic analyses of in-situ cast concrete floors when checking their vibration serviceability.

3.2 Fundamentals

Mass, damping and stiffness are the key dynamic properties of any real structure which are, by their very nature, distributed. The description of the dynamic behaviour of such a system is difficult as it requires knowledge of the movement of an infinite number of points on the structure.

Nevertheless, by suitably discretising a distributed system into elements of a finite size (finite elements), which are connected at a limited number of points (nodes) the problem can be simplified considerably. The focus of the analysis is now reduced to a consideration of the movement of a finite number of nodal points in the direction of the prescribed DOFs at each node.

3.2.1 Equations of Motion

During the discretisation, mass, damping and stiffness properties are lumped at each of N pre-selected DOFs. The problem of complex analysis of a distributed parameter system is now simplified to the analysis of a lumped parameter MDOF system. By carefully selecting the location of nodal points and DOFs which are of interest, the movement of the whole structure can be defined in sufficient detail at each instant of time by a displacement vector $\{x(t)\}$. The elements of $\{x(t)\}$ are unknown functions $x_i(t)$ (i=1,...,N) describing the movement of each DOF as a function of time.

The limiting MDOF case is a SDOF system where only one DOF is considered to be sufficient to describe the movement of the whole distributed system. Ewins (1995), however, maintains that "...very few practical structures could realistically be modelled by a SDOF system". In addition, the literature review in Chapter 2 clearly demonstrated that this modelling practice in the case of cast in-situ concrete floors is likely to be unsuitable due to the appearance of closely spaced modes of vibration and difficulties in lumping mass, stiffness and damping properties to a single DOF.

After applying the prescribed time-varying loads $\{f(t)\}$, as well as the equilibrium, compatibility and stress-strain conditions (NAFEMS, 1992a) to all DOFs, the following well known matrix equation can be obtained:

$$[M]\{\ddot{x}(t)\}+[C]\{\dot{x}(t)\}+[K]\{x(t)\}=\{f(t)\} \qquad \text{Equation 3.1}$$

The vector $\{x(t)\}$ is the unknown in this matrix equation. Various methods for the development of this matrix equation, fundamental in the dynamic analysis of damped MDOF systems, are given elsewhere (Clough & Penzien, 1993; Cook et al., 1989; Petyt, 1990). The FE method implemented through commercially available FE codes is, however, the most common (NAFEMS, 1992b). The key assumptions made in the development of this matrix equation are that a linear time invariant dynamic system is being analysed. This leads to mass $[M]$, damping $[C]$ and stiffness $[K]$ matrices being time independent. The superposition principle and Maxwell's reciprocity theorem, therefore, apply. These assumptions are justifiable in the case of heavy concrete floors under low level human induced excitation where stress levels are minute (Wyatt, 1989; Eriksson, 1994).

Matrix equation 3.1 can be understood as a statement that equilibrium of inertial $\{f_I(t)\}$, damping $\{f_D(t)\}$, elastic (or stiffness, or restoring) forces $\{f_E(t)\}$ and external forces $\{f(t)\}$, acting in the direction of each DOF, is satisfied at each instant of time t (NAFEMS, 1992b; Bathe, 1996):

$$\{f_I(t)\}+\{f_D(t)\}+\{f_E(t)\}=\{f(t)\} \qquad \text{Equation 3.2}$$

where

$$\{f_I(t)\}=[M]\{\ddot{x}(t)\} \qquad \text{Equation 3.3}$$

$$\{f_D(t)\}=[C]\{\dot{x}(t)\} \qquad \text{Equation 3.4}$$

$$\{f_E(t)\}=[K]\{x(t)\}. \qquad \text{Equation 3.5}$$

For N DOFs, matrix equation 3.1 comprises N second order ordinary linear differential equations, known as the equations of motion. Normally, these are coupled which means that at least one unknown displacement function from vector $\{x(t)\}$ and/or its derivatives feature in more than one differential equation. Whereas the formulation of mass and stiffness matrices $[M]$ and $[K]$ is based on the summation of physical properties of the individual discretised elements, the damping matrix $[C]$ cannot be formulated in the same way. Nevertheless, in the case of a wide range of civil engineering structures, including floors, it is convenient to assume that the damping is viscous meaning that the damping force vector $\{f_D(t)\}$ is directly proportional to the velocity vector $\{\dot{x}(t)\}$ (Equation 3.4). As will shortly be seen, this almost certainly does not represent the actual damping mechanism which physically dissipates vibration energy from the real floor structural system. However, it is a good modelling approximation and is very useful from a mathematical point of view as it simplifies the solution of the equations of motion.

3.2.2 Solution of Equations of Motion

Vast efforts were made in the past devising methods to solve equations of motion formulated by the FE method. Generally speaking, the existing methods can be divided into two groups: (1) mode superposition (or modal solution), and (2) direct (or step-by-step) time integration methods.

Of greatest interest in this investigation is the linear dynamic response of floors engaging only a limited number of the lowest modes of vibration. In addition, relatively long excitation and response time histories, lasting typically more than 50 periods of the lowest mode of vibration, will have to be produced. Considering these two requirements and NAFEMS (1992b) recommendations, mode superposition has been selected as the principal and more efficient solution method.

3.2.2.1 MODE SUPERPOSITION SOLUTION

Without going into the details of the development of the mode superposition method, only the key ideas, terminology and formulas, used extensively in the thesis, will be introduced here. Much more detailed accounts of these aspects are given elsewhere (Clough & Penzien, 1993; Meirovitch, 1980). The notation used follows as closely as possible the one adopted by the DTA (Ewins, 1995).

The mode superposition solution for the unknown vector $\{x(t)\}$ in Equation 3.4 can be assumed as:

$$\{x(t)\} = [\Psi]\{q(t)\} \qquad \text{Equation 3.6}$$

where: $[\Psi]$ is a modal matrix and $\{q(t)\}$ is termed a generalised coordinate vector. In general, for a discrete system with N DOFs, the modal matrix $[\Psi]$ is comprised of N eigen vectors $\{\psi\}_r$ (r=1,...,N). Each of these, paired with one of up to N distinct eigenvalues ω_r^2, is a solution of the following undamped eigenvalue problem:

$$[[K]-\omega^2[M]]\{\bar{X}\} = \{0\} \qquad \text{Equation 3.7}$$

where $\{\bar{X}\}$ is a vector of unknown time-independent displacement amplitudes. Hence:

$$[[K]-\omega_r^2[M]]\{\psi\}_r = \{0\} \qquad \text{Equation 3.8}$$

The time-independent modal vectors $\{\psi\}_r$ have orthogonality properties enabling the modal matrix $[\Psi]$ to 'diagonalise' matrices $[M]$ and $[K]$, as follows:

$$[\Psi]^T[M][\Psi] = [\,m_r\,] \qquad \text{Equation 3.9}$$

$$[\Psi]^T[K][\Psi] = [\,k_r\,] \qquad \text{Equation 3.10}$$

Being orthogonal, the modal vectors $\{\psi\}_r$ are linearly independent and form a basis in N-dimensional space. This means that any other N-dimensional vector from this space, such as the vector of unknown

displacements $\{x(t)\}$, can be expressed as a linear combination of time-independent modal vectors. This is the basis of an expansion theorem (Meirovitch, 1980), which can be stated as:

$$\{x(t)\} = \sum_{r=1}^{N} \{\psi\}_r q_r(t) \qquad \text{Equation 3.11}$$

Equation 3.11 is a coordinate transformation linking vectors $\{x(t)\}$ and $\{q(t)\}$, and is, in fact, just another way of representing Equation 3.6.

The main reason for introducing the above coordinate transformation is that it is able to de-couple the equations of motion. This is done by pre-multiplying Equation 3.1 by $[\Psi]^T$ and by replacing vectors of unknown displacements, velocities and accelerations by appropriate terms calculated from Equation 3.6. The result is the following set of differential equations:

$$[m_r]\{\ddot{q}_r(t)\} + [\Psi]^T[C][\Psi]\{\dot{q}_r(t)\} + [k_r]\{q_r(t)\} = [\Psi]^T\{f(t)\} \qquad \text{Equation 3.12}$$

In order to de-couple the equations fully, the matrix product $[\Psi]^T[C][\Psi]$ should be a diagonal matrix $[c_r]$ leading to N independent linear differential equations:

$$m_r\ddot{q}_r(t) + c_r\dot{q}_r(t) + k_r q_r(t) = P_r(t), \qquad \text{Equation 3.13}$$

where

$$P_r(t) = \sum_{j=1}^{N} \psi_{jr} f_j(t) \qquad \text{Equation 3.14}$$

is defined as a generalised load for mode r or, simply, the r^{th} modal force. Equation 3.13 corresponds to a SDOF system and, in the case of an undercritically-damped system, its solution can be represented as (Clough & Penzien, 1993):

$$q_r(t) = q_{r,transient}(t) + q_{r,forced}(t) \qquad \text{Equation 3.15}$$

where

$$q_{r,transient}(t) = e^{-\zeta_r\omega_r t}\left[q_r(0)\cos(\omega_{rd}t) + \left(\frac{\dot{q}_r(0) + q_r(0)\zeta_r\omega_r}{\omega_{rd}}\right)\sin(\omega_{rd}t)\right] \qquad \text{Equation 3.16}$$

and

$$q_{r,forced}(t) = \frac{1}{m_r\omega_{rd}}\int_0^t P_r(\tau)e^{-\zeta_r\omega_{rd}(t-\tau)}\sin(\omega_{rd}(t-\tau))d\tau \qquad \text{Equation 3.17}$$

In the case of homogeneous initial conditions when $q_r(0) = 0$ and $\dot{q}_r(0) = 0$, the transient response $q_{r,transient}(t)$ vanishes and the complete modal response $q_r(t)$ corresponds to the forced vibration response $q_{r,forced}(t)$. In the case of more complex modal forces $P_r(t)$, commercial FE packages usually solve Equation

3.13 numerically by direct integration which is much easier for a SDOF system than for an MDOF system (Equation 3.1).

When all N generalised coordinates $q_r(t)$ are known, the unknown displacement vector $\{x(t)\}$ can be obtained by the superposition of modal responses $q_r(t)$ using either Equation 3.6 or Equation 3.11.

3.2.2.2 De-Coupling of Equations of Motion

Obviously, the key condition for de-coupling and, therefore, for simplifying the original set of equations of motion is that the matrix product $[\Psi]^T[C][\Psi]$ is a diagonal matrix $[c_r]$. Typically, commercial FE packages allow this 'diagonalisation' of the matrix $[C]$ to be done in one of two ways: (1) explicitly, by specifying damping coefficients c_r (or ζ_r) directly for each mode of vibration in Equation 3.13, or (2) implicitly, by assuming that the damping matrix can be expressed as the following linear combination of mass and stiffness matrices:

$$[C] = \alpha[M] + \beta[K] \qquad \text{Equation 3.18}$$

where α and β are pre-determined constants. The former approach corresponds to a modal damping model, and the latter to a proportional damping model where

$$c_r = \alpha m_r + \beta k_r \qquad \text{Equation 3.19}$$

The name for the latter damping model comes from its assumed proportionality to mass and stiffness. This model is also known as the Rayleigh damping model.

3.2.3 Analysis Software Selection

Apart from being used in the calculation of the transient dynamic response in the time domain (Equation 3.1), the mode superposition techniques can also be used for frequency domain calculations which are often required in some methods for checking floor vibration serviceability. The mode superposition methods, employed for the frequency domain calculations using FE analysis, are described in detail by Petyt (1990).

Naturally, the commercially available FE package to be used in this investigation had to have mode superposition analysis options capable of performing both types of forced response analyses: transient time domain and harmonic frequency domain analyses. In addition, the software had to posses utilities, such as extensive graphical, pre- and post-processing capabilities, as recommended by NAFEMS (1992a; 1992b), in order to perform quality assured numerical modelling. Also, a very important and rather specific requirement was an easy link between the FE analysis and the software used in the experimental work, as outlined in Chapter 4. Having in mind all these requirements, as well as the financial constraints for this project, a decision was made to opt for the widely used ANSYS FE code.

3.3 FE Modelling of Concrete Floors

As previously stated, there is a lack of knowledge regarding the modelling of boundary conditions, and walking excitation when checking vibration serviceability of in-situ concrete floors. In the case of prestressed concrete floors, further attention is required regarding issues such as the effects of prestressing and cracks on the floor vibration performance. In addition to this, the modelling of damping could well be particularly problematic since it is not well understood, but may be of paramount importance in controlling floor response in resonant or near-resonant conditions, as is the case in low-frequency floors. Finally, the FE modelling of the floor's orthotropic behaviour requires careful consideration. Modelling assumptions having a bearing on these issues will be discussed in this section.

3.3.1 Selection of Finite Elements

For FE modelling of the floors investigated in this thesis, the following types of ANSYS finite elements (ANSYS, 1995c) were used:

- Linear elastic beam (or bar) elements denoted as BEAM4 and BEAM44 (Figure 3.1a). Both elements are uniaxial 3D elements with six degrees of freedom at each node. BEAM44 has a node offset capability which makes it suitable for modelling slab beams which are relatively narrow and deep. BEAM4 elements were mainly used for modelling the columns.
- SHELL63 (Figure 3.2), was the main type of ANSYS shell elements used. It is a 4-noded element with six degrees of freedom at each node allowing both bending and membrane action. SHELL63 elements were used in the modelling of wide and shallow beams, typical in post-tensioned floors (Figures 2.2 and 2.3). They were used for modelling both isotropic and orthotropic behaviour of the flat plates (Figure 2.4) and beam-and-slab floor systems (Figure 2.3). Having six degrees of freedom at each node, all beam and shell elements used are fully compatible and suitable for analysis of 3D structures.

Spring damper (COMBIN14) and lumped mass (MASS21) elements were also used as additional elements in various parametric investigations. Whilst MASS21 (Figure 3.1c) is a single node element with all six degrees of freedom, COMBIN14 is a 2-node element which may have stiffness corresponding to either three translations (linear spring) or three rotations (rotational spring) at each node, depending on the option selected

A more detailed description of all elements is given in the ANSYS User's Manual (ANSYS, 1995c) and will not be repeated here.

3.3.2 Modelling of Stiffness

Resolution of some of the uncertainties in the modelling of in-situ cast columns and walls, and of orthotropic properties of floors with wide and shallow beams is one of the objectives of this work. However, modelling of the effects of prestressing in concrete elements, including floors, seems to be another issue where a number of authors have expressed different opinions.

3.3.2.1 Geometric Stiffness and Effects of Prestressing

Some authors, such as Maguire (1984) and Eriksson (1994), maintain that prestressing, as a compressive axial load, has the ability to reduce natural frequencies. This is because of the second order effects which reduce the elastic stiffness and which, ultimately, can cause buckling (Figure 3.3a). Indeed, Clough and Penzien (1993), for example, showed that compressive axial force reduces the elastic stiffness $[K]$ of a structural system via the so called geometric stiffness matrix $[K]_G$, as shown in the following equation:

$$[M]\{\ddot{x}(t)\}+[C]\{\dot{x}(t)\}+([K]-[K]_G)\{x(t)\}=\{f(t)\} \qquad \text{Equation 3.20}$$

The resulting reduced stiffness is called the effective stiffness $[K]_E$:

$$[K]_E=[K]-[K]_G \qquad \text{Equation 3.21}$$

However, it is important to note here that this phenomenon cannot be a result of axial forces from internal prestressing. Internally prestressed structures, including floors, where the prestressing tendons have an intimate contact with the surrounding concrete cannot buckle as the tendon profile follows faithfully the deformed shape of the prestressed element (Figure 3.3b). Therefore, no additional eccentricity can be created due to the deformation, that is - there are no second order effects. This is a specific property of internally prestressed concrete elements well documented in the classical work of Leonhardt (1962), and confirmed by Hurst (1988), and Khan and Williams (1995).

Therefore, the writer concluded that the second order effects due to prestressing should not be taken into account when analysing dynamic properties of internally prestressed concrete floors.

3.3.2.2 Modulus of Elasticity for Concrete in Dynamic Calculations

The dynamic modulus of elasticity of concrete $E_{c,dyn}$ is a traditionally uncertain parameter in dynamic FE analysis. Some attempts to quantify it will be outlined here.

Maguire (1984) compiled information from five sources to determine $E_{c,dyn}$ for a concrete having a compressive strength of 35.8 MPa. The values obtained varied between 36.5 GPa and 39.2 GPa. The selected value for FE modelling was $E_{c,dyn}=38\text{GPa}$. It is interesting to note that Wyatt (1989) independently recommends the same value for a normal weight concrete when checking the vibration serviceability of composite steel-concrete floors. Other proposals for the dynamic modulus of elasticity, found in the literature

pertinent to the dynamic performance of floors, typically recommend the increase of the static modulus by 10-25% (Bachmann & Amman, 1987; Eriksson, 1994; Amman & Nussbaumer, 1991; Maguire, 1995).

A draft of the Lloyd's Register structural assessment guidelines (Maguire, 1995) contains a very practical discussion as to the values of Young's modulus of elasticity to be used in dynamic calculations. Firstly, it was observed that $E_{c,dyn}$ depends on the stress-strain regime under short term loading such as wind or traffic. Having this in mind, it was pointed out that the dynamic modulus obtained from dynamic testing of full-scale structures seems to be more appropriate than the modulus obtained from static testing (inappropriate strain rate) or from ultrasonic pulse velocity testing (inappropriate strain level). However, it has been noted that experimental data from full-scale testing are scarce. Therefore, $E_{c,dyn}$ will be treated as an uncertain modelling parameter and an attempt will be made to determine it more reliably through a comprehensive full-scale testing programme which has been scheduled to accompany all FE modelling exercises in this investigation.

3.3.2.3 Upper and Lower Bound Analyses

The modelling of the cracks in concrete slabs is another aspect where no firm guidelines exist. Meyer and Will (1987) suggested that gross concrete cross sections should be assumed in the FE models of both classically reinforced and prestressed concrete structures. However, cracks, if they occur, may reduce the floor stiffness considerably (Grace & Kennedy, 1990). Therefore, the writer concluded that it is prudent not to neglect the possibility for cracking, especially in the case of classically reinforced floors.

Dynamic modulus of elasticity and cracking, together with the boundary conditions, are examples of uncertain paramcters which may have significant effect on the floor's stiffness. Recognising the problem, it has been suggested to adopt both upper and lower bound stiffnesses in FE dynamic analyses (Meyer & Will, 1987; NAFEMS, 1992a; Spence & Kenchington, 1993). Meyer and Will justified this by saying:

> "Even though bounding of the stiffness does not guarantee bounds on the response, the resulting ranges of expected upper and lower bound response values are likely to be more meaningful than single values."

3.3.3 Modelling of Mass

When modelling the mass of a relatively heavy and rigid item placed or attached to the floor (e.g. machinery), manual lumping using a point mass finite element, such as MASS21 in ANSYS, is recommended. However, a mass originating from the self weight of flexible structures, such as concrete slabs, should be modelled as distributed through the finite elements used to represent the elements with such homogeneously distributed mass (Ridlon & Meyer, 1987). This is done by assigning mass to each finite element, usually through its material density. The density parameter can be varied to accommodate, if

appropriate, the relatively small (non-structural) and distributed mass of the imposed load (NAFEMS, 1992a).

When checking the vibration serviceability of concrete floors caution is necessary in specifying the mass corresponding to such imposed (live) gravity load. This is because, in general, two types of dynamic FE analyses may be performed:

- FE analysis at the design stage when no real-life structure exists. In this case only 10-25% of the assumed imposed gravity loads, as given in the design codes (Murray, 1975; Wyatt, 1989), should be converted into equivalent mass, and
- FE analyses aimed at simulating the measured dynamic behaviour of an existing floor structure. In this case the imposed loading which physically existed during the testing should be estimated as accurately as possible and converted into the equivalent mass in the FE model.

The finite element representation of mass can be either lumped or consistent. Theoretically speaking, both methods are suitable for vibration analysis of concrete floors. However, the consistent mass method tends to be more expensive and unnecessary when only the lowest modes of vibration are excited (NAFEMS, 1992a), as is the case of low-frequency floors under human-induced excitation. Therefore, the lumped mass model, where the mass is associated only to the translational degrees of freedom and where the mass matrix is diagonal, will be used whenever possible.

3.3.4 Damping Modelling

All real vibrating structures lose the kinetic and potential energies which are stored in them. Any method of dispersing vibration energy in a vibrating system is generically termed damping. In the case of low-frequency floors, damping has the potential to reduce significantly the resonant or near-resonant response due to walking excitation. On the other hand, in high-frequency floors, it increases the decay rate in the case of free-vibration response between subsequent footsteps. In both cases the effects of damping are beneficial and it is prudent to model it as accurately as possible.

Unfortunately, the actual physical phenomena and mechanisms which cause damping are not well understood (NAFEMS, 1992a; Spence & Kenchington, 1993). Damping tends to be a result of an engagement of several energy dissipating mechanisms within the structure, the individual contributions of which are extremely difficult to assess. Consequently, the modelling of damping is not as exact as the modelling of mass or stiffness. However, NAFEMS literature (NAFEMS, 1992a; NAFEMS, 1992b; Spence & Kenchington, 1993) provides excellent state-of-the-art guidelines on the treatment of damping when conducting a dynamic FE analysis. Only the most important aspects, often overlooked in the literature on vibration serviceability of floors, will be summarised here.

3.3.4.1 RESONANCE CONSIDERATIONS

Although an order of magnitude lower than the inertia and stiffness forces, the damping force tends to be important when a structure vibrates at resonance. This is because at resonance the inertia forces $\{f_I(t)\}$ cancel stiffness forces $\{f_E(t)\}$ and the only force which remains to oppose the external excitation $\{f(t)\}$ is the damping force $\{f_D(t)\}$ (see Equation 3.2), as discussed in more detail by NAFEMS (1992b). At near-resonance conditions, this is approximately satisfied. However, it is to be expected that the importance of the damping force diminishes, in comparison to the stiffness and inertia forces, as the response becomes more non-resonant.

3.3.4.2 PHYSICAL SOURCES OF DAMPING

When considering damping, a clear distinction should be made between sources to which damping can physically be attributed, and the mathematical models used to simulate them.

Large structures, such as floors, lose vibration energy in two principal ways: (1) through 'dissipation' within the boundaries of the structure, and (2) through 'dispersion' of vibration energy which is propagated away from the structure (Ungar, 1988). Wyatt (1989) calls the second type of damping "lateral dispersion" whereas Ohlsson (1988b) uses the term "geometrical damping".

As every floor is uniquely connected to the rest of the structure, the 'dispersion' part of damping is dependent upon the precise form of this connection and cannot be generalised easily. More general and useful for future designs is knowledge of energy-dissipation damping (Ohlsson, 1988b), uncoupled from the 'dispersion' part. Unfortunately, one of the most difficult problems related to gaining such knowledge is the measurement of energy 'dissipation' only. Any practically achievable damping measurement on a real floor structure, which is a part of a larger building, will measure damping as a compound effect of 'dispersion' and 'dissipation' with no practical means of distinguishing between them, as noted by Ungar (1988). Such damping, Ungar called the "effective damping".

In the case of floors, 'dissipation' loss can be attributed to two causes: loss in the body of the material and loss at discontinuities and connections. According to Spence and Kenchington (1993), the word "structural damping" is used to describe the combined effects of these 'dissipation' losses because, again, it is difficult to separate them. Interface friction and mechanical hysteresis are typical examples of structural damping defined in this way. However, older literature (Maguire, 1984) considers structural damping as representing only the loss at connections. From the above examples, it is obvious that there is trend towards proliferation of terminology in structural dynamics (NAFEMS, 1992a). This trend is particularly problematic in the case of damping where numerous different prefixes to the word 'damping' are used in an inconsistent way.

3.3.4.3 ANALYTICAL MODELS OF DAMPING IN THE MODE SUPERPOSITION METHOD

Generally speaking, analytical models of damping used in the mode superposition method tend not to represent the exact physical source of vibration energy loss. Instead, they are mathematically convenient representations of damping as a global structural property. The already introduced modal and proportional (or Rayleigh) damping approaches represent the two most commonly used models suitable for dynamic FE analysis of floors. Of these two, the former has more physical meaning than the latter as it can be measured by experimental modal testing. In addition, the vast majority of experimentally measured floor damping values were (meant to be) modal damping. Furthermore, the anticipated outcome of the full-scale modal testing of floors in this research are the modal damping values estimated from MDOF parameter estimation procedures (Spence & Kenchington, 1993) for each experimentally identified mode. Therefore, it is prudent to adopt FE models having damping based on the modal damping ratios, as such models are able to simulate directly the measured floor dynamic behaviour.

3.3.5 Floor Excitation Modelling

As specified in Chapters 1 and 2, a single person walking is the governing loading case (when checking the vibration serviceability of relatively quiet office floors) which is going to be examined in this thesis. If an FE analysis is used to predict the floor dynamic response, in order to fully utilise the power of the FE method and time invested in the development of the FE model, it is prudent to adopt walking excitation models which are as detailed and as realistic as possible.

In general, two such models exist: the time domain, and the frequency domain models (Mouring & Ellingwood, 1994). An excellent overview of these models is given by Eriksson (1994).

3.3.5.1 SINGLE PERSON WALKING EXCITATION: TIME DOMAIN MODELS

Time domain models are developed assuming that walking is a perfectly periodic activity which can be modelled as the sum of a number of discrete Fourier components. The frequency of a fundamental harmonic corresponds to the pacing rate whereas the frequencies of higher harmonics are integer multiples of the fundamental frequency. Recently, Bachmann et al. (1991b; 1995b) collated the somewhat varying data from the literature and proposed that the vertical load $F_p(t)$ due to a single person walking be expressed as:

$$\begin{aligned} F_p(t) = G &+ \alpha_1 G \sin(2\pi f_s t) \\ &+ \alpha_2 G \sin(4\pi f_s t - \varphi_2) \\ &+ \alpha_3 G \sin(6\pi f_s t - \varphi_3), \end{aligned} \qquad \text{Equation 3.22}$$

where G is the weight of the person (usually assumed to be between 700N and 800N), $\alpha_i G$ is the loading amplitude corresponding to the i^{th} harmonic ($i = 1, 2, 3$), f_s is the pacing rate (between 2.0 Hz and 2.4 Hz),

and φ_2 and φ_3 are the phase angles of the second and third harmonics. The amplitude coefficients and phase angles for the first and higher harmonics are given in Table 3.1.

Table 3.1: Amplitude coefficients and phase angles to be used in Equation 3.22.

Frequency	α_1	α_2	φ_2 [degrees]	α_3	φ_3 [degrees]
2.0 Hz	0.4	0.1	90	0.1	90
2.4 Hz	0.5	0.1	90	0.1	90

When using the values from Table 3.1 to calculate α_1, a linear interpolation between 0.4 and 0.5 is to be assumed. This corresponds to pacing rates between 2.0 Hz and 2.4 Hz. A large scatter exists in experimentally determined phase angles φ_2 and φ_3 (Bachmann & Ammann, 1987). In order to obtain an "upper bound solution", Rainer et al. (1995) suggest selecting a single harmonic from Equation 3.22 to excite the steady-state resonance of an applicable mode of floor vibration. Such calculated responses should then be compared with the applicable vibration assessment criteria. This procedure has been classified by Rainer et al. as "more advanced design rules".

Alternatively, the complete force $F_p(t)$, as defined in Equation 3.22, can be taken into account assuming that the fundamental or higher floor resonance is excited exactly by one of its harmonics. When using all harmonics it is interesting to note that Bachmann and Ammann (1987) suggested varying the phase angles φ_2 and φ_3 in order to obtain "the most unfavourable combination of the different harmonics". However, they failed to mention that this phase adjustment is meaningful only if a transient analysis is required. Phase angles do not affect the RMS response if a steady-state vibration is assumed in the vibration serviceability calculations. Some examples showing how the variations of φ_2 and φ_3 change $F_p(t)$ are given in Figure 3.4.

ISO 10137 (ISO, 1992) and Rainer et al. (1988b) propose different coefficients and applicable frequency ranges compared to those presented in Table 3.1. However, Rainer and Pernica (1986) also propose the 4th harmonic amplitude to be included in the calculations as and when necessary. The "dynamic load factor", that is the Fourier coefficient, recommended for the 4th harmonic is $\alpha_4 = 0.05$.

Willford (1997) adopted a similar calculation strategy, which assumes pure resonance conditions excited by one of the first three harmonics of walking. However, he suggested the lower bound of a normal pacing frequency to be reduced from 2.0 Hz to 1.2 Hz. Frequency ranges, corresponding to the higher harmonics, had to be adjusted accordingly, as shown in Table 3.2.

Table 3.2: Harmonic amplitudes proposed by Willford (1997).

Harmonic [i]	Frequency [Hz]	$\alpha_i G$ [N]
1	1.2 - 2.4	240
2	2.4 - 4.8	96
3	4.8 - 7.2	48

3.3.5.2 SINGLE PERSON WALKING EXCITATION: FREQUENCY DOMAIN MODELS

By considering walking as a perfectly periodic activity, an assumption is made that the excitation energy is concentrated only at discrete frequencies corresponding to the fundamental and a number of higher harmonics of walking. This is a deterministic model of the walking excitation.

However, by indirectly measuring the continuous excitation due to a single person walking, Eriksson (1994) showed that there is a spread of excitation energy around frequencies which nominally correspond to the pacing rate and its integer multiplies (Figure 3.5). Even when the pacing rate was strictly controlled by a metronome, a spread of energy occurred indicating that the walking excitation is a sort of narrow-band random phenomenon. In this case the walking force can be represented in terms of its auto-spectral density (ASD) denoted as $S_{ff}(\omega)$. This force ASD can be used to calculate the acceleration response ASD using the following well known equation (McConnell, 1995):

$$S_{aa}(\omega) = |A(\omega)|^2 S_{ff}(\omega) \qquad \text{Equation 3.23}$$

Introducing an acceleration auto-correlation function as:

$$R_{aa}(\tau) = \lim_{T\to\infty} \frac{1}{T} \int_{-T/2}^{+T/2} a(t)a(t+\tau)dt \qquad \text{Equation 3.24}$$

it is obvious that when $\tau = 0$:

$$R_{aa}(0) = \lim_{T\to\infty} \frac{1}{T} \int_{-T/2}^{+T/2} a^2(t)dt \qquad \text{Equation 3.25}$$

Clearly, $R_{aa}(0)$ is a mean square value of $a(t)$ averaged over a period T, that is:

$$R_{aa}(0) = a_{RMS}^2 \qquad \text{Equation 3.26}$$

On the other hand, using the Wiener-Khintchin transform pair (McConnell, 1995):

$$R_{aa}(\tau) = \frac{1}{2\pi} \int_{-\infty}^{+\infty} S_{aa}(\omega) e^{-i\omega\tau} d\omega \qquad \text{Equation 3.27}$$

$$S_{aa}(\omega) = \int_{-\infty}^{+\infty} R_{aa}(\tau) e^{i\omega\tau} d\tau \qquad \text{Equation 3.28}$$

and putting $\tau = 0$ in Equation 3.27 one obtains:

$$R_{aa}(0) = \frac{1}{2\pi} \int_{-\infty}^{+\infty} S_{aa}(\omega) d\omega \qquad \text{Equation 3.29}$$

Considering equations 3.23, 3.26 and 3.29, the RMS acceleration can be calculated as:

$$a_{RMS} = \sqrt{\frac{1}{2\pi}\int_{-\infty}^{+\infty}|A(\omega)|^2 S_{ff}(\omega)d\omega} \qquad \text{Equation 3.30}$$

Equation 3.30 is a means of taking into account the spread of excitation energy in $S_{ff}(\omega)$ around the pacing frequency $\omega_s = 2\pi f_s$ and its positive integer multiples (Figure 3.5) when calculating the RMS acceleration.

Eriksson (1994) introduced a number of simplifications in order to make the use of Equation 3.30 more user friendly. For the "one person walking" loading case, he cautiously suggested that the excitation power contained within the width of ASD peaks (Figure 3.5) could be modelled by an equivalent single harmonic force F_{RMS} assumed to excite pure resonance. The amplitude values of F_{RMS} are selected in such a way so that the steady-state resonant acceleration response due to F_{RMS} has the same RMS value as the response due to $S_{ff}(\omega)$. When doing this, the energy spread around only one peak (Figure 3.5) in $S_{ff}(\omega)$has been considered when estimating amplitudes of F_{RMS} as a function of frequency. These amplitudes are given in Table 3.3.

Table 3.3: Equivalent RMS force representing a single person walking (Eriksson, 1994).

Excitation frequency f interval [Hz]	F_{RMS} [N]
0-2.5	220
2.5-10.0	180(1/f)

Eriksson suggested that the harmonic force F_{RMS} should be tuned to excite the resonance of the "weakest mode" of the structure and should be treated as stationary, that is treading in place, preferably at an antinode of the appropriate mode shape. Eriksson neglected the possible effects of closely spaced modes of vibration noting that "...this effect is not assumed to be sufficiently common to be considered". This statement is quite questionable in the case of concrete floors where even Eriksson (1994) himself frequently reported close modes of vibration which were experimentally identified. In addition, experimental validation of this frequency domain walking model presented in his thesis is not conclusive as human subjects were not trying to excite spot-on resonances of the floors they were walking on. Clearly, there is a scope for such a validation to be performed in this research work.

3.3.5.3 SPEED OF WALKING

The above mentioned assumption, that the human induced loading due to walking does not move and is applied at the worst possible point, is very popular as it simplifies calculations and can commonly be found in literature. Bachmann and Ammann (1987) explain this stating:

> "The relatively slow forward speed has hardly any effect on the vertical excitation of the structure as investigations have confirmed. (...) If one were to consider the effect that the forward speed of a single walking or running person has on a forced vibration, the response would be transient with smaller amplitudes, since the steady state is not reached before the person leaves the structure".

It is important to note here that the references which were used by Bachmann and Ammann to support this view were related to footbridges and not to massive concrete floors. Nevertheless, modelling of a moving load due to walking is difficult, but is justifiable if an FE analysis is used. Smith (1988) described the application of a time varying force travelling with a constant speed across a continuos beam. The forward speed depends on the pacing frequency and the stride length and this complex relationship is given in Figure 3.6 (Bachmann & Ammann, 1987). These will be taken into account when modelling the moving excitation due to walking. With regard to this it is interesting to note that Wyatt (1989) maintains that the normal pacing rate is predominantly 1.6 Hz (and not 2.0 Hz) in offices.

Finally, it should be stressed that a similar frequency domain approach has been adopted by Mouring and Ellingwood (1994; 1996) when investigating the effects of crowd loading on busy floors, as found in shopping malls. The two authors, however, introduced a number of simplifications including the assumption that the floor responds in single mode only. Although the ABAQUS FE code was used in the investigation, no study was presented to justify this assumption. Models for walking excitation caused by groups of people, which were recently developed by Mouring and Ellingwood are, nevertheless, more appropriate for crowd loading and will not be used in this work.

3.4 FE Modelling Feasibility Studies

FE modal analysis aimed at calculating the undamped natural frequencies and mode shapes is the backbone of the mode superposition technique. A poor analytical modal model, which does not correspond to its measured counterpart, is almost certainly going to produce inaccurate response calculations. Such poor analytical results could well be a consequence of errors in modelling the mass and overall stiffness properties.

Therefore, two feasibility studies were carried out in order to gain experience in floor modelling and check the performance of ANSYS FE code when calculating the natural frequencies and mode shapes of concrete floors. The calculated results were validated against the experimental results obtained by Caverson (1992) from modal testing of two prototype floors. Structural details of these floors and results of these two feasibility studies were published at an early stage of this research (Pavic et al., 1994; 1995a; 1995b) and will not be repeated here. Only the main findings are stated below.

3.4.1 Wycombe Entertainment Centre Car Park (Pavic et al., 1994)

The first structure is an in-situ cast post-tensioned floor built in High Wycombe with a 210 mm thick slab forming a typical panel 12.05 m long and 7.3 m wide. Statically, it is a one-way acting system (of the kind

shown in Figure 2.3) between a series of parallel band beams which are 665 mm wide and 650 mm deep (inclusive of slab thickness). Both full-scale modal testing and FE modelling showed that the band beams provide considerably less restraint to a floor panel than is commonly assumed. It was somewhat surprising to see that the first mode of vibration was clearly bending the slab in the longer 12.05 m (along the band beams) , instead of the shorter 7.3 m direction (between the band beams). This clearly shows that one-way static load bearing action in the shorter direction is not happening in the fundamental mode of vibration. Khan and Williams (1995) reported this particular work and its conclusion in their recently published textbook on the design of PT floors.

In order to match the measured frequencies more closely, the wide and shallow band beams had to be modelled by SHELL63 instead of BEAM44 elements. The slab FE models utilising BEAM44 elements were considerably less stiff. Also, the non-structural facade wall 'supporting' the edge of the slab had to be modelled as a line support (by means of series of pin-supports), otherwise significant differences between the calculated and measured fundamental frequencies would have occurred. Interestingly, the slab edge and the wall were in reality only connected by means of a 'soft joint', typically used in the design of PT floors in order to allow floor movements without damaging the wall. Such a joint was not designed to bear any static loading, but it appears that it 'worked' as a support for low-level vibration excitation. Clearly, boundary conditions applicable to static analysis seem to be inappropriate for vibration serviceability analysis of this floor. Wyatt (1989) noted that similar behaviour should be expected in the case of composite steel-concrete floors.

The above conclusions were made by qualitatively comparing the first five measured and calculated frequencies and mode shapes corresponding only to a single bay. Unfortunately, the quality of Caverson's (1992) experimental data did not allow more detailed comparison of mode shapes and natural frequencies.

3.4.2 Trigonos Phase V Car Park, Swindon (Pavic et al., 1995a; 1995b)

The second prototype floor investigated was the top floor of a multi-storey car park in Swindon. The structure is not cast in-situ but comprises a series of precast pre-tensioned double-T concrete elements spanning 16.3m. These are simply supported by the main precast pre-tensioned inverted-T elements, which is normal practice in pre-cast construction.

This time, relatively narrow and deep double-T ribs were successfully modelled with BEAM44 elements whereas SHELL63 was used for the flange. Very reasonable results were obtained for the first six modes of vibration although the quality of experimental data again hampered a more detailed study. Lower values for dynamic modulus of elasticity were assumed for SHELL63 elements in order to accommodate less stiff RC topping and asphalt layers poured over the double-T flange. However, columns were modelled as pin-supports and this caused an apparent lack of stiffness in the FE model which was to some extent compensated for by using relatively large values of dynamic moduli of elasticity (42 GPa for SHELL63 and

49 GPa for BEAM44). With hindsight, a better balance between more realistic (i.e. stiff) boundary conditions and lower moduli of elasticity would have been preferable in this modelling exercise.

However, the main aim of both exercises was to help the writer to gain expertise in dynamic testing and confidence in applying the above proposed FE modelling guidelines. It appears that this aim has been achieved at least with regard to the basic undamped free vibration FE analysis of floors.

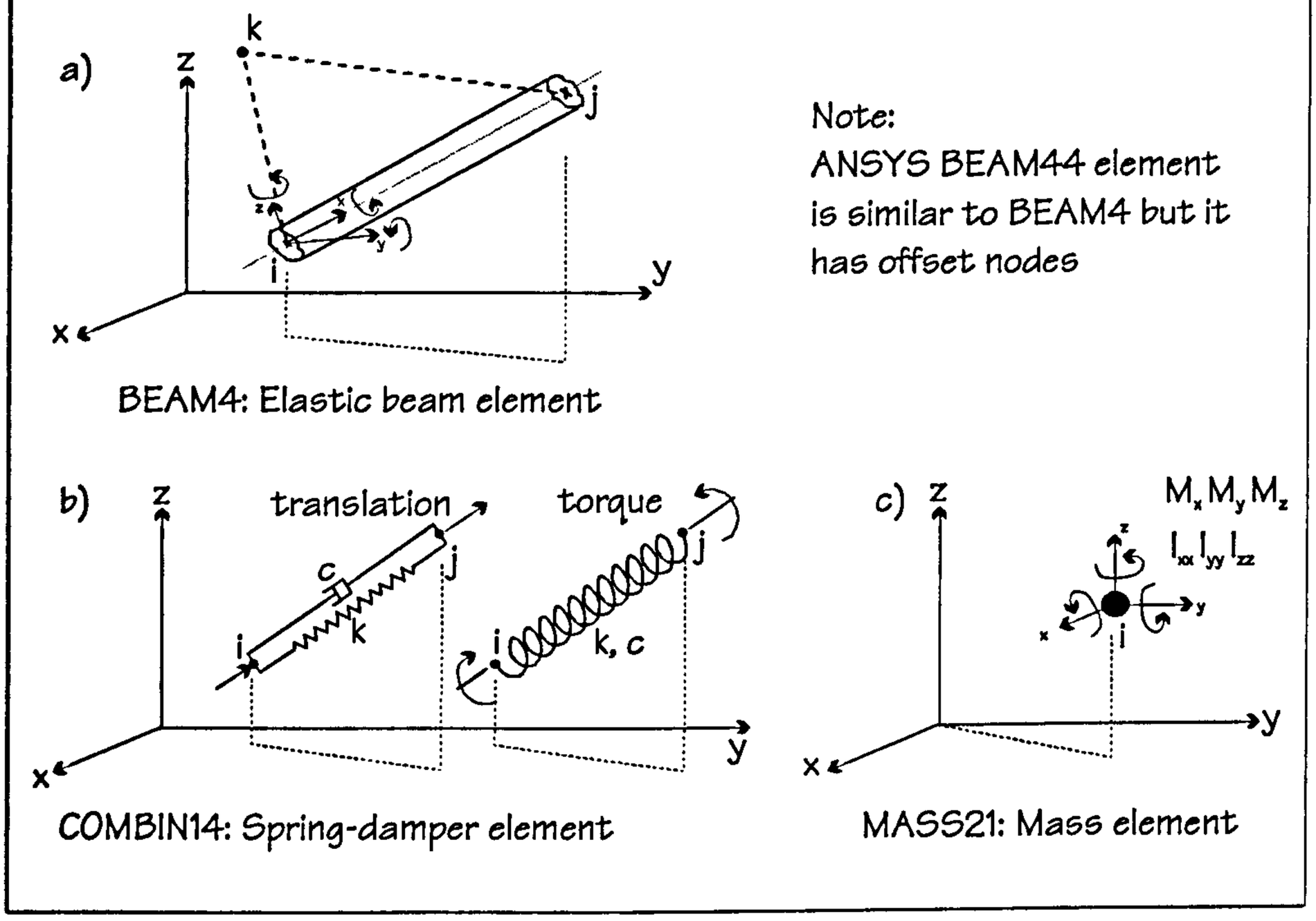

Figure 3.1: ANSYS beam, spring and mass elements (after ANSYS, 1995c).

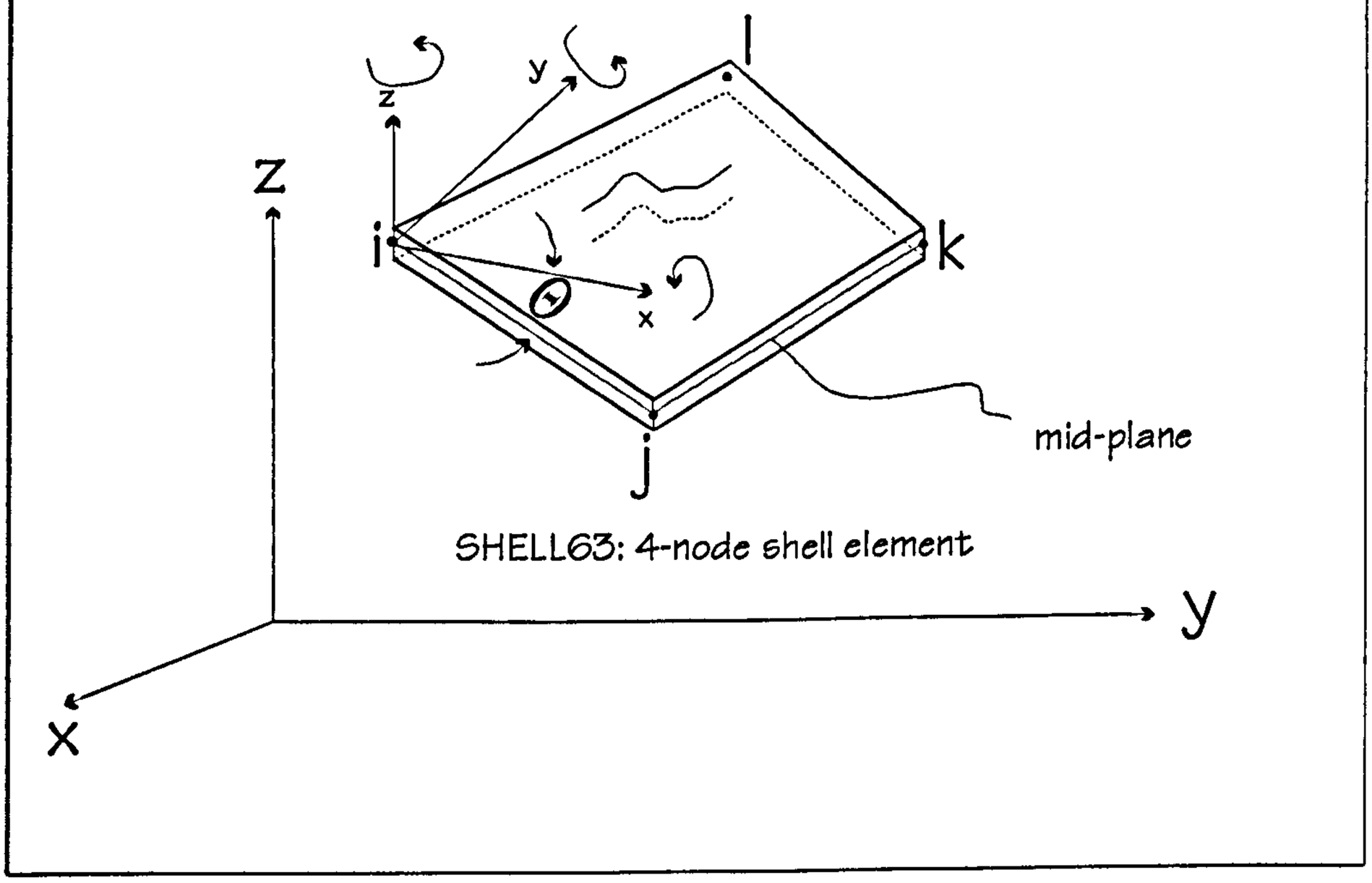

Figure 3.2: ANSYS shell element used (after ANSYS, 1995c).

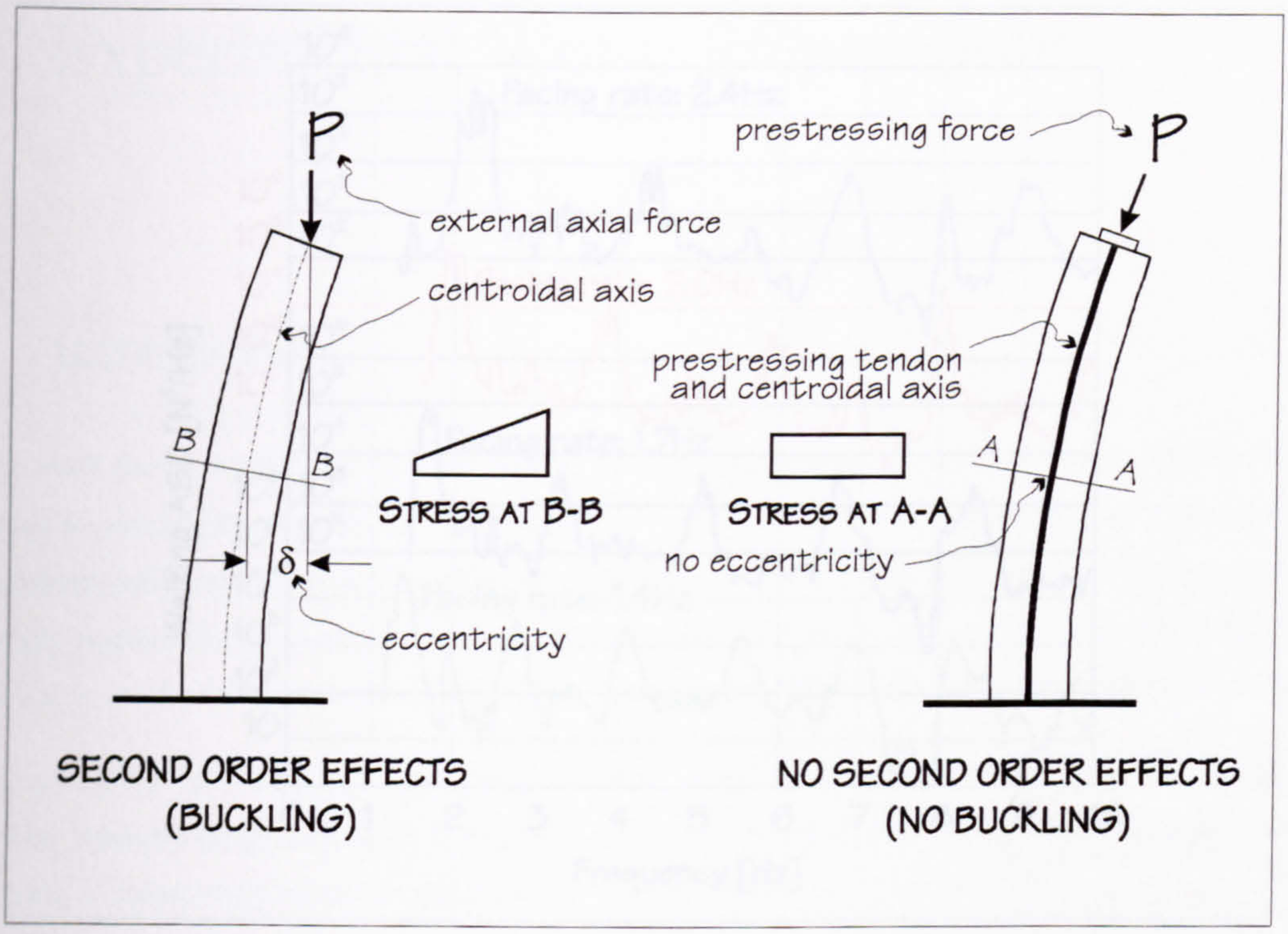

Figure 3.3: Axially loaded and internally prestressed concrete element (after Hurst, 1988).

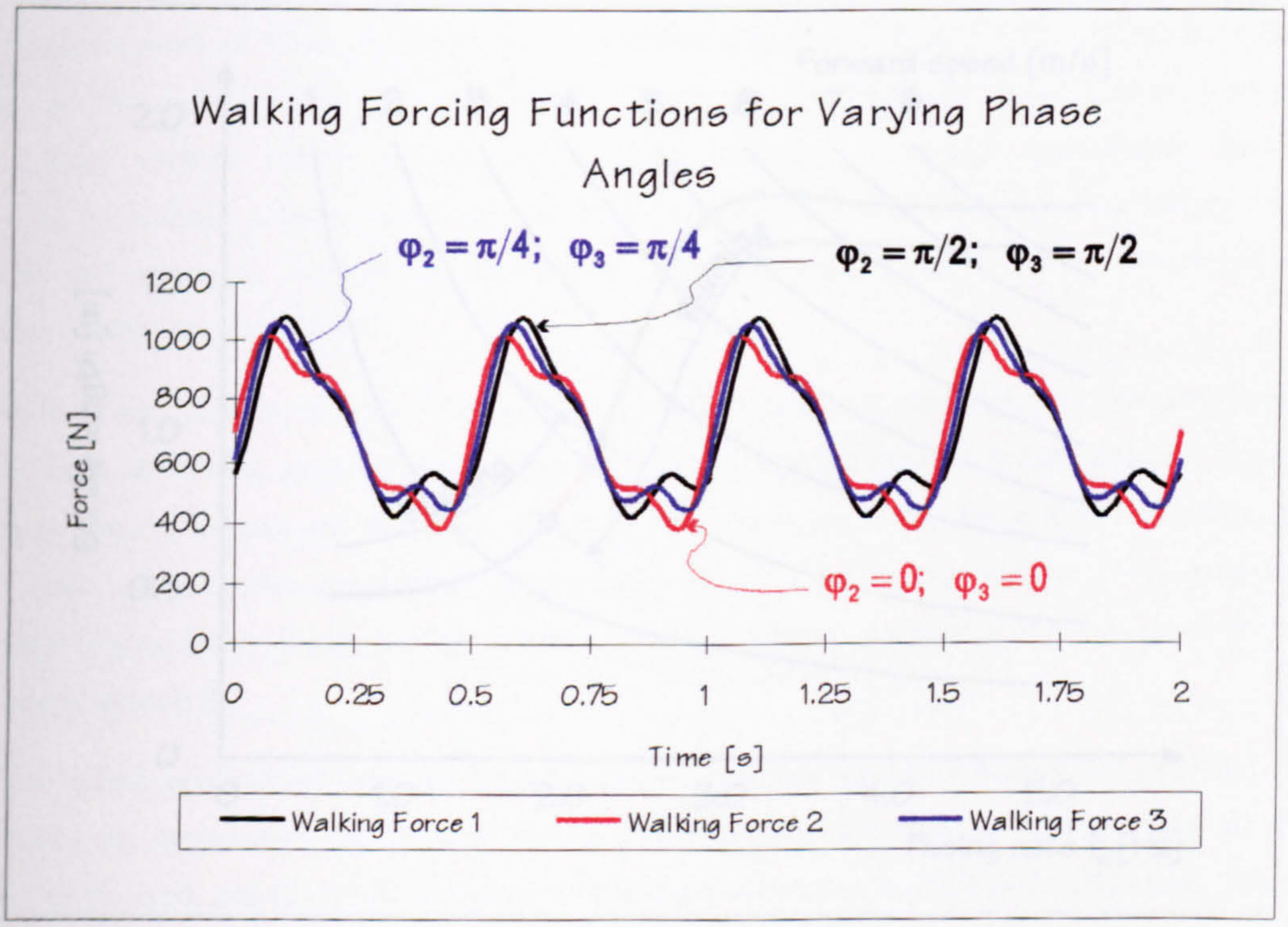

Figure 3.4: Deterministic forcing function.

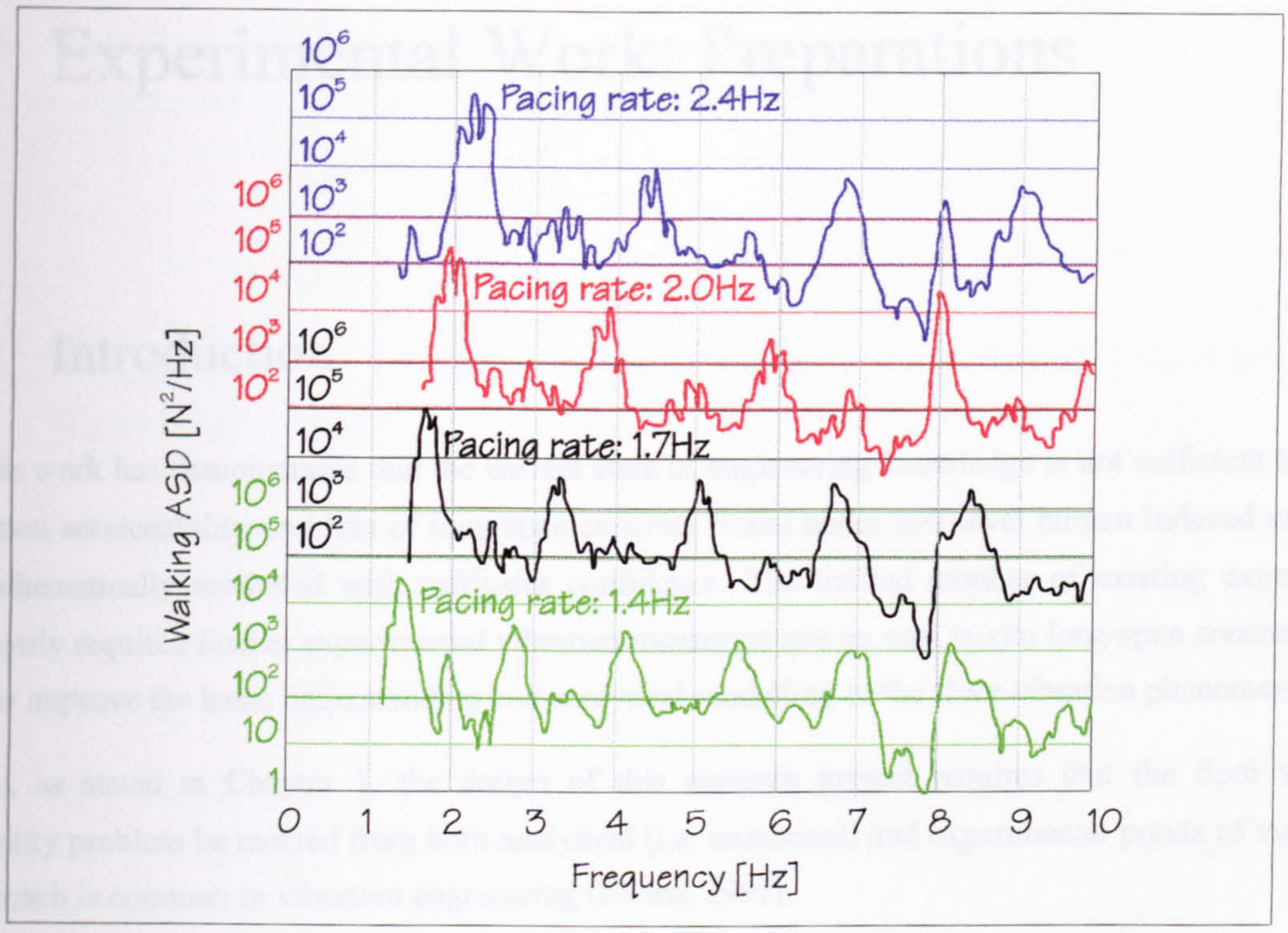

Figure 3.5: ASDs of a narrow-band excitation force imposed by a single person walking (after Eriksson, 1994)

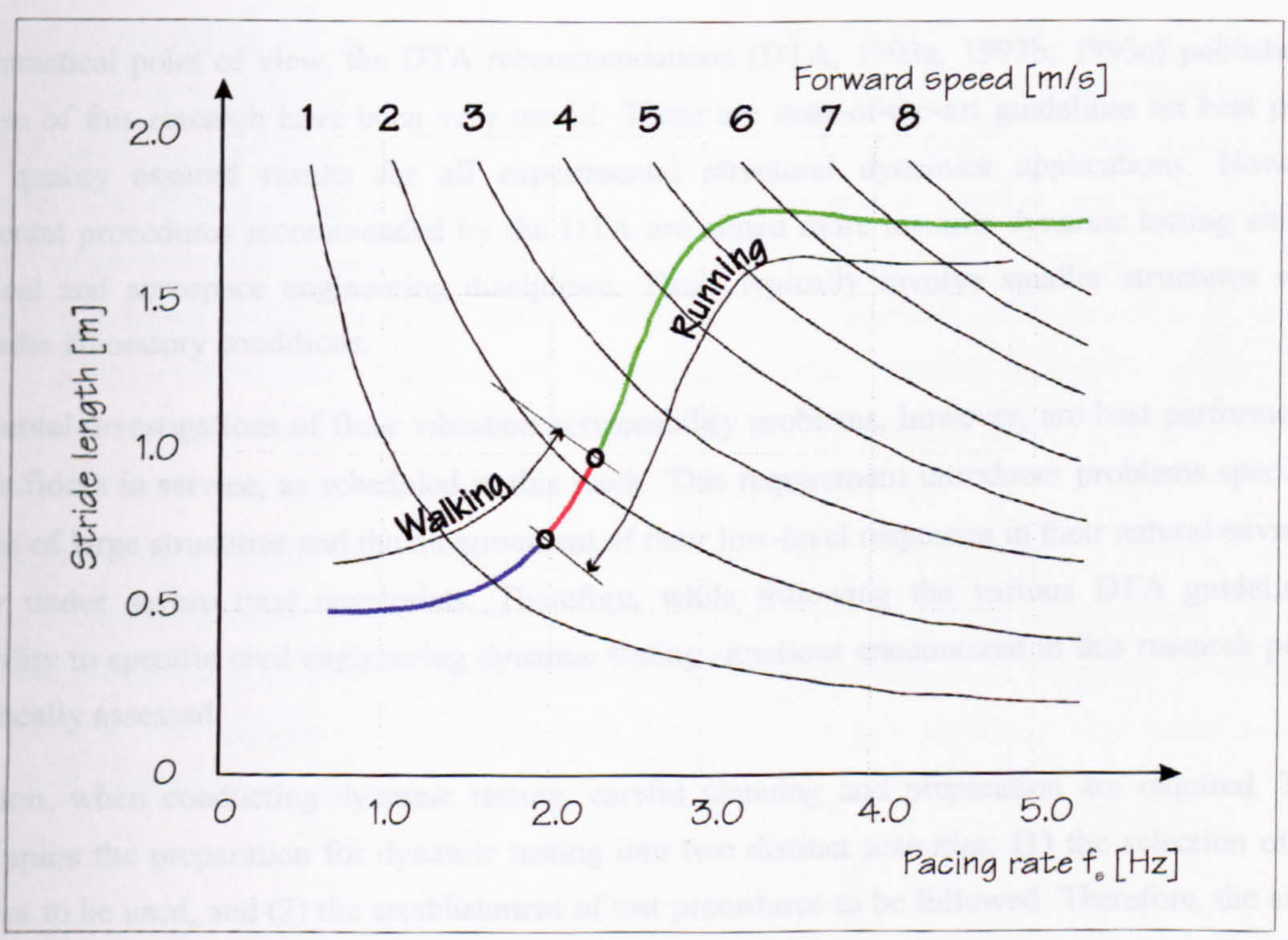

Figure 3.6: Relationship between the walking speed, pacing rate and stride length (after Bachmann & Ammann, 1987).

4 Experimental Work: Preparations

4.1 Introduction

So far, this work has demonstrated that the current state of engineering knowledge is not sufficient to enable the vibration serviceability problem of long-span concrete floors under low-level human induced excitation to be mathematically modelled with sufficient confidence. The limited number of existing experimental results clearly requires further experimental vibration measurements on cast in-situ long-span concrete floors in order to improve the basic understanding and analytical modelling of the floor vibration phenomenon.

Therefore, as stated in Chapter 1, the design of this research project requires that the floor vibration serviceability problem be tackled from both analytical (i.e. numerical) and experimental points of view. This dual approach is common in vibration engineering (Ewins, 1995).

This chapter is devoted exclusively to the preparations for the experimental part of the research. These preparations account for a considerable portion of the total research time because no experimental facilities suitable for this kind of work were available when the research commenced.

From a practical point of view, the DTA recommendations (DTA, 1993a; 1993b; 1993c) published during the course of this research have been very useful. These are state-of-the-art guidelines on best practice to provide quality assured results for all experimental structural dynamics applications. However, the experimental procedures recommended by the DTA are aimed more towards dynamic testing situations in mechanical and aerospace engineering disciplines. These typically involve smaller structures which are tested under laboratory conditions.

Experimental investigations of floor vibration serviceability problems, however, are best performed on real full-scale floors in service, as scheduled in this work. This requirement introduces problems specific to the excitation of large structures and the measurement of their low-level responses in their natural environments, typically under severe time constraints. Therefore, while following the various DTA guidelines, their applicability to specific civil engineering dynamic testing situations encountered in this research project has been critically assessed.

In addition, when conducting dynamic testing, careful planning and preparation are required. The DTA (1993c) splits the preparation for dynamic testing into two distinct activities: (1) the selection of items of equipment to be used, and (2) the establishment of test procedures to be followed. Therefore, the aim of this chapter is to describe the necessary groundwork undertaken to commission the appropriate hardware and software testing facilities taking into account the various project constraints. The descriptions of the testing procedures adopted are given in Chapter 5 for each individual test as the exact experimentation steps varied

slightly from test to test, depending on the in-situ conditions and on the available instrumentation, which was constantly developing and improving throughout the research.

4.2 Selection of Vibration Measurement System: General Considerations

Although no attempt is made here to master and detail the instrumentation electronics, some considerable attention has been paid to the selection of appropriate facilities and development of the various measurement system components having regard for the specific problems associated with the dynamic testing of large scale civil engineering structures.

The initial factor which governs the selection of test facilities is the type of vibration measurements that are to be made. Generally speaking, there are four such types of engineering measurement which are currently performed (Serridge & Licht, 1987). These are:

1. Vibration endurance and shock testing or environmental vibration testing. Typically used in mechanical, aerospace, electronic or electrical engineering, this determines endurance of a component to the vibration environment which is likely to be encountered in service;
2. Machine health monitoring and fault diagnosis. This is the measurement of an actual vibration level on a running machine in operation which may be used to give a warning of possible machine malfunction;
3. Human vibration measurement. This is the measurement of vibrations to which human beings are exposed. The measured vibration levels are then related to human comfort and health criteria using various national or international standards; and
4. Structural dynamic testing. Using the dynamic excitations and responses, or responses only, measured at various points on the existing structure, its key dynamic properties, such as natural frequencies, mode shapes and damping, can be experimentally determined. Terms such as modal testing or experimental modal analysis are frequently used in literature to describe this activity.

This research involves the last two types of vibration measurements. Whilst human vibration measurement comprises an assessment of vibration levels by analysing only a single measurement channel, the experimental modal analysis requires in principle simultaneous analysis of at least two channels (Ewins, 1995). Therefore, the decision to select equipment capable of doing both single- and simultaneous dual-channel signal analysis was made.

4.2.1 Components of Measurement System

Over the last half century, the development of vibration measurement instrumentation has had three distinct phases (Buzdugan et al., 1986). Firstly various mechanical devices were used. These were superseded by analogue electrical instruments, utilised to produce, measure and analyse continuous electrical signals from vibration tests. Finally, the typical vibration measurement systems in use today are based on developments in solid state electronics and digital signal processing.

Normally, human vibration measurements and structural dynamic testing require various electronic instruments to be selected and linked to form the instrumentation system. In principle, this system can be rationalised into six parts performing: (1) sensing, (2) conversion, (3) transmission, (4) storage, (5) analysis, and (6) display tasks (Figure 4.1). However, because of modern advances in instrumentation, system elements integrating two or more of the six functions are now commercially available.

For example, the first measuring step is the transformation of a measured mechanical quantity (a measurand), such as force or accceleration, into a corresponding electrical signal. This is termed sensing which is performed by a sensor. The raw signal from a sensor is usually not suitable for transmission, storage or analysis and its conversion into a more suitable electrical form is required (Broch, 1984; Serridge & Licht, 1987; Change, 1995; Dally et al., 1993). The signal sensing and conversion elements may be incorporated in a single device called a transducer (Dally et al., 1993; Usher & Keating, 1990). The output of this is an electrical signal directly proportional to the mechanical quantity measured which can then be transmitted and recorded on a mass storage device (e.g. analogue tape recorder) in order to be analysed at later date. Alternatively, signals can be analysed immediately and displayed on a readout device.

Another example of the integration of several elements within the modern vibration measurement system is the digital spectrum analyser. In the past, different types of dynamic measurements, such as single-channel vibration level measurements or dual-channel structural dynamic testing, normally required slightly different instrumentation systems (Keast, 1967). This is not the case any longer. When equipped with a suitable internal memory, spectrum analysers can perform storage, analysis and display tasks of measurand data converted into digital form, utilising both single- and dual-channel signal analysis procedures. This removes the inconvenience of physically setting up different measurement chains for single- and dual-channel analyses. It is very important to use such opportunities when commissioning field testing equipment as it is advantageous to make it as integrated as possible. A lesser number of items reduces the time required to set-up the equipment and for possible trouble-shooting on site. These two practical aspects are crucial for successful field testing time management.

4.2.2 Properties of the Measurement System

Electrical signals obtained from dynamic testing and passed through the various elements of the measurement chain must contain all the required information on structural vibration levels and dynamic properties. Therefore, it is essential to assemble a measurement system which can produce, transmit and analyse signals with as little distortion as possible. The level of signal distortion is governed by the properties of the components of the measurement system, of which the most important are: operating frequency range, linearity, dynamic range and sensitivity. The same properties may be defined for the chain as a whole, treating it as a linear system which maps input $x_i(t)$ to the output $x_o(t)$, as shown in Figure 4.2.

It is of paramount importance to be aware of these characteristics because they define limits of the measurement system. Vibration measurements producing signals outside these limits are bound to be erroneous. However, certain types of vibration measurements produce signals having more or less common characteristics. For example, vibration testing of full-scale civil engineering structures typically produces a low-level structural dynamic response having a low-frequency content. Therefore, when commissioning a measurement system for recording and analysing such vibrations it is important to have a good understanding of their likely level and frequency content, so as to match these to the measurement system characteristics (Shock and Vibration Measurement Technology, undated).

4.2.2.1 Operating Frequency Range

The instrumentation chain shown in Figure 4.1 can be represented as a 'black box' system (Figure 4.2). As stated above, sensing, conversion, transmission, storage and analysis functional blocks act together and jointly modify an input $x_i(t)$ creating the output signal $x_o(t)$. Each element of the measurement chain modifies the signal via its own input/output characteristic defined by the element's frequency response properties (Keast, 1967; Beckwith et al., 1995). The measurement system frequency response characteristic (Figure 4.3) has magnitude and phase spectra showing how the frequency components of the input signal are altered. Flat parts of the magnitude and phase spectra define the operating frequency range of the whole instrumentation system. If an attempt is made to measure an $x_i(t)$ having frequency components outside this 'flat' range, they will be distorted in amplitude or phase or in both. It is, therefore, essential to ensure that each and every element of the measurement system has frequency response characteristics which do not distort input signals in the frequency range of interest.

4.2.2.2 Measurement System Linearity

The ultimate goal for each element and the whole of the measurement chain is to produce an output signal $x_o(t)$ which is proportional to the input $x_i(t)$. That way a simple linear relationship can be established between instantaneous input and output values of the measurand. Knowing this relationship as well as the system output $x_o(t)$, typically given in Volts, it is possible to determine the system mechanical input $x_i(t)$.

However, this simple measurement principle is valid only as long as amplitudes of the input signal do not exceed certain limit, i.e. as long as the equipment is operating in the linear range (Figure 4.4).

When the amplitudes of the input signal are higher than the linear range limit, then the measurement system is said to be overloaded (or saturated) and the output signal is obviously distorted producing erroneous end results (Figure 4.4). This particular distortion of a measurement signal is called signal clipping. It is therefore important to make measurements in such a way that the measurement system is not overloaded. As to the linearity, when setting up a new measurement system, it is worthwhile considering the maximum values of the time-varying mechanical quantities which are likely to occur in practice. When this has been established, the instrumentation chain components can be selected in such a way that the possible highest values of the measurand are still in the linear range.

4.2.2.3 MEASUREMENT SYSTEM DYNAMIC RANGE

If a single harmonic input signal is passed through the measurement chain, its measurable amplitude must always be within certain bounds. The lower amplitude bound is determined by the level of the inevitable electrical noise present in the measurement system or transducer - the noise floor (Buzdugan et al., 1987; Keast, 1967; Shock and Vibration Measurement Technology, undated) as illustrated in Figure 4.5a.

The upper amplitude bound is determined by the permissible amount of signal distortion (termed harmonic distortion) due to clipping, as discussed above. These two values, the lower and the upper amplitude bounds, define the so-called system dynamic or operating range for a given frequency (Figure 4.5b). When these values are plotted against frequency, a typical area describing measurable harmonic amplitudes can be constructed (Figure 4.5c).

4.2.2.4 OTHER PROPERTIES OF MEASUREMENT SYSTEM AND ITS COMPONENTS

Apart from the system linearity, frequency and dynamic range, Buzdugan et al. (1987), Smith (1989) and Beckwith et al. (1995) discuss other characteristics of the measurement system and its components such as: sensitivity, instability (or consistency, or repeatability), and resolution (or discrimination).

Of these, the sensitivity is particularly important. It represents the ratio of electrical output to mechanical input to the transducer or to the whole measurement system. Therefore, the sensitivity may be defined for both transducers (transducer sensitivity) and the measurement system (system sensitivity).

Endevco (Shock and Vibration Measurement Technology, undated) short course notes specify that the transducer sensitivity is:

> "...probably the most important single characteristic of any transducer: does it have an appropriate sensitivity for the level to be measured?"

4.3 Modal Testing and FE Model Correlation

Of the two vibration testing activities scheduled for this work: (1) human vibration measurements, and (2) structural testing, the latter is generally more complex and demanding, especially regarding its use in civil engineering applications. Therefore, it is described below in more detail.

4.3.1 Interdisciplinarity

Although, as its name suggests, modal testing may be perceived to be purely an experimental technique, Allemang and Brown (1993) maintain that it has a strong interdisciplinary character linking areas such as signal conditioning from electrical engineering, theory of mechanics and vibrations (including FE modelling) from structural engineering and parameter estimation from applied mathematics. Therefore, modal testing is not only experimental, but is an analytical activity as well.

Modern approaches to experimental modal analysis include analytical, usually FE, modelling of the structure to be tested and a vibration parameter estimation phase as indispensable elements of the modal testing activity. For example, FE modelling prior to testing is prudent in order to establish the best position for transducers in order to avoid the so called 'spatial aliasing' of measured mode shapes (Friswell & Mottershead, 1995; NAFEMS, 1992b), and to have estimates of natural frequencies and mode shapes of the test structure to help the test setup (DTA, 1993b; 1993c). Hence, Ewins (1995) stresses that the subject of modal testing requires a "thorough integration" of: (1) the theoretical basis of vibration, (2) the accurate measurement of vibration, and (3) realistic and detailed data analysis.

This is probably the reason why modal testing, used nowadays as a standard design tool in aerospace and mechanical engineering industries, is typically performed by two groups of specialists: experimentalists and analysts, who join their expertise covering the various phases of modal testing. The first group is usually concerned only with experimental data collection and analysis, whilst the second group correlate these results with (independent) mathematical modelling usually using FE analysis. In order for testing to succeed when conducted in this way, the two groups of modal testing personnel must communicate with each other and carefully co-ordinate their activities (DTA, 1993b).

In this research project, however, the test preparation, field data collection, their analysis and correlation with the FE modelling all were performed by the writer. However, by the very nature of the modal testing techniques selected and used (instrumented hammer excitation, to be described later), the writer had to be helped by the member(s) of the field testing crew when physically gathering experimental data.

4.3.2 Concepts Employed

Excellent introductory overviews of the concepts of modal testing are given by Ramsey, (1975; 1976), Ewins (1975; 1976a; 1976b; 1979; 1995), DTA (1993b; 1993c), Dossing (1988a; 1988b), Allemang and Brown (1993), and many others. According to these, experimental modal analysis exploits the fact that an analytical model used to simulate structural linear dynamic behaviour, can typically be formulated in one of the following three ways (Ewins, 1995; DTA 1993c):

- As a spatial model, where the dynamic behaviour of the structure is described by its mass, stiffness and damping properties;
- As a modal model, where the dynamic behaviour of the structure is given in terms of its modal parameters; and
- As a response model which is typically represented by a set of frequency response functions which can be used to describe the structural responses to known excitations.

Theoretically, knowledge of any of these three models allows for the establishment of the other two as long as the structure remains linear (DTA, 1993c). In addition, when any of these models is known, the structural response to a given excitation can be obtained. Therefore, Ewins (1979; 1995) defines two routes to vibration analysis: (1) the theoretical route; and (2) the experimental route (Figure 4.6).

4.3.2.1 THEORETICAL VS. EXPERIMENTAL VIBRATION ANALYSIS ROUTES

Following the theoretical route, the structure is firstly described as a spatial model by assuming its mass, stiffness and damping properties. A modal model can then be extracted by means of theoretical modal analysis achieved by mathematical eigenvalue/eigenvector extraction. Finally, a response model is obtained from the modal model typically utilising the mode superposition method. FE analysis is nowadays usually employed when following this route to vibration analysis, as outlined in Chapter 3.

Following the experimental route, the structure itself must exist so that the response model can be established from experimental measurements of structural excitations and responses. In order to establish the necessary set of FRFs describing the response model, a Fourier transform is typically applied to the pairs of simultaneously measured structural excitations and responses. Experimentally measured FRFs are then used to establish a modal model of the test structure by fitting assumed mathematical models into them. This procedure is called vibration parameter estimation or, simply, parameter estimation. Finally, a spatial model can again be constructed from the established modal model, by means of system identification (Ewins, 1979).

Figure 4.6 shows that the modal model falls between the spatial and the response model. It is relatively easy obtainable following both the analytical and the experimental routes. Therefore, this is the point where the assumed analytical spatial FE models are usually verified against the estimated experimentally determined modal properties. The two modal models developed for the same structure following the theoretical and

experimental routes are typically compared by correlating their modal properties. However, theoretically and experimentally obtained structural response models could be compared also by examining their corresponding pairs of FRFs.

The main aim of the experimental part of this research is the confirmation of existing mathematical models and the possible establishment of more realistic ones for the analysis of the vibration serviceability phenomenon of long-span cast in-situ concrete floors. Hence, the main thrust of the modal testing work presented here has been directed towards the establishment of the floor modal models from full-scale modal testing and their correlation with the corresponding FE models.

4.3.2.2 General Linear Dynamic System: Input/Output Concepts

The analysis of a general constant parameter linear dynamic system is usually concerned with finding the system output (i.e. response) $x(t)$ to a known input (i.e. excitation) $f(t)$ (Figure 4.7). If an arbitrary excitation $f(t)$ is applied as an input, the system transforms it producing the corresponding output $x(t)$. This transformation is mathematically predictable and is governed by the constant properties of the so-called system descriptor (Dossing, 1988a).

In the time domain, this input/output relationship can be established using the system descriptor termed the impulse response function (IRF). In the frequency domain inputs and outputs are related via the well known descriptor called the FRF. The Fourier transform pair F and F^{-1} typically serves as a link between the time and the frequency domains (Figure 4.7).

When compared with the time-domain counterparts, the frequency domain model for the input/output analysis is very efficient (Dossing, 1988a). If the system properties are known, its FRF $H(\omega)$ is also known. For example, a harmonic input of frequency ω to a linear system characterised by $H(\omega)$ will have a harmonic output of the same frequency (Figure 4.9). More generally, for a given input spectrum $F(\omega)$, the output spectrum can be calculated by simply multiplying the two known functions of frequency $F(\omega)$ and $H(\omega)$:

$$X(\omega)=H(\omega)\cdot F(\omega) \qquad \text{Equation 4.1}$$

This is why a set of frequency response functions is in fact the response model of a linear system which enables the output response to a given input to be calculated. By establishing the input/output relationship in this way and by inverse transforming the $X(\omega)$, an involved calculation of a convolution integral obtaining the response $x(t)$ to the excitation $f(t)$ in the time-domain is avoided.

More importantly, Equation 4.1 can be also written as:

$$H(\omega)=\frac{X(\omega)}{F(\omega)}, \qquad \text{Equation 4.2}$$

indicating that the frequency response function $H(\omega)$, if not known, can be measured. This can be done by simultaneously gauging the system excitation $f(t)$ and its response $x(t)$, and by calculating their spectral properties utilising principles of dynamic signal analysis.

4.3.3 Signal Analysis

For the purpose of practical signal analysis of vibration measurements, excitation and response signals in the instrumentation system can be divided conveniently into two main groups: deterministic, which may be either periodic or transient; and random (McConnell, 1978; 1995). This classification is shown in Figure 4.8. For the interpretation of signal analysis results, it is of paramount importance to know which of the signal types has been analysed. Signal temporal parameters typically measured are: temporal mean, temporal mean square, temporal root mean square, temporal auto-correlation and temporal cross-correlation. Similarly, signal spectral parameters usually measured are frequency spectra as well as auto- and cross-spectral densities. Mathematical manipulations using these measurable signal parameters lead to all the experimental results required in this research, such as floor vibration levels (single-channel analysis) or frequency response functions (dual-channel analysis).

Nowadays, practical signal analysis is almost invariably conducted using signal digitisation and discrete Fourier transforms (DFT) of which most popular is the fast Fourier transform (FFT) method (Brigham, 1974; Randall, 1987a; McConnell, 1995). Signal analysis is a separate scientific and engineering subject discussed in many standard textbooks and research papers and will not be covered here in greater detail. Nevertheless, mastering of its core principles and terminology is one of the requirements for conducting quality assured dynamic testing (Ewins, 1995; DTA, 1993c; Allemang & Brown, 1993).

4.3.4 Vibration Parameter Estimation

4.3.4.1 Non-Parametric and Parametric Models

In modal testing, digital signal processing leads to the so called non-parametric model of the structure, because it is "represented in terms of measured data" (DTA, 1993c). The non-parametric model is, in fact, the structural response model obtained by performing the following data gathering steps: (1) generation of analogue time histories by the measurement transducers, (2) digital sampling of measured time-histories, (3) calculation of the spectral properties of the digital signals, and (4) production of a set of discrete FRFs.

Usually, modern spectrum analysers used for this kind of input-output signal analysis produce frequency response functions each of which is defined by hundreds if not thousands of complex data points. Therefore,

the digital signal processing stage of the modal testing typically produces non-parametric models of the test structures defined by a large amount of numerical data.

Generally, when modelling the large volume of test results from a structure, some kind of data reduction is required. The outcome of this data reduction is a limited set of numbers which is capable of representing the bulk of the numerical measured data. These numbers are called parameters and the new model they represent is called a parametric model. The procedure for extracting the parametric model from its non-parametric counterpart is termed parameter estimation.

In the case of modal testing such a parametric model is, in fact, the modal model. As already mentioned, the procedure for its extraction from experimental measurements is logically termed vibration parameter estimation.

4.3.4.2 THE OBJECTIVE OF VIBRATION PARAMETER ESTIMATION

Being the experimental response model of a given structure, a set of measured FRFs contains all the information required for the establishment of a modal model. This 'modal information carrier' ability of FRFs will be briefly demonstrated here. It establishes the basis for the majority of the sophisticated MDOF vibration parameter estimation procedures. These procedures had to be employed in this project due to specifics in the dynamic behaviour of concrete floors, such as high modal density. Detailed development of the concepts presented here are given elsewhere (Maia et al., 1997; DTA, 1993b; 1993c; Ewins, 1995)

It can be demonstrated (Ewins, 1995) that the receptance FRF $\alpha_{jk}(\omega)$ is a function of constant modal parameters, by developing the following expression:

$$\alpha_{jk}(\omega)=\sum_{r=1}^{N}\frac{(\psi_{jr})(\psi_{kr})}{(k_r-\omega^2 m_r)+i(\omega c_r)} \qquad \text{Equation 4.3}$$

which may also be written as:

$$\alpha_{jk}(\omega)=\sum_{r=1}^{N}\frac{\frac{1}{m_r}(\psi_{jr})(\psi_{kr})}{(\omega_r^2-\omega^2)+i(2\omega\omega_r\zeta_r)} \qquad \text{Equation 4.4}$$

Similarly, if instead of viscous damping (ζ_r), hysteretic (or structural) damping model (η_r) is assumed, the previous equation changes into:

$$\alpha_{jk}(\omega)=\sum_{r=1}^{N}\frac{\frac{1}{m_r}(\psi_{jr})(\psi_{kr})}{(\omega_r^2-\omega^2)+i(\omega_r^2\eta_r)} \qquad \text{Equation 4.5}$$

Expressions for the mobility $Y_{jk}(\omega)$ and accelerance $A_{jk}(\omega)$ FRFs can be easily obtained as:

$$Y_{jk}(\omega) = i\omega\alpha_{jk}(\omega) \qquad \text{Equation 4.6}$$

and

$$A_{jk}(\omega) = -\omega^2\alpha_{jk}(\omega) \qquad \text{Equation 4.7}$$

Equations 4.4-4.7 show that, no matter whether the FRFs are obtained from the displacement, velocity or acceleration structural responses, they all contain information about all the relevant modal properties of the MDOF structure: the natural frequencies ω_r, the mode shapes $\{\psi\}_r$ and the modal damping ratios ζ_r or loss factors η_r, depending on which damping model is assumed in the mathematical model (Ewins, 1995). Any one of the three forms of FRF equation may, therefore, serve as a basis for the theoretical model representing the measured FRFs if the unknown constant parameters: ω_r, $\{\psi\}_r$ and ζ_r (or η_r) are determined so that there is a good fit of the theoretical FRF curves into the corresponding measured ones. Therefore, determination of the modal parameters for a number of modes of vibration by curve-fitting set of measured FRFs is the objective of the parameter estimation phase of modal testing. Richardson (1984) refers to this parameter estimation process as - curve fitting.

4.3.4.3 PARAMETER ESTIMATION: GENERAL CONSIDERATIONS

The majority of parameter estimation procedures used in practice today are based on the analysis of frequency response functions in the frequency domain (DTA, 1993c). DTA recommends the general procedure which should be followed when undertaking curve fitting. The parameter estimation basic steps are:

Step 1: Graphical presentation and inspection of the measured data;

Step 2: Selection of a suitable mathematical model, such as those given in Equations 4.3-4.7 applicable for frequency domain analysis, considered to be capable of representing the vibration properties of the structure tested to a sufficient degree of accuracy; and

Step 3: Estimation of the vibration parameters required to produce the minimum difference between the mathematical FRF model selected above and the measured FRF data.

The ability to inspect graphically the measured data prior to the parameter estimation is important in order to assure the quality of the curve fitting. The DTA (1993b) further stresses:

> "There is sometimes a danger of manipulating data into parametric models without first checking the non-parametric model. The experienced test engineer knows the correct form that time histories, frequency spectra and FRFs take and can spot a non-conforming example. Consequently, it is important to look at visual displays of data as they are manipulated through their various stages."

Hence a decision has been made to commission experimental analysis facilities which would allow the graphical inspection of the measured data prior to the parameter estimation. Also, due to the nature of field

modal testing in civil engineering, this qualitative data inspection should be possible 'in-situ'. This is because poor 'raw' experimental data quality preventing successful parameter estimation usually results in inconvenient repetition of the whole field trip which, sometimes, may be impossible. Also, in this particular research project, the in-situ estimated natural frequencies and mode shapes were required prior to performing the walking response measurements, as explained in Chapter 5.

If a frequency domain parameter estimation approach is to be followed, then a decision to analyse only one or a number of FRFs simultaneously has to be made fairly early in the analysis. Even if only one FRF is to be analysed two options generally exist: (1) to assume and extract only one mode at time from it, adopting an SDOF mathematical model, or (2) to assume and extract several modes simultaneously using an MDOF approach.

On the other hand, the simultaneous analysis of all measured FRFs can be done in two different ways, depending on whether the FRFs were collected using: (1) a Single-Input, Multiple-Output (SIMO) or (2) a Multiple-Input, Multiple-Output (MIMO) approach. In the SIMO approach, a single column or row of the FRF matrix is measured at a time. On the other hand, in the MIMO approach several rows or columns of the FRF matrix are measured simultaneously.

The options for general parameter estimation are further compounded by specific algorithms within each option. Even the simplest SDOF parameter estimation method can be done employing at least three different frequency-domain procedures such as: (1) half-power (or peak-picking), (2) circle fit, and (3) line-fit methods.

Experimental modal analysis software packages capable of handling vast amount of numerical data, and having powerful graphical interfaces producing still and animated graphical output, are nowadays typically used for parameter estimation. Moreover, modern computer curve-fitters usually provide a multitude of vibration parameter estimation methods. All of them should lead to the same result to within an acceptable error and, not surprisingly, DTA (1993c) insists on using at least two curve fitting methods in order to produce quality assured estimates.

Whilst some SDOF parameter estimation algorithms, such as the 'half-power method' are simple to understand and use, they have limitations especially with regard to the analysis of FRFs from structures having closely-spaced modes. Some other curve-fit methods, which are essentially hybrids between the SDOF and MDOF methods (such as the circle-fit with the capacity to subtract the effect of modes already identified), perform better (Maia et al., 1997). Finally, MDOF parameter estimation procedures capable of simultaneously identifying more than one mode can cope with this problem much better. Therefore, the capability for applying these more advanced procedures should be considered as a prerequisite for the parameter estimation software which is to be used in experimental modal analysis of concrete floors. Interestingly, as shown in the literature review (Chapter 2), the vast majority of full-scale experimental dynamic tests performed on floors, reported in the literature, were based on variations of SDOF parameter

estimation procedures which performed poorly introducing large errors in the estimated modal parameters, particularly in damping ratios.

Numerical procedures used in these most sophisticated methods stem from applied mathematics and Ewins (1995) states that:

> "It is seldom necessary (and is often impossible) for the modal analyst to have an intimate knowledge of the detailed working of the numerical processes but it is important that he is aware of the assumptions which have been made, and of the limitations and implications."

Bearing in mind the limited research time scales and the objectives of using modal testing only as a research tool in this thesis, the writer has adopted this 'black box' approach, but has a sound understanding of the underlying principles employed.

4.3.5 FE Model Correlation

Validation of theoretical models against experimental data is usually a goal in many engineering disciplines. Likewise, uncertainties in numerical modelling of the vibration serviceability phenomenon in long-span concrete floors required the validation of a number of analytical FE models in order to gain more confidence in their performance. A procedure termed analytical or FE model correlation (DTA, 1993c) is used when validating assumed structural dynamic models against their experimental counterparts.

With regard to the terminology employed, it is worthwhile mentioning that Ewins (1995) and DTA (1993c) recognise the comparison and correlation of theoretical and experimental structural dynamic properties as two significantly different activities. Whilst the comparison is a qualitative process of simply observing similarities and differences between two sets of data, the correlation is a more complex activity. The correlation involves combining the two sets of data aimed at quantifying the differences between them and the sources causing these differences.

In this thesis, the correlation of analytical and experimental modal models will be performed by: (1) graphically comparing their natural frequencies and mode shapes, and (2) numerically comparing their mode shapes using the modal assurance criterion (MAC) and the coordinate modal assurance criterion (COMAC). These procedures are described in more detail by Ewins (1995) and Maia et al. (1997) and are incorporated, sometimes as a separate module, in commercially available software used for further processing of modal testing data. Therefore, the decision to use an integrated software having both parameter estimation and model correlation capabilities was made.

Finally, the differences between the experiments and analysis established using FE model correlation may be corrected in the analytical/FE model either manually by trial and error, or by employing a whole set of systematic and programmable procedures. Both methods are generically termed FE model updating. Friswell and Mottershead (1995) introduced FE model updating as the "technology of the 90s". In this research, due

to time and budgetary constraints, only a limited manual correction of FE models has been performed. Nevertheless, automatic FE model updating could have an important application in civil engineering structural dynamics problems, but it is beyond the scope of this thesis.

4.4 Modal Testing in Civil Engineering

The DTA (1993b, 1993c) insists on formulating the aims of modal testing very early in the testing process as a pre-condition for good quality results. Clarification of the aims for full-scale modal testing in civil engineering is important because, although based on the same theoretical principles as for mechanical and aerospace engineering, significant differences exist. These inevitably arise from the dissimilar design processes of mechanical/aerospace and civil engineering structures (Pavic & Waldron, 1996b).

4.4.1 Mechanical/Aerospace vs. Civil Engineering Applications

In the mechanical/aerospace industries: (1) mass production of identical structures and components is common; (2) design and manufacturing tolerances and safety margins are relatively small; (3) uncertainties as to the material properties are greatly reduced; and (4) design and manufacturing processes are more carefully monitored. Consequently, the preparation of expensive tools for mass production, costly structural prototyping and prototype modal testing, aiming at fine structural modifications and improvements to the design, are standard practice. This is where experimental modal analysis plays a significant role.

On the other hand, the nature of civil engineering structures, their size, purpose, constituent materials, cost, design and construction methods are such that much higher tolerances and structural safety factors must usually be adopted. Moreover, prototyping as part of the design process in civil engineering is rarely an option due to its prohibitively high cost. Therefore, modal testing of large as-built civil engineering structures is hardly ever used as a tool in the structural design process. Instead, it is more of a research tool for gaining knowledge and experience of the actual behaviour of existing full-scale structures which could be used in their assessment, or in the future for similar generic designs (Severn et al., 1988).

Maguire (1984) demonstrated this approach when investigating the dynamic behaviour of elevated piled tanks which were found to vibrate "in a translational fashion about the tops of their pile caps". This dynamic action, which could overstress the supporting elements during earthquakes had not commonly been anticipated in the design of such structures. Conclusions like this are, obviously, extremely valuable for the future design and dynamic modelling of similar structures.

When discussing applications of experimental results from dynamic testing of full-scale civil engineering structures, Reese and Kawahara (1993) clearly support this role of full-scale experimental modal analysis stating:

> "Most civil engineering structures are unique. Testing these types of typically large structures presents challenges to the engineers and technicians because it is not possible to first build and test a prototype. Each structure is generally one-of-a-kind, although there may be a number of common similar components. Testing these structures can be useful in advancing the state of the art of analysis and design for an entire class of structures."

Severn et al. (1988), Maguire (1984), and Reese and Kawahara (1993) are three examples which illustrate the general philosophy commonly behind full-scale dynamic testing in civil engineering. Their opinions strongly underpin the idea, advocated in this thesis as well, of conducting modal testing in order to gather new knowledge about the actual as-built dynamic behaviour of long-span cast-in-situ concrete floors.

4.5 Commissioning of Experimental Facilities

DTA (1993c) warns that:

> "The task of equipment selection is a key to successful modal testing - in fact, any testing - and yet it often receives little or insufficient consideration. Much time and effort may be spent at a later date trying to correct errors introduced by the incorrect choice of instrumentation."

Moreover, McConnell (1995) states that vibration measurement instruments could be the "Achilles' heel" of the vibration testing process. This is especially so in relatively less common measurement situations such as the prototype dynamic testing in civil engineering.

4.5.1 Dual-Channel Input-Output Modal Testing System

A scheme of a generic modal testing system, being in fact a dual-channel measurement chain, is shown in Figure 4.10. Apart from the curve-fitting stage towards the end, each of these two channels clearly corresponds to the single instrumentation chain shown in Figure 4.1. Typically, a sensor capable of measuring force, mounted on a suitable mechanical exciter, is at the beginning of the input measurement chain. The output measurement chain starts with a displacement, velocity or acceleration sensor. A multi-channel tape recorder is commonly used as the (analogue) input/output mass data storage device. A dual-channel FFT spectrum analyser usually plays both the dual-channel analysis and display roles although the analysis block of the scheme could contain a PC instead of the analyser. The last curve-fitting step may also be performed either in the spectrum analyser or in the PC. Nevertheless, modal testing systems where both a

spectrum analyser (for dual-channel analysis and display) and a PC (for curve fitting) are used are also common (Heylen et al., 1997).

4.5.2 Modal Testing Standardisation Requirements

The availability of high quality modal testing data, systematically gathered, processed, reported and stored, obviously assists in reducing uncertainties in the FE modelling being based on the correlation with experiments. Severn et al. (1988) suggested the setting-up of a global database which would contain results from full-scale experimental dynamic tests of civil engineering structures performed throughout the world. This is, however, a tremendous task and a vision which may only be achieved in the next century.

One of the reasons why this idea of a global database is currently impractical is that dynamic tests of full scale structures have not been performed and reported in a unified manner. This makes the subsequent extraction of data and their interpretation by different users very difficult if not impossible. This diversity of terminology and practices in structural dynamic testing has already been observed in the even more developed area of modal testing of mechanical and aerospace structures, where it is more critical. Recognising this problem, the UK Department of Trade and Industry launched the DTA in 1990. The DTA's brief was, and still is, to "promote harmonisation and standardisation of dynamic testing" (DTA, 1996) across various engineering disciplines including civil engineering.

In this thesis an attempt has been made to, whenever possible, use notation and terminology, and test-out the recently introduced general DTA testing recommendations. This is done by applying them to the experimental modal analysis of prototype concrete floors, considered to be a rather specialised modal testing application.

In order to help decide on the aims and objectives of modal testing, critical for obtaining high quality results, DTA (1993b; 1993c) introduces five categories, so called "levels", of modal testing:

Level 0: This is the simplest level of modal testing, comprising only an estimation of natural frequencies and damping ratios. No mode shape calculation is required. An example of this category used in floor dynamics is the well known heel-drop test, sometimes used to estimate the first natural frequency (CSA, 1989; Ellis, 1992);

Level 1: Estimation of natural frequencies, damping ratios and the general qualitative form of the mode shapes. Caverson (1992) and Pernica (1987) demonstrated the use of this level of modal testing to investigate floor vibrations;

Level 2: Measurement of all modal parameters in a sufficiently accurate manner to enable mode shapes to be computer animated. Although it does not require normalisation of mode shapes, the computer animation is a very powerful tool for comparing measured and calculated mode shapes (ICATS, 1995; 1997; Ewins, 1995; Dossing, 1988b). This level of modal testing

requires numerous and fairly precise measurements producing a set of FRFs which are typically required in order to extract modal parameters and use them to visualise the measured modes of vibration. An animation option may be built in the modal analysis facility which is usually either a higher class spectrum analyser or a PC;

Level 3: Measurement of a modal model of the structure including normalised mode shapes. As for the Level 2 testing, thorough checks of data quality during measurements are needed since the modal model should be of sufficient quality to enable FE model correlation; and

Level 4: Highest quality measurements of the modal model are required for direct use in response prediction and modification assessment typically employed in the mechanical and aerospace engineering disciplines.

The Level 0 test, although the least time consuming, does not offer sufficient information to satisfy the research needs for establishing more reliable analytical models. Moreover, as outlined in Chapter 2, major misinterpretations of the heel-drop results were caused by inappropriate floor damping parameter estimation procedures used mainly during the 1960s and 1970s by researchers in the North America. The DTA Levels 1 and 2 of modal testing are also not suitable as they do not produce normalised mode shapes which are required for reliable FE model correlation using modal test data. Therefore, a decision to set-up experimental and analytical facilities capable of achieving Level 3 modal testing quality has been made.

4.5.3 Special Requirements and Constraints

Apart from the general technical requirements, such as the quality of data achievable from modal testing, the new dynamic testing facilities had to satisfy a number of important special requirements and constraints related to the specifics of this project.

Firstly, the total project budget was obviously a major factor influencing the strategy for this research in general, and the selection of the facilities and their development in particular. For example, the limited human resources available governed the decision to set up the testing system from readily available components. Therefore, a decision to opt for commercially available modal testing facilities (hardware and software) was made.

When performing field modal testing of a full-scale floor structure, the timing is of paramount importance. The writer's experience gained during the preparatory phase of this project was that contractors and building owners, if not properly compensated, were prepared to allow only very limited access time to the structure. By their very nature, the testing activities disturb normal use of the floor, either during construction or during everyday service. Unfortunately, the research project budgetary constraints did not allow for compensation or hire of the structures tested. This created a conflict with the need to adopt high quality, but more time

consuming, modal testing procedures in order to satisfy the DTA Level 3 requirements, which had to be resolved.

Harsh field testing conditions and the availability of limited manpower on site were anticipated requiring the equipment to be rugged, portable and easily (dis)mountable.

The requirement for alternative battery-powered equipment was set in order to provide the flexibility to test structures where a 240V supply was either not available or not allowed.

Rapid advances in digital electronics, computer technology and instrumentation in general over the last five years (Heylen et al., 1997) ruled in favour of facilities allowing easy future upgrades.

In addition, modal testing facilities, allowing full 'in-situ' experimental modal and FE analyses, were required to meet the DTA (1993b, 1993c) quality assurance criteria for performing various checks and trial analyses on-site prior to full experimental FRF data acquisition.

Some instrumentation chains used in dynamic measurement and testing comprise sensors requiring special low-noise cables which are expensive. Whilst the cost of such transmission systems maybe acceptable in laboratory conditions, where the connection lines are short, instrumentation of large civil engineering structures, especially floors, may require tens if not hundreds of metres of such cables. This would make the use of systems utilising expensive low-noise cabling unacceptable and therefore the logical requirement for cheap but low-noise long transmission lines was set.

Elements of the modal testing instrumentation chain may develop faults. This is a fact of life reported by renowned experts in the field, such as Maguire (1984) and Farrar et al. (1994), and has also been the writer's frequent experience, as is reported in Chapter 5. Therefore a requirement for efficient trouble-shooting requiring a minimum number of components in the measurement chain was set. Moreover, when doing field testing away from base, a fault in a relatively cheap but not replaceable item, such as the transducer power source or the micro-dot cable connector commonly used with accelerometers, is very frustrating and could lead to abandonment of the whole experiment. The cost of such a decision is an order of magnitude higher than the cost of the failed part. Following Maguire's (1984) advice, the requirement to purchase affordable key spare parts was also set.

Finally, the writer decided not to rely on the technical advice provided by the equipment suppliers. Therefore, a condition for equipment pre-purchase trials was set. This was done because the prospective suppliers often had very limited knowledge as to the application of their products to the DTA Level 3 modal testing of full-scale concrete floors which is a fairly rare experimental exercise. This requirement was met by either borrowing various equipment items from other institutions prior to their purchase or by requesting at least a two-week trial period from the prospective suppliers.

4.5.4 General Selection from Multitude of Options

An extensive review of manufacturers producing various components of the general modal testing system has been published by the SEM (1989). An inspection of this Guide revealed that vibration exciters, such as hammers and shakers, could be purchased from at least 17 manufacturers; 41 companies were producing vibration response transducers; instrumentation tape recorders were available from at least 6 suppliers; whilst 18 different manufacturers were offering FFT spectrum analysers. Moreover, in general, each manufacturer produced a wide range of options. For example, Endevco produces 48 different types of piezoelectric accelerometers and Bruel & Kjaer produces 21 various acceleration pick-ups. A similar multitude of options was offered by all manufacturers for each and every component in the modal measurement chain. This large number of commercially available system components made the task of selection very difficult.

Nevertheless, the number of options reduced considerably when the above-mentioned general and special project requirements and constraints were introduced. For example, only seven manufacturers were able to meet the portability condition for the FFT spectrum analyser, whilst Endevco Corporation produced only a handful of accelerometers suitable for this civil engineering type of vibration measurement.

Finally, it should be noted that the selection process did not follow the sequence of the elements in the measurement chain i.e. first choosing exciters and motion transducers, then signal transmission cables, then data storage, and, finally, data analysis facilities. Although the selection of each key element of the measurement chain is, for the sake of clarity, presented here in this order, these elements should not be prioritised and should always be considered as a part of the whole measurement system.

4.6 Vibration Excitation Devices

The first practical step following the requirements for achieving the DTA Level 3 quality in modal testing is the production of a set of FRFs for the floor structure tested. For this first step to be made, the structure has to be repeatedly excited and both its excitation and response simultaneously measured and further processed.

Interestingly, in a recently published review of dynamic full-scale testing in civil engineering, Ellis (1992) states that the data obtained from the dynamic full-scale tests can be used to "check the accuracy of mathematical models", which is one of the aims of this thesis. However, he does not advocate strongly the input-output dual-channel approach based on gathering and analysing simultaneously a set of FRFs when validating structural FE analytical models. He mentions that this method is extensively used in modal testing of cars and aircraft and is often combined with complex finite element analysis, but he concludes that these techniques "still have little application within buildings".

So, Ellis accepts the checking of analytical models against experiments as an important reason for conducting prototype dynamic testing. But, as further analysis of his paper reveals, he practically advocates measurement of modal properties of full-scale structures using a dual-channel analysis of their dynamic responses only. This is usually done with one 'reference', and one 'traveller' response transducer. In this approach, it should be noted, the establishment of the full response model of the structure by experiment (Figure 4.6) is omitted, and the modal model is estimated directly and not always accurately. For years this procedure has been and still is common in dynamic testing of large civil engineering structures because of the practical difficulties associated with measuring FRFs on such structures. Nevertheless, response measurements alone do not produce a proper structural response model (i.e. a set of complex FRFs) as indicated in Figure 4.6. Having no measured FRFs, these 'response only' techniques are to some extent easier to perform in practice, but they are not particularly suitable for the detection of closely spaced modes of vibration (Ewins, 1995) which typically occur in long-span concrete floors (Eriksson, 1994; Pavic et al., 1995a; 1995b; Pavic and Waldron, 1996a).

Therefore, in order to detect the closely spaced modes, a theoretically more sound and appropriate dynamic testing procedure has been employed in this research work. It is based on measuring the structural response model (i.e. FRFs) from which the vibration parameters are estimated, following the DTA recommended experimental route (Figure 4.6). As Ellis states, this procedure is a standard in the more advanced modal testing applications found in mechanical and aerospace engineering, but is not widely used in the construction industry which, according to Maguire (DTA, 1996) "has a fairly conservative reputation" with regard to the use of prototype dynamic testing technology. Therefore, this research has yet another purpose - to provide new case studies assessing the performance of the combined dynamic FE modelling and the advanced (FRF based) modal testing in civil engineering.

In order to succeed, the provision of a sufficient and measurable excitation of large floor structures weighing hundreds of tonnes has obviously been a matter requiring serious consideration. This problem strongly influences the selection of an excitation method in dual-channel input-output modal testing, which, in turn, governs the choice of key components and procedures which the testing facilities have to be able to accommodate.

4.6.1 Excitation Method Selection

An excellent overview of controlled excitation techniques for FRF measurements was published in 1977 by Brown et al. The survey, prepared for the US Society of Automotive Engineers, firstly observes that the number of possible excitation techniques for FRFs has been "greatly increased" by the advent of the digital spectrum analyser. It then classifies the possible excitation signals into four categories: (1) random, (2) periodic, (3) transient, and (4) operating. Dismissing the operating excitation on the basis that "input forces are very difficult to measure", Brown et al. list advantages and disadvantages of various excitation functions

comparing them on the basis of simplicity, testing time, cost and accuracy. The requirements for greater simplicity, shorter experimentation time and lower testing costs on one side, and greater accuracy on the other are, obviously, contradictory. Therefore, a compromise is usually required when selecting the method of modal testing excitation. Recognising the unbeatable performance of broadband excitations for speed of testing, Brown et al. concluded that "either pure random, periodic random or impact testing is the best." Therefore, a criterion for broadband excitation allowing fast field modal testing had been set.

Generally speaking, the testing techniques where the structural excitation is not measured could not be used as they do not produce FRFs. This reduces the available excitation methods to only two practical options.

The first is an instrumented large shaker which, attached to the floor, produces measurable floor excitation in some of the periodic, random or transient forms described by Brown et al. (1977). The second option is a sufficiently large instrumented impactor of the kind used in civil engineering applications by Maguire (1984), Brownjohn (1988), Caverson (1992), Eriksson (1994), Caetano and Cunha (1993), Agardh (1991, 1994), Bono et al. (1996), Raghavendrachar and Aktan (1992), and Green and Cebon (1993).

In this research the cheaper instrumented impact exciter was used. This choice was mainly governed by the limited research budget. Nevertheless, the broadband excitation criterion has been met by the selection of this exciter.

4.6.2 Selection of Dytran 5803A Instrumented Impact Hammer

With regard to the impulsive excitation device, two options existed: to develop in-house our own exciter such as the one made and used by Agardh (1994) or Eriksson (1994), or to buy a large hand held instrumented sledge hammer offered off-the-shelf by numerous manufacturers (SEM, 1989).

The already stated requirement for minimum development work governed a preference to be given to a manufactured hand-held instrumented sledge hammer for pre-purchase trials. Dytran UK allowed a two-week trial period for their largest model 5803A impactor suitable for floor testing (Dytran, 1995). After successful trials carried out along the recently published guidelines (ISO 7626-5, 1994; DTA, 1993b; 1993c) a decision to commission this particular exciter was made.

A detailed description of the hammer is given in the manufacturer's documentation (Dytran, 1992; 1995; Operating Guide Model 5803A Instrumented Impulse Hammer Twelve Pound Sledge, undated) and will not be repeated here. However, some practical aspects of the hammer operation will be described here as they strongly influenced its selection.

4.6.3 Signal Conditioning Electronics

The Dytran model 5803A impact hammer is usually called 'instrumented' because it has a piezoelectric force sensor mounted in its 12-pound (5.4 kg) head which is made of cast iron.

Generally speaking, electrical sensors used in modern vibration engineering typically comprise two 'sensing' devices or stages. The first device is a detector which usually transforms the mechanical measurand (force, acceleration, velocity, etc.) into some form of time varying motion. The second stage converts this motion, which is often a displacement, into a more suitable time-varying electrical signal. In the case of the hammer piezoelectric force cell, the first-stage detector is a very stiff SDOF spring-mass system built-in the hammer head which 'senses' the applied impact force as the dynamic displacement of the mass. This mass displacement is acting upon the stiff spring made of piezoelectric material and produces stress within it, which generates an electrical charge proportional to the stress. The basic role of the secondary 'sensing' device is, therefore, to 'collect' this electrical charge and produce an electrical signal which is analogous to the applied external force.

The electrical signal produced in this way is of a very low power and its size can further be reduced by the effects of the cables and other electronic components in the measurement chain. In order to prevent this happening, so called signal pre-amplifiers are used (Smith et al., 1996). For the sake of consistency it should be mentioned here that Ewins (1995) and a few other authors use the term 'amplifier' instead of 'pre-amplifier' to describe the same device. The purpose of (pre-)amplifiers is to convert the weak electrical signal into a form which is more suitable for passing along the measurement chain. These are elements performing the conversion step in the typical vibration measurement chain shown in Figure 4.1.

A word of extreme caution is necessary here because there are two types of pre-amplifiers typically used with piezoelectric sensors to achieve this: the voltage pre-amplifier and the charge pre-amplifier (Ewins, 1995; Smith at al, 1996). The two essentially differ in the way they convert the weak signal from the sensor. The voltage pre-amplifier does this in such a way that the sensitivity of the overall measurement system depends on the length and characteristics of the transmission cable. In other words, different cables produce different sensitivities which is unacceptable for field vibration measurements of the kind scheduled in this research. Fortunately, the charge pre-amplifier converts the weak piezoelectric charge into a usable electrical signal which is practically independent of the transmission cable properties and a hammer having this preamplifier is a suitable choice.

When checking which of the two types of pre-amplifier should be used with a particular piezoelectric sensor (in this case a force sensor, but it may be an accelerometer as will be seen later), the terminology is again rather confusing because different manufacturers use different names as trademarks for essentially the same thing. This amplifies the common problem of unclear terminology in vibration engineering as is fully recognised by the DTA (1993a) stating that:

> "...users and suppliers call their equipment by variety of names, depending on the background of the organisation and current fashion."

For example, Dytran's equivalent of the pre-amplifier capable of driving long cables is called the LIVM system which stands for the Low Impedance Voltage Mode system. Other similarly ambiguous abbreviations which may be found in the technical literature representing basically the same type of pre-amplifier arrangement are ICP, IEPE, ISOTRON, etc. The inconsistent terminology typically found in the technical and manufacturers' literature makes the selection of the equipment more complex and may easily lead to mistakes. The writer found the equipment pre-purchase trials a very useful safeguard against such errors.

The weak signals generated by piezoelectric force sensors should be passed through the charge pre-amplifier as soon as possible. Maguire (1984) used force (and acceleration) piezoelectric transducers having separate pre-amplifier boxes which had to be remotely placed close to the transducers and, therefore, required special protection from dust, moisture, etc. The pre-amplifiers were occasionally developing faults and, presumably, were inconvenient to carry around. They were also, to some extent, less safe under site conditions because it appears that they utilised 240V mains power.

From today's perspective such systems could be characterised as cumbersome. Rapid developments in micro electronics have enabled the charge pre-amplifiers to be designed as miniature integrated electronic circuits, usually battery powered, which can be built into sealed piezoelectric transducer casings. Such built-in charge pre-amplifiers are very convenient for field testing as they do not require carrying separate pre-amplifier boxes around which may slow down the testing. Serridge and Licht (1987) and Randall (1996) use the term "line-drive pre-amplifier" instead of the built-in (or in-built) charge pre-amplifier.

The Dytran model 5803A hammer features the LIVM built-in electronics. Therefore, it (nominally) satisfies the criteria for transmitting electrical signals generated by the force sensor along very long and inexpensive cables with very little distortion, and for easy site handling.

4.7 Vibration Response Transducers

In order to measure vibrations of concrete floors due to various excitations, it is necessary first to decide which time-varying motion is to be measured.

Two basic types of motion exist: linear motion and angular motion. Although possible, angular motion is notoriously difficult to measure (Ewins, 1995) and the scope of this research did not require it. Hence, one of the three time-varying linear motion parameters, displacement, velocity or acceleration, had to be selected together with an appropriate transducer.

4.7.1 Relative vs. Absolute Transducers

Detailed overviews of the types and principles of operation of vibrometers (for measurement of time varying velocity or displacement) and accelerometers are given in numerous standard texts (Buzdugan et al., 1987; Beckwith et al., 1995; Chu et al., 1996, Dally et al., 1996; McConnell, 1995; Usher & Keating, 1990) and will not be repeated here. However, the process of selecting a transducer suitable for vibration measurement in this research will be outlined.

All linear motion transducers can be conveniently divided into two groups (Usher & Keating, 1990; Chu et al., 1996) depending on whether or not they need a reference point: (1) relative (or fixed-reference) transducers and (2) absolute (or mass-spring) transducers.

As its name suggests, a relative transducer measures relative linear motion between two points. If one of those two points has a known movement (preferably no movement at all) then the unknown movement of the other point can be deduced. The point at which movement is known is termed the reference point. On the other hand, an absolute motion transducer does not require the reference point. It measures absolute motion of the point to which it is attached, where the reference is the past position of that point (usually at the moment when the measurement started). If a vibrometer is used to measured dynamic displacement or velocity (Beckwith et al., 1995), then it can work either as a relative transducer or as an absolute transducer. However, if an accelerometer is selected, then it typically works only as an absolute transducer (User & Keating, 1990).

Due to the nature of field dynamic testing, absolute transducers were preferred for this research. Whereas it may be easy to find or construct a fixed reference point in laboratory conditions, this is very difficult when performing short field dynamic testing of full-scale concrete floors.

Therefore, a decision to opt for the absolute displacement, velocity or acceleration transducer was made.

4.7.2 Selection of the Motion Measurement Parameter

Theoretically speaking, measurement of any of the three time-varying vibration motion parameters could lead to the other two by differentiating or integrating the time-varying signal, as appropriate (McConnell & Riley, 1993). The crucial difference between displacement and velocity transducers, and accelerometers lies in the dynamic properties of the mechanical primary sensing stage (Figure 4.11). Also, it is important which type of mechanical motion of the primary stage is actually 'sensed' by the secondary stage of the transducer. The secondary stage, as mentioned earlier, converts the mechanical motion of a primary stage into an analogous electrical signal directly proportional to the motion (Beckwith et al., 1995).

Absolute transducers typically utilise a mass, frequently termed 'seismic mass', as a part of the primary stage which is mounted in the transducer casing forming a SDOF system (Figure 4.11). From descriptions given

by Usher and Keating (1990), Beckwith et al. (1995) and Buzdugan et al. (1987), it can be concluded that the secondary stage of such a transducer is either a relative displacement or velocity meter which somehow gauges the corresponding relative motion between the seismic mass and the housing. This motion occurs when the supporting structure, that is the housing which is firmly attached to it, moves.

If the vibration frequencies measured are greater than the natural frequency of the seismic transducer SDOF system two options exist. Firstly, if a relative displacement is measured by the secondary device, its signal is directly proportional to the displacement of the moving structure for the range of excitation frequencies above the natural frequency ω_{ot} of the primary SDOF system (Curve A, Figure 4.12). Secondly, if relative velocity is measured by the secondary stage, then its signal is proportional to the velocity of the moving structure for the frequencies above ω_{ot} (Curve A, Figure 4.12).

On the other hand, if the vibration frequencies measured are lower than ω_{ot}, the measurement of relative displacement produces an electrical signal proportional to the acceleration of the supporting structure (Curve B, Figure 4.12).

In all three cases mentioned, it is important to note that the proportionality between the generated signal and the corresponding motion measured actually means that the sensitivities should be as constant as possible for all frequencies either above or below ω_{ot} (Figure 4.12), depending on which transducer is used. However, in reality, this requirement is only approximately satisfied. The frequencies for which this condition is satisfied within a pre-defined error margin determine the operational frequency range of the transducer.

4.7.2.1 ABSOLUTE TRANSDUCERS MEASURING TIME-VARYING DISPLACEMENTS

In order to increase the lower end of their frequency range of operation, these transducers should have their natural frequencies as low as possible because the useful frequencies are only well above ω_{ot}. This means that the primary stage of this instrument has, in fact, to be a relatively large mass supported by relatively soft springs. The large inertia of this SDOF system means that the mass remains in place while the transducer housing moves when measuring frequencies above ω_{ot}.

A linear variable differential transformer (LVDT) may be used as the secondary sensing element (Dally et al., 1993). Buzdugan et al. (1987) describe other relative displacement sensors, such as capacitance probes, which may be used as the secondary stage. Chu et al. (1996) describe in detail the principles of operation of the LVDT-based absolute displacement measurement transducer which they call 'differential-transformer pickup'. Relatively large relative motion between the mass and the transducer casing typically occur in all transducers of this kind.

4.7.2.2 ABSOLUTE TRANSDUCERS MEASURING TIME-VARYING VELOCITIES

These are based on the principle of electromagnetic induction caused by the relative movement of a magnetic field and a conductor. The relative movement sensed is in fact the relative velocity between the mass and the

transducer housing (Figure 4.12). The voltage generated by the induction is proportional to the relative velocity, which is, in turn, proportional to the velocity of the vibrating structure for frequencies above ω_{ot}.

4.7.2.3 ABSOLUTE TRANSDUCERS MEASURING TIME-VARYING ACCELERATIONS

Transducers for measuring vibratory acceleration are most commonly used in vibration engineering today. Various accelerometer designs differ in principle only in the sensors used as the secondary transducer stage measuring the relative displacement between the seismic mass and the accelerometer housing (Figure 4.12). The following two designs are most common in civil engineering applications:

- Servo (or force-balanced) accelerometers. These utilise a relative displacement transducer, such as an LVDT or capacitance sensor, which generates a feedback (or servo-loop) signal. This signal drives a coil which generates a force restoring the seismic mass to its original position. Acceleration, which is proportional to this restoring force, is measured as the restoring signal.
- Piezoelectric accelerometers. These utilise the piezoelectric effect in exactly the same way as the already introduced piezoelectric load cells do, the only difference being the nature of the force which causes the mass of the SDOF primary stage to move dynamically. By sensing this force, the piezoelectric element, which is actually the stiff spring of the SDOF absolute transducer (Figure 4.11), gauges the relative displacement between the mass and the accelerometer housing. This displacement is, nevertheless, directly proportional to the support (i.e. structural) acceleration (Curve B, Figure 4.12) for the useful range of frequencies below ω_{ot}. Therefore, the piezoelectric element has a dual role in a piezoelectric accelerometer. Firstly, as a 'spring' it is a part of the primary mechanical SDOF stage of the transducer. Secondly, as a 'relative displacement transducer' it forms the secondary stage together with the associated electronics.

When deciding which motion parameter to measure (displacement, velocity or acceleration) it is important to chose the one which is actually required by the vibration problem being investigated (Ellis, 1992). Applying this principle, with regard to the modal testing part of this experimental work, any motion parameter could have been used. However, considering the assessment of the vibration serviceability of floors, most of the assessment criteria and scales are based on the acceleration levels. Therefore, this consideration indicated a preference for accelerometers.

In addition, vibrometers are in general more fragile than accelerometers. This is because the SDOF system they utilise as the primary mechanical stage must be much 'softer' than for an accelerometer. As a consequence, the large mechanical moving parts of vibrometers are prone to wear and fatigue failure. Endevco (Shock and Vibration Measurement Technology, undated) states that new piezoelectric accelerometer designs are much more robust and usually outperform vibrometers in the low-frequency region. This is an important observation because poor performance in the lower frequency region was the main problem of early piezoelectric accelerometer designs.

With regard to the research project brief, a conclusion was reached that vibrometers have serious disadvantages and no obvious advantages when compared with modern accelerometers. Therefore, the decision was made in principle to commission accelerometers as the vibration response transducers.

4.7.3 Selection of Accelerometer Design

Servo accelerometers are very popular in the civil engineering sector. For years they were the most precise and sensitive acceleration transducers available (Usher & Keating, 1990). Typical operational frequency ranges of these accelerometers are between 0 and 50 Hz only, and their sensitivity goes down to micro-g acceleration. These characteristics, together with excellent linearity, made them almost perfect transducers for this research.

However, these transducers are also as fragile as the vibrometers. Relatively cheap and much more robust piezoelectric accelerometers able to compete with the highly sensitive servo accelerometers, have recently been made commercially available (Shock and Vibration Measurement Technology, undated). Hence, when compared with servo accelerometers, a slight advantage was given to ultra-sensitive piezoelectric accelerometers.

Piezoelectric accelerometers are by far the most commonly used vibration response transducers today. A quick overview of the product ranges of large manufacturers, such as Endevco, Bruel & Kjaer and Dytran, revealed that each supplier offered at least one piezoelectric accelerometer suitable for this research. These transducers satisfy practically all general and specific requirements which will be briefly outlined in the following section.

4.7.4 Piezoelectric Accelerometer Requirements for Floor Vibration Measurements

Chu et al. (1996) recommend considerations of the following parameters when selecting an accelerometer: (1) sensitivity, (2) resolution, (3) transverse sensitivity, (4) amplitude linearity and limits, (5) frequency range, (6) physical size, and (7) environmental effects (temperature, humidity, acoustic noise and strain sensitivity). Some of these considerations are clearly related to the requirements of vibration measurement in the mechanical and aerospace engineering disciplines where accelerometer properties such as its mass, size, resistance to high humidity and temperature, and low-transverse sensitivities are more important.

However, following these recommendations, the writer formulated more focused conditions which the piezoelectric accelerometers to be used for measuring vibrations of concrete floors had to satisfy. These are based on the literature reviewed and the writer's experience gained during the preparatory phase of this research.

4.7.4.1 ACCELEROMETER DYNAMIC RANGE REQUIREMENTS

When measuring point mobility of full-scale concrete floors using hammer excitation, Caverson (1992) typically measured peak accelerations of approximately up to 0.2g. Heel-drop tests typically produced 0.05g, while peak accelerations due to walking were approximately 0.007g. Eriksson (1994) measured a walking acceleration time history on a prototype concrete floor which peaked at 0.004g. This was quite comparable with Caverson's data.

On the other hand, in order to ensure maximum flexibility in the measurement system, all accelerometers had to be able to measure accelerations of up to 1g. To conclude, it was determined that the accelerometers had to be able to measure accelerations as low as 0.00001g and as high as 1g.

4.7.4.2 ACCELEROMETER FREQUENCY RANGE REQUIREMENTS

Considering results presented by Caverson (1992), Eriksson (1994) and others who tested floors in the past, it was estimated that the typical frequency range of interest when testing full-scale concrete floors, should be between approximately 3 Hz and 30 Hz, approximately, for hammer and human induced excitations. Therefore, a requirement for an accelerometer to have flat frequency response between 1 Hz and 50 Hz has been set.

4.7.4.3 ACCELEROMETER SENSITIVITY REQUIREMENTS

The requirement for a low operational frequency range typically means that the sensitivity of the transducer is inevitably higher. These more sensitive sensors also tend to have lower electrical noise levels (Wilcoxon Research, 1995). However, due to the fact that fairly low levels of acceleration (milli-g) were expected to be measured, a requirement for sensitivity of at least 1V/g has been set. This was done to ensure that the signals corresponding to very small accelerations are above the electrical noise of the measurement system with unity gains set on all signal conditioning devices.

However, sometimes manufacturers claim high sensitivities of transducers which, actually, correspond to gains of the signal conditioning electronics higher than 1. For example, Wilcoxon Research (1996) states that their "ultra highly sensitive" Model 731/P31 seismic accelerometer and amplifier has "selectable sensitivities of 10, 100 and 1000 V/g". The sensitivity of this system corresponding to unity gain is, in fact, only 10V/g, the other two "sensitivities" correspond to gains of 10 and 100. With regard to low-level measurements a statement like this can be quite misleading as higher signal conditioning gains tend to amplify electrical noise together with the low-level measured signals. This means that low-level signals can still be buried in noise if the transducer's unity gain sensitivity is not sufficient (even if the highest gain nominally generating 1000V/g is selected).

To conclude, when selecting a transducer it is important to be aware that there is a difference between the 'sensitivity' and the 'gain' of a transducer and signal conditioning system. Whereas sensitivity is a measure

of the ability of a transducer to measure low-level signals, the gain plays an important role in making such low-level voltages 'readable' by other parts of the measurement system. This is so because the storage, analysis and display parts of an instrumentation system (Figure 4.1) have their own electrical noise levels above which the transducer's electrical signal must be.

4.7.4.4 ACCELEROMETER SURVIVABILITY AND OTHER REQUIREMENTS

In order to ensure robustness of the accelerometer during field operation a shock limit of at least 500g has been set.

Cheap cabling, easy future upgrades of the signal conditioning electronics and compatibility with the rest of the measurement chain (Figures 4.1 and 4.10) are some of the specific requirements which the piezoelectric accelerometers had also to satisfy.

4.7.5 Selection of Piezoelectric Accelerometer Design

Having formulated the specific requirements of the accelerometer to be used in this research, a suitable piezoelectric accelerometer design had to be selected.

Accelerometers were first made in the 1950s. Since then they have undergone tremendous development which, in the case of piezoelectric accelerometers, has resulted in approximately a thousand or more models being available today. However, not all models are suitable for all applications and a careful selection is required. In order to help decide which piezoelectric accelerometer design and model to select manufacturer Endevco (Shock and Vibration Measurement Technology, undated), for example, divide vibration acceleration measurements into the following typical categories:

- mini-structure measurements
- low-g measurements
- shock measurements
- high-frequency measurements
- machine monitoring measurements
- high-temperature measurements
- nuclear measurements
- low-temperature measurements
- general vibration measurements.

Measuring concrete floor vibrations falls into the "low-g" and not the "general vibration measurements" group, as may be perceived. The "general vibration measurements" are performed usually in

mechanical/acrospace engineering disciplines and transducers optimised for such exercises typically do not posses the required sensitivity and frequency range for detecting low-level low-frequency concrete floor vibrations.

Early piezoelectric accelerometer designs suffered from low sensitivity and signal to noise ratio problems when measuring frequencies below 100 Hz. This made early measurements of frequencies below, say, 5 Hz using piezoelectric accelerometers "almost impossible" (Shock and Vibration Measurement Technology, undated). Older textbooks and papers tend to present piezoelectric accelerometers as not particularly suitable for the measurement of frequencies below, approximately, 10 Hz. However, recent advances in their design over the last decade have remedied these problems. Nowadays, piezoelectric accelerometers capable of measuring frequencies down to 0.1 Hz are commercially available.

Licht et al. (1987) explain that the main thrust in the improvement of the piezoelectric accelerometer design was concentrated on the elimination of quite large electrical signals generated by (1) non-vibratory motion, such as temperature variations, and (2) vibratory motion, such as the accelerometer case straining due to bending.

Almost all piezoelectric accelerometers commercially available today utilise either the compression design or the shear design (Licht et al., 1987). Externally they look practically the same. Early accelerometer designs were compression type (Figure 4.13) where the electrical charge produced in the piezoelectric element is proportional to the normal stress. However, piezoelectric material under shear can also generate electrical charge proportional to the shearing force, so this characteristic can also be used when designing a piezoelectric accelerometer (Figure 4.13).

It is now well established that the compressive designs are much more susceptible to transverse vibrations, strain of the accelerometer housing and external temperature when compared to their shear counterparts (Licht et al., 1987; Smith et al., 1996; Serridge & Licht, 1987). This is particularly important when measuring low-level vibrations where relatively small unwanted signals can completely obscure the signal from the actual minute measurand deteriorating its signal-to-noise ratio. This was the reason why early compressive designs were failing to measure low-level low-frequency accelerations.

For the low-g measurements, as required by this research, the shear accelerometer design is the recommended choice.

4.7.5.1 ACCELEROMETER SIGNAL CONDITIONING ELECTRONICS

Similarly as for the piezoelectric load cells introduced earlier, piezoelectric accelerometers require special consideration of the signal conditioning electronics. In order to make possible transmission of the accelerometer signals through very long cables with as little as possible distortion, piezoelectric accelerometers with built-in charge amplifiers should be selected. Detailed discussions of these internally amplified piezoelectric sensors and specifics of their operation are given in several standard textbooks and

papers (McConnell, 1995; Dally et al., 1993; Serridge & Licht, 1987; Chu et al., 1996; Randall, 1996). Certain practical consequences of some of these issues with regard to the instrumented hammer testing have been highlighted by Pavic and Waldron (1996b).

4.7.6 Selection of Piezoelectric Accelerometer Model

Three models of piezoelectric accelerometers were looked at in greater detail, and assessed against the specifications outlined earlier. These are:

1. Bruel & Kjaer Model 4370,
2. Endevco Model 7754-1000, and
3. Dytran Model 3100B24.

4.7.6.1 BRUEL & KJAER MODEL 4370

This accelerometer was recommended by the technical personnel of Bruel & Kjaer (UK) who were briefed in detail about the type of the vibration measurements on concrete floors for which the accelerometer was required. After its arrival for the pre-purchase trials, an inspection of the accelerometer and its technical documentation was performed. Having nominal sensitivity of only 100 mV/g and no internal built-in electronics, signals produced by this accelerometer were very sensitive to the movements of even a very short micro-coaxial cable with which the accelerometer was delivered. Performance of the accelerometer at low frequencies was also far from satisfactory. It was concluded that, despite the technical advice given by Bruel and Kjaer technical division, their Model 4370 was not suitable.

4.7.6.2 ENDEVCO MODEL 7754-1000

Endevco was the first company to have started production of low-noise shear accelerometers. Endevco accelerometers, such as Model 7751-500, having 500 mV/g sensitivity are traditionally used in the civil engineering sector (Farrar et al., 1994). In 1993 Endevco launched a state-of-the-art piezoelectric ISOTRON™ (i.e. with built-in electronics) accelerometer Model 7754-1000. This is a hermetically sealed device preventing internal contamination due to environmental factors such as humidity and dust. It also has high nominal sensitivity of 1V/g, which makes it the most sensitive Endevco piezoelectric accelerometer with integral electronics. Its state-of-the-art signal conditioning allows a very good near-DC frequency response with only 5% distortion between 0.2 Hz and 400 Hz. Moreover, it utilises the patented Endevco ISOSHEAR™ (shear) design which is insensitive to most non-vibratory inputs and was purposely designed to compete with servo accelerometers. It is meant to be used in seismic, building and deep space vibration measurements, the application areas traditionally reserved for servo accelerometers in the past. Also, apart from the excellent signal-to-noise ratio and low-frequency response, Model 7754-1000 has one indisputable

advantage over many other absolute transducers suitable for low-frequency measurements. It has a guaranteed shock survivability of 1000g, which makes it very robust.

4.7.6.3 DYTRAN MODEL 3100B24

This model is, officially, denoted as "seismic" (Dytran, 1992; 1995), which implies that it is highly sensitive. It has a nominal sensitivity of 1 V/g and built-in electronics which satisfies two of the previously described selection criteria. However, Model 3100B24 is a 'noisy' compression type piezoelectric acceleromcter having a broadband noise floor which is 40 times higher than the noise floor of Endevco Model 7754-1000. It also has a poorer low-frequency response. Finally, it can survive shocks of only 200g.

Pre-purchase trials of the Endevco 7754-1000 accelerometer confirmed its very good performance and a decision was made to commission a pair of Model 7754-1000 with matching Model 102 ISOTRON signal conditioning and Model 109 low-noise power source. The cost per channel was high (£1800) and not more than two high quality transducers of this kind could be afforded by the research project budget at the time. Important properties of this accelerometer are summarised in Table 4.1.

In addition, despite all the problems encountered with the Dytran accelerometer, a (reluctant) decision has been made to commission as a backup a pair of 3100B24 together with Dytran Model 4105 battery powered current source for driving the internal accelerometer electronics. The price per channel utilising this accelcrometer was only £700 (Table 4.1). Pre-purchase trials performed with this accelerometer put side by side high-spec Endevco 7754-1000 showed that Dytran 3100B24 produces noisier signals at low-level vibrations (for frequencies of 2 Hz and higher), but the results were still very reasonable, which gave more confidence in this transducer.

Table 4.1: Summary of important properties of the commissioned accelerometers

Relevant accelerometer characteristics	Endevco model 7754-1000	Dytran model 3100B24
Nominal sensitivity	1V/g	1V/g
Frequency range (±5%)	From 0.2 Hz to 400 Hz	From 2 Hz to 1000 Hz
Linearity range	From 0.000001g to 5g	From 0.001g to 5g
Battery powering option	Yes	Yes
Broadband noise level	0.00001g RMS	0.0004g RMS
Survivability	1000g	200g
Price per channel	£1800	£700

4.8 Accelerometer Mounting and Signal Transmission

Serridge and Licht (1987) state that totally incorrect vibration measurements may result from careless accelcromcter mounting and poor signal transmission. In addition, Endevco course notes (Shock and

Vibration Measurement Technology, undated) claim that "connectors and cables are usually the weak link in any instrumentation chain". Therefore, it is not surprising that accelerometer manufacturers typically publish lengthy general explanations of how to properly mount an accelerometer to the vibrating structure and connect it to the rest of the measurement chain (Serridge & Licht, 1987; Dytran 1992; 1995). These will not be repeated here. However, the nature of the field measurements in this project required some additional special considerations of accelerometer mounting and cabling. These will be briefly outlined here.

4.8.1 Accelerometer Mounting onto Concrete Floors

Numerous technical papers warn that, in order to measure structural vibrations accurately, an accelerometer has to physically follow the movement of the structure. In addition, the literature offers a range of techniques for fixing an accelerometer to the vibrating structure by methods such as direct studs, cement, self-adhesives, magnets and beeswax mounting (ISO, 1987; BSI, 1989). The selection of each of these methods depends on the specifics of the vibration measurement being performed. Even the far reaching DTA Handbook on Guidelines to Best Practice on Instrumentation (1993a), covering all aspects of dynamic measurements across engineering disciplines, does not offer anything other than these mounting techniques which are typically used in mechanical and aerospace engineering applications where high frequency and high-acceleration levels are normally encountered.

However, these methods were not considered to be suitable when measuring vertical vibrations of full-scale concrete floors. Practicalities, such as the limited testing time and likely reluctance of the floor owners and/or users to allow any local damage to be caused to the concrete slabs, effectively prevented any of the mounting solutions suggested. Fortunately, other accelerometer attachment methods exist and are perfectly acceptable when measuring vertical vibrations of concrete floors.

These methods utilise mounting of an accelerometer on a heavy base plate which freely sits on a floor without any special attachments (Figure 4.14). The plate is supported at three points only to ensure its stability. An accelerometer, with its sensitive axis positioned in the vertical direction, should be firmly attached to the base plate by any of the standard methods described above. Direct stud mounting (DTA, 1993a) was used successfully on a 2 kg base plate made of steel (Figure 4.14). An accelerometer set-up in this way measures the base plate movements with sufficient accuracy. The base plate is under gravity load from self weight. When the floor starts vibrating, the base plate will faithfully follow the floor movements provided that its peak acceleration is less than 1g. Concrete floors normally satisfy this condition.

This accelerometer mounting method is typically used in the civil engineering applications (bridges, dams, floors, etc.) where vertical low-level accelerations are commonly measured. University of Bristol (Caverson, 1992) and EMPA (Cantieni, 1996) both frequently use this simple set-up. Updating of International Standard 5348 (ISO, 1987), British Standard (BSI, 1989) and the DTA (1993a) instrumentation handbook is obviously

required in order to promote this type of accelerometer mounting in the vibration engineering community where appropriate.

4.8.2 Accelerometer Signal Transmission and Connections

Caverson (1992) used relatively long micro-coaxial cables which consisted of numerous shorter cables linked via micro-dot connectors (Figure 4.15). Having been actively involved in Caverson's field tests, the writer quickly became aware of the frequent problems caused by connection faults in the signal lines, mainly due to dirt, dust and water at the micro-dot connection points. Concluding that these connectors are not suitable for field work, especially if there are lots of them, it was decided to set up the transmission lines in the new testing kit using standard coaxial cable (which is approximately 10 times cheaper than the micro-coaxial cable used by Caverson). In order to ensure easy site handling with a minimum number of connectors, it was decided to use pieces of either 50 m or 100 m long coaxial cables which would be connected together if longer signal transmission was required. Instead of the micro-dot connectors, BNC connectors mounted at the ends of coaxial cables were used (Figure 4.15). The writer used this cabling set-up as a member of the field testing team involved in the vibration measurement of a long-span footbridge at Aberfeldy, Scotland (Pimentel, 1997). Unfortunately, the BNC connectors proved to be extremely unreliable as 70% of them failed after a week of intensive field work requiring daily setting up and dismantling of the long signal lines. The reason for this was the poor resistance of the BNC connections to the pulling forces which inevitably develop during the site handling of the coaxial cables.

Therefore, the failing BNC connectors were replaced by more robust XLR connectors supplied by RS Components (1997). Figure 4.15 shows the micro-dot, BNC and XLR connectors. Performance of the XLR connector proved to be satisfactory.

4.9 Data Storage, Analysis and Display Facilities

Vast technical literature exists explaining the purpose and operation of data storage, analysis and display facilities, the last three elements of the measurement system (Figures 4.1 and 4.10). Therefore, only some specific aspects of the commissioning of the data storage, analysis and display facilities, directly related to this work will be outlined here.

4.9.1 Data Storage

Since short field testing times were anticipated, only limited signal processing and data analysis could be performed on site, mostly to ensure good quality data (Pavic & Waldron, 1996b; Pavic et al., 1997), but also to determine relevant parameters for the vibration response measurements due to walking. Therefore, a tape recorder, which allows storage of large amounts of analogue data, and their subsequent off-site digital re-sampling and analysis, had to be commissioned. This is important because selecting the best signal sampling and digital analysis parameters, such as frequency resolution, sampling speed and windowing, is basically a time consuming trial and error procedure (Pandit, 1991) which is difficult to perform during site testing.

Unfortunately, due to severe financial constraints it was not possible to use such a device in all field tests performed. However, when possible, either a 4-channel RACAL Store 4 (RACAL, 1979) or an 8-channel RACAL StorePlus VL (RACAL, 1993) was used. The usage of the former, which was more than 20 years old device, proved to be quite problematic, as reported in Chapter 5. It should be noted that the cost of data storage for the new RACAL StorePlus VL, which utilises VHS tapes, is an order of magnitude lower than for the obsolete RACAL Store 4 tape recorder.

4.9.2 Analysis and Display of Signals

Twenty years ago, in his review paper, Hudson (1977) recognised that mini computers have been a major step forward in the development of dynamic testing of full-scale civil engineering structures. He, also, stressed the importance of in-situ data processing and analysis by saying:

> "...the possibility of completing the analysis of test results on the spot during the course of the test before equipment and instrumentation has been removed is a major advantage of such (mini computer based) systems."

This important comment heavily influenced the selection of the appropriate analysis and display facilities as will be described.

An analyser is usually used to perform the signal analysis and display functions of the instrumentation chains shown in Figures 4.1 and 4.10. With regard to the selection of an appropriate analyser, capable of doing both single- and dual-channel signal analysis, DTA (1993a) emphasises that the problem of semantics also exists in the technical literature about signal analysers because:

> "An essentially similar piece of equipment may have a variety of names, e.g. FFT, spectrum, Fourier, dynamic-signal analyser may all be used to identify a single piece of equipment."

The Diagnostic Instruments PL202 (PL20 Series FFT Analyser/DSO Applications Manual, undated; PL202 Realtime FFT Analyser Getting Started Guide, undated) portable spectrum analyser has been selected for this project. Although there are many commercially available FFT analysers, a decision to commission this

particular instrument was not very difficult to make. Firstly, only seven manufacturers making portable spectrum analysers were found in 1994. These were: Hewlett Packard, Bruel & Kjaer, Onosokki, Zonic A & D, Hakuto, Lars & Davies and Diagnostic Instruments. Diagnostic Instruments are a leading manufacturer of portable spectrum analysers and their model PL202 satisfied basically all of the requirements such as fast push-button set-up, straightforward use, robustness, low cost and existence of an interface to high quality parameter estimation software (ICATS, 1995; 1997). It is worthwhile mentioning here that over the last three years its hardware and software were upgraded three times leading to a fully refurbished model Diagnostic Instruments model DI2200 FFT analyser (DI-2200 Real Time FFT Analyser/DSO Operating Manual, undated; Long Time Record DI-Card Operating Manual, undated). This proves that the instrument selected also satisfied the requirement for easy upgrades in order to follow fast developments in the field of portable instrumentation.

4.9.3 Modal Analysis Facilities

As already generally outlined, there are two routes to modal analysis: the experimental route, and the theoretical route (Figure 4.6). Both types of modal analysis had to be performed in this research.

Figure 4.10 indicates that the process of modal testing involves the interfacing of several measurement and analysis phases. The DTA (1993a) recognises that this interfacing is "often very difficult to achieve effectively". This is particularly true when linking FE modelling and modal testing phases. Due to time limitations for this project which did not allow for any development of these interfaces, it was decided to commission a commercially available packages for which all interfaces with the already selected hardware and software facilities existed. As already mentioned in Chapter 3, ANSYS FE code was selected for the FE modelling. On the other hand, for the experimental modal analysis ICATS (1995; 1997) suite of programmes was selected.

FE models from ANSYS can be easily exported and further manipulated by ICATS utility software. This compatibility between ICATS and ANSYS is a consequence of the fact that ANSYS has been used for more than 25 years in mechanical and aerospace engineering disciplines. ANSYS has powerful state-of-the-art vibration analysis options and it is capable of performing all FE modelling and analysis procedures required for advanced floor vibration serviceability investigations, as outlined in Chapter 3.

One of the special requirements which the curve fitting software to be selected had to satisfy was its ability to be run on site during field testing in order to comply with the DTA QA requirements (1993b; 1993c). Hence, ICATS as a PC based curve fitting package which could be run on a portable notebook PC was a natural choice. PC software is cheaper and easier to upgrade than the hard-wired firmware which is sometimes built into spectrum analysers. More than 20 upgrades of the ICATS software were received in the last 5 years. In addition, it should be stressed that the actual full 'modal analysis' and 'further analysis'

stages shown in Figure 4.10 are not meant to be performed in-situ and a desktop PC in the base with the same modal analysis software is an optimal solution.

This selection concluded the preparatory phase of the experimental research work presented in this thesis.

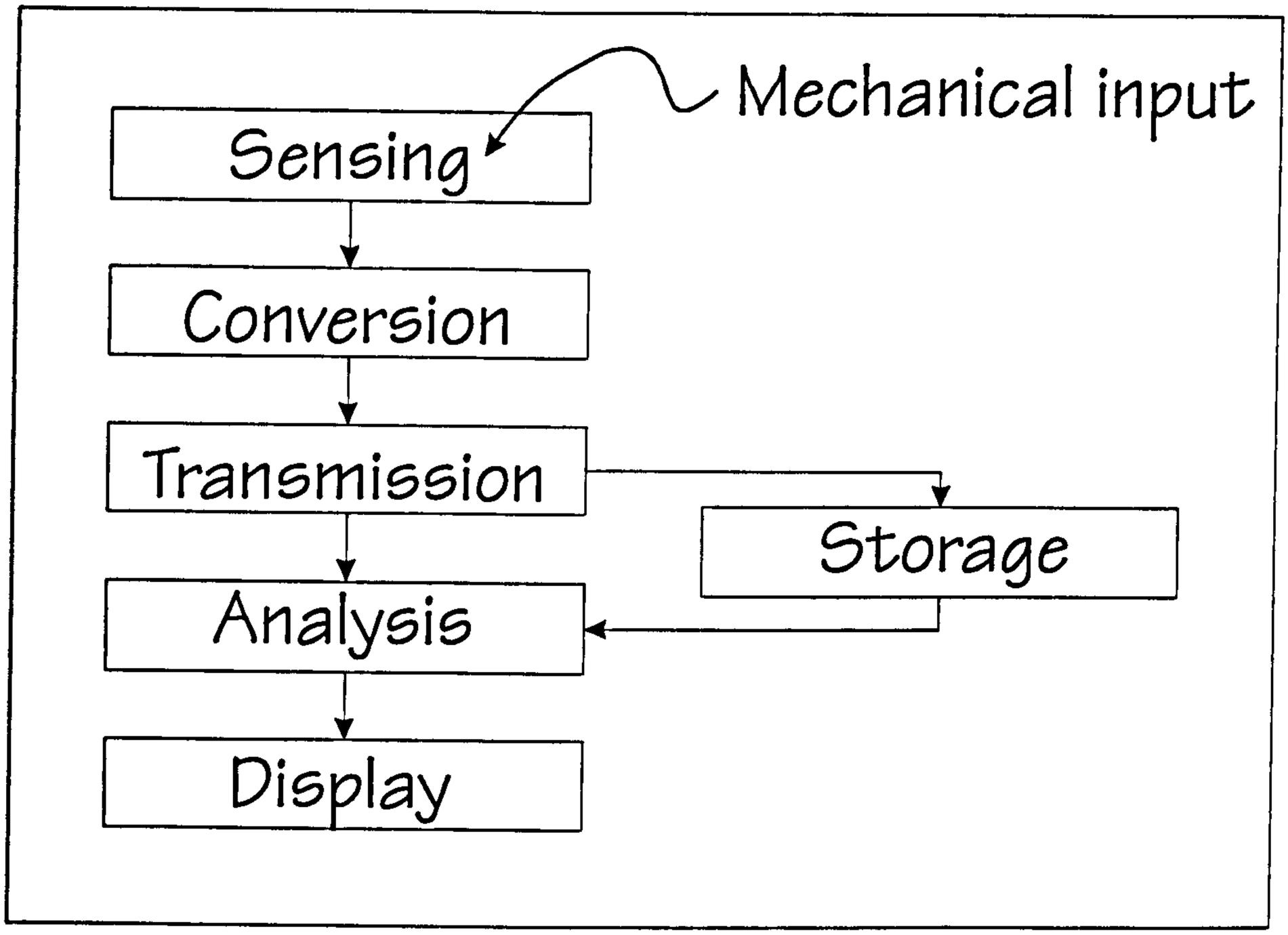

Figure 4.1: Measurement system.

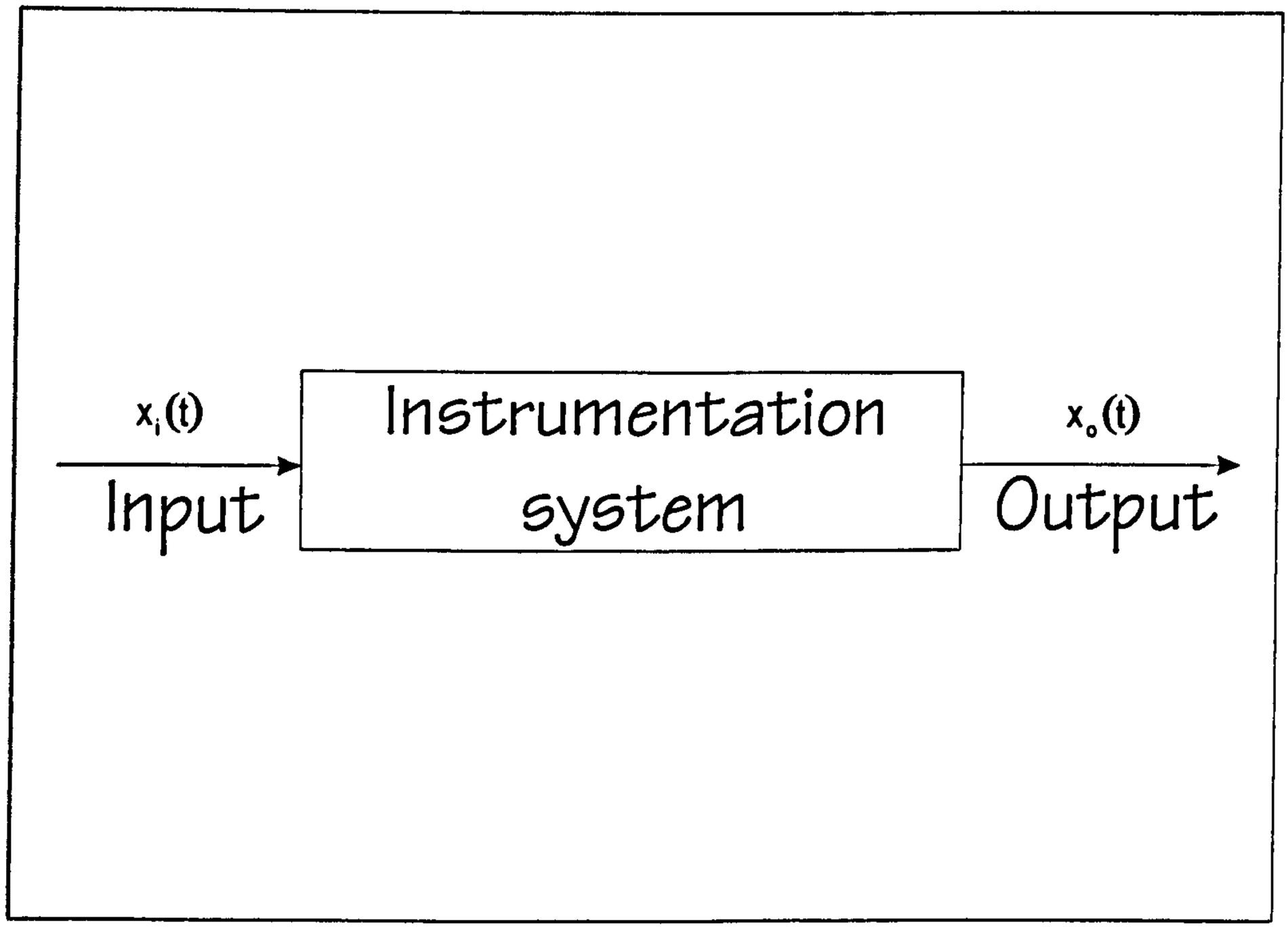

Figure 4.2: Input-output block scheme of an instrumentation system.

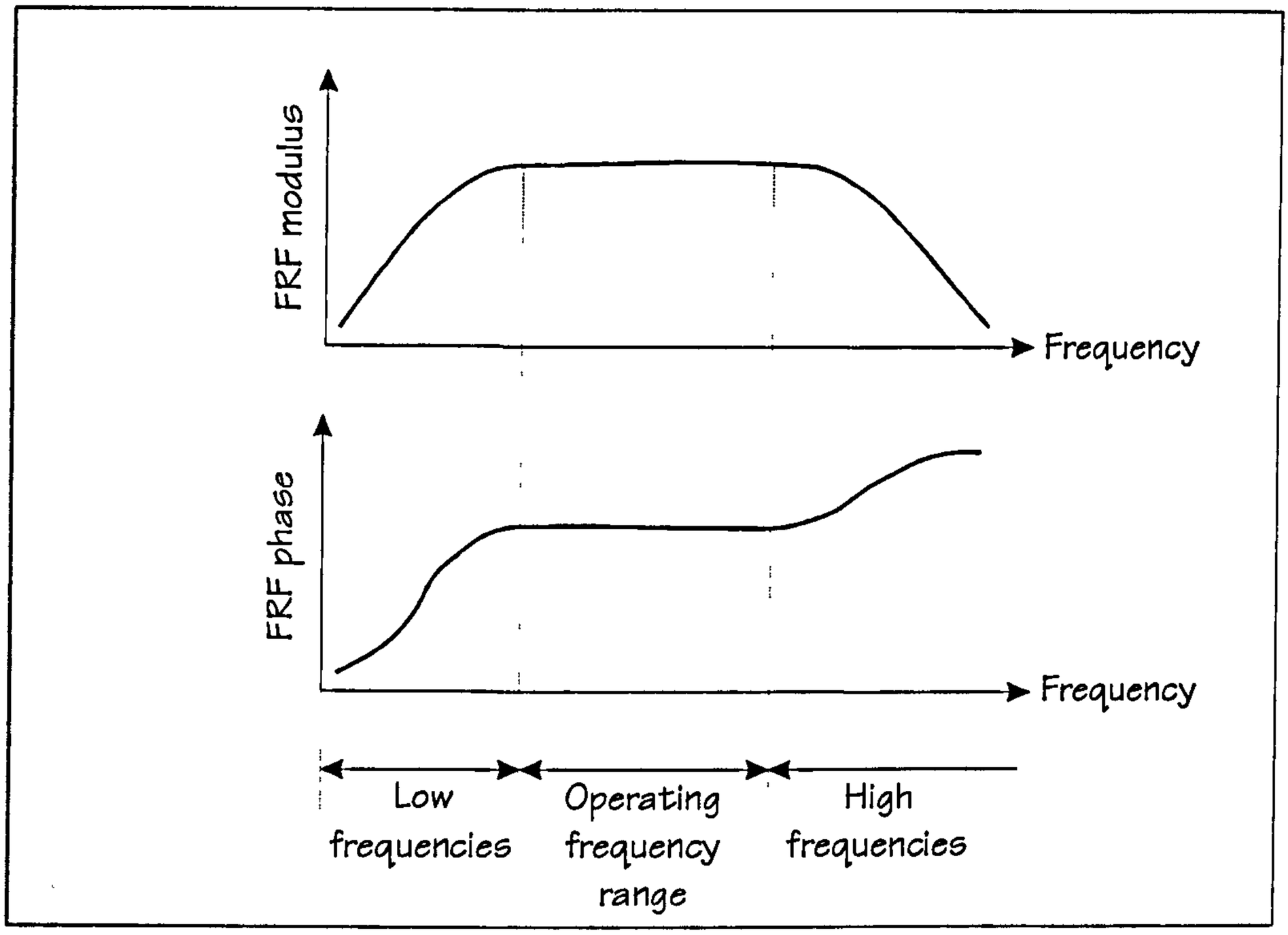

Figure 4.3: Operating frequency range (after Keast, 1967).

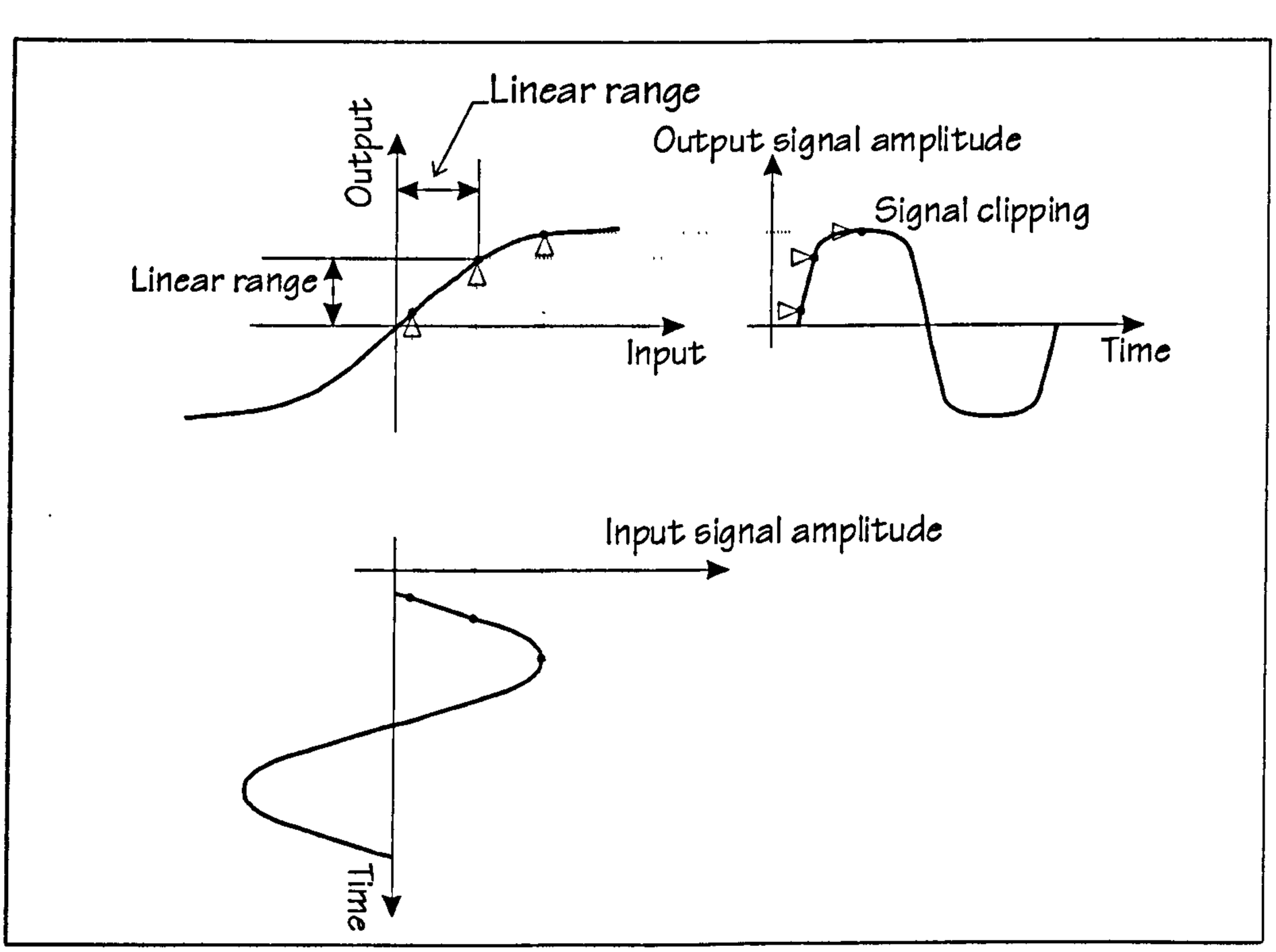

Figure 4.4: Linearity and operating ranges (after Keast, 1967).

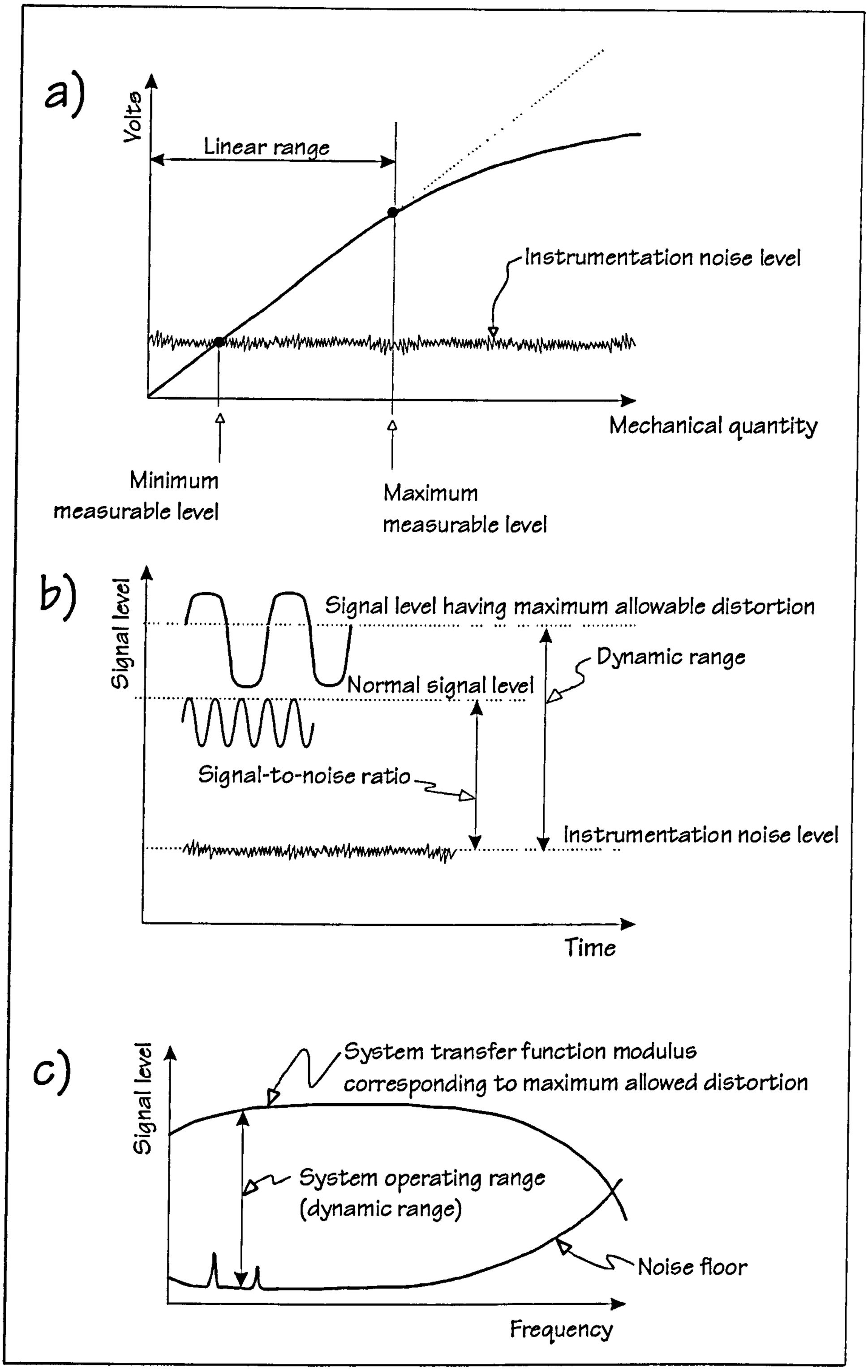

Figure 4.5: Noise and operating levels (after Smith et al, 1996; Keast, 1967).

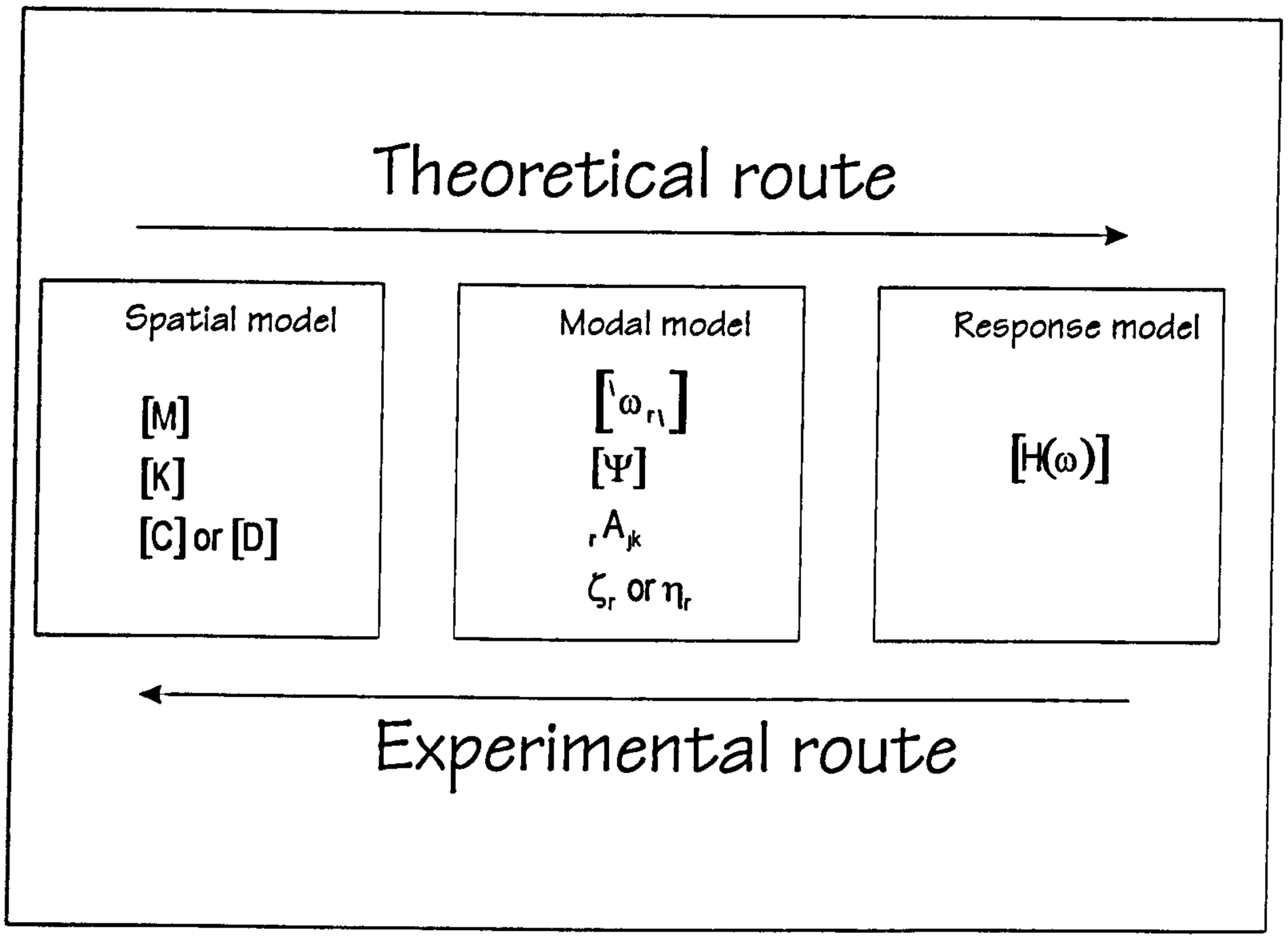

Figure 4.6: Theoretical and experimental routes to modal analysis (after Ewins, 1995).

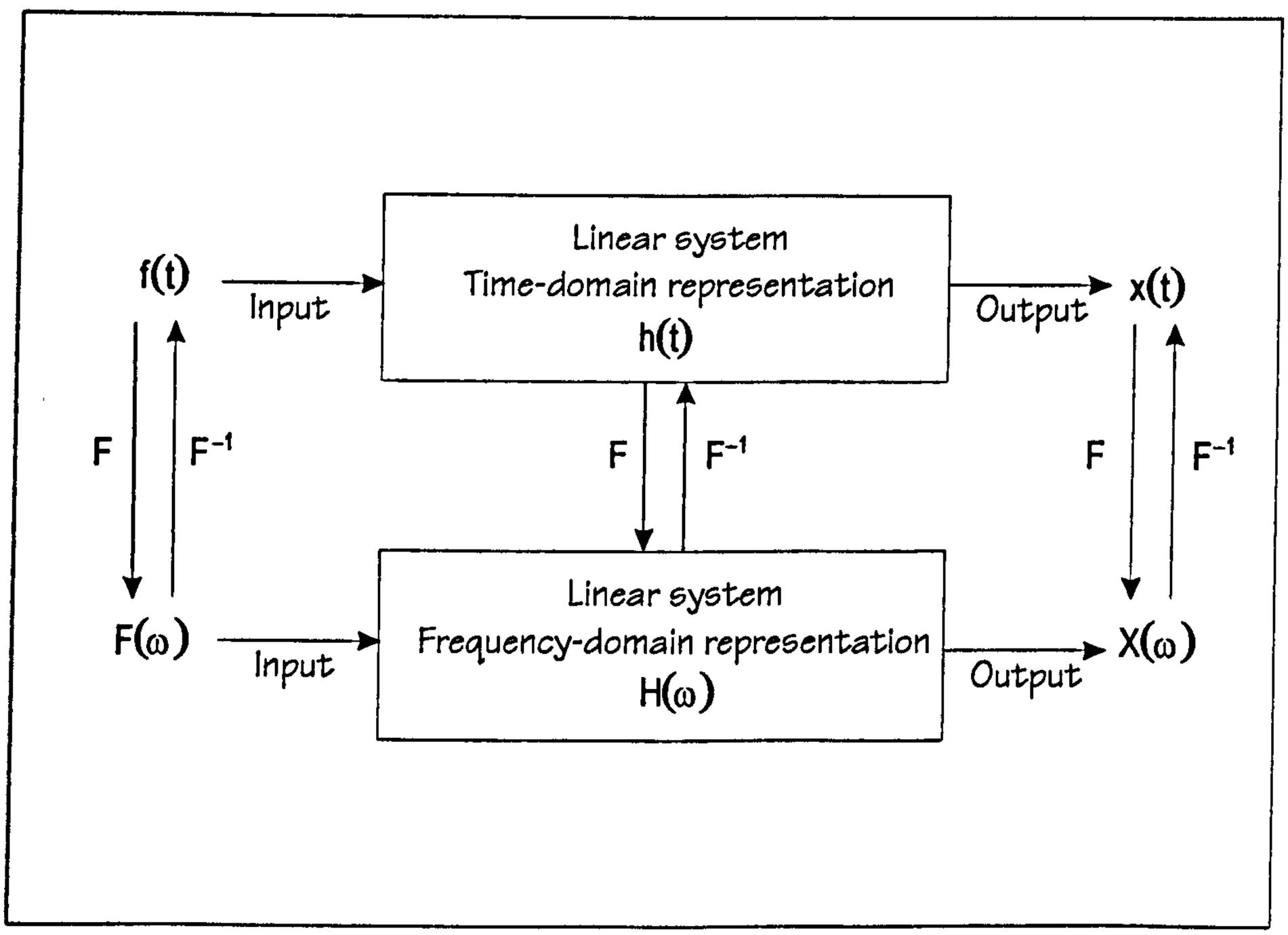

Figure 4.7: Liner system time and frequency domain representations (after McConnell, 1995).

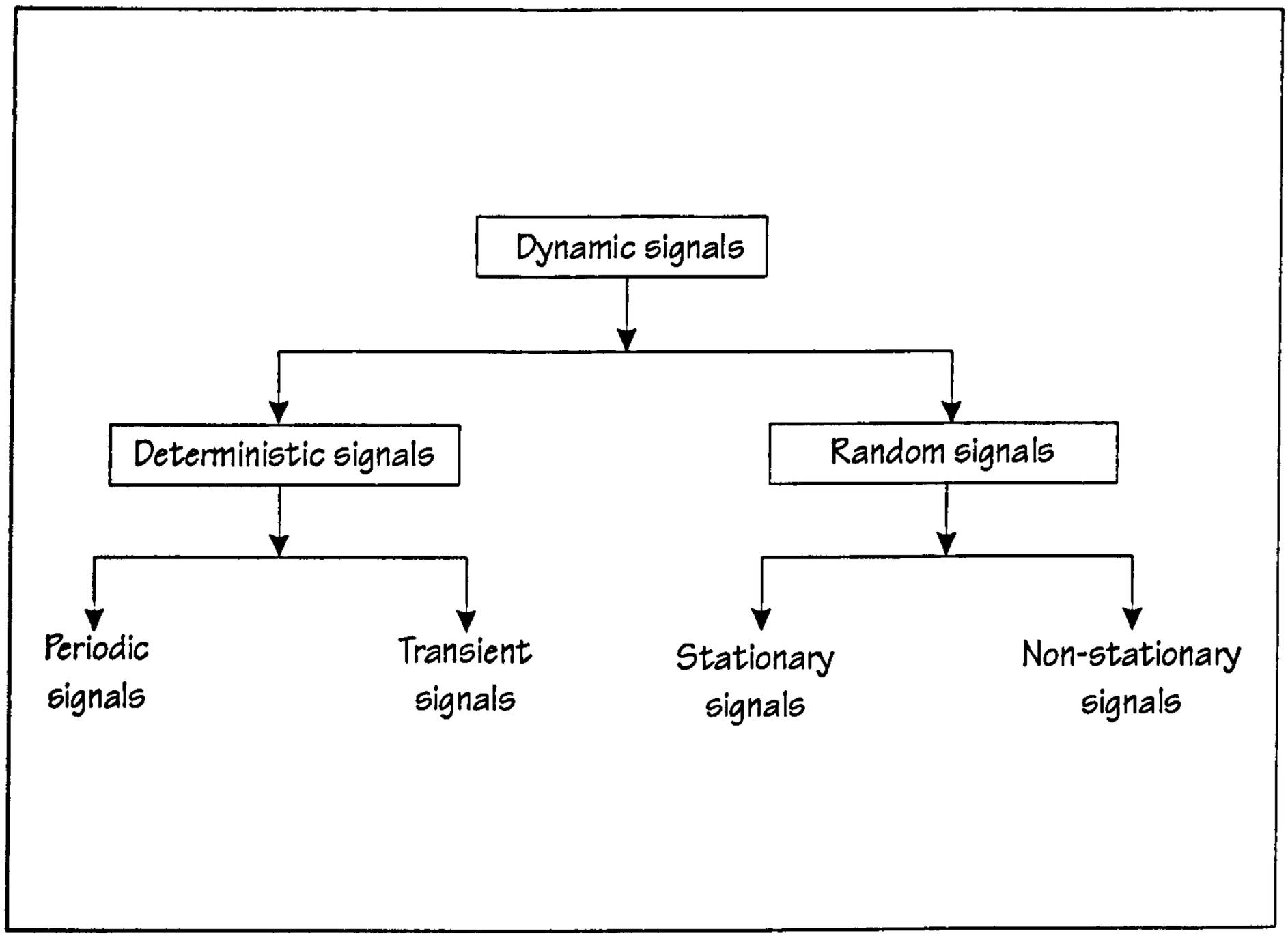

Figure 4.8: Classification of dynamic signals in vibration engineering (after McConnell, 1995).

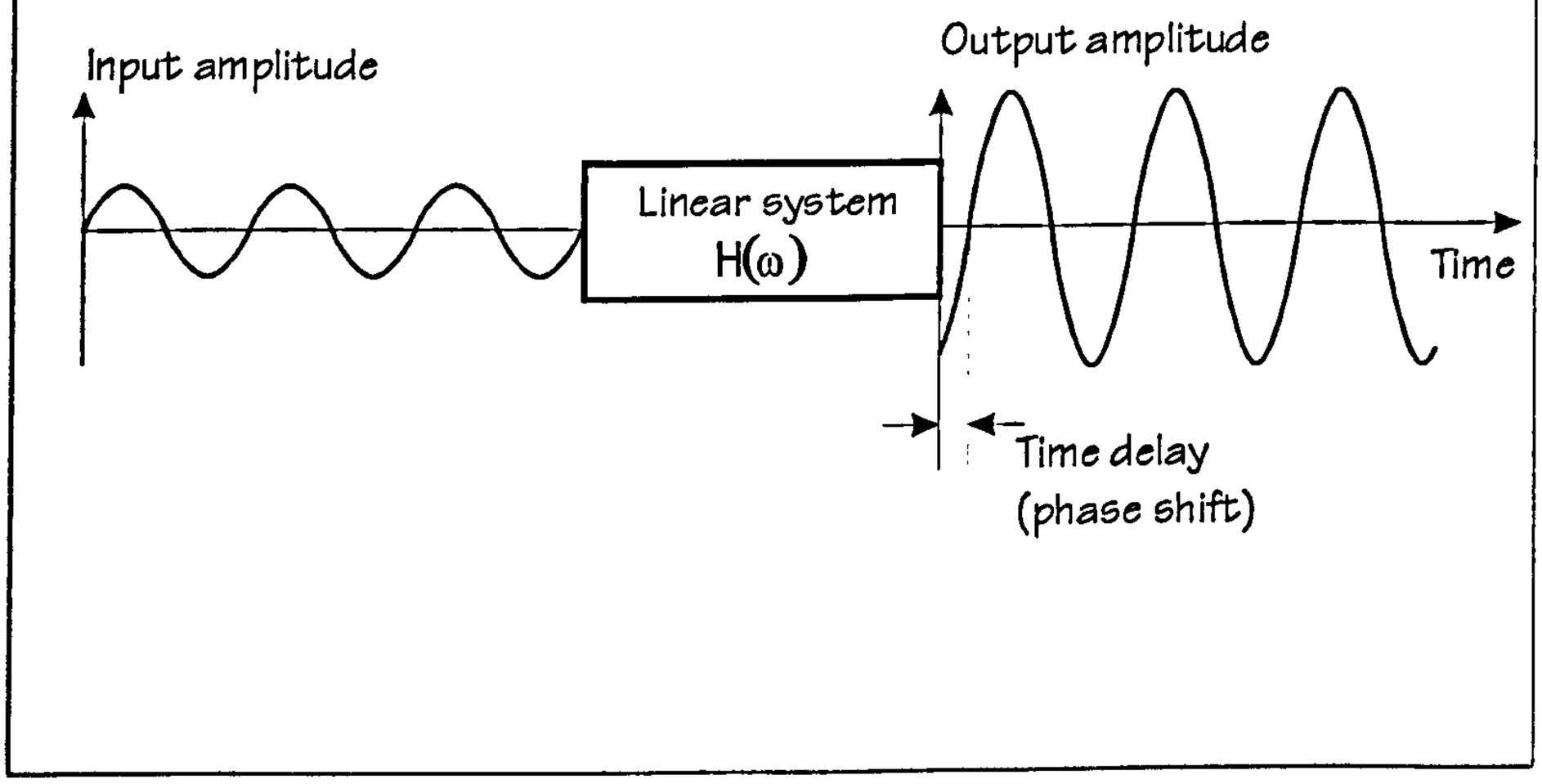

Figure 4.9: Modification of a harmonic input by a linear system FRF (after Dossing, 1988a).

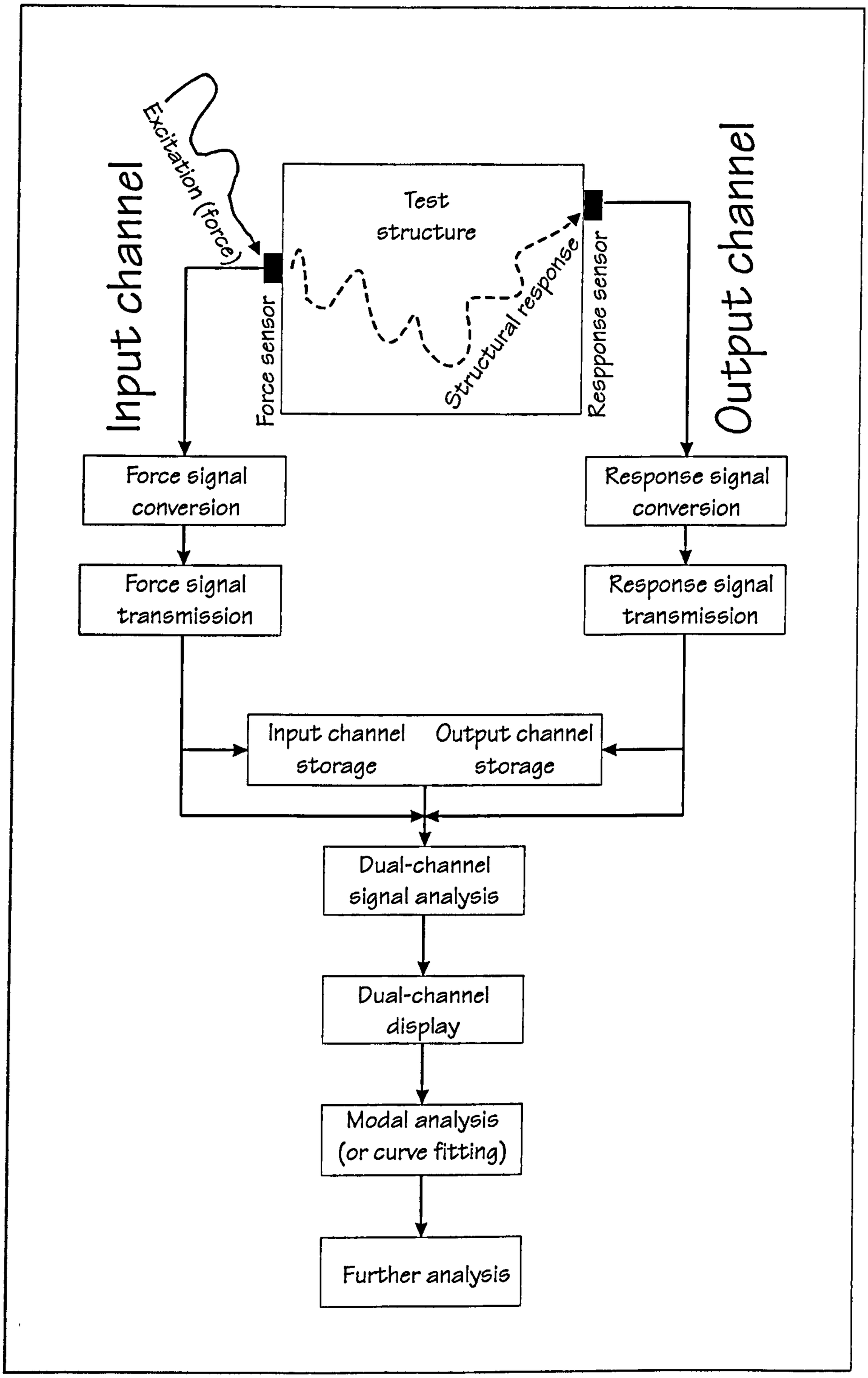

Figure 4.10: Modal testing instrumentation system.

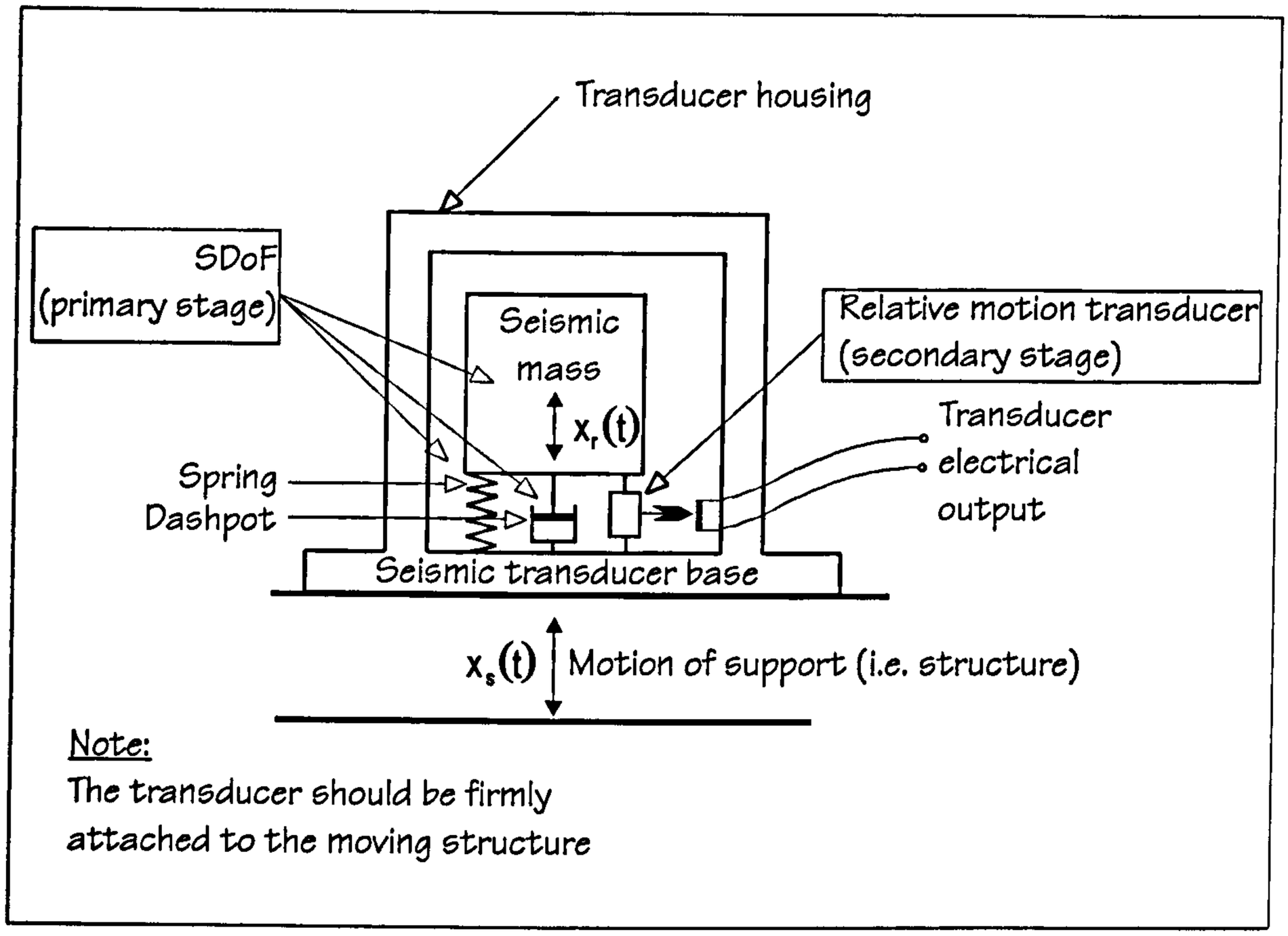

Figure 4.11: Operational scheme of a seismic (or absolute) motion transducer (after Beckwith et al, 1993).

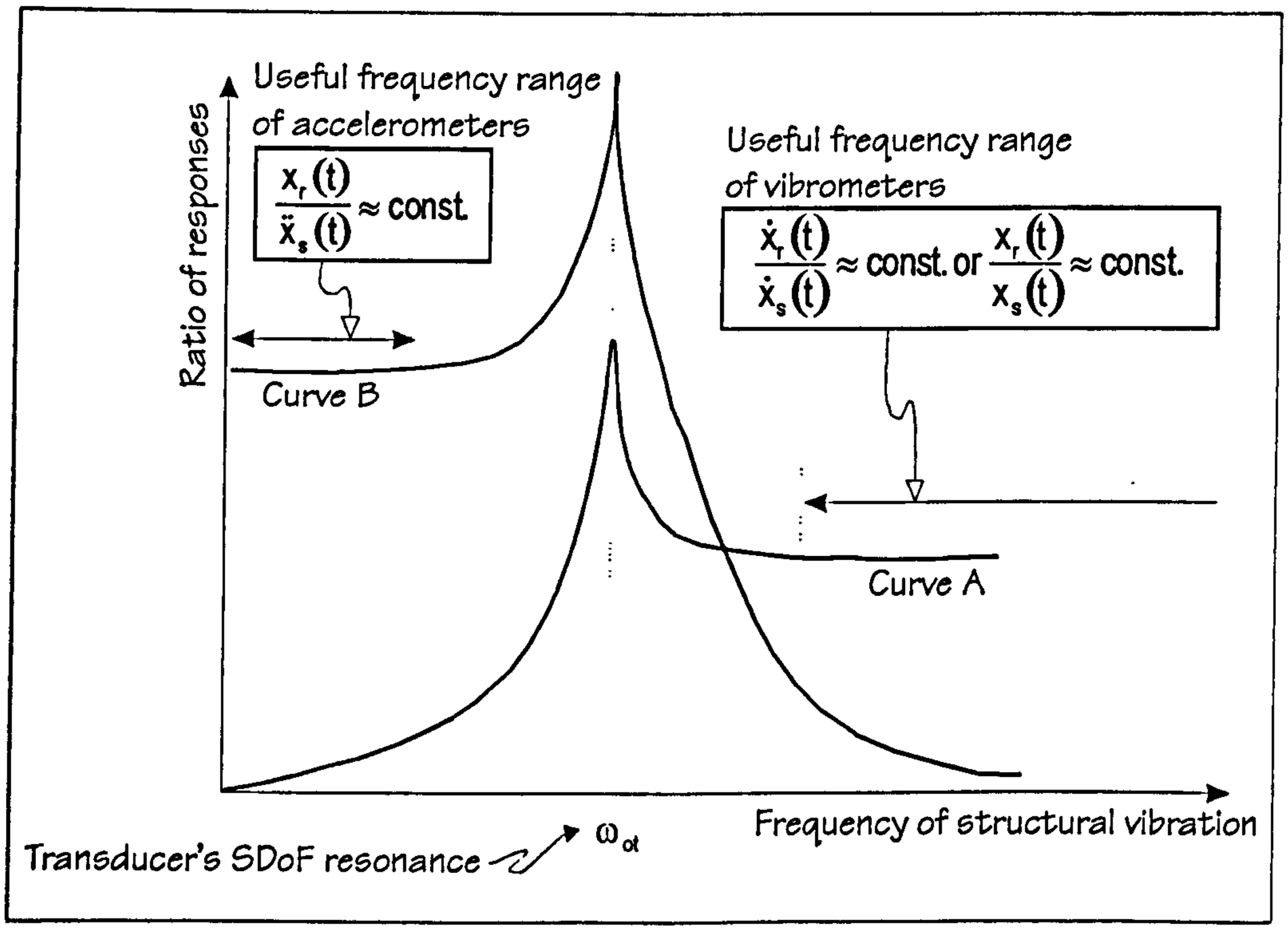

Figure 4.12: Two types of frequency responses of seismic motion transducers, depending on the parameters used to describe the support and response motion (after Serridge and Licht, 1987).

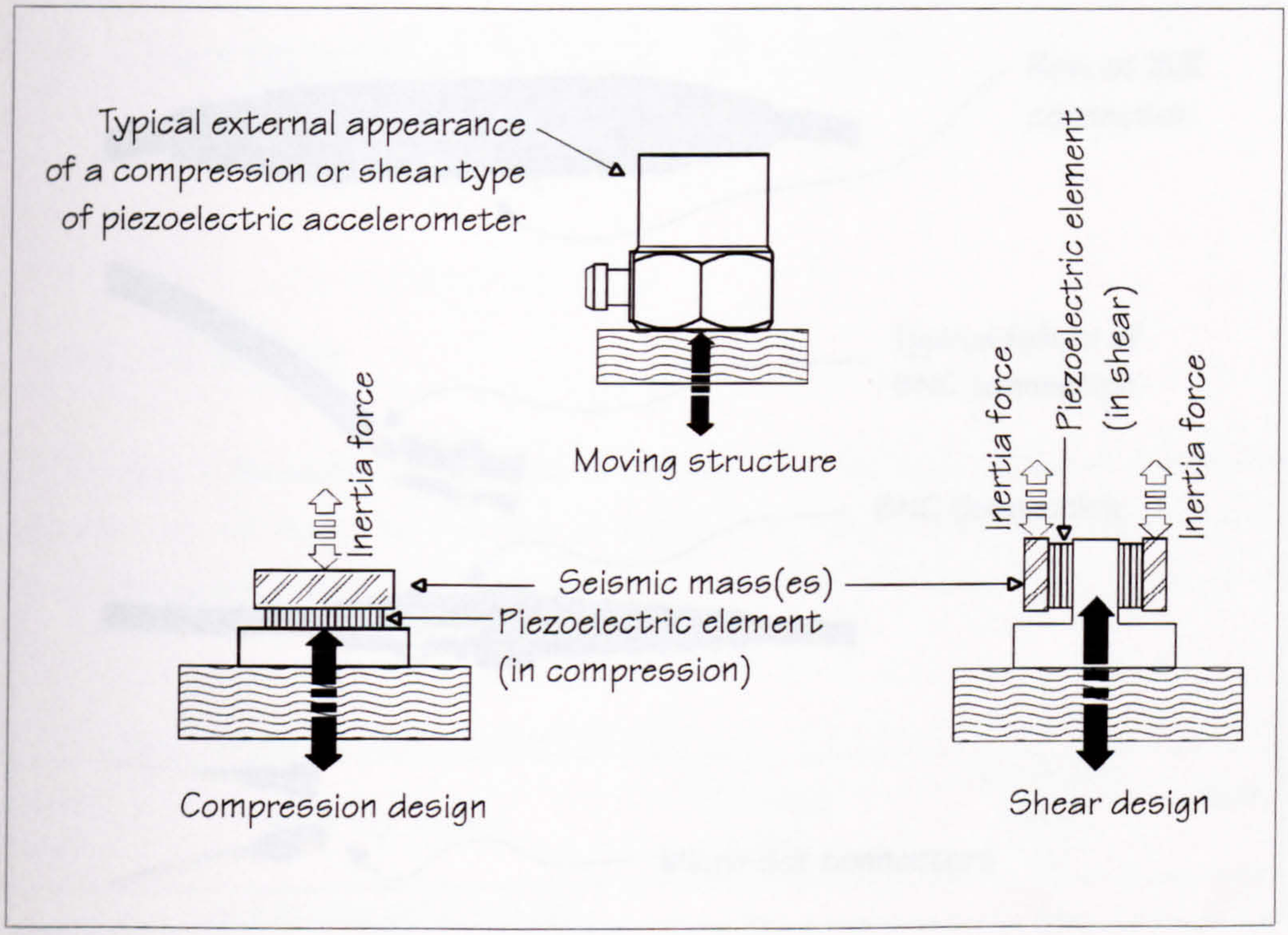

Figure 4.13: Compression and shear designs of piezoelectric accelerometers (after Licht et al, 1987).

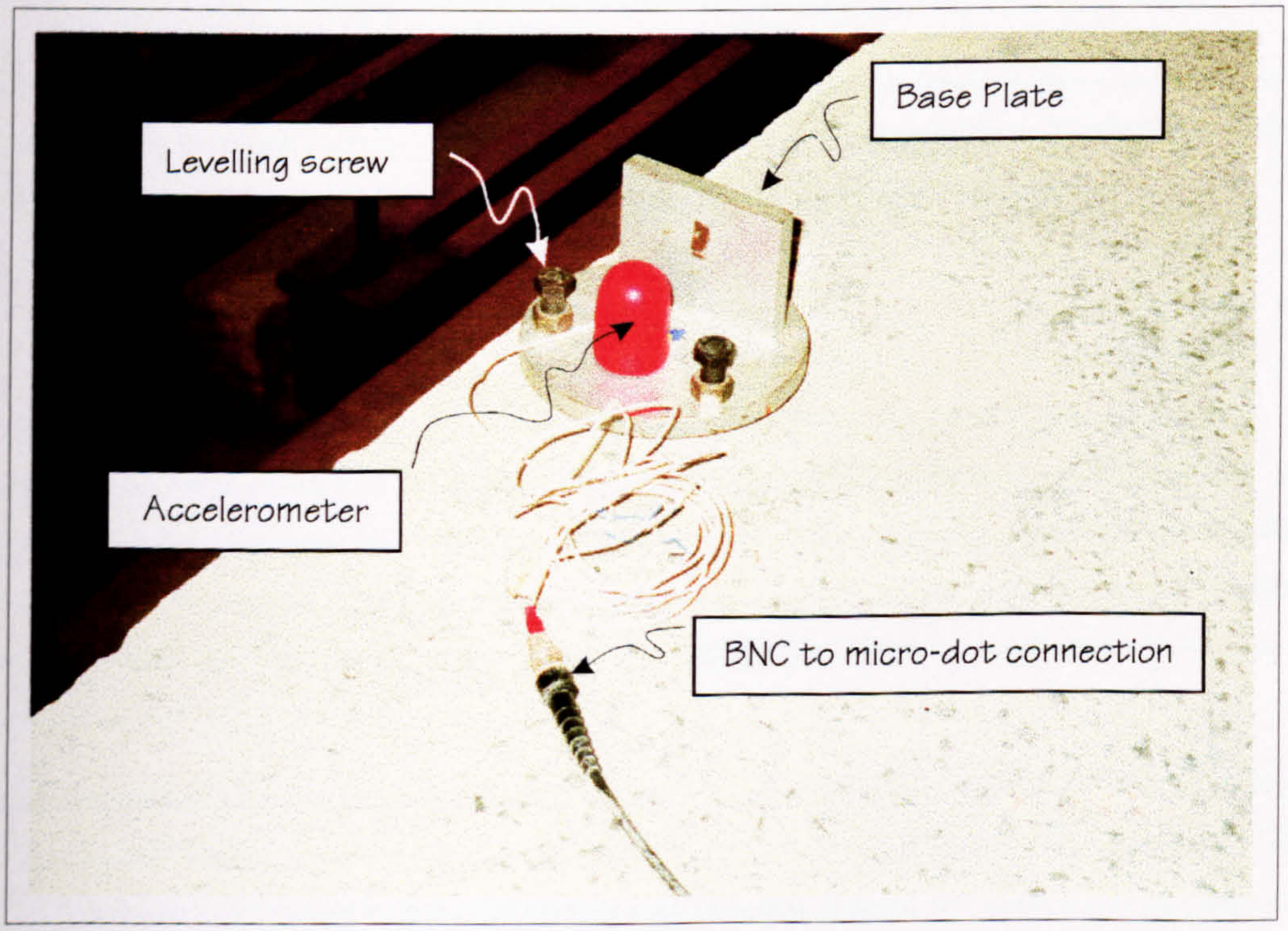

Figure 4.14: Accelerometer attachment base

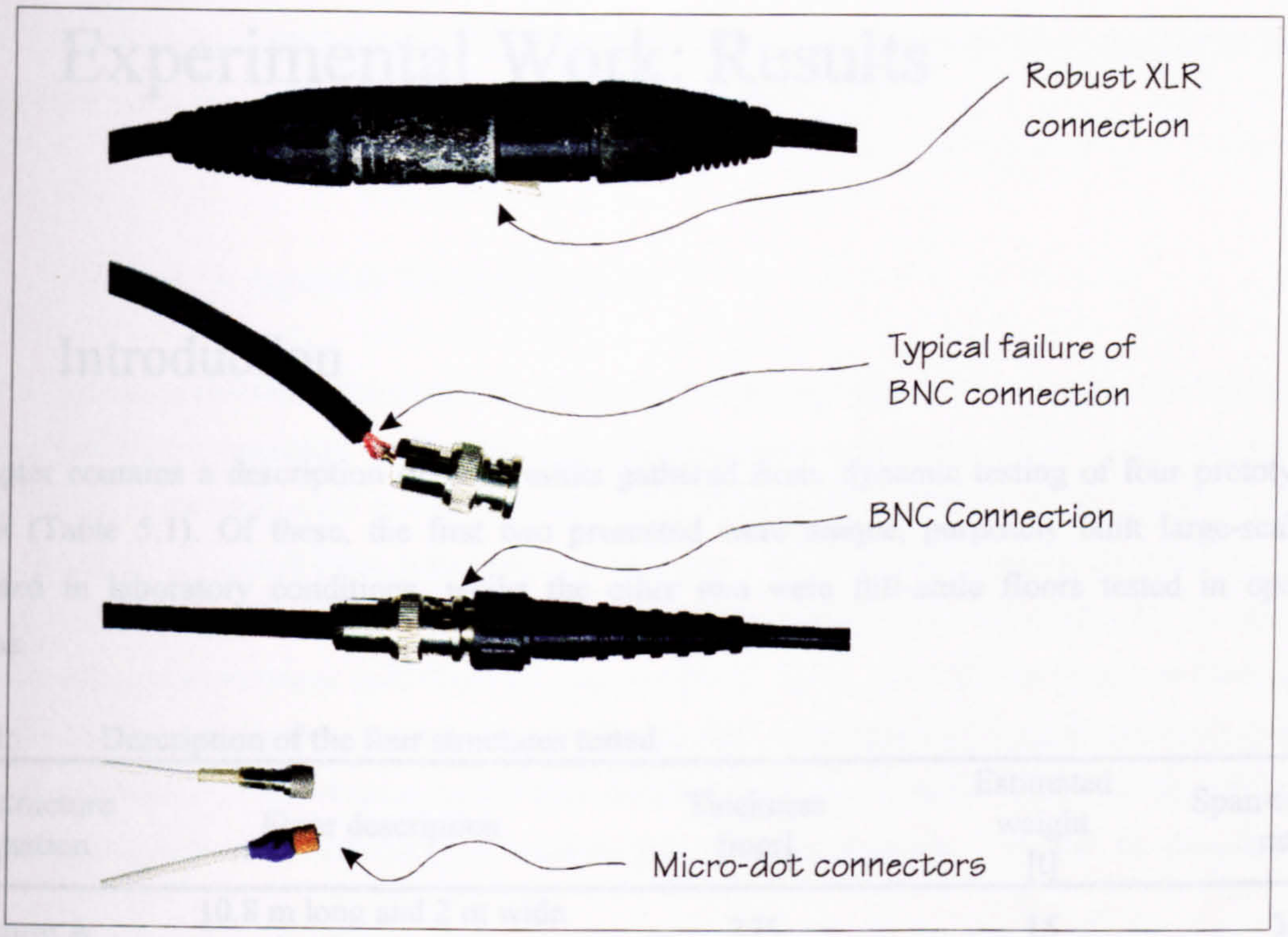

Figure 4.15: Micro-dot, BNC and XLR cable connectors.

5 Experimental Work: Results

5.1 Introduction

This chapter contains a description of, and results gathered from, dynamic testing of four prototype floor structures (Table 5.1). Of these, the first two presented were unique, purposely built large-scale floors investigated in laboratory conditions, whilst the other two were full-scale floors tested in open space conditions.

Table 5.1: Description of the four structures tested

Floor structure designation	Floor description	Thickness [mm]	Estimated weight [t]	Span-to-depth ratio
Structure A	10.8 m long and 2 m wide cast in-situ PT slab strip	275	15	39
Structure B	15 m x 15 m cast in-situ reinforced HSC floor	250	135	36
Structure C	14.5 m long and 31 m wide cast in-situ PT ribbed floor	Slab: 100 Band-beam rib: 350	530	41
Structure D	47.5 m x 37.5 m cast in-situ PT flat slab	225	1000	36

Modal testing using hammer impulse excitation was performed on each structure. In addition, when possible, acceleration response measurements mainly due to walking excitation were made.

5.1.1 Aims of Modal Testing

The modal testing was performed in order to measure the natural frequencies, mode shapes and modal damping ratios of the prototype floor structures tested. Apart from using the measured modal properties to improve analytical FE models of the structures tested, the purpose of which was outlined in Chapter 1 and is described in detail in Chapter 6, these properties were also used to help and guide the response measurements.

The in-situ estimated modal properties served to indicate excitation conditions in which a single-person walking across the test structure produces the largest possible, but realistic, floor response. The natural frequencies measured were used to tune the pacing rate of a test subject (by means of a metronome) so that one of the walking excitation harmonics excited the floor resonance as precisely as possible. In addition, the measured mode shapes served to determine the walking path(s) suitable for producing maximum floor responses when someone walked along them with a pacing rate which excited the corresponding mode of

vibration. Ideally, these walking paths should pass through the antinode (absolute maximum amplitude) point(s) of each mode shape of interest.

5.1.2 Aims of Response Measurements

The floor acceleration response measurements due to 'tuned' pacing rates were conducted for several reasons. Firstly, to establish the accuracy of the assumption of resonance conditions due to single-person walking excitation, which is currently used in many guidelines for checking the vibration serviceability, as reported in Chapter 2. Secondly, to assess these responses in accordance with the latest vibration assessment procedures (BSI, 1992; ISO, 1997). These vibration serviceability ratings were then compared with the assessments made by the relevant assessment guidelines for cast in-situ PT floors given by the Concrete Society (1994). Only the description of response tests and general comments regarding the typical measured acceleration responses are presented in this chapter, whilst their detailed discussion is given in Chapter 6. Compared with modal testing, response measurements are considerably easier to perform, and will be described in less detail.

5.2 General (Modal) Testing Procedure

Generally speaking, the practical execution of modal testing comprises the following phases (DTA, 1993b; Heylen et al., 1997): (1) definition of objectives and test planning, (2) setting up, (3) preliminary investigation, (4) test measurements (i.e. data acquisition), (5) critical review of collected data, (6) data analysis comprising vibration parameter estimation and presentation of results, and (7) interpretation of results and, if required, utilisation of experimentally measured data. In addition, validation of results and implementation of quality control procedures should be performed throughout all these phases.

5.2.1 Definition of Objectives and Test Planning

This phase comprises all preparatory work required before the equipment is setup. In the case of field testing, it includes a site survey long before the equipment is taken out of a laboratory, and test organisation. The writer found this task to be extremely time-consuming, but also of crucial importance, particularly with regard to the health and safety (Hartley & Pavic, 1996) and QA (DTA, 1993b) requirements.

With regard to the QA, it is interesting to mention the following statement by the DTA (1993b):

"It is tempting, particularly with on-site testing, to capture as much data as possible for later analysis back in the comfort of the laboratory. However, this is usually a very inefficient method, often resulting in the complete data set being scrapped as transducers were found to be overloading, or not working. At the very minimum, trial tests should be performed and analysed on site."

The DTA (1993b) accompanied this very explicit warning with a comprehensive description of a QA system, which should be adopted when doing any kind of laboratory or field based modal testing. These quality control measures were adopted in this research, but with some modifications to take into account the specific circumstances typically occurring in the field testing of floors.

5.2.2 Setting-up, Preliminary Investigation and Data Acquisition

Implementation of the QA measures recommended by the DTA (1993b) and ISO (1994) is crucial during the setting-up, preliminary investigation and data acquisition modal testing steps. The following QA steps have been implemented during the preliminary investigation and/or data acquisition phases:

1. "pre-test analysis" (Heylen et al., 1997) comprising relatively crude FE modal analysis of each structure prior to its testing,
2. visual inspection of typical excitation and response signals in the time-domain during the preliminary investigation,
3. checking the suitability of the excitation spectra during the preliminary investigation,
4. visual inspection of measured FRFs in the frequency-domain throughout the data acquisition phase aimed primarily at checking if the effects of noise and uncorrelated extraneous excitation are being averaged out,
5. investigation of optimum instrumentation gain settings during preliminary investigation, and non-stop monitoring of over- and under-ranging of signals acquired by the measurement system,
6. prevention of signal aliasing by the application of anti-aliasing filtering on both excitation and response measurement channels throughout the preliminary and data acquisition phases,
7. reduction or elimination of signal leakage by an application of appropriate signal windowing or data acquisition periods throughout the preliminary and data acquisition phases,
8. visual inspection of the shape of some point mobility FRFs $H_{jj}(\omega)$ during the preliminary investigation,
9. checking how well the reciprocity condition (Dossing, 1988b) is satisfied by visually inspecting pairs of reciprocal FRFs $H_{jk}(\omega)$ and $H_{kj}(\omega)$ during the preliminary phase,

10. checking how well the linearity, also known as homogeneity, condition (Dossing, 1988b) is satisfied by visually inspecting pairs of nominally identical FRFs, $H^{(1)}_{jk}(\omega)$ and $H^{(2)}_{jk}(\omega)$, which correspond to relatively low and relatively high levels of excitation during the preliminary phase, and

11. checking how well the repeatability condition is satisfied by comparing measurements of two pairs of nominally identical FRFs, $H^{(1)}_{jk}(\omega)$ and $H^{(2)}_{jk}(\omega)$, made immediately one after another (in the preliminary investigation), and at the beginning and at the end of the full FRF data acquisition.

5.2.2.1 PRE-TEST ANALYSIS

The aim of the pre-test (FE) analysis is to identify likely shapes and natural frequencies of the modes of vibration to be measured. This helps the initial selection of digital data acquisition parameters. It also enables the visualisation of mode shapes (likely to be measured) in order to reduce the possibility for spatial aliasing and improve the observability of the experimentally measured modal properties (NAFEMS, 1992b).

Spatial aliasing occurs when the experimentally measured DOFs are not able to produce clearly identifiable mode shapes corresponding to each measured natural frequency. The confusion between two or more experimentally measured mode shapes usually occurs when there is an insufficient number of measured DOFs. A good way to reduce the possibility of spatial aliasing is to calculate the so called 'Auto-Modal Assurance Criterion', or Auto-MAC (DTA, 1993c), between all possible vector pairs $\{{}_A\phi\}_r$ and $\{{}_A\phi\}_p$ of the analytically calculated mode shapes. The elements of these two vectors correspond only to the limited number of measured DOFs. The Auto-MAC is calculated using the following formula:

$$\text{Auto-MAC}\left(\{\phi\}_r,\{\phi\}_p\right)=\frac{\left|\{\phi_A\}_r^T\{\phi_A\}_p\right|^2}{\left(\{\phi_A\}_r^T\{\phi_A\}_r\right)\left(\{\phi_A\}_p^T\{\phi_A\}_p\right)}, \qquad \text{Equation 5.1}$$

which developed form is:

$$\text{Auto-MAC}\left(\{\phi\}_r,\{\phi\}_p\right)=\frac{\left|\sum_{j=1}^{n}\left({}_A\phi_{jr}\right)\left({}_A\phi_{jp}\right)\right|^2}{\left(\sum_{j=1}^{n}\left({}_A\phi_{jr}\right)\left({}_A\phi_{jr}\right)\right)\left(\sum_{j=1}^{n}\left({}_A\phi_{jp}\right)\left({}_A\phi_{jp}\right)\right)}. \qquad \text{Equation 5.2}$$

If the selected measurement DOFs are sufficient to produce linearly independent mode shapes and avoid the spatial aliasing in the first, say, m modes of interest, then diagonal elements of the corresponding $m \times m$ Auto-MAC matrix should have values of 1.0 (i.e. 100%). When a MAC value, corresponding to two mode shapes $\{\phi\}_r$ and $\{\phi\}_p$, equals to 1.0 this means that one mode shape is, in fact, the other multiplied by a constant, that is the two mode shapes are identical i.e. they are linearly dependent. This is why the diagonal values of the Auto-MAC matrix, corresponding to two identical mode shapes, must be 1.0. In addition, a comparison of two linearly independent mode shape vectors $\{\phi\}_r$ and $\{\phi\}_p$ should produce off-diagonal

values of Auto-MAC matrix which are zero or close to zero (Friswell & Mottershead, 1995). The DTA (1993b) advises that if the values of non-diagonal elements are above 0.6, than there is a likelihood that the selected measurement DOFs will cause spatial aliasing and confusion of mode shapes in the frequency region of interest.

If a roving exciter is used, as is the case in this research, in addition to spatial aliasing, the observability of the measured mode shapes may be impaired by the response measurements made close to or at mode shape nodal points. However, analytically obtained mode shapes are likely to indicate where nodal points for certain modes of interest occur and these points should be avoided when placing stationary accelerometers.

5.2.2.2 OTHER QA REQUIREMENTS

The rationale behind the remaining of the above listed QA measures is firstly to ensure that the floor tested is a reasonably linear and time-invariant structure, so that experimental modal analysis, which is based on these assumptions, is able to produce meaningful results. In addition, they should reduce the effects of noise and signal processing errors typically caused by the instrumentation dynamic range limitations, signal aliasing and leakage (Heylen et al., 1997).

Further details about these QA checks are outlined by the DTA (1993b, 1993c), Heylen et al. (1997) and ISO (1994) and will not be repeated here. However, some illustrations of how well the QA checks were satisfied are presented for each of the four floor structures tested.

In general, the experimentally determined modal parameters reported in this thesis can be considered to be fairly consistent unless is otherwise stated. They have been confirmed by performing a number of SDOF and at least one MDOF parameter estimation exercises using either a single or, in the latter case, a group of the measured FRFs at a time. The ICATS (1995) MODENT software module was used to carry out the calculations in accordance with the parameter estimation algorithms and best practice procedures described in detail by the DTA (1993b; 1993c), Ewins (1995), Maia et al. (1997) and Heylen et al. (1997).

5.2.3 System Calibration

In addition to the above-mentioned QA measures, DTA (1993b) advises overall calibration of the system using a suspended mass to be performed "between the preliminary investigation and the main data collection part of the test". The procedure recommended is based on Newton's second law:

$$f(t) = m \cdot a(t), \qquad \text{Equation 5.3}$$

where: m [kg] is the known suspended mass, $f(t)$ [N] is the force applied to the suspended mass by the exciter, and $a(t)$ [m/s^2] is the acceleration of the suspended mass due to force $f(t)$. The acceleration is

measured by an accelerometer in the direction of the force. From a theoretical point of view, the accelerance FRF of this SDOF suspension system is a real constant $A(\omega)$:

$$A(\omega) = 1/m\,. \qquad \text{Equation 5.4}$$

Such a measured accelerance modulus should, therefore, be close to the known constant ($1/m$) and its phase close to zero. This property can then be used to check the accuracy of the nominal sensitivity values, reported by the manufacturers of the modal testing hardware. This is done in accordance with the fairly straightforward procedure, details of which are given in a number of texts on modal testing (Halvorsen & Brown, 1977; Ewins, 1995, Maia et al., 1997; Dossing, 1988b).

5.2.3.1 PRACTICAL PROBLEMS

The writer found this QA requirement to be practically impossible to satisfy when doing field testing under the circumstances pertinent to this research. The reasons were the lack of both time and facilities to manipulate and suspend a relatively large calibration mass required. Whereas the lack of time is easy to accept as a difficulty, the latter problem, for the case when Dytran 5803 5.4 kg instrumented sledge hammer is used as the exciter, deserves further explanation.

Let us assume that 13 kN is roughly the maximum force, which is going to be applied by the sledge hammer to the suspended mass, as determined from the manufacturer's technical documentation (Operating Guide Model 5803A Instrumented Impulse Hammer Twelve Pound Sledge, undated). The accelerations of the mass are, naturally, measured by the selected Endevco and Dytran accelerometers, as described in Chapter 4. These accelerometers have a 5g linear range and, therefore, the minimum mass required to prevent accelerations which are over-ranged is:

$$m_{min} = \frac{F_{max\ assumed}}{a_{max.allowed}} = \frac{13 \cdot 10^3}{5 \cdot 9.81} = 265\text{kg} \qquad \text{Equation 5.5}$$

The assumption of the 13 kN peak force is realistic because it corresponds to approximately 50-60% of the hammer's linear force range (22.2 kN). The minimum required mass of 265 kg is, obviously, very large (see Figures 5.1 and 5.2) and difficult to manage. This is a consequence of the fact that relatively large forces must cause relatively low accelerations. Although the minimum calibration mass can be reduced if a lower maximum force is assumed, such a force is not realistic and is difficult to apply in practice by manually operating a 5.4 kg sledge hammer (Figure 5.2).

5.2.3.2 INVESTIGATION OF EFFECTS OF LONG CABLES

Being practically unable to perform the system calibration in-situ between the preliminary investigation and data acquisition phases, it was decided to use the nominal instrumentation sensitivities (i.e. those specified by the manufacturers) in all measurements. As this is far from being an ideal solution, particularly with

regard to the possibly detrimental effects of long leads in the measurement system (Maia et al., 1997), which could be required in field testing, occasional system calibrations were performed under laboratory conditions. The main aim of these exercises was to increase confidence in the results of field measurements, as it is impractical to replicate the exact instrumentation set-up during each and every field test in order to use the experimentally determined calibration factors.

For this, a concrete cube weighing exactly 3096 kN (m=316 kg) was cast (Figure 5.1) and was suspended from a crane in a laboratory (Figure 5.2). The accelerometer was firmly attached to the block via a mounting stud protruding from a steel plate embedded in the concrete (Figure 5.1). When investigating the effects of long cables, two different cabling configurations were tried. The first was with a hammer and accelerometer each connected to the data acquisition system through 250 m of coaxial cables, which is considered to be a relatively long length. The second configuration had the lengths of connecting cables reduced to 100 m.

Twenty hammer hits were applied and the measured accelerance FRFs averaged by a spectrum analyser (Figure 5.3) between 0 and 500 Hz. The data sampling rate was 1280 samples per second over 1.6 s leading to the total of 2048 points acquired per each channel. No signal windowing was applied. Typical hammer excitation and acceleration response signals acquired with unity gains on all signal conditioning equipment are shown in Figure 5.4.

Somewhat surprisingly, the pair of Dytran accelerometers demonstrated poor performance with 250 m long coaxial cables. Figure 5.5 shows that an FRF (Equation 5.4) measured with long cables has very distorted modulus and phase, particularly in the lower frequency region. On the other hand, when shorter cables were used, much better quality of the calibration FRF was obtained (Figure 5.6). The FRF modulus is approximately flat and the FRF phase is close to zero.

As expected, the calibration FRFs for both high-spec Endevco accelerometers showed almost no dependence on the cable length and their shape was as theoretically expected and was similar to that shown in Figure 5.6.

5.2.3.3 LESSONS LEARNED AND CONCLUSIONS

Although the manufacturer's data suggested that Dytran accelerometers perform well with much longer cables, the system calibration exercise revealed that these transducers should not be used when the required cable lengths are more than 100m. Fortunately, the circumstances of the field work carried out on all prototype floors presented in this thesis did not require cable lengths of more than 50 m per channel.

For the modal testing systems comprising the instrumented sledge hammer and any of the accelerometers used, differences of no more than $\pm 10\%$ between the nominal and experimentally obtained FRF scaling factors have normally been observed during occasional system calibrations using a suspended mass. In addition to the inability to perform the calibration in field conditions, such relatively small differences are another reason why the nominal FRF scaling factors were adopted. For unity gain set on all channels, the nominal sensitivities and the corresponding FRF scaling factors calculated are given in Table 5.2.

Designations given to the five accelerometers used are from A1 to A5. It should be mentioned here that the A5 accelerometer replaced its A3 counterpart which was accidentally dropped and damaged beyond repair in the course of this research.

Table 5.2: Nominal hammer and accelerometer sensitivities, and FRF scaling factors for hammer testing

Device	Sensitivity	FRF scaling factor. Units: $(m/s^2)/N$ per (V_{output}/V_{input})
Sledge Hammer	0.236 mV/N	N/A
Endevco A1	979 mV/g @ 20 Hz	0.00236
Endevco A2	971 mV/g@ 20 Hz	0.00238
Dytran A3	915 mV/g@ 20 Hz	0.00253
Dytran A4	965 mV/g@ 20 Hz	0.00240
Dytran A5	1038 mV/g@ 20 Hz	0.00223

5.3 Vibration Testing of Post-Tensioned Concrete Slab Strip (Structure A)

The first prototype floor structure presented, Structure A, is the simplest, but also the last tested, in April 1998. It is a PT slab strip, 2 m wide and 11.2 m long, spanning 10.8 m between the supports (Figure 5.7). The main aim of this purposely built slab was to study the effects of various configurations of false floors on the vibration performance of long span concrete slabs as part of another research project carried out by the University of Sheffield and a number of industrial partners (Waldron et al., 1997). However, the opportunity was seized to use this slab in its bare state when the damping could be assumed to be the lowest and to perform modal testing and walking response measurements.

5.3.1 Structural Description

In essence, this is a simply supported beam purposely designed to have a fundamental natural frequency around 4.5 Hz. This was done so that the third harmonic of somewhat slower walking and the second harmonic of relatively fast walking could produce as large as possible a response of this slab. Structure A can, therefore, be considered as a low-frequency floor (Wyatt, 1989).

5.3.1.1 SPAN-TO-DEPTH RATIO

The 275 mm thick slab was designed by PSC Freyssinet (UK) Ltd and it is prestressed by 12 single-strand unbonded tendons. The tendons have one 'live' and one 'dead' anchor and were alternatively prestressed from both ends (Figure 5.8). The total estimated weight of the slab is 15 tonnes.

The amount of prestressing and its position were selected so that the full slab self weight is balanced. Being a 'single-span floor', and having span-to-depth ratio of almost 40 (10.8/0.275=39.3), this configuration can be considered to be fairly slender with regard to vibration serviceability following the Concrete Society (1994) guidelines.

5.3.1.2 ENVIRONMENTAL AND BOUNDARY CONDITIONS

In order to reduce the environmental effects, the slab was placed indoors (Figure 5.9). In addition, as perfect as possible 'knife edge' supports along the ends of the strip (Figure 5.10) were designed in order to reduce the uncertainties in the FE modelling of this structure.

5.3.2 Modal Testing

Although the structure was simple and located indoors in one of the University of Sheffield laboratories, testing time scales were stringent as a false floor had to be mounted on the structure almost immediately after its construction. Therefore, to produce good quality experimental data first time, full modal testing QA procedures were carried out.

5.3.2.1 PRE-TEST ANALYSIS

A relatively crude FE model, based on grillage analogy, was developed prior to the testing. The aim of this model was to predict roughly the natural frequencies and mode shapes in order to help develop the test grid and position the accelerometers so that all modes of vibration which are of interest were observable. The test grid comprising 27 points which was investigated is shown in Figure 5.11.

The FE grillage model was created by dividing the slab into five beam-like strips along its 10.8 m long length. These strips were modelled using ANSYS BEAM4 elements all being 0.275 m deep and 0.2m, 0.5m, 0.6m, 0.5 m and 0.2 m wide, respectively (Figure 5.11). The mass of the whole structure was allocated to these longitudinal beams. In addition, 11 cross-beams were created (Figure 5.12). All cross beams were assumed to be without mass but possessing varying stiffnesses. The beams were 0.275 m deep and had widths between 0.1 m and 1.5 m (Figure 5.11).

Dynamic modulus of elasticity for concrete was assumed to be 38 GPa, whereas the density was taken as 2400 kg/m^3 (Wyatt, 1989). Supports were modelled as pinned allowing free rotation, but preventing translations in all three directions.

The calculated natural frequencies and the description of the first six modes of vibration are shown in Table 5.3. The corresponding analytical mode shapes are shown in Figure 5.13.

Table 5.3: Structure A - Calculated natural frequencies in pre-test analysis.

Mode No.	Natural frequency [Hz]	Mode description
1	4.3	1st vertical bending mode
2	17.0	2nd vertical bending mode
3	38.1	3rd vertical bending mode
4	45.7	1st torsional mode
5	48.3	1st horizontal bending mode
6	67.7	4th vertical bending mode

The Auto-MAC calculations presented in Figure 5.14 show that the grid selected was likely to be capable of distinguishing the first 10 mode shapes including the first three vertical bending modes and the first torsional mode. The four accelerometers available for this test were positioned as indicated in Figure 5.15, according to the following:

- Accelerometer (A2) at TP14 is required in order to measure accurately the 1st mode of vibration which is of greatest interest;
- Accelerometer (A1) at TP16 is likely to measure the first three vertical bending modes of vibration, and can serve to confirm the measurements of the 1st mode using A2;
- Accelerometer (A4) at TP22 should be able to pick everything that A1 and A2 are measuring, which can be used as an additional check of A1 and A2 measurements, and to measure torsional modes;
- Accelerometer A5 at TP9 serves to indicate if and how much the right support moves. This was done because a visual inspection prior to testing revealed that, due to imperfections in construction, there was an approximately 500 mm long gap under TP9 between the 'knife edge' (steel angle section) support and the upper bearing plate (see the slab strip support detail in Figures 5.7 and 5.10).

5.3.2.2 Excitation and Data Collection

The floor was impacted by a sledge hammer, the operator of which was sitting in a chair and trying to be very still during data capture after the impact. This is the standard way in which the hammer was operated in this research (Figure 5.16).

The data from the one hammer and four accelerometer channels were recorded on an analogue RACAL VL VHS tape recorder. In addition to being analogue recorded, the hammer (H) and one accelerometer (A1) channels were monitored in parallel using the DI2200 portable digital oscilloscope and spectrum analyser (Figure 5.16).

5.3.2.3 PRELIMINARY INVESTIGATION AND NOTE ON EXPONENTIAL WINDOWING

A typical hammer blow and the corresponding acceleration response sampled at 512 points per second (200 Hz baseband analysis) are shown in Figure 5.17. No windowing was applied and anti-aliasing filtering was switched on, as appropriate. Figure 5.17 clearly shows that after 8 s of data acquisition the vibrations still did not die out, which indicated that the slab was likely to have a very low damping and that there was a need to use a longer data acquisition time and exponential windowing in order to artificially dampen the response measurements and produce better quality FRFs.

The DI2200 spectrum analyser applies the exponential window function $w_{exp}(t)$ to both the input and output channels. In this particular instrument the windowing function is defined by specifying the TC constant in the following formula:

$$w_{exp}(t) = e^{-\left(\frac{TC}{T_{acq}}\right)t}, \qquad \text{Equation 5.6}$$

where T_{acq} is the data acquisition time. The value of TC can be an integer between 0 (no exponential windowing) and 10. The greater the TC, greater the exponential decay. Theoretically speaking, the only consequence of the application of the exponential windowing in the hammer modal testing is an (artificial) increase of modal damping ratios in the measured FRFs (ISO, 1994). However, it is possible to recover the real damping afterwards by applying the following formula (ISO, 1994):

$$\zeta_r = \zeta_{r,windowed} - \frac{TC}{T_{acq}} \cdot \frac{1}{2\pi f_r}, \qquad \text{Equation 5.7}$$

where $\zeta_{r,windowed}$ is the modal damping ratio for the r^{th} mode of vibration estimated from the 'windowed' FRFs.

After several attempts based on trial and error, the main data acquisition parameters were selected. These are shown in Table 5.4.

Table 5.4: Structure A - Main digital data acquisition parameters adopted for FRF measurements

Parameter description	Parameter value
Data acquisition time	16 s
Frequency resolution	0.0625 Hz
Frequency range of interest	1-51 Hz
Total number of samples	2048
Number of frequency lines	800
Number of averages	5
Exponential window time constant (TC)	10

At this stage, a 'standard' strength of the hammer blow was established and agreed with the hammer operator so that the likelihood for overloading of the electronics was reduced. The FRFs measured were not scaled to appropriate units at this stage as these served only the qualitative assessment of the measurements.

Figure 5.18 shows the result of the so called 'immediate repeatability' check of the FRF. The writer found this check particularly useful in field conditions when extraneous unmeasured excitation, such as wind, can spoil the FRF measurements. If there is a great difference between two nominally identical FRFs measured immediately one after another, then it is recommended to stop the testing and investigate the problem further. A pair of point mobilities measured at TP16 and shown in Figure 5.18 was assessed as acceptable regarding this check. Also, it was noted that three peak values of these two FRFs corresponding to frequencies of 4.6 Hz, 17.0 Hz and 37.9 Hz correlate well with the pre-test FE analysis (4.3 Hz, 17.0 Hz and 38.1 Hz) for the first three bending modes (Table 5.3).

Figure 5.19 shows a reciprocity check between TP16 and TP22 considered to be satisfactory. However, it should be mentioned that although the shape of these two FRFs is very similar, certain differences between the FRF peaks exist. These differences were attributed to the effects of noise in the measurements and to the presence of the hammer operator at different positions on the slab.

Figure 5.20 shows a satisfactory homogeneity check performed using again two point mobility FRFs corresponding to TP16. Relatively soft hammer impacts were used for the first (the blue line) FRF $H^{(1)}_{16,16}(\omega)$, which, obviously, is noisier than the second (the red line) FRF produced by strong hammer blows. However, it is interesting to note that the TP16 point mobility FRF peak corresponding to 17.0 Hz was significantly lower than the peak in the nominally identical point mobility FRF measured while performing the 'immediate repeatability' check (Figure 5.18). The other two peak values at 4.6 Hz and 37.9 Hz shown in Figures 5.19 and 5.20 correlate much better. This was attributed to the different positions of the hammer operator while performing these two checks.

All point mobility FRFs must have an anti-resonance between the pairs of subsequent resonances. Anti-resonances between the modal peaks should be clearly observable as characteristic 'troughs' in log-log plots (Ewins, 1995). The existence of these anti-resonances in point mobility FRFs is a good indication that the FRF measurements are likely to be valid, as illustrated in Figure 5.21. This was termed the FRF shape check.

Having performed the FRF shape check, and although the differences in some of the peaks of other FRFs were notable, all preliminary QA checks were deemed satisfactory and a decision to acquire the full set of FRFs using the data acquisition parameters given in Table 5.4 was made.

At the end of the full FRF data acquisition, which lasted four hours, another measurement of the point mobility at TP16 was made and this result was compared with its nominally identical counterpart measured just before the full hammer swipe started. This comparison is shown in Figure 5.22 and was considered as a satisfactory 'end-of-test' repeatability check.

5.3.2.4 FRF DATA ACQUISITION AND INITIAL DATA ANALYSIS

At the end of the main hammer sweep, a collection of 81 FRFs forming 3 rows of the FRF matrix was used to estimate the modal properties of the test structure. The fourth row of the FRF matrix produced by the accelerometer at the support (TP9) was not used due to poor signal-to-noise ratio.

A visual inspection of the scaled point mobilities (the damping effects of exponential window not removed) corresponding to TP14 (Figure 5.23), TP16 (Figure 5.24) and TP22 (Figure 5.25) showed that characteristic resonant phase change occurred at five distinct frequencies. Therefore, it was initially estimated that there had been at least five modes of vibration between 1 Hz and 51 Hz which were picked up by this experimental set up.

Figure 5.26 shows the first five estimated mode shapes. The estimated natural frequencies and modal damping ratios, the latter obtained after removing the effects of the exponential window, obtained by an MDOF curve-fitting are shown in Table 5.5.

It is interesting to note here that the shape of mode 1, the 1st vertical bending mode, shown in Figure 5.26 is not 'smooth'. This is due to the complexity of this mode, as indicated in Figure 5.27. This matter required immediate attention as the complex modes could be a result of analysis and/or measurement errors (Imregun & Ewins, 1995).

Table 5.5: Structure A - The estimated natural frequencies and modal damping ratios.

Mode No.	Description	Natural frequency [Hz]	Modal damping ratio ζ [%]
1	1st vertical bending mode	4.5	0.59
2	2nd vertical bending mode	17.0	0.56
3	1st torsional ('rocking') mode	26.1	1.76
4	2nd torsional ('bending') mode	29.1	1.41
5	3rd vertical bending mode	37.6	1.22

5.3.2.5 COMPLEXITY OF THE FIRST MODE OF VIBRATION

The complexity of the first mode of vibration was, almost certainly, caused by the presence of the hammer operator on the slab.

This is, to some extent, corroborated by measurements of the modal damping ratio for the first mode using heel-drop excitation and response at TP14 which is the maximum modal amplitude for the 1st mode of vibration. Figure 5.28 shows the acceleration peak amplitudes featuring in the approximate logarithmic decrement formula (Thompson, 1993):

$$\zeta \approx \frac{1}{n} \ln\left(\frac{a_o}{a_n}\right), \qquad \text{Equation 5.8}$$

used to estimate the modal damping ratio for the 1st mode of vibration. In Equation 5.8, n is the number of cycles elapsed between the acceleration peak values a_o and a_n. As the 1st mode of vibration is well separated from the higher modes, application of Equation 5.8, has been considered as valid. Three pairs of peak values were used to estimate the same modal damping ratio for the fundamental mode and the values calculated are shown in Table 5.6.

The average of the three values in Table 5.6 is $\zeta_1 = 1.03\%$ and is greater than the average value of 0.59% (Table 5.5) estimated from MDOF curve fitting of 27 FRFs. This demonstrates the potential of a stationary human body to affect modal damping values, especially when positioned at the point where maximum modal amplitude occurs. The writer speculates that the fact that the hammer operator moved from point to point across the slab resulted, in average, in the lower damping ratio estimated from a set of FRFs. This movement introduced either relatively weak non-linearities or non-proportional damping, or both, resulting in the complex 1st mode of vibration (Imregun & Ewins, 1995).

Table 5.6: Structure A - Estimated 1st mode damping ratios using amplitude decay after a heel-drop.

Number of cycles elapsed	First mode damping ratio ζ_1 [%]
10	1.13
20	0.95
40	1.01

Another proof that the presence of a human body may create complex modes of vibration has been produced by Reynolds (1999) who tested Structure A in identical bare condition but using the shaker excitation, instead of the manually operated sledge hammer. No humans were present on the structure. The first mode shape measured by Reynolds had identical frequency and was almost perfectly real resulting in a 'smooth' mode shape.

Finally, it should be mentioned that the DTA (1993b) requires that the effects of the measurements on the structure tested, such as the mass and stiffness of transducers attached, must be evaluated. It is interesting to note here that in the case of the relatively large Structure A, tested with a manually operated sledge hammer, the problem appeared not to be the physical properties of the excitation and/or response transducers, but of the human being on the structure while operating the exciter.

5.3.3 Response Measurements

Having estimated the fundamental natural frequency at 4.5 Hz, the shape (Figure 5.26) and the point where the maximum response of the first mode occurs (TP14), it was determined that the walking path which would generate the greatest response at TP14 should be as close as possible to the mid-line of the slab strip (see Figures 5.26 and 5.29). Three types of forced excitation tests were performed.

Firstly, a continuous walking (back and forth the along walking path) lasting two minutes. This was done in order to simulate a 'busy' floor environment and to create as steady a state as possible response conditions by a single person walking. Two sets of tests were performed:

- with a pacing rate of 135 steps per minute so that the second harmonic of the walking forcing function excited the floor resonance at 4.5 Hz, and
- with a pacing rate of 90 steps per minute so that the third harmonic excited the resonance.

Secondly, vibrations were measured at TP14 due to just a single traversing of the strip. Again, the prescribed pacing rates were either 135 or 90 steps, depending on the relevant harmonic which had to be generated.

Finally, an acceleration response to a single-person treading 135 times per minute in place at TP14 was recorded at the same point. Making only 90 steps in place per minute proved to be difficult for the test subject and can be considered as unrealistic.

Only one person generated these responses. The aim of these tests for all four structures tested was to establish if the tests were repeatable and what were the general response trends. The aim was not to produce statistically reliable data, because this would require more testing time than was available when investigating all four floor structures.

5.3.3.1 ACCELERATION RESPONSES TO CONTINUOUS WALKING LASTING 120 S

Figure 5.30 shows a typical acceleration response at TP14 due to 120 s of walking of an average male weighing 75 kg who tuned his pacing rate so that the 2nd harmonic of walking excited the structure as close as possible to its first resonance. The test subject, who had considerable experience in such exercises, did his best to match the prescribed rate of 135 paces per minute controlled by a beeping metronome. The acceleration signal sampling rate was 256 samples per second.

In addition to 120 s long acceleration time histories, RMS trend analysis for 'moving' data blocks lasting 10 s was performed, as proposed by Eriksson (1994). As outlined in Chapter 2, in order to produce results comparable with the work of others, the 10 s RMS average of measured accelerations is going to be the main parameter for assessing and comparing the floor vibrations. The 'moving' of 10 s blocks over 120 s of acceleration time history ensures that the largest 10 s RMS value is going to be found. For easier presentation, units adopted for this parameter are 'gRMS' presented in percentages. DATS (1995) signal analysis software was used for these extensive calculations. Figure 5.30 shows one such 10 s RMS trend analysis whereby maximum of 3.1% gRMS acceleration was measured 99.2 s after the start of walking.

Generally, it was established that the maximum gRMS values measurements from continuous walking were relatively well repeatable. An illustration of this is given in Figure 5.31 where the same test subject repeated the same test for another 120 s and produced a maximum of 2.95% gRMS acceleration. By inspecting a number of acceleration time histories and RMS trend analysis graphs of the kind shown in Figures 5.30 and

5.31, it was concluded that it was unlikely that prolonged continuous walking for more than 120 s would produce significantly different peak gRMS values.

The pacing set at 90 steps per minute, performed by the same test subject, produced a peak of only 0.92% gRMS (Figure 5.32). This value was verified by a repeated test which resulted in a peak of 0.85% gRMS (Figure 5.33).

5.3.3.2 Acceleration Responses to Single Crossing and Treading In-Place.

Typical acceleration time histories corresponding to single crossings of the slab strip are shown in Figures 5.34 (135 paces per minute) and 5.35 (90 paces per minute). The former lasted approximately 5 s whilst the duration of the latter was about 8 s. Again, the third harmonic of walking produced considerably lower responses then the second.

Finally, Figure 5.36 shows a typical response to transient stomping at TP14 which simulated the 2nd harmonic of walking and lasted about 7 s. Surprisingly, although the application of the force was non-stop at the maximum modal amplitude, the maximum 10 s gRMS value was not higher than for transient walking along the slab covering lower as well as higher modal amplitudes at 135 paces per minute (Figure 5.34). A 22 s non-stop stomping at TP14 produced a fairly constant response after a build-up of vibrations, resulting in the maximum of 1.76% gRMS, in the example shown in Figure 5.37.

5.3.3.3 Summary of Response Measurements on Structure A

In addition to the results discussed above, a summary of all walking and stomping response measurements is given in Table 5.7 for typical pairs of the four types of excitation. Although the variations in the maximum gRMS values between pairs of nominally identical tests were considerable for shorter excitations, the following trends could be established:

1. a single pass walking excitation generally produces lower responses than its multiple-pass excitation counterpart,
2. the 3rd harmonic of walking excitation, which is of particular interest when checking the floor vibration serviceability (Wyatt, 1989), generates a significantly lower response than the 2nd harmonic, and
3. tuned stomping produces a considerably lower response than the corresponding continuous walking.

Table 5.7: Structure A - Summary of response measurements in terms of maximum 10 s gRMS.

Type of excitation	2nd harmonic excitation		3rd harmonic excitation	
	Test 1	Test 2	Test 1	Test 2
Continuous walking for 120 s	3.10%	2.95%	0.92%	0.85%
Transient walking over one length lasting	1.29%	1.72%	0.42%	0.44%
Stomping @TP14 for 6 s	1.14%	0.65%	N/A	N/A
Stomping @TP14 for 20 s	1.76%	1.55%	N/A	N/A

5.4 Vibration Testing of a Reinforced HSC Flat Plate (Structure B)

The second prototype floor structure, Structure B, was a cast in-situ floor made of HSC. This was an experimental slab designed as a part of an EU funded BRITE EURAM demonstration project on HSC. The floor was, probably, the strongest concrete slab ever produced in the UK (Price, 1996). The slab was cast indoors on 10 October 1995 in a large workshop at Taywood Engineering in West London. Its de-commissioning took place in June 1998. The writer seized a unique opportunity, given by Taywood Engineering and Ove Arup & Partners, the latter being the principal designers of the floor (Feltham, 1995), to dynamically test this exceptional structure.

5.4.1 Structural Description

The floor was a 15 m symmetric 250 mm thick square plate, being directly supported by four 300×300mm` columns. The columns were 1.6 m high and set in 3.0 m from the floor edges (Figure 5.38). They were founded on 400 mm deep and 2.0 m square footings, which, in turn, were supported by the workshop's strong floor. The slab boundary conditions along the edges of the 3.0 m cantilevers were completely free. Also, 1.0 m high safety handrails were clamped approximately every 3.0 m along all four edges (Figure 5.38). The slab was classically reinforced with two layers of meshed unstressed reinforcement placed in the bottom and/or top zones of the slab depth, as appropriate (Figure 5.39).

Spanning 9.0 m between the columns, the slab's span-to-depth ratio was 36, which can be considered to be quite slender for a cast in-situ PT floor and to be extremely slender for a classically reinforced concrete floor.

An investigation of the dynamic properties and vibration serviceability performance of such a slender cast in-situ concrete floor is, clearly, very relevant to this research.

5.4.2 Field Test(s) Planning

As a part of an EU funded research project, which was completely separate from the research reported in this thesis, the floor had to be loaded twice and its serviceability performance examined in terms of deflections and cracking. Firstly, only three days after casting, the slab was loaded to 1.5 kN/m^2 plus dead weight, and, then, 28 days after casting to 13.125 kN/m^2 including dead load (Price, 1996). The loading was applied by a system of 36 hydraulic jacks and prestressing bars, which passed through the slab and were anchored in a strong floor underneath (Figure 5.40). The first load was considered to be light and was meant only to cause deflections with no cracking of the slab. However, the second, much increased, load was aimed at causing extensive deformation and cracking. Both loading conditions were, nevertheless, within the design serviceability loading limits (Price, 1996).

In the context of this two-phase static testing, it was interesting to compare the floor's vibration performance at the following three distinctive stages in the life of this structure:

- Stage 1: immediately after the slab was cast;
- Stage 2: between the light and the heavy loading; and
- Stage 3: after the heavy loading.

5.4.2.1 SPECIAL CIRCUMSTANCES

Severe time constraints played an important role in the planning of the dynamic testing. For example, as there were only three days between the slab casting and the application of the first loading, it was not feasible to carry out Stage 1 dynamic testing. Therefore, only the remaining two stages were possible to be investigated. In addition, being unique, a number of other investigations were scheduled to take place on the HSC floor. This, and the available funding, reduced the time available for the dynamic investigation during Stage 2 to two days, and during Stage 3 to three days. Also, although the slab was located indoors, the testing conditions were not up to normal laboratory standards as no heating existed and the workshop itself was very noisy due to other activities. The worst example of this was the running of an aircraft engine only 50 m away from the place where the slab was erected. While the engine was running no dynamic testing of the floor was possible. Also, other frequent sources of noise had the potential to affect the quality of experimental data, as will be seen later.

5.4.2.2 SITE VISIT

One site visit prior to even preliminary field modal testing is recommended (DTA, 1993c) in order to gain familiarity with the test structure and its environment. This is fully supported by the writer's experience in that up to half of the total site time can actually be devoted to activities such as accessing the structure, the equipment (un)packing, (dis)connecting, setting-up, checking and trouble-shooting. Familiarity with the test structure, its site and environment can reduce uncertainties associated with these time consuming activities, and this is very important if the test is to be completed during the allotted time period.

Also, when using hammer excitation on floors, the first site visit can be used, if possible, to do some quick FRF measurements in order to ascertain whether additional floor 'de-rattling' procedures are necessary. It is well known that hammer impact testing is particularly sensitive to rattling of the structure being hit (Halvorsen & Brown, 1977). Floors usually have non-structural elements attached which may rattle, introducing non-linearities and thus giving poor test results.

The HSC floor site was visited for a brief period of only four hours on 24 October 1995. A number of quick FRF reciprocity and homogeneity checks were performed by a two-strong test crew using the sledge hammer as the exciter. Although the prestressing bars were removed, it appeared that the very presence of 36 hydraulic jacks loosely positioned on the top surface of the floor (Figure 5.40) caused the structure to fail the reciprocity check. Problems were experienced with the homogeneity checks as well. Hence, a 'de-rattling' procedure, in the form of stripping the floor surface of everything 'non-structural', apart from the safety handrails (required by safety regulations), was suggested and was carried out over a couple of days by the Taywood Engineering personnel. The first site visit was also used to check the essential geometric properties of the structure being tested, the levels of excitation due to background noise and the availability of a 240 V electrical power supply.

5.4.2.3 PRE-TEST ANALYSIS

The FE model developed in the pre-test analysis utilised SHELL63 elements to represent the HSC flat plate. As no cracks were anticipated in the slab, isotropic properties were assumed for this element. Following the spirit of a number of floor vibration serviceability guidelines, including those given by the Concrete Society (1994), the relatively thin 300×300mm columns (Figure 5.38) were modelled as pin-supports (Figure 5.41). Similarly to the grillage model developed for Structure A (Figure 5.12), the pre-test analysis FE model was relatively crude. It consisted of 36 elements having a uniform thickness of 250 mm and the model had just enough nodes to match the adopted experimental test-grid of 49 points shown in Figure 5.42.

Values of the dynamic modulus of elasticity and density of the HSC used in the pre-test analysis were based on ultrasonic pulse velocity and concrete density measurements made by Taywood Engineering Ltd (Price, 1995). The average ultrasonic pulse velocity through six HSC specimens made when the floor was cast was 4983 m/s, whereas the average material density was 2465 kg/m^3. The dynamic modulus of elasticity $E_{c,dyn}$

was then calculated using Equation 5.9 (Neville, 1995), which links it with the ultrasonic pulse velocity V through concrete specimens having density ρ_c and Poisson's ratio ν_c.

$$E_{c,dyn} = \frac{V^2 \rho_c (1+\nu_c)(1-2\nu_c)}{(1-\nu_c)} \qquad \text{Equation 5.9}$$

For Poisson's ratio values increasing from 0.16 to 0.25 (Neville, 1995) the values of $E_{c,dyn}$ decrease from 57.5 GPa to 51 GPa, respectively, when Equation 5.9 is used. It should be stressed that the equation is applicable only to homogeneous, isotropic linear elastic materials (Neville, 1995). These figures might appear high to a concrete designer used to operating with static elastic moduli in the range 20-30 GPa for normal concretes.

However, Lyndon and Iacovou (1995) recently reported that HSC can have a significantly increased dynamic modulus of elasticity when compared with the values obtained from normal strength concrete. The HSC considered here was designed to be concrete grade C110. In fact, only three weeks after the casting, when the dynamic testing took place, its strength was already at 115 MPa (Price, 1996). Given these considerations, it was decided to adopt $E_{c,dyn} = 50$ GPa in the pre-test analysis.

Table 5.8: Structure B - Calculated natural frequencies in pre-test analysis

Mode No.	Natural frequency [Hz]
1	4.8
2	5.3
3	7.9
4	7.9
5	10.9
6	10.9
7	11.9
8	12.4
9	15.9
10	17.1

The initially calculated mode shapes and natural frequencies are shown in Figure 5.43 and are summarised in Table 5.8. The Auto-MAC matrix calculations based on the pre-test FE model indicated that the test grid was likely to be suitable for the prevention of spatial aliasing (Figure 5.44).

5.4.2.4 INSTRUMENTATION, EXCITATION AND DATA COLLECTION

It should be mentioned here that in October 1995, when the first round of Stage 2 tests took place, no tape recorder was available to the writer. The only data acquisition device available was the dual-channel spectrum analyser Diagnostic Instruments PL202. The spectrum analyser internal memory was limited to only 512 KB and no long-term digital sampling was possible. This limited the data acquisition to only two channels, each containing up to 4096 data points per record.

The limited facilities for this test (Figure 5.45), together with the severe testing time constraints, required a careful selection of the FRF reference point which would be able to identify all modes of vibration, excitable by normal walking.

This problem was compounded by the fact that the calculated natural frequencies indicated that repeated or closely spaced modes of vibration may occur in the real structure. By inspecting the first four calculated modes (Figure 5.43), modes 1 and 2 can be considered as close, whereas modes 3 and 4 are repeated. In this particular case, when selecting the FRF reference point, the full value and importance of a pre-test analysis can be demonstrated quite effectively.

Typically, without performing any FE analysis and by exercising 'engineering judgement', an obvious choice for the reference point to measure the 1st mode of vibration would be TP25, the slab's mid-point (Figure 5.42). However, the FE analysis clearly showed that the very same point could easily be a non-moving nodal point for modes 1, 3 and 4 (Figure 5.43). Therefore, the FRFs measured with the accelerometer at the slab's mid-point would, quite possibly, miss three out of the first four modes of vibration, including the very important fundamental mode.

Having this in mind, a decision was made to place the reference accelerometer at TP5, which appeared to move considerably in modes 1, 3 and 4 (Figure 5.43), and to perform one hammer swipe over the 49 test points. Then, in order to comply with the DTA (1993b; 1993c) requirement to measure more than one column/row of the FRF matrix, another hammer swipe was made with TP25 as the reference point. The main aim of second swipe was to ensure that the 2nd mode of vibration was identified properly, as TP5 appeared to have a fairly small response in this mode (Figure 5.43). Clearly, if more than two simultaneous data acquisition channels existed, there would be no need to perform another time consuming and tiring (when there is only one hammer operator, as was the case here) hammer swipe. The layout of the hardware setup used when testing Structure B is shown in Figure 5.46.

5.4.3 Modal Testing of the Uncracked HSC Slab at Stage 2

The research schedule for the uncracked HSC slab allowed for 31 October and 1 November 1995 to be devoted to dynamic testing. This meant that only approximately 24 hours of effective field work was available for the preliminary investigation, full FRF data acquisition and the vibration response measurements due to walking. Considering such extremely short time scales and the problems with modal testing experienced during the site visit, a decision was made to focus on the modal testing and, time permitting, perform a limited number of response measurements.

5.4.3.1 PRELIMINARY INVESTIGATION

At the very beginning of the preliminary investigation during the first day of testing, the Endevco dual-channel signal conditioning unit developed a fault. Therefore, a decision to use a spare Dytran, instead of Endevco, accelerometer was made on the spot. However, the troubleshooting of this fault took a considerable amount of time. As a consequence, no time remained in the second day of dynamic testing for the response measurements. These, by their very nature, had to be performed at the end of the modal testing and initial parameter estimation after the natural frequencies and mode shapes (i.e. the critical walking paths) had been determined in-situ.

After replacing the Endevco accelerometer, setting up its Dytran counterpart and amending the test documentation to account for these changes, a number of quick QA measurements was performed. The general procedure used was very similar to the case of the previously described Structure A. The main aim of these QA checks was twofold. Firstly, to select the digital data acquisition parameters for acquiring good quality FRF data (Table 5.9). Secondly, to establish the quality of FRF data which could be obtained from a notably quite noisy environment.

The acquisition parameters shown in Table 5.9 are those that were adopted when performing FRF measurements having TP5 as the reference. However, when TP25 was used as the reference, the principal aim was to identify only the 2nd mode of vibration and, therefore, the frequency resolution was not the prime consideration. Therefore, instead of 0.05 Hz, the resolution for the second measurement was 0.1 Hz. As a consequence, the data acquisition times, number of data samples and frequency lines were halved for the same frequency range of interest. This was quite desirable considering the limited testing time and spectrum analyser internal memory available.

Table 5.9: Structure B - Main digital data acquisition parameters adopted for FRF measurements when TP5 is the reference point.

Parameter description	Parameter value
Data acquisition time	20 s
Frequency resolution	0.05 Hz
Frequency range of interest	1-21 Hz
Total number of samples	1024
Number of frequency lines	400
Number of averages	5
Exponential window time constant (TC)	8

Examples of the FRF reciprocity and linearity checks are shown in Figures 5.47 and 5.48. The quality of the FRF data was, obviously, not ideal as the appropriate pairs of the FRF curves should be identical. In general, while performing the FRF averages, the individual FRFs shifted noticeably. This shift was probably a consequence of one or more of the following factors:

- The noisiness of the environment causing unmeasured excitation
- The presence of the hammer operator on the floor
- The possible rattling of the safety handrails which were clamped onto the edge of the floor

- The improper sampling of the hammer excitation signal by the portable spectrum analyser used after being passed through anti-aliasing filters when performing modal testing on structures having low natural frequencies. This issue was discussed recently by Pavic and Waldron (1996b), Pimentel (1997) and Pavic et al. (1998), and will not be repeated here.

As it was generally observed that the shift between subsequent FRFs reduced as the number of averages was increased, it was concluded that these effects could be treated as an uncorrelated 'noise'. This was filtered out by FRF averaging using the H1 estimator built into the spectrum analyser used (McConnell, 1995). However, the testing time constraints did not allow for more than five FRF averages to be performed.

Finally, an example of a satisfactory point mobility FRF shape check is shown in Figure 5.49, although the region between the second and third peaks (8.2-14.8 Hz) showed some rather peculiar behaviour.

5.4.3.2 FRF Data Acquisition and Initial Data Analysis

Two FRF sweeps followed by limited data analysis took the whole of the second day of testing. In total, 98 FRFs were acquired over 49 test points, half of these with TP5 as a reference, and half with TP25 as a reference.

As the FRF data were generally noisy and there was a strong indication that the structure may have a number of close modes of vibration, one of the mode indicator functions (MIF) available in ICATS (1995; 1997) was used to pinpoint the frequencies which may correspond to the modes of vibration. This helps the selection of the frequency ranges of interest when performing either SDOF or MDOF single or multi-FRF parameter estimation exercises (Heylen et al., 1997).

In this case, a very simple MIF, denoted as $|H_{j,sum}(\omega)|$, and defined as the sum of the moduli of all measured FRFs, was selected. A mathematical expression of this MIF is:

$$|H_{j,sum}(\omega)| = \sum_{k} |H_{jk}(\omega)| \qquad \text{Equation 5.10}$$

Two MIFs were calculated. Firstly for the row of the FRF matrix corresponding to TP5 as the reference response point (j=5), and, then, for the row where TP25 was the reference (j=25). The calculated $|H_{5,sum}(\omega)|$ and $|H_{25,sum}(\omega)|$ MIFs are plotted in Figure 5.50. The two curves effectively integrate information available in all the collected FRFs. The peaks in the two MIFs indicate the frequencies of the possible modes of vibration. By visually examining Figure 5.50, it appeared that the two lowest modes of vibration could, indeed, be closely spaced (5.8 Hz and 6.0 Hz). Other higher modes were clearly visible at 8.2 Hz, 14.8 Hz, 17.1 Hz and 18.4 Hz. Finally there was a group of small peaks possibly indicating a number of closely spaced modes of vibration between 9.0 Hz and 11.0 Hz.

Having established where to look for the modes of vibration, a number of parameter estimation exercises identified 12 modes between 1 Hz and 21 Hz. Their properties are shown in Table 5.10 (natural frequencies and modal damping ratios), and in Figures 5.51 (modal complexity) and 5.52 (mode shapes).

Table 5.10: Structure B (Uncracked) - The estimated natural frequencies and modal damping ratios.

Mode No.	Frequency [Hz]	Modal damping ratio ζ [%]
1	5.8	0.51
2	6.0	0.54
3	8.2	1.19
4	10.5	1.12
5	10.8	1.00
6	10.9	1.65
7	11.2	0.36
8	11.6	0.23
9	12.3	0.30
10	14.8	0.73
11	17.1	0.39
12	18.4	2.08

By visually inspecting the FE calculated and experimentally estimated modes shapes (Figures 5.43 and 5.52), the first three estimated modes resembled the FE modes 1, 2 and 4. Also, there was a clear correlation between analytical modes 9 and 10 and experimental modes 10 and 11, respectively. However, experimental modes 4-9 (highlighted in Table 5.10) had much less consistent modal parameters than modes 1-3, and 10 and 11.

Regarding the complexity of the modes (Figure 5.51) it should be noted that the higher modes 10 and 11 were almost perfectly real whilst the other modes, estimated from the same FRF data, developed various degrees of complexity. It is possible that this phenomenon was, again, caused by the presence of the hammer operator on the floor, as was the case in Structure A. Unfortunately, no evidence was produced to corroborate this possibility.

Finally, and most importantly, a notable difference was observed between the measured (Table 5.10) and analytically calculated (Table 5.8) natural frequencies for the first three modes of vibration. Nevertheless, having in mind the very good correlation between the lowest three calculated and measured mode shapes, the writer was satisfied that modal data of sufficient quality had been obtained during the two-day testing. The differences, clearly indicating a lack of stiffness in the analytical model, could easily be attributed to inaccuracies in the relatively crude FE model. Further, more detailed correlation and updating exercises aimed at obtaining a more reliable analytical model of Structure B at Stage 2 will be presented in Chapter 6.

5.4.3.3 LESSONS LEARNED

The two-day test in London was the first field work for which the writer was in charge and two important lessons were learned.

Firstly, the failure to gather response data was quite frustrating, but also indicated that a two-day testing period was overambitious, especially when something went wrong. The QA preliminary investigations, the full FRF data collection and the walking response measurements are three quite distinct activities requiring,

under the circumstances pertinent to this research, at least a day of field work per floor. Therefore, similar subsequent field tests on this and other floor structures were planned to last at least three days.

Secondly, the quick one-day site visit proved to be extremely useful. Without it, an attempt to do the full modal testing of the floor with the hydraulic jacks on it would have failed completely. As a consequence, the short two-day research slot and the financial resources to do it would have been lost.

5.4.4 Modal Testing of the Cracked HSC Slab at Stage 3

The second round of testing of the HSC floor took place after the 13.5 kN/m^2 total static loading had been applied to the floor. This was achieved by 36 hydraulic jacks which were computer controlled in order to ensure as uniform as possible 'surface loading' across the whole area of the slab (including the cantilevers). The floor was subsequently tested dynamically over three days between 22 and 24 February 1996.

5.4.4.1 CRACKING PATTERNS

The 13.5 kN/m^2 loading caused extensive cracking in the floor. These remained visible even after the loading was removed. The crack patterns on the top and bottom surfaces of the slab were examined in detail by the Taywood Engineering personnel. Information about the cracking available at the time of dynamic testing is given in Figure 5.53. However, the state of cracking in the slab above columns C1 and C2 was not available.

The writer's interpretation of the cracking patterns is that they conform to the way the reinforcement mesh was layered. As the top mesh had bars in the N-S direction lower than in the E-W direction, this made the N-S direction 'weaker' for the action of negative bending moments which put the top surface of the slab under tension. This tension opened a long E-W crack on the top surface (Figure 5.53a). The bottom mesh also had N-S bars lower than E-W bars. However, for the action of positive bending moments, the E-W direction is now 'weaker'. This caused the cracks due to moments which bend the slab in this 'weaker' direction to be spread over a more narrow N-S strip (Figure 5.53b).

The static loading caused extensive cracking at the top of all four columns as well (Figure 5.54). The cracking propagation conformed to the state of biaxial bending, combined with an axial compression force, of the square 300×300mm column cross sections.

5.4.4.2 PRELIMINARY INVESTIGATION

Having to investigate such a heavily cracked structure, the prime concern was its (non)linearity. A number of checks was made and, considering the adverse environmental circumstances, the results were as good as for the same slab when it was uncracked. So, for the relatively low-levels of excitation and response, the structure could be considered as linear.

Regarding the digital data acquisition parameters selected for this second round of testing, the only changes to the values used in the first round (Table 5.9) was an increased number of averages from 5 to 10 and an increased exponential window time constant from TC = 8 to TC = 10. Better testing time management allowed for more averages whereas the new time constant was the maximum which could be applied by the portable spectrum analyser. This was done in order to improve the signal-to-noise ratio during the 20 s of data acquisition per each hammer impact.

5.4.4.3 FRF DATA ACQUISITION AND INITIAL DATA ANALYSIS

The same test grid comprising 49 points was used as for the first round of testing (Figure 5.42). Two rows of 49 elements of the FRF matrix were measured by performing two separate hammer swipes. Although a 4-channel RACAL Store 4 tape recorder was made available for this round of testing, an electro-mechanical fault prevented its efficient use during the FRF data acquisition which took place during the second day of testing. However, the nature of the fault was such that it was possible to use the tape recorder for the vibration response measurements due to walking during the last day of testing. Therefore, the FRFs were acquired using only the dual-channel DI2200 spectrum analyser. This is the reason why two hammer swipes were performed.

As it was anticipated that the cracking would change the stiffness distribution in the slab, and considering the results of the preliminary analysis, it was decided to use points TP5 and TP35 as the FRF reference points.

After the FRF swipes, two MIFs, $|H_{5,sum}(\omega)|$ and $|H_{35,sum}(\omega)|$, defined previously in Equation 5.10, were calculated and their plots are shown in Figure 5.55. As the lowest modes of vibration were of particular interest, the functions were visually examined and the lowest peak identified was at 5.0 Hz. However, a small 'bulge' on the left side of the peak at 5.0 Hz in $|H_{35,sum}(\omega)|$ indicated the possibility that an even a lower mode of vibration existed.

To check this, another pair of MIFs, $Im^2(H_{5,sum}(\omega))$ and $Im^2(H_{35,sum}(\omega))$, being the summations of the squared imaginary parts of FRFs (ICATS, 1995; 1997), was used. A mathematical expression of this new form of MIF, which is a readily available utility in the ICATS software, is:

$$Im^2(H_{j,sum}(\omega)) = \sum_k (Im(H_{jk}(\omega)))^2 \qquad \text{Equation 5.11}$$

where j is the FRF reference point. Two plots of this function corresponding to TP5 (j=5) and TP35 (j=35), as the reference points, are shown in Figure 5.56. Another peak at 4.7 Hz is now clearly visible, but only in $Im^2(H_{35,sum}(\omega))$ indicating that TP5 this time was not a particularly suitable reference point for measuring the fundamental mode of vibration.

After processing two rows of 49 FRFs and combining the results, 11 modes were identified. Their properties are shown in Figure 5.57 and in Table 5.11.

The majority of modes was identified using TP35 as the reference point. The lowest two modes clearly show that the slab firstly bends in the less stiff E-W direction and then in the stiffer N-S direction. This would be expected if the mode shapes were interpreted as the displacement configuration which minimises the potential and maximises the kinetic energy in each mode of vibration (NAFEMS, 1992b).

Table 5.11: Structure B (Cracked) - The estimated natural frequencies and modal damping ratios.

Mode No.	Frequency [Hz]	Modal damping ratio ζ [%]
1	4.7	0.64
2	5.0	0.74
3	7.1	1.14
4	7.2	0.82
5	8.8	1.31
6	8.9	1.45
7	9.1	1.44
8	12.7	0.11
9	13.0	0.62
10	15.6	0.77
11	15.9	1.38

Although there was a number of peaks in the FRFs between 9.4 Hz and 12.7 Hz, these failed to produce any consistent modal estimates. An example of such uncertain estimates is mode 8 in Figure 5.57, which has a peculiar mode shape and a very low damping value. This may indicate that this modal estimate is unrealistic. However, the shape of this mode resembled to some extent that of mode 9. This could indicate that mode 8 really existed, and was caused by the slight orthotropy in the slab developed by cracking. It was close to mode 9, but could not be estimated accurately using TP35 and TP5 as the reference points. Mode 9 is also interesting, as it was almost perfectly real whereas all of the other modes developed a certain degree of complexity.

The preliminary investigation, two full FRF swipes and initial data analysis, performed by a two-strong test crew, took the first two days of field work.

5.4.5 Stage B Response Measurements on the Cracked HSC Slab

For the response measurements made during the last day of testing on 24 February 1996, only one test subject was used - the same person as for Structure A.

5.4.5.1 DATA ACQUISITION

An old RACAL Store 4 tape recorder was used in parallel with the Diagnostic Instruments PL202 spectrum analyser which was operating in a digital oscilloscope mode. The tape recorder was used in order to acquire simultaneous acceleration records on three channels and to gather vibration response data over periods

longer than 64 s. The 64 s was the maximum duration possible for data acquisition by the spectrum analyser. Later, after the testing, the spectrum analyser was upgraded with new software and hardware (Long Time Record DI-Card Operating Manual, undated) allowing much longer data acquisition times. Therefore, the data presented here were digitally re-sampled from the magnetic tapes using the enhanced spectrum analyser and further processed using the DATS (1995) software in a similar way as for Structure A.

5.4.5.2 WALKING PATHS AND MEASUREMENT POINTS

Prior to the response measurements, there was only time to partially process half of the collected FRF data. These processed FRFs had TP35 as the reference point. The first three modes, estimated at 4.7 Hz, 5.0 Hz and 7.1 Hz, were easily identifiable. Considering the values of the three natural frequencies these three modes were assumed to be excitable by normal walking. Mode 4 and higher, shown in Figure 5.57, were estimated after returning to base. Therefore, only the frequencies and shapes of the first three modes were available to the writer on site so as to establish the walking paths, pacing rates and measurement points which would be able to produce and register 'nominally' the greatest acceleration responses. These are summarised in Table 5.12 and in Figure 5.58.

The only type of walking in the six tests was continuous normal walking back and forth along the paths with a prescribed pacing rate controlled by a metronome for several minutes. Every effort was made to restrict the response measurements of vibration only to those due to walking with as little as possible additional extraneous excitation. Mode 3, having a 7.1 Hz natural frequency, could not be excited by the second harmonic of normal walking as it would require 213 ($=60 \cdot 7.1/2$) steps per minute, which is unrealistically fast.

Table 5.12: Structure B - Schedule of continuous walking response measurements.

Test No.	Mode and frequency excited	Excitation harmonic (pacing rate)	Walking path	Maximum modal amplitude	Measurement points
1.1	1 (4.7 Hz)	2^{nd} (141 spm)	TP46-TP4	@TP25	@TP25, 43, 49
1.2	1 (4.7 Hz)	3^{rd} (94 spm)	TP46-TP4	@TP25	@TP25, 43, 49
2.1	2 (5.0 Hz)	2^{nd} (150 spm)	TP43-TP49	@TP46	@TP46, 22, 28
2.2	2 (5.0 Hz)	3^{rd} (100 spm)	TP43-TP49	@TP46	@TP46, 22, 28
3.1	3 (7.1 Hz)	3^{rd} (142 spm)	TP49-TP1	@TP22	@TP22, 27, 28
3.2	3 (7.1 Hz)	4^{th} (107 spm)	TP49-TP1	@TP22	@TP22, 27, 28

Generally, 120 s of acceleration data again proved to be sufficient to provide a reliable trend of RMS acceleration averages over 10 s long data blocks. This is demonstrated in Figures 5.59 and 5.60 which jointly show 240 s of acceleration response at TP43 in Test 1.1. Figure 5.59 contains the data pertinent to the first 120 s whilst Figure 5.60 the data recorded during the remaining 120 s. By visually examining the acceleration time histories in these two figures the records look similar. In addition, the 10 s RMS trend analysis produced a peak of 0.370% gRMS from the first 120 s of data, whereas the remaining 120 s produced 0.338% gRMS representing a difference of less than 10%, same as for Structure A. In both cases,

however, the 10 s RMS trends showed a considerable fluctuation between, approximately, 0.2% and 0.4% gRMS.

As expected, the maximum acceleration response recorded in Test 1.1 occurred at TP25, the point of maximum amplitude for mode 1 (Figure 5.61). This resulted in a 0.418% gRMS peak.

Similar analyses were performed on 18 acceleration time histories acquired at three pre-selected measurement points (Figure 5.58) in each of the six tests (Table 5.12). For each of the three modes of interest, the measurement points corresponded to the three mode shape amplitudes which were, at the time of testing, assessed to be the largest (in an absolute sense). The results of these analyses, in terms of 10 s RMS acceleration peaks, are shown in Table 5.13.

Two results in Table 5.13 deserve particular attention. Firstly, the highest response in all 18 tests was 0.512% gRMS and was produced in Test 2.1 by exciting mode 2 and not the fundamental mode 1. The acceleration time record leading to this result is shown in Figure 5.62. Equally interesting are the strong responses at TP22 to the 3rd and even the 4th 'harmonics' of normal walking which were exciting mode 3 at 7.1 Hz in Tests 3.1 and 3.2, respectively. These acceleration responses are shown in Figures 5.63 and 5.64, respectively. The responses in Test 3.1 are almost at the same level as the responses in the fundamental mode, whereas the responses to the 4th harmonic in Test 3.2 are considerably greater that than the responses to the 3rd harmonic in Test 1.2. These are only slightly lower than the responses to the 3rd harmonic in Test 2.2.

Table 5.13: Structure B (Cracked) - Summary of results of 10 s RMS trend analyses of 120 s long acceleration time histories.

Test No.	Mode and frequency excited	Excitation harmonic (pacing rate)	Walking path	Measurement point	10 s RMS peak acceleration [gRMS]
1.1	1 (4.7 Hz)	2nd (141 spm)	TP46-TP4	TP25	0.418%
1.1	1 (4.7 Hz)	2nd (141 spm)	TP46-TP4	TP43	0.370%
1.1	1 (4.7 Hz)	2nd (141 spm)	TP46-TP4	TP49	0.368%
1.2	1 (4.7 Hz)	3rd (94 spm)	TP46-TP4	TP25	0.200%
1.2	1 (4.7 Hz)	3rd (94 spm)	TP46-TP4	TP43	0.176%
1.2	1 (4.7 Hz)	3rd (94 spm)	TP46-TP4	TP49	0.173%
2.1	2 (5.0 Hz)	2nd (150 spm)	TP43-TP49	TP46	0.512%
2.1	2 (5.0 Hz)	2nd (150 spm)	TP43-TP49	TP28	0.489%
2.1	2 (5.0 Hz)	2nd (150 spm)	TP43-TP49	TP22	0.479%
2.2	2 (5.0 Hz)	3rd (100 spm)	TP43-TP49	TP46	0.373%
2.2	2 (5.0 Hz)	3rd (100 spm)	TP43-TP49	TP22	0.342%
2.2	2 (5.0 Hz)	3rd (100 spm)	TP43-TP49	TP28	0.339%
3.1	3 (7.1 Hz)	3rd (142 spm)	TP49-TP1	TP22	0.410%
3.1	3 (7.1 Hz)	3rd (142 spm)	TP49-TP1	TP28	0.368%
3.1	3 (7.1 Hz)	3rd (142 spm)	TP49-TP1	TP27	0.218%
3.2	3 (7.1 Hz)	4th (107 spm)	TP49-TP1	TP22	0.332%
3.2	3 (7.1 Hz)	4th (107 spm)	TP49-TP1	TP28	0.309%
3.2	3 (7.1 Hz)	4th (107 spm)	TP49-TP1	TP27	0.167%

These results independently confirm Eriksson's (1994) finding that it is important to consider all modes of vibration, and not only the fundamental mode, which can be excited by normal walking. Also, it was

interesting to see that the 4th harmonic of walking is capable of causing such a strong response in a floor structure. A further discussion of these important issues will be presented in Chapters 6 and 7.

5.5 Vibration Testing of a Post-Tensioned Ribbed Slab (Structure C)

Structure C was the first floor in a real-life building to be investigated. The writer was approached by the floor designers in March 1995, after they found that the floor failed the vibration serviceability check proposed by the CSTR43. The floor, being very slender indeed (span-to-depth ratio of almost 40), was intended to support high-quality offices in a building located in the centre of London. However, the constraints of this multi-million pound project did not allow for usual remedial measures, such as an increase of the floor depth, or inclusion of additional columns, to be employed.

Having little confidence in the CSTR43 guidelines, the floor designers wanted to know what the actual vibration performance of the floor would be if it was built as originally proposed. An informed decision to build the floor anyway, and as slender as originally planned, was made after a sophisticated but limited linear dynamic FE analysis of the floor was carried out by the writer. This analysis indicated that it was likely that the floor would have a satisfactory vibration serviceability performance. After the floor was built the writer verified this analysis by prototype modal testing and vibration response measurements. The description and results of this very challenging experimental investigation will be presented here.

5.5.1 Structural Description

The floor investigated was in fact one of a number of nominally identical floors in a six-storey building which was designed and erected in 1995 and 1996. The building had two near symmetric and physically separated parts denoted as 'South' and 'North'. Each part consisted of five nominally identical floors. Details of one of the floors on the 'North' side, which was experimentally investigated, are given in Figure 5.66.

Structurally, each floor had two areas:

- The 'main' area, being approximately 31 m wide in the E-W direction and 14.5 m long in the N-S direction; and
- The 'core' area being 31 m wide in the E-W direction and having varying length in the N-S direction.

General horizontal stability of the floor and of the whole building was provided by the system of walls and lift shafts as well as orthogonal structural frames comprising horizontal beams rigidly connected to wide columns along the floor edges.

5.5.1.1 'MAIN' AREA

The floor in the main area consisted of a partly ribbed slab, post-tensioned only in the direction of the ribs, spanning 14.5 m in the N-S direction. The PT ribs, 650 mm wide, of 350 mm overall depth at approximately 1.0 m centres in the E-W direction, were cast integrally with a 110 mm thick concrete slab. This arrangement formed a monolithic T beam cross section having 1.0 m wide flange. Furthermore, the system of 26 transversely connected (via the 110 mm thick flange) parallel T beams spanning 12 m in the N-S direction (defined as the 'ribbed' zone in Figure 5.66) was supported along the inner edge of the 'ring' zone (Figure 5.66) with a 350 mm thick solid slab. This slab was approximately 1.25 m wide. The outer edge of the 'ring' zone was supported by 1050 mm deep and 300 mm wide beams. These beams were themselves supported either by wide columns along the edge of the slab, or by walls and facade beams in the 'core' area.

5.5.1.2 'CORE' AREA

The 'core' area comprised a 300 mm thick solid concrete slab having a number of openings designed to permit the passage of stairs, lifts and services. These openings were also used to gain access during the tensioning of the prestressing tendons coming from the wide shallow ribs in the 'main' area. The 'core' area slab was supported either by walls or by beams. The boundary between the 'core' area and the 'main' area was stiffened by 850 mm deep and 500 mm (or 200mm) wide reinforced concrete beams running in the E-W direction. The main structural role of these beams was to accept and transfer the vertical reaction forces from the prestressing tendons which changed curvature in the zone where the 'core' area met the 'main' area.

5.5.2 Field Test Planning

As the testing had to be performed during the building construction, the selection of the exact floor level to be tested was left to the building frame contractor. Level 3 North side was selected and the contractor cleared this floor space twice for the purpose of dynamic tests, firstly in December 1995 and, then, in June 1996. Two slots of three effective working days were allocated to do these tests. The difference between these two rounds of tests was the state of the floor and of the building site itself.

5.5.3 December 1995: Modal Testing of Bare Floor in Unclad Building

5.5.3.1 Special Circumstances, Environmental and Boundary Conditions

A two-strong testing crew performed the first round of tests in December 1995 under extremely cold and windy weather conditions, in the middle of a very active building site. The floor level tested was not clad and the temperature during the testing was around 0^{0}C.

The floor tested was supported only by a building frame made of cast in-situ reinforced concrete. No facade and internal partitions existed. The floor was completely bare with no services attached underneath.

No suitable means of lifting mechanically the equipment to the 3rd floor existed, so every piece had to be manually carried by the test crew. In addition, being a high-profile location in the centre of London, transportation and unloading of the equipment to the building site was difficult as parking restrictions were strictly enforced. Also, difficulties were experienced while using 110 V power supply provided by the contractor as no 240 V petrol generator was allowed to be used in this active building site. In addition, security issues required the work to be carried out only during daytime while other workers were on the site i.e. while the building site was active. This inevitably resulted in poorer quality of the FRF experimental data due to unmeasured extraneous excitation. Finally, because the extraneous excitation was present practically continuously, it was not possible for any representative vibration responses due to a single person walking to be measured.

These were just some of practicalities which affected the field testing of Structure C in December 1995. Although these difficulties were to some extent anticipated after a one-day site inspection prior to the testing, they put additional pressure on the test crew leading to a much slower acquisition of relatively low quality data.

5.5.3.2 Pre-Test Analysis

A test grid comprising 76 points (Figure 5.65) was investigated in the pre-test analysis. The FE model developed in the pre-test analysis (Figure 5.67) was considerably more complex than the models used for floor Structures A and B. The model was developed by employing a solid modelling technique available in the ANSYS FE code (ANSYS, 1995a). By defining the so called 'keypoints' in the FE model at the locations of all of the selected test points, each test point was mapped to a single node in the FE model. Similarly, as for Structures A and B, vertical modal displacements at these 76 nodes, obtained through analytical FE modal analysis, were then used to calculate an Auto-MAC matrix and check the spatial aliasing.

Although some rotational restraint existed at every support point of the real floor structure in the pre-test analysis, to follow the spirit of CSTR43, it was again assumed that all support points for the FE model were pinned (Figure 5.67). This was assumed at the points where the floor was supported not only by columns and

walls, but also by edge beams. This was done to simplify the initial modelling and avoid using beam elements at this stage. Apart from being pin-supported, the connection along the boundary between the 'main' and 'core' areas was assumed to be fully continuous. All floor openings were treated as permanent holes. Appropriate rotations were restrained along the support lines corresponding to walls.

As no additional information about the concrete material properties existed, the dynamic modulus of elasticity of concrete, designed as grade 50, was taken as 38 GPa, whilst the concrete density was taken as 2400 kg/m^3.

When analysed as a 3D system, the 'ribbed' zone of the 'main' area acted structurally as an orthotropic plate having greater bending stiffnesses in the main span (N-S) direction than in the lateral (E-W) direction. This orthotropy was modelled by using SHELL63 elements. However, the main problem was how to determine the lateral stiffnesses for this finite element which would represent the effects of the 110 mm integral slab. When 'smeared' over the 1 m width of the slab, the series of 350 mm deep T beams have an order of magnitude greater bending stiffness than the 110 mm thick slab spanning in the lateral E-W direction. However, the configuration of this ribbed floor was unusual because the ribs were wide and shallow and there was only approximately a 350 mm gap between them (Figure 5.67). This means that the wide and shallow beams could stiffen the E-W direction as well. The lateral stiffness of this in-situ cast concrete floor was one of the generally unknown FE modelling parameters about which little has been published. Therefore, an attempt is made in Chapter 6 to determine it through FE model updating based on the experimental measurements. At this stage, for the purpose of pre-test analysis, the lateral stiffness was modelled in the pre-test analysis by taking into account only the 110 mm slab (Szilard, 1974).

The stiffness of the remainder of the floor surface in the 'ring' zone and 'core' area was modelled using isotropic SHELL63 elements having 350 mm and 300 mm thicknesses respectively. Slightly different permanent surface loads which existed in the core area were modelled by adjusting the density of material in SHELL63 elements. In total, four different groups of SHELL63 elements were used to represent the various differing properties of this floor. These are indicated by different colours in Figure 5.67.

Figure 5.68 shows a satisfactory Auto-MAC matrix based on the calculation (Equation 5.1) of the first 10 mode shapes shown in Figure 5.69. It should be mentioned here that a number of more refined meshes was tried as well. However, these did not produce any noteworthy difference in the lowest modes of vibration considered to be of greatest interest here. The natural frequencies calculated are summarised in Table 5.14.

Table 5.14: Structure C - Calculated natural frequencies in pre-test analysis

Mode No.	Natural frequency [Hz]
1	5.2
2	5.5
3	6.6
4	7.9
5	9.3
6	11.5

Mode No.	Natural frequency [Hz]
7	13.9
8	14.4
9	14.8
10	16.8

Being shorter and supported by many walls and beams, the 'core' area was not moving very much in any of the first 10 modes calculated. Through the continuity (i. e. rotation restraining) conditions along the boundary between it and the 'main' area, the 'core' area clearly stiffened the 'main' area. The first four natural frequencies calculated indicated that the floor could be considered as a 'low-frequency' one excitable by the 3rd or 4th harmonic of normal walking.

5.5.3.3 EXCITATION AND DATA COLLECTION

During the first round of testing in December 1995 another attempt was made to use the old 4-channel RACAL Store 4 tape recorder (Figure 5.70) and simultaneously acquire one hammer and three accelerometer analogue signal channels (Figure 5.71). Unfortunately, right at the beginning of the testing, an accident happened when workers from the floor above unintentionally unloaded rubble through a floor opening directly onto the tape recorder. The tape recorder was damaged and could not be used any more in this round of testing. Therefore, the only data acquisition facility available was the dual-channel spectrum analyser DI2200.

5.5.3.4 PRELIMINARY INVESTIGATION

A full set of QA checks was performed, as there was a major concern that considerable extraneous excitation would prevent any meaningful FRF measurements.

To illustrate this, three examples are given. Firstly, Figure 5.72, shows a 16 s acceleration response at TP32 to a heel-drop applied at TP38. It can be seen that the floor vibrated before the heel drop and, approximately 12 s after the data acquisition started, the floor was again excited by a tool which was dropped on the floor below. It should be noted here that a heel-drop, in principle, causes peak accelerations which are an order of magnitude greater than the response due to normal walking. Therefore, a visual inspection of Figure 5.72 indicates that vibration responses to ambient excitations were roughly of the same magnitude as, or even larger than, the acceleration responses due to normal walking. Under such circumstances no meaningful measurements of the walking responses was possible.

Another direct consequence of relatively large extraneous excitation is given in Figure 5.73 which shows an 'immediate repeatability' QA check. This check was made by subsequent measurements of two, nominally identical, FRF transfer mobilities between TP32 and TP35. The second series of 10 averages was completed two minutes after the first. The last illustration is given in Figure 5.74 which is a 'reciprocity' QA check between TP32 and TP38. Obviously, the FRFs collected during the QA checks were not ideal.

However, by examining the data collected during the QA checks, it was concluded that the extraneous excitation could be treated as uncorrelated as the difference between the supposedly identical FRFs was being reduced by calculating more averages. It was decided to perform 10 averages per point as the testing time constraints did not allow for more. The key data acquisition parameters determined during the preliminary investigation and adopted for modal testing of Structure C are given in Table 5.15.

Table 5.15: Structure C - Main digital data acquisition parameters adopted for FRF measurements with TP32 as the reference point.

Parameter description	Parameter value
Data acquisition time	10 s
Frequency resolution	0.1 Hz
Frequency range of interest	1-21 Hz
Total number of samples	512
Number of frequency lines	200
Number of averages	10
Exponential window time constant (TC)	10

Another outcome of the QA checks was a reduction of the test grid from 76 to only 33 points. All test grid points in the 'core' area and along the edges of the 'main' area were abandoned due to very poor quality of the FRFs corresponding to these points. Application of the sledge hammer excitation at these points, situated at relatively stiff areas of the floor (edge beams, columns, lift shafts, 'core' area, etc.), could not excite the floor properly. Therefore, the test grid comprised three rows of 11 points: from TP17 to TP27, from TP30 to TP40, and from TP43 to TP53 (Figure 5.65).

Finally, it should be mentioned that due to unforeseen interruptions caused by working in an active building site, the cold weather conditions, problems in establishing valid test grid points and difficulties in communication with the hammer operator in a very noisy environment, the preliminary investigation took almost two out of the three scheduled field testing days.

5.5.3.5 FRF Data Acquisition and Initial Data Analysis

As it was determined that it would not be possible for meaningful response measurements to be made due to extraneous excitation, the last day of testing was devoted entirely to the modal testing. A hammer swipe (Figure 5.71), having the accelerometer at TP32 as the selected single reference point, lasted six hours. There was no time to perform another sweep and acquire another row of the FRF matrix. The acquired FRF data were, nevertheless, processed in situ in order to spot any flaws and, if required, repeat a limited number of measurements. This was done because the repetition of any FRF measurement after return to base was not possible.

After acquiring all 33 FRFs, a MIF, based on the squared imaginary parts of the FRFs measured (Equation 5.11), was calculated and is shown in Figure 5.75. Although produced from 'noisy' FRFs of the kind shown in Figures 5.73 and 5.74, the MIF clearly indicated that six modes of vibration have been picked by the experimental set-up used. A quick in-situ processing of the FRFs using MDOF parameter estimation

(ICATS, 1995) produced results shown in Figure 5.76. The estimated mode shapes were very encouraging, as they appeared to correlate very well with the pre-test analysis results. This was sufficient to conclude that FRF data of usable quality was collected.

After returning to base, the FRF data were re-processed, the effects of the exponential window removed, and the complexity of the modes examined. The natural frequencies and modal damping ratios are given in Table 5.16, whereas the complexity of the modes is shown in Figure 5.77.

Table 5.16: Structure C (Unclad) - The estimated natural frequencies and modal damping ratios after the first round of modal testing in December 1995.

Mode No.	Frequency [Hz]	Modal Damping Ratio ζ [%]
1	6.0	0.75
2	6.5	1.02
3	8.1	0.92
4	9.7	N/A
5	11.6	0.75
6	14.3	0.64
7	17.2	0.89

By comparing the pre-test FE (Figure 5.69) and experimental (Figure 5.76) mode shapes, it appears that the measurements missed the fourth analytical mode. This happened because the reference point TP32 was close to the nodal line of this mode. However, by re-examining the FRFs measured it appeared that this mode had a frequency of 9.7 Hz. Also, similarly as for Structure B, the measured natural frequencies (Table 5.16) were considerably lower than those predicted by the pre-test FE model (Table 5.14).

5.5.3.6 LESSONS LEARNED

One of the numerous lessons learned was to use hands-free operated radios in similar situations in the future in order to improve communication with the hammer operator.

5.5.4 June 1996: Modal Testing of a Bare Floor in the Clad Building

5.5.4.1 ENVIRONMENTAL AND BOUNDARY CONDITIONS

In June 1996, the building was completely clad and it was possible to perform the tests after hours when the building site was not in operation. This resulted in a much quieter environment leading to better quality FRFs and the ability to acquire more representative walking response measurements. Many of other problems experienced during the first round of testing did not occur again. This time, the floor surface was again bare, but complete services, including air-conditioning ducts and piping, were attached underneath (Figure 5.78). Also, as the building was clad, a number of non-structural masonry facade walls existed between the RC

columns. The brickwork was erected full height between the 1050/300 mm edge beams and was supporting large window frames. These architectural details are not shown in Figure 5.66.

This was the first test when the writer had an opportunity to use the newly acquired 8-channel RACAL VL (Figure 5.79) tape recorder. All this and the experience with the test site resulted in more effective testing time management which allowed more detailed modal testing and response measurements to be made.

This was, however, hampered to some extent by the fault of one of the four accelerometers (Dytran A4 accelerometer), so that only three response channels were recorded. Interestingly, the fault, manifested on site by large low-frequency drifts of time-domain signals, could not be replicated after returning to base and no further action was taken to repair this accelerometer.

5.5.4.2 PRELIMINARY INVESTIGATION

All FRF measurements in the second round of testing were performed overnight, starting after 7pm. Preliminary investigation was done in the same way as for the first round of testing, and its results will not be elaborated in greater detail. It suffices to say that an outcome of this investigation was to use the same data acquisition parameters as in the first round of testing (Table 5.15). It is interesting to note that, compared with the first round of testing, the averaging produced much more stable FRFs towards the 10^{th} (last) average, as illustrated in Figure 5.80.

5.5.4.3 FRF DATA ACQUISITION AND INITIAL DATA ANALYSIS

For the main hammer swipe, the same reduced test grid of 33 points was used (Figure 5.65). The hammer swipe took one night of testing. Three rows of the FRF matrix were measured having TP32, TP38 and TP51 as references. In addition to being recorded on the tape recorder, signals from the hammer and one accelerometer channel (TP32) were processed in parallel on the spot by the spectrum analyser. At the end of the modal testing 33 FRF acquired in this way were processed.

A MIF (Equation 5.11), which corresponded to TP32 as the reference, was calculated in-situ and is one of the three MIFs shown as the red line in Figure 5.81. The peaks in this MIF proved to be natural frequencies of 7 modes of vibration which frequencies and mode shapes are shown in Figure 5.82, including the complexity for the estimated modes. After return to base, further processing of all of the acquired FRFs confirmed the natural frequencies and mode shapes estimated in-situ. Two more MIFs were calculated using Equation 5.11, this time for TP38 and TP51 as the reference points, and are also shown in Figure 5.81. The estimated frequencies are summarised together with the modal damping ratios in Table 5.17.

Table 5.17: Structure C (Clad) - The estimated natural frequencies and modal damping ratios after the first round of modal testing in June 1996.

Mode No.	Frequency [Hz]	Modal damping ratio ζ [%]
1	6.4	0.95
2	6.9	1.29
3	8.2	1.00
4	10.2	N/A
5	11.9	1.93
6	15.0	1.86
7	17.4	2.32
8	18.2	0.89

Compared with the first round of testing (Table 5.16), all natural frequencies increased, clearly showing that the floor structure was somehow stiffened between December 1995 and June 1996. Although there is a general trend towards increased damping in the second round of testing, the estimated modal damping ratios of all lower modes of vibration excitable by normal walking were less than 1.5%, even with some services attached underneath the floor.

Another interesting point is that the 4th mode of vibration was missed again, although not one but three reference points were used. It appears that all three accelerometers were on nodal lines of this mode. Two of them were on the same N-S grid line from TP25 through TP38 to TP51 (Figure 5.65). With a hindsight, these two accelerometers should not have been on the same N-S line. However, a visual inspection of the calculated MIFs (Figure 5.81), showed that the frequency of this mode was likely to be around 10.2 Hz. This is consistent with its lower 9.7 Hz counterpart estimated from the data gathered from the first round of testing of the unclad building (Table 5.16).

Finally, it should be mentioned that using TP51 as the reference point produced poorer quality FRFs than when TP32 and TP38 were used as the references.

5.5.5 June 1996: Response Measurements

The very quiet overnight environment allowed walking response measurements to be made. A quick check showed that vibrations due to ambient excitation were about an order of magnitude lower than the vibrations measured while somebody was walking on the floor.

The main focus of the measurements was the excitation of the two lowest modes of vibration by the 3rd harmonic of walking. The effects of the 4th walking harmonic on the 3rd mode of vibration at 8.2 Hz were not investigated.

Figure 5.82 shows three walking paths selected to excite modes 1 and 2. Whereas all three paths were relevant for mode 1, only WPs 1 and 3 were considered in the case of mode 2. According to the floor designer's brief, WP1, running in the E-W direction, was unlikely to exist in a real-life situation but was

investigated because it provided the longest time for a single walker to build up the vibrations. WP2 was much shorter, but was also more realistic as it linked the lift shafts (Figure 5.66) and people using the floor were likely to use this path. The diagonal WP3 was less realistic than WP2, but was longer and it passed through the area where modes 1 and 2 were likely to have maximum modal amplitudes.

Table 5.18: Structure C - Summary of results of 10 s RMS trend analyses of 120 s long acceleration time histories.

Test No.	Mode and frequency excited	Excitation harmonic (pacing rate)	Walking path	Measurement point	10 s RMS peak acceleration [gRMS]
1.1a	1 (6.4 Hz)	3rd (128 spm)	1	TP32	0.0770%
1.1b	1 (6.4 Hz)	3rd (128 spm)	1	TP35	0.0841%
1.1c	1 (6.4 Hz)	3rd (128 spm)	1	TP38	0.0855%
2.1a	2 (6.9 Hz)	3rd (138 spm)	1	TP32	0.0954%
2.1c	2 (6.9 Hz)	3rd (138 spm)	1	TP38	0.0860%
3.1a	1 (6.4 Hz)	3rd (128 spm)	2	TP32	0.0550%
3.1b	1 (6.4 Hz)	3rd (128 spm)	2	TP35	0.0820%
3.1c	1 (6.4 Hz)	3rd (128 spm)	2	TP38	0.0577%
4.1a	1 (6.4 Hz)	3rd (128 spm)	3	TP32	0.0449%
4.1b	1 (6.4 Hz)	3rd (128 spm)	3	TP35	0.0532%
4.1c	1 (6.4 Hz)	3rd (128 spm)	3	TP38	0.0608%
5.1a	2 (6.9 Hz)	3rd (138 spm)	3	TP32	0.0558%
5.1c	2 (6.9 Hz)	3rd (138 spm)	3	TP38	0.0629%

Again, every effort was made for an average male test subject weighing 75 kg, who has considerable experience in similar exercises, to make the prescribed number of steps per minute. The pacing rate was controlled by a metronome. When the pace was unintentionally lost, tests were repeated. Therefore, the measured responses, presented in Table 5.18 in terms of peak 10 s RMS trend values, correspond to the best possible attempt to excite, as much as possible, the two lowest modes of vibration this floor by normal walking.

Interestingly, the maximum response of 0.0954% gRMS did not occur in the fundamental mode of vibration, but in the 2nd mode, while walking along WP1. Acceleration time history and RMS trend analysis which led to this result are shown in Figure 5.83. However, a considerable peak response of 0.0820% gRMS was caused in the fundamental mode while walking along WP2 (Figure 5.84). Although longer than WP2, WP3 did not produce as high responses in tests 4.1 and 5.1.

5.6 Vibration Testing of PT Flat Slab (Structure D)

Structure D is the last and the largest cast in-situ concrete floor investigated in this research. Its testing took place in August 1996. The preparations for the testing, including a selection of the structure, gathering the technical information about it and obtaining permission for its testing, lasted almost a year.

The main aim of the testing was to investigate vibration performance of a beamless flat slab floor. Although this is a common post-tensioned concrete floor configuration, its dynamic behaviour has not been researched very much in the past, when compared with other floor configurations which have beams.

5.6.1 Structural Description

Structure D was the top floor (Level 3b) of a 24-hour multi-storey car park in the centre of Birmingham, UK. Its dimensions were 47.5 m in the E-W direction and 37.5 m in the N-S direction (Figure 5.85). A typical panel spanned 8.0m, was 7.5 m wide and consisted of a 225 mm thick slab which was prestressed in two orthogonal (E-W and N-S) directions. The total weight of this relatively slender prestressed PT concrete floor, having a span-to-depth ratio of 36, was about 1000t. End spans in the E-W direction were shortened from 8.0 m to 3.8 m. Being a large car parking area located about 15 m above the ground, the slab had stocky upstanding edge beams forming up to a parapet 1.54 m high around its perimeter. These beams were designed to prevent accidental falling of vehicles.

The horizontal stability of the floor was provided by two cores made of normally reinforced concrete, denoted as 'Stairwell' and 'British Rail Duct' in Figure 5.85, and by the system of orthogonal frames comprising the columns and the corresponding floor column strips. Whilst the 300x300 mm edge columns had 600x600 mm heads, the main columns were 450x450 mm and having heads flared up to 800x800 mm.

5.6.2 Field Test Planning

Being the top level of a 24h car park, this was the first floor structure tested in a completely open space environment as no cladding or floor above existed. Naturally, under such circumstances, and being in the city centre of Birmingham, the main concern was the effects of extraneous excitation.

Having good experience with overnight testing of Structure C, permission was sought to test Structure D after 7pm. In addition, the floor had to be completely free of cars as their presence might have affected the measurements. Willing to help free of charge, the car park management allowed the modal and response testing to take place between 7pm on Saturday 17 August and 5am on Monday 19 August 1996. The car park Level 3b was fenced off in advance to prevent other people from using it.

5.6.2.1 Site Visit

During the site visit before the testing, it was noted that the limited headspace would require two estate cars for transportation instead of one high roof van, which was usually used for field tests. Otherwise, as no lifts existed, it would be difficult and time-consuming to carry the test equipment manually to the third floor of

the car park. In addition, no power supply was available requiring the use of a transportable power generator which had to be placed away from the floor tested. This, in turn, required long power leads.

An underground railway station existed four levels below the car park and the excitation caused by trains entering and leaving the station was so noticeable that it was possible to hear the trains. Fortunately, as the testing was scheduled overnight, when the station was not used frequently, this form of extraneous excitation did not cause particular problems.

Finally, the site visit was used to inform the local police about the forthcoming overnight work for security reasons.

5.6.3 Modal Testing

After the site visit, during which it was not feasible to perform any quick hammer testing, it was clear that, as in all other tests, there would be not a lot of time to carry out the field work. However, as for the second round of testing of Structure C, it was possible to engage three people, including the writer, to perform the testing. This eased the pressure on individual members of the test crew. Nevertheless, to gather the required data in only 36 continuous hours available for this testing, required very careful planning.

5.6.3.1 PRE-TEST ANALYSIS

Two FE models were developed in the pre-test analysis. Both of them utilised only isotropic ANSYS SHELL63 elements. As no additional information existed about the concrete designed to be grade C40, a dynamic modulus of elasticity of 38 GPa was assumed together with a concrete density of 2400 kg/m^3. The columns, supporting walls, and edge beams (Figure 5.85) were modelled using pin-supports (Figure 5.86). To simplify the model, the pin-supported boundary conditions were assumed to be perfectly symmetric, of the kind shown in Figure 5.86.

Modal analysis of the first FE model, whose mesh, in addition to the boundary conditions, was perfectly symmetric (not shown in Figure 5.86), produced 14 modes of vibration between 7 Hz and 9 Hz. The natural frequencies of these modes are listed in Table 5.19.

Table 5.19: Structure D - Calculated natural frequencies in pre-test analysis

Mode No.	Natural frequency [Hz]
1	7.03
2	7.47
3	7.79
4	7.85
5	7.89
6	8.00
7	8.31

Mode No.	Natural frequency [Hz]
8	8.36
9	8.79
10	8.80
11	8.88
12	8.92
13	8.96
14	8.99

This indicated that the floor might have plenty of closely spaced modes of vibration. In addition, mode shapes looked very similar which would, probably, require a relatively dense test grid across the whole slab surface to avoid spatial aliasing. This created a problem of not having enough time to perform the hammer swipe across the complete floor surface. Also, there was a serious uncertainty about whether the measurements of transfer mobilities between remote points on the test grid spread across the whole floor area would produce any meaningful results. Such a test grid should have covered almost 1800 m^2 of a thousand-tonne structure exited by a manually operated hammer weighing only 5.4 kg.

Considering all this, a decision was made to test a relatively dense test grid comprising 59 points and covering approximately only one quarter of the floor area (shaded bottom-right area in Figure 5.87). This would reduce the uncertainty about the ability to excite the test area properly. The numbering of the test grid was devised to speed up the movement of the hammer operator. Also, the test grid did not contain the points above the columns and close to the edge beams where a normal hammer blow was not expected to excite the slab sufficiently. This was done considering the experience gained from the previous field tests.

Nevertheless, it was likely that this test-grid, covering a considerably reduced area of the floor, would increase the likelihood of spatial aliasing. This is because only a portion of the slab had to be used to provide information about mode shapes corresponding to the whole slab. Although the first pre-test FE model produced perfectly symmetric or anti-symmetric mode shapes, realistically, experimental mode shapes could not be assumed to be perfectly (anti-)symmetric. This is due to imperfect boundary conditions (walls, ramp, etc.) spoiling the symmetry of the real-life structure. As a consequence, the information from one quarter of the floor could not be easily extrapolated to cover the whole area by simply assuming (anti-)symmetry of the modes.

This is a well known problem of 'incompleteness' of the experimental model which happens when only a portion of the structure is tested (NAFEMS, 1992b).

5.6.3.2 CHECK OF THE SPATIAL ALIASING

To check if the 59 test points are going to be sufficient to describe the measured mode shapes and avoid the spatial aliasing of experimental mode shapes, an Auto-MAC matrix was calculated using a refined pre-test FE model. This is the model shown in Figure 5.86. The only difference between it and the first pre-test FE model (which indicated the likelihood of closely spaced modes of vibration) was that one quarter of it was

re-meshed to create nodes corresponding to the test points (Figure 5.87). This refinement did not practically affect any of the mode shapes and natural frequencies of interest calculated using the first model with the perfectly symmetric mesh. The first 14 of 30 mode shapes calculated, corresponding only to the limited test-grid area are shown in Figure 5.88. This presentation of the mode shapes calculated using the FE model, which represented the whole floor, was chosen to simplify the comparison with the measured mode shapes,

To check if 59 test points were going to be enough to avoid spatial aliasing, exactly 8011 of 8070 DOFs in each of calculated FE mode shapes covering the whole floor area, were deleted. The FE mode shapes were reduced to only 59 vertical displacements corresponding to the adopted test grid area only. The Auto-MAC matrix calculated after this reduction of the FE model is shown in Figure 5.89. Clearly, there is a number of off-diagonal mode shape pairs having Auto-MAC of more than 60% indicating that it would be difficult to distinguish between them. A comparison of four pairs of such 'problematic' mode shapes is also given in Figure 5.89. For example, an element of the Auto-MAC matrix corresponding to modes 2 and 5 is 65% indicating that these two modes could be swapped and/or mistaken for each other. Indeed, a visual inspection of modes 2 and 5 in Figure 5.88 confirms this as the two modes look very similar. It appeared that 59 test points corresponding to one quarter of the floor were likely not to be enough to avoid the spatial aliasing of the measured mode shapes. More test points to describe the experimental mode shapes were required to reduce the possible problem of spatial aliasing. Unfortunately, 59 points were the practical upper limit of the number of points on Structure D that it was possible to test within the severely limited time scales.

On the other hand, Figure 5.90 shows the Auto-MAC matrix obtained after the FE mode shapes, reduced to only 59 elements, were expanded back to the full set of FE DOFs using the ICATS (1995) software which is based on the procedure described by Imregun and Ewins (1995), and Maia et al. (1997). Naturally, the MAC matrix is now almost diagonal demonstrating clearly the limitations of the reduced number of test points to describe the mode shapes of Structure D. This fact had to be borne in mind when interpreting the modal test results. As the main aim of the modal testing was to identify as many of the lowest modes of vibration as possible, TP1, TP3, TP26 and TP51 (Figure 5.87) were selected as the references for four rows of the FRF matrix planned to be measured. This was done by a visual inspection of modes shown in Figure 5.88.

5.6.3.3 PRELIMINARY INVESTIGATION

The test equipment used for testing Structure D is shown in Figure 5.91. It can be seen that, instead of one, two notebook PCs were used this time. One PC was used for downloading the measured FRF data from the spectrum analyser whereas the other was used for the curve fitting of incomplete sets of downloaded FRFs. This was done to speed up the in-situ initial data analysis. It was anticipated that parameter estimation for this structure, possibly having many closely spaced modes of vibration, was going to be a difficult and time consuming task so data acquisition and analysis had to be done in parallel.

The data acquisition 'centre' was positioned on the slab tested, but not within the test grid. The equipment was placed in a small area above one of the columns in the top right corner of the floor (see Figure 5.87). The aim was to reduce the effects of the presence of the test crew on the floor during the measurements.

The first QA check during the first day of field work was the check of ambient vibration levels lasting 20 minutes. The measurement took place at about 7:30pm in broad daylight and sunshine. This detail is important as during this measurement accelerometer A4 developed a fault similar to the one already seen when testing Structure C in July 1996. Large low frequency drifts of the kind shown in Figure 5.92 made the selection of an appropriate dynamic range for this accelerometer impossible. Therefore, accelerometer A4 was discarded from the remaining measurements.

Later, it was established that one common circumstance while testing Structures C and D (when A4 failed) was a relatively high air temperature of about 20-30^{0}C. It appears that the compression (as opposed to shear) design of this accelerometer proved to be particularly sensitive to higher environmental temperatures, as mentioned in Chapter 4. This was probably the reason why in cooler laboratory conditions this problem could not be replicated. Interestingly, nominally identical Dytran accelerometer A3 also showed some low frequency drifting, but of a much lesser magnitude. Both A1 and A2 Endevco accelerometers were not prone to this problem. After noting this behaviour, as a precaution, high pass filtering was applied when processing the acceleration response data using DATS (1995) signal processing software after the testing. This filtering removed frequencies lower than 1 Hz in all acceleration response measurements. Nevertheless, very little change between the properties of unfiltered and filtered signals was observed.

The instrumented sledge hammer was operated in a similar way as for the other tests, the only difference being the hands-free voice-activated radio communication used to pass instructions to and from the hammer operator more easily (Figure 5.93).

The preliminary investigation took place during the first night of testing which was very calm. Without going into details of these checks, some illustrations of the results produced while performing them are presented. Figure 5.94 shows an FRF reciprocity check between TP 1 and TP 3, which were relatively close to each other. Figure 5.95 shows the reciprocity check using transfer mobility measurement between two remote points: TP1 and TP 51. In both cases, although the floor was the heaviest of the four structures and was tested in a completely open space environment, the checks produced remarkably good results. Finally, Figure 5.96 shows a satisfactory homogeneity check when measuring point mobility at TP1 using soft and hard hits.

As all FRFs measured in the preliminary investigation were 'settling down' quickly, 10 averages and an exponential window constant of only TC = 5 were deemed to be sufficient for the main hammer swipe over 59 points (Table 5.20).

Table 5.20: Structure D - Main digital data acquisition parameters adopted for the in-situ FRF measurements when TP1 is the reference point.

Parameter description	Parameter value
Data acquisition time	10 s
Frequency resolution	0.1 Hz

Parameter description	Parameter value
Frequency range of interest	1-21 Hz
Total number of samples	512
Number of frequency lines	200
Number of averages	10
Exponential window time constant (TC)	5

5.6.3.4 FRF Data Acquisition and Initial Data Analysis

Being encouraged by the quality of the measurements in the preliminary investigation, the writer decided not to wait until the evening of the second day of testing to start the main hammer swipe. Hence, the hammer swipe was performed between 11am and 5pm on Sunday 18 August 1996. That day was warm, and also very calm so the FRFs measured still performed well. The three accelerometers available were positioned at TP1, TP3 and TP26. Their signals and the corresponding hammer analogue signal were stored on four VHS tapes recorded by the RACAL VL tape recorder (Figure 5.91). In parallel, signals from the hammer and the accelerometer positioned at TP1 were processed by the spectrum analyser. This resulted in 59 FRFs (acquired using the parameters shown in Table 5.20) at the end of the modal testing swipe.

Interestingly, towards the end of testing it was noted that the plastic tip of the hammer was very soft and practically half-melted. This happened as a result of the hammer hitting the car park surface, which was warmed by intensive afternoon sunshine, more than 600 times. The tip had to be replaced. Also, while testing TP 47, a coaxial lead connecting the BNC socket at the end of the hammer handle with one of the long cable reels failed and had also to be replaced. This again proved that cables with BNC connectors are not suitable for field work of the kind performed in this research.

A MIF $\mathrm{Im}^2\left(H_{l,sum}(\omega)\right)$, calculated on the spot using imaginary parts of all measured FRFs $H_{l,j}(\omega)$ (j=1,...,59), is shown in Figure 5.97. As the first clear peak was observed at 8.5 Hz, the frequency range of interest was set between 7 and 17 Hz. The MIF indicated at least seven frequencies (8.5 Hz, 8.9 Hz, 9.9 Hz, 10.5 Hz, 11.9 Hz, 12.7 Hz and 16.7 Hz) likely to correspond to modes of vibration in this region (Figure 5.97). A number of less emphasised peaks also existed, clearly showing that the floor as a dynamic system may be characterised as having a high modal density. The pre-test FE analysis, again, revealed prior to the test an important feature of the test structure.

After performing MDOF curve fitting by using the whole set of 59 directly measured FRFs, the first two modes of vibration excitable by normal walking which were identified had natural frequencies at 8.52 Hz and 8.92 Hz. Their mode shapes are shown in Figure 5.98. Naturally, and as for all other floor structures tested, only the in-situ estimated modes were used to establish the walking paths (Figures 5.87 and 5.98) and pacing rates.

5.6.3.5 FURTHER FRF DATA ANALYSIS

After returning to base, an additional two rows of the FRF matrix, having TP3 and TP26 as the reference points, were calculated by replaying analogue data from the four VHS tapes. Having re-analysed in total three sets of 59 FRFs each, the estimated natural frequencies and mode shapes are shown in Figure 5.99, whereas the natural frequencies and modal damping ratios are summarised in Table 5.21. Figure 5.99 also shows the reference points used for identification of each particular mode of vibration. All modes of vibration developed considerable complexity.

Table 5.21: Structure D - The estimated natural frequencies and modal damping ratios after the first round of modal testing in June 1996.

Mode No.	Frequency [Hz]	Modal damping ratio ζ [%]
1	7.99	1.57
2	8.52	0.93
3	8.72	0.84
4	8.92	1.48
5	9.28	1.20
6	9.94	0.71
7	10.39	1.11
8	11.07	1.99
9	11.17	0.63
10	11.93	1.23
11	12.65	1.22
12	16.72	0.79

In addition to $\mathrm{Im}^2(H_{1,sum}(\omega))$, two new MIFs, $\mathrm{Im}^2(H_{3,sum}(\omega))$ and $\mathrm{Im}^2(H_{26,sum}(\omega))$, were calculated (Figure 5.100) and used in this rather difficult modal identification of Structure D. The three MIFs in Figures 5.97 and 5.100 clearly show that numerous modes were likely to exist in the frequency range of interest. Different reference points were useful to indicate different modes of vibration, but they also created a number of identical modes with slightly different natural frequencies and damping factors. As the experimental mode shapes were not perfect, it was extremely difficult to judge which modes are identical and which are not identical but closely spaced. The repetition of curve fits, the use of animation and the Auto-MAC calculations to compare pairs of experimental modes, helped eliminate identical modes estimated from different rows of FRFs. The final 12x12 Auto-MAC matrix, generated using 12 experimentally estimated modes, is shown in Figure 5.101. All off-diagonal values are less than 60% indicating that the 12 experimental modes are reasonably orthogonal, as would be expected.

Finally, it should be said that a visual inspection of analytical and experimental modal properties shown in Figures 5.88 and 5.99, reveals once again that the pre-test FE model lacked stiffness as its natural frequencies were considerably lower than the measured ones.

5.6.4 Response Measurements

The main focus of the walking response measurements was on the excitation of the two modes of vibration shown in Figure 5.98 and estimated from the FRF data available in-situ. Visually, the mode shapes of these two modes correlated well with the two lowest modes calculated in the pre-test analysis (Figure 5.88). Based on this information, two walking paths were prescribed (Figures 5.87 and 5.98).

Walking at a rate of 128 steps per minute along WP1 would excite the 8.52 Hz mode by the 4th harmonic of walking. The excitation by the 3rd harmonic would require a pacing rate of 170 spm, which was too fast for normal walking. Similarly, WP2, walking at 134 spm, was designed to excite the 8.92 Hz mode again by the 4th harmonic. As in the previous tests, the pacing rate was controlled by a beeping metronome and every effort was made by an experienced average male walker of 75 kg to maintain the prescribed pace. Walking along one length of WP1 lasted approximately 24 s, whilst slightly faster walking along the longer WP2 was taking in average 28 s. A short survey of ambient vibration levels was performed before each walking test and lasted approximately 20-30 s (see Figures 5.102 and 5.103). The level of ambient excitation was considerable as would be expected from an open-space car park structure. This point had to be borne in mind when interpreting results from this set of response measurements. Nevertheless, the acceleration response data was processed in the same way as for Structures A, B and C.

A summary of the peaks of 10 s RMS trend analyses of the accelerations, recorded at TP1, TP3 and TP26 during the most successful attempts to excite the floor resonances by walking is shown in Table 5.22.

Table 5.22: Structure D - Summary of results of 10 s RMS trend analyses of 120 s long acceleration time histories.

Test No.	Mode (frequency excited)	Excitation harmonic (pacing rate)	Walking path	Measurement point	10 s RMS peak acceleration [gRMS]
1.1a	1 (8.52 Hz)	4th (128 spm)	1	TP1	0.1579%
1.1b	1 (8.52 Hz)	4th (128 spm)	1	TP3	0.1164%
1.1c	1 (8.52 Hz)	4th (128 spm)	1	TP26	0.0847%
2.1a	2 (8.92 Hz)	4th (134 spm)	2	TP1	0.2200%
2.1b	2 (8.92 Hz)	4th (134 spm)	2	TP3	0.1980%
2.1c	2 (8.92 Hz)	4th (124 spm)	2	TP26	0.1059%

The acceleration time histories leading to the maximum responses registered at TP1 in both tests are shown in Figures 5.102 and 5.103. The figures show that each pass along the single length of WPs 1 and 2 produced similar peaks of the calculated 10 s RMS acceleration trends. Surprisingly, although the floor was almost twice heavier than Structure C, and excitation was not by the 3rd but by the 4th harmonic of walking, the peak 10 s RMS responses were consistently greater than for Structure C. Also, the higher mode of vibration at 8.92 Hz was more excited than the lower mode at 8.52 Hz. Further analysis and discussion of these phenomena will be given in Chapters 6 and 7.

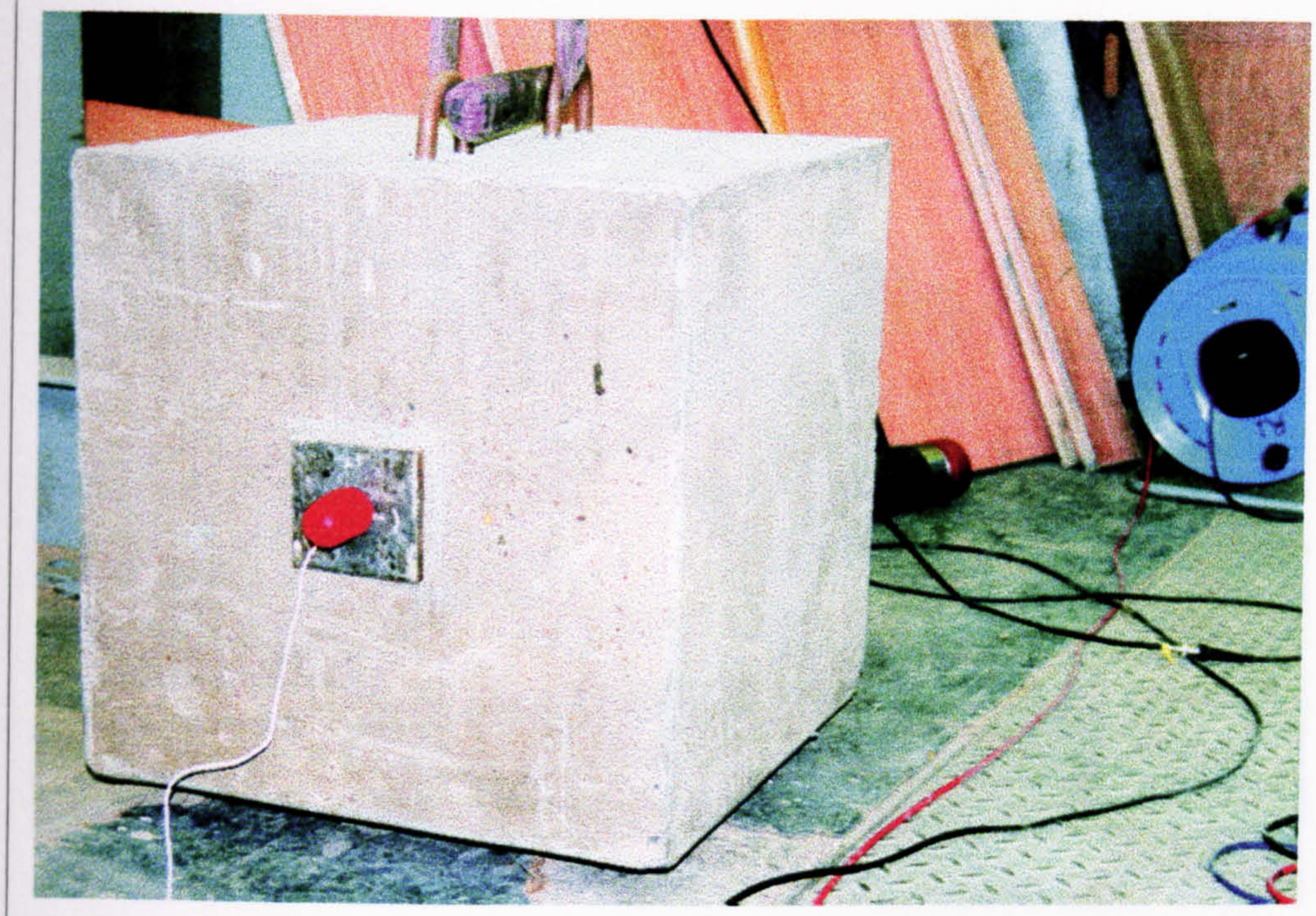

Figure 5.1: System calbiration - Concrete cube weighing 316kg used in the measurement system calibration.

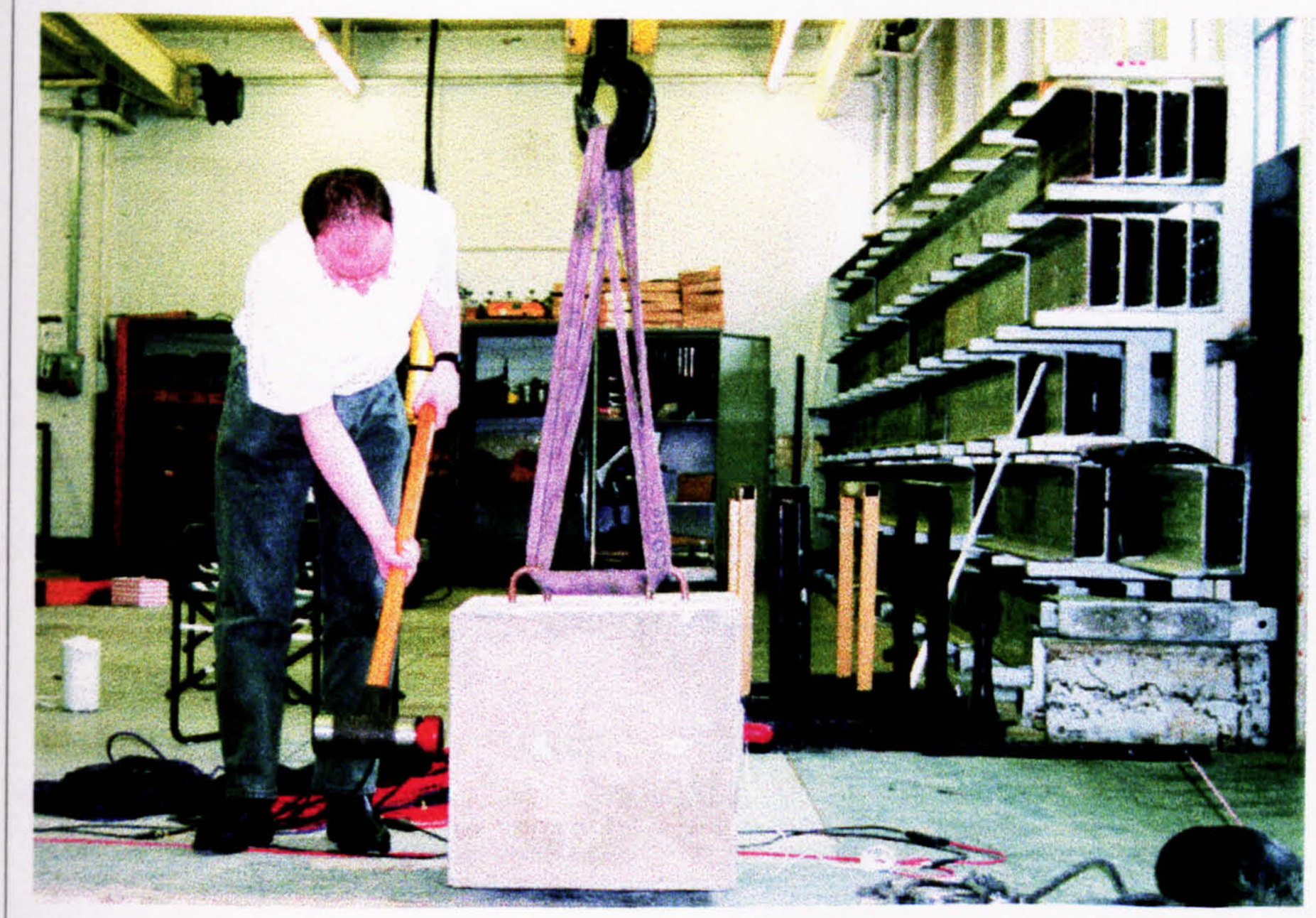

Figure 5.2: System calibration - Excitation of the suspended

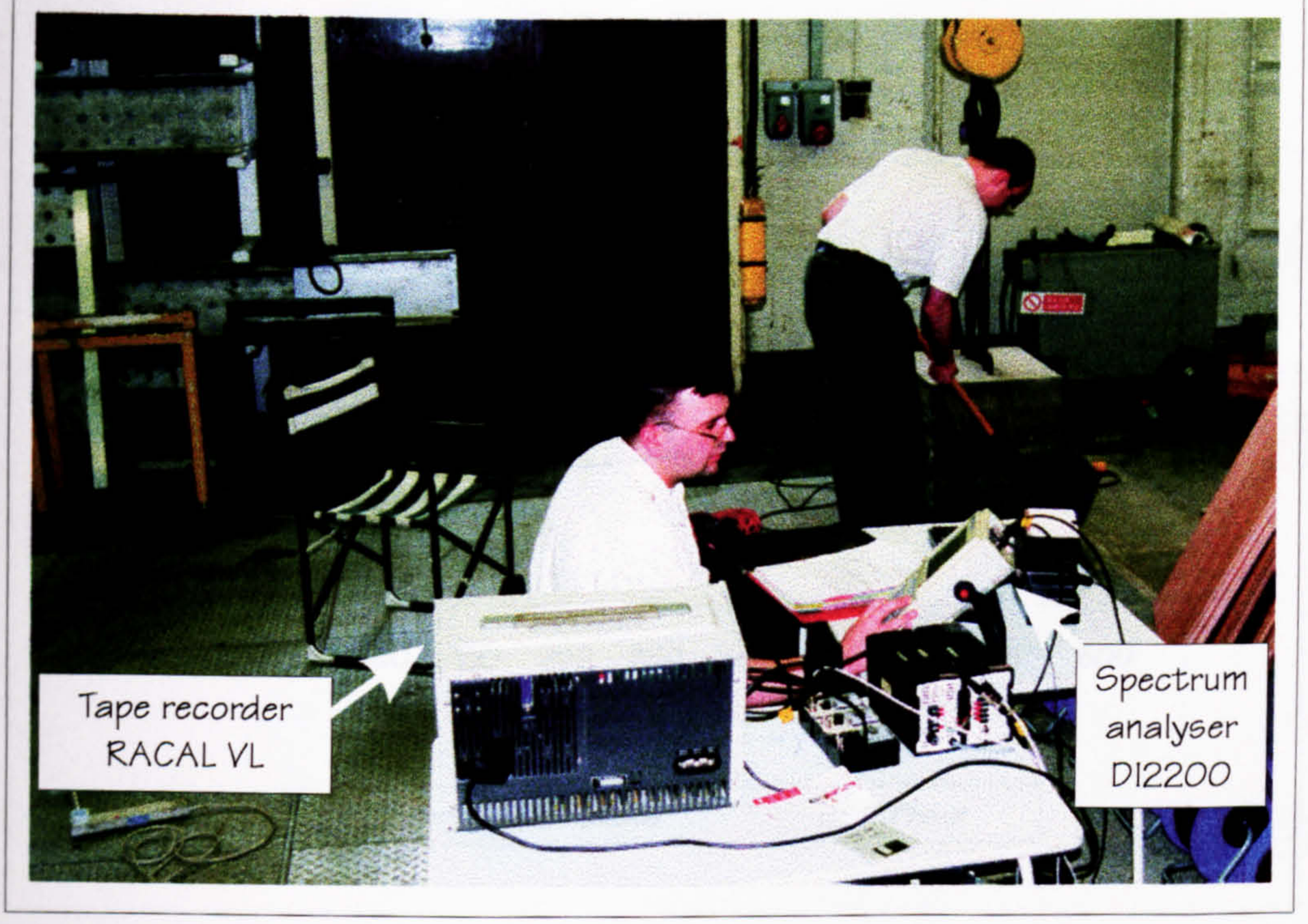

Figure 5.3: System calibration - Hardware layout for data

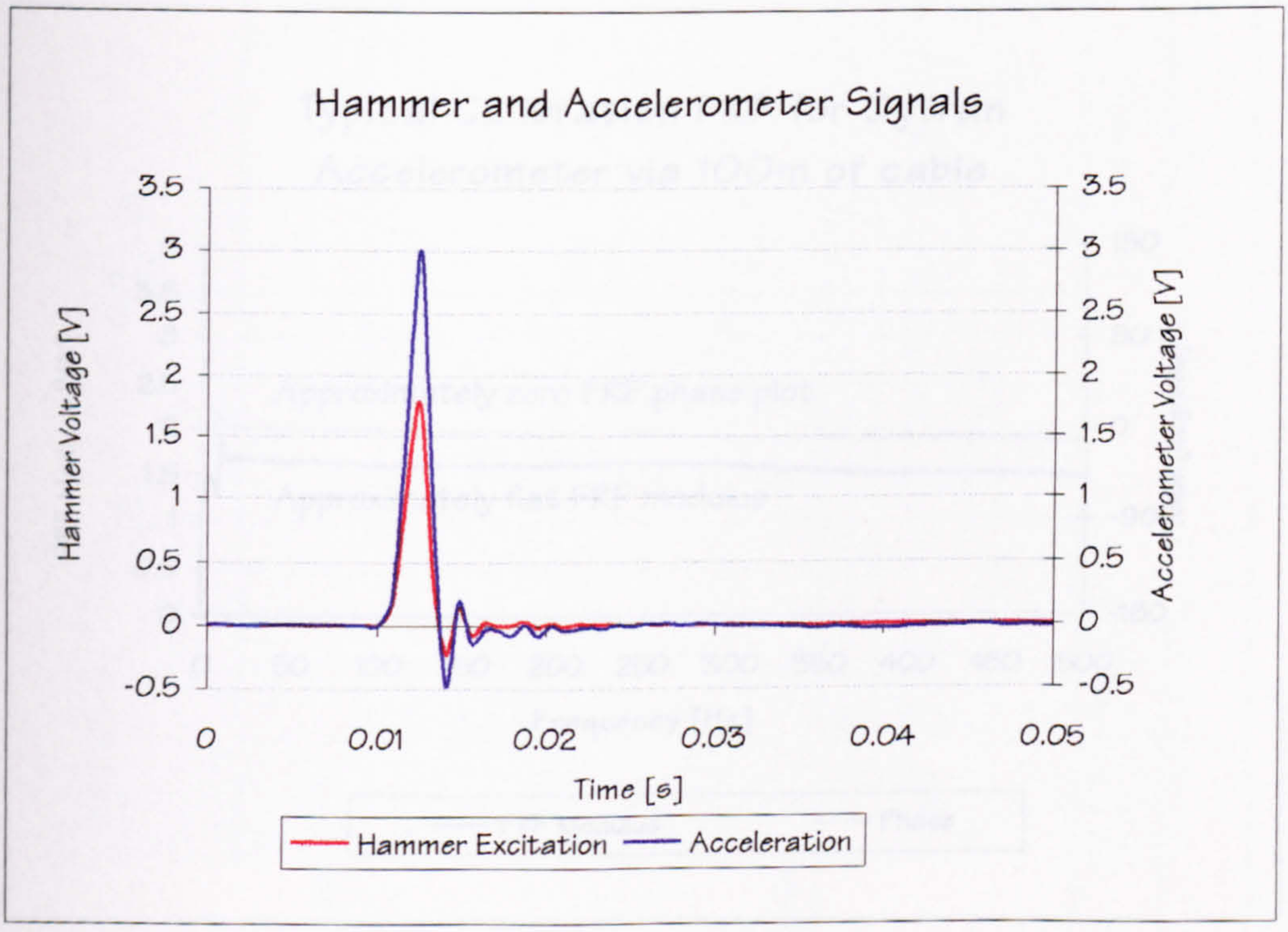

Figure 5.4: System calibration - Typical hammer and accelerometer voltage signals acquired.

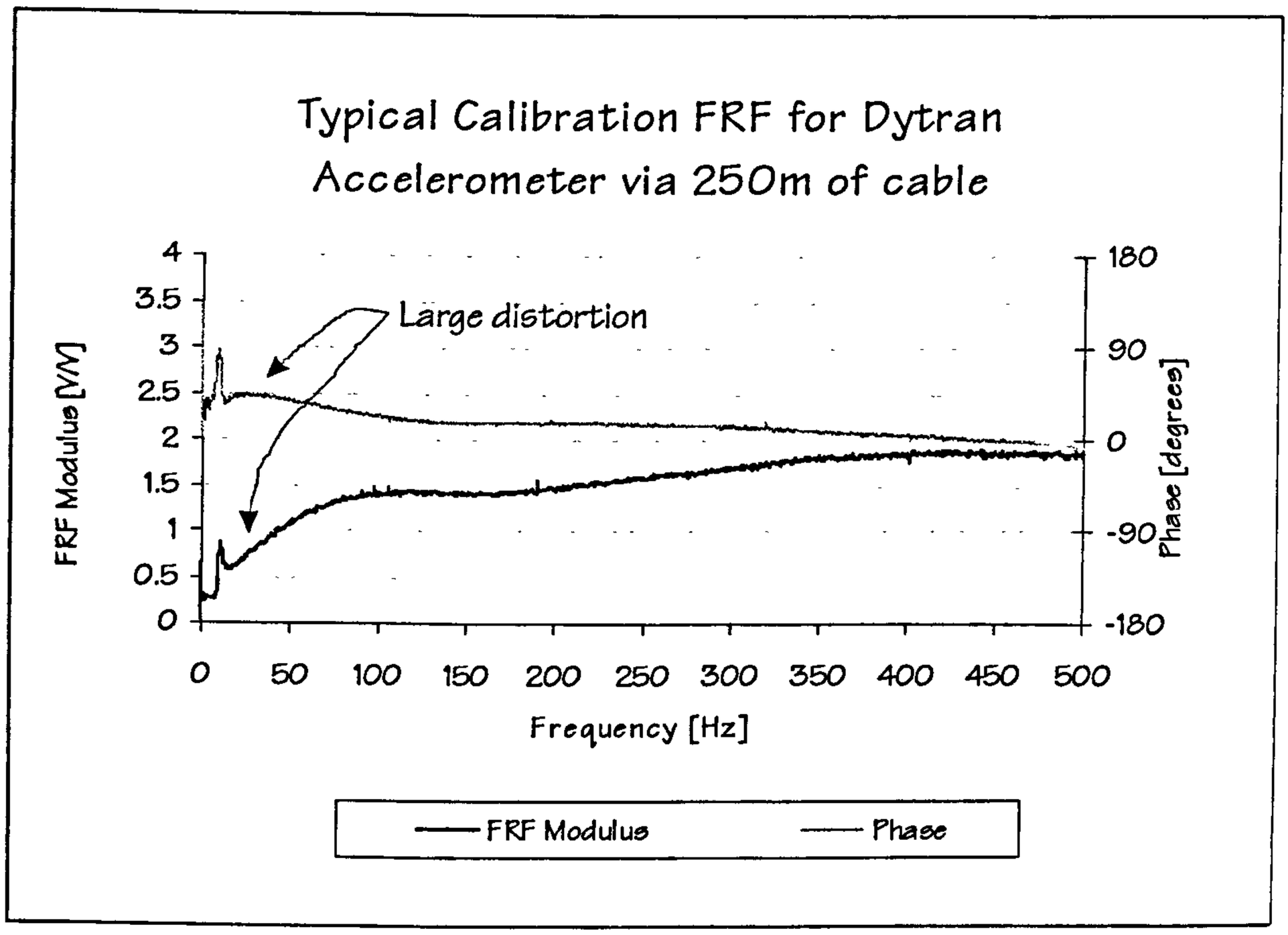

Figure 5.5: System calibration - Large distortion of the calibration FRF occurred when both channels were acquired through 250m of coaxial cable each.

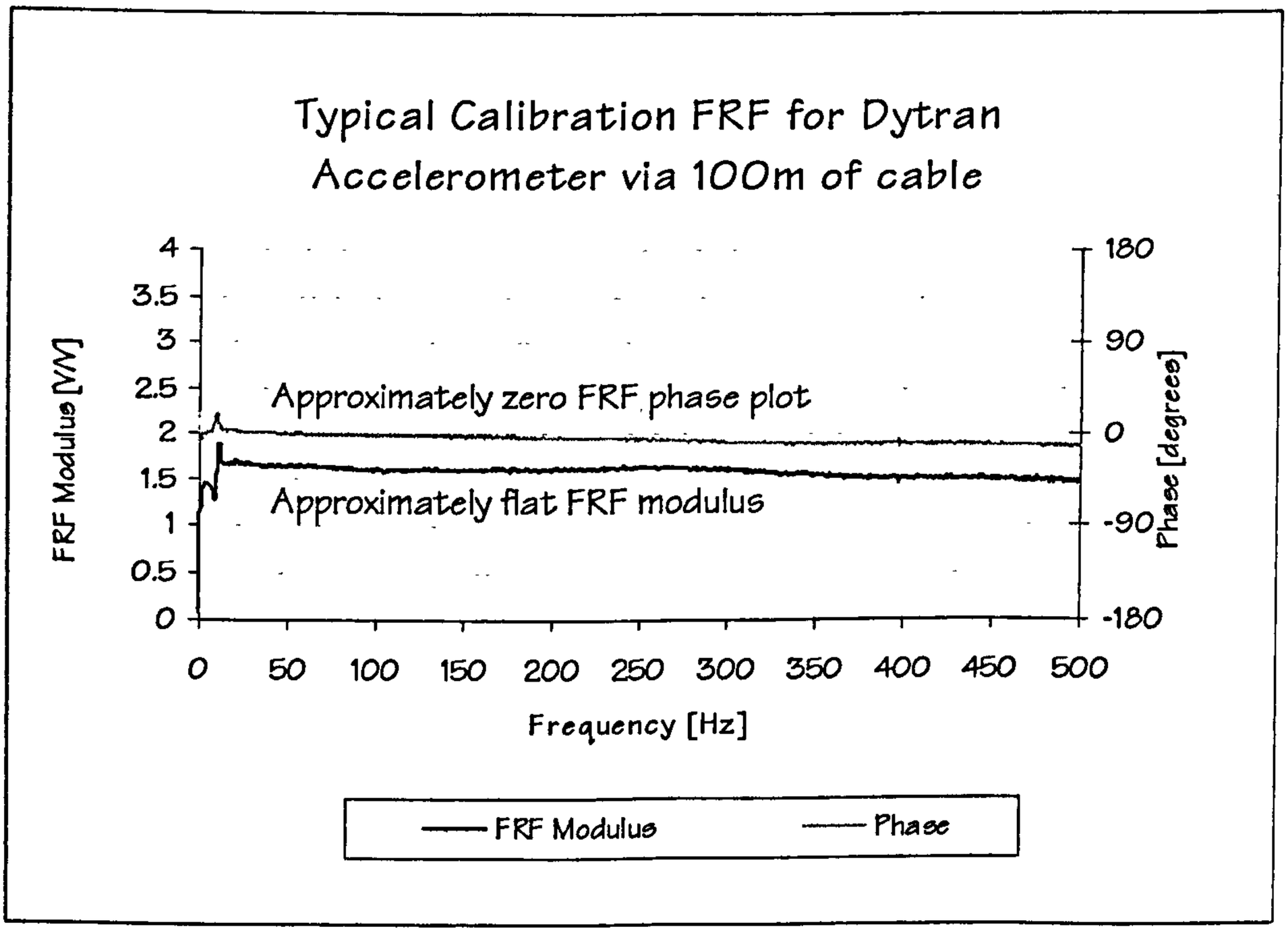

Figure 5.6: System calibration - Improved calibration FRF measured when both channels were acquired through a shorter length (100m) of coaxial cable each.

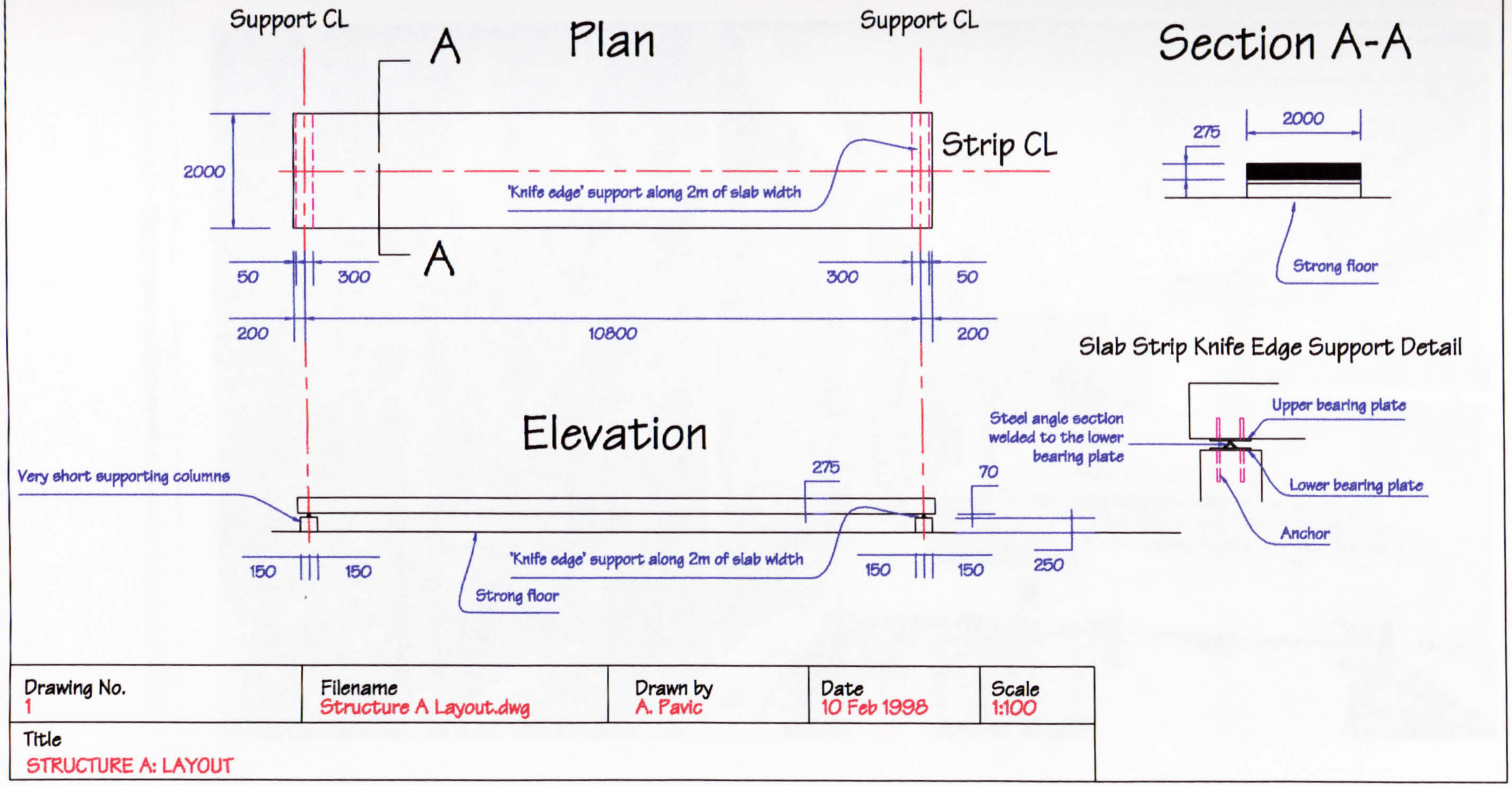

Figure 5.7: Structure A - Layout.

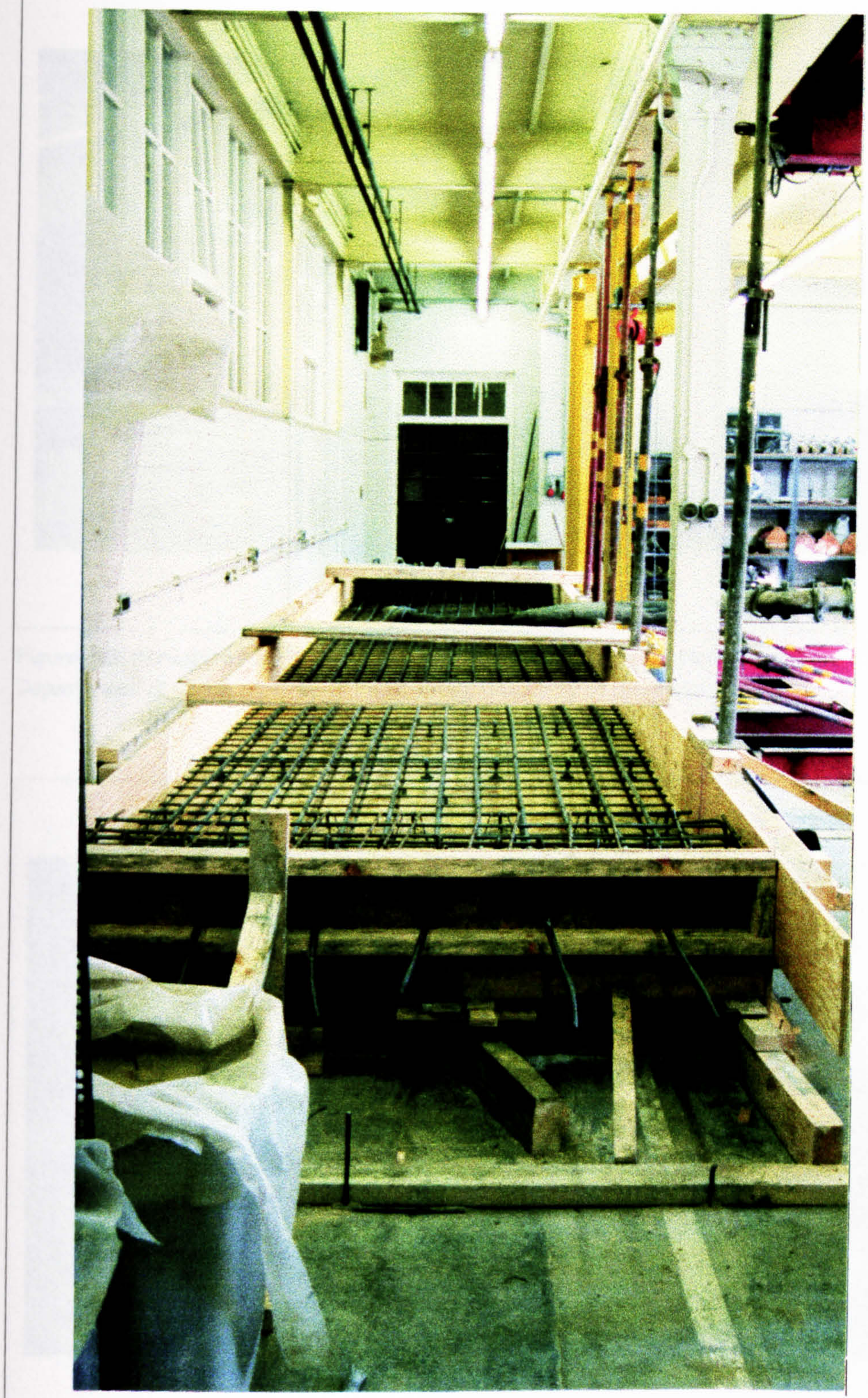

Figure 5.8: Structure A - Tendon and reinforcement placement prior to concreting.

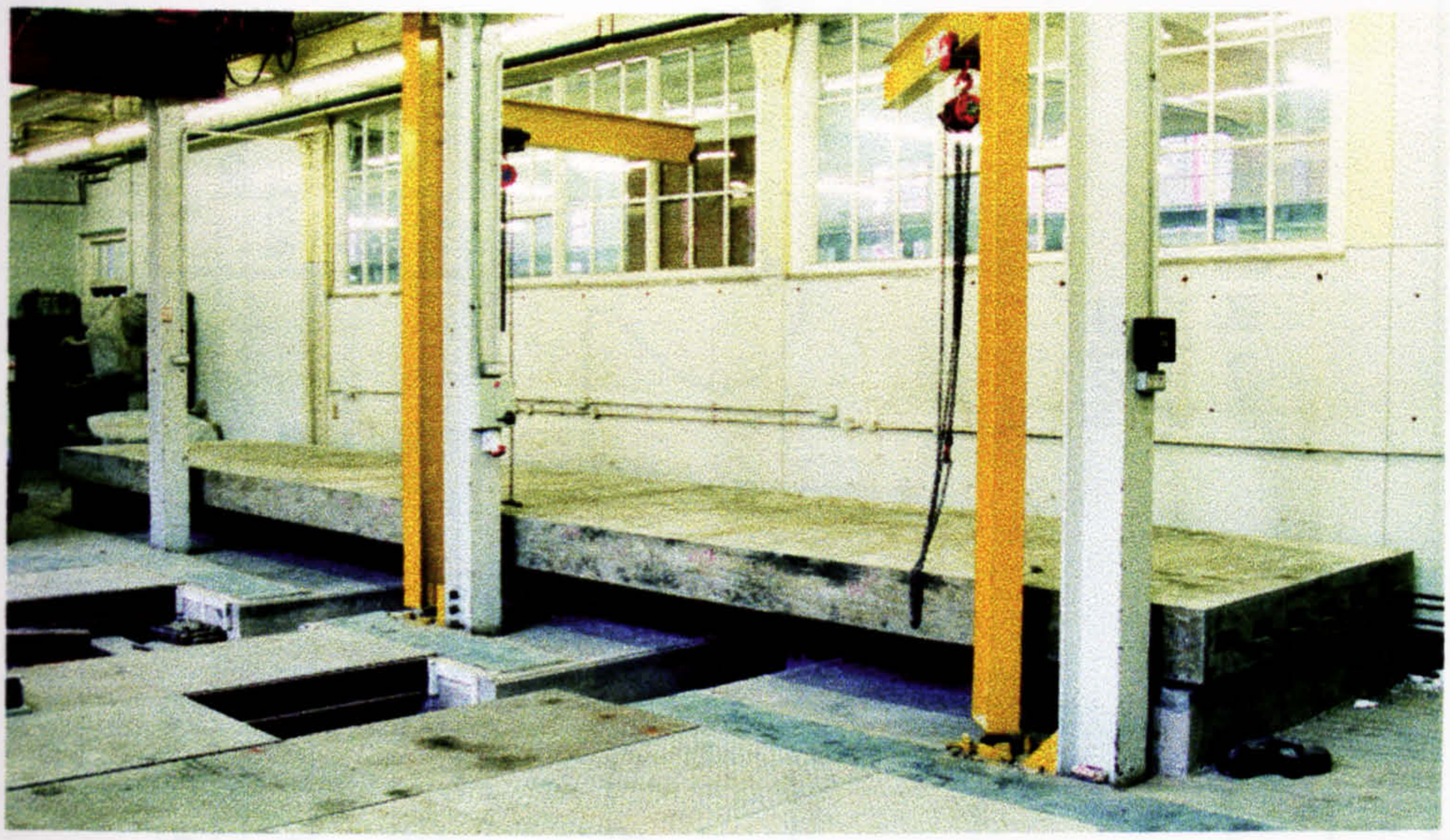

Figure 5.9: Structure A - PT slab strip erected within the Strong Floor laboratory, Department of Civil & Structural Engineering, University of Sheffield.

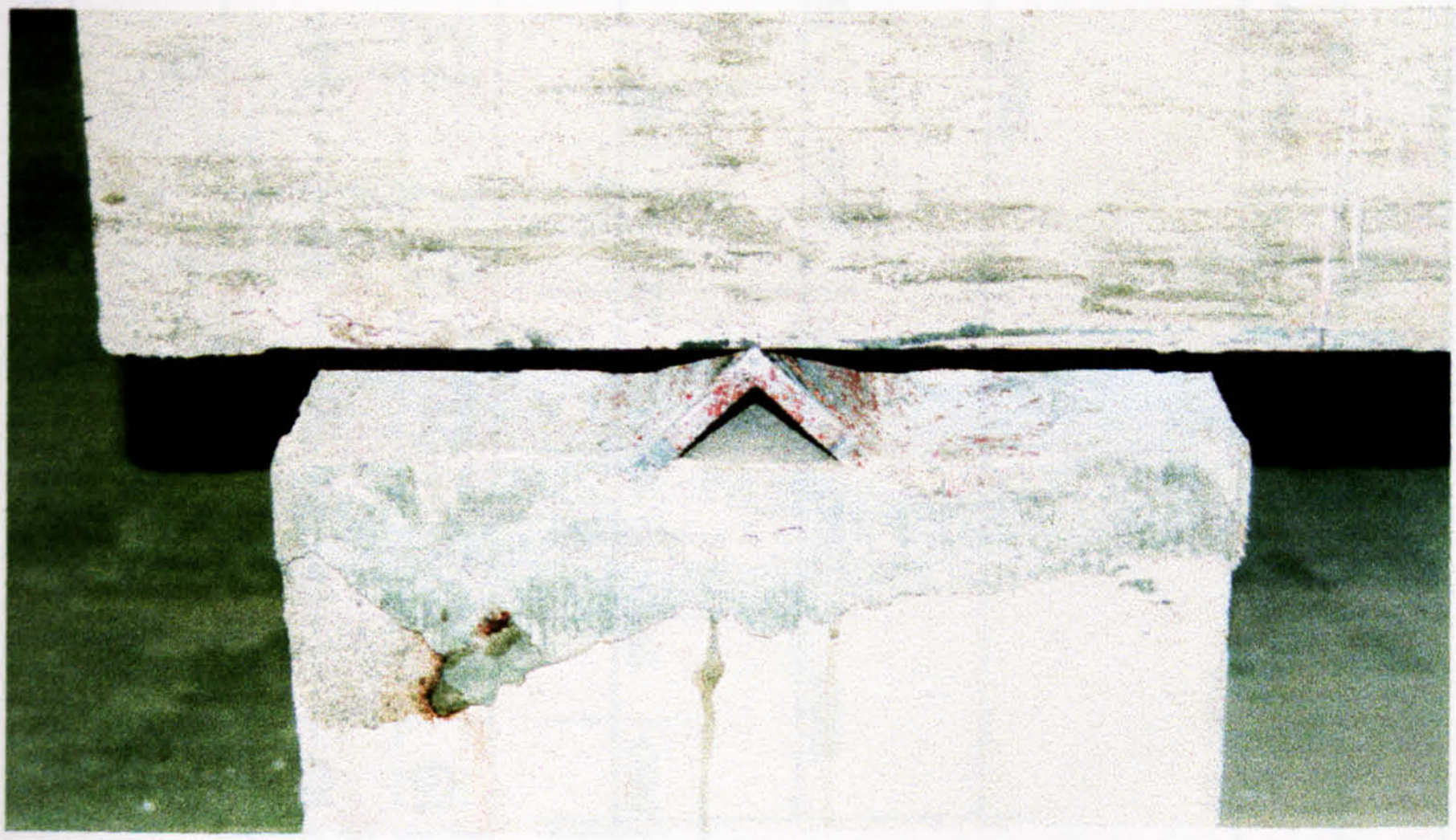

Figure 5.10: Structure A - 2m long steel angle section acting as a 'knife edge' support of the slab strip.

Floor Structure A: Test Grid and Grillage Modelling

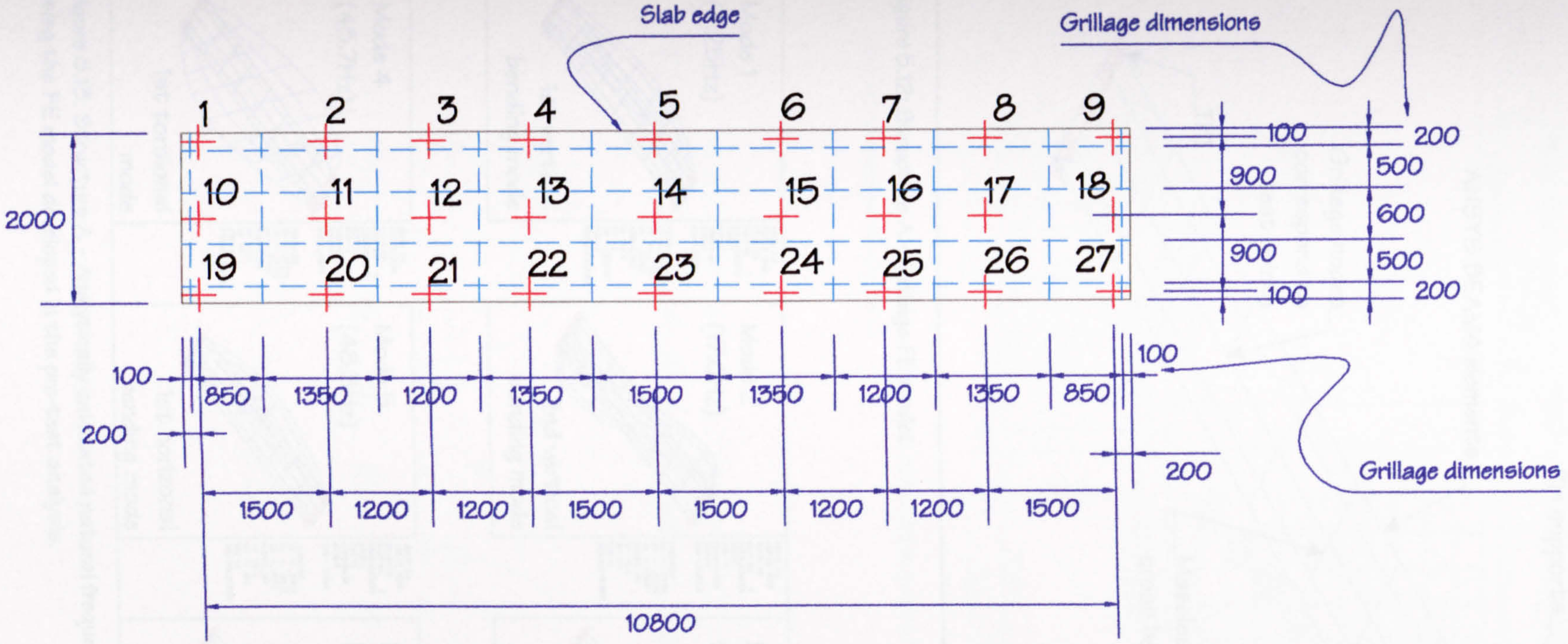

Note:
All dimensions are in [mm]

Drawing No.	Filename	Drawn by	Date	Scale
2	Structure A - Test Points.dwg	A. Pavic	10 Feb 1998	1:75

Title
STRUCTURE A: MODAL TESTING GRID AND GRILLAGE FE MODELLING

Figure 5.11: Structure A - Test grid and FE grillage modelling.

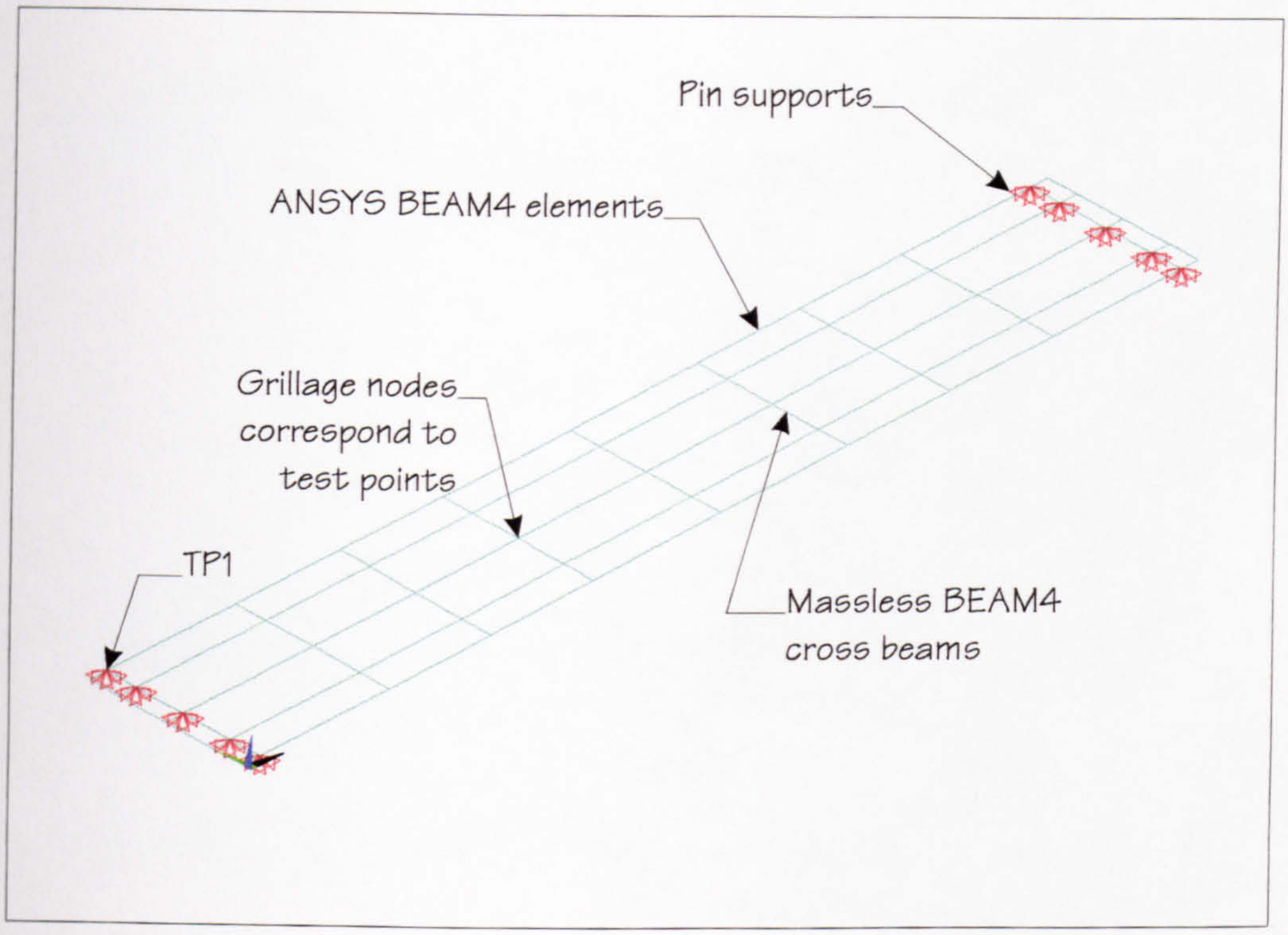

Figure 5.12: Structure A - Grillage FE model.

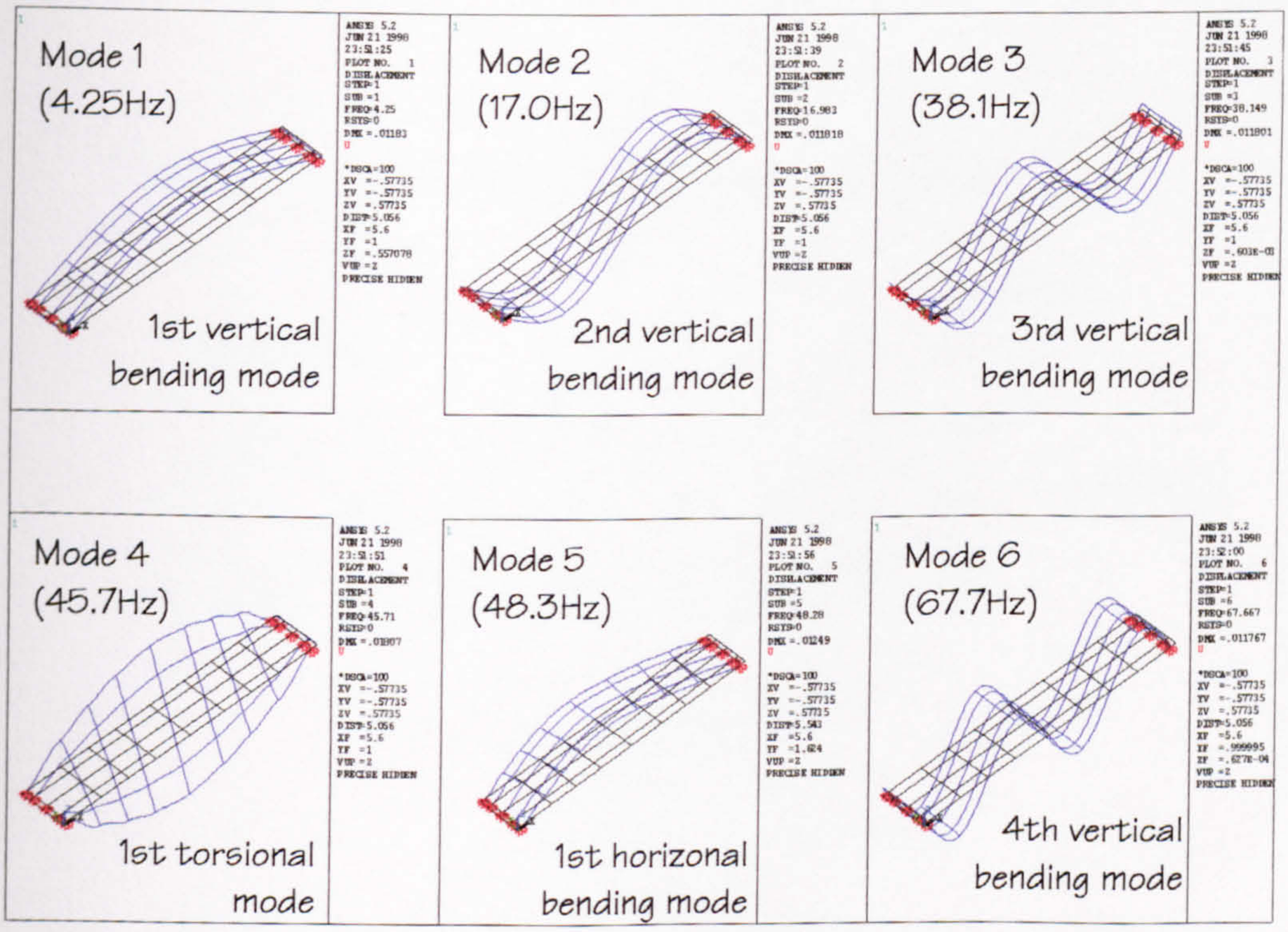

Figure 5.13: Structure A - Analytically calculated natural frequencies and mode shapes using the FE model developed in the pre-test analysis.

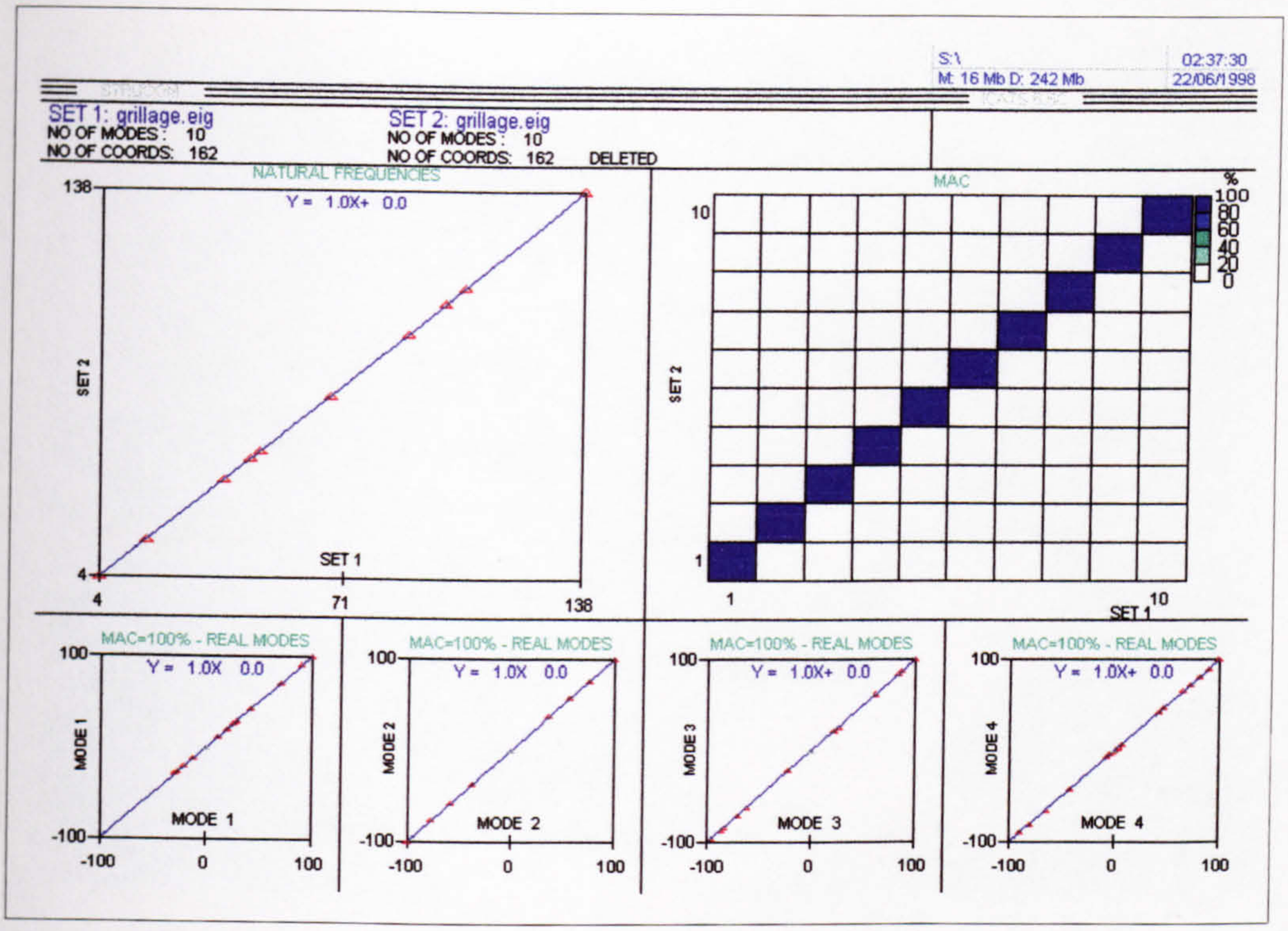

Figure 5.14: Structure A - Auto-MAC for the selected experimental grid and the first ten calculated modes of vibration.

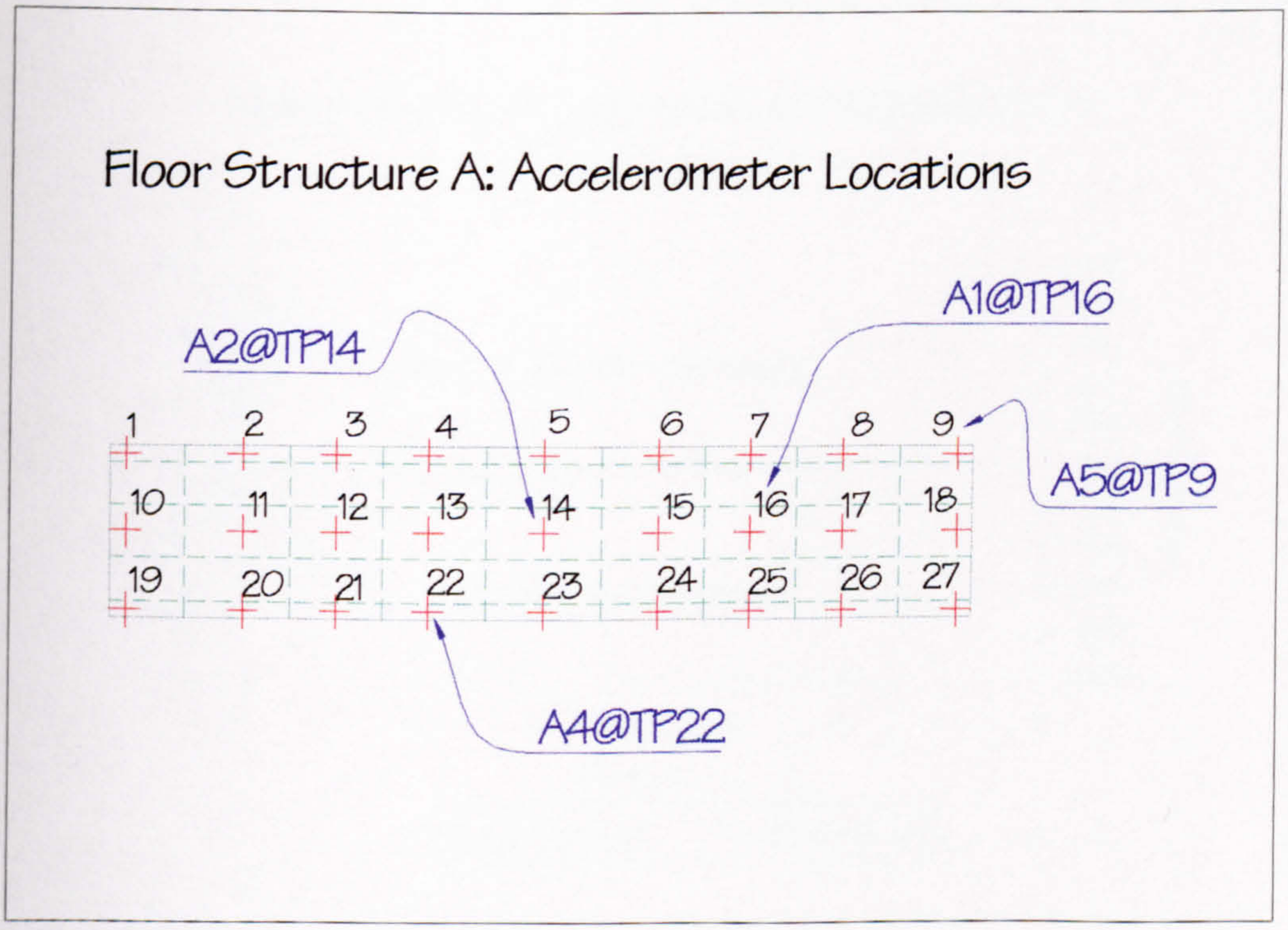

Figure 5.15: Structure A - Accelerometer locations.

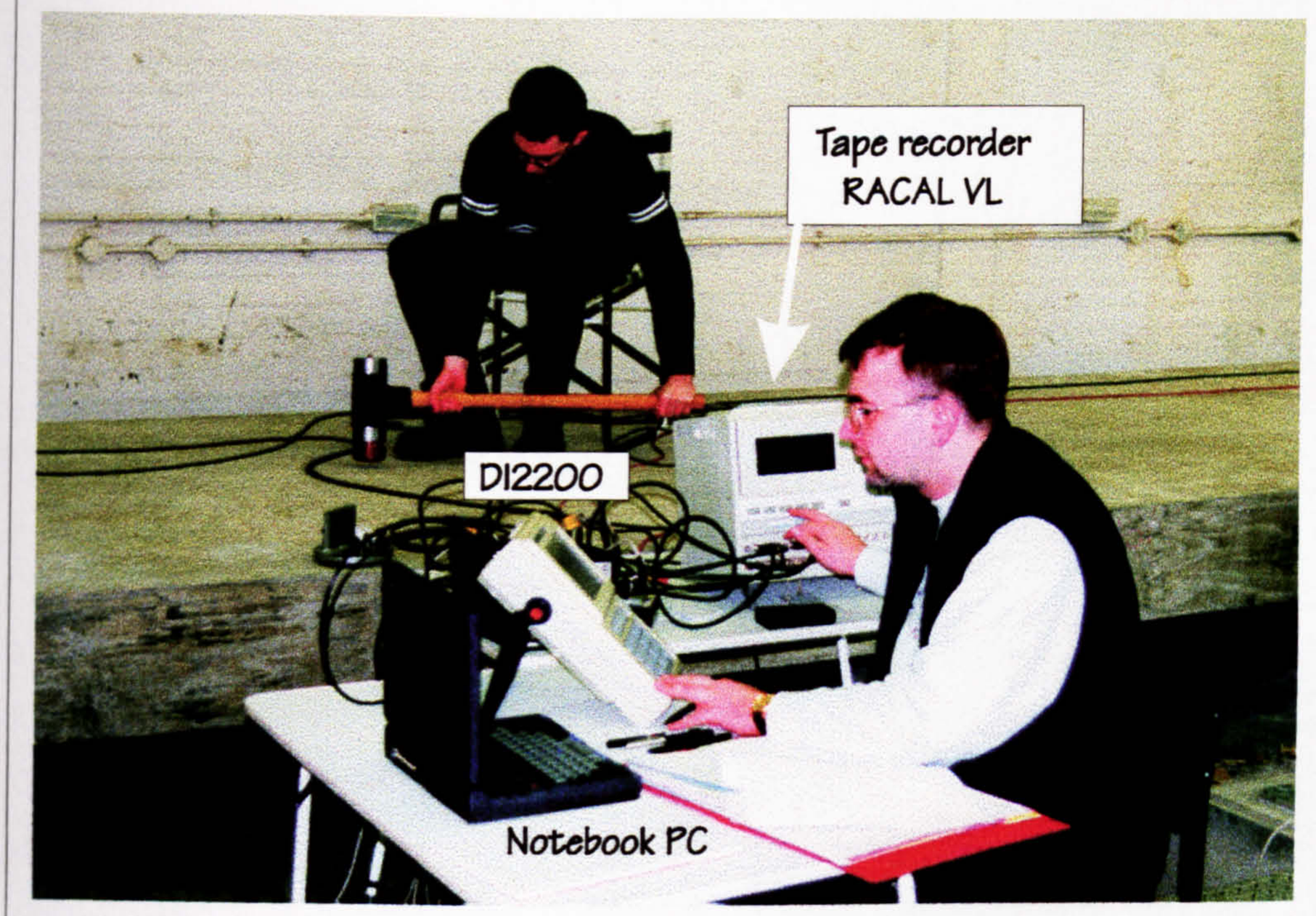

Figure 5.16: Structure A - Hammer testing and data acquisition setup.

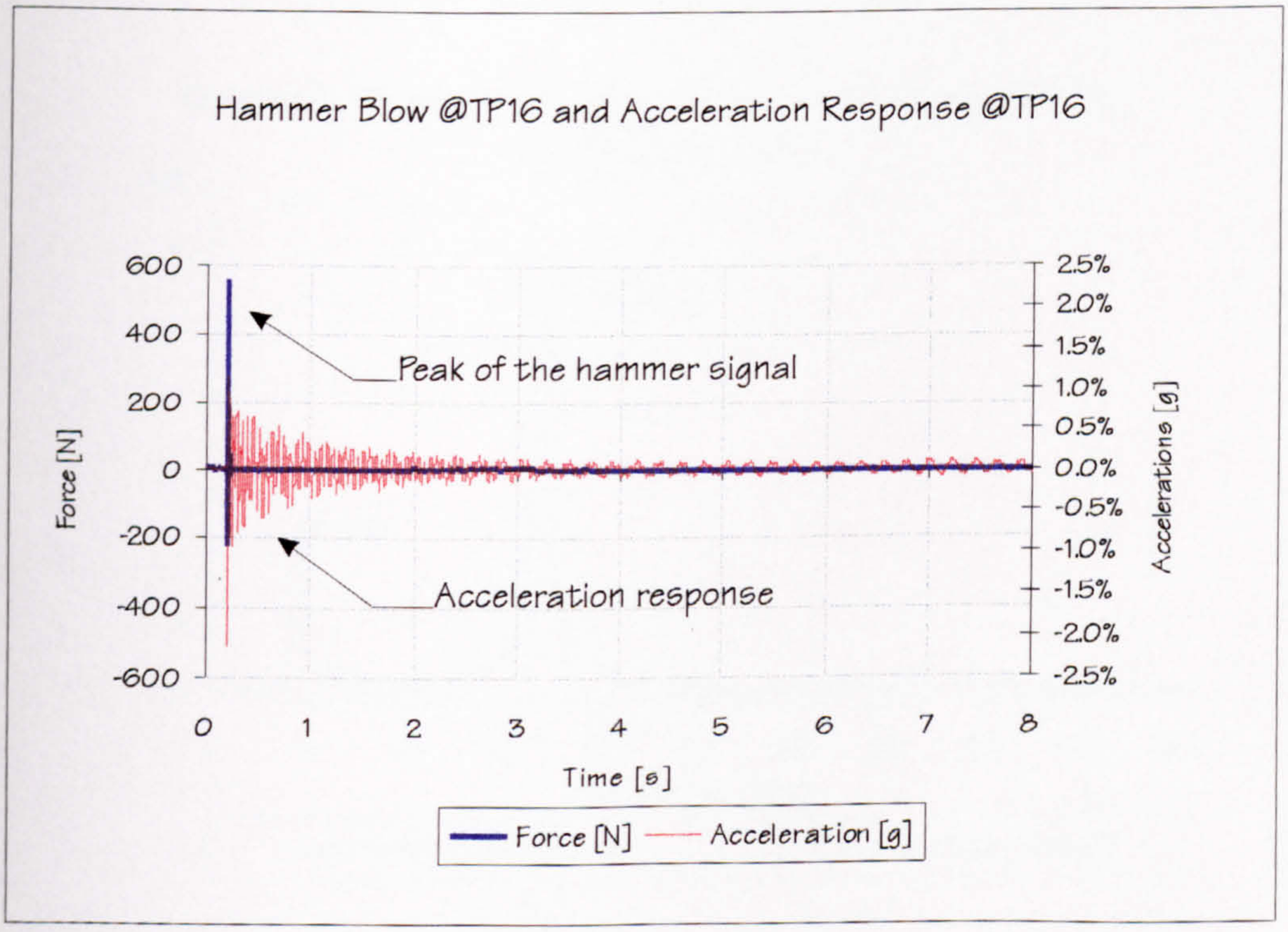

Figure 5.17: Structure A - Typical time-domain signals representing the hammer blow and acceleration response.

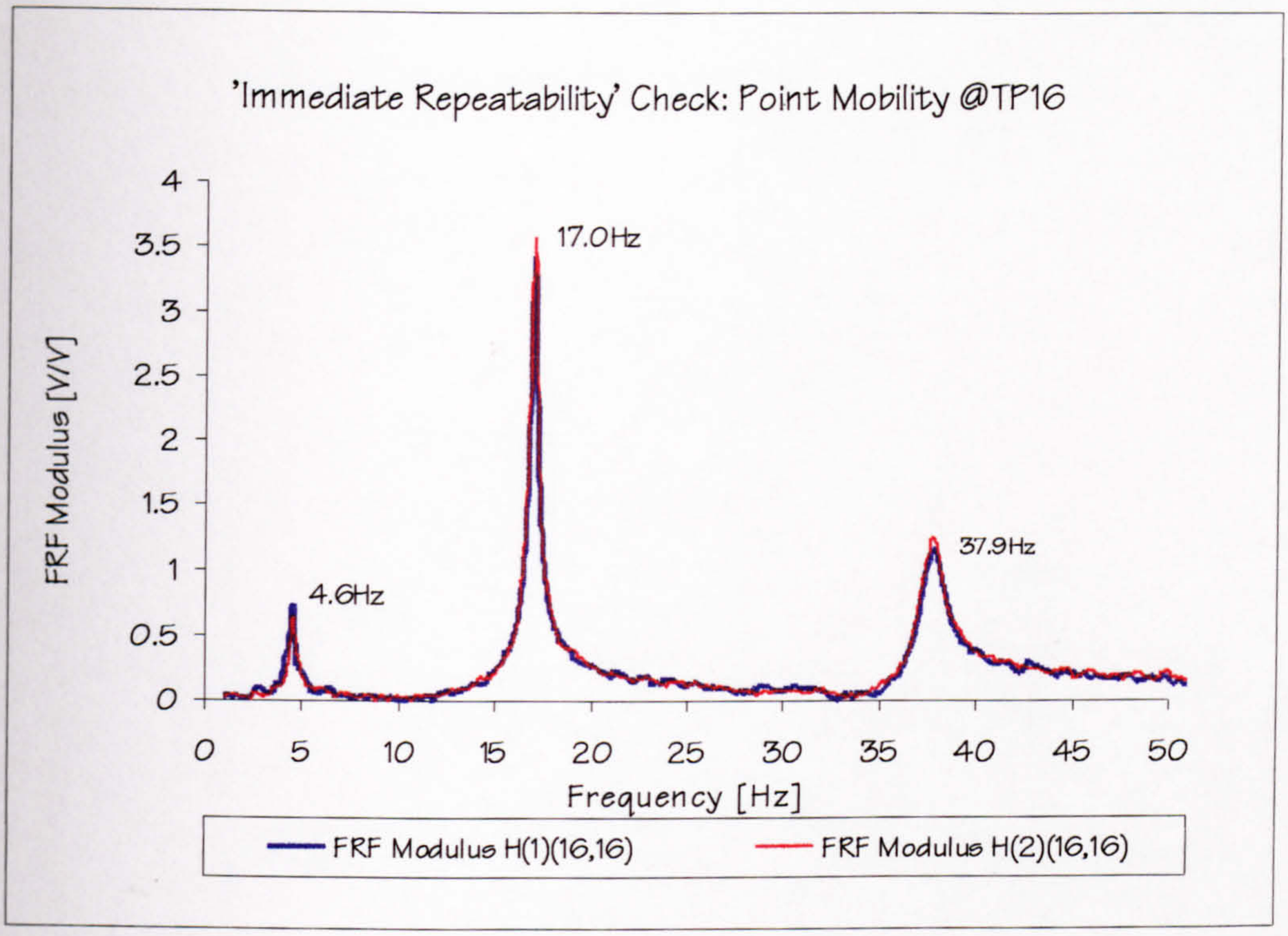

Figure 5.18: Structure A - 'Immediate repeatability' check.

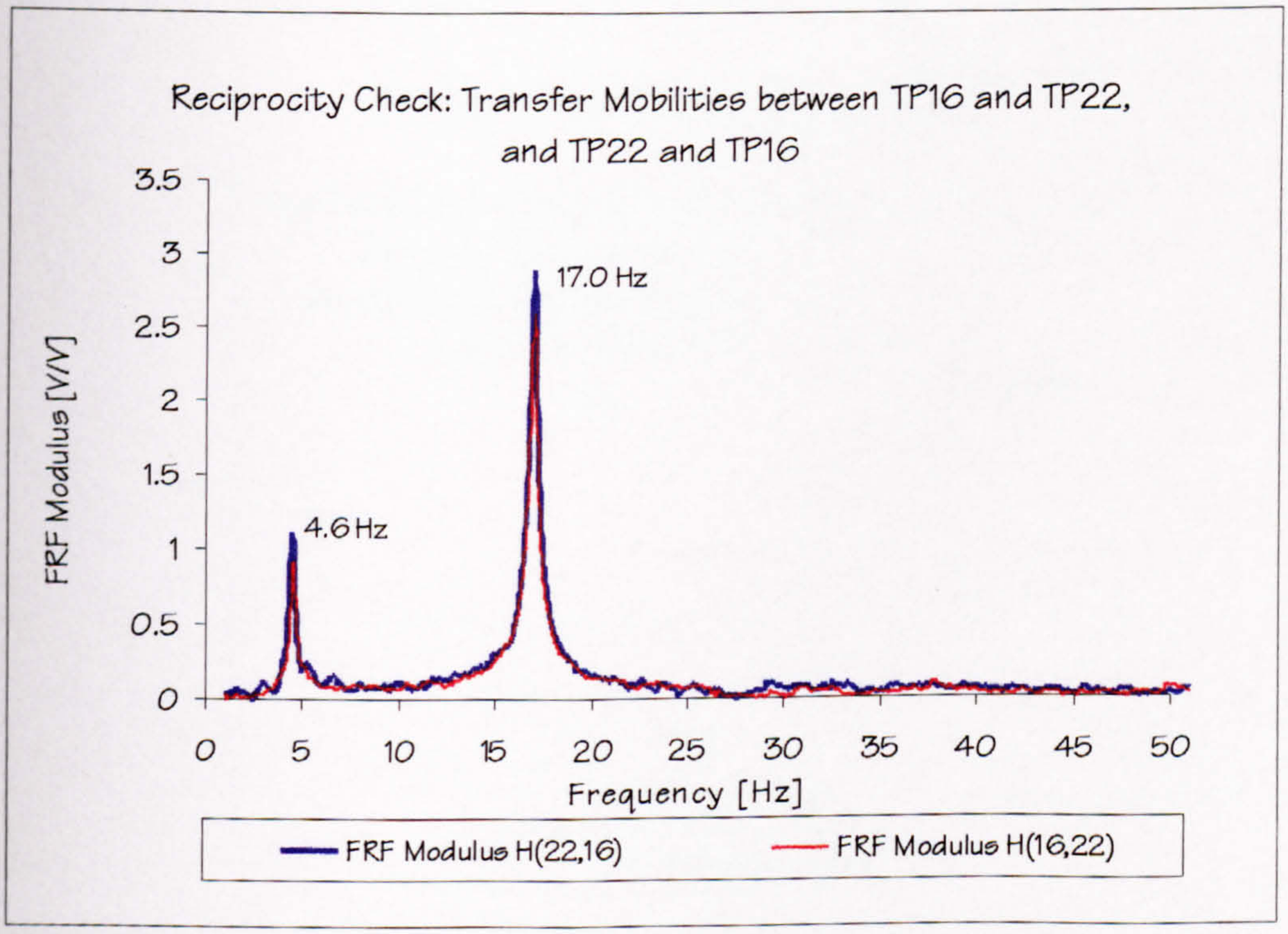

Figure 5.19: Structure A - Reciprocity check.

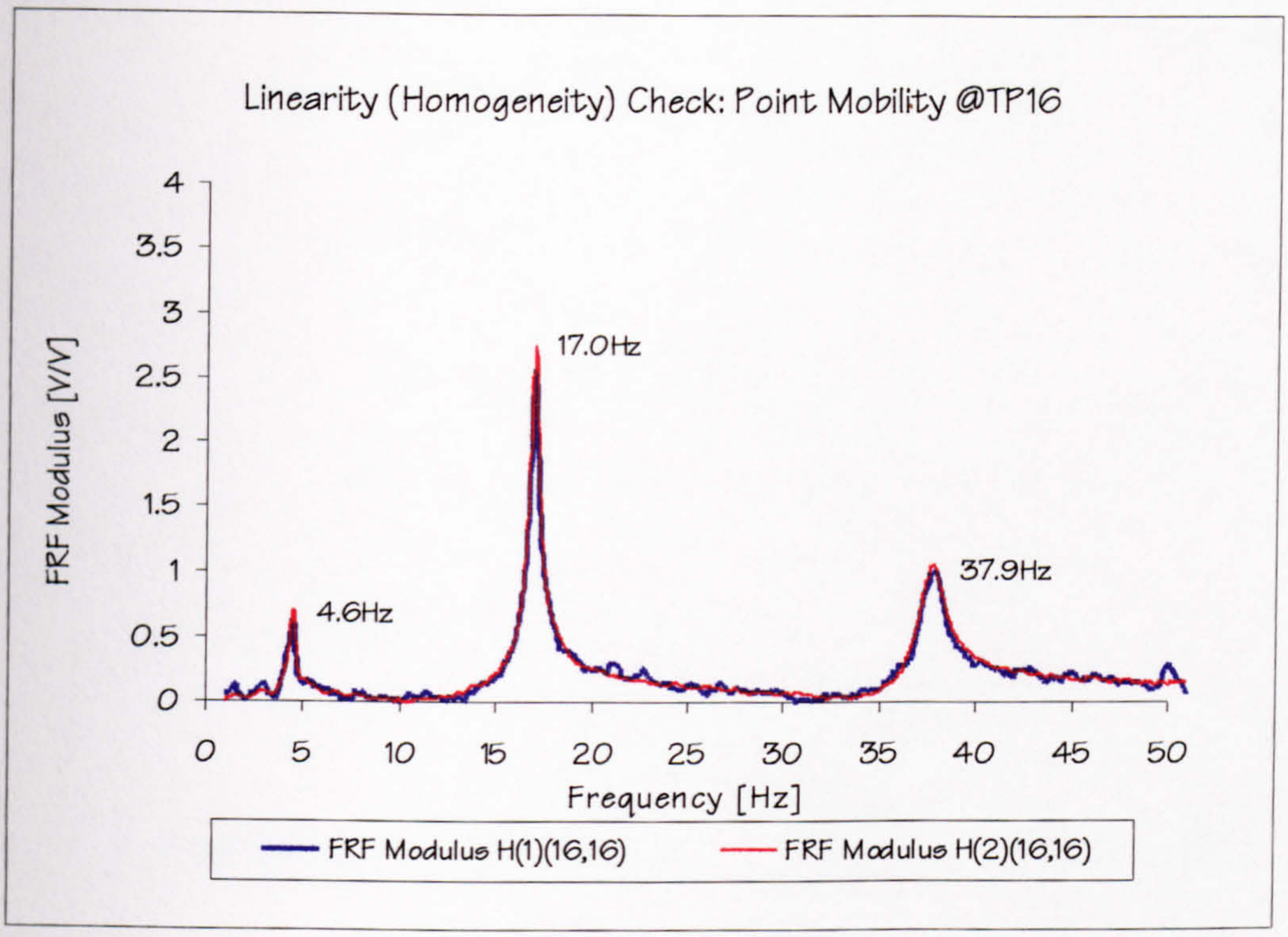

Figure 5.20: Structure A - Linearity (or homogeneity) check.

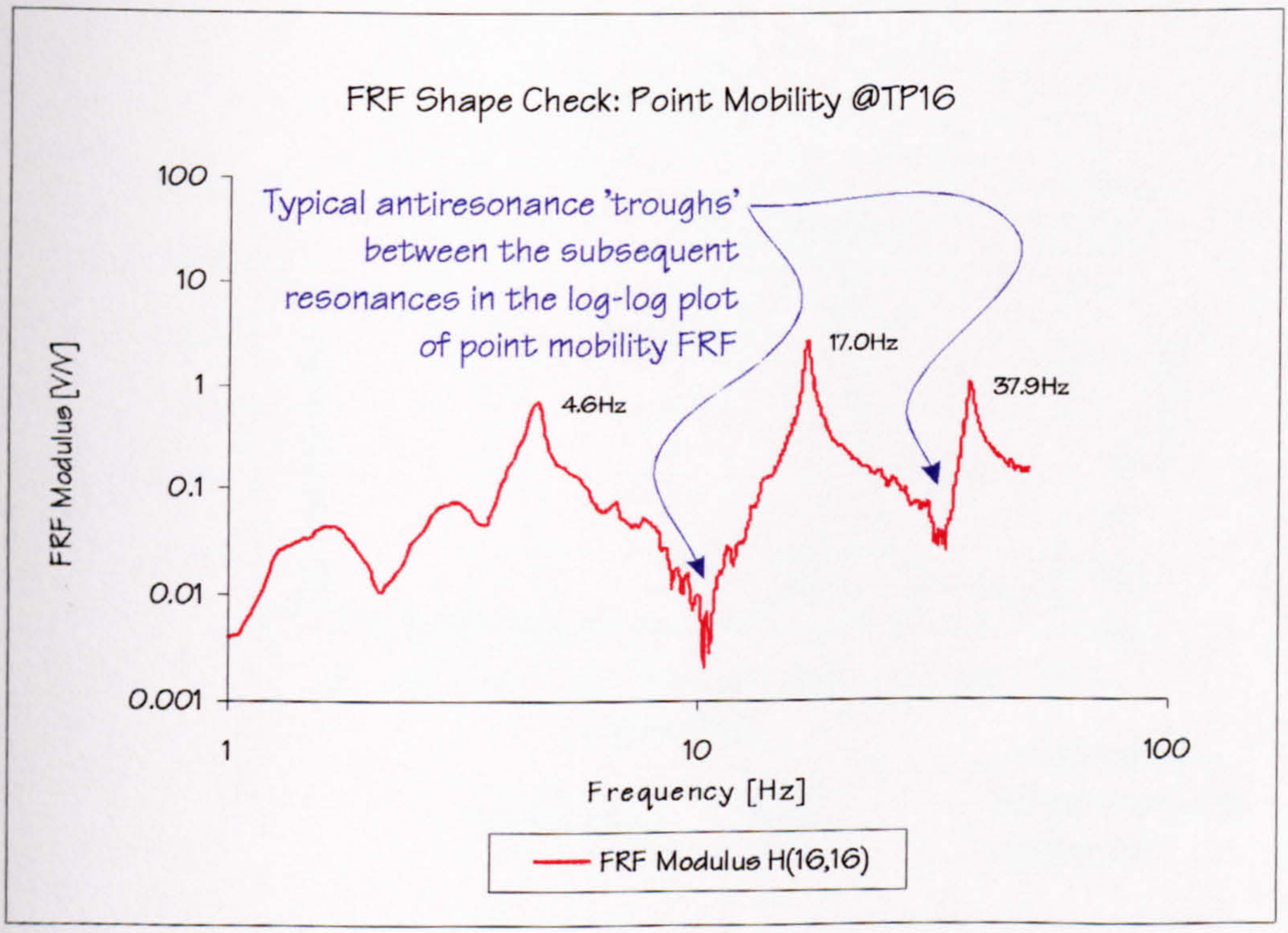

Figure 5.21: Structure A - Point mobility FRF shape check.

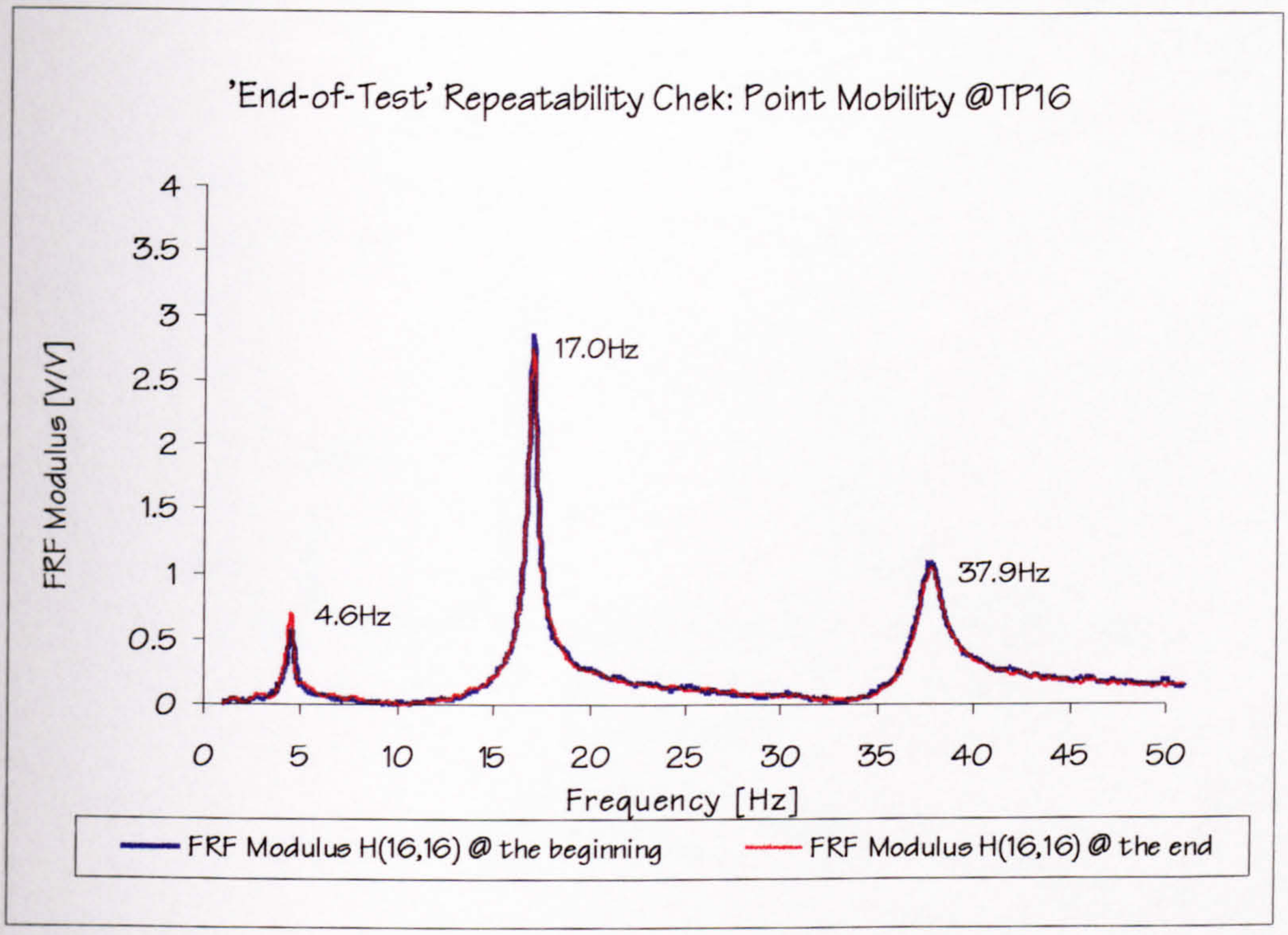

Figure 5.22: Structure A - 'End-of-test' repeatability check.

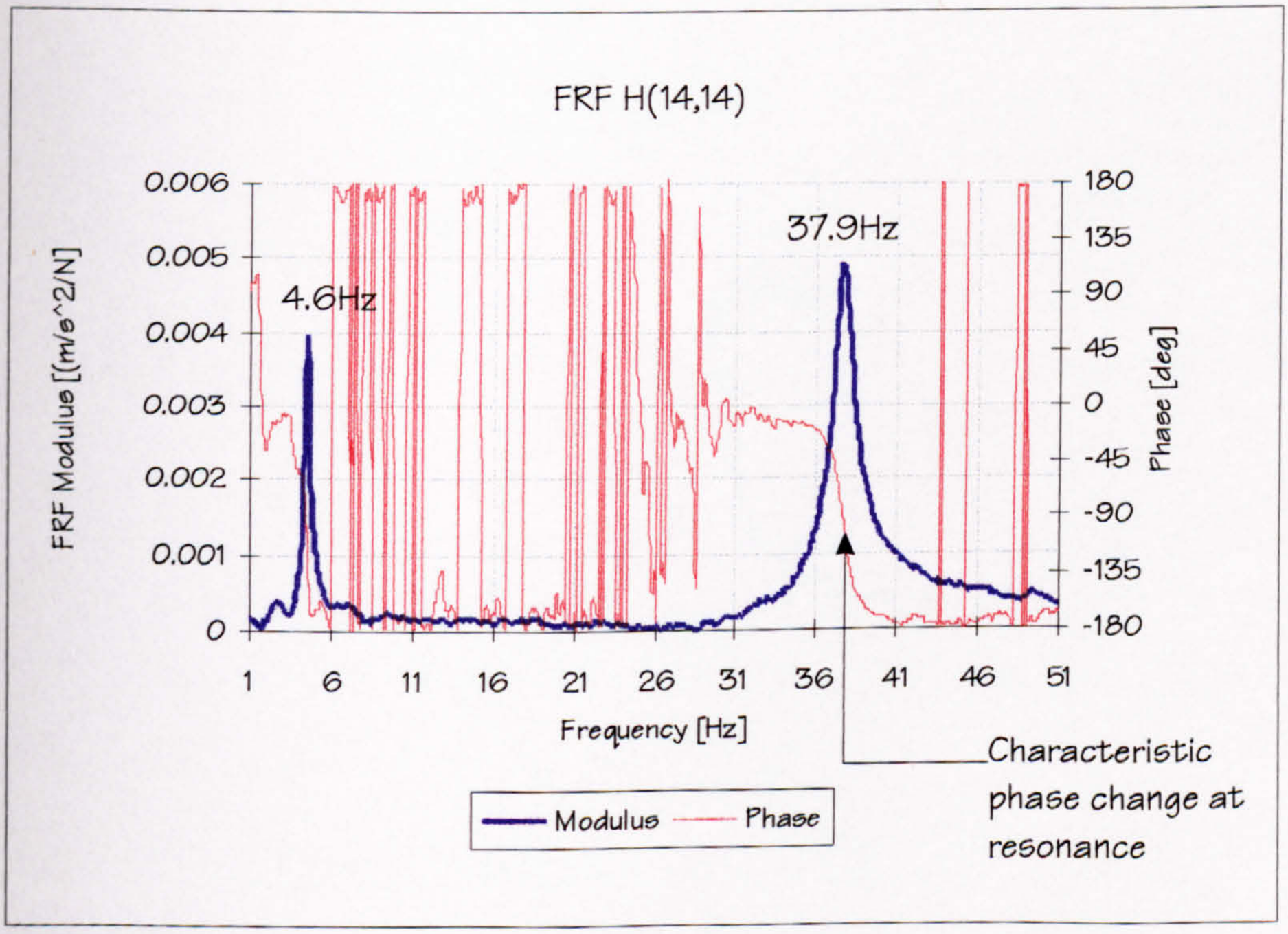

Figure 5.23: Structure A - Point mobility @TP14.

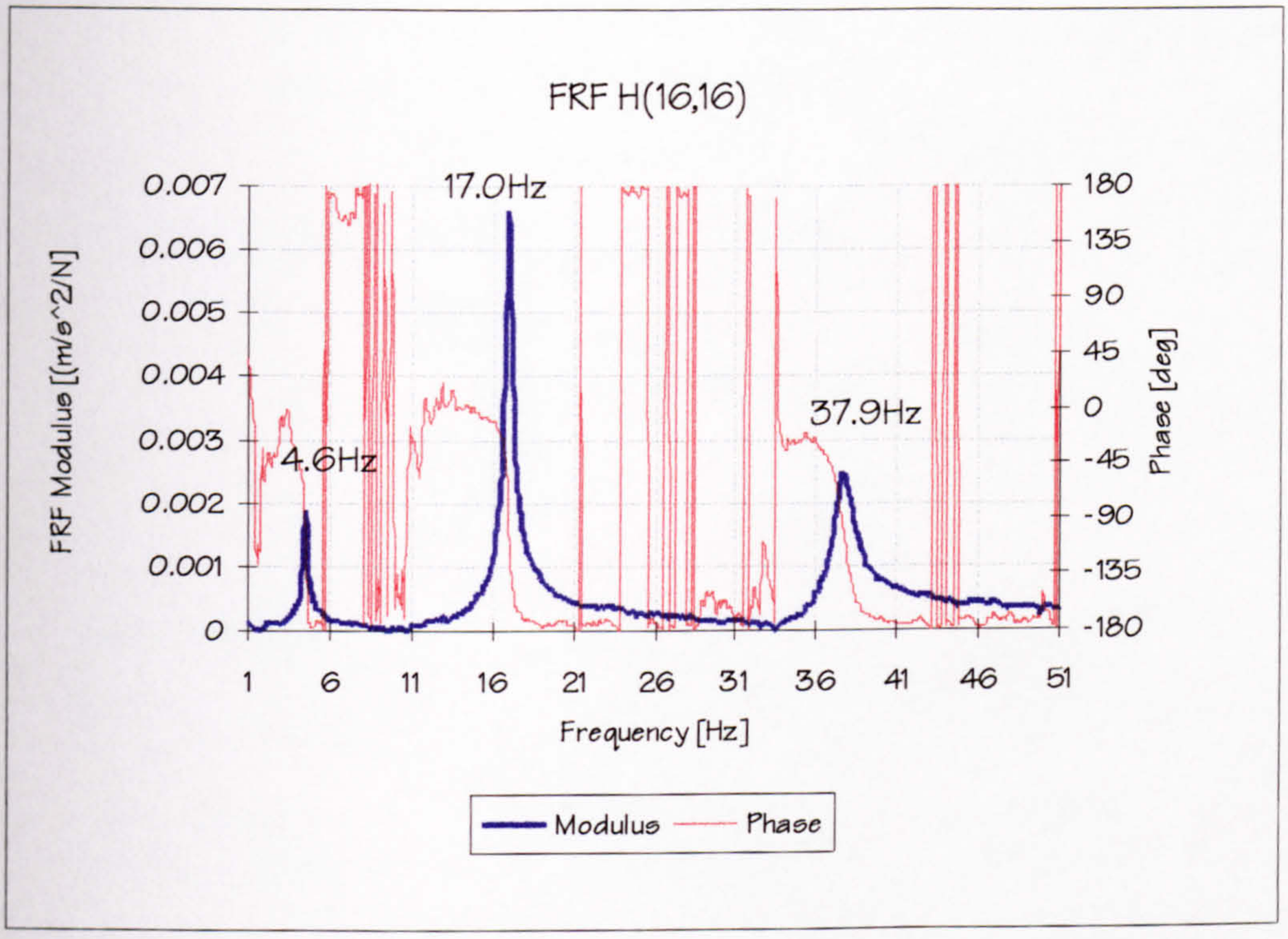

Figure 5.24: Structure A - Point mobility @TP16.

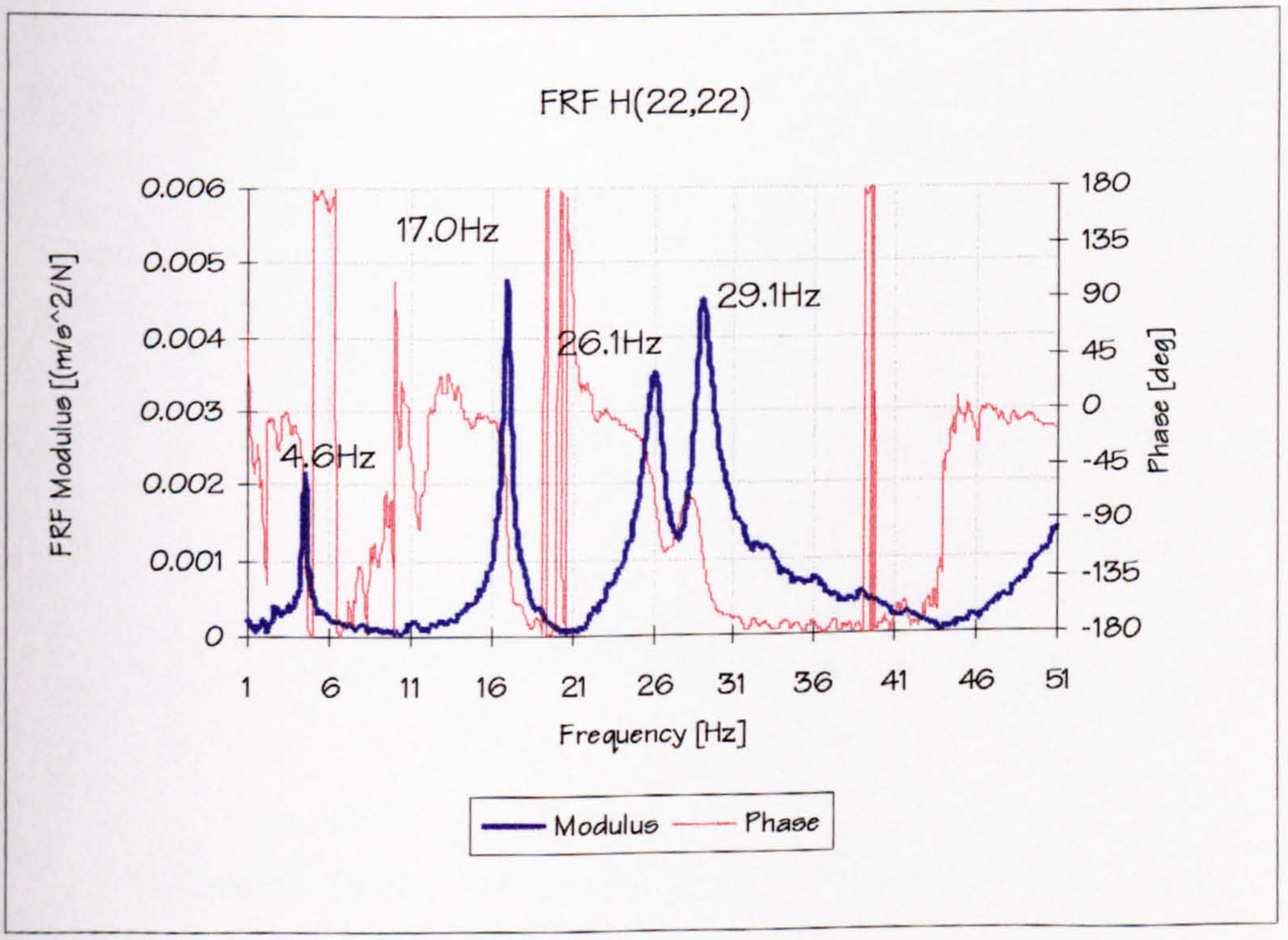

Figure 5.25: Structure A - Point mobility @TP22.

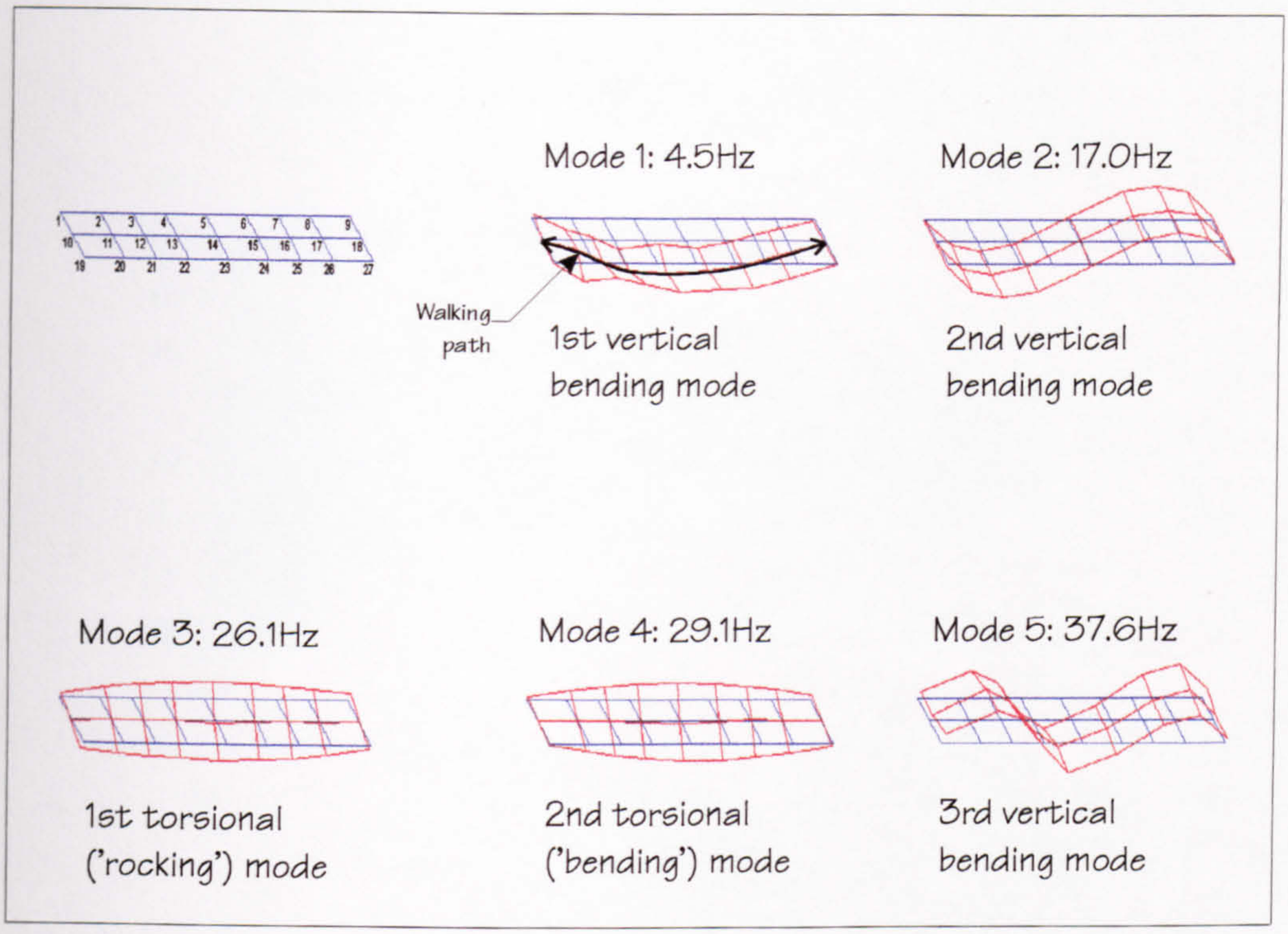

Figure 5.26: Structure A - Experimentally measured natural frequencies and mode shapes.

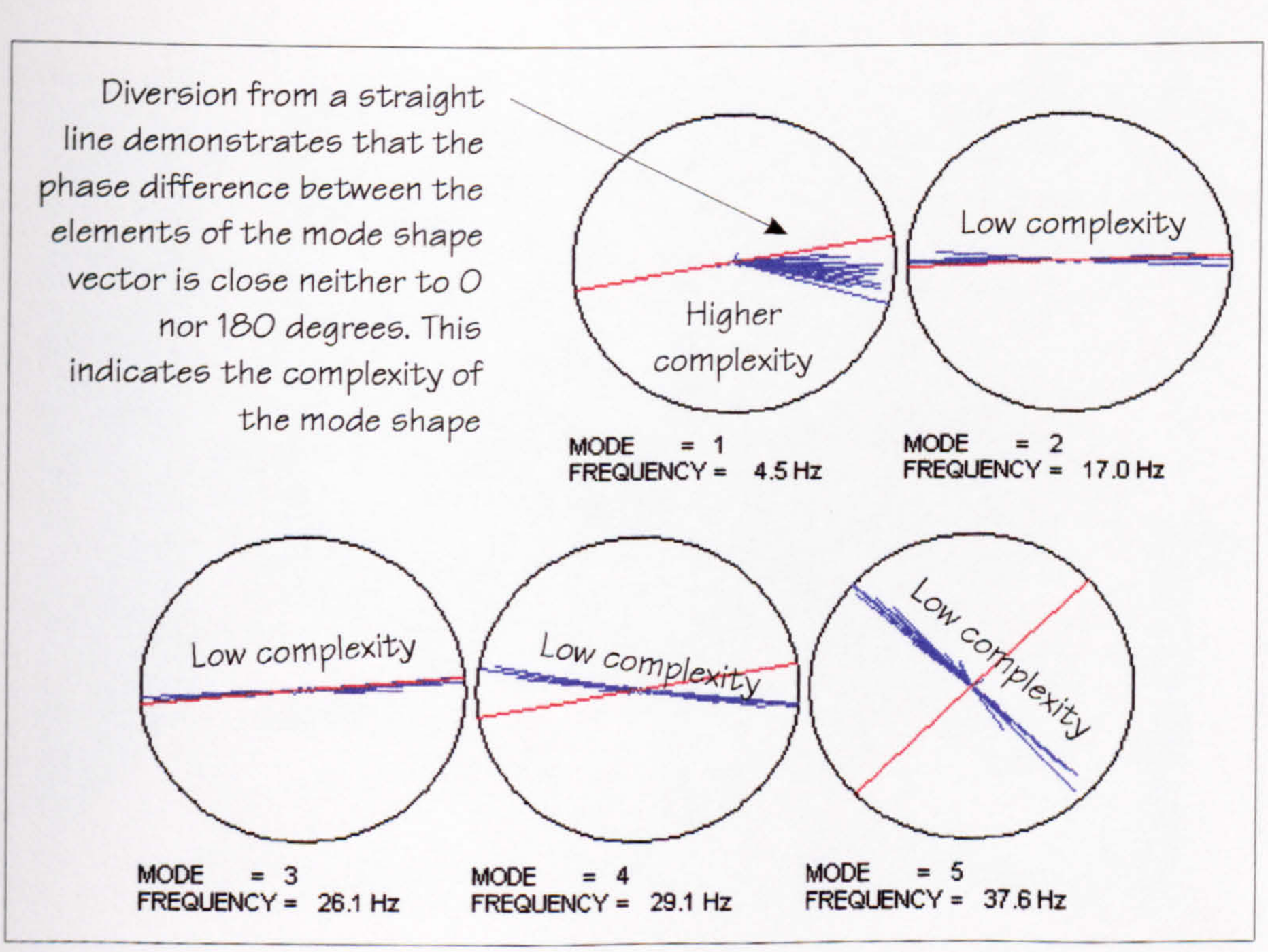

Figure 5.27: Structure A - Indication of modal complexity for the first five measured modes of vibration.

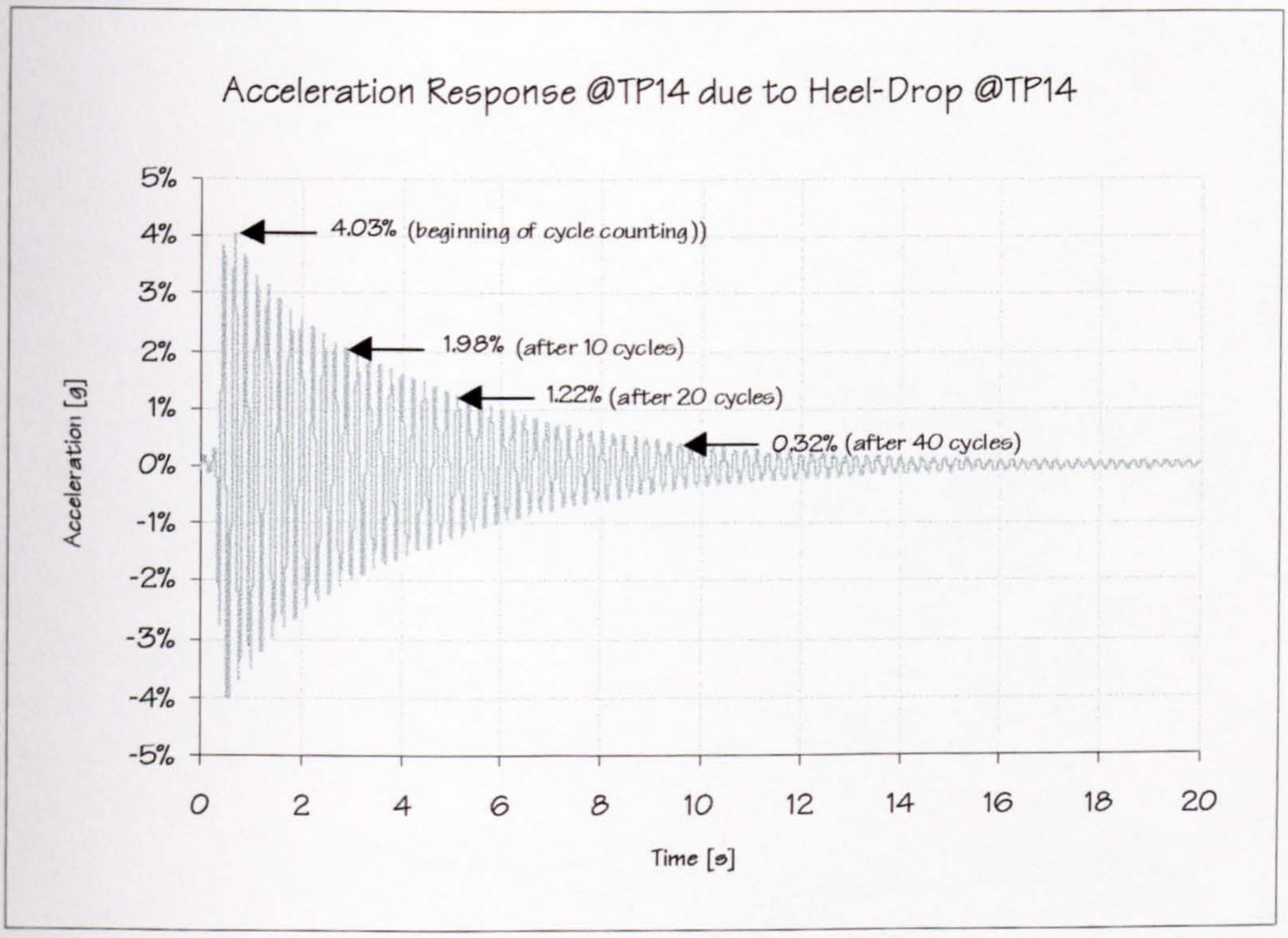

Figure 5.28: Structure A - Typical response to a heel-drop.

Figure 5.29: Structure A - Excitation of the structure by walking as close as practical to the slab strip mid-line.

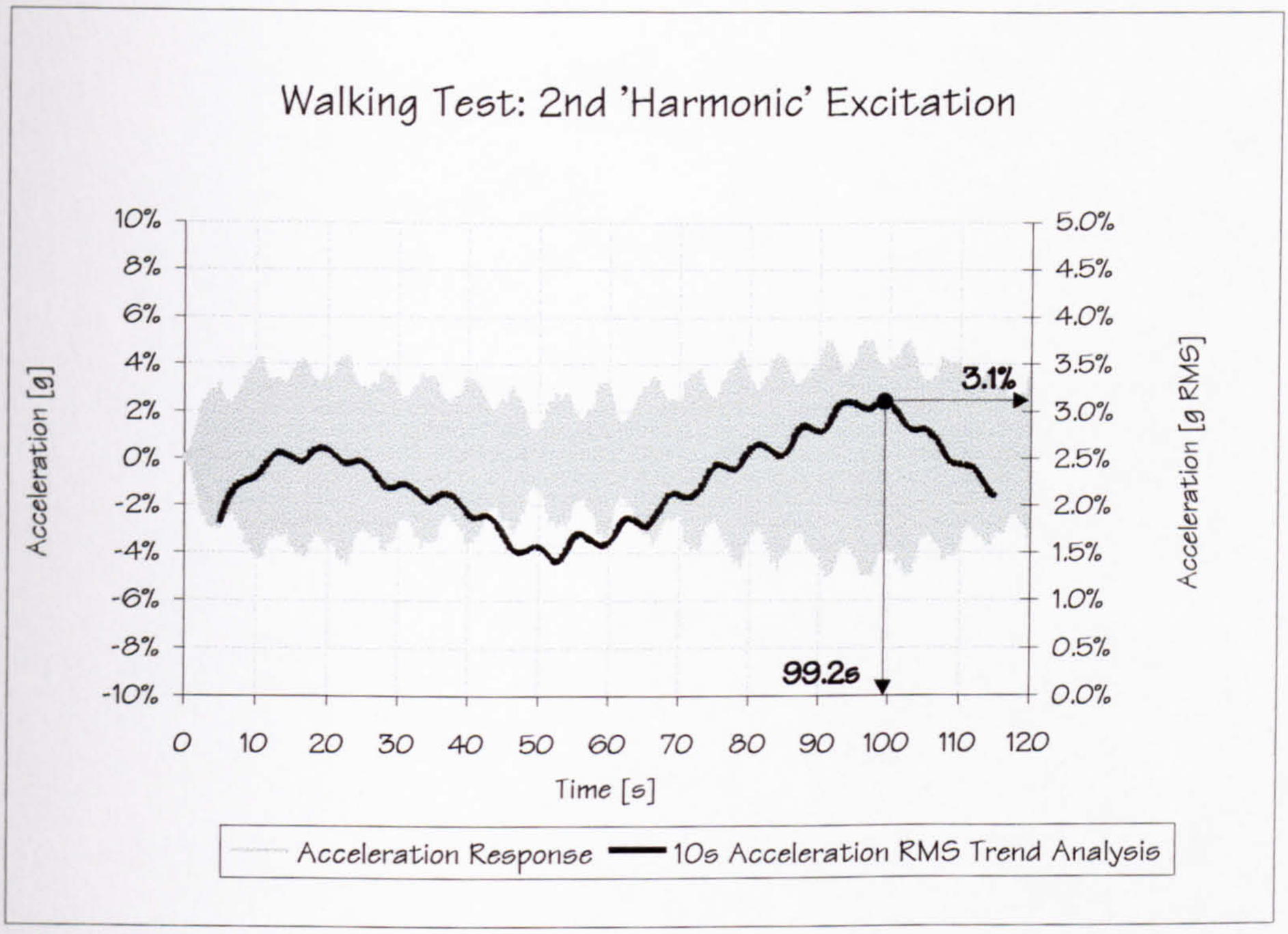

Figure 5.30: Structure A - Acceleration response @TP14 (mid point) and 10s RMS trend analysis due to excitation by the 2nd 'harmonic' of walking (an average male traversing the slab continuously for two minutes at a rate of 135 steps per minute).

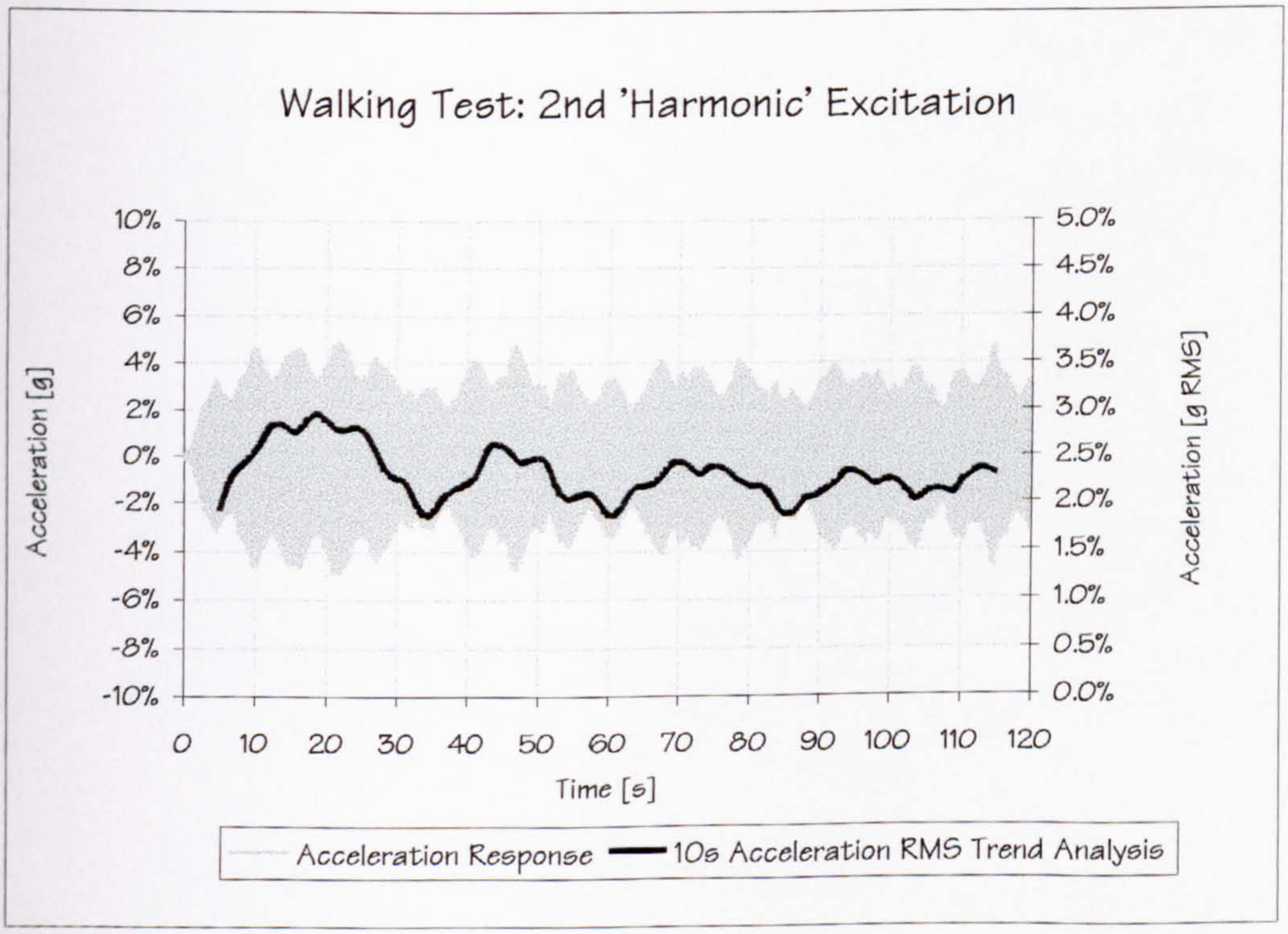

Figure 5.31: Structure A - Acceleration response @TP14 (mid point) and 10s RMS trend analysis due to repeated excitation by the 2nd 'harmonic' of walking (an average male traversing the slab continuously for two minutes at a rate of 135 steps per minute).

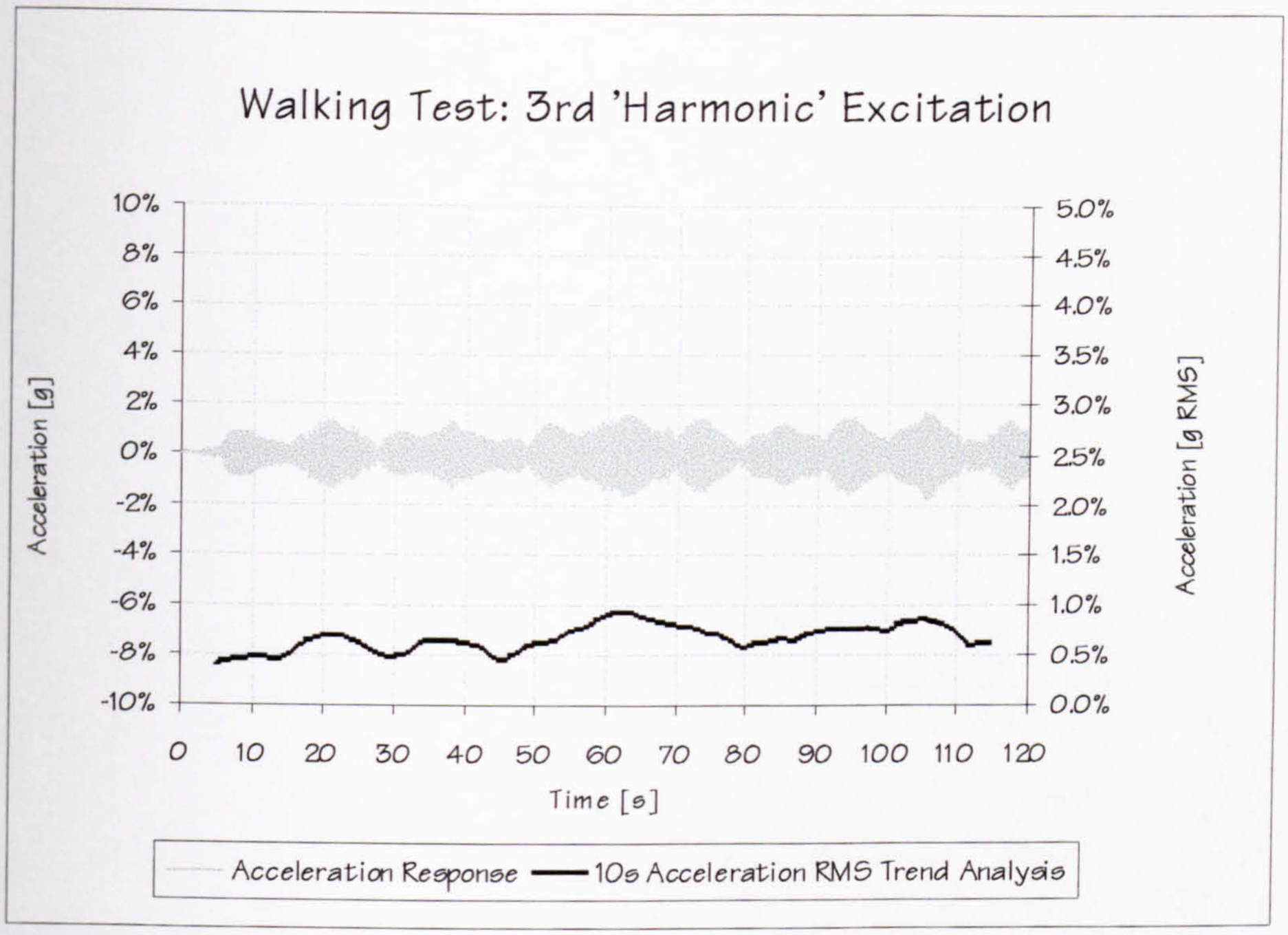

Figure 5.32: Structure A - Acceleration response @TP14 (mid point) and 10s RMS trend analysis due to excitation by the 3rd 'harmonic' of walking (an average male traversing the slab continuously for two minutes at a rate of 90 steps per minute).

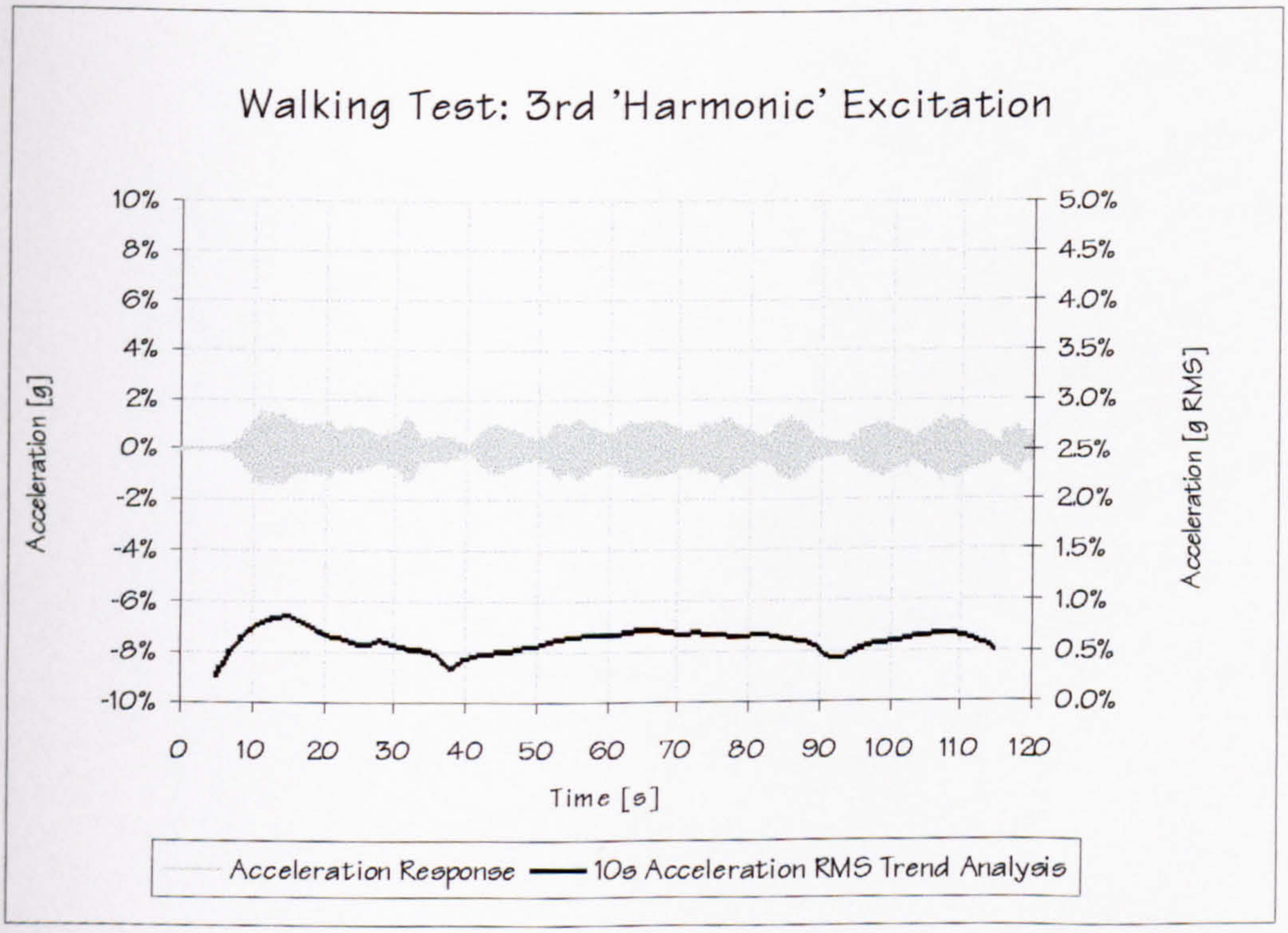

Figure 5.33: Structure A - Acceleration response @TP14 (mid point) and 10s RMS trend analysis due to repeated excitation by the 3rd 'harmonic' of walking (an average male traversing the slab continuously for two minutes at a rate of 90 steps per minute).

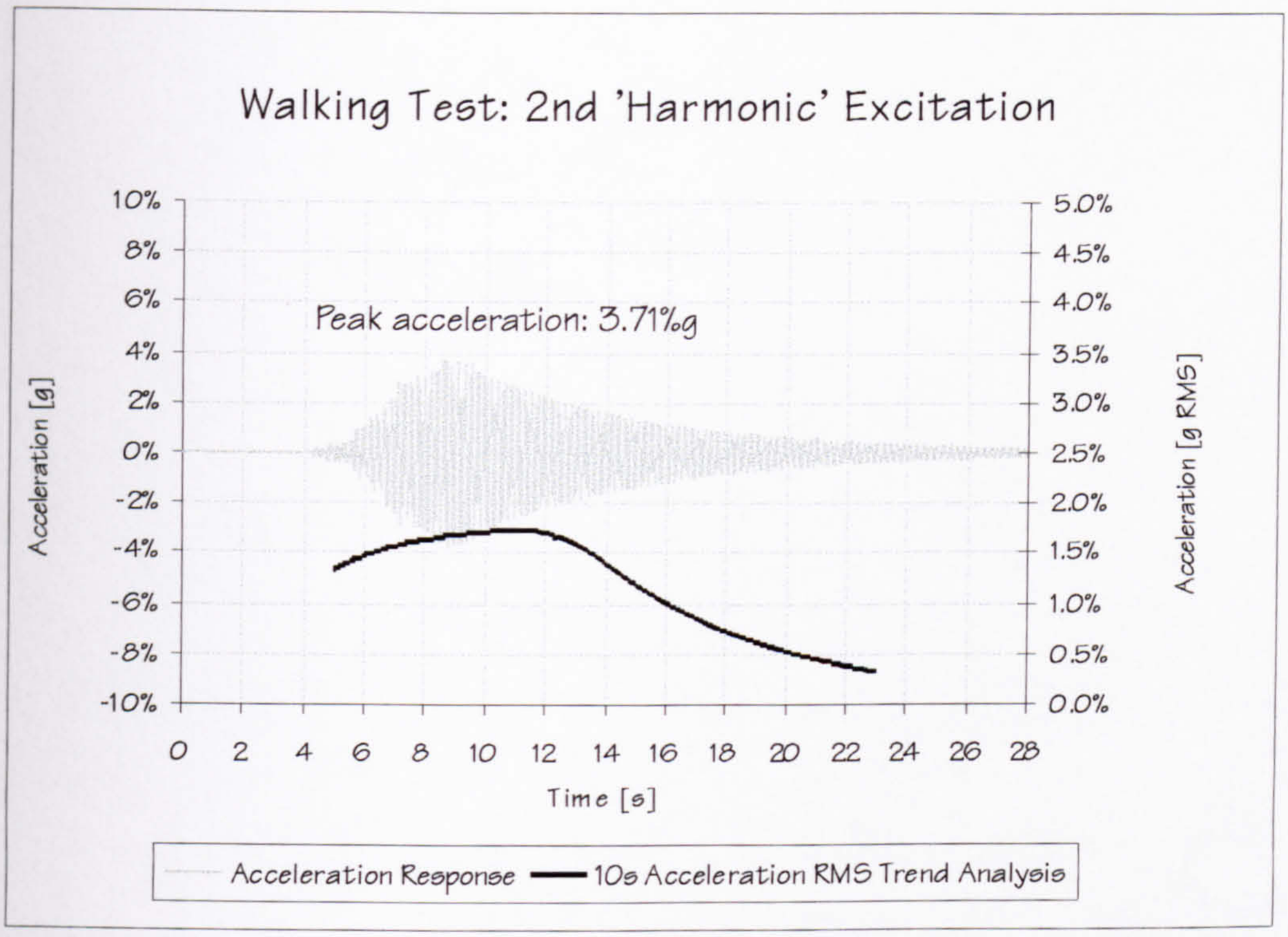

Figure 5.34: Structure A - Acceleration response @TP14 (mid point) and 10s RMS trend analysis due to excitation by the 2nd 'harmonic' of transient walking (an average male traversing the slab for approximately 5s at a rate of 135 steps per minute).

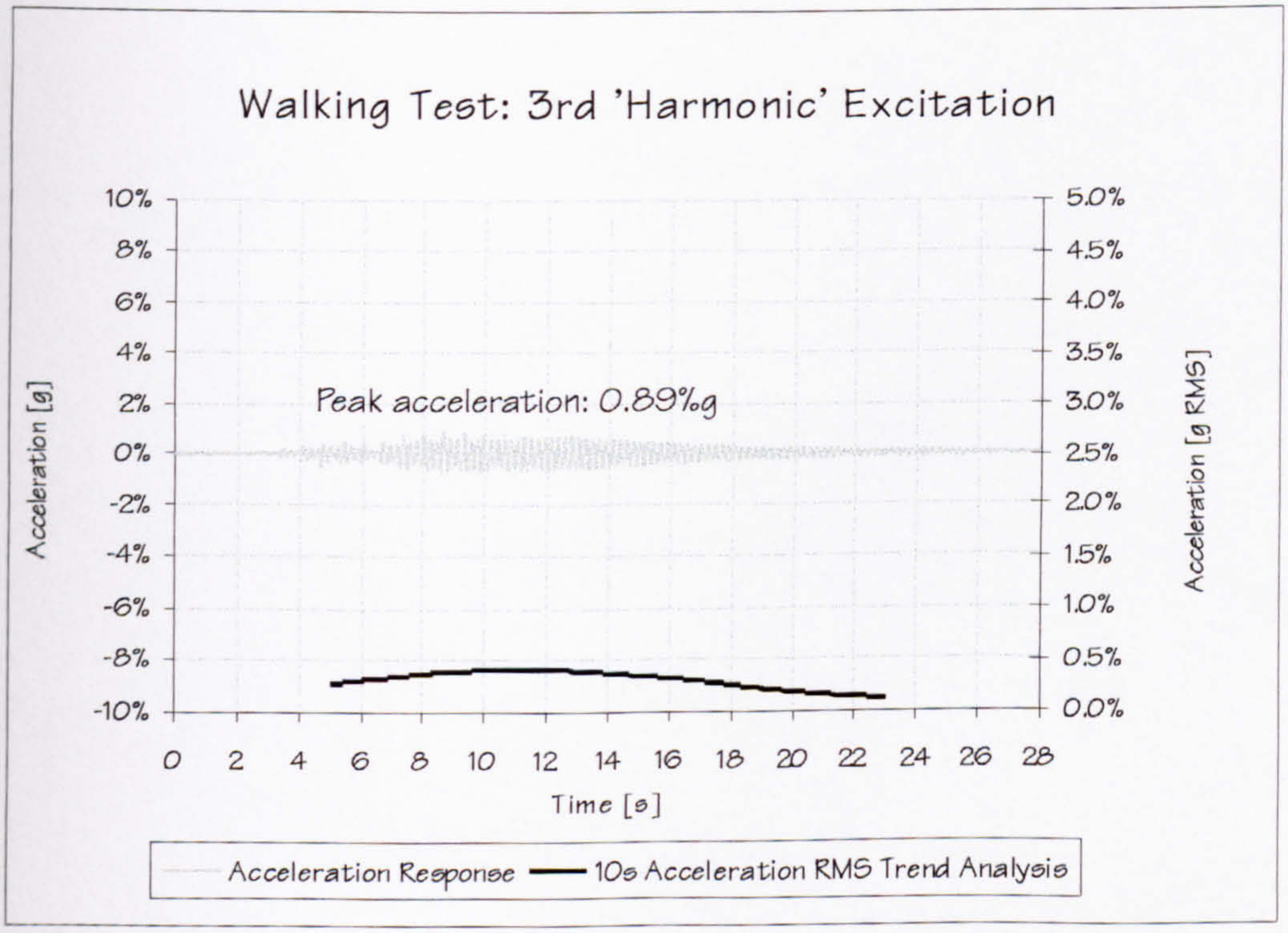

Figure 5.35: Structure A - Acceleration response @TP14 (mid point) and 10s RMS trend analysis due to excitation by the 3rd 'harmonic' of transient walking (an average male traversing the slab for approximately 8s at a rate of 90 steps per minute).

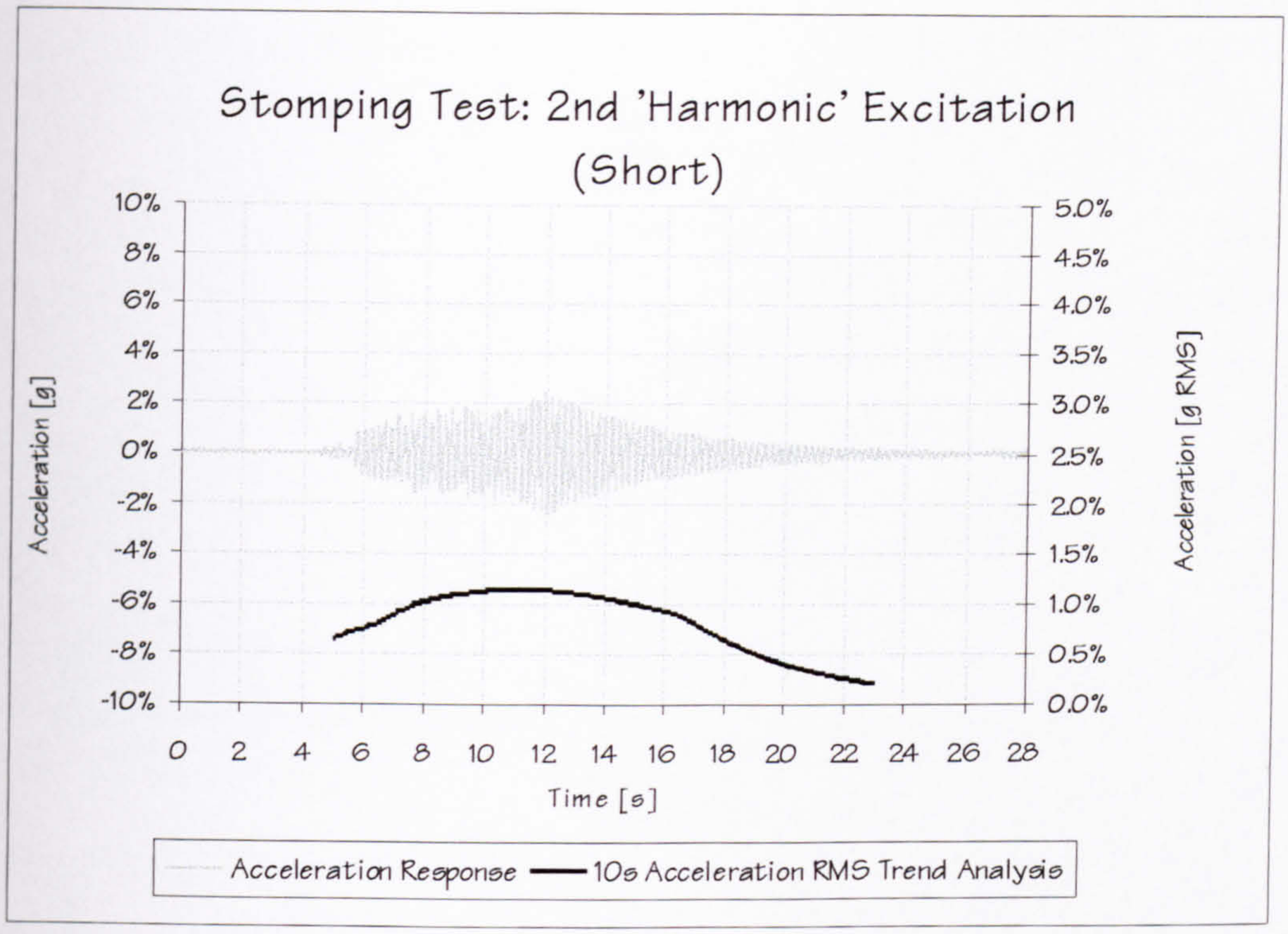

Figure 5.36: Structure A - Acceleration response @TP14 (mid point) and 10s RMS trend analysis due to excitation by treading in place @TP14 at a pace corresponding to the 2nd 'harmonic' of walking (an average male stomping for approximately 7s at a rate of 135 steps per minute).

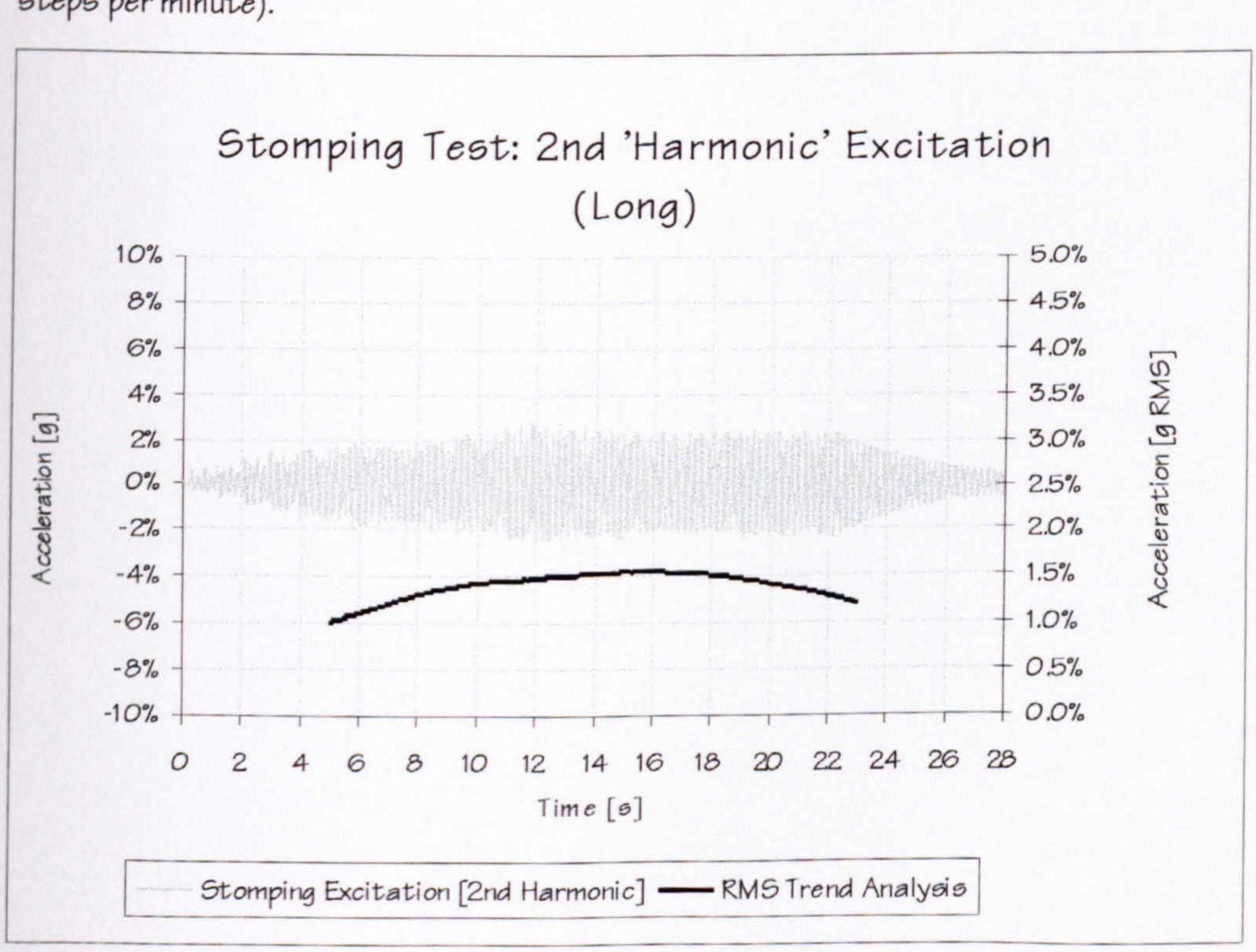

Figure 5.37: Structure A - Acceleration response @TP14 (mid point) and 10s RMS trend analysis due to excitation by treading in place @TP14 at a pace corresponding to the 2nd 'harmonic' of walking (an average male stomping for approximately 22s at a rate of 135 steps per minute).

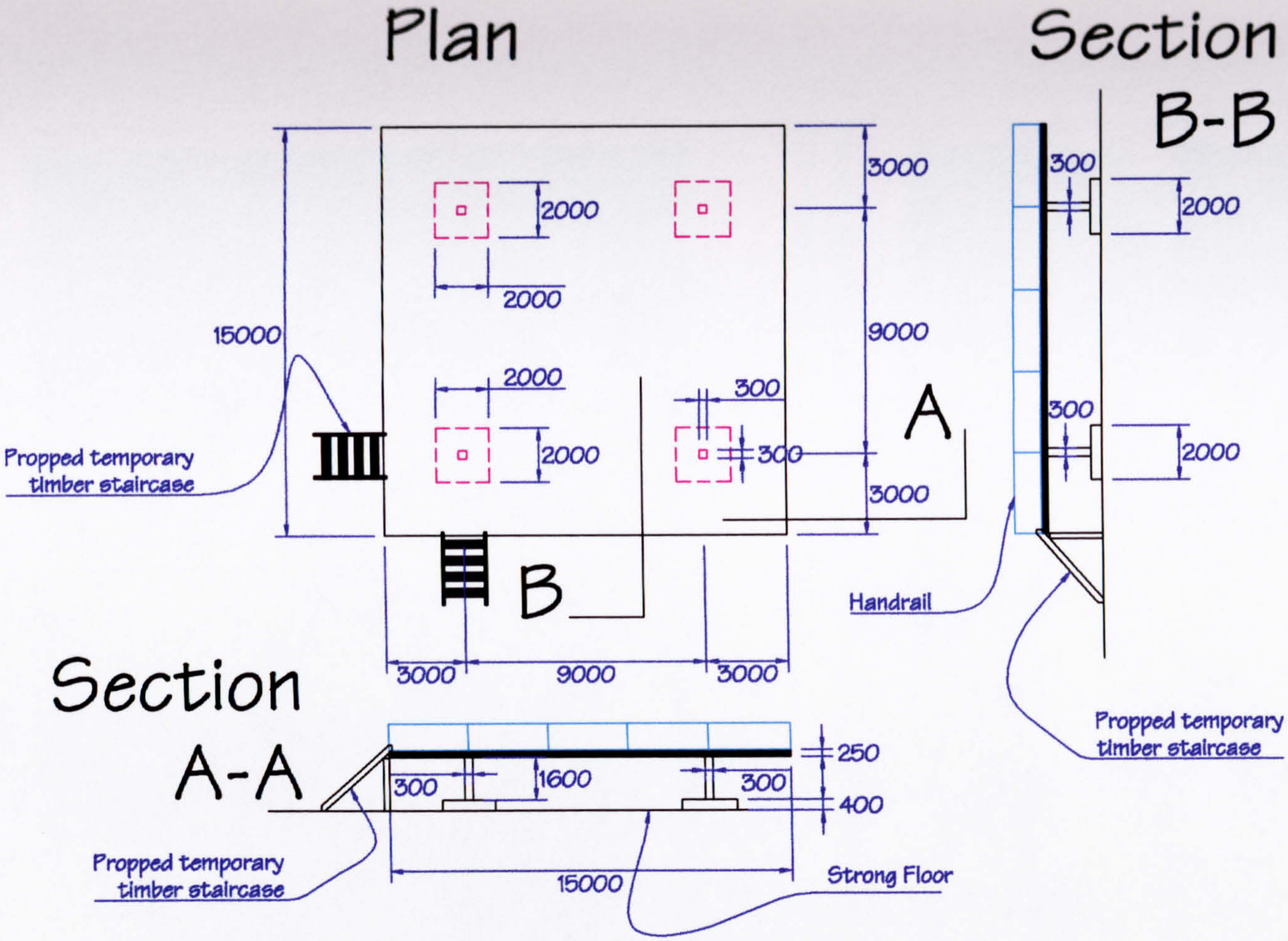

Drawing No.	Filename	Drawn by	Date	Scale
3	Structure B - Layout.dwg	A. Pavic	10 Oct 1995	1:250

Title
STRUCTURE B: GENERAL ARRANGEMENT DRAWING

Figure 5.38: Structure B - Layout of classically reinforced in-situ cast HSC floor.

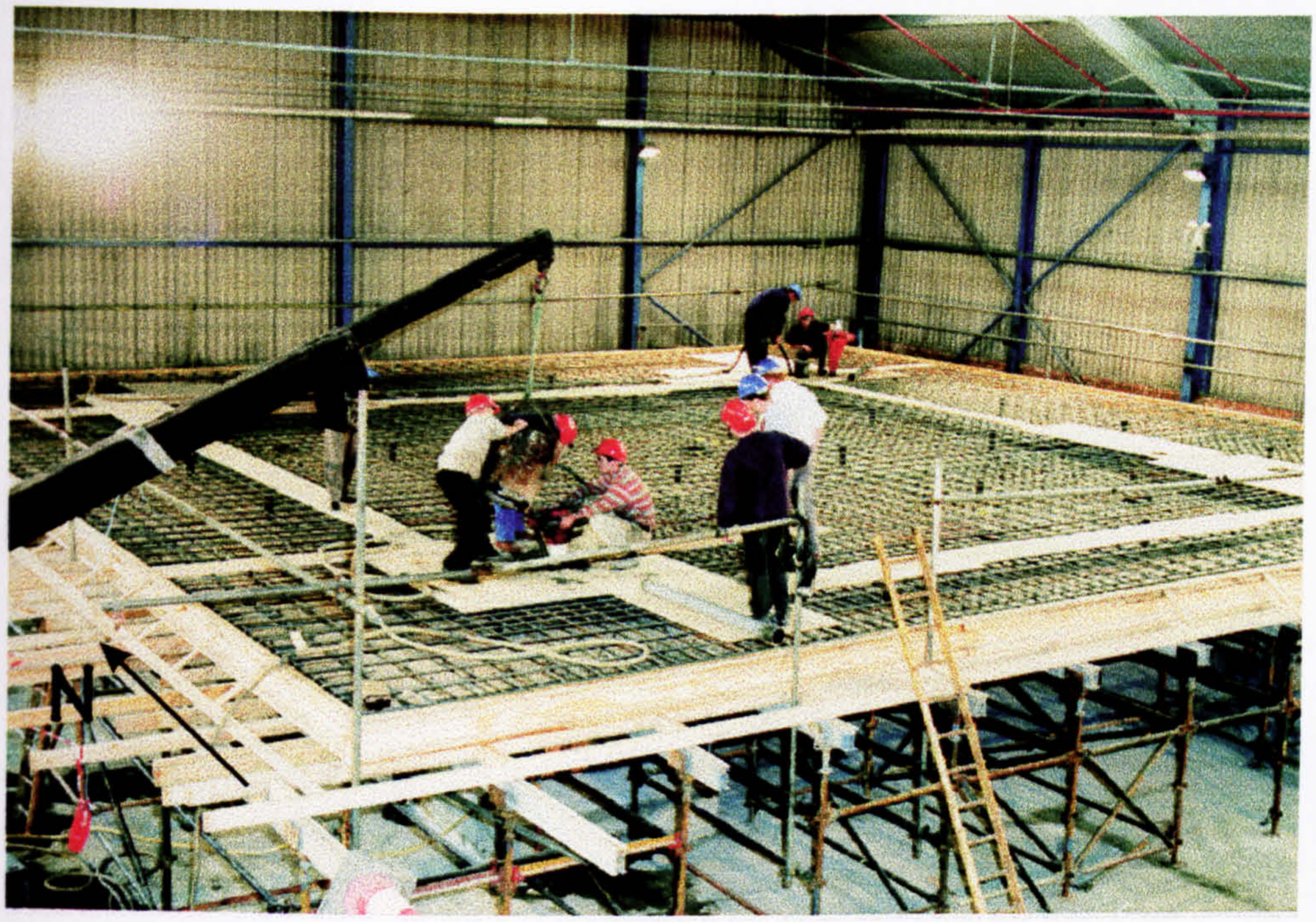

Figure 5.39: Structure B - Reinforcement placement and casting of columns prior to slab concreting (courtesy of Taywood Engineering Ltd).

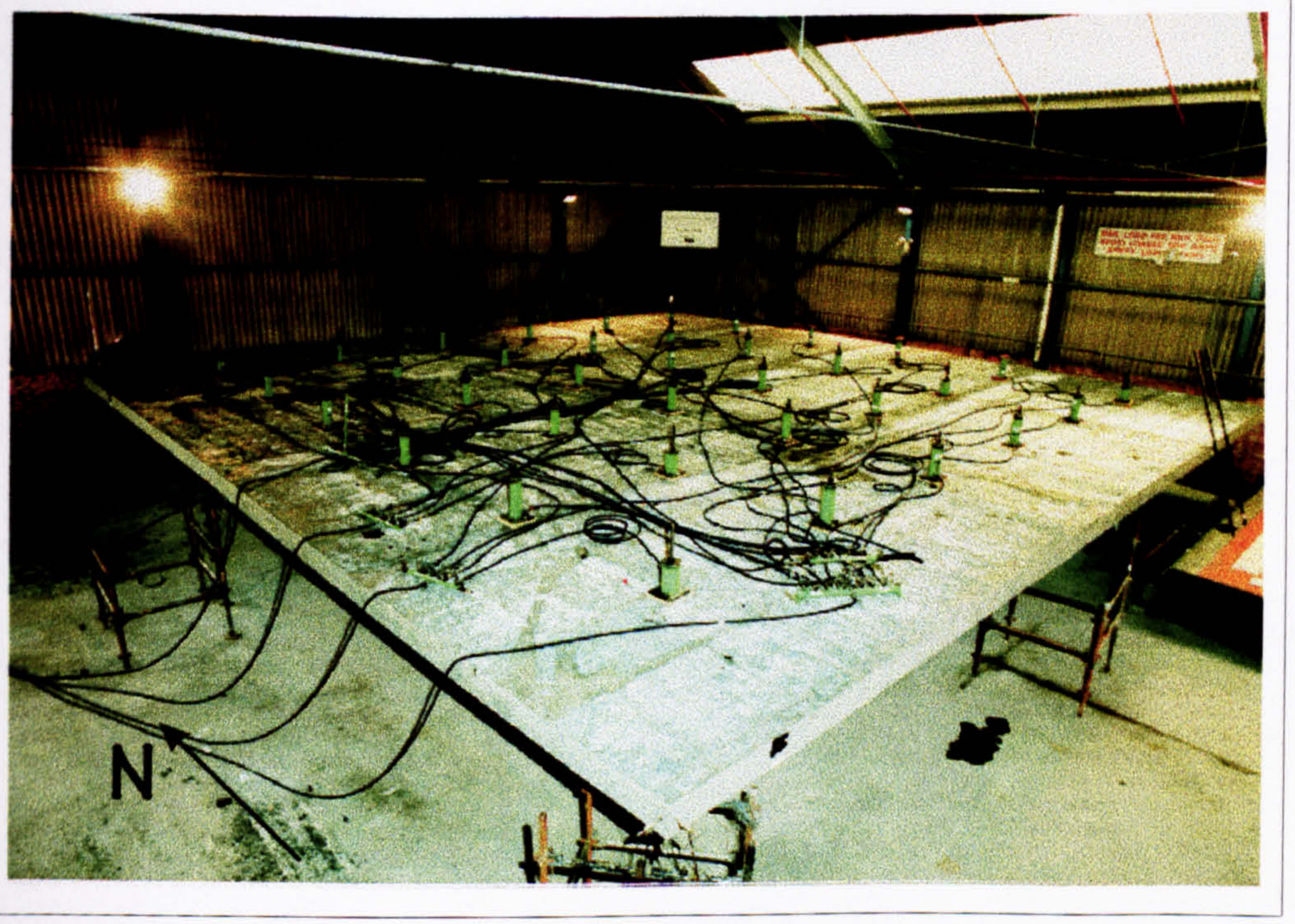

Figure 5.40: Structure B - Static loading test setup using 36 hydraulc jacks (courtesy of Taywood Engineering Ltd).

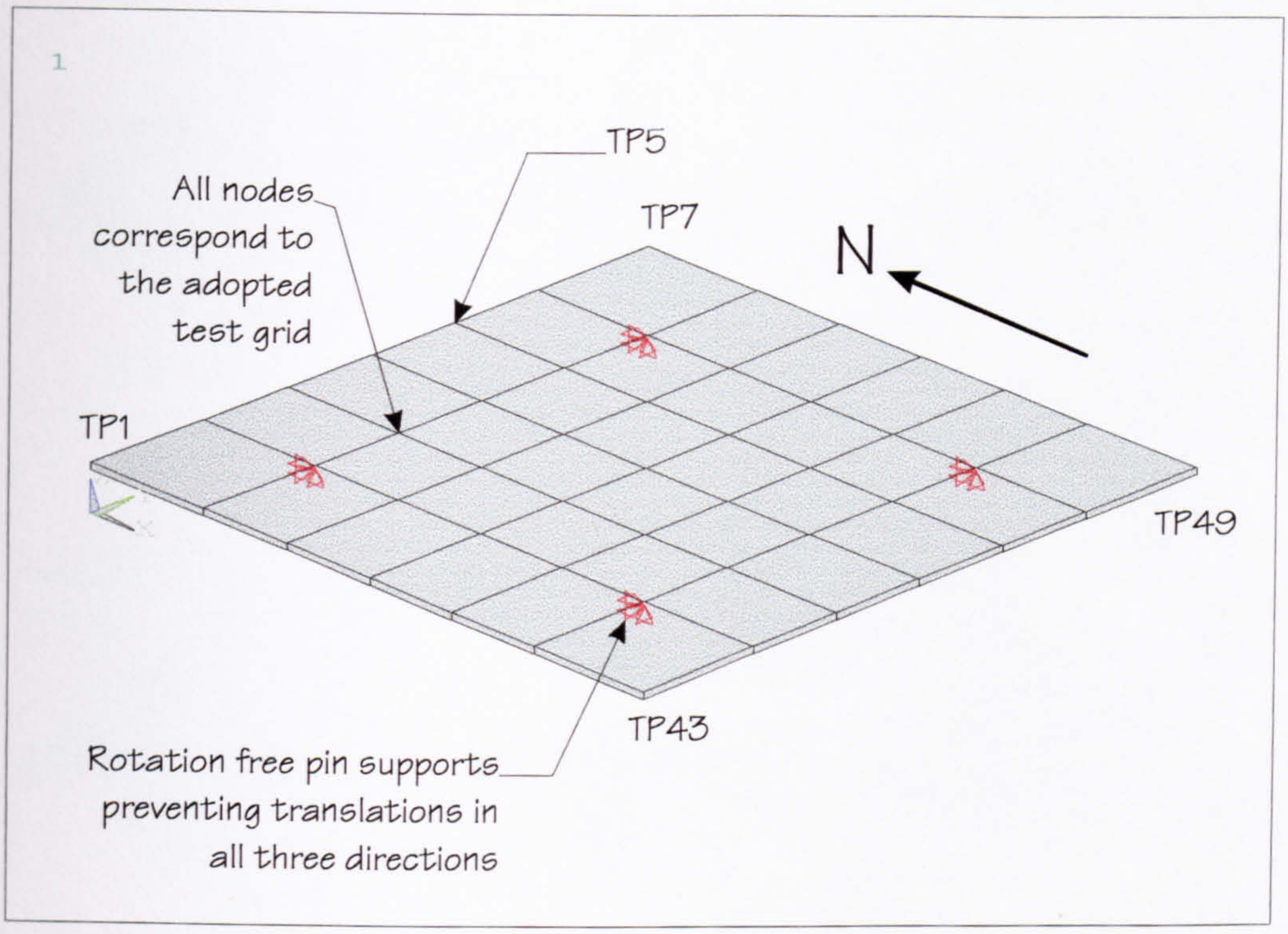

Figure 5.41: Structure B - FE model developed for pre-test analysis.

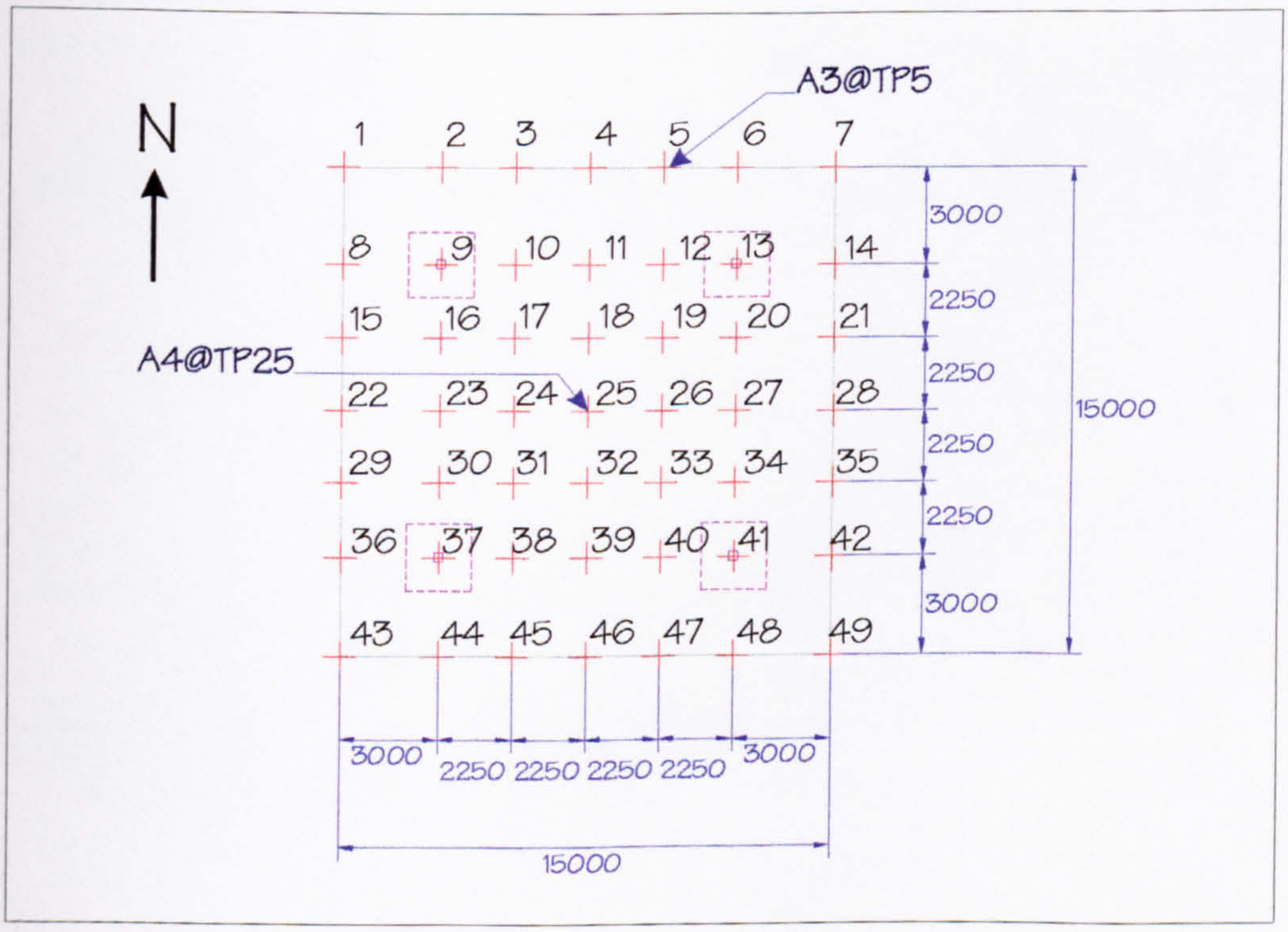

Figure 5.42: Structure B - Test grid and accelerometer locations.

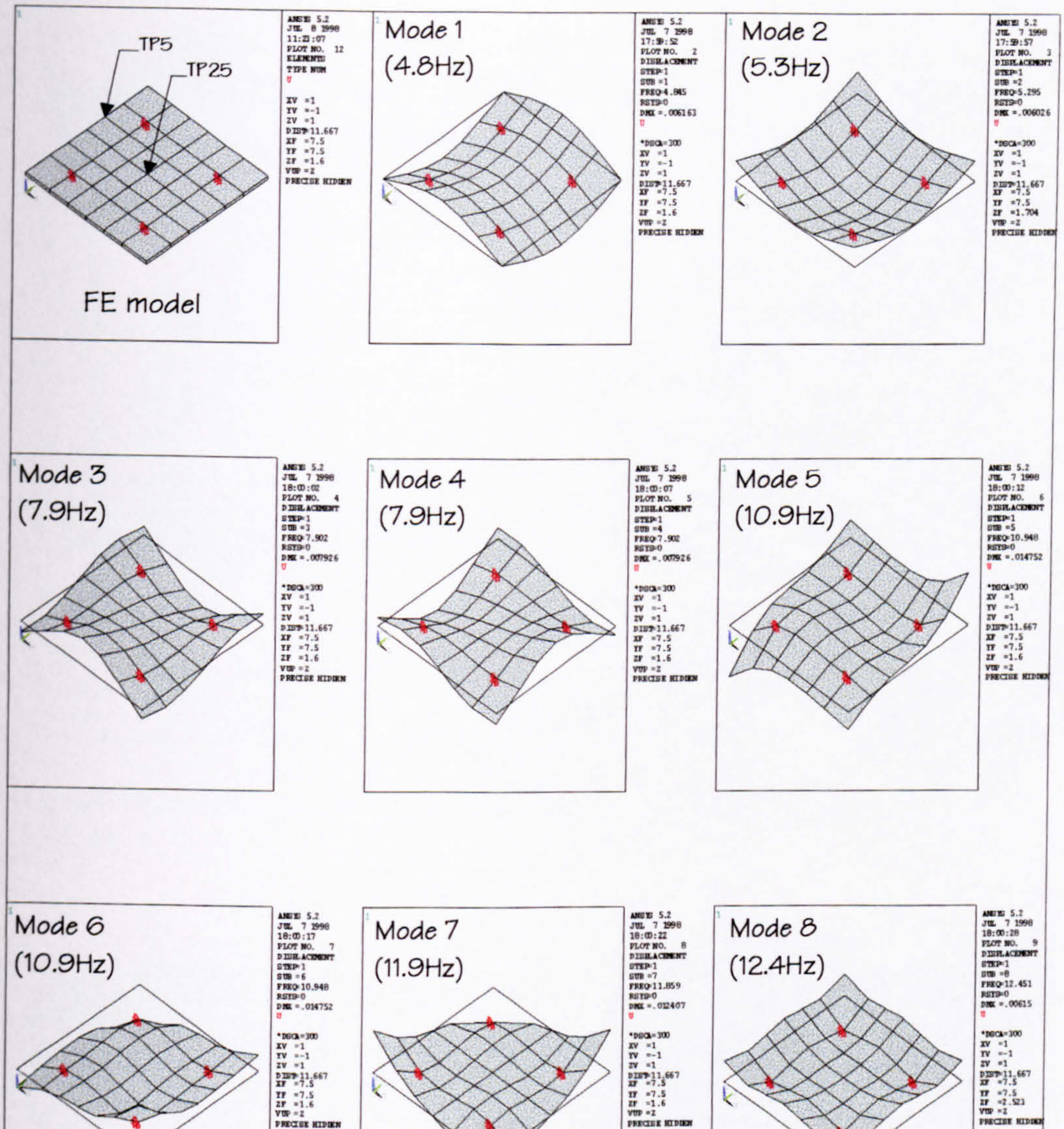

Figure 5.43: Structure B - Analytically calculated natural frequencies and mode shapes using the pre-test analysis FE model.

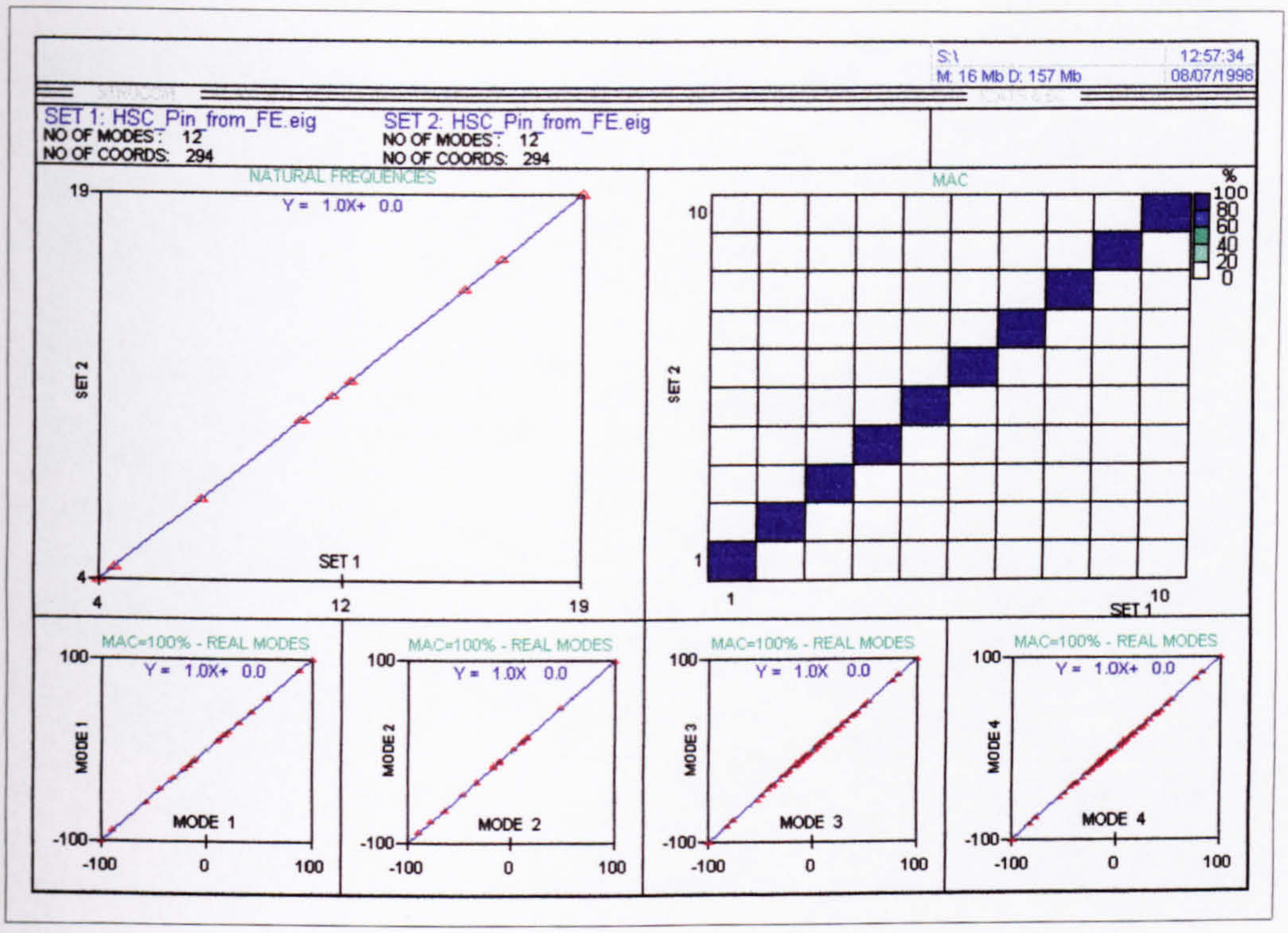

Figure 5.44: Structure B - Satisfactory Auto-MAC calculations for the test grid selected.

Figure 5.45: Structure B (Uncracked) - Limited equipment, consisting of a dual-channel spectrum analyser and portable PC (for in-situ parameter estimation), used for field testing of this structure.

Figure 5.46: Structure B (Uncracked) - Hammer excitation and data acquisition.

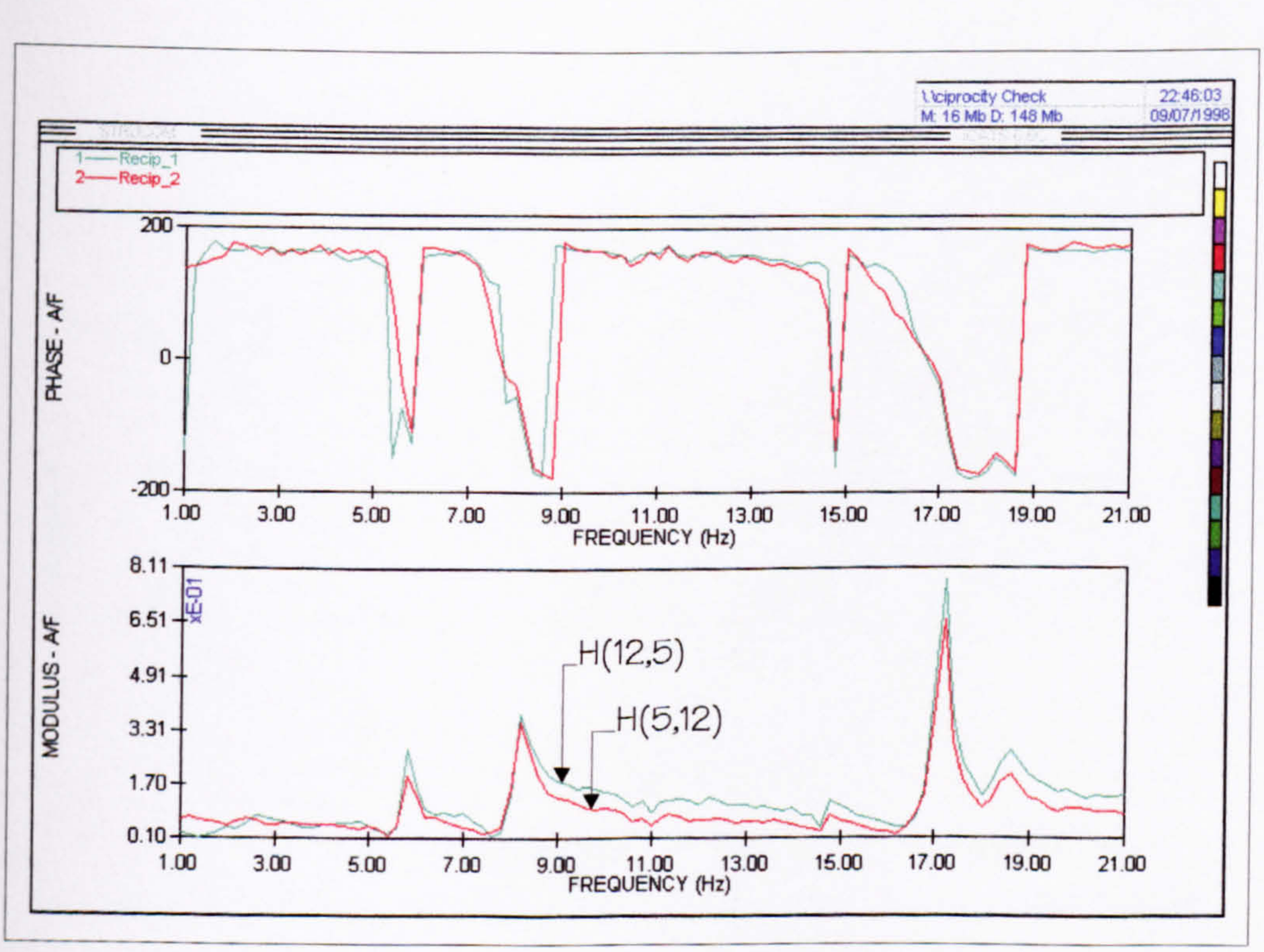

Figure 5.47: Structure B (Uncracked) - Reciprocity check (between TP5 and TP12).

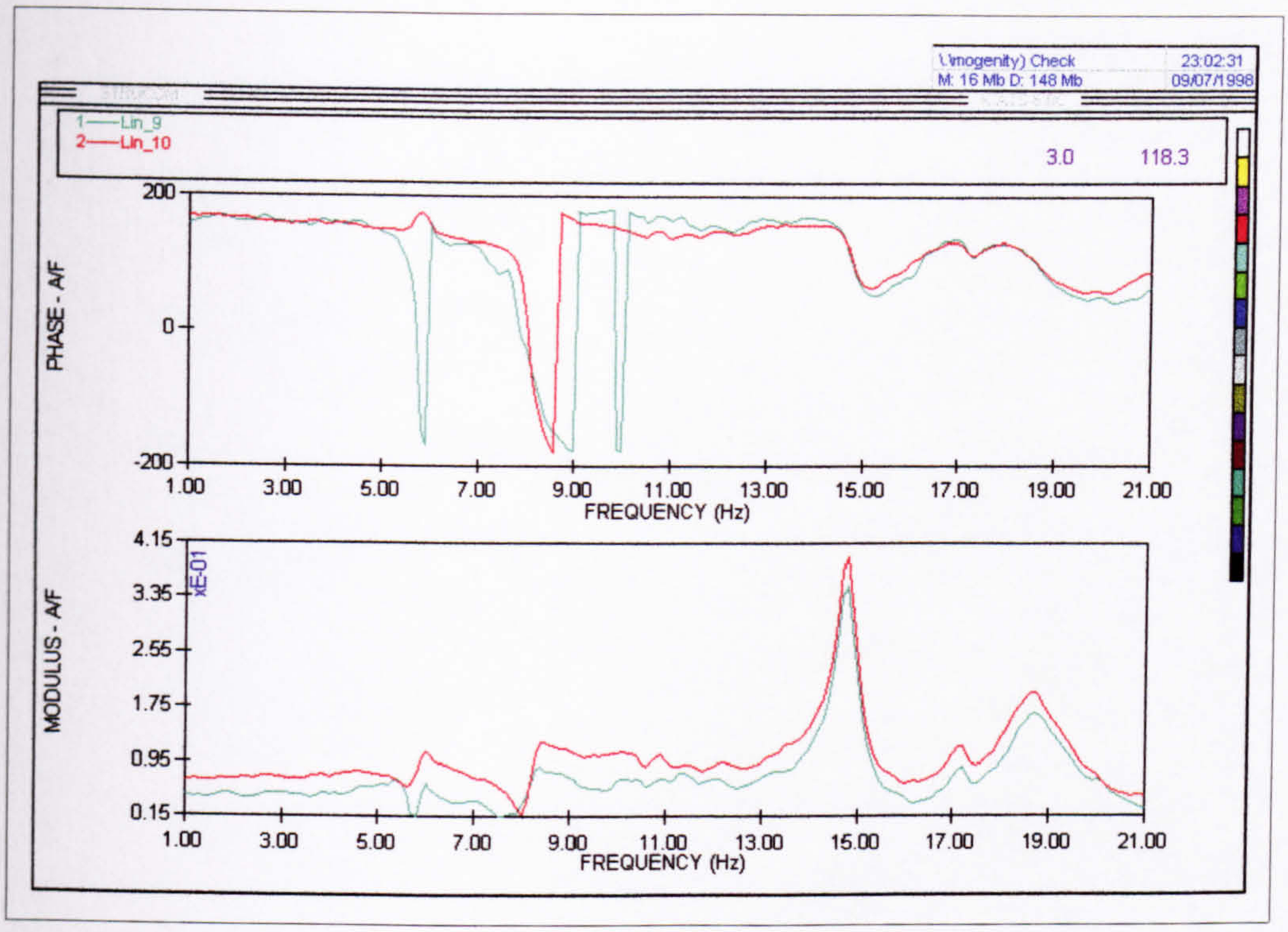

Figure 5.48: Structure B (Uncreacked) - Linearity (homogeneity) check of transfer mobility H(18,5) between TP5 and TP18.

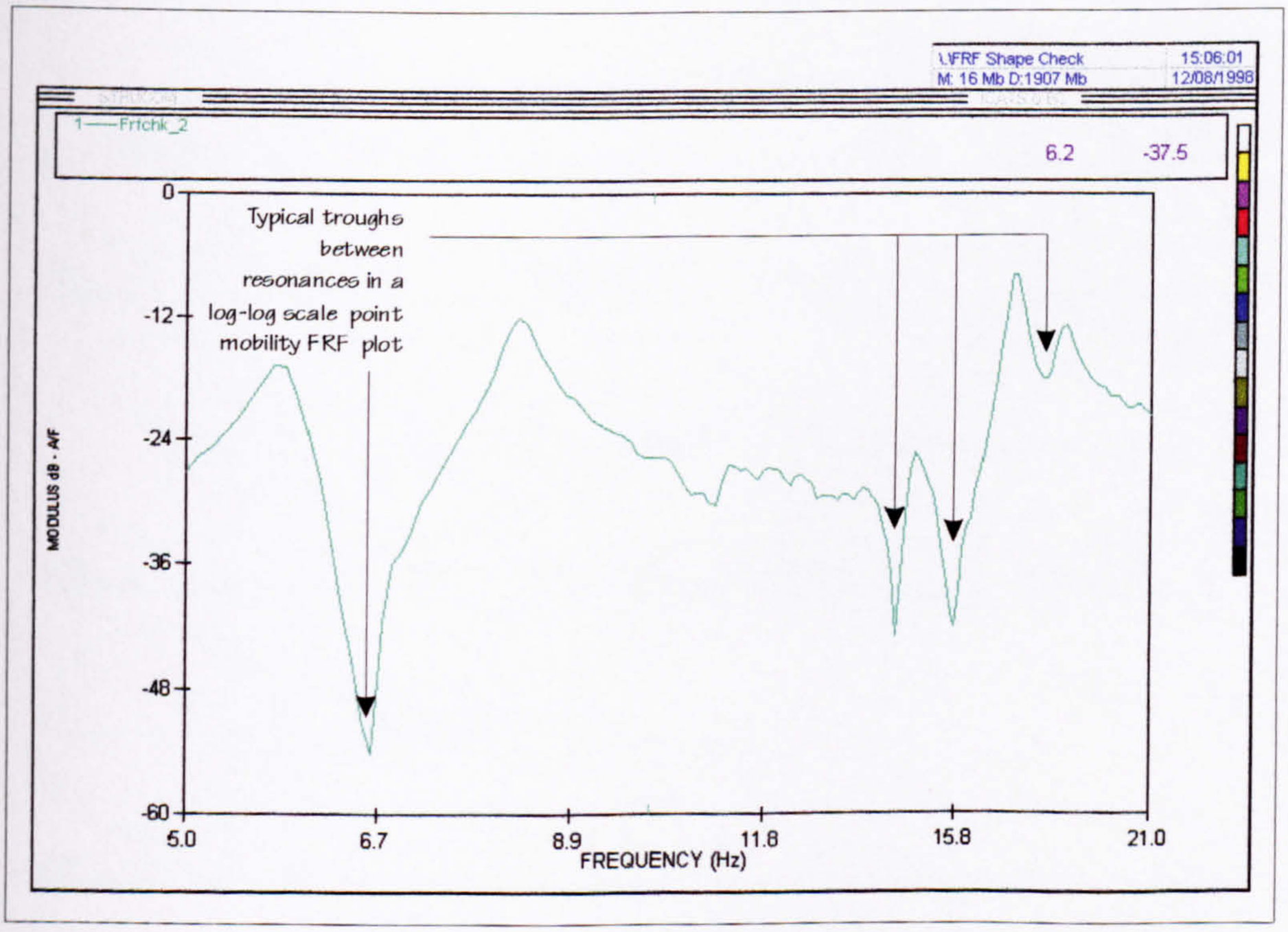

Figure 5.49: Structure B (Uncracked) - FRF shape check for point mobility H(12,12) at TP12.

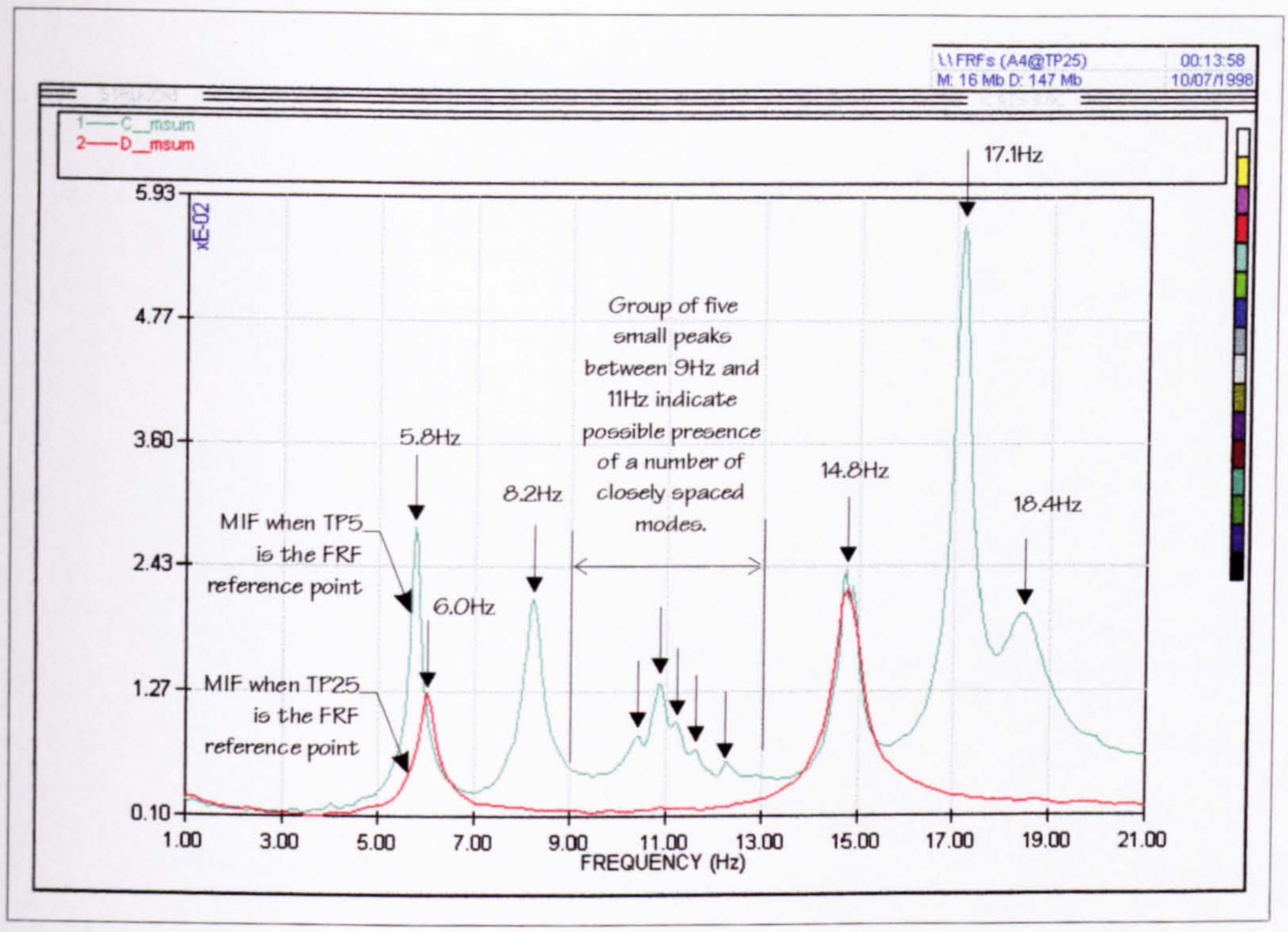

Figure 5.50: Structure B (Uncracked) - Calculation of Mode Indicator Functions (MIFs) based on the summation of FRF moduli for two sets of 49 FRFs corresponding to TP5 and TP25, respectively.

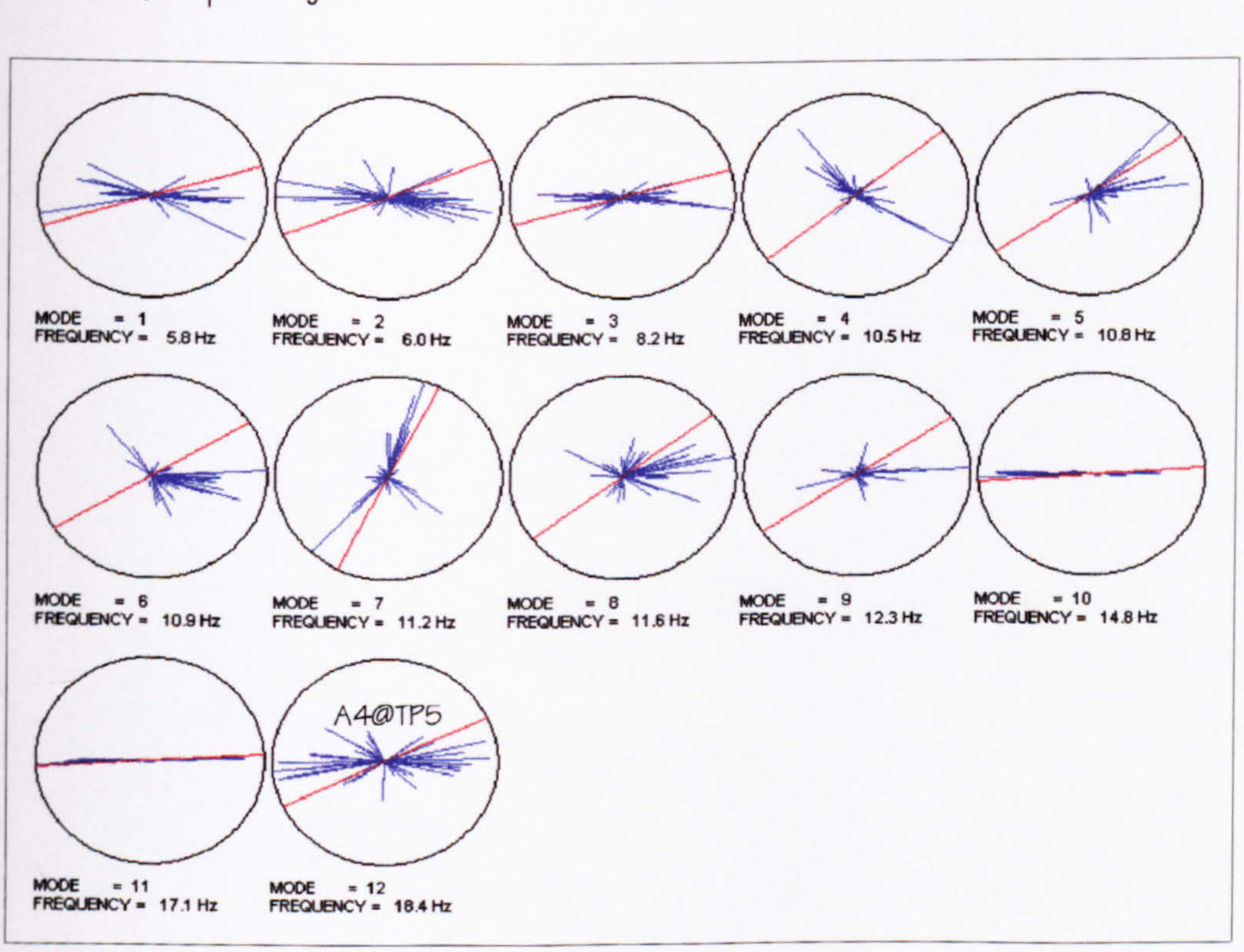

Figure 5.51: Structure B (Uncracked) - Complexity of the estimated modes of vibration.

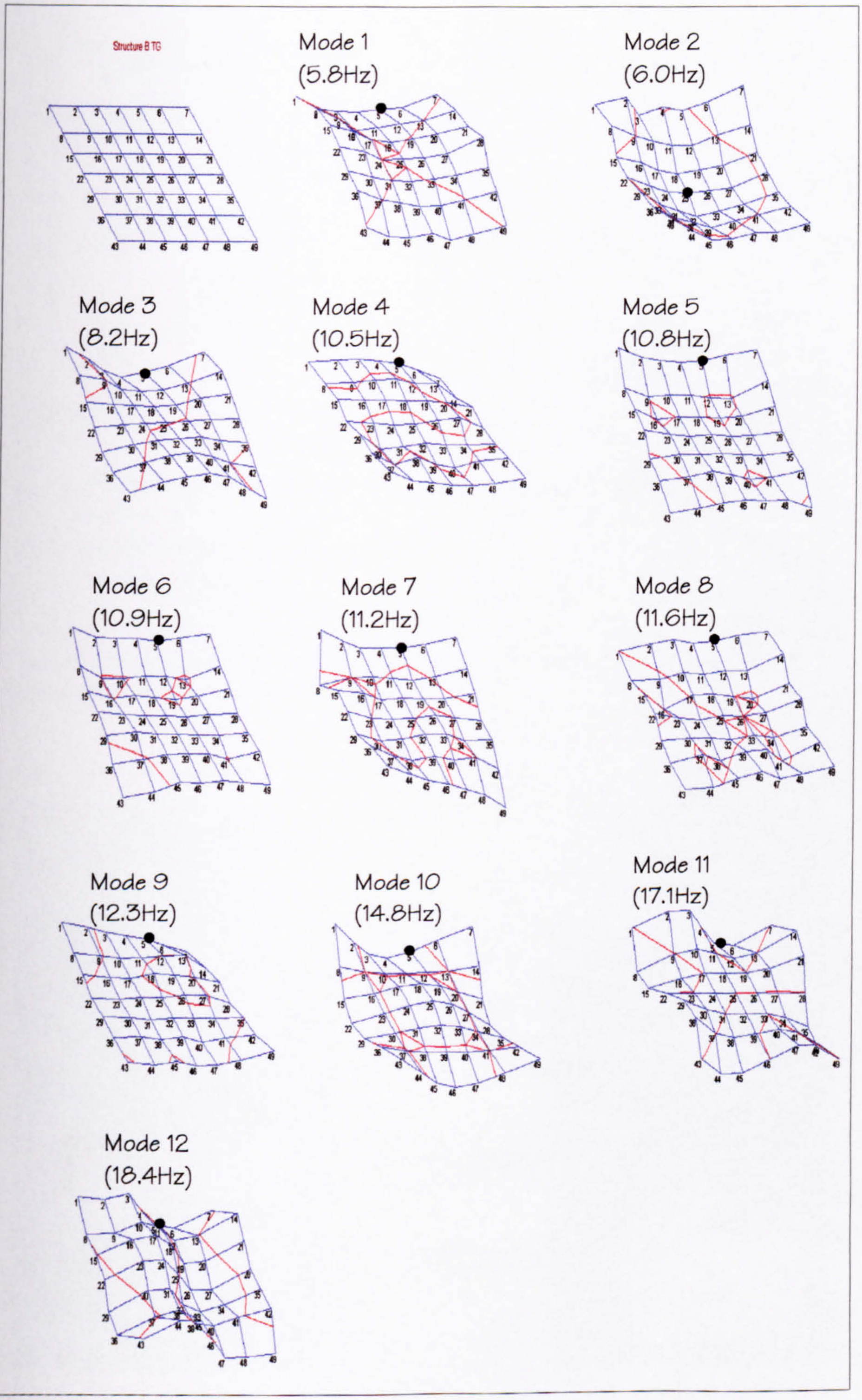

Figure 5.52: Structure B (Uncracked) - Experimentally measured modes of vibration.

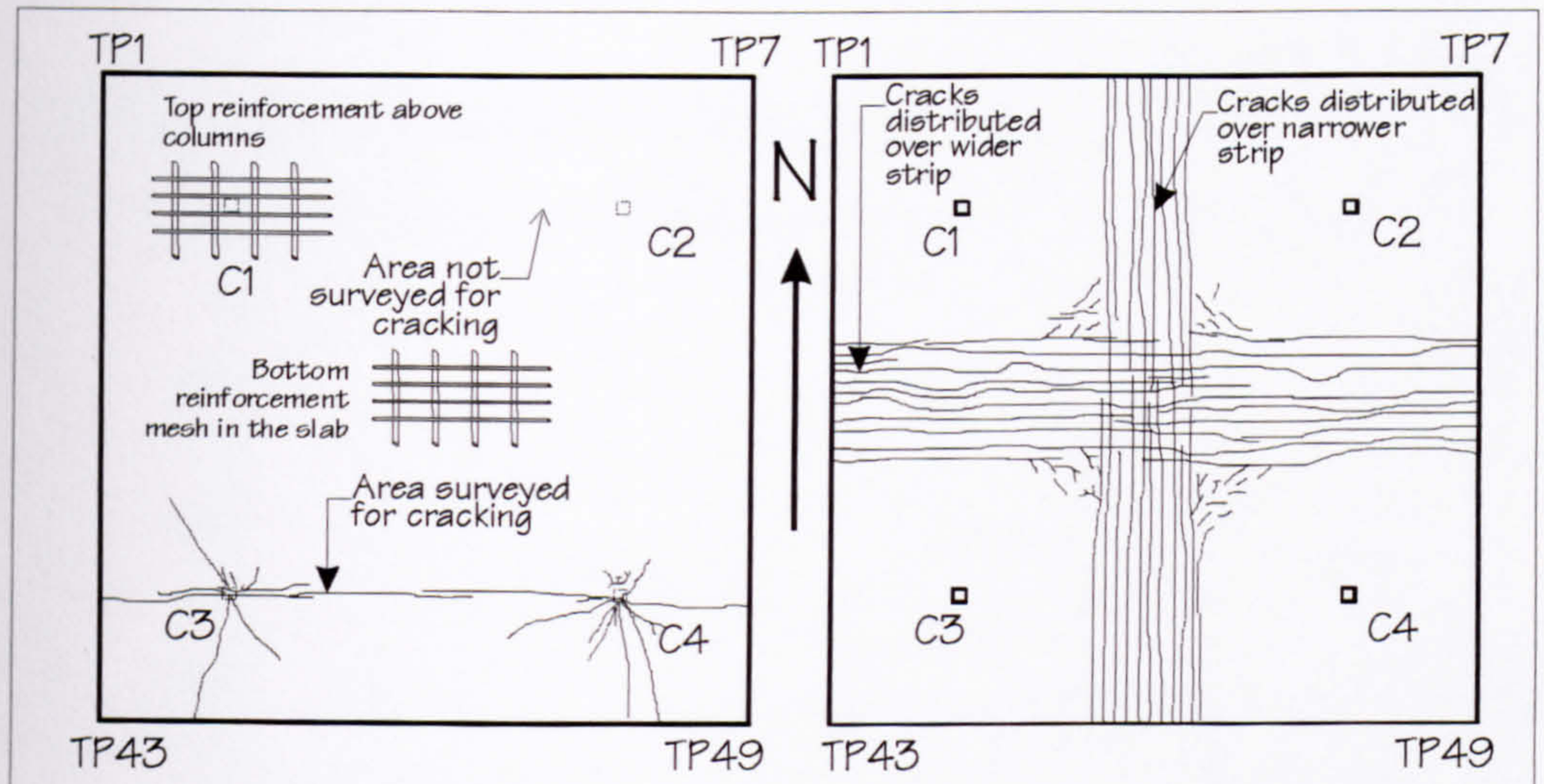

a) Cracking pattern at the top surface of the slab (only partial information available at the time of testing)

b) Cracking pattern at the bottom surface of the slab

Figure 5.53: Structure B (Cracked) - Visible cracking pattern on the top (left) and bottom (right) surface of the HSC floor.

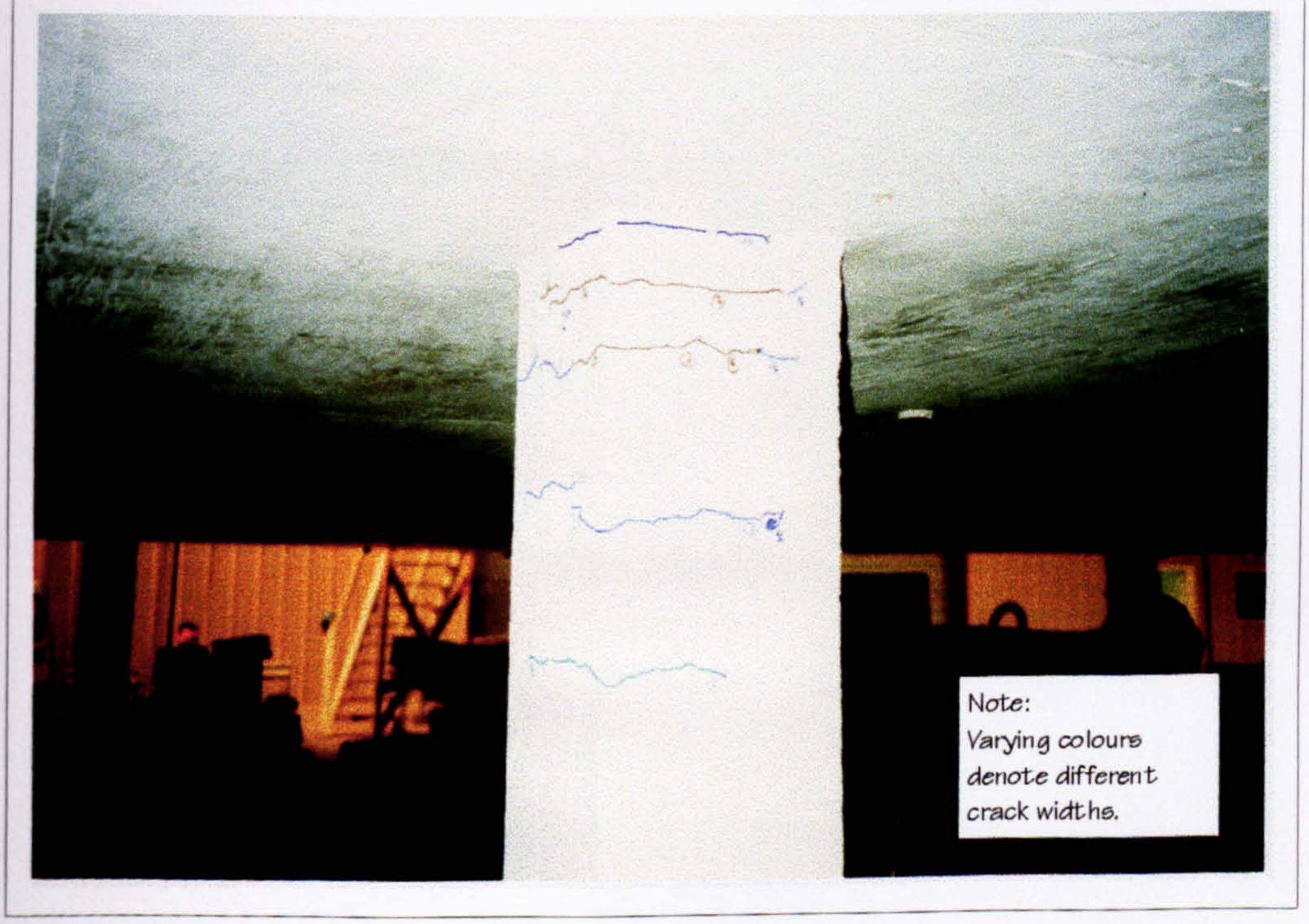

Figure 5.54: Structure B (Cracked) - Cracking in column C2 looking from the North.

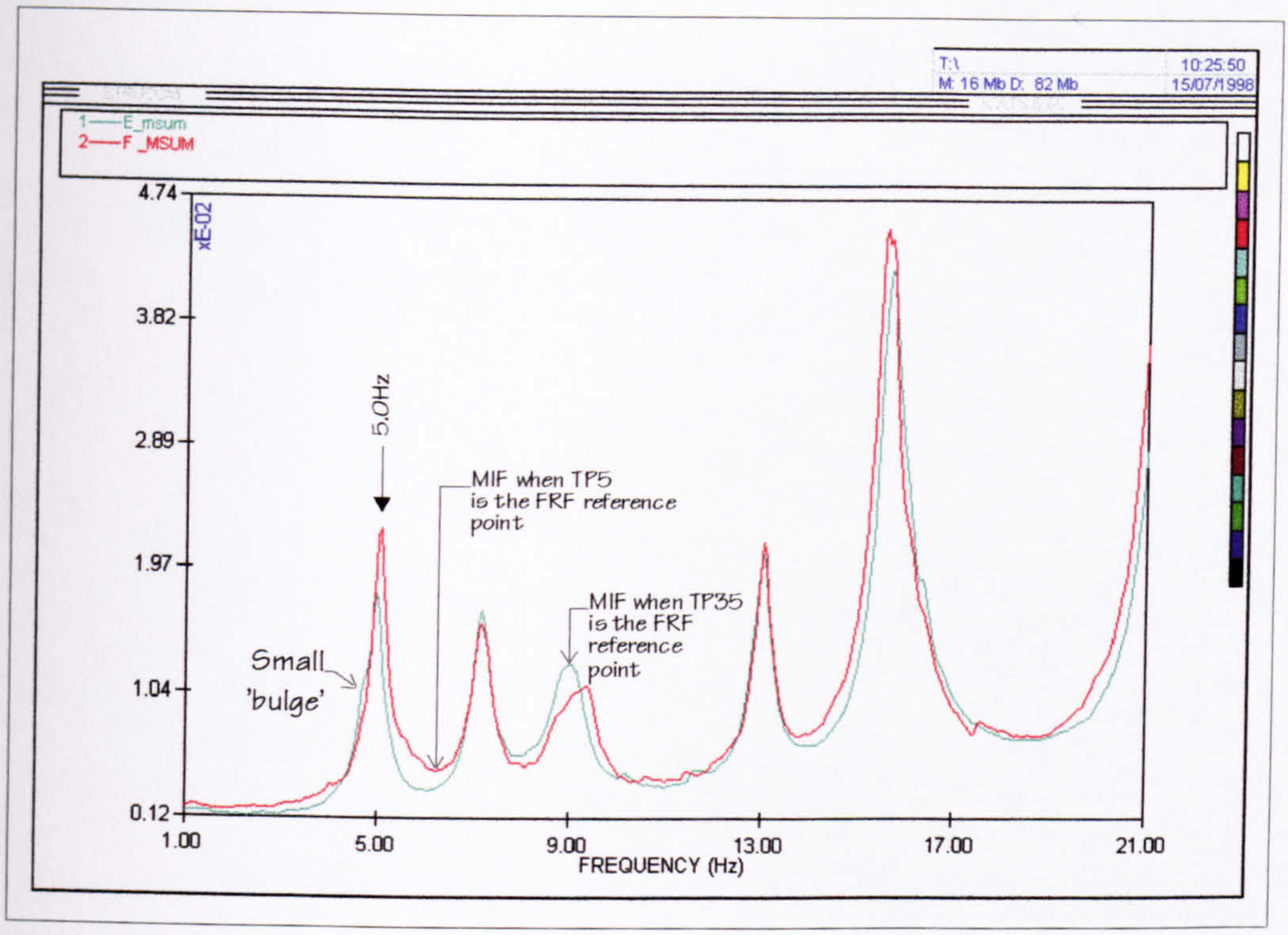

Figure 5.55: Structure B (Cracked) - Two MIFs, being the summation of all measured FRF moduli in one row of FRF matrix, calculated for TP35 and TP5 as the FRF reference

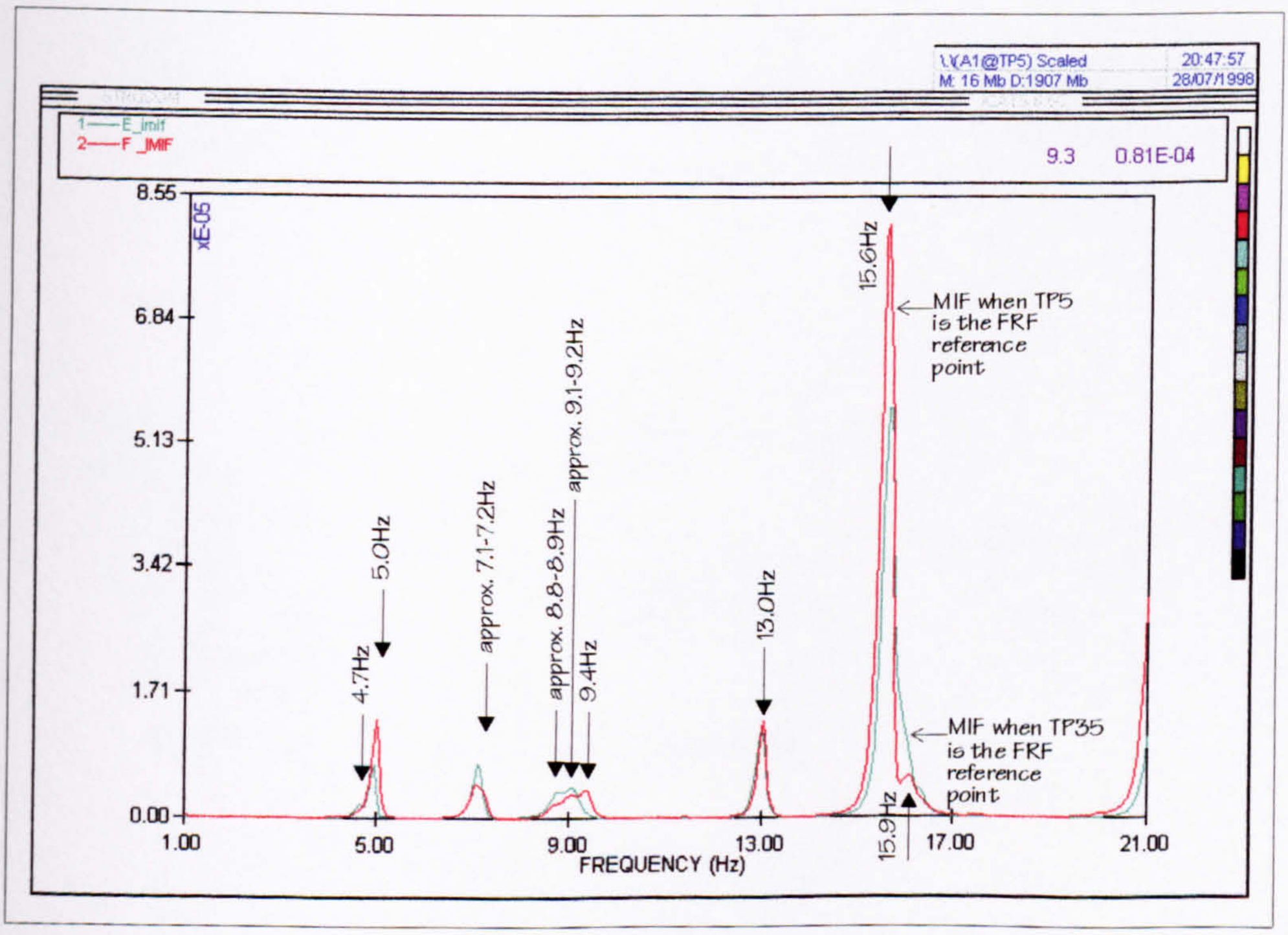

Figure 5.56: Structure B (Cracked) - Two MIFs, being the summation of squared imaginary parts of all FRFs in one row of FRF matrix, calculated for TP35 and TP5 as the FRF reference points.

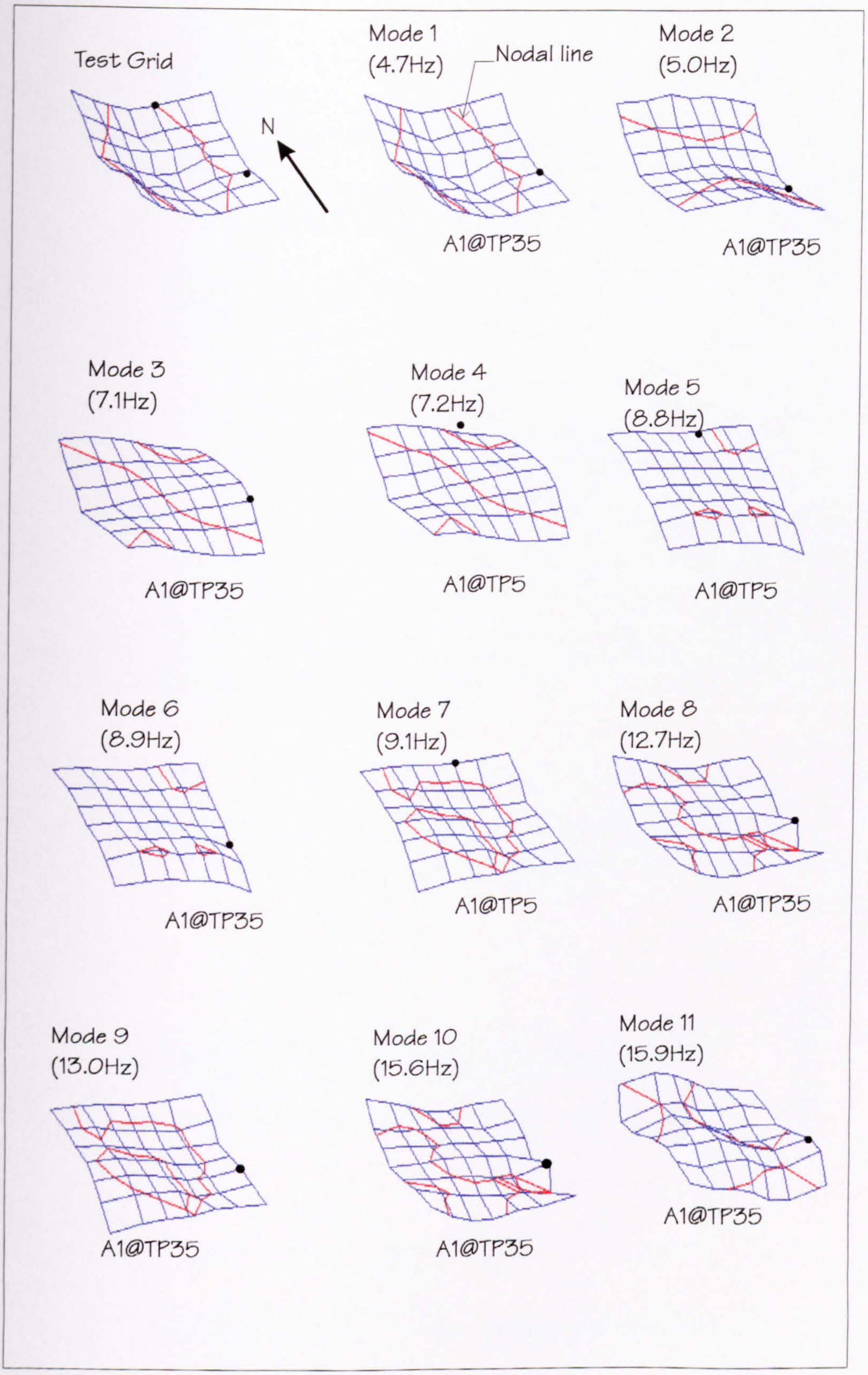

Figure 5.57: Structure B (Cracked) - The experimentally estimated mode shapes and natural frequencies. Black dots show which FRF reference point was used to identify the particular mode of vibration.

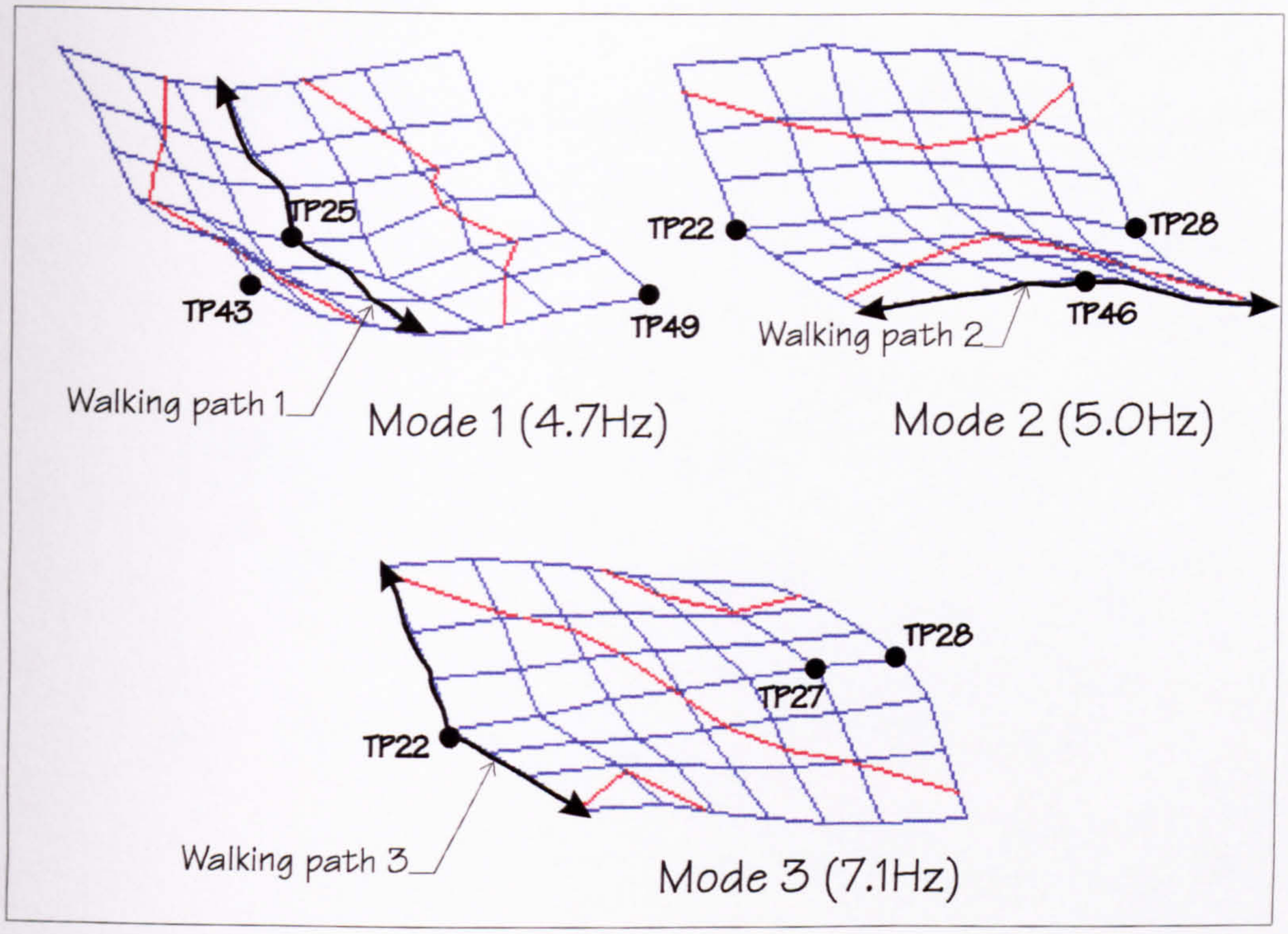

Figure 5.58: Structure B (Cracked) - Walking paths and the location of the response measurement accelerometers.

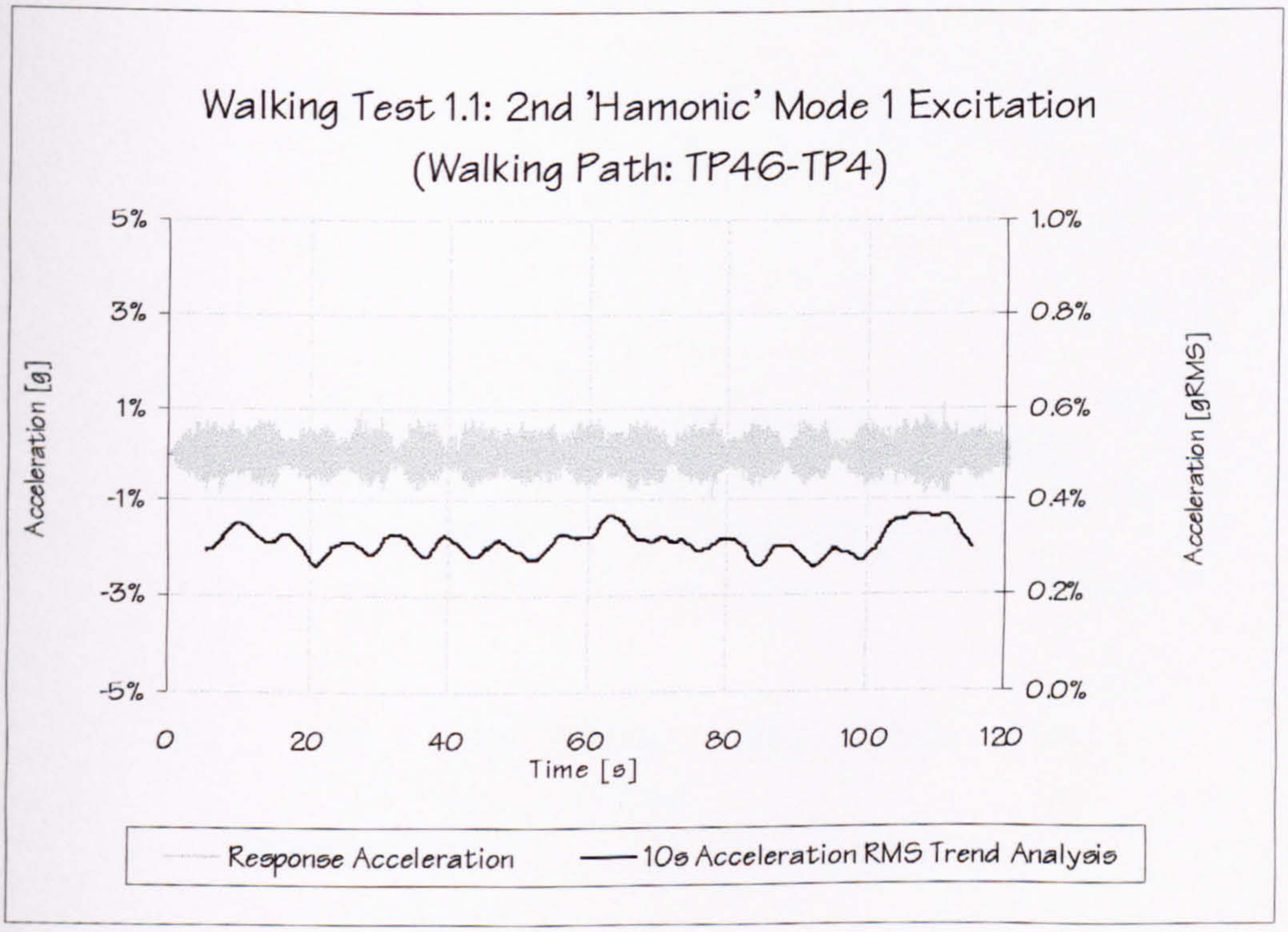

Figure 5.59: Structure B - The first 120s block of acceleration time history due to walking in Test 1.1 (registered at TP43).

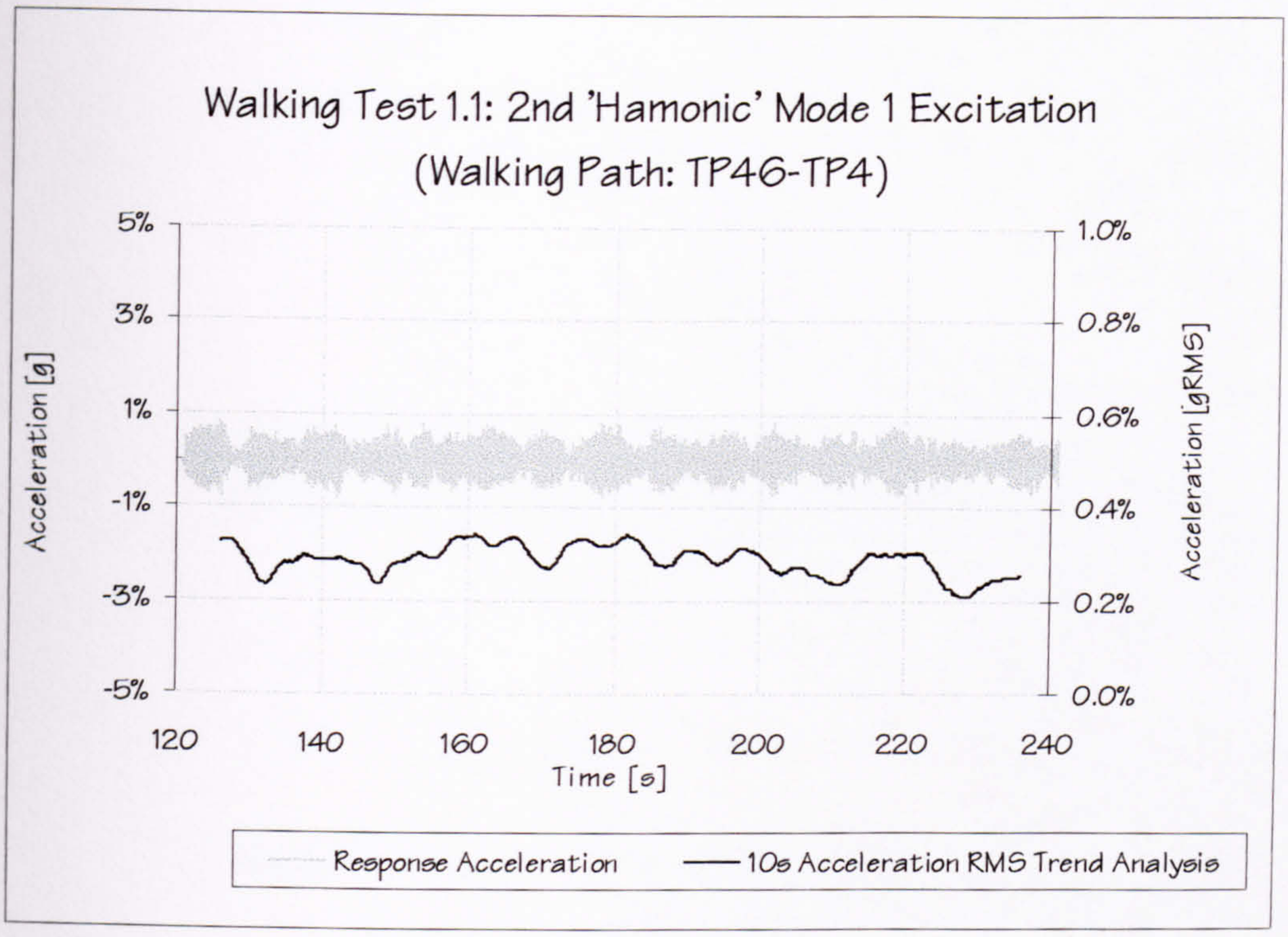

Figure 5.60: Structure B - The second 120s block of acceleration time history due to walking in Test 1.1 (registered at TP43).

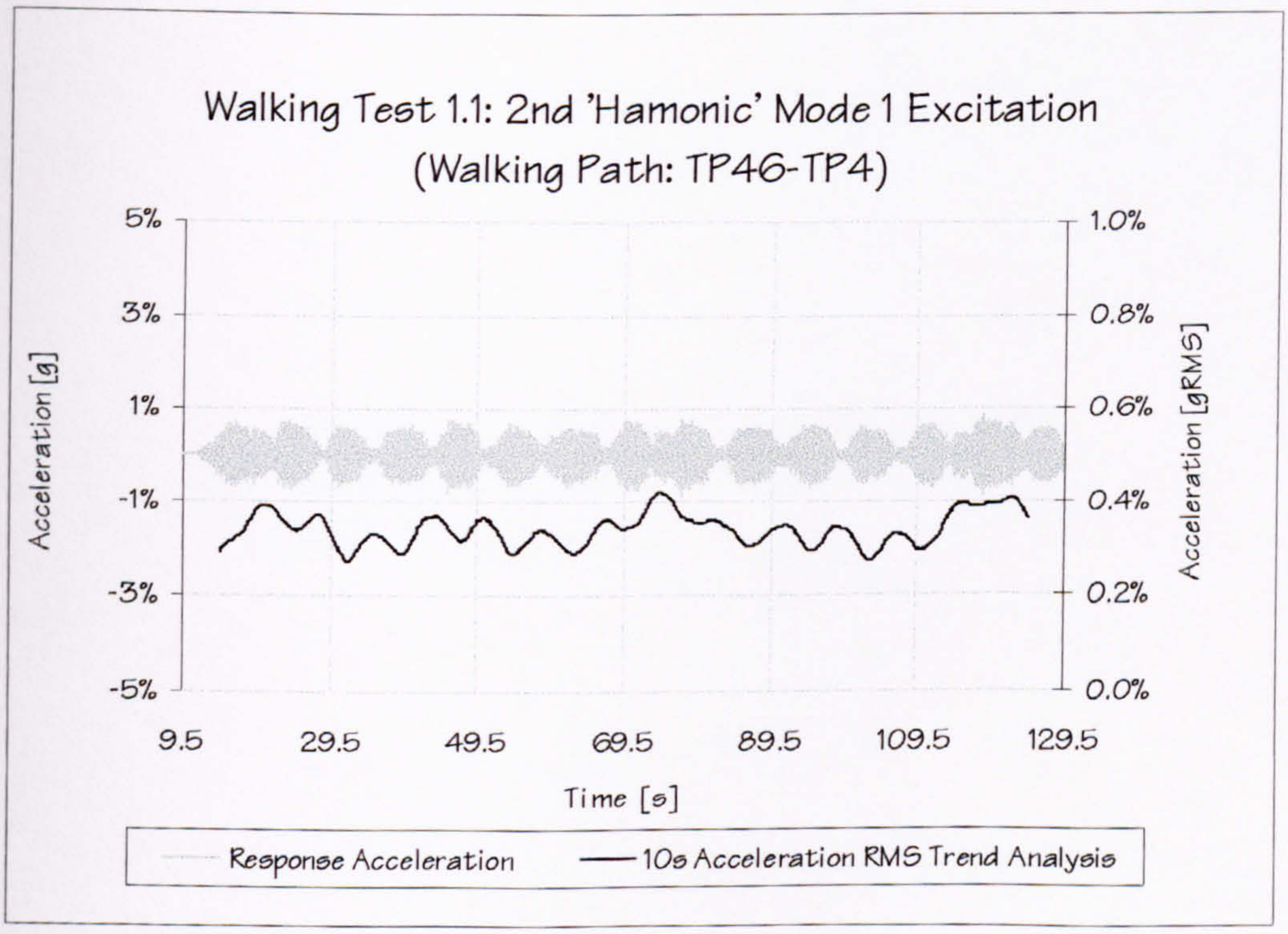

Figure 5.61: Structure B - Maximum acceleration response obtained in Test 1.1 (registered at TP25).

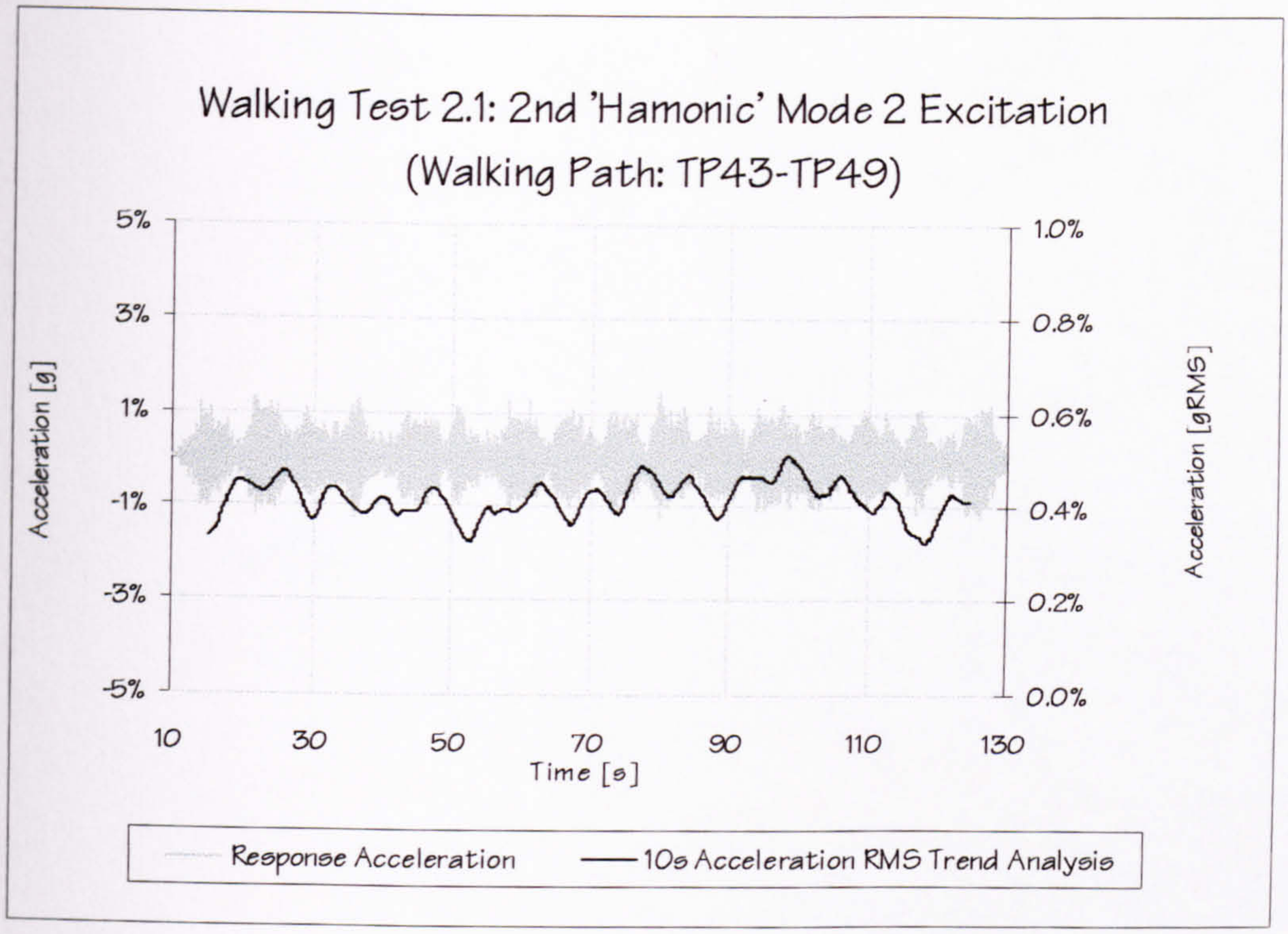

Figure 5.62: Structure B - Maximum acceleration response obtained in Test 2.1 (registered at TP46).

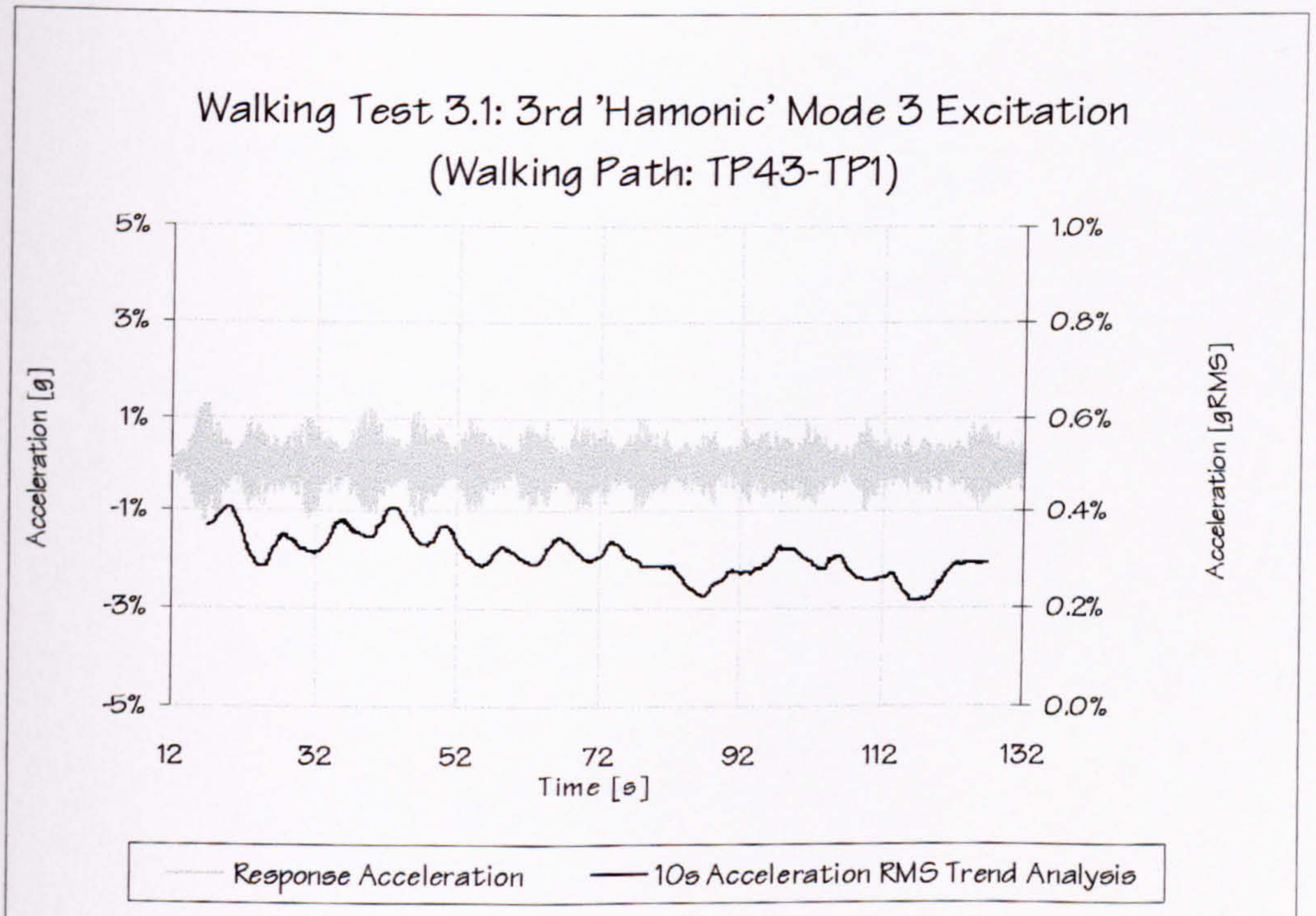

Figure 5.63: Structure B - Maximum acceleration response obtained in Test 3.1 (registered at TP22).

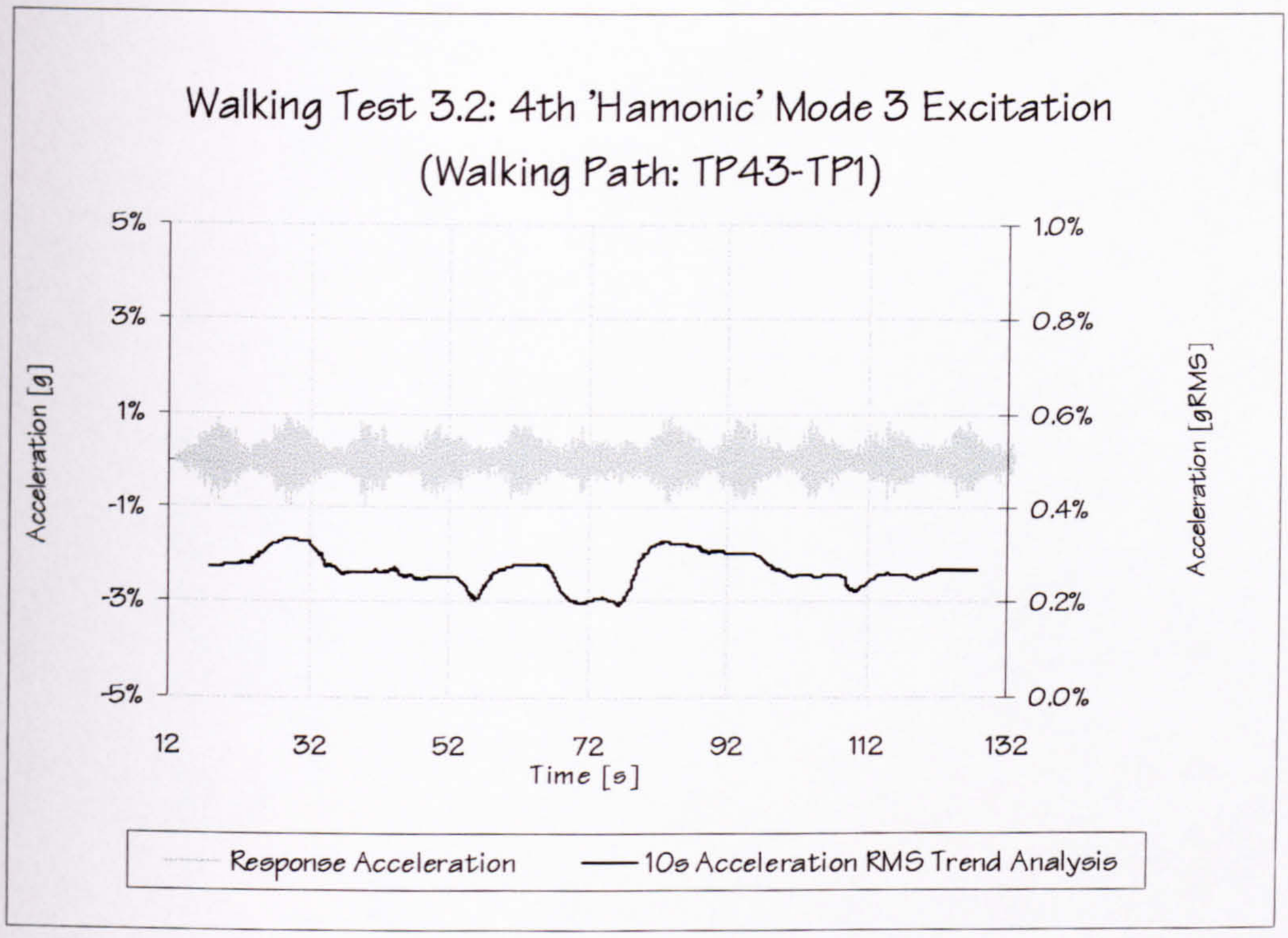

Figure 5.64: Structure B - Maximum acceleration response obtained in Test 3.2 (registered at TP22).

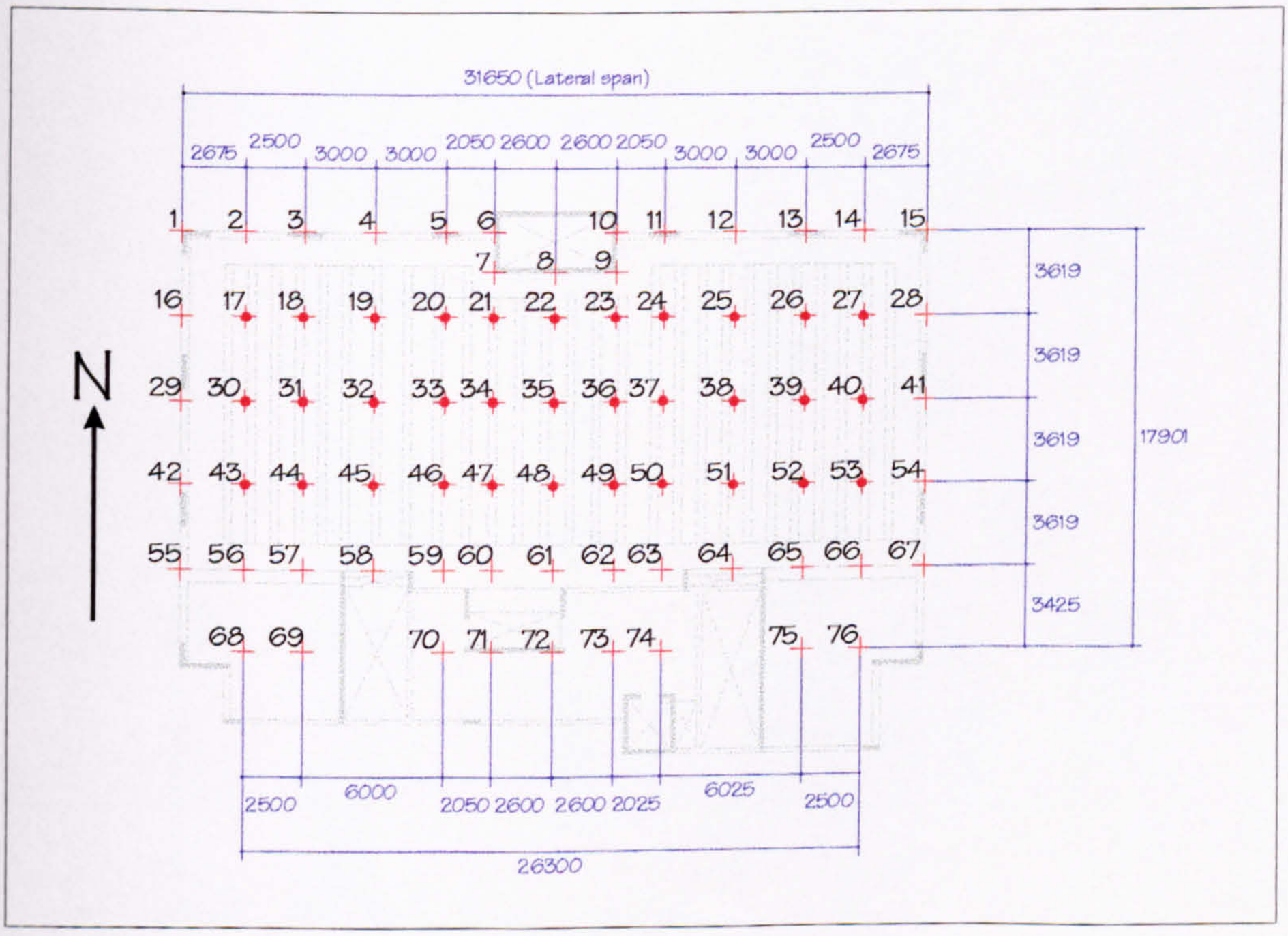

Figure 5.65: Structure C - Test grid.

Section A-A

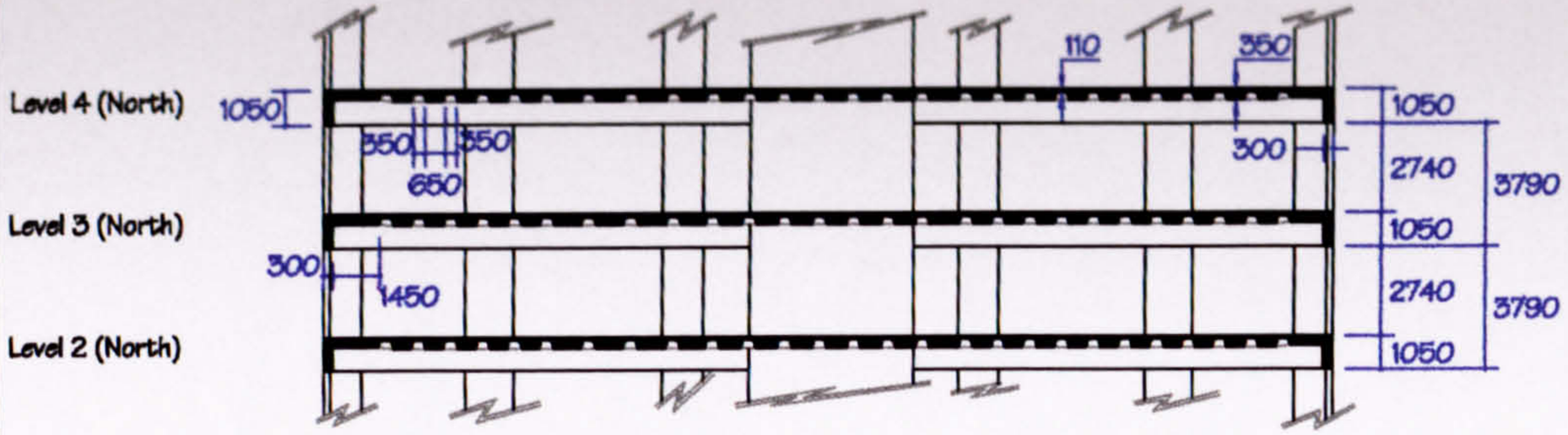

Section B-B

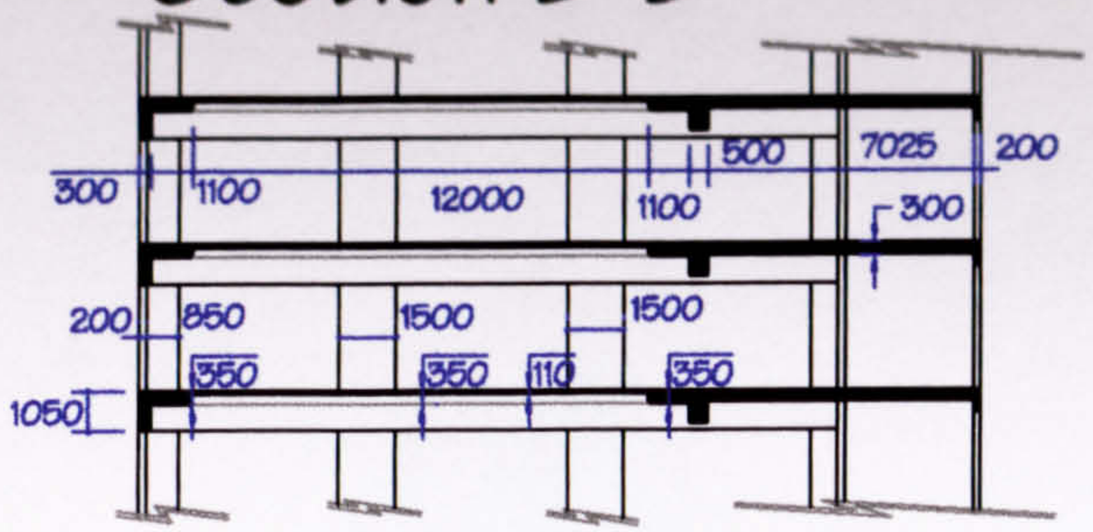

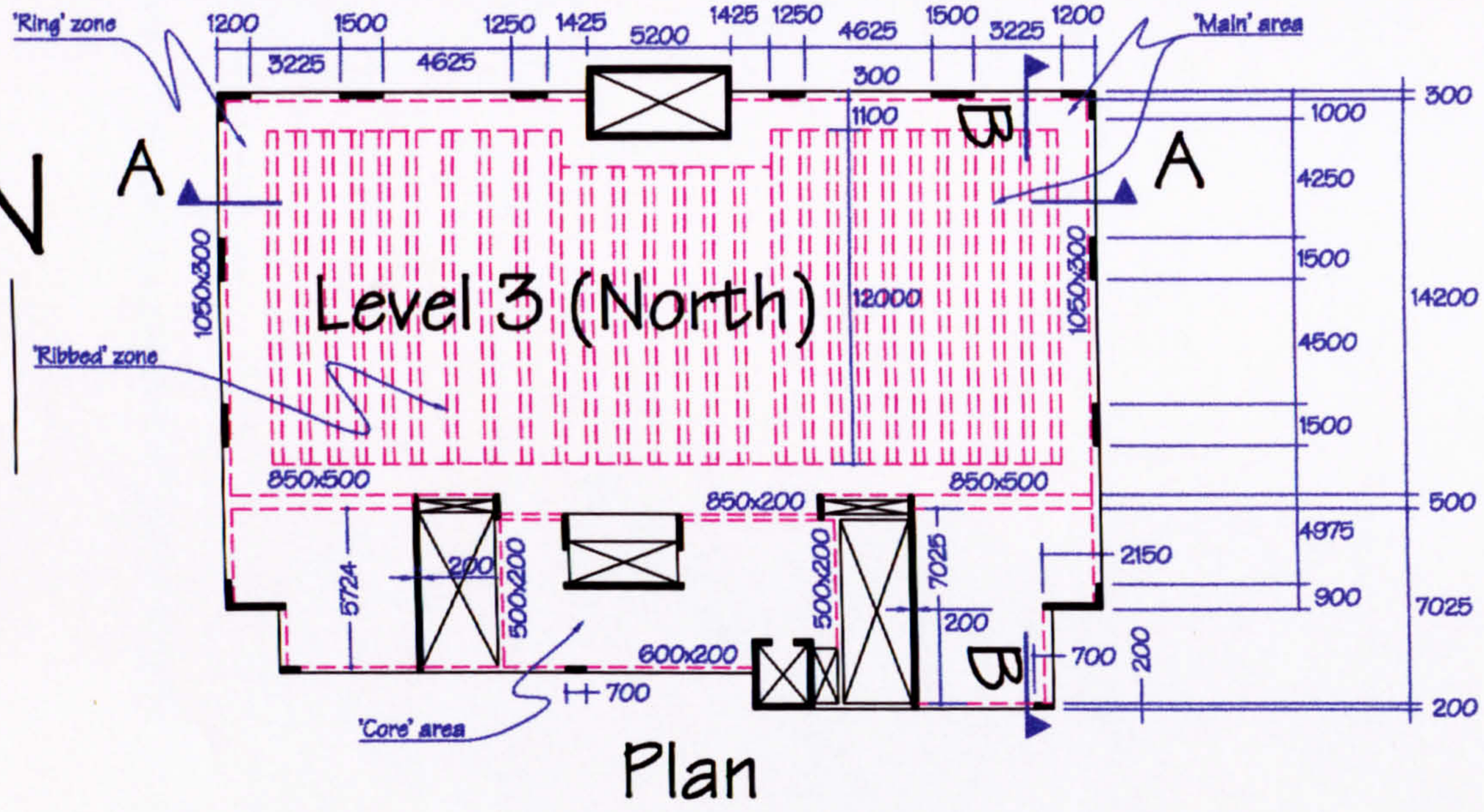

Plan

Note:
Ribs are not of equal width. The width is mainly 650mm, but varies between 650mm and 1200mm

Concrete grade: C50

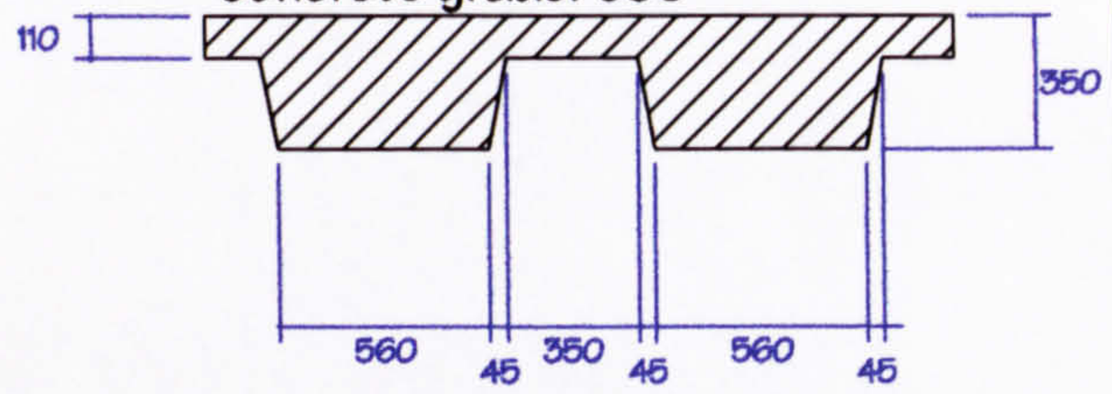

Typical Rib Detail
(Scale 1:33)

Drawing No.	Filename	Drawn by	Date	Scale
4	Parnell GA Drawing.dwg	A. Pavic	10 Oct 1995	1:333

Title
STRUCTURE C GENERAL ARRANGEMENT DRAWING: SIMPLIFIED FOR FINITE ELEMENT MODELLING

Figure 5.66: Structure C - Layout of in-situ cast post-tensioned concrete floor.

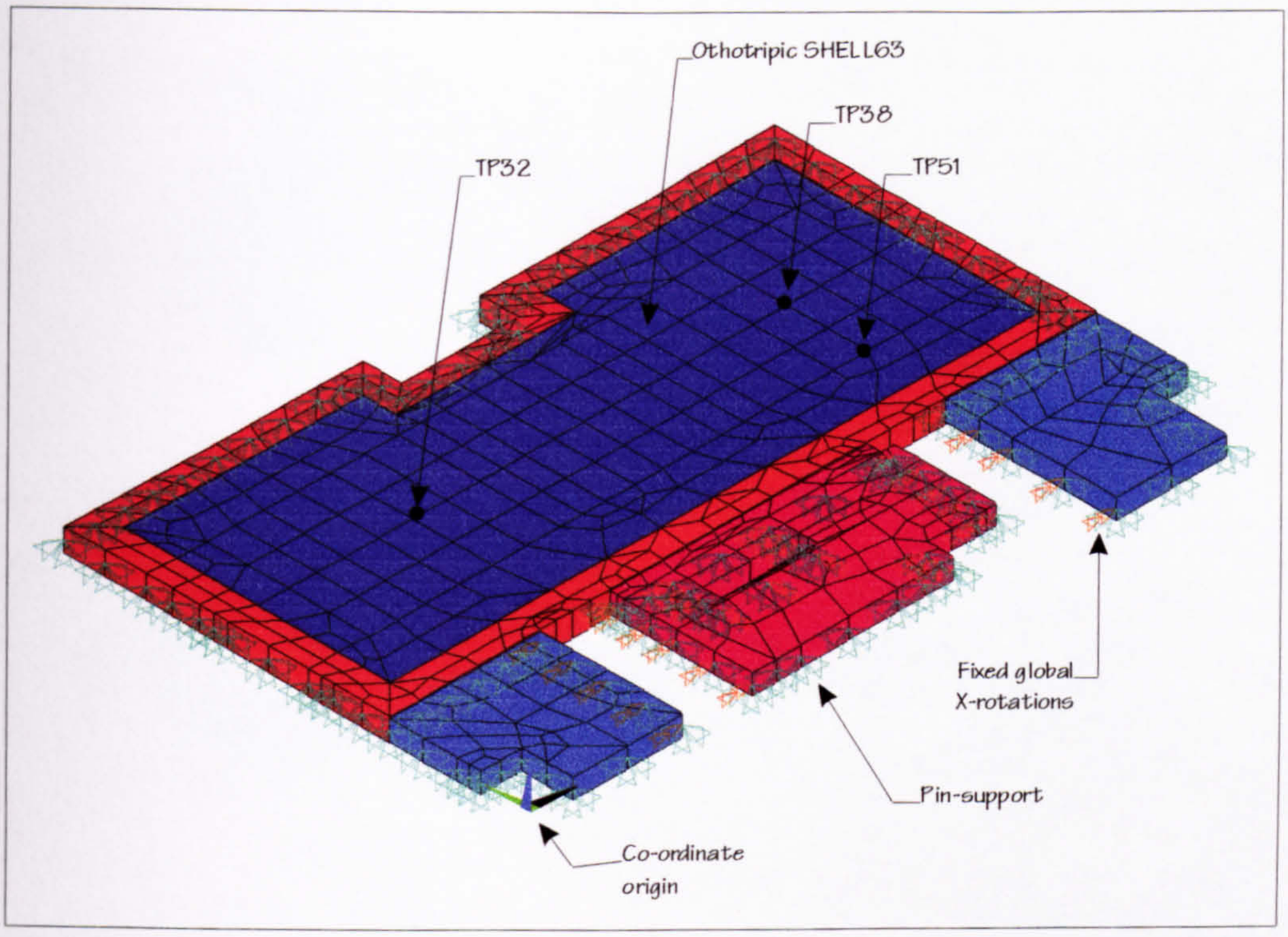

Figure 5.67: Structure C - FE model developed for the pre-test analysis using SHELL63 elements only.

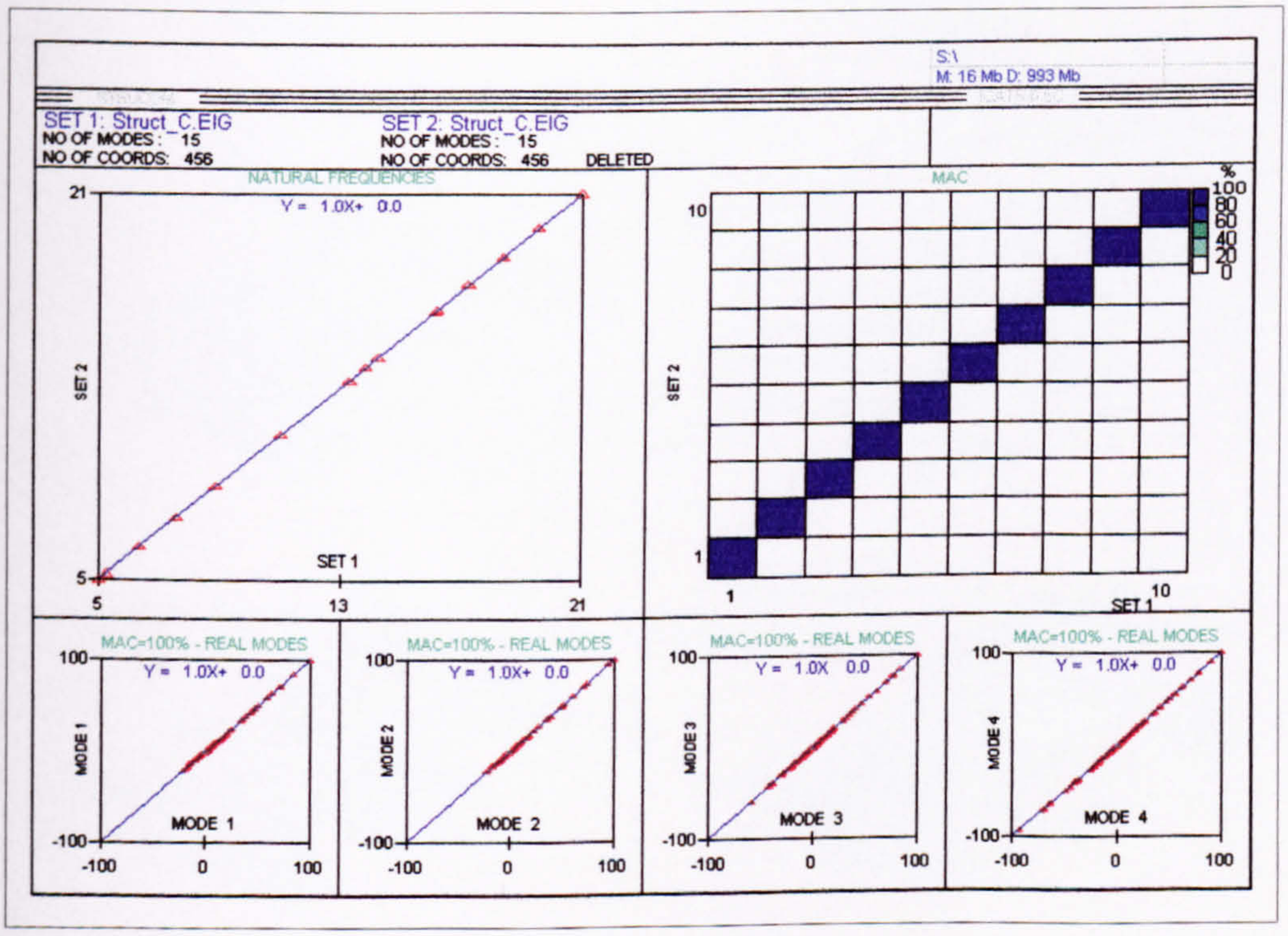

Figure 5.68: Structure C- Satisfactory Auto-MAC calculations for the test grid selected.

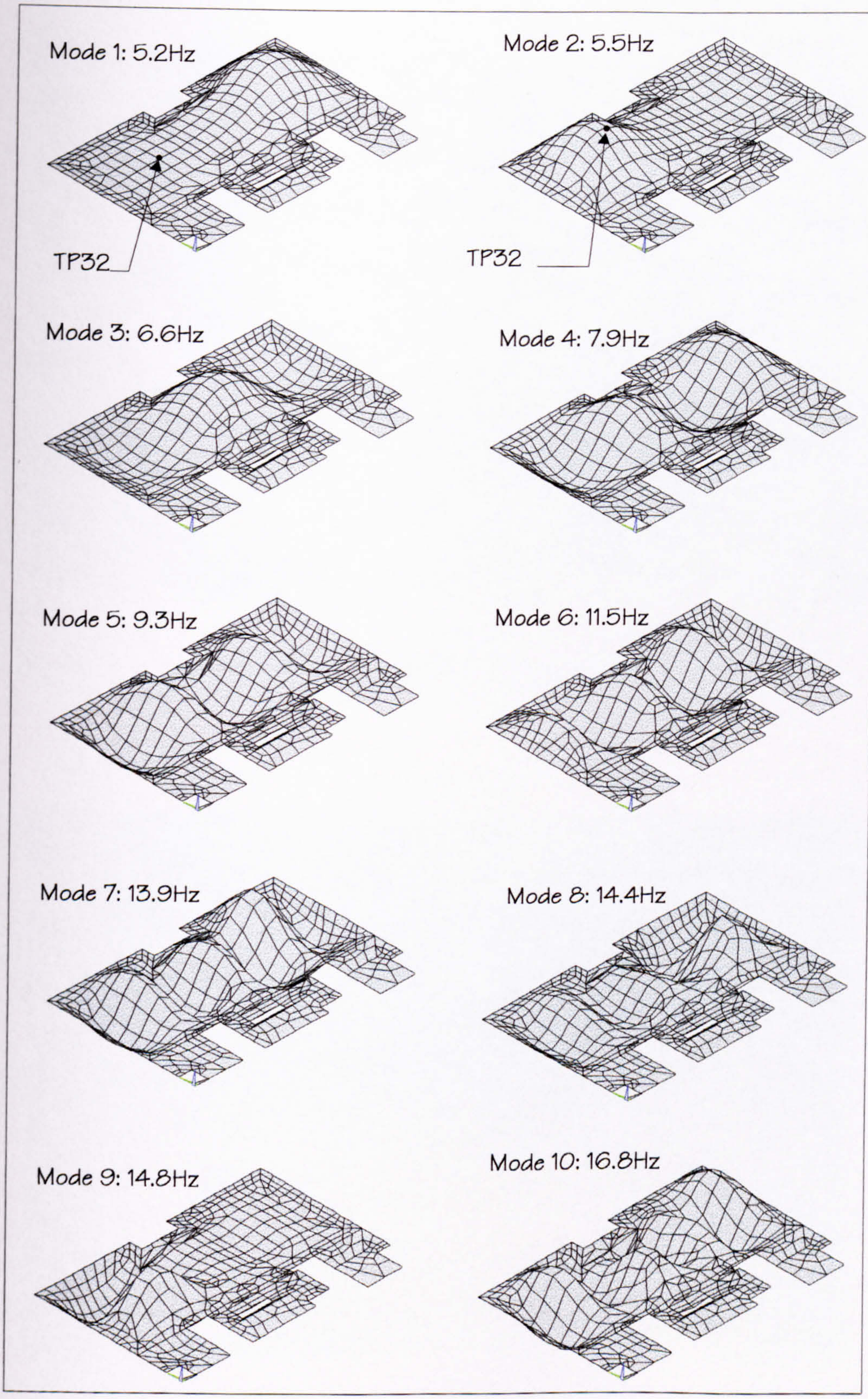

Figure 5.69: Structure C - Analytically calculated natural frequencies and mode shapes using the pre-test analysis FE model.

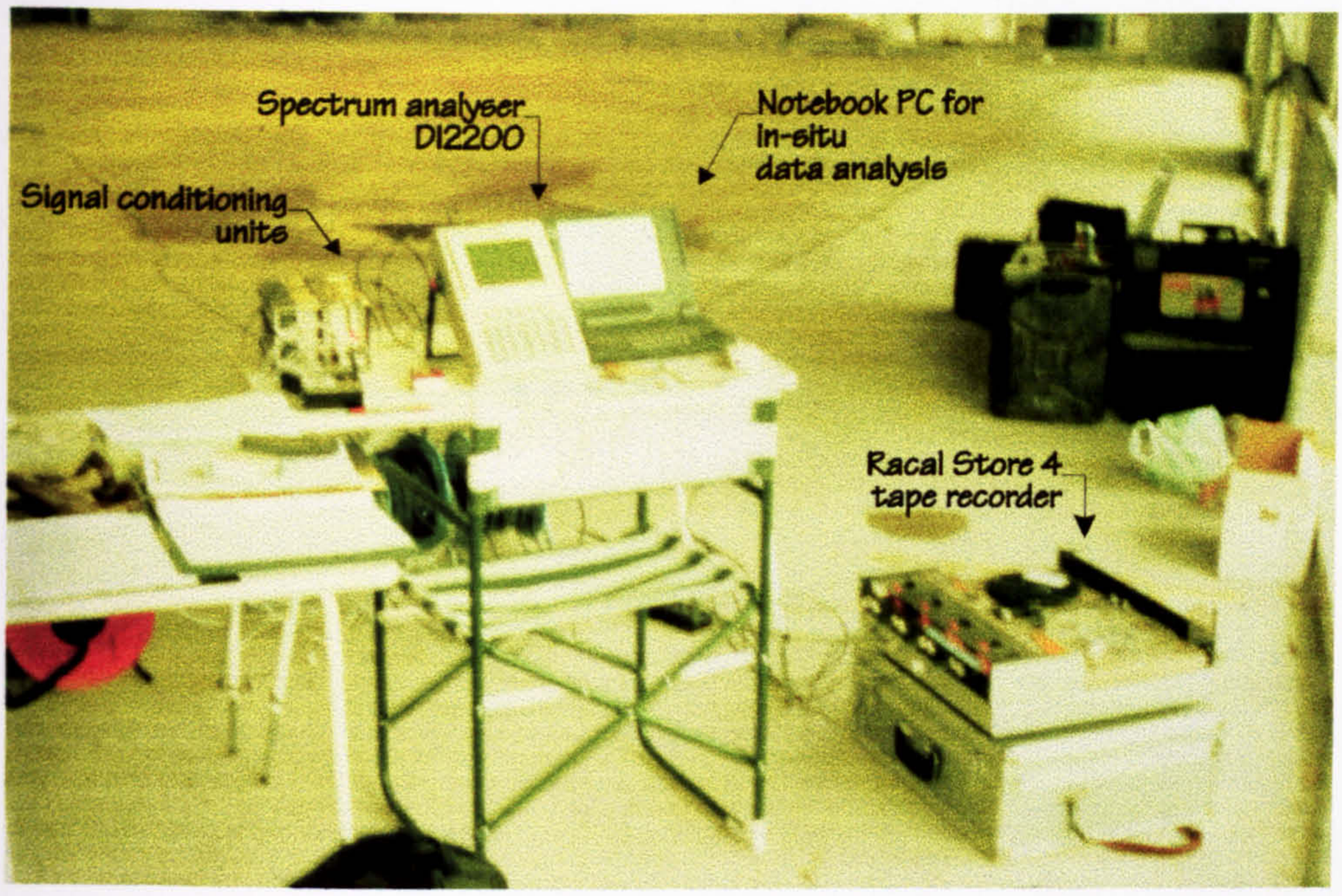

Figure 5.70: Structure C (Unclad) - Hardware for data acquisition setup.

Figure 5.71: Structure C (Unclad) - Hammer excitation at TP35.

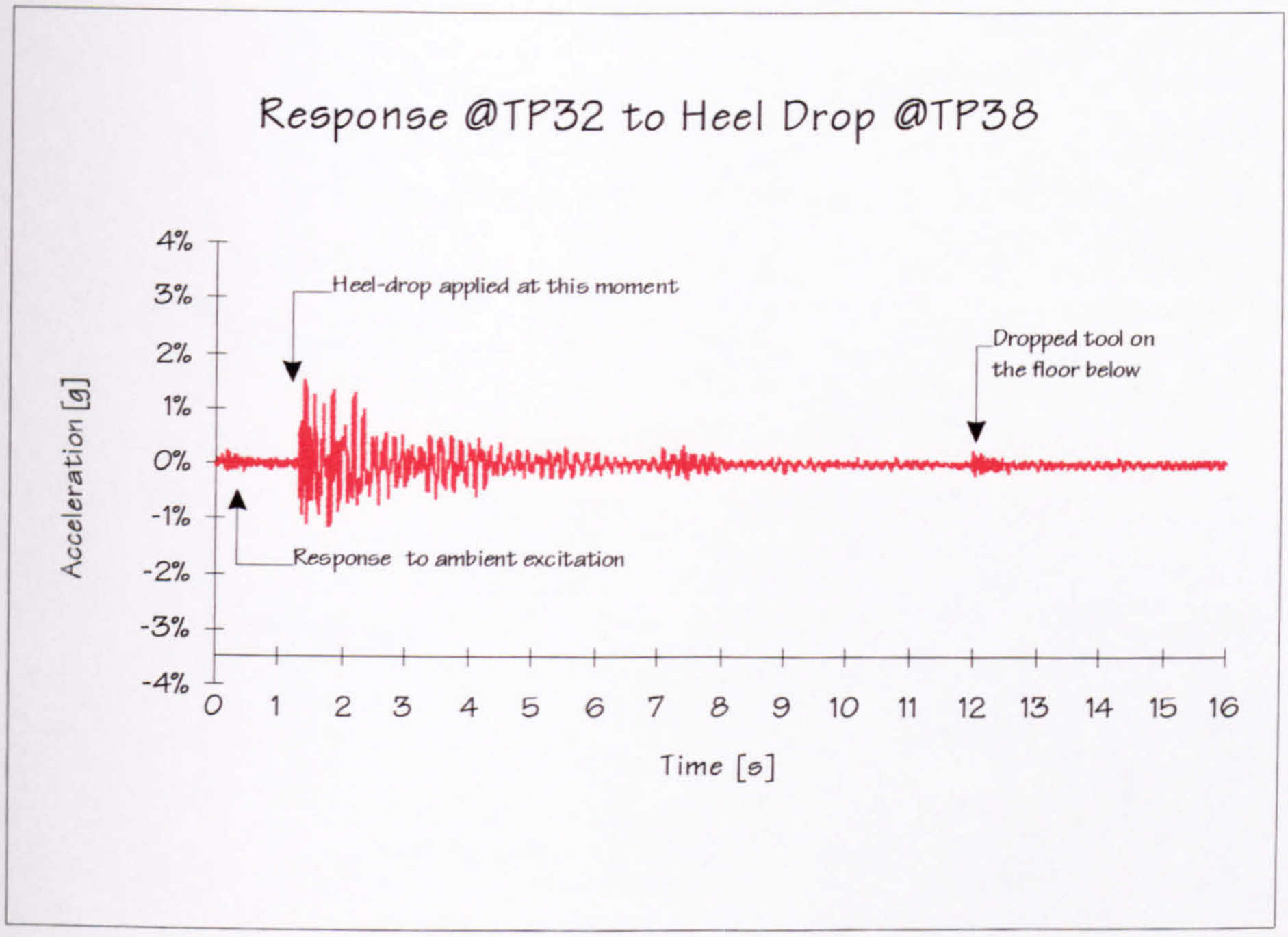

Figure 5.72: Structure C (Unclad) - Acceleration response at TP32 due to heel drop at TP32 and other ambient excitation.

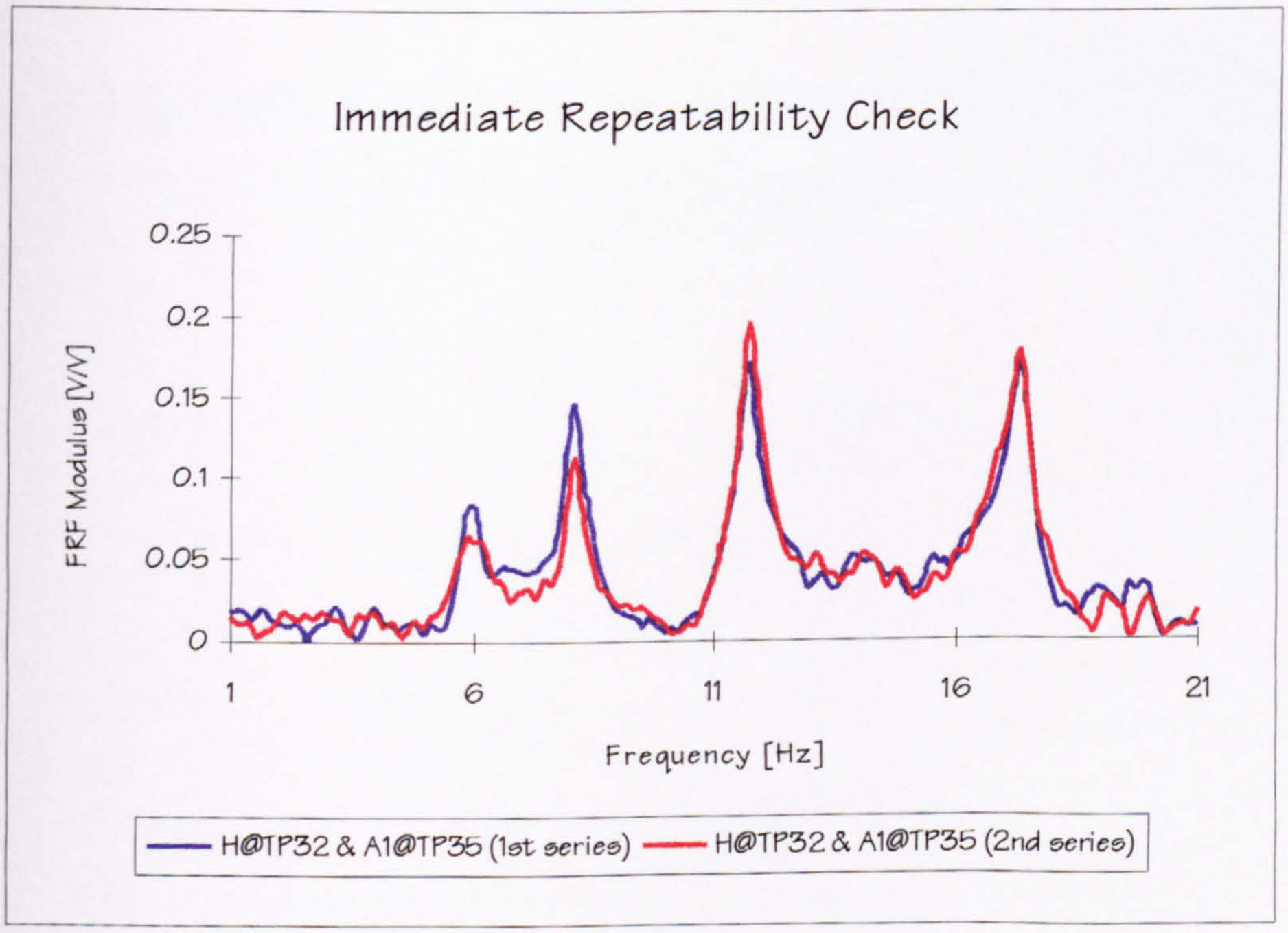

Figure 5.73: Structure C (Unclad) - 'Immediate repeatability' check..

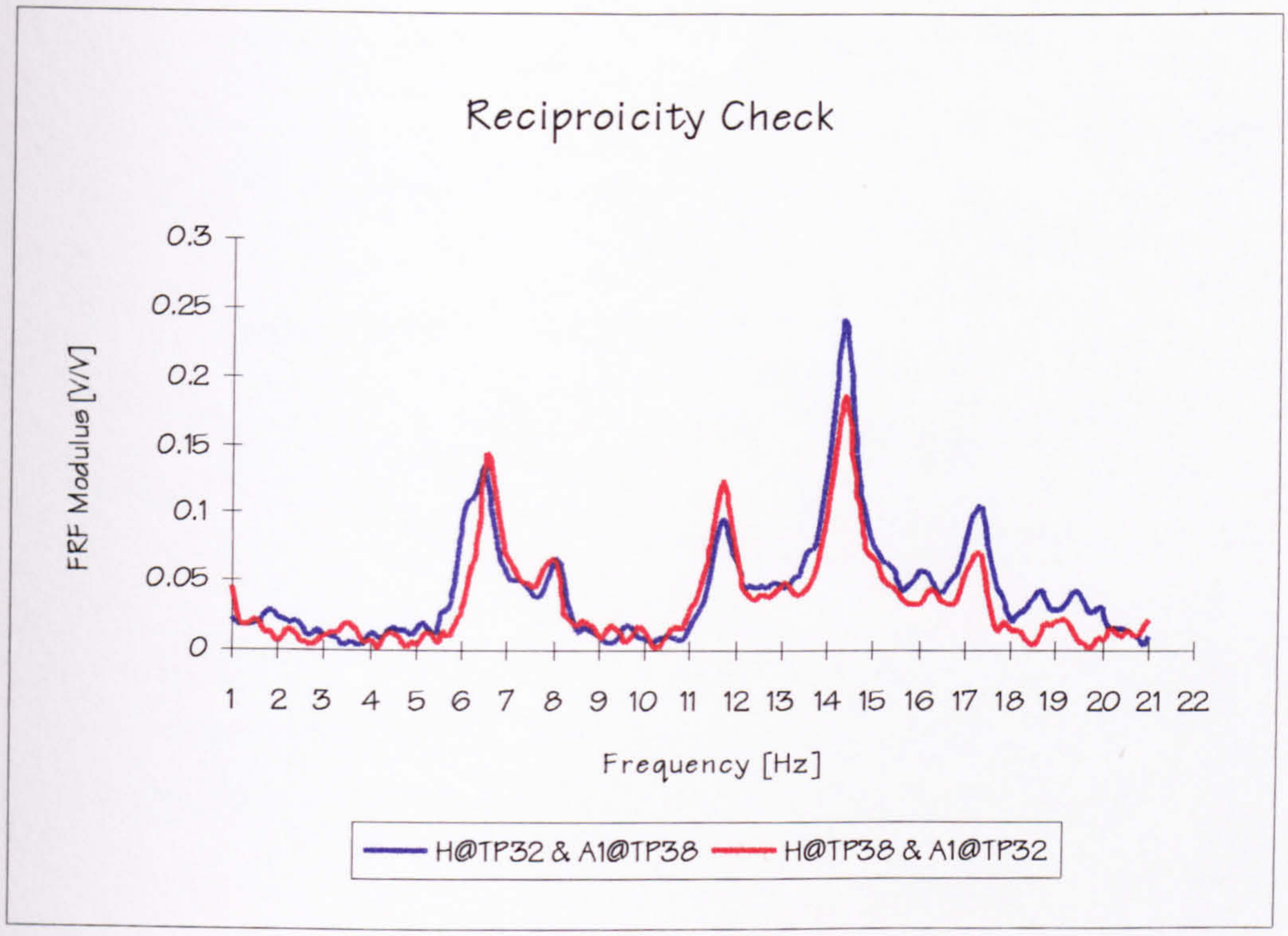

Figure 5.74: Structure C (Unclad) - Reciprocity check between TP32 and TP38.

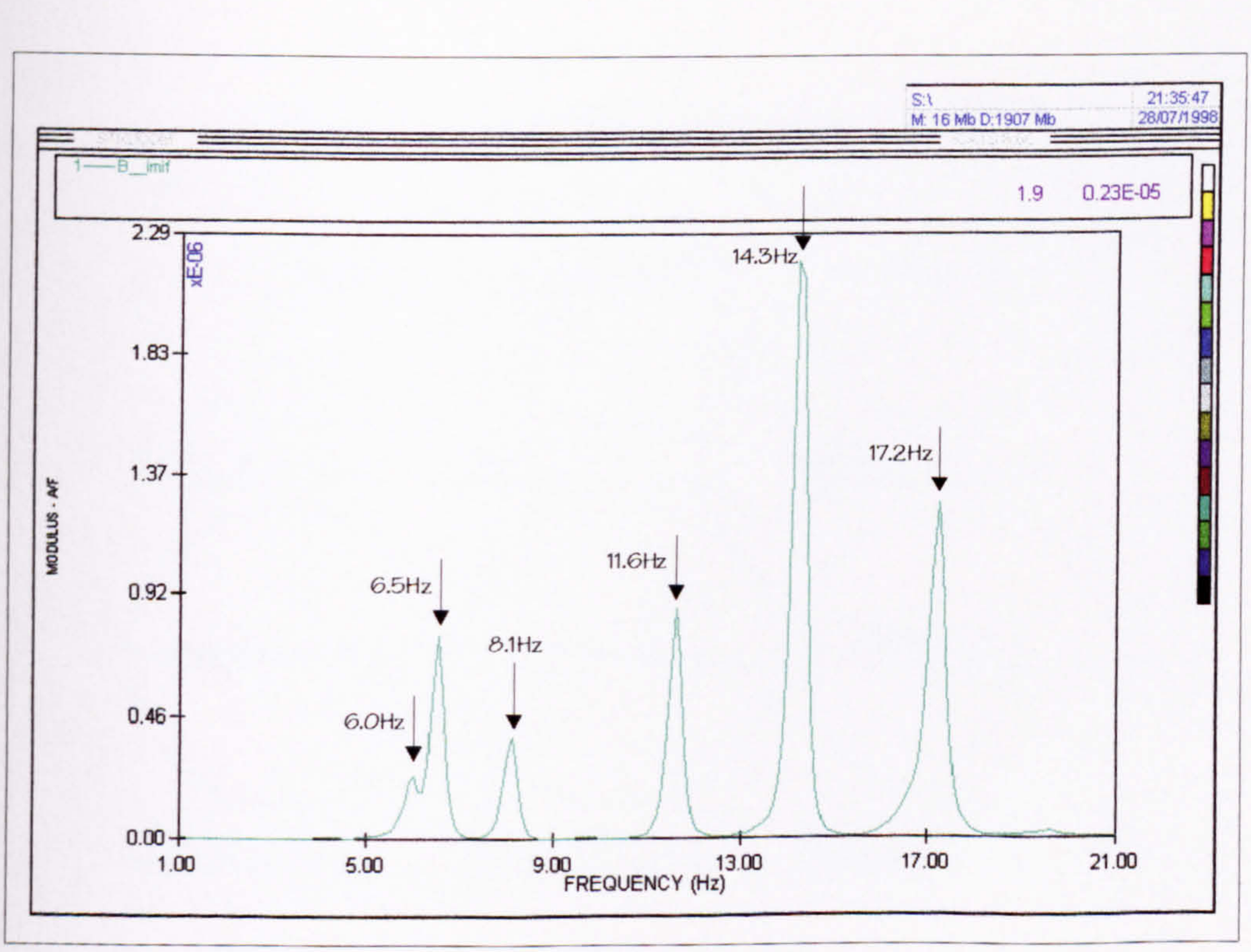

Figure 5.75: Structure C (Unclad) - A MIF, being the summation of squared imaginary parts of all FRFs having TP32 as the reference point, clearly identified the likely frequencies of six modes of vibration.

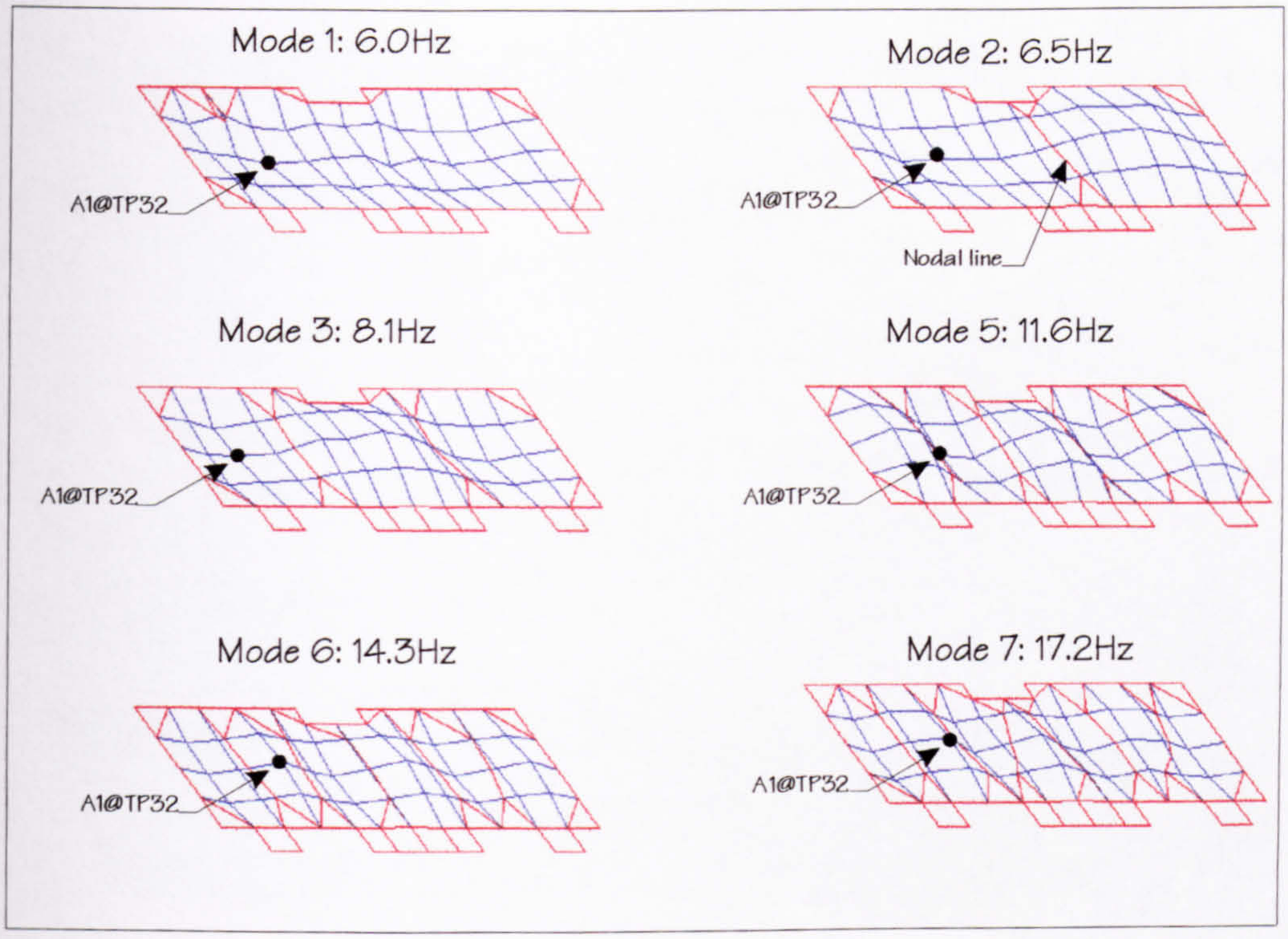

Figure 5.76: Structure C (Unclad) - The experimentally estimated mode shapes and natural frequencies. Mode 4 could not be measured.

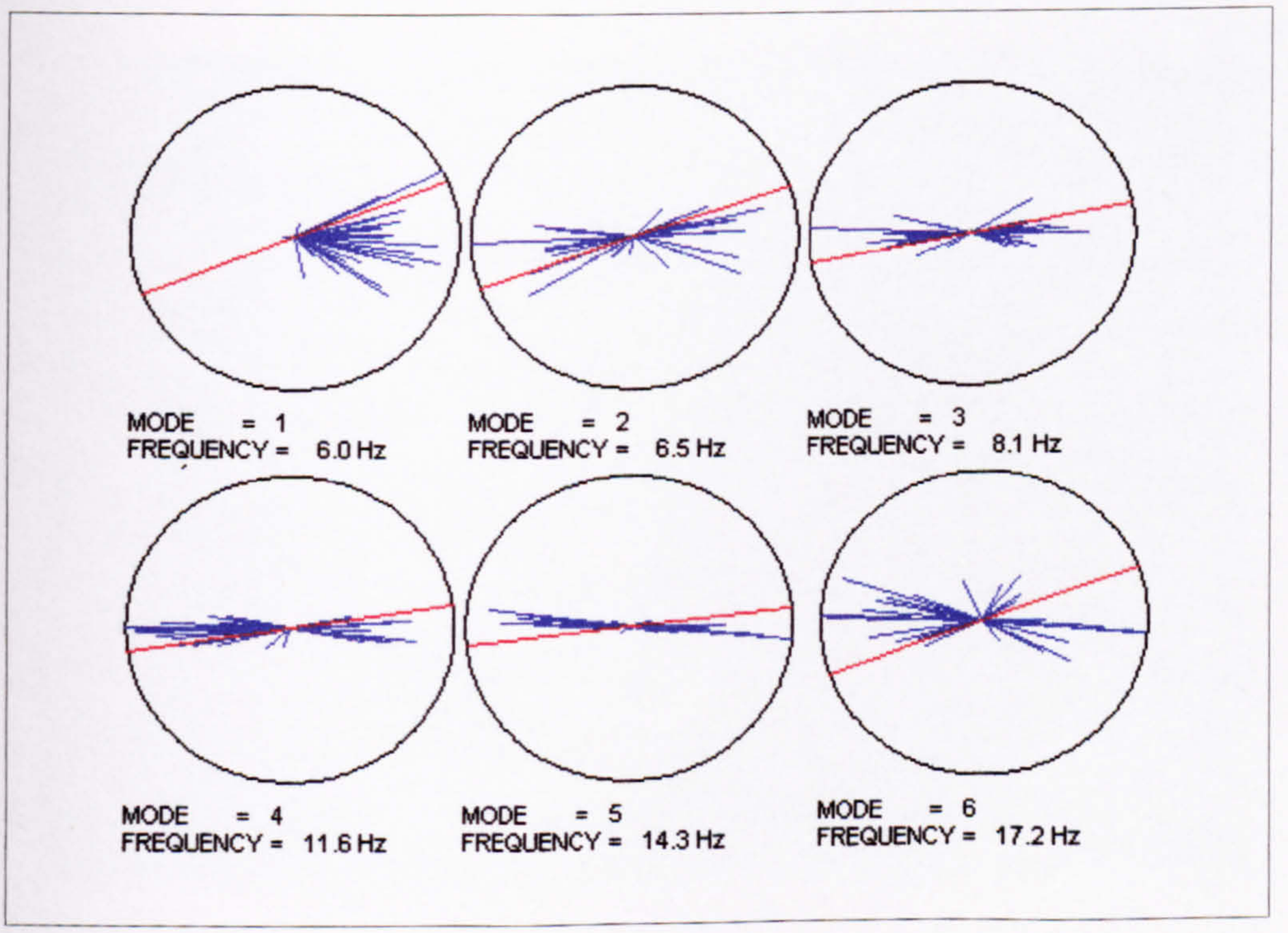

Figure 5.77: Structure C (Unclad) - Complexity of the estimated modes of vibration.

Figure 5.78: Structure C (Clad) - Installations and piping underneath the floor.

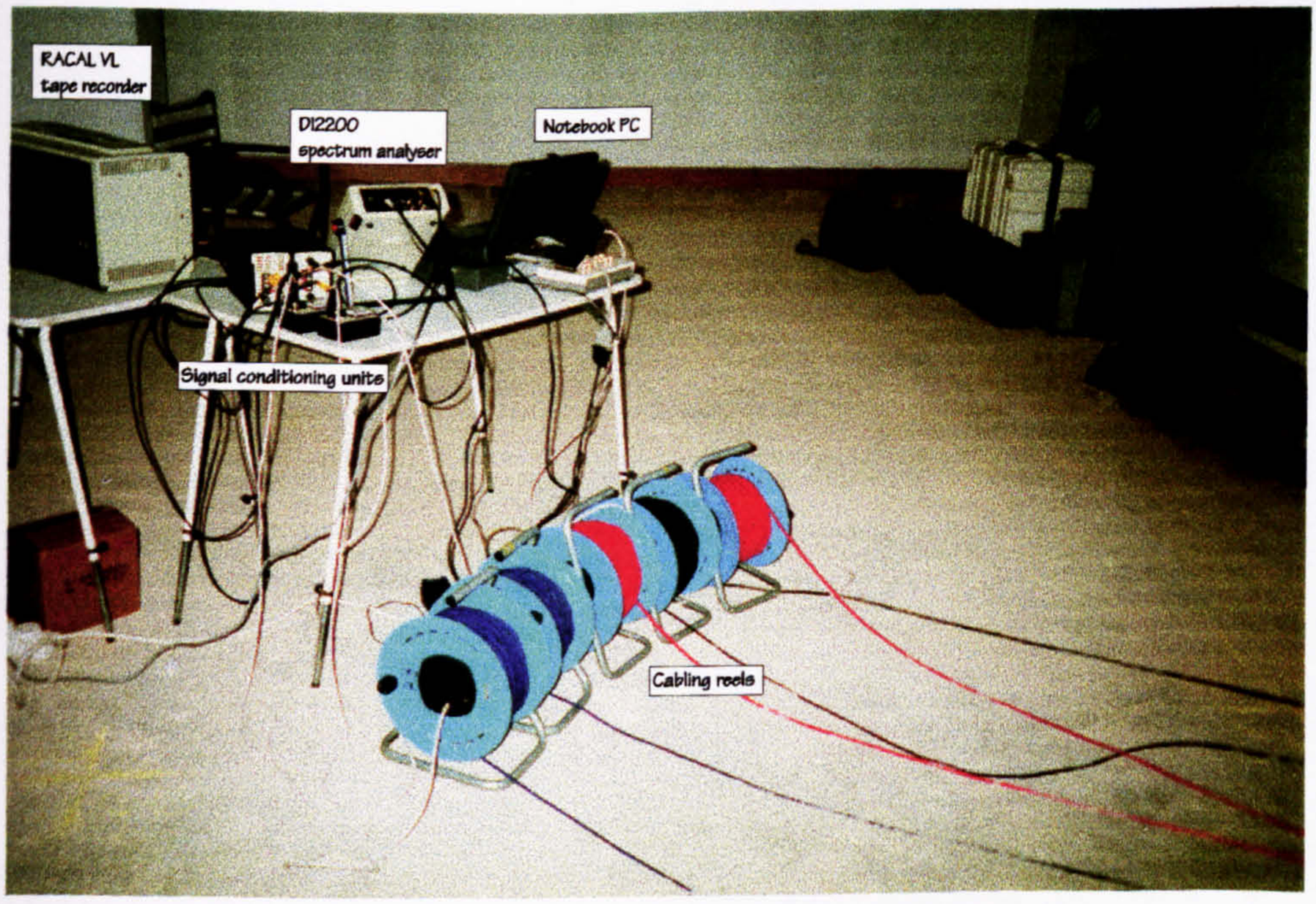

Figure 5.79: Structure C (Clad) - Hardware used for data acquisition.

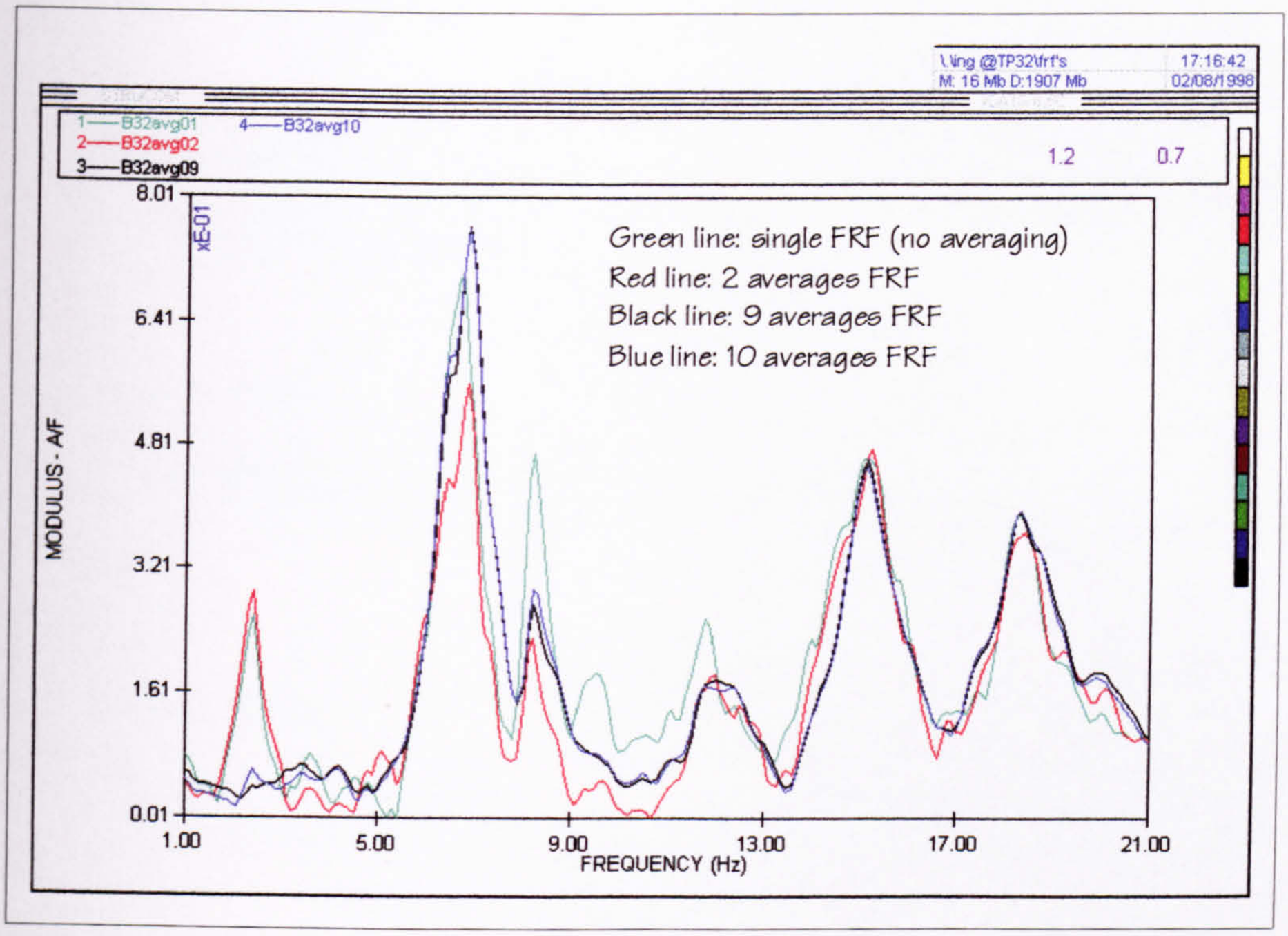

Figure 5.80: Structure C (Clad) - The effects of averaging point mobility FRF measured at TP32 during the second round of testing in June 1996.

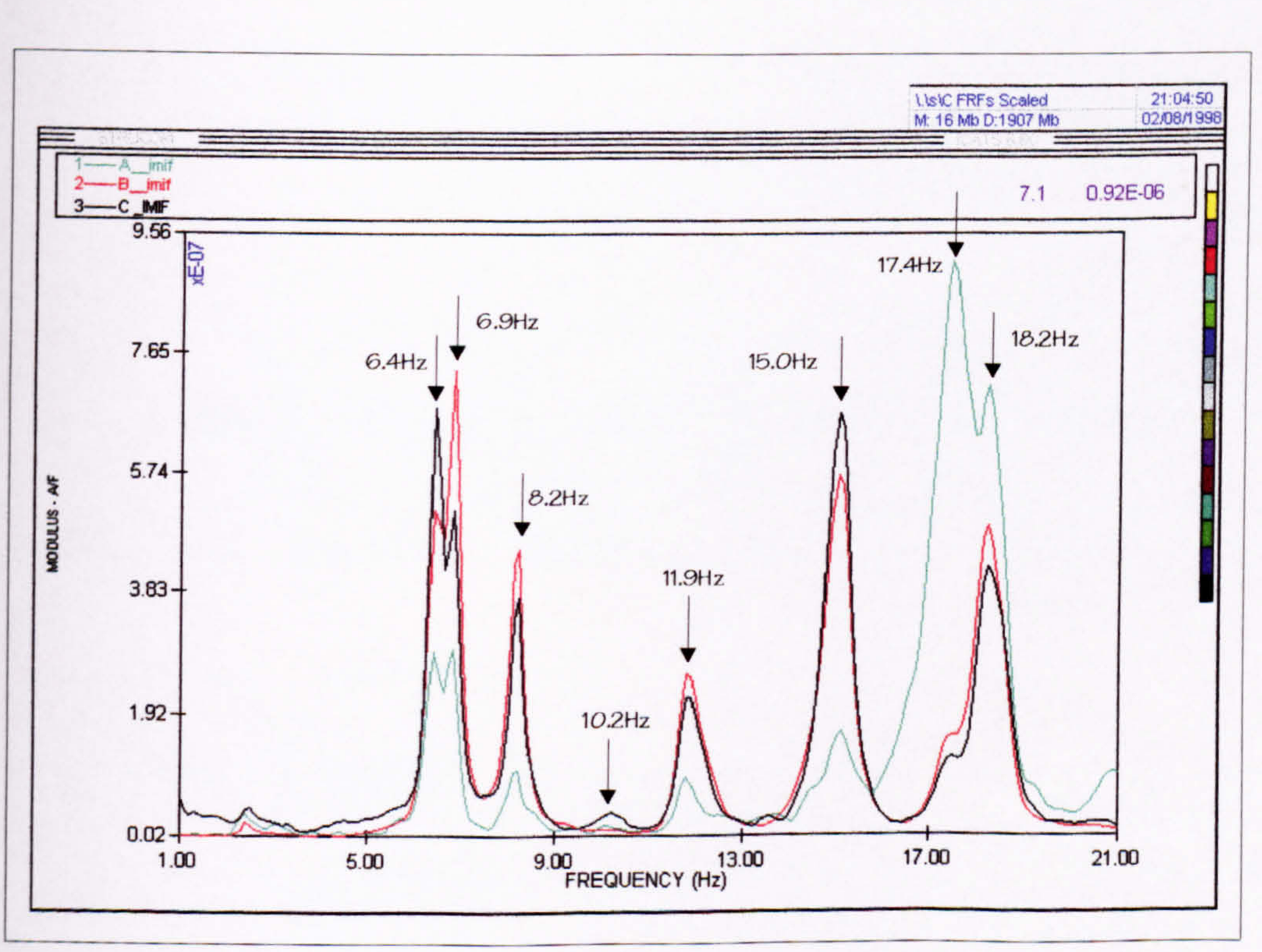

Figure 5.81: Structure C (Clad) - Three MIFs having TP32 (red line), TP38 (black line) and TP51 (green line) as the reference points.

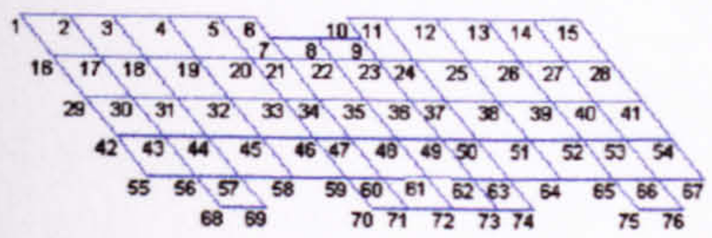

Mode 1: 6.4Hz

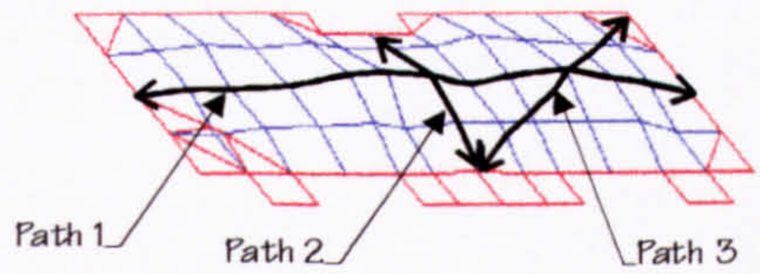

Mode 2: 6.9Hz

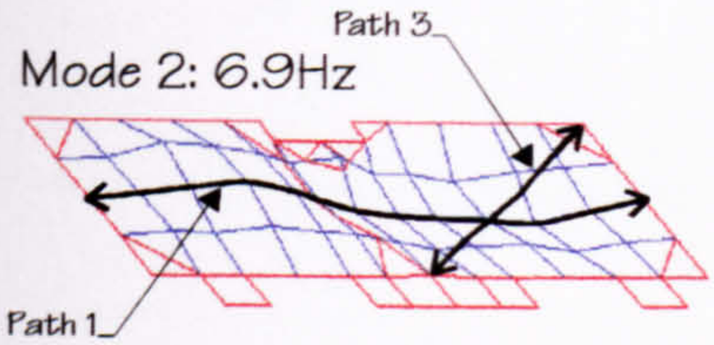

Mode 3: 8.2Hz

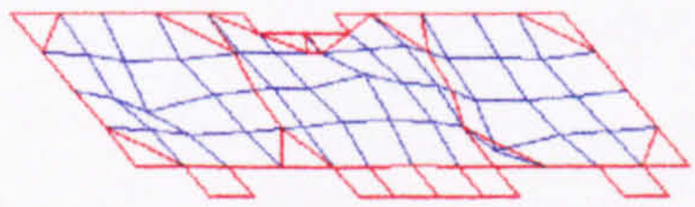

Mode 4: 11.9Hz

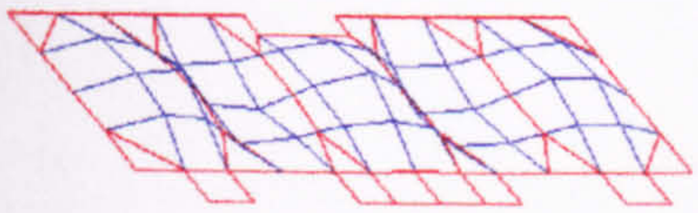

Mode 5: 15.0Hz

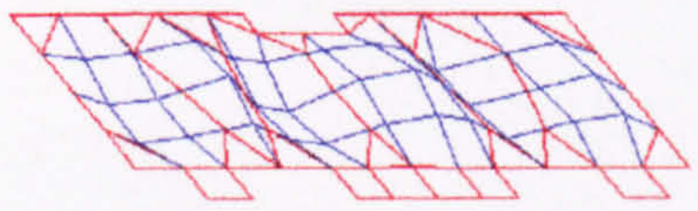

Mode 6: 17.4Hz

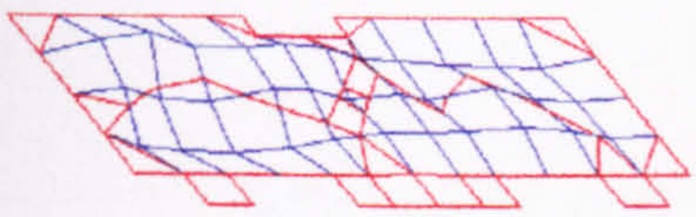

Mode 7: 18.2Hz

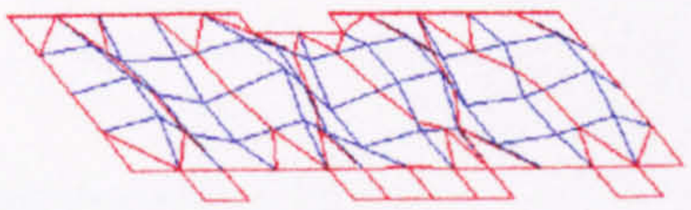

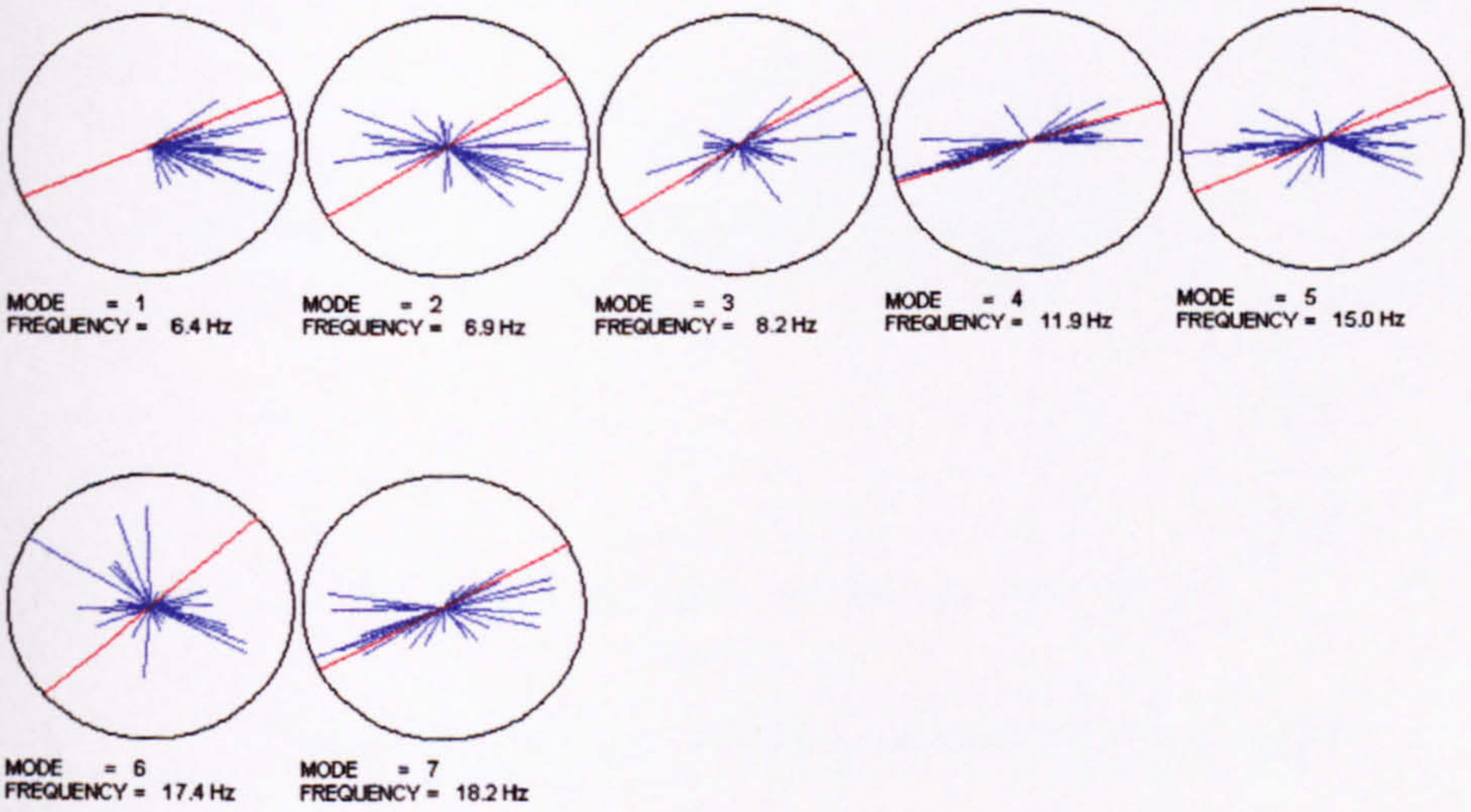

Figure 5.82: Structure C (Clad) - The experimentally estimated mode shapes and natural frequencies after the second round of testing in June 1996, including walking paths and indication of modal complexity.

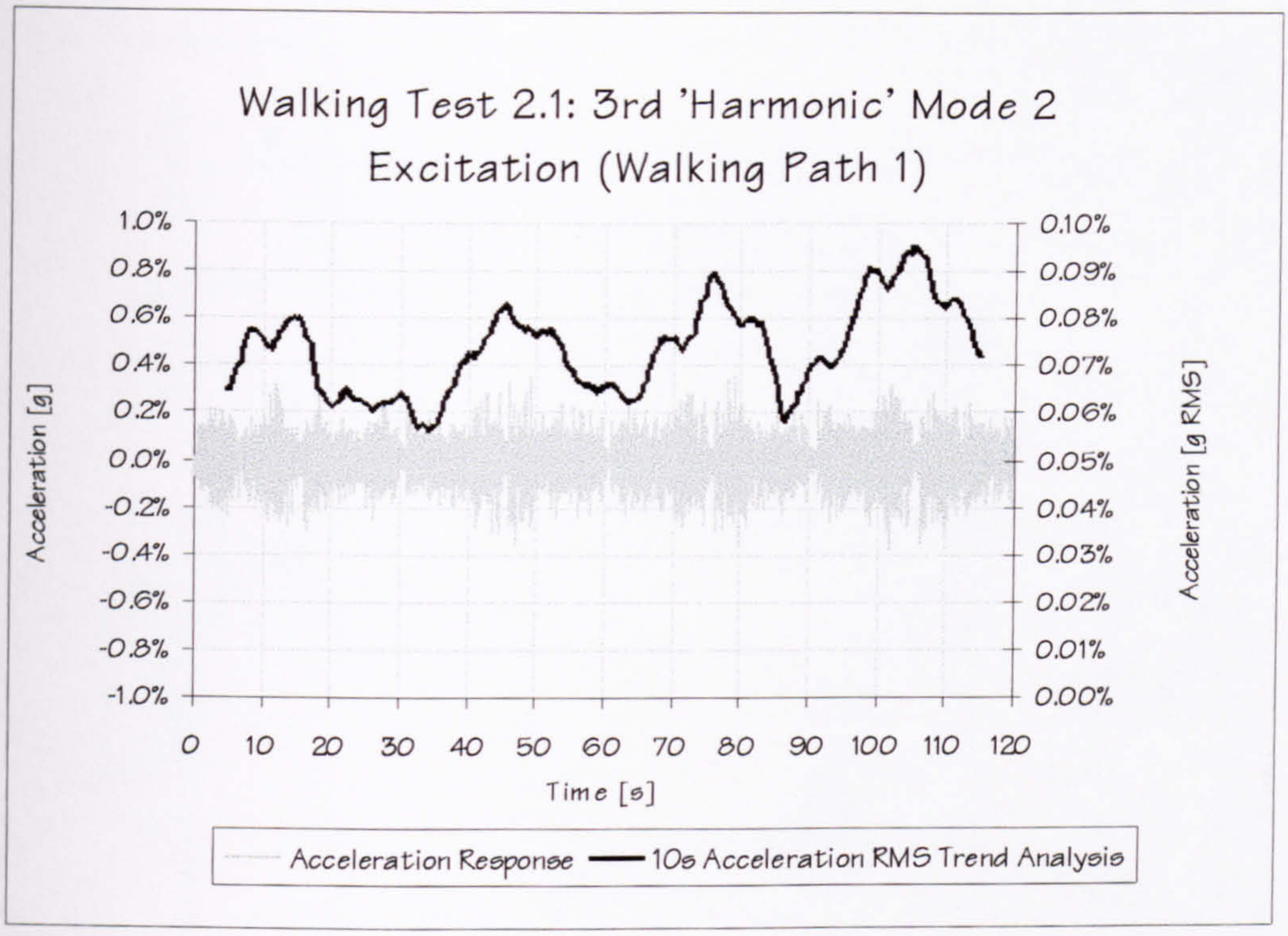

Figure 5.83: Structure C - Maximum acceleration response obtained in Test 2.1 (registered at TP32).

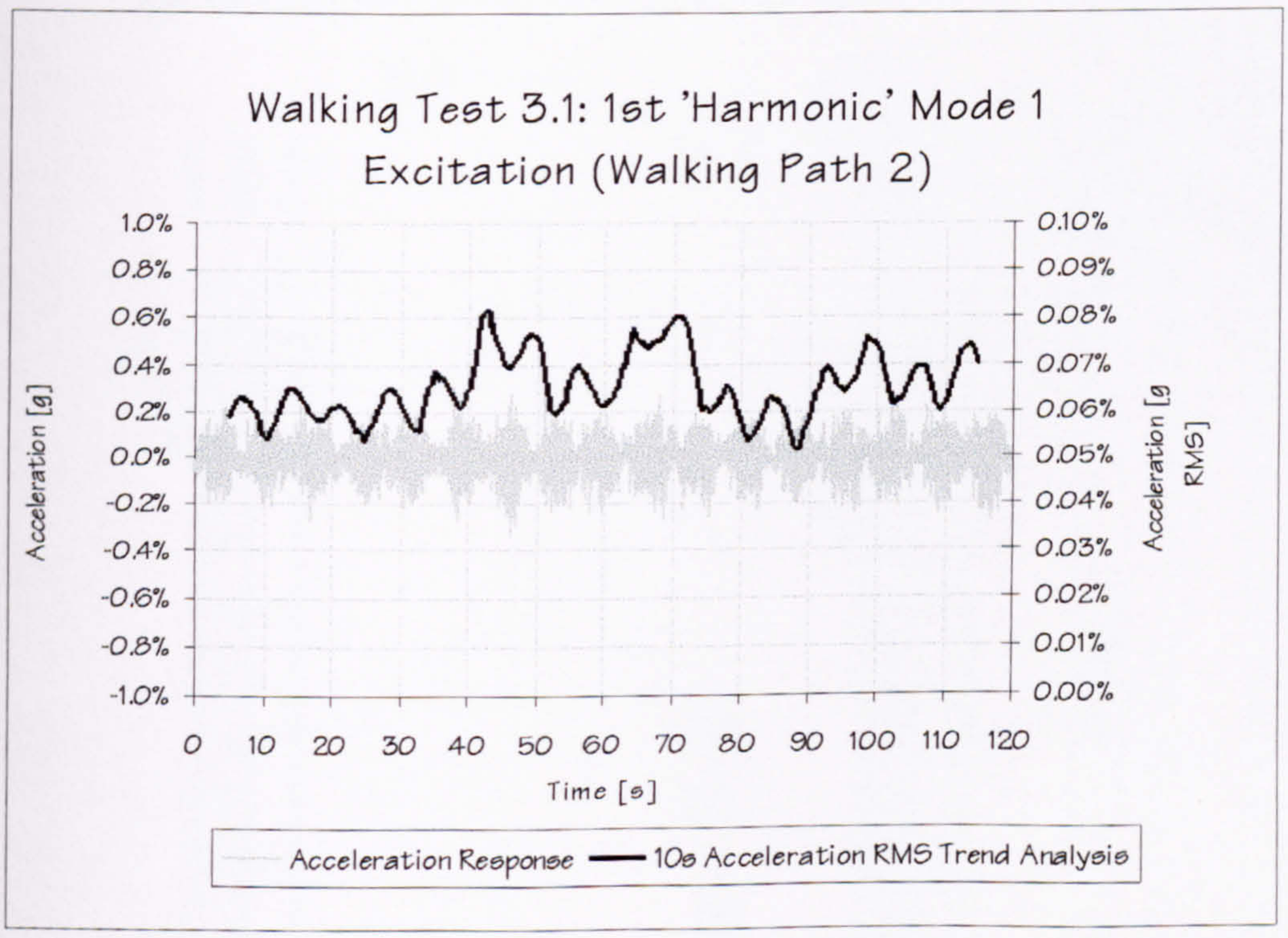

Figure 5.84: Structure C - Maximum acceleration response obtained in Test 3.1 (registered at TP35).

Section A-A

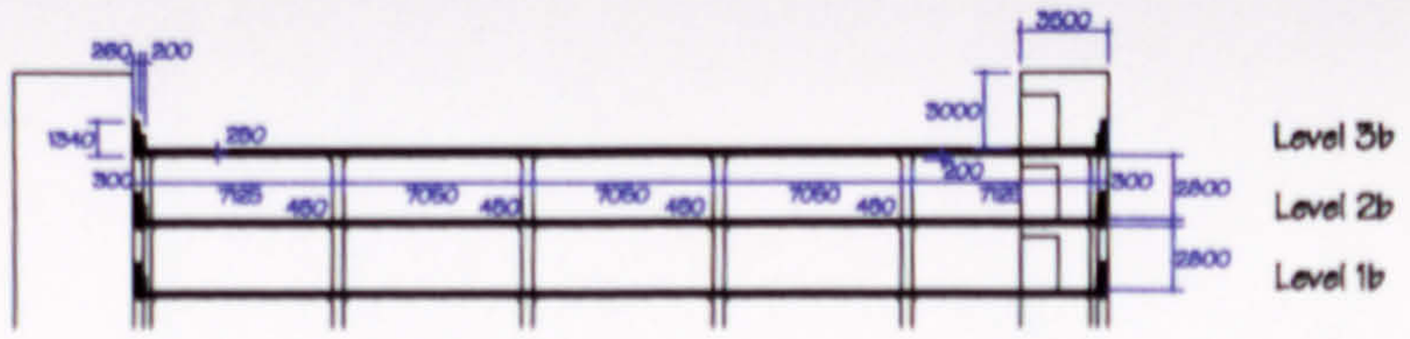

Plan A

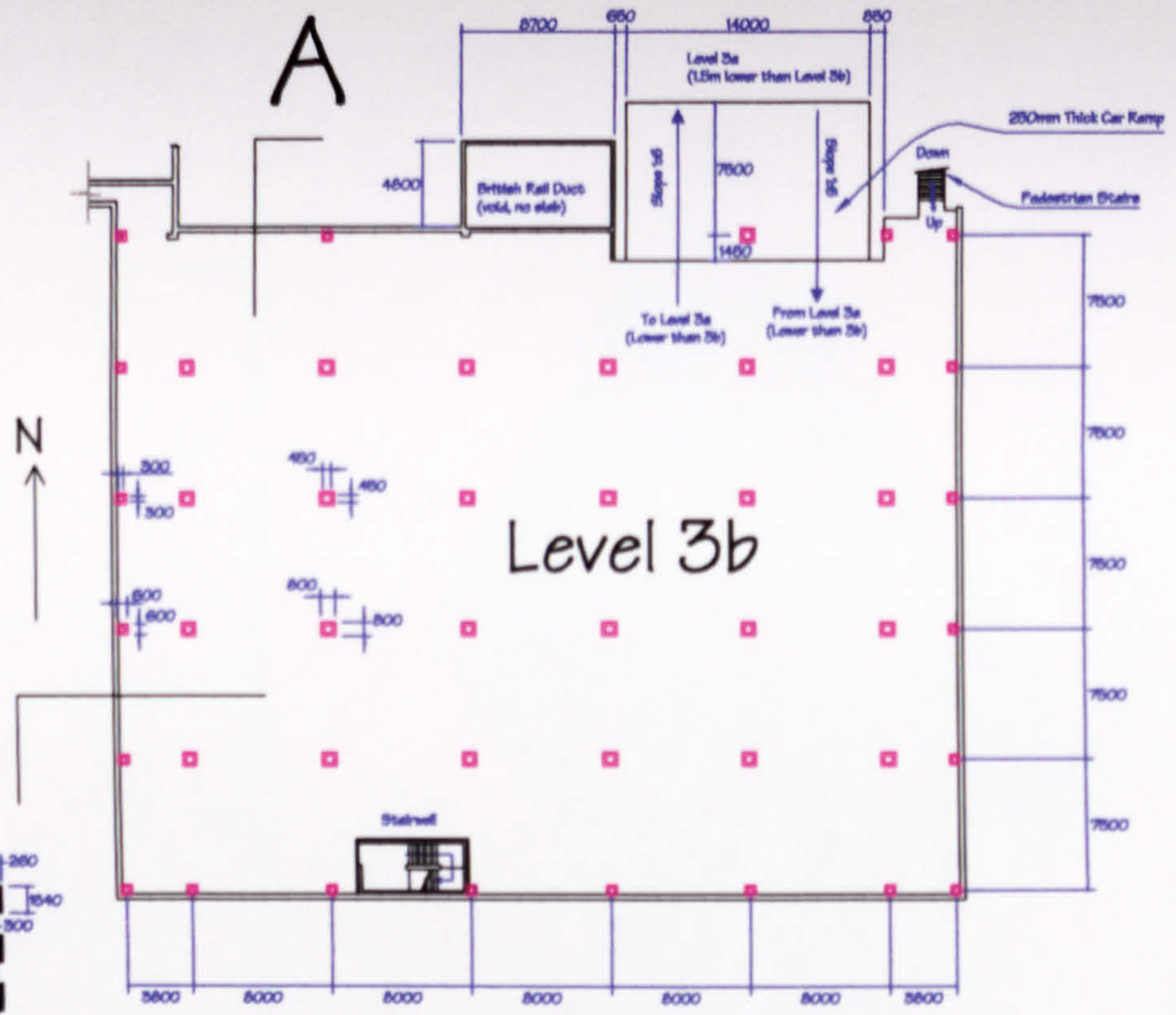

Section B-B

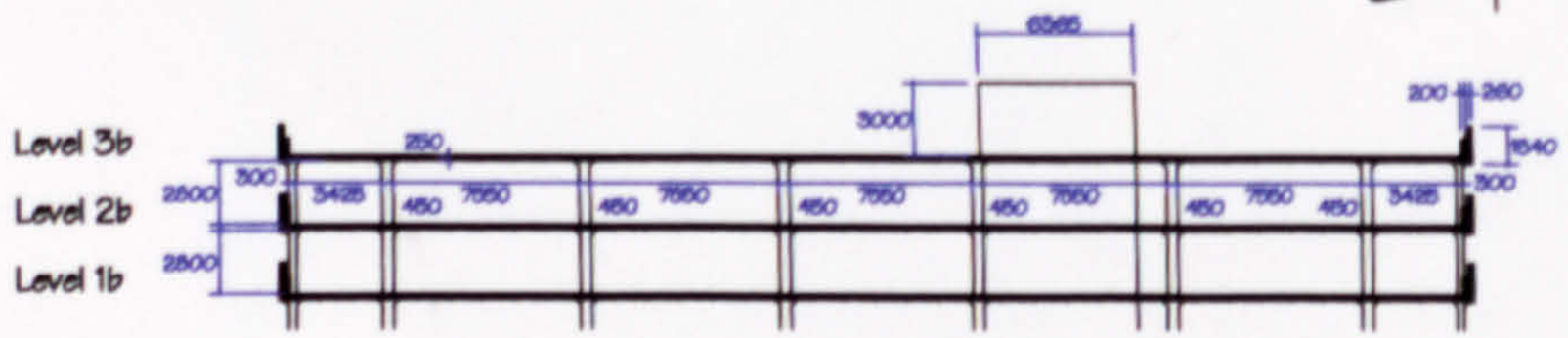

B

Drawing No.	Filename	Drawn by	Date	Scale
5	Structure D - GA Drawing.dwg	A. Pavic	15 Feb 1996	1:500

Title
STRUCTURE D GENERAL ARRANGEMENT DRAWING: SIMPLIFIED FOR FINITE ELEMENT MODELLING

Note:
Concrete grade: C40

Figure 5.85: Structure D - Layout of in-situ cast post-tensioned flat slab.

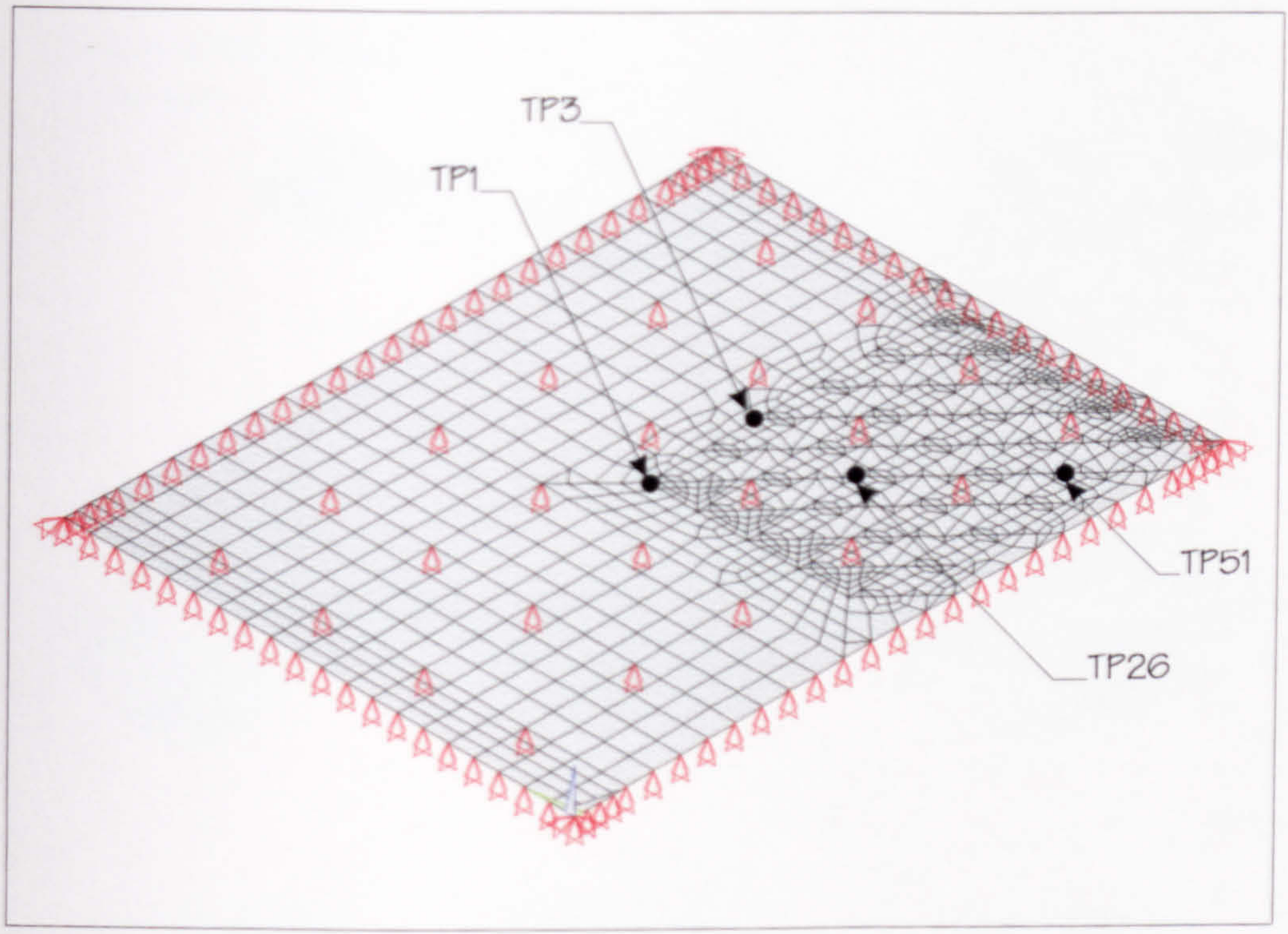

Figure 5.86: Structure D - A refined pre-test FE model having nodes at all test points.

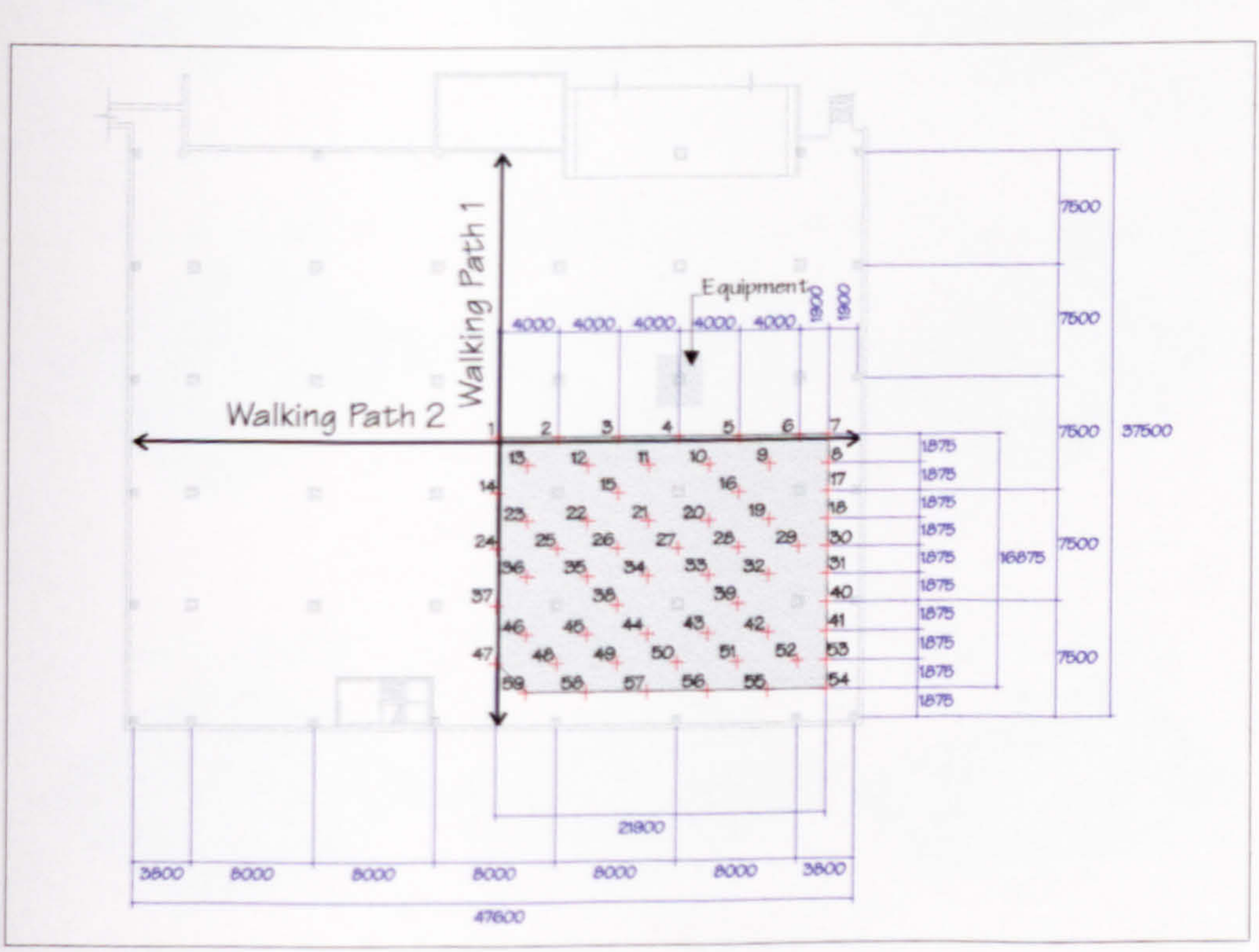

Figure 5.87: Structure D - Test grid, walking paths and location of the test equipment.

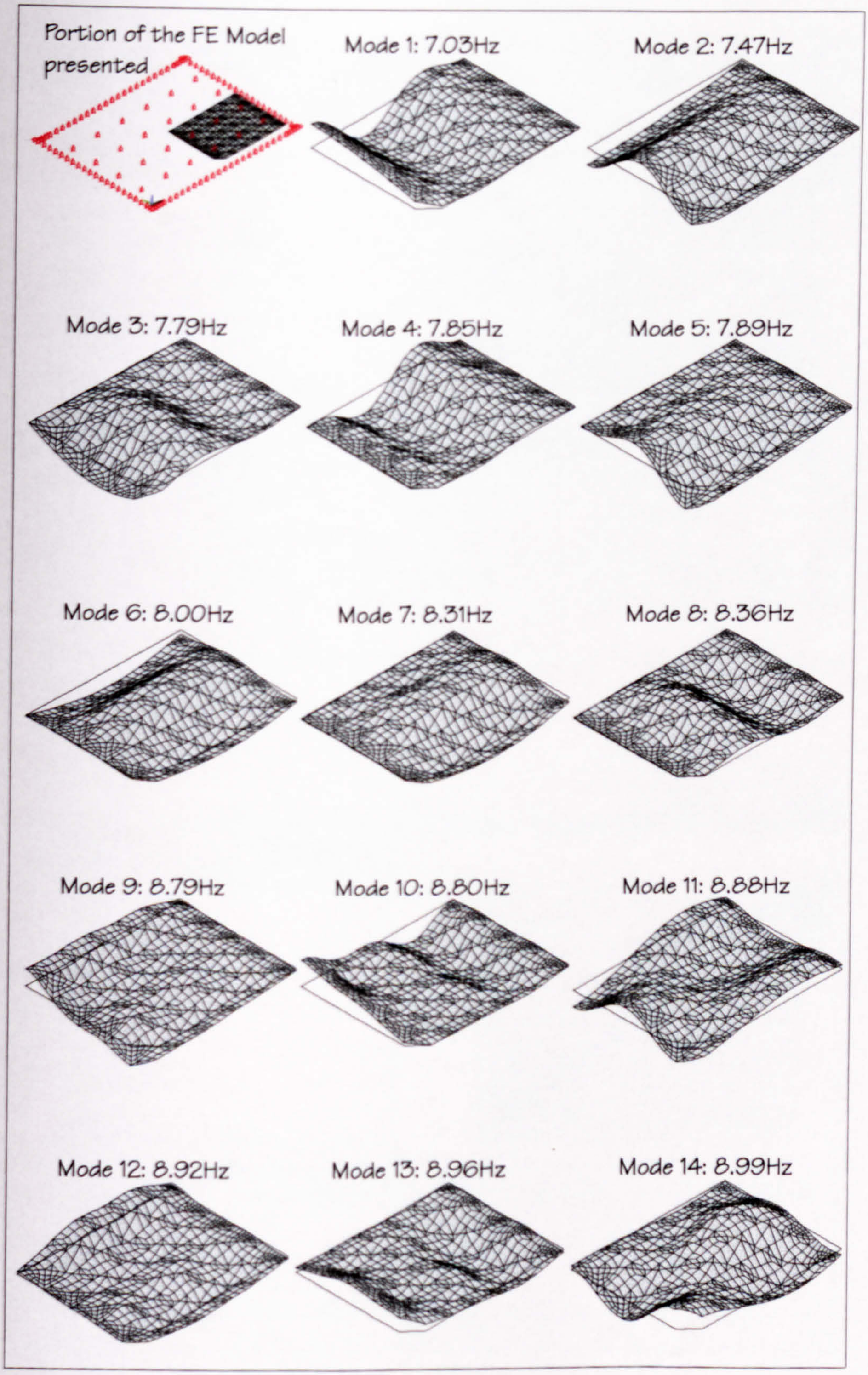

Figure 5.88: Structure D - Analytically calculated natural frequencies and mode shapes using the pre-test analysis FE model

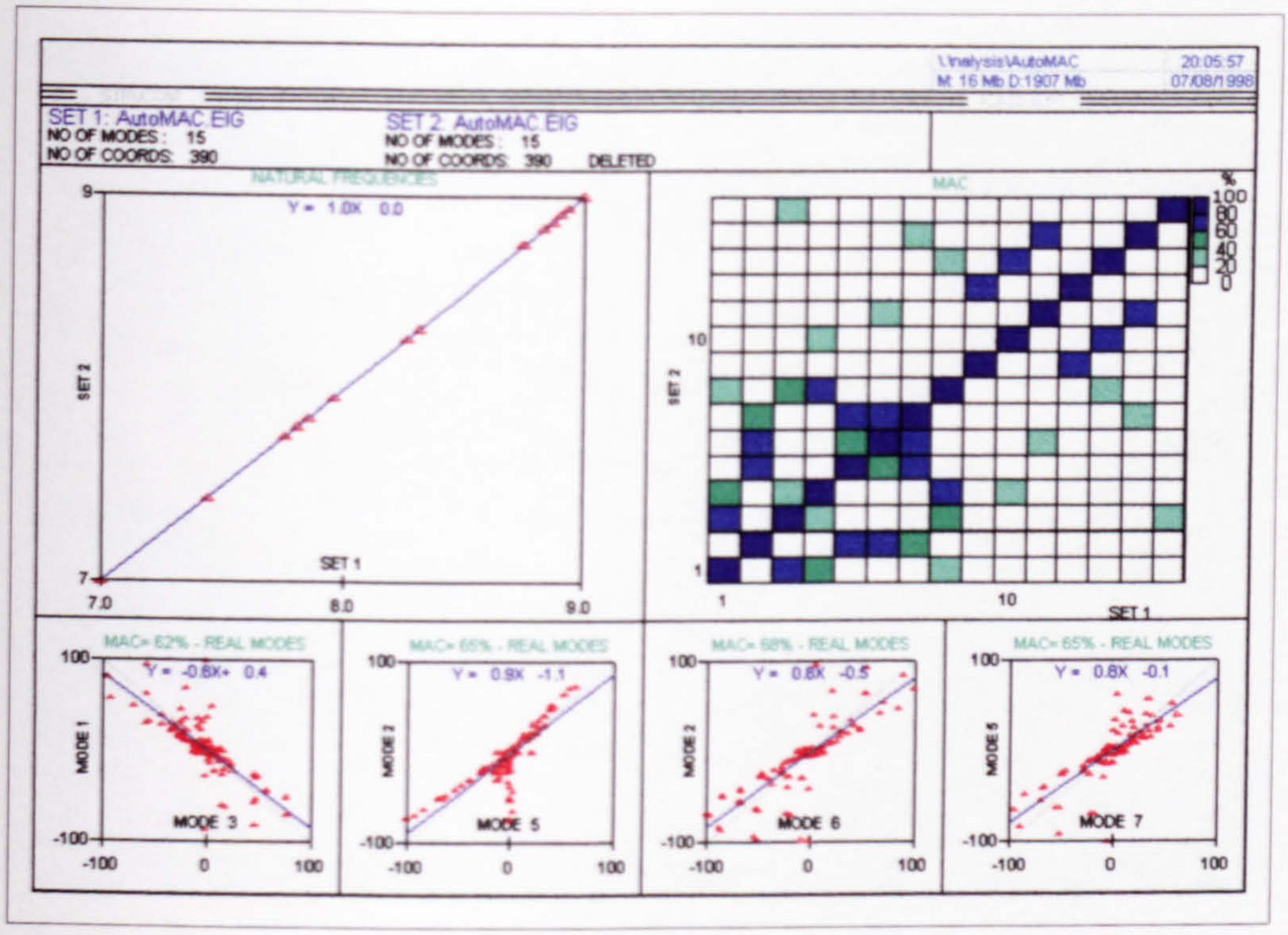

Figure 5.89: Structure D - Auto-MAC matrix obtained from FE mode shapes reduced to the test grid co-ordinates.

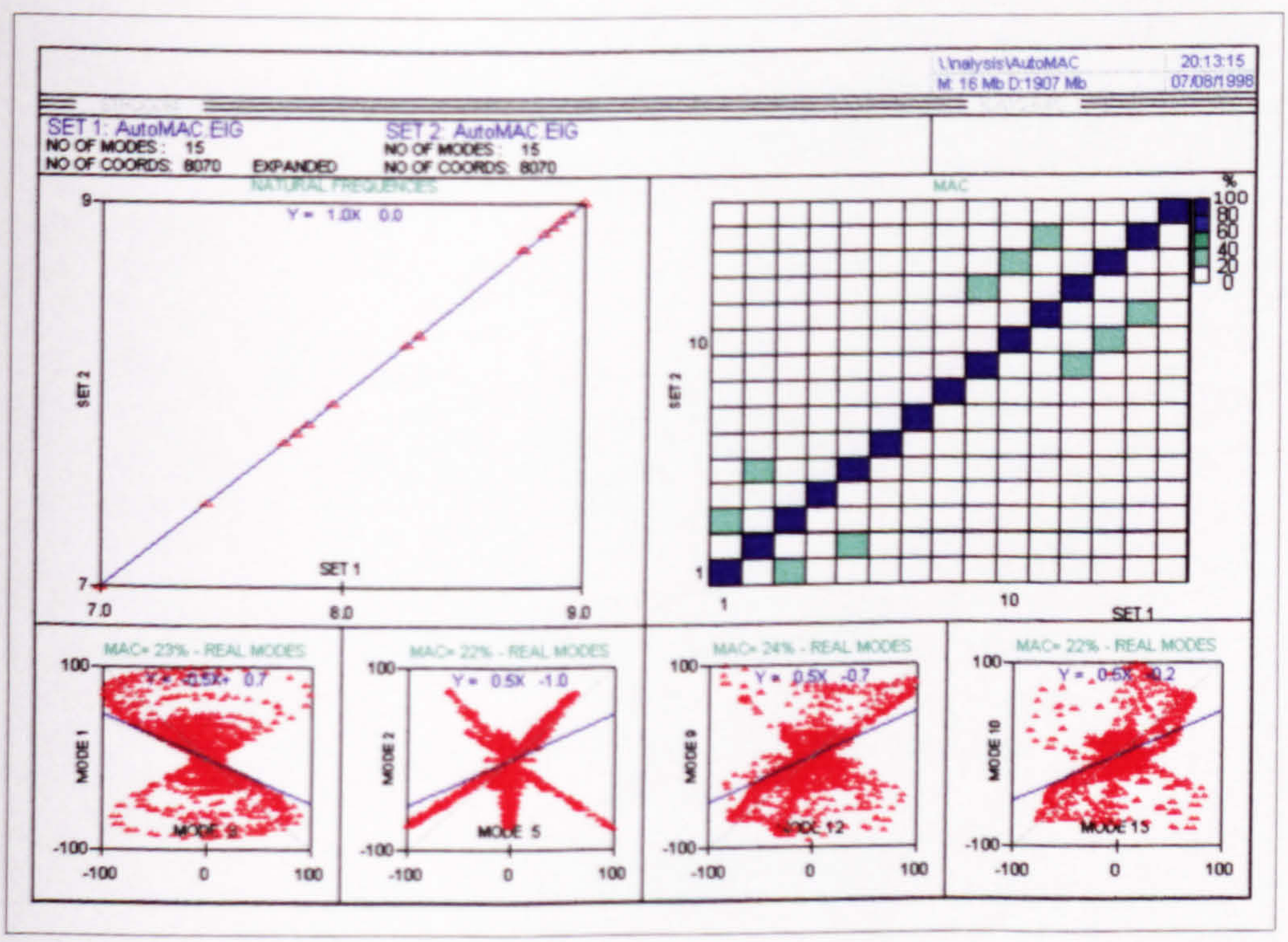

Figure 5.90: Structure D - Auto-MAC matrix obtained from expanded FE mode shapes which were reduced to the test grid co-ordinates.

Figure 5.91: Structure D - Hardware used for data acquisition.

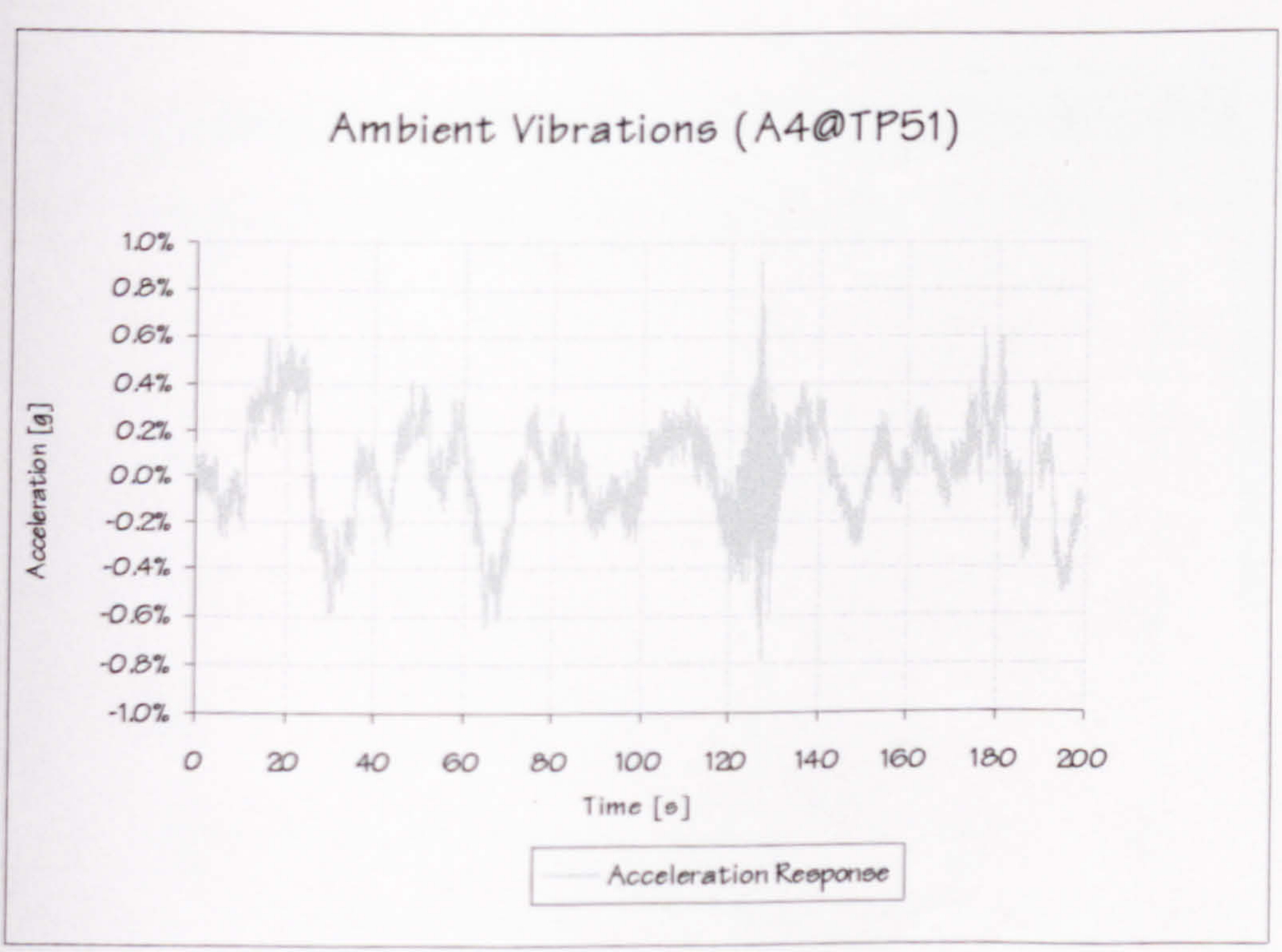

Figure 5.92: Structure D - Low-frequency drifting of signals from accelerometer A4.

Figure 5.93: Structure D - Hammer test operator receiving instructions via the hands-free voice-activated two-way radio head set.

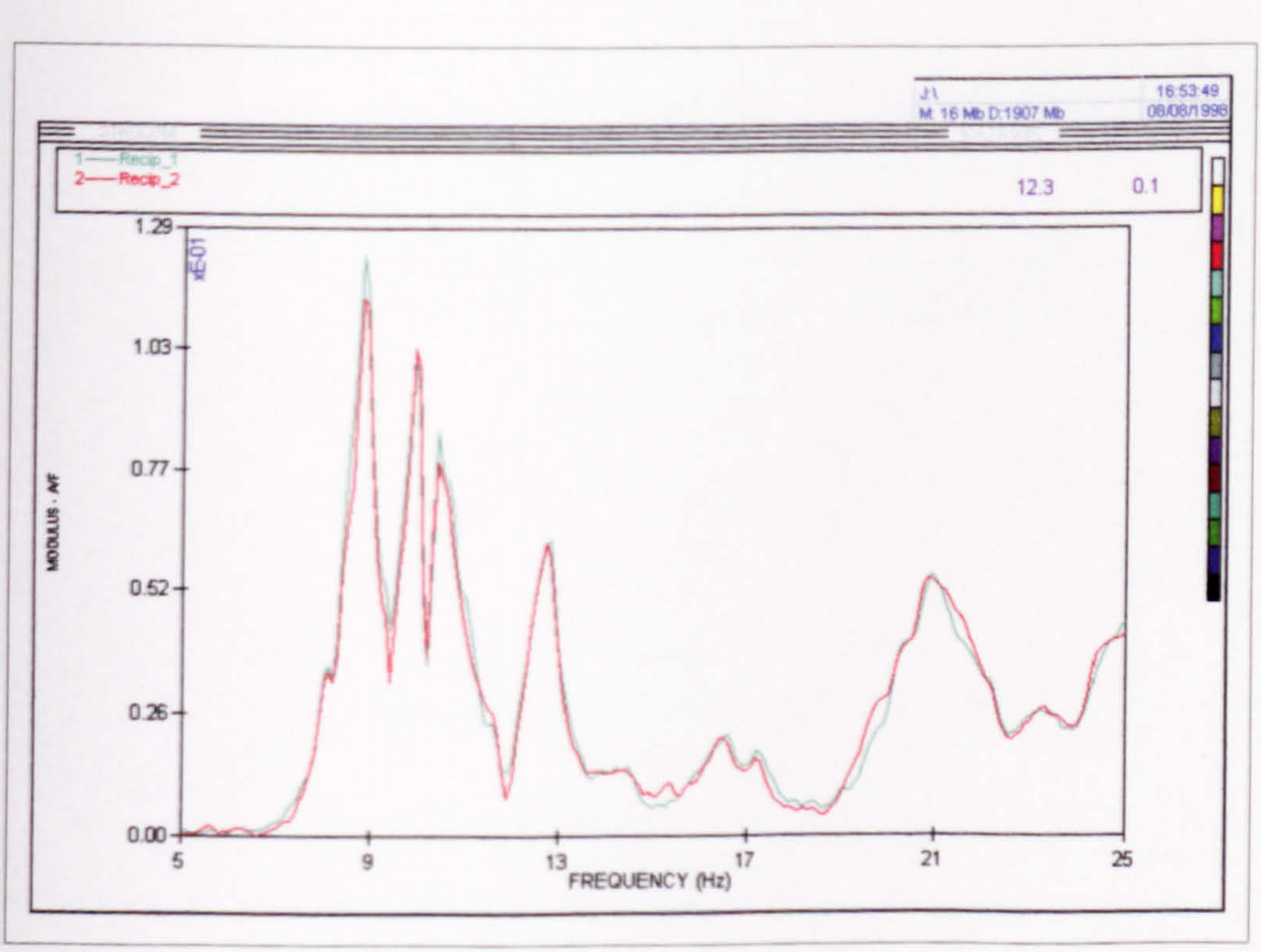

Figure 5.94: Structure D - Reciprocity check using transfer mobilities between TP1 and TP3.

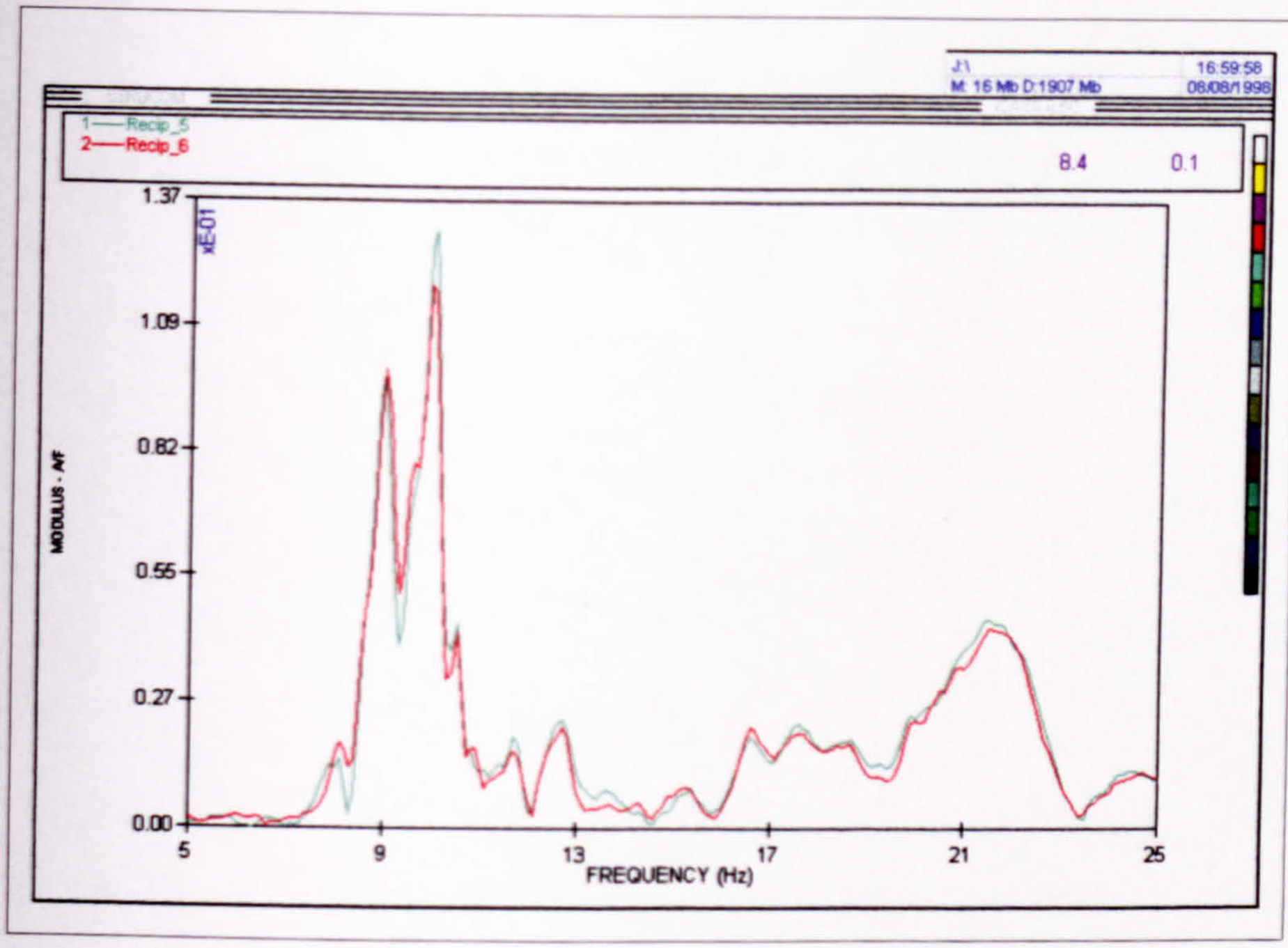

Figure 5.95: Structure D - Reciprocity check using transfer mobilities between TP1 and TP51.

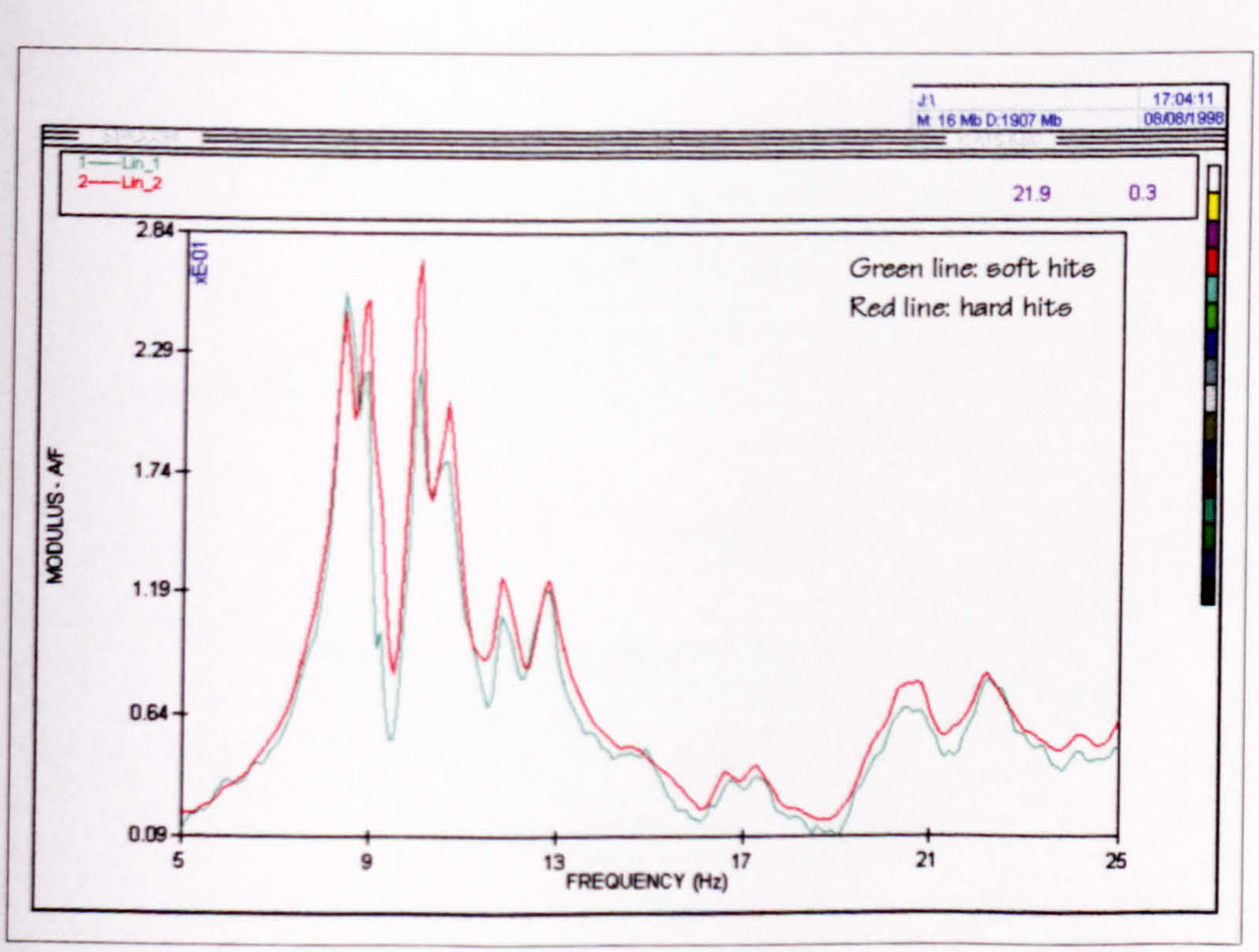

Figure 5.96: Structure D - Homogeneity check using two point mobility FRFs measured at TP1.

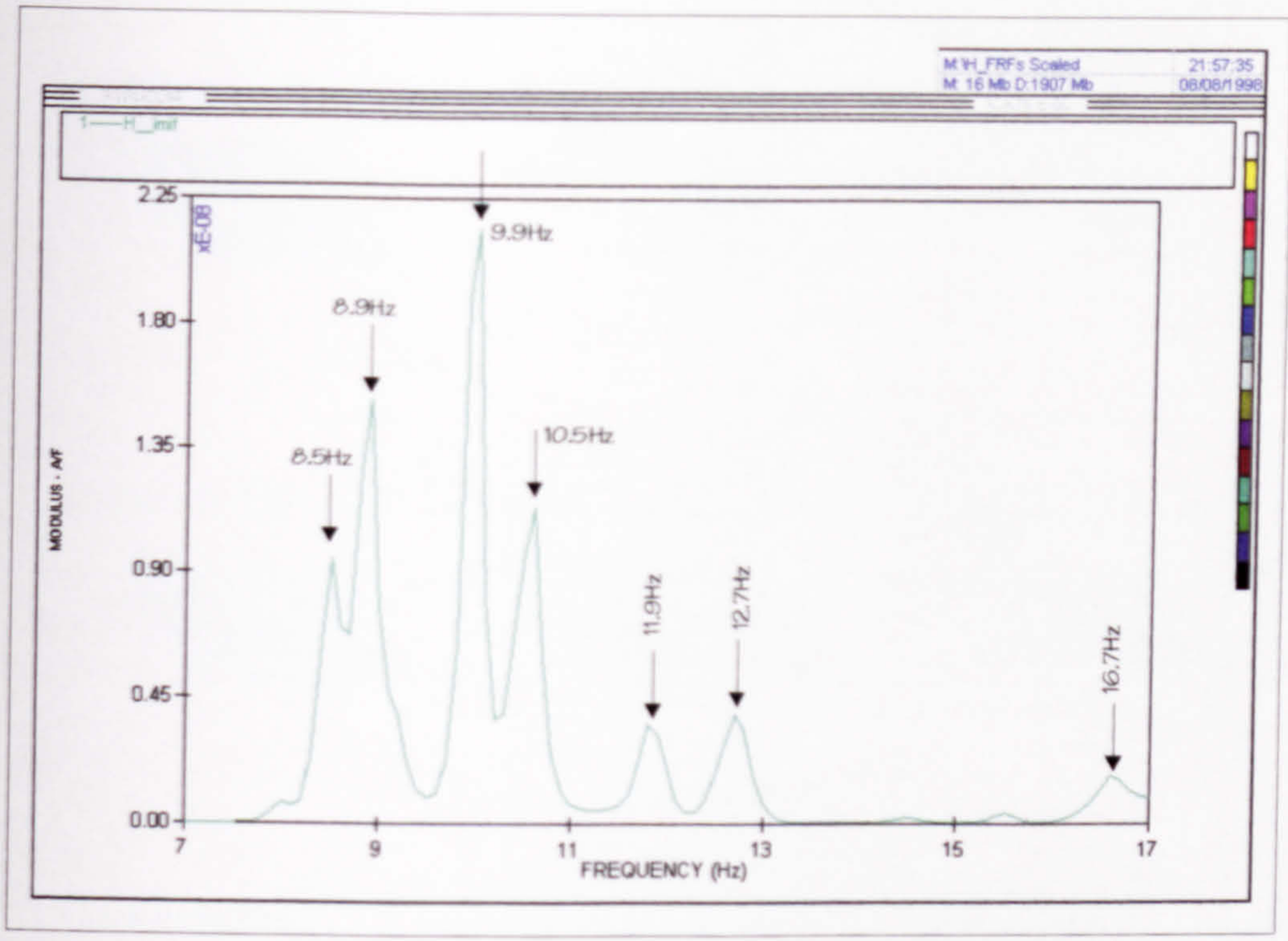

Figure 5.97: Structure D - An in-situ calculated MIF having TP1 as the reference point.

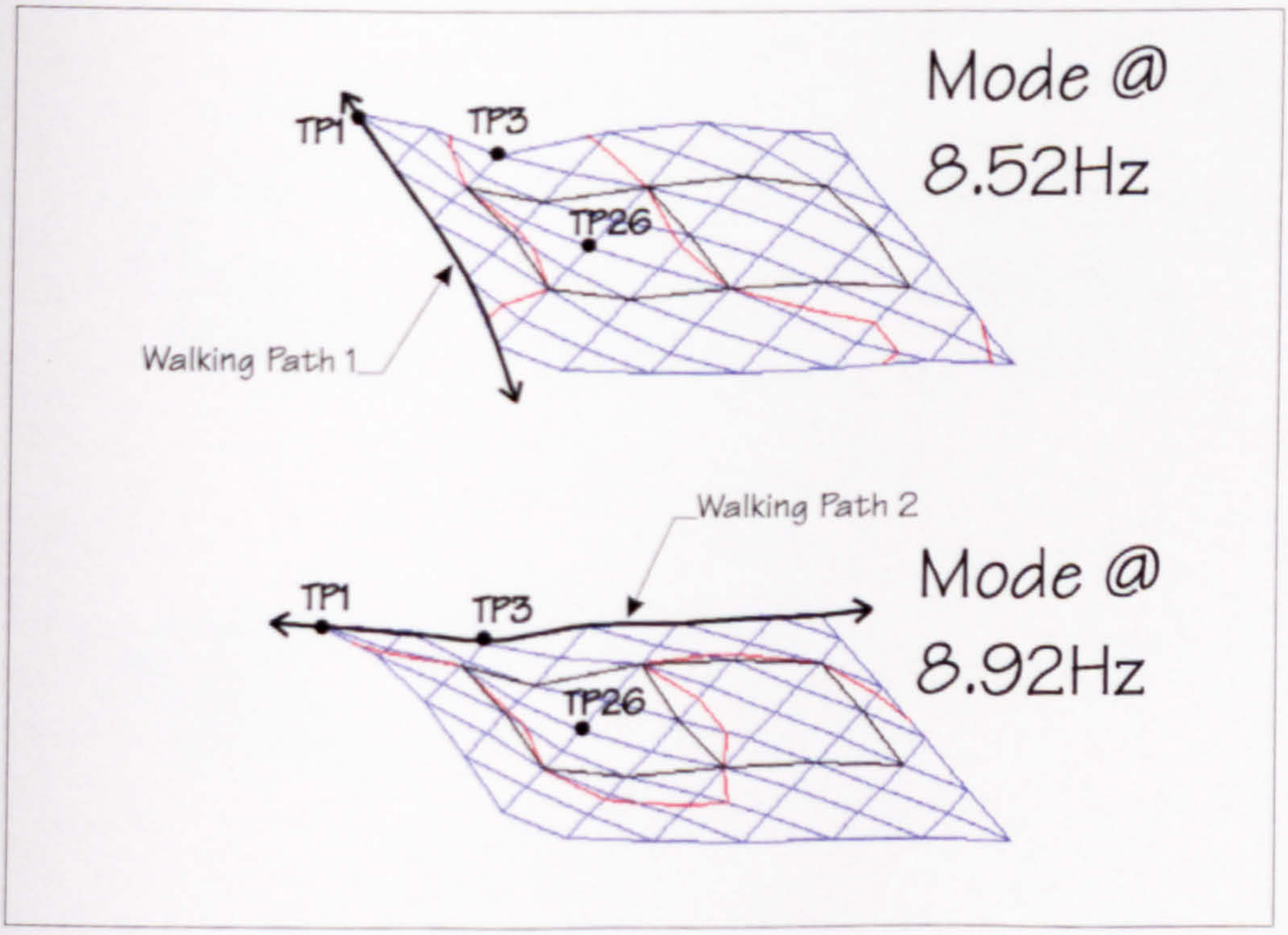

Figure 5.98: Structure D - In-situ identified mode shapes to be excited by normal walking.

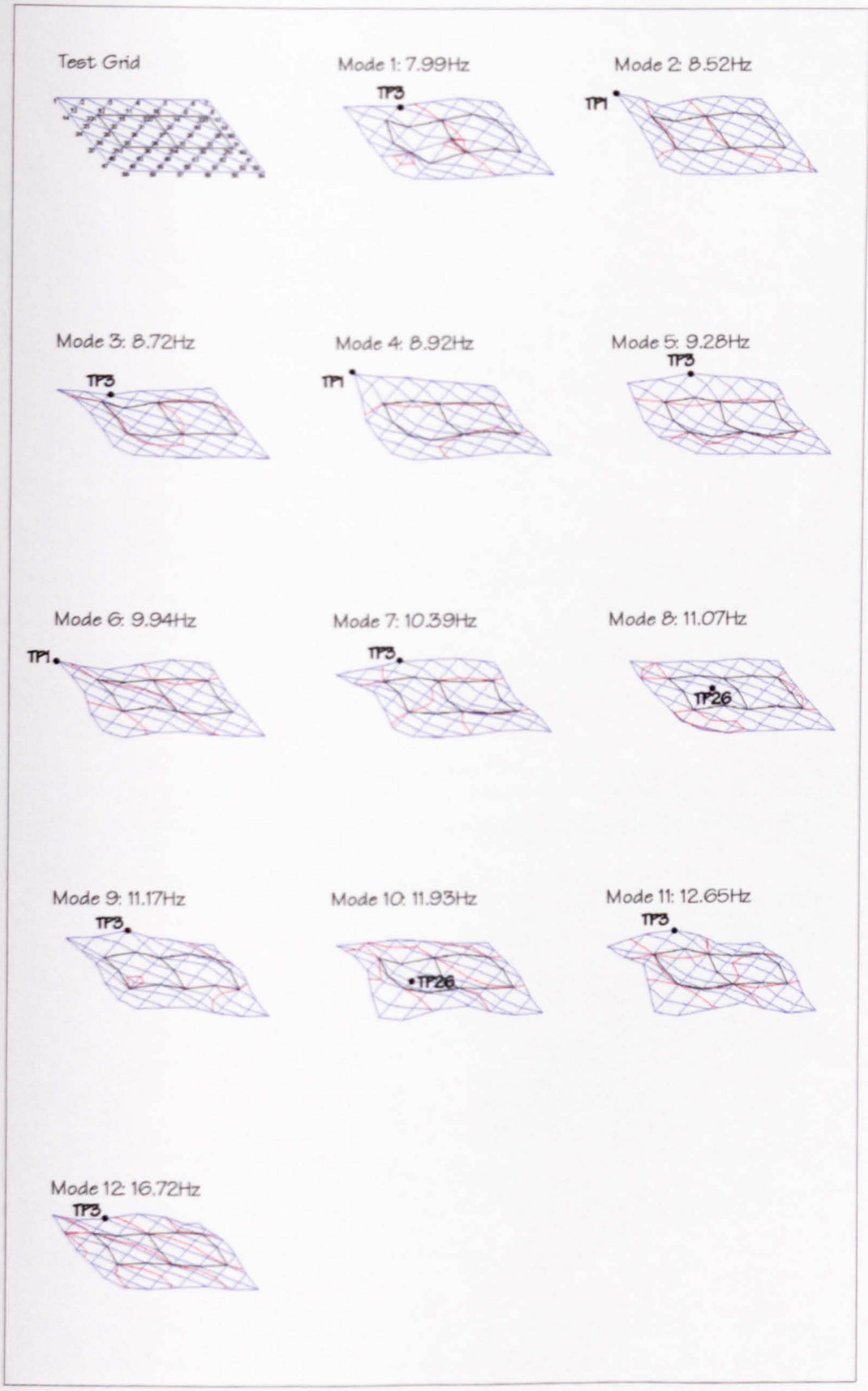

Figure 5.99: Structure D - Experimentally measured mode shapes and natural frequencies.

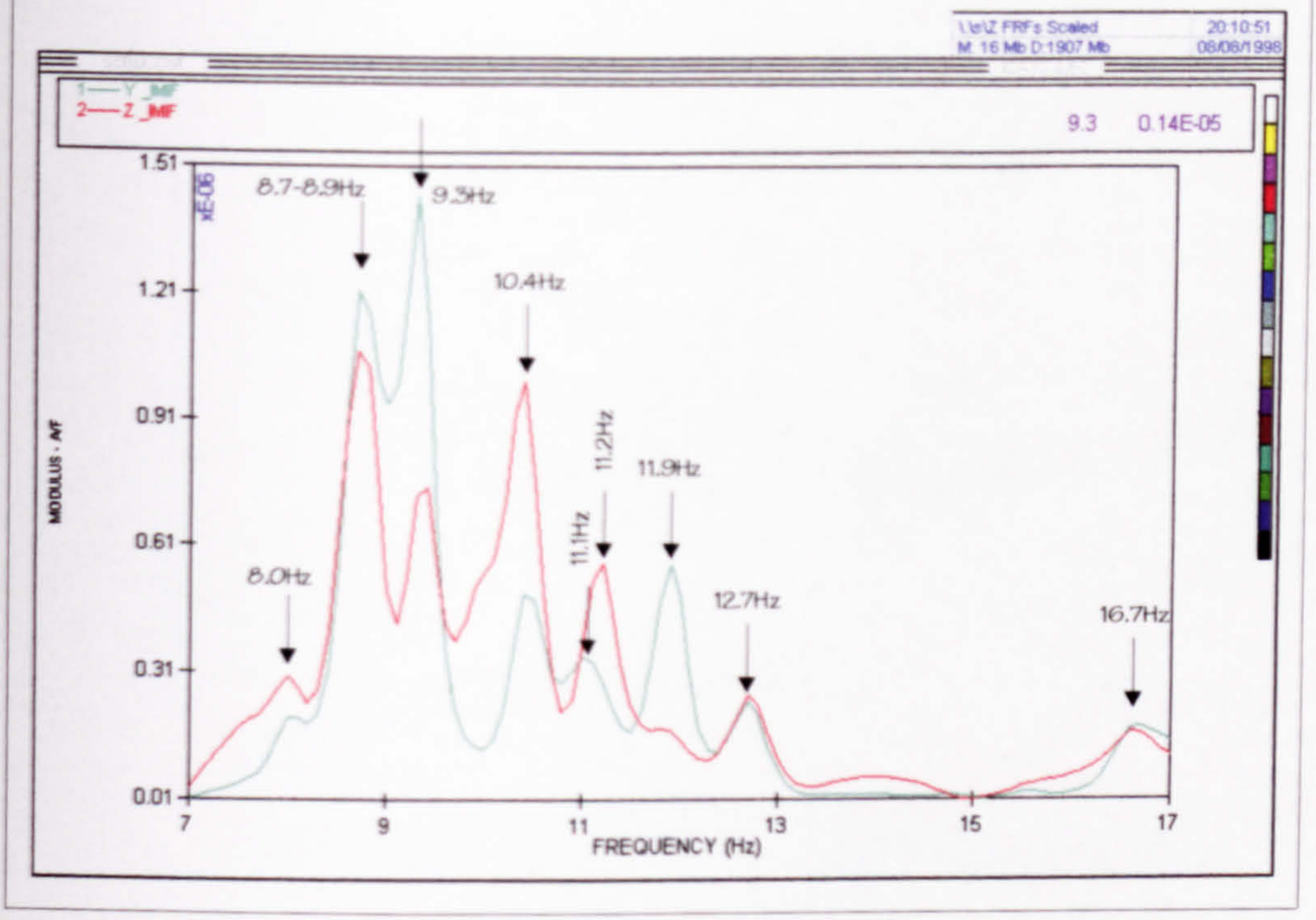

Figure 5.100: Structure D - Two MIFs produced after return to base and corresponding to TP26 (green line) and TP3 (red line).

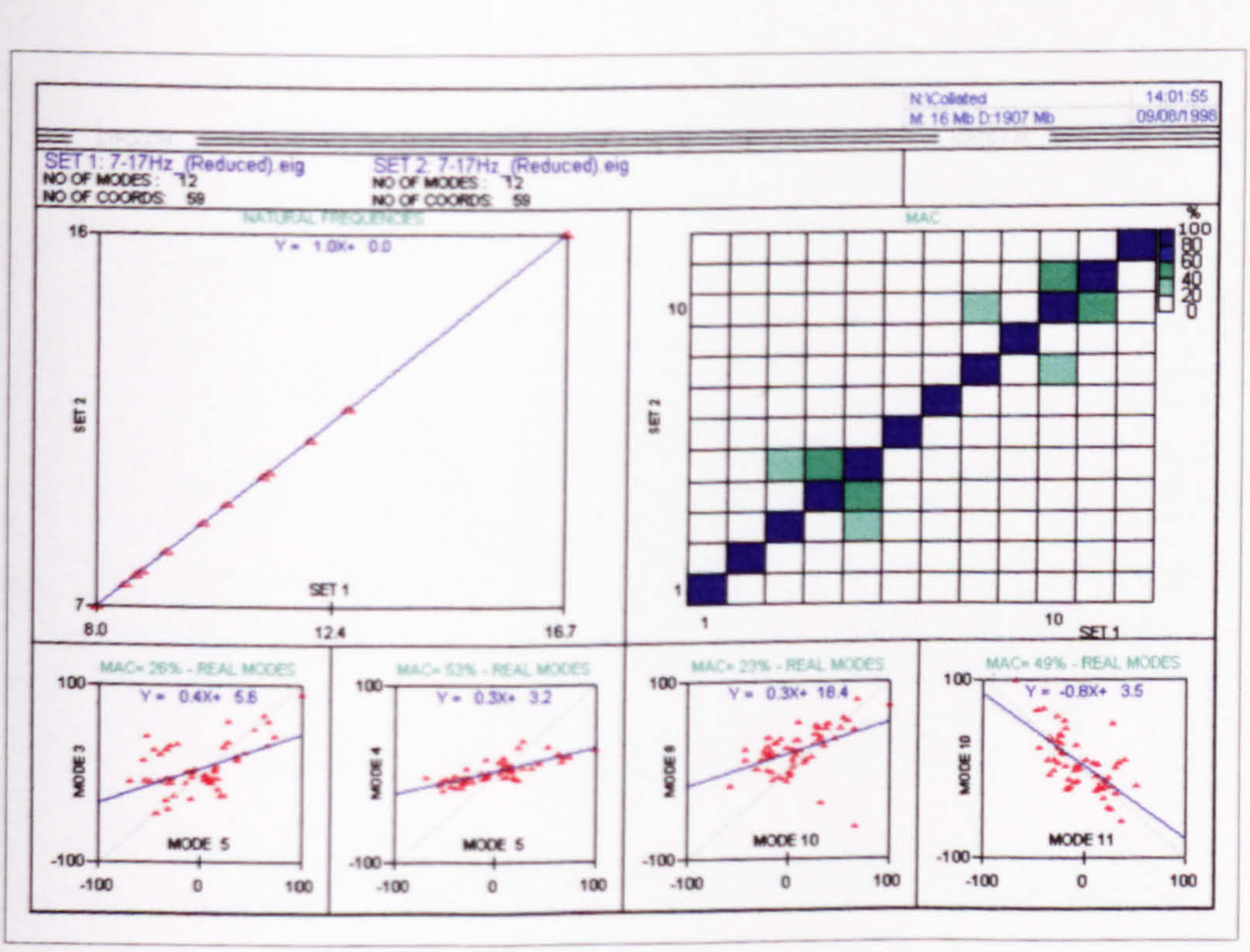

Figure 5.101: Structure D - Auto-MAC matrix calculated using 12 experimentally estimated mode shapes.

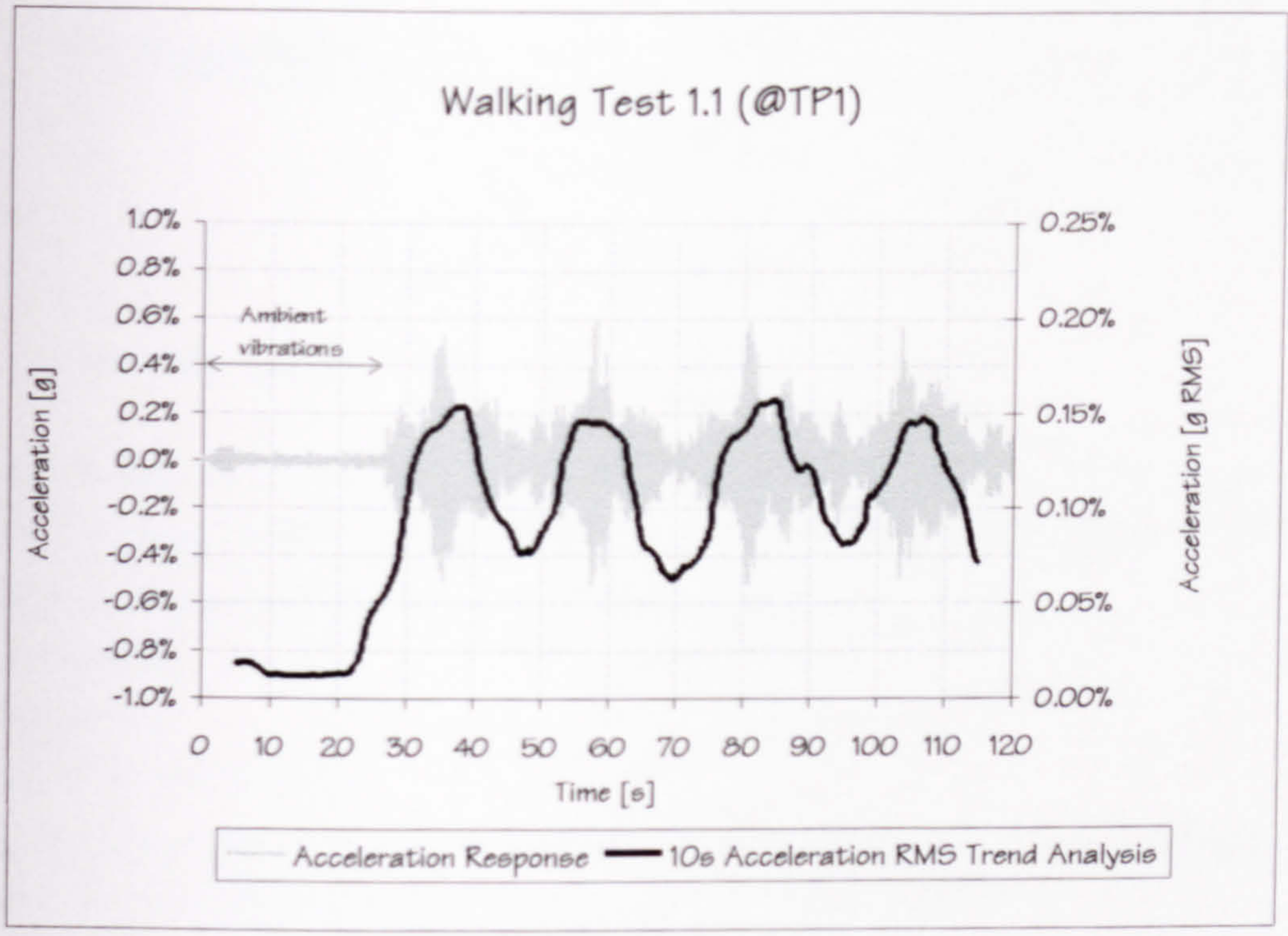

Figure 5.102: Structure D - Maximum response due to walking along Path 1 recorded at TP1.

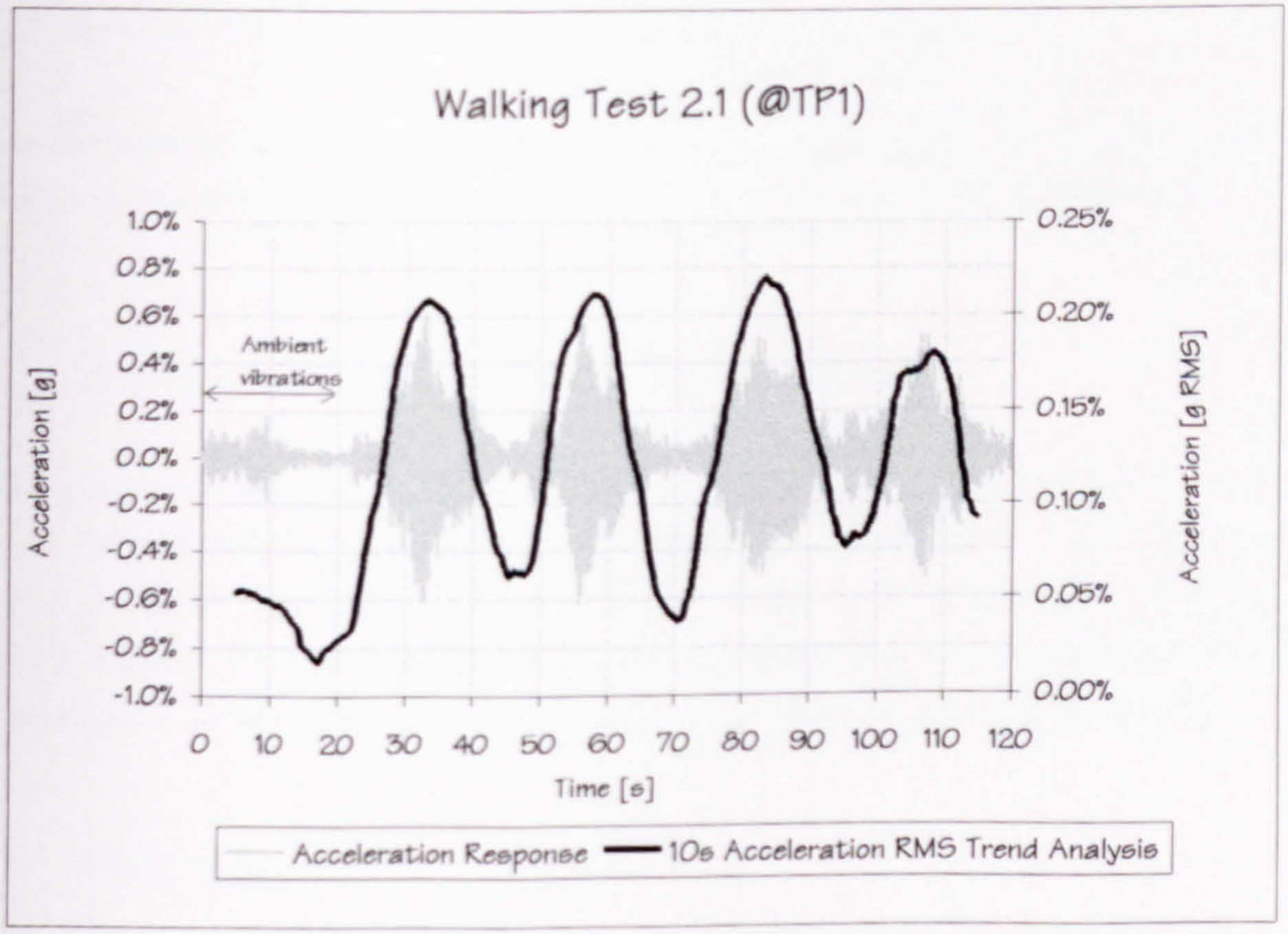

Figure 5.103: Structure D - Maximum response due to walking along Path 2 recorded at TP1.

6 Parametric Investigations

6.1 Introduction

This chapter describes the development of updated FE models which then served as test-beds for numerical simulations of walking excitation. The simulations were made by changing various parameters, including:

1. the nature of the forcing function (stationary or moving; steady-state or transient),
2. pacing frequency,
3. step length, and
4. position of the walking path.

Based on the comparison of these analytically calculated responses with their experimentally obtained counterparts, the performance of the selected excitation models will be assessed.

6.2 Structure A: Parametric Investigations

The general procedures used for the 'manual' FE model updating and analytical response calculations are presented first in considerable detail for Structure A, which was the simplest structure tested.

6.2.1 Structure A: FE Model Correlation and Updating

By comparing pre-test analytical results (Table 5.3 and Figure 5.13) with the measured modal properties (Table 5.5 and Figure 5.26), the measured and calculated frequencies for the 2nd and 3rd bending modes can be seen to correlate very well. However, the main interest here is in the first mode excitable by normal walking, which had a measured natural frequency (4.5 Hz) higher than that calculated (4.3 Hz). Therefore, the FE model had to be 'tuned' to match the experimental data which were assumed to be correct.

6.2.1.1 Material Properties

The discrepancy between the measured and initially calculated fundamental frequencies was attributed partly to the concrete density of 2400 kg/m^3 assumed in the pre-test analysis. As the modal and dynamic response tests were performed immediately after the slab was built, it was not practical to measure the density of the

concrete specimens taken during the casting of the slab and use this in the pre-test analysis. However, after the testing, specimens of known volume were weighed and it was established that 2300 kg/m^3 material density was a more appropriate value for the FE modelling. This increased the first calculated natural frequency to 4.4 Hz. In addition, to match the measured frequency of 4.5 Hz, $E_{c,dyn}$, another global material property which affects all modes of vibration, was increased from 38.0 GPa to 40.7 GPa.

6.2.1.2 MODEL MESHING

The amended material properties were used to re-calculate the natural frequencies using FE model 1 shown in Figure 6.1. The FE model was developed using ANSYS SHELL63, instead of BEAM4 elements used in the pre-test FE model. Although the pre-test modelling based on the grillage analogy produced quite reasonable results, the utilisation of SHELL63 was considered to be more appropriate and easier having in mind the practicalities when performing a manual FE model updating. Such shell elements were modelled as isotropic and had constant thickness of 275 mm.

The meshing was performed by the solid modelling technique where the number of divisions of solid modelling lines was controlled so that a model of a reasonable size was produced without losing accuracy. This was achieved by performing a number of trial studies in accordance with the NAFEMS (1992b) QA guidelines during which the mesh density and shape of the elements were varied.

Although the adopted mesh of FE model 1 shown in Figure 6.1 may look odd, during these trial QA runs it produced practically the same lowest natural frequencies and mode shapes as the more regular, detailed and expensive meshes. Apart from this, the adopted mesh also satisfied two additional requirements. Firstly, it had nodes at the geometric locations of the 27 test points, and, secondly, it had nodes every 0.3 m along the walking path line (Figure 6.1). The latter was required as the updated FE model had to be used to simulate responses due to a spatially varying force which moves from node to node along the walking path (representing a single pedestrian), and which also varies with time during this movement (Figure 6.7).

A comparison of the first five natural frequencies, measured on the prototype floor and calculated using FE model 1, is shown in Table 6.1.

Table 6.1: Structure A - Comparison of correlated (measured and calculated) natural frequencies using updated FE models 1 and 2.

Mode No.	Description	Measured frequency [Hz]	Pre-test grillage FE model [Hz]	Updated FE model 1 [Hz]	Updated FE model 2 [Hz]
1	1st vertical bending mode	4.5	4.3	4.5	4.5
2	2nd vertical bending mode	17.0	17.0	18.0	18.0
3	1st torsional ('rocking') mode	26.1	No correlation	No correlation	No correlation
4	2nd torsional ('bending') mode	29.1	45.7	35.8	34.4
5	3rd vertical bending mode	37.6	38.1	40.8	40.6

The results in Table 6.1 show that the FE model based on SHELL63 elements seems to be more appropriate to represent the torsional mode than the grillage model. However, although the first natural frequency of FE model 1 is now matched with its experimental counterpart, the correlation between the measured and calculated natural frequencies for the 2nd and 3rd vertical bending modes has worsened, compared with the pre-test model.

6.2.1.3 Boundary Conditions

This indicated that boundary conditions, as another important modelling parameter, might require updating too. Considering that a visual inspection of the 'knife edge' line supports of the slab showed that they were imperfect, the gaps observed, as mentioned in Chapter 5, were modelled by removing the pin-supports as appropriate. This is resulted in the model 1 being amended to model 2, as shown in Figure 6.1.

The most significant effect of the change in the boundary conditions was the reduction of the frequency of the torsional mode. The frequencies of the fundamental and the 2nd (vertical bending) modes were practically unaffected by this change, whilst the reduction of the natural frequency corresponding to the 3rd vertical bending mode was relatively small.

Further improvement of the FE model was likely to be possible by replacing the pin-supports by rotational and translational elastic springs and adjusting their properties to fit even better the experimental data. However, considering the dynamic properties of this particular structure and the purpose of the exercise, further improvement of the FE model was not deemed necessary. This is because Structure A has a well separated fundamental mode of vibration which was practically the only mode excited by walking. Also, in addition to matching the measured fundamental natural frequency, the updated FE model was capable of representing the modal mass m_1 of this mode quite well.

The latter was established by using the measured row of the FRF matrix which corresponded to the mid-span point (TP14, Figure 5.11) as the reference. Curve fitting was used to experimentally determine modal mass $m_{1,x}$ (ICATS, 1995; 1997). This procedure will be outlined.

6.2.1.4 CALCULATION OF MODAL MASS: EXPERIMENTAL APPROACH

Recalling the various types of FRF receptance equations given in Chapter 4 (Equations 4.4 or 4.5), the numerator for each element of the sum of modal contributions corresponding to, say, the r^{th} mode may be written as:

$$ {}_rA_{jk} = \frac{1}{m_r}(\psi_{jr})(\psi_{kr}) \qquad \text{Equation 6.1} $$

where ${}_rA_{jk}$ is termed the modal constant. For the FRF point mobility measurement which is made at the antinode (maximum displacement) point of the unity scaled shape of the r^{th} mode, it can be assumed that $j = k$ and that:

$$ (\psi_{jr}) = (\psi_{kr}) = 1.0 \qquad \text{Equation 6.2} $$

In this case, the modal constant ${}_rA_{jj}$, estimated from the curve fitting, will be:

$$ {}_rA_{jj} = \frac{1}{m_r} \cdot 1.0 = \frac{1}{m_r} \qquad \text{Equation 6.3} $$

where m_r is the modal (or effective) mass corresponding to the unity scaled r^{th} mode shape. Obviously, this modal mass can be calculated as an inverse of the modal constant ${}_rA_{jj}$.

Hence, to determine experimentally the modal mass for the fundamental mode of Structure A, an assumption was made that the pertinent antinode was at the slab strip mid-point (TP14). This was one more reason why this point was useful as the FRF reference point. The experimentally estimated modal mass $m_{1,X} = 6289\text{kg}$ compares favourably with the analytically (by ANSYS) calculated modal mass of $m_{1,A} = 6739\text{kg}$ for the unity scaled fundamental mode of model 2.

Matching the modal properties of the experimental and analytical fundamental mode of Structure A by changing the global material properties, such as the density and dynamic modulus of elasticity, affected the correlation of the higher modes to some extent. This is not particularly relevant in the case of the relatively simple Structure A, where only the fundamental mode is considered to be important. However, for the other, more complex structures tested, there was a need to establish how well not only the fundamental, but also the higher analytical and experimental modes correlated. For this, four methods for comparing the modal properties were used (ICATS, 1995; 1997; Ewins, 1995): (1) comparison of natural frequencies, (2) graphical comparison of mode shapes, (3) the Modal Assurance Criterion (MAC) and (4) the Co-Ordinate Modal Assurance Criterion (COMAC). These correlation methods are available in the ICATS suite of programmes and will be briefly introduced here, using Structure A as an example.

6.2.1.5 COMPARISON OF NATURAL FREQUENCIES, MAC, MODE SHAPES AND COMAC.

Tabulating and plotting of experimental vs. analytical natural frequencies is a simple but effective way of comparing the two sets of data. Table 6.1 and Figure 6.2 show that the experimental frequencies (data Set 1) for the 2nd and higher modes are all lower than their analytical counterparts (data Set 2).

The MAC matrix element corresponding to the ith experimental $\{\phi_X\}_i$ and jth analytical $\{\phi_A\}_j$ mode shape is defined as (Maia et al., 1997):

$$MAC\left(\{\phi_X\}_i, \{\phi_A\}_j\right) = \frac{\left|\{\phi_X\}_i^T \{\phi_A^*\}_j\right|^2}{\left(\{\phi_X\}_i^T \{\phi_A^*\}_j\right)\left(\{\phi_X\}_i^T \{\phi_A^*\}_j\right)} . \qquad \text{Equation 6.4}$$

Figure 6.2 shows the MAC matrix for Structure A. It indicates a very good correlation (MAC of 80% or greater) between the 1st, 2nd , and 5th experimental (data Set 1), and 1st, 2nd and 4th analytical (data Set 2) mode shapes, respectively.

However, caution is necessary when interpreting these results, as the MAC matrix also shows that the 3rd analytical mode shape (torsion-bending at 34.4 Hz) correlates well with two experimental modes (torsion-rocking at 26.9 Hz, and torsion-bending at 29.1 Hz). It is likely that imperfect and relatively complex boundary conditions allowing vertical displacement caused the torsion-rocking experimental mode to occur before the torsion-bending mode. The torsion-rocking could not be simulated by FE model 2 which was pin-supported. Therefore, the good MAC correlation between the 3rd modes in Sets 1 and 2 is actually false and should be discarded. All (un)correlated pairs of experimental and analytical modes of vibration, as indicated by the MAC matrix (Figure 6.2), are shown in Figure 6.3.

Whilst the MAC provides a good measure of global correlation between the mode shapes, when the correlation is not so good it fails to pinpoint geometrically the source of the error i.e. the DOFs generating the lack of correlation. Such a localisation of the error can be done by calculating the COMAC for each correlated DOF (Maia et al., 1997). The number of COMAC values, typically, matches the number of experimentally measured DOFs. Each COMAC value, which ranges between 0 and 1, assesses the performance of the corresponding DOF averaged over the set of correlated mode pairs. The COMAC for ith DOF in the mode shape is defined as (Maia et al., 1997):

$$COMAC(i) = \frac{\left(\sum_{j=1}^{n_{CMP}} \left|\left({}_A\phi_{ij}\right)\left({}_X\phi_{ij}\right)^*\right|\right)^2}{\left(\sum_{j=1}^{n_{CMP}} \left|\left({}_A\phi_{ij}\right)\right|^2\right)\left(\sum_{j=1}^{n_{CMP}} \left|\left({}_X\phi_{ij}\right)\right|^2\right)} \qquad \text{Equation 6.5}$$

where n_{CMP} is the number of the correlated mode pairs. Lower values of the COMAC indicate poorer performance of the particular DOF and possible errors either in its measurement or modelling.

In the case of Structure A, there are four correlated mode pairs (circled in Figure 6.2), so $n_{CMP} = 4$. Figure 6.2 shows the COMAC values for the measured DOFs of 27 test points. It indicates that the DOFs corresponding to the support points (TP1, TP10, TP18, TP19 and TP27) do not correlate well between experiment and analysis. These zones could have benefited from additional improvements of the boundary conditions in the analytical model, as mentioned earlier.

6.2.2 General Considerations of Response Calculations

To simplify the response calculation problem, practically all guidelines on the modelling of a single person walking treat the excitation as a stationary force. Not surprisingly, this is the key assumption of the three walking excitation models to be investigated in this thesis. These are:

- Walking Model 1 (WM1): proposed by the CEB (1991) and described by Bachmann et al. (1991b, 1995b) (Equation 3.22 and Table 3.1),
- Walking Model 2 (WM2): proposed by Eriksson (1994) (Table 3.3), and
- Walking Model 3 (WM3): proposed by Willford (1997) (Table 3.2).

These three walking excitation models are not the only ones available in the literature, as indicated in Chapter 2. However, due to the time limitations for this project, only these three models were selected to test their performance against experimental results for the following specific reasons.

Firstly, WM1 is interesting as it has been officially recommended by the CEB as appropriate for checking the vibration serviceability of concrete structures including long-span concrete floors. As such, this model deserves detailed scrutiny in this thesis. Secondly, WM2 is the result of very recent state-of-the-art research (Eriksson, 1994). However, as recommended by its developer, it requires further and independent performance testing, which will be done here. Finally, WM3 is used by Ove Arup & Partners, one of the biggest UK consultants in day-to-day design and, as such, would benefit from experimental verification. All three models consider a single person walking and are described in detail in Chapter 3.

An additional common feature of these excitation models is that the dynamic force caused by human walking may be assumed to be a sinusoid which frequency excites the steady-state resonance. Also, to simulate the worst case scenario, the force should, preferably, be applied at the antinode point of the mode excited (Eriksson, 1994; CEB, 1991).

However, the models differ considerably in the range of frequencies and amplitude of the sinusoid which represents the 'offending' harmonic of walking which excites the floor resonance (Figure 6.4). Sometimes this is a function of the weight of the person (WM1), sometimes it is not (WM2 and WM3) in which case an average person's weight (typically from 700 to 800 N) is implicitly assumed.

An assessment of the performance of such different excitation models which are, in principle, representing the same thing (i.e. an average person walking) is clearly warranted. This was done by performing the following two types of response analysis using the ANSYS FE code:

Type 1: Harmonic analysis in the frequency domain. Here, a stationary steady-state sinusoid having 1.0 N amplitude is applied at the antinode point of the pertinent mode. Assuming pure steady-state conditions, a point mobility FRF corresponding to this point is calculated. Its peaks are then scaled to accommodate for the different amplitudes of the sinusoids representing the walking excitation models investigated.

Type 2: Time domain transient analysis assuming a moving excitation force. Here, the same force models as in the previous steady-state analysis are moved along prescribed walking paths for a prescribed amount of time and with a prescribed speed.

However, to investigate the effects of the time required for steady state vibrations to build up, Structure A only was also subjected to a third type of excitation. Here, a single resonant sinusoid (WM2 and WM3), or a number of harmonics, of which one is resonant (WM1), as proposed by the CEB (1991) (Equation 3.22), are exciting an antinode of the appropriate mode shape only for a prescribed amount of time. Therefore, the response to this stationary excitation is transient in essence and requires time-domain calculations.

6.2.3 Structure A: Harmonic Analysis

Figure 6.5 shows the point mobility FRF corresponding to the middle of the slab strip. This was the antinode of the fundamental mode shape calculated using the updated FE model 2. The first five analytical modes shown in Figure 6.3 were used in the FRF calculation together with the measured modal damping ratios for the correlated experimental modes (Table 5.5). The peaks at 4.5 Hz and 40.6 Hz correspond to the analytically calculated 1st and 3rd vertical bending modes (Figure 6.3). The FRF peak value at 4.5 Hz is 0.0123 m/s^2 (0.125% g). After being scaled, the resulting acceleration responses are shown in Table 6.2.

Table 6.2: Structure A - Analytically calculated maximum steady-state resonant responses exciting the 4.5 Hz resonance.

Walking Model	Excitation amplitude [N]	Sinusoidal peak acceleration [% g]	RMS acceleration [% gRMS]
1 (excitation by 2nd harmonic)	75	9.4	6.6
1 (excitation by 3rd harmonic)	75	9.4	6.6
2	56	7.0	4.9
3	96	12.0	8.5

It should be noted that in the case of WM1, out of the three harmonics (Equation 3.22), only the 2nd or the 3rd harmonic was taken into consideration, which is a simplification suggested by the CEB (1991). In the case of

Eriksson's WM2, the RMS force amplitude of $F_{RMS} = 180/f$ [N] was multiplied by the FRF peak to obtain the RMS accelerations given in Table 6.2.

A comparison of the estimated responses in Table 6.2 with the measured values (Table 5.7) is given in Tables 6.3 and 6.4 for the 2nd and 3rd harmonic excitation, respectively.

Table 6.3: Structure A - A comparison of analytically calculated and experimentally measured maximum responses for the resonant excitation caused by the 2nd harmonic of walking excitation ($f_s = 2.25$Hz).

Walking model	Analytically calculated response [% gRMS]	Measured response to continuous excitation [% gRMS] (Error)	Measured response to transient excitation [% gRMS] (Error)
1	6.6	3.10 (113%)	1.72 (284%)
2	4.9	3.10 (58%)	1.72 (184%)
3	8.5	3.10 (174%)	1.72 (394%)

Table 6.4: Structure A - A comparison of analytically calculated and experimentally measured maximum responses for the resonant excitation caused by the 3rd harmonic of walking excitation ($f_s = 1.50$Hz).

Walking model	Analytically calculated response [% gRMS]	Measured response to continuous excitation [% gRMS] (Error)	Measured response to transient excitation [% gRMS] (Error)
1	6.6	0.92 (617%)	0.42 (1471%)
2	4.9	0.92 (432%)	0.42 (1066%)
3	8.5	0.92 (823%)	0.42 (1923%)

The experimental results indicate that very large overestimation errors are possible when compared with those determined analytically. This is particularly true for shorter transient excitations where the overestimation varied between about 2 to 20 times, depending on which walking harmonic excites the structure and which excitation model is used. Also, it appears that the continuous experimental excitation could not manage to establish the steady-state resonant conditions assumed by all three walking models. Although the 2nd harmonic of continuous excitation was relatively well modelled leading to smaller errors (Table 6.3), the responses to the 3rd harmonic were overestimated roughly between 4 and 8 times (Table 6.4).

According to Wyatt (1989), the 3rd harmonic excitation is particularly important when checking the vibration serviceability of building floors, so the comparisons presented indicate the potential for the walking excitation models to be overconservative when steady-state resonance is assumed.

6.2.4 Structure A: Transient Analysis under Stationary Walking Excitation

Figure 6.6 shows the build up of the acceleration response due to a stationary 4.5 Hz sinusoid of 1.0 N amplitude exciting resonance at the mid-point. Only the fundamental mode was assumed to participate in the response and the modal damping ratio was taken as 0.59% (Table 5.5). After approximately 6 seconds, which corresponds to the duration of a single pass across the floor corresponding to a pacing rate of $f_s = 2.25Hz$ (2^{nd} harmonic of walking creates the resonance), the acceleration peak response was 0.0075 m/s2 (0.076% g). This is only 60% of the resonant peak acceleration (Figure 6.6).

This quantifies the possible significance of the time required to build up the resonant response in floors having low-frequency and low damping. In principle, if this parameter was taken into consideration, then predicted responses corresponding to the 2^{nd} harmonic of transient walking which lasted approximately 6 s could safely be reduced to 60% of their original steady-state value. This would make the excitation models more reliable and would reduce the large overestimation error in the case of short lived excitation. However, this modelling is still not realistic as it considers the walking as treading in place.

6.2.5 Structure A: Transient Analysis under Moving Excitation

By the very nature of walking, the point of application of force moves as the walker traverses the floor. Therefore, the physically most representative walking forcing function, but also the most difficult to model, is one which changes in time and moves in space.

Considering that Structure A could be excited either by the 2^{nd} or by the 3^{rd} harmonic of walking, and that the stride length depends on the pacing rate (Figure 3.6), an attempt was made to simulate this situation using the updated FE model 2. To do this, ANSYS (1995a; 1995b) Parametric Design Language (APDL) was employed to develop a relatively simple programmable routine within the FE code which simulates the moving force along the prescribed walking paths.

6.2.5.1 The Moving Force Modelling

The idea behind this simulation is based on that used by Smith (1988) to calculate responses of footbridges under a human-induced moving load. The simulation assumes that a single point force spends a prescribed time interval at a single FE node on the walking path. This interval is equal to the time T_s required for making a single step, where:

$$T_s = \frac{1}{f_s} \qquad \text{Equation 6.6}$$

During the period T_s, the force acting on a single node is assumed to vary only with time as it is stationary. After each time interval T_s, the force instantaneously advances to another node along the walking path for the prescribed length and continues to change in time (Figure 6.7).

Compared with Smith's formula, developed for a simplified SDOF system, the advantage of the procedure developed here using APDL programming is that it is backed by the powerful FE code. This makes it very flexible and applicable to a very wide range of 2D and 3D structures, and it takes into account as many modes of vibration as necessary.

However, to simplify the FE model updating and the APDL programming, it was assumed in all simulations that an average person makes a single step of 0.6 m during a slow walk when $f_s \leq 2.0\text{Hz}$, whilst the step is 0.9 m during the fast walking assumed to happen when $f_s > 2.0\text{Hz}$. This is consistent with the graphical data given in Figure 3.6. Therefore, a walking path having equidistant nodes every 0.3 m was suitable for simulating both pacing rates, and was incorporated in the updated FE model, as mentioned before.

In the case of slower walking simulations, the force moved two 0.3 m segments every 0.67 s ($=1.5^{-1}$s) whilst in the case of the faster walking the force moved three segments every 0.44 s ($=2.25^{-1}$s). These times corresponded to a single stride. Therefore, to cross the 10.8 m beam, the force was applied for a total of 12 s when f_s=1.50 Hz, and 5.3 s for a pacing rate of 2.25 Hz. The developed APDL software routine allowed for the change of the pace length while keeping the pacing frequency constant. For example, walking with the pacing rate of f_s=1.50 Hz could be done in 8 s instead of 12 s if the stride length was assumed to be 0.9 m instead of 0.6 m. This is more realistic in terms of what was actually observed during the measurements (Figure 5.35), but is less realistic in terms of what is shown in Figure 3.6.

6.2.5.2 Structure A: WM1 Simulating a Single Crossing

Figure 6.8 shows the acceleration response to the excitation from WM1 tuned to the pacing rate of 2.25 Hz which lasted 5.3 s. Due to the relatively short acceleration time histories calculated, the comparison between the experiments and analytical modelling is given in terms of peak acceleration responses instead of 10 s gRMS values.

The stride length assumed was 0.9 m and all three excitation harmonics (Equation 3.22) were taken into account. The figure shows the time required to build the vibration and this, together with the calculated peak acccleration of 0.3635 m/s^2 (3.71% g), compare favourably with the measured response shown in Figure 5.43. Interestingly, and apparently only by chance, the measured peak response was also 3.71% g.

Figure 6.9 shows the simulation of the 3rd harmonic excitation ($f_s = 1.50\text{Hz}$) using WM1 where the force moved 0.6 m per stride. As the excitation model WM1 assumes the same dynamic loading factors for the 2nd and 3rd harmonics ($\alpha_2 = \alpha_3 = 0.1$), and as the slower moving force spent more time on the structure, the calculated response to the 3rd harmonic excitation was greater than for the 2nd harmonic excitation (Figure 6.8). This is contrary to what was observed in the experiments where the 2nd harmonic excitation produced a

considerably greater response. The simulated peak response to the 3rd harmonic excitation of 0.505 m/s^2 (5.15% g) (Figure 6.8) is almost six times greater than its measured counterpart of only 0.89% g(Figure 5.35). In the case when the length of a single stride is extended to 0.9 m, the simulated peak response was reduced to 0.439 m/s^2 (4.48% g), but this is still five times greater than the maximum experimentally observed peak response.

6.2.5.3 STRUCTURE A: WMS 2 & 3 SIMULATING A SINGLE CROSSING

WMs 2 and 3 are based on a single sinusoid and are the same in nature, the only difference being the amplitude of the sinusoids at various frequencies (Figure 6.6). Therefore, the responses to WM2 excitation were scaled as appropriate to obtain their counterparts for WM3.

As WMs 2 and 3 are not meant to be used as 'moving' forces, they do not make assumptions about the pacing frequency f_s and the duration of walking. Therefore, assumptions had to be made as to how the sinusoidal force moves. The obvious choice was to investigate the same three cases as for WM1. Firstly the fast walking at 2.25 steps of 0.9 m each per second, then the slower walking at 1.50 steps of 0.6 m each per second, and, finally, 1.50 steps of 0.9 m each per second.

After scaling the results to obtain responses to WM3, a comparison of the experimental and analytical peak responses is shown in Table 6.5.

Table 6.5: Structure A - Comparison of experimental peak responses with their analytical counterparts for moving WMs 2 and 3, single pass.

Excitation harmonic	Maximum measured experimental peak acceleration [% g]	Peak response for WM2 [% g] (Error)	Peak response for WM3 [% g] (Error)
2nd (f_s = 2.25Hz) 0.9 m/stride	3.71	2.48 (-33%)	4.25 (15%)
3rd (f_s = 1.50Hz) 0.6 m/stride	Not measured	3.74 (N/A)	6.41 (N/A)
3rd (f_s = 1.50Hz) 0.9 m/stride	0.89	3.14 (252%)	5.39 (506%)

Again, the results in Table 6.5 show that even the moving forces of WMs 2 and 3 overestimate significantly the responses to slower walking of 1.5 strides per second (3rd harmonic), which could be important for floor vibration checks. Nevertheless, the possibly beneficial effects of the transient analysis of moving loads are evident, as the amount of error has been considerably reduced when compared with the steady-state resonant modelling using the same forcing function (Table 6.4).

6.2.5.4 STRUCTURE A: WM1 SIMULATING MULTIPLE CROSSINGS LASTING 120 S

The ANSYS APDL routine developed for simulating a single strip crossing was used to generate several passes along the slab-strip (from 'Start' to 'End' and back, as shown in Figure 6.1). The total duration of the simulation was 120 s. Figure 6.10 shows the simulated acceleration response at mid-point of the slab strip to the 2nd harmonic of WM1 excitation. The stride length was assumed to be 0.9 m, as appropriate for the pacing rate of 2.25 steps per second. The 10 s RMS trend analysis of the 120 s long acceleration time history having a maximum of 2.1% gRMS is shown in Figure 6.14. This is lower than the measured peak value of 3.1% gRMS (Figure 5.35). The general shapes of the measured (Figures 5.30 and 5.31) and calculated (Figure 6.10) acceleration time history are however comparable.

Regarding the simulation of the 3rd harmonic excitation, Figure 6.11 shows the calculated acceleration time history assuming a 0.6 m stride length only. Its RMS trend analysis is shown in Figure 6.14 and should be compared with the measured data shown in Figures 5.32 and 5.33, and in Table 5.7. The calculated peak of 2.3% gRMS is 2.5 times higher than 0.92% gRMS, which was the maximum measured RMS acceleration. Although the amount of overestimation error in calculating the 3rd harmonic responses has been reduced from 617% (see Table 6.4) to 250%, after the excitation was assumed to be transient and moving instead of steady-state and stationary, the error is still significant. This is, again, a strong indication that there may be problems in the modelling of the 3rd harmonic in WM1. This is particularly so as the calculated peak RMS responses shown in Figure 6.14 are higher for the slower 3rd than for the faster 2nd harmonic excitation, which is totally inconsistent with the experimental data shown in Table 5.7.

6.2.5.5 STRUCTURE A: WMS 2 & 3 SIMULATING MULTIPLE CROSSINGS LASTING 120 S

Similar analysis as for WM1 was performed for the remaining two walking models. Figures 6.12 and 6.13 show 120 s of simulated acceleration response to WM2. The assumed pacing rates were 2.25 (0.9 m stride) and 1.50 steps (0.6 m stride) per second, respectively. The corresponding pair of 10 s RMS trend analyses are given in Figure 6.15. The comparison between the measured and calculated peak gRMS values is given in Table 6.6. This table also contains results pertinent to WM3, produced after the appropriate scaling of WM2 data.

Table 6.6: Structure A - Comparison of the measured and calculated RMS trend peaks obtained for moving WMs 2 and 3, multiple passes.

Excitation harmonic	Measured peak RMS acceleration [% gRMS]	Calculated peak RMS acceleration using WM2 [% gRMS] (Error)	Calculated peak RMS acceleration using WM3 [% gRMS] (Error)
2nd ($f_s = 2.25$Hz) (0.9 m/stride)	3.10	1.56 (-50%)	2.67 (-14%)
3rd ($f_s = 1.50$Hz) (0.6 m/stride)	0.92	1.66 (80%)	2.84 (209%)

These results will be discussed further in Chapter 7.

6.3 Structure B: Parametric Investigations

The parametric investigations pertinent to Structure B were:

1. FE model correlation and updating of uncracked Structure B,
2. FE model correlation and updating of cracked Structure B, and
3. Response simulations using the latter updated model.

6.3.1 Structure B (Uncracked): FE Model Correlation and Updating

The aim of the manual updating of uncracked Structure B was to match the lowest three measured modes of vibration with their analytical counterparts. The first FE model updating step, taken to address the observed lack of stiffness in the pre-test FE model, was to model the 300x300 mm columns.

The FE modelling was initially performed using a regular symmetric mesh of isotropic SHELL63 elements. The four columns, having 1.6 m clear height (Figure 5.38), were modelled using four identical BEAM4 elements. The columns were assumed to be rigidly connected to the HSC slab and fully fixed at their bottoms (Figure 6.16). The main FE model tuning parameters were the length of the columns, assumed to be fully fixed at their bases, and the dynamic modulus of elasticity of concrete assumed to be the same in the slab and columns.

After a number of trial and error attempts, a length of 1.925 m of column system lines and a dynamic modulus of elasticity $E_{c,dyn} = 46.7$ GPa for the HSC produced analytical modes which correlated well with the selected three lowest measured modes of vibration. This is illustrated in Figures 6.17 and 6.18. The MAC matrix in Figure 6.17 shows that the 3rd analytical mode shape (data Set 2) did not correlate with any of the measured modes (data Set 1), whereas the 4th analytical mode clearly corresponded to the 3rd measured mode (Figure 6.18).

This updating exercise showed that:

1. high-strength concrete can be expected to have a significantly increased dynamic modulus of elasticity compared to concretes of normal strength, and these increased values may be used in vibration serviceability calculations,
2. the in-situ cast columns supporting uncracked in-situ cast concrete floors can be expected to have a significant stiffening effect and should not be modelled as pin-supports, and

3. if the concrete floor of a flat plate configuration is uncracked, very reasonable FE modelling can be achieved by using isotropic shell elements, such as SHELL63 in ANSYS.

6.3.2 Structure B (Cracked): FE Model Correlation and Updating

Considering the cracking patterns in the slab and columns (Figures 5.53 and 5.54) and the required walking paths (Figure 5.58), FE model 2 was developed (Figure 6.19). The slab of this model consisted of four rectangular areas (Areas 1, 2, 3 and 4) and one square area around the columns (Area 5). The dimensions of these areas and the orthotropic stiffness of the SHELL63 elements in the five areas could differ between the areas and could be parametrically changed during the updating. In addition, the cracked tops (25% of the height) of the four columns were modelled with BEAM4 elements whose bending stiffness could be parametrically changed and be different from that of the BEAM4 elements representing the lower uncracked portion of the columns. The three walking paths shown in Figure 6.19 were established in a similar way as for Structure A, and equidistant nodes were distributed every 0.3 m along each of them. The first analysis performed using FE model 2 (Figure 6.19) was to check it against the results produced by the already verified model 1 (Figure 6.16), when identical material and stiffness (i.e. uncracked) conditions were assumed. Model 2 produced the relevant natural frequencies and mode shapes practically identical to model 1 proving that it was a good starting point for the manual updating aimed at simulating the cracked conditions.

Subsequent exercises related to modelling of the cracked conditions proved to be much more difficult and time consuming compared to their counterpart for the uncracked case. The main updating parameters used were:

1. the dimensions of the five cracked areas,
2. the five pairs of orthotropic bending stiffnesses corresponding to the five areas,
3. the dynamic modulus of elasticity for HSC, and
4. the bending stiffness of the cracked tops of the columns.

The results of the updating pertinent to the bending stiffnesses in the five areas are given in Table 6.7.

Table 6.7: Structure B (Cracked) - Updated parameters related to the properties of the five areas.

Area	Rectangular area dimension in x direction [m]	Rectangular area dimension in y direction [m]	Percentage of 'uncracked' bending stiffness in x direction	Percentage of 'uncracked' bending stiffness in y direction
1*	n/a	n/a	100%	100%
2	12.6	3.0	100%	58%
3	2.4	12.0	40%	100%
4	2.4	3.0	40%	75%
5	3.6	3.6	90%	35%

*Area 1 is uncracked

In addition, the updated dynamic modulus of elasticity was 47.5 GPa (increased from 46.7 GPa for uncracked model) and the cracked column bending stiffness was reduced to 78% of its uncracked stiffness. The last result indicates that even the visibly cracked HSC columns could be able to retain a significant portion of their uncracked stiffness for the level of excitation applied during the modal testing.

The updated FE model representing the cracked state of Structure B is shown in Figure 6.20. The calculated analytical mode shapes for the lowest 10 modes of vibration are shown in Figure 6.22 and the calculated unity-scaled modal masses for these 10 modes are presented in Table 6.8.

Table 6.8: Structure B (Cracked) - The analytically calculated natural frequencies and modal masses using the updated FE model.

Mode	Natural frequency [Hz]	Modal mass [kg]
1	4.69	34,390
2	4.96	46,980
3	6.81	13,642
4	7.14	14,569
5	9.57	7,768
6	10.14	7,536
7	10.27	23,536
8	10.43	6,666
9	13.03	10,607
10	15.47	17,657

Note: Highlighted are the analytical modes well correlated with the experimental data.

The comparison of analytical and measured natural frequencies, MAC and COMAC are given in Figure 6.21. It appears that the improved analytical FE model would have benefited from further updating, especially a refinement of distribution of stiffness in Areas 2 and 3. However, this would be difficult to do manually and an automatic updating procedure supported by appropriate software would be more efficient. This is, however, beyond the scope of this thesis.

Nevertheless, a visual comparison of mode shapes (Figure 6.23) shows that the manually updated FE model managed to capture the main features of the measured modes of vibration excitable by walking at 4.7 Hz, 5.0 Hz and 7.1 Hz. Also, it simulates remarkably well two higher measured modes at 13.0 Hz and 15.6 Hz. All this increases the confidence in this FE model as to its suitability to simulate walking excitations.

6.3.3 Structure B (Cracked) - Harmonic Analysis

Figure 6.24 shows three point mobility FRFs, calculated using the updated FE model, at antinodes of the analytical modes 1, 2 and 4 (Figure 6.22). These antinodes are in fact at the exact geometric locations of test points TP25 (mode 1), TP46 (mode 2) and TP22 (mode 4). Moreover, to simulate responses measured at the other two locations in each test (Table 5.13) additional transfer mobilities were created (Figures 6.25-6.27). For example, Figure 6.25 shows point and transfer mobilities used to simulate responses while walking along

WP1. When using these FRFs it has been assumed that the excitation is always at TP25 (antinode), and that responses are at the points where the accelerometers were positioned (TP25, 43 and 49). Similarly, Figures 6.26 and 6.27 present the three FRFs used to simulate walking along WPs 2 and 3. A summary of harmonic forces and FRF peaks used in these simulations is shown in Table 6.9.

Table 6.9: Structure B (Cracked) - A summary of harmonic forces and FRF peak values used to simulate resonant excitation by WM1, 2 and 3.

Test	Accel @TP	Excitation harmonic	Natural frequency excited [Hz]	WM1 Force [N]	WM2 Force [N]	WM3 Force [N]	FRF; FRF Peak [m/s^2]
1.1a	25	2nd	4.7	75	54	96	H(25,25); 0.00104
1.1b	43	2nd	4.7	75	54	96	H(43,25); 0.00101
1.1c	49	2nd	4.7	75	54	96	H(49,25); 0.00100
1.2a	25	3rd	4.7	75	54	96	H(25,25); 0.00104
1.2b	43	3rd	4.7	75	54	96	H(43,25); 0.00101
1.2c	49	3rd	4.7	75	54	96	H(49,25); 0.00100
2.1a	46	2nd	5.0	75	51	48	H(46,46); 0.00117
2.1b	28	2nd	5.0	75	51	48	H(28,46); 0.00124
2.1c	22	2nd	5.0	75	51	48	H(22,46); 0.00130
2.2a	46	3rd	5.0	75	51	48	H(46,46); 0.00117
2.2b	22	3rd	5.0	75	51	48	H(22,46); 0.00124
2.2c	28	3rd	5.0	75	51	48	H(28,46); 0.00130
3.1a	22	3rd	7.1	75	36	48	H(22,22); 0.00302
3.1b	28	3rd	7.1	75	36	48	H(28,22); 0.00301
3.1c	27	3rd	7.1	75	36	48	H(27,22); 0.00168
3.2a	22	4th	7.1	n/a	36	48	H(22,22); 0.00302
3.2b	28	4th	7.1	n/a	36	48	H(28,22); 0.00301
3.2c	27	4th	7.1	n/a	36	48	H(27,22); 0.00168

Table 6.10 presents a comparison of measured and simulated acceleration responses in terms of (10 s) gRMS values.

Table 6.10: Structure B (Cracked) - A comparison of experimentally measured and analytically calculated maximum acceleration responses for the resonant excitation by WM1, 2 and 3 assumed to be stationary.

Test	Excitation harmonic	Natural frequency excited [Hz]	Measured [% gRMS]	WM1 simulation [% gRMS] (Error)	WM2 simulation [% gRMS] (Error)	WM3 simulation [% gRMS] (Error)
1.1a	2nd	4.7	0.418	0.562 (34%)	0.405 (-3%)	0.720 (72%)
1.1b	2nd	4.7	0.370	0.546 (48%)	0.393 (6%)	0.699 (89%)
1.1c	2nd	4.7	0.368	0.541 (47%)	0.389 (6%)	0.692 (88%)
1.2a	3rd	4.7	0.200	0.562 (181%)	0.405 (102%)	0.720 (260%)
1.2b	3rd	4.7	0.176	0.546 (210%)	0.393 (123%)	0.699 (297%)
1.2c	3rd	4.7	0.173	0.541 (212%)	0.389 (125%)	0.692 (300%)
2.1a	2nd	5.0	0.512	0.632 (24%)	0.428 (-16%)	0.405 (-21%)
2.1b	2nd	5.0	0.489	0.670 (37%)	0.454 (-7%)	0.429 (-12%)
2.1c	2nd	5.0	0.479	0.703 (47%)	0.476 (-1%)	0.450 (-6%)
2.2a	3rd	5.0	0.373	0.632 (69%)	0.428 (-15%)	0.405 (9%)

Test	Excitation harmonic	Natural frequency excited [Hz]	Measured [% gRMS]	WM1 simulation [% gRMS] (Error)	WM2 simulation [% gRMS] (Error)	WM3 simulation [% gRMS] (Error)
2.2b	3rd	5.0	0.342	0.670 (96%)	0.454 (33%)	0.429 (25%)
2.2c	3rd	5.0	0.339	0.703 (107%)	0.476 (40%)	0.450 (33%)
3.1a	3rd	7.1	0.410	1.632 (298%)	0.778 (90%)	1.045 (155%)
3.1b	3rd	7.1	0.368	1.627 (342%)	0.775 (111%)	1.041 (183%)
3.1c	3rd	7.1	0.218	0.908 (317%)	0.433 (99%)	0.581 (167%)
3.2a	4th	7.1	0.332	n/a	0.778 (134%)	1.045 (215%)
3.2b	4th	7.1	0.309	n/a	0.775 (151%)	1.041 (237%)
3.2c	4th	7.1	0.162	n/a	0.433 (167%)	0.581 (259%)

These results show that WM1 again overestimated all responses, and particularly those pertinent to the 3rd harmonic excitation (Tests 1.2, 2.2 and 3.1). Performance of WM1 regarding the 2nd harmonic excitation was relatively reasonable. However, another shortcoming of WM1 is that it does not have a provision for the 4th harmonic of excitation, which, as shown by Test 3.2 measurements, may be an issue. In the case of the cracked Structure B, this issue was raised almost certainly due to very low modal mass corresponding to the mode of vibration at 7.1 Hz excited in Tests 3.1 and 3.2. The modal mass of 14,569 kg (Table 6.8) is only approximately 10% of the total mass of the floor. This illustrates that it is of utmost importance to analyse not only the fundamental, but all modes of vibration excitable by normal walking.

As to the performance of WM2 it can be seen that it overestimates the responses to the 4th harmonic of walking, and performs much better than WM1 regarding the response to the 3rd harmonic of excitation.

Finally, WM3 is very conservative regarding the 3rd and 4th harmonic excitation of modes having natural frequencies of 4.7 Hz and 7.1 Hz. However, it appears that a sudden halving of forcing amplitudes at 4.8 Hz (Table 3.2 and Figure 6.4) was not warranted.

6.3.4 Structure B (Cracked) - Transient Analysis under Moving Excitation

The three walking models were used to simulate the measured responses assuming that the excitation force moves along one of the three walking paths. The pacing rates were adjusted to excite an appropriate mode at 4.7, 5.0 or 7.1 Hz. The step lengths were adjusted similarly as for Structure A: to 0.6 m if a pacing rate was less than 2 steps per second, or to 0.9 m if $f_s > 2$ Hz. Due to computing limitations, acceleration time histories lasting only 60 s (instead of the measured 120 s) were calculated and processed further. Only responses at the respective antinodes of modes at 4.7 Hz (TP25), 5.0 Hz (TP46) and 7.1 Hz (TP22) were calculated. Figure 6.28 shows the simulation of Test 1.1a using WM1 excitation moving along WP1 (Figure 6.19). Using the same walking model, maximum responses in other tests were simulated over 60 s and five RMS trend analyses are shown in Figure 6.29. Similarly, Figure 6.30 shows an example of the calculated acceleration time-history corresponding to WM2 excitation of the mode at 7.1 Hz while moving along WP3 (Figure 6.19). Figure 6.31 shows the results of all six acceleration trend analyses which correspond to the

maximum responses achieved in simulations of Tests 1.1a, 1.2a, 2.1a, 2.2a, 3.1a and 3.2a. Responses to WM3 were obtained by scaling the results from WM2, as appropriate. Table 6.11 summarises and compares the maximum values of all measured and calculated RMS trend analyses for the cracked Structure B.

Table 6.11: Structure B (Cracked) - A comparison of analytically calculated and experimentally measured maximum responses for the excitation by WM1, 2 and 3, assumed to be moving.

Test	Excitation harmonic	Natural frequency excited [Hz]	Measured [% gRMS]	WM1 simulation [% gRMS] (Error)	WM2 simulation [% gRMS] (Error)	WM3 simulation [% gRMS] (Error)
1.1a	2nd	4.7	0.418	0.342 (-18%)	0.231 (-45%)	0.579 (39%)
1.2a	3rd	4.7	0.200	0.362 (81%)	0.236 (18%)	0.592 (196%)
2.1a	2nd	5.0	0.512	0.428 (-16%)	0.198 (-61%)	0.264 (-48%)
2.2a	3rd	5.0	0.373	0.389 (4%)	0.215 (-42%)	0.287 (-23%)
3.1a	3rd	7.1	0.410	0.536 (31%)	0.222 (-46%)	0.420 (2%)
3.2a	4th	7.1	0.332	n/a	0.260 (-22%)	0.490 (48%)

One measured and three simulated 10 s RMS trend analyses corresponding to Test 1.2a are shown in Figure 6.32. As indicated in Table 6.11, this figure shows that even when modelled as a moving load, WM3 significantly overestimates the response, whereas WM2 is a fair representation of the measured RMS trend. However, Figure 6.33 shows that in the case of Test 3.1a, WM3 is a very good representation of the measured trend, while WM2 underestimates it. In Tests 1.2a, 2.2a and 3.1a WM1 overestimates the response to the 3rd harmonic excitation, but to a much lesser extent then when assumed to be a stationary resonant excitation (Table 6.10).

6.4 Structure C: Parametric Investigations

The parametric investigations pertinent to Structure C were:

1. FE model correlation and updating of the unclad Structure C,
2. FE model correlation and updating of the clad Structure C, and
3. response simulations using the latter updated model.

6.4.1 Structure C (Unclad): FE Model Correlation and Updating

The main aim of the FE model updating was to match the first three measured and calculated modes as well as was practicably possible. The starting model for the manual updating was the pre-test FE model and a comparison of its natural frequencies and those measured for the first three modes is given in Table 6.12.

Table 6.12: Structure C (Unclad) - Comparison of measured and updated natural frequencies.

Mode No.	Pre-test FE model natural frequency [Hz]	Measured natural frequency [Hz]	Updated FE model frequency [Hz]
1	5.2	6.0	6.0
2	5.5	6.5	6.5
3	6.6	8.1	8.1

The first three initially calculated (Figure 5.69) and measured (Figure 5.76) mode shapes correlate well. However, their frequencies do not compare well and the first two columns of frequencies in Table 6.12 show not only discrepancies between the corresponding frequency values, but also discrepancies in the intervals between them.

The values of measured frequencies and their separations indicated that simply changing a global property, such as the dynamic modulus or the density of concrete, which were assumed to be consistent throughout the structure, was not likely to produce much improved results. Therefore, in addition to the concrete dynamic modulus and density, a number of other updating parameters was selected. These were:

1. the floor lateral stiffness,
2. the column bending stiffness and boundary conditions at the end of the columns,
3. the stiffness of the floor support at the lift shaft at the North edge of the floor (Figure 5.66); this was necessary as special steel dowels allowing horizontal movements and preventing vertical displacements served as the connection between the PT slab and the lift shaft, and
4. the torsional stiffness of the edge beams around the 'main' floor area.

The updating involved about 50 simulations leading to a finally updated model having much improved natural frequencies, as shown in Table 6.12. The updated model is shown in Figure 6.34. There were three main conclusions of this very interesting but time-consuming exercise.

Firstly, an unrealistic change of a global updating parameter (say the dynamic modulus of concrete) which led to matching one natural frequency also resulted in unmatched values for the other two frequencies.

Secondly, the updated FE model had to feature columns and these were modelled as elastic bar elements rigidly connected to the slab, having a full (clear) height up to the floor above and down to the floor below to which they were assumed to be fully fixed. During the updating exercises it became clear that the FE models where columns were modelled as pin-supports did not permit the first three natural frequencies to be matched while keeping other updating parameters within their realistic boundaries.

Finally, the frequency separation between the modes was particularly sensitive to the changes in the lateral floor stiffness, and, to a lesser extent, to the changes in bending stiffness of the columns along the East and West edges and in the torsional beam stiffnesses along the same edges. This behaviour can be explained if the floor's mode shapes $\{\phi_r\}$ are thought of as vectors which minimise the Rayleigh quotient $\lambda_r \left(= \omega_r^2\right)$ given as:

$$\lambda_r = \omega_r^2 = \frac{\{\phi_r\}^T[K]\{\phi_r\}}{\{\phi_r\}^T[M]\{\phi_r\}} \qquad \text{Equation 6.7}$$

where ω_r^2 is the r^{th} natural frequency of the floor. If lower modes are of interest, as is the case when considering the floor's vibration serviceability, Equation 6.7 indicates that λ_r will tend to be minimised when its numerator $\{\phi_r\}^T[K]\{\phi_r\}$ is minimised and denominator $\{\phi_r\}^T[M]\{\phi_r\}$ is maximised. These terms are proportional to the strain and kinetic energies (NAFEMS, 1992b), respectively, when the structure vibrates harmonically in one of its modes of vibration. This is the reason why the lowest floor mode shape is always curving gently, so that strain energy is low, but most of it is moving, hence the kinetic energy is high. The next higher mode shape will tend to preserve the kinetic energy as much as possible, but also add as little as possible strain energy. This is precisely the reason why the fundamental and several of the higher modes of Structure C shown in Figures 5.69 and 5.76 bend more in the less stiff lateral direction while essentially preserving the same smooth half-wave deformation shape in the much stiffer N-S direction. The stiffer direction essentially controls the lowest Rayleigh quotient i.e. the frequency of the fundamental mode of vibration if the floor is relatively 'weak' in the lateral direction, as is the case with Structure C. Therefore, in order to increase the frequency separation between the fundamental and the higher modes, whilst keeping the frequency of the fundamental mode more or less unchanged, it is necessary to increase stiffness in the lateral direction, as this stiffness has little influence on the frequency of the fundamental mode and is engaged much more in the higher modes.

Figure 6.35 shows the comparison between the measured results and those from the updated FE model. Five pairs of modes were used for the correlation and it is clear that for the first three pairs, the natural frequencies match well with the corresponding MAC values all above 80%. This indicates significantly improved reliability of the analytical modelling compared to the pre-test model, the development of which was based mainly on engineering judgement. A list of starting and final updated parameters is given in Table 6.13. The list indicates some fundamental properties related to the dynamic behaviour of in-situ cast PT floors which will be discussed further in Chapter 7.

Table 6.13: Structure C (Unclad) - Starting and final FE model updating parameters.

Updated parameter	Starting model and/or value	Final model/value
Dynamic modulus of concrete	38.0 GPa	40.5 GPa
Concrete density	2400 kg/m^3	2400 kg/m^3
North lift shaft vertical stiffness	Pin support (infinite stiffness)	$750 \cdot 10^6$ N/m per each of five vertical COMBIN14 springs
Columns	Pin support (infinite vertical and no rotational stiffness)	BEAM4 uniaxial beam having 1500/200 mm cross section; full column height of 2·2.79 m modelled; column ends fully fixed
Lateral floor stiffness in E-W direction	10% of the stiffness in the ribbed N-S direction	25% of the stiffness in the ribbed N-S direction
Torsional stiffness of edge beams	Stiffness K_T corresponding to a rectangular 1050/300 mm cross section	$5 \cdot K_T$

6.4.2 Structure C (Clad): FE Model Correlation and Updating

The main aim of the FE model updating, based on the experimental results gathered during the second round of modal testing of a bare floor in the clad building, was to create a more reliable analytical model suitable for the simulation of walking responses which were also measured during this round of dynamic testing in June 1996.

As natural frequencies changed between the bare floor in the unclad and clad building, it was clear that the previously updated FE model having the fundamental mode at 6.0 Hz would no longer be suitable for the simulation of walking responses measured on the floor now having the first measured natural frequency of 6.4 Hz. Table 6.14 shows a comparison of the first three natural frequencies measured in the unclad and clad building.

Table 6.14: Structure C - Comparison of the first three measured natural frequencies for the bare floor in the unclad (December 1995 measurements) and clad (June 1996 measurements) building.

Mode No.	Unclad building [Hz]	Clad building [Hz]
1	6.0	6.4
2	6.5	6.9
3	8.1	8.2

Obviously, something changed between December 1995 and June 1996 which caused the stiffening of the floor system and increases in the natural frequencies of interest. Apart from the temperature, which was 20^0C higher in June than in January, other visible changes were the presence of the installations underneath the floor (Figure 5.78) and the façade wall. These are difficult to model and it was hoped that the updating exercise would provide a better understanding of the effects of the installations and façade and of their modelling. Also, it was possible that some other unforeseen factors might have affected the natural frequencies.

A very good starting point for this round of FE model updating was the already updated FE model for the floor in the unclad building (Table 6.12 and Figure 6.34).

After several trial and error attempts the following parameters were selected for updating:

- The dynamic modulus of concrete;
- The lateral floor bending stiffness;
- The main longitudinal floor bending stiffness;
- Material density to take into account the weight of additional installations;
- The stiffness of columns along the East, West and North floor outer edges (Figure 5.66).

After approximately 70 simulations, an updated FE model was developed. Its correlation with the measured mode shapes and natural frequencies are shown in Figure 6.36. Seven pairs of experimental and analytical modes correlated quite well in terms of mode shapes and natural frequencies, and a visual comparison of the

first three correlated mode pairs is shown in Figure 6.37. A list of measured and updated frequencies in given in Table 6.15.

Table 6.15: Structure C (Clad) - Measured, starting model and updated model frequencies, and unity scaled modal mass of the updated FE model.

Mode No.	Measured natural frequency [Hz]	Starting FE model natural frequency [Hz]	Updated FE model natural frequency [Hz]	Modal mass of updated modes [kg]
1	6.4	6.0	6.4	72,649
2	6.9	6.5	6.9	56,264
3	8.2	8.1	8.2	49,286
4	10.2	10.5	10.2	60,455
5	11.9	12.9	12.4	59,745
6	15.0	15.7	15.3	61,952
7	17.4	16.0	17.4	55,753

A list of starting and final updated parameters which led to the much improved matching of frequencies and mode shapes in the updated FE model is presented in Table 6.16. All updated parameters are within reasonable boundaries.

Table 6.16: Structure C (Clad) - Starting and final FE model updating parameters.

Updated parameter	Starting model and/or value	Final model/value
Dynamic modulus of concrete	40.5 GPa	42.7 GPa
Additional mass of installations	0 kg/m^3	10 kg/m^3
North lift shaft vertical stiffness	Pin support (infinite stiffness)	750·10^6 N/m per each of five vertical COMBIN14 springs
North lift shaft rotational stiffness along the longer lift shaft edge	Pin support (infinite stiffness)	5·10^6 kNm/m per each of three torsional COMBIN14 springs
Columns	BEAM4 element having 1500/200 mm cross section; full column height of 2·2.79 m modelled; column ends fully fixed	BEAM4 element having starting bending and axial stiffness values (artificially) increased four times; full column height of 2·2.79 m modelled; column ends fully fixed
Main floor stiffness in N-S direction in 'ribbed' area	'Smeared' stiffness modelled with SHELL63 elements corresponding to 1 m spaced 350 mm deep and 650 mm wide beams with a 110 mm thick slab	16% increased staring 'smeared' stiffness
Lateral floor stiffness in E-W direction	25% of the stiffness in the ribbed N-S direction	14% of the increased stiffness in the ribbed N-S direction
Torsional stiffness of edge beams	$5 \cdot K_T$	$5 \cdot K_T$

It should be mentioned that the relatively high dynamic modulus for concrete increased further. This increase probably accounts for the effect of concrete ageing, whilst the relatively high absolute value may be explained by the fact that concrete designed as C50 actually achieved strength of approximately 70 MPa (Bennett, 1997).

Another interesting observation is that the main stiffness of the ribbed area increased by 16%, whilst the ratio of the lateral to main bending stiffness of the floor decreased from 25% to 14%. This re-distribution of stiffness may be explained by the stiffening effects of the services which were attached to the soffit of the floor (Figure 5.78). Also, as the whole floor area was cast without any construction joints it is possible that due to creep and shrinkage in the longer E-W direction (which was not prestressed), some micro-cracking occurred in the N-S direction. This micro-cracking could have reduced the relative stiffness of the E-W direction compared to the N-S direction. These are, however, only educated guesses and no additional proof to support them has been obtained.

Finally, the reason for the significant increase in the bending stiffness of the columns probably reflects the stiffening effects of the façade.

The updated FE model having the natural frequencies shown in Table 6.15 was subsequently used for the harmonic and transient simulations of the walking responses to WM1, WM2 and WM3 excitation.

6.4.3 Structure C (Clad): Harmonic Analysis

Figure 6.38 shows two point mobilities corresponding to the antinodes of the 1st and 2nd analytical modes of vibration. These antinodes are very close to TP38 and TP32 which were established as the antinodes of the 1st and 2nd measured modes (Figure 5.82), respectively. Consequently, TP38 and TP32 are also the test points where the maximum measured RMS acceleration responses occurred (Table 5.18).

Table 6.17: Structure C (Clad) - A summary of harmonic forces and FRF peak values used to simulate resonant excitation by WM1, WM2 and WM3.

Test	Accel @	Excitation harmonic	Natural frequency excited [Hz]	WM1 force [N]	WM2 force [N]	WM3 force [N]	FRF; FRF peak [m/s^2]
1.1c	TP38	3rd	6.4	75	40	48	H(38,38); 0.000728
2.1a	TP32	3rd	6.9	75	37	48	H(32,32); 0.000700

Table 6.18 presents the simulated acceleration responses in terms of (10 s) gRMS values obtained after scaling the FRF peaks.

Table 6.18: Structure C (Clad) - A comparison of analytically calculated and experimentally measured responses for the excitation by WM1, 2 and 3, assumed to be stationary.

Test	Excitation harmonic	Natural frequency excited [Hz]	Measured [% gRMS]	WM1 simulation [% gRMS] (Error)	WM2 simulation [% gRMS] (Error)	WM3 simulation [% gRMS] (Error)
1.1c	3rd	6.4	0.0855	0.394 (360%)	0.208 (143%)	0.252 (195%)
2.1a	3rd	6.9	0.0954	0.378 (297%)	0.186 (95%)	0.242 (154%)

These results show that the 3rd harmonic modelling using WM1 and WM3 overestimate the response considerably, particularly in the case of WM1, whereas WM2 performs slightly better.

6.4.4 Structure C (Clad): Transient Analysis under Moving Excitation

Similarly as for Structures A and B, the three walking models were assumed to move with a constant speed along WPs 1 and 2 (Figure 6.34). Along each straight path, equidistant nodes spaced every 0.3 m exist. Experimentally investigated WP3 (Figure 5.82) was not modelled due to computational limitations. As the natural frequencies of the two modes were above 6 Hz, the pacing rates required were greater than 2 Hz leading to the assumed step length of 0.9 m. Limitations in the computing power available also governed the decision to simulate only 60 s of acceleration responses due to walking instead of 120 s which were measured. However, as in the case of Structures A and B, the 60 s simulated acceleration time-history proved to be sufficient to establish clearly the response trends.

Of five groups of experimental tests, only Tests 1.1, 2.1 and 3.1 (along WP1 and 2) were simulated and the responses were calculated at the FE nodes corresponding to the geometric locations where the measurements were made (Table 5.18). In addition, the responses were also calculated at theoretical antinode points for modes 1 and 2, respectively. This was done to obtain the maximum theoretical responses for comparison with the response simulations which were measured at the three points: TP32, TP35 and TP38. This is because TP32 and TP38 were not exactly at the theoretical antinodes of modes 1 and 2, calculated using the updated FE model.

An example of an acceleration response simulation to moving WM1 walking excitation is given in Figure 6.39 whilst RMS acceleration trends for antinode responses to WM1 simulation of Tests 1.1, 2.1 and 3.1 are shown in Figure 6.40. Similarly as for WM1, the response to a 'rolling' sinusoid representing WM2 was calculated (Figure 6.39) and three 10 s RMS trend analyses corresponding to antinodes of modes 1 and 2 are presented in Figure 6.41. A summary of all simulations in terms of maximum 10 s RMS accelerations is given in Table 6.19.

Table 6.19: Structure C (Clad) - A comparison of analytically calculated and experimentally measured maximum responses for the excitation by WM1, 2 and 3, assumed to be moving.

Test	Excitation harmonic	Natural frequency excited [Hz]	Measured [% gRMS]	WM1 simulation [% gRMS] (Error)	WM2 simulation [% gRMS] (Error)	WM3 simulation [% gRMS] (Error)
1.1*	3rd	6.4	n/a	0.134 (n/a)	0.070 (n/a)	0.085 (n/a)
1.1a	3rd	6.4	0.0770	0.110 (43%)	0.054 (-21%)	0.065 (-22%)
1.1b	3rd	6.4	0.0841	0.119 (41%)	0.069 (-13%)	0.083 (-2%)
1.1c	3rd	6.4	0.0855	0.133 (56%)	0.062 (-18%)	0.075 (-17%)
2.1*	3rd	6.9	n/a	0.110 (n/a)	0.050 (n/a)	0.065 (n/a)
2.1a	3rd	6.9	0.0954	0.110 (15%)	0.050 (-41%)	0.065 (-61%)
2.1c	3rd	6.9	0.0860	0.108 (26%)	0.047 (-36%)	0.061 (-53%)

Test	Excitation harmonic	Natural frequency excited [Hz]	Measured [% gRMS]	WM1 simulation [% gRMS] (Error)	WM2 simulation [% gRMS] (Error)	WM3 simulation [% gRMS] (Error)
3.1*	3rd	6.4	n/a	0.110 (n/a)	0.054 (n/a)	0.065 (n/a)
3.1a	3rd	6.4	0.0550	0.081 (47%)	0.041 (-17%)	0.050 (-12%)
3.1b	3rd	6.4	0.0820	0.109 (33%)	0.053 (-27%)	0.064 (-34%)
3.1c	3rd	6.4	0.0577	0.094 (63%)	0.048 (-10%)	0.058 (1%)

*Response calculated at a theoretical antinode point for the analytical FE mode excited.

The results show that for the natural frequencies of 6.4 and 6.9 Hz, the performance of WM1 (3rd harmonic) modelling improved when the excitation was assumed to be moving. The same assumption led to the general underestimation of responses using WM2 and WM3.

6.5 Structure D: Parametric Investigations

Parametric investigations pertinent to Structure D were its FE model correlation and updating, and the response calculations.

6.5.1 Structure D: FE Model Correlation and Updating

The main aim of the FE model updating was to find analytical modes of vibration which match the experimentally measured floor modes at 8.52 Hz and 8.92 Hz, which were excited by the 4th harmonic of walking in the experiments (Figure 5.98). As with Structures A, B and C, described previously, the starting model was the pre-test FE model (Figure 5.86). This model was refined through the following six phases:

Phase 1: Equidistant nodes at 0.3 m were generated along WPs 1 and 2 (Figure 5.87 and Figure 6.42). The model remained fully pinned (as was the pre-test model), with no edge beams and no ramp. The slab was modelled with 225 mm thick isotropic SHELL63 elements assuming material density of 2400 kg/m^3 and dynamic modulus of 38 GPa.

Phase 2: Same as the Phase 1 model, but with the ramp modelled as having a fully fixed far edge (Figure 6.42).

Phase 3: Same as the Phase 2 model, but with upstanding edge beams modelled (Figure 6.42).

Phase 4: Same as the Phase 3 model, but with columns modelled (though not column heads). Column supports modelled as fully fixed (Figure 6.42).

Phase 5: Same as the Phase 4 model but with column heads modelled as short bar elements (Figure 6.42).

Phase 6: Same as the Phase 5 model but with orthotropic shell elements where the bending stiffness in the N-S direction was reduced to 87% of the stiffness in the E-W direction.

For each of the six updating phases, natural frequencies, MAC and COMAC values were calculated using the 59 test points and the portion of the FE model which corresponded to it (Figures 5.87 and 6.45). Due to the high modal density of this structure, the 'manual' updating proved to be very difficult, particularly with regard to the interpretation of the MAC matrix. For example, the finally updated FE model had 20 modes between 8.51 Hz and 10.82 Hz (Table 6.20, and Figures 6.44 and 6.45) of which only four were matched with the measured modes (Figure 6.46). Figure 6.43 shows the pairing of the natural frequencies of these four correlated experimental (data Set 1) and analytical (data Set 2) mode pairs which are circled in the MAC matrix as well as the corresponding COMAC values. Analytical modes 1 and 3, clearly, matched the two modes excited by walking, which was the principal aim of this exercise.

Table 6.20: Structure D - Measured, initial model and updated model frequencies, and unity scaled modal mass of the updated FE model.

Mode No.	Measured natural frequency [Hz]	Starting FE model natural frequency [Hz]	Updated FE model natural frequency [Hz]	Modal mass of updated modes [kg]
1	7.99	7.03	8.51	99,328
2	8.52	7.47	8.92	109,731
3	8.72	7.79	8.93	99,818
4	8.92	7.85	9.26	71,656
5	9.28	7.89	9.30	56,550
6	9.94	8.00	9.34	54,548
7	10.39	8.31	9.39	73,185
8	11.07	8.36	9.44	94,750
9	11.17	8.79	9.52	13,157
10	11.93	8.80	9.54	46,306
11	12.65	8.88	9.60	34,349
12	16.72	8.92	9.64	12,045
13	n/a	8.96	9.65	123,780
14	n/a	8.99	9.78	106,341
15	n/a	n/a	9.86	50,859
16	n/a	n/a	10.11	32,332
17	n/a	n/a	10.28	24,315
18	n/a	n/a	10.37	99,525
19	n/a	n/a	10.48	70,915
20	n/a	n/a	10.82	34,093

The first measured mode at 7.99 Hz was a relatively weak one and it is possible that it is a mode corresponding to the lower floor levels, which is, probably, the reason why it could not be replicated by the FE model which neglected other floor levels. The relatively coarse test mesh which failed to capture some of the local modes (Figures 6.44 and 6.45) was probably the main reason why a better correlation between the measurements and analysis was not achieved.

The list of starting (Phase 1 model) and final (Phase 6 model) updating parameters is given in Table 6.21.

Table 6.21: Structure D - Starting and final FE model updating parameters.

Updated parameter	Starting model and/or value	Final model/value
Dynamic modulus of concrete	38 GPa	37.71 GPa
Concrete density	2400 kg/m^3	2300 kg/m^3
Columns	Pin support (infinite stiffness)	BEAM4 element having square cross section; full column height of 3.05 m modelled; column ends fully fixed
Column heads	Not modelled	Modelled using a 0.4 m long elastic beam element with a square cross section having the bending stiffness 9.5 greater than the column stiffness
Floor bending stiffness in N-S direction	Same as the bending stiffness in the E-W direction	87% of the bending stiffness in the E-W direction
Ramp	Not modelled	Modelled with SHELL63 elements; fully fixed lower end of the ramp
Stairwell	Not modelled	Modelled with fully fixed edges

This updating exercise provided an insight into some rather interesting features of the vibration behaviour of Structure D.

Firstly, as with structures B and C having cast in-situ columns, to achieve this level of correlation with the experiments it was necessary to model the columns, which proved to be a major source of the slab's overall stiffness. In addition, the column heads appeared to be an important modelling feature as the calculated frequencies were particularly sensitive to the assumed bending stiffness of the relatively short column heads.

Secondly, whereas the total calculated weight of the slab, excluding the edge beams and columns, was about 1020 tonnes, the largest unity-scaled modal mass was only about 12% of this, as shown in Table 6.20. Moreover, the same table also identifies modes having natural frequency lower than 10 Hz and possibly excitable by the 4th harmonic of walking, which have a modal mass as low as 5% of the total floor mass.

Finally, locating the prestressing tendons in two orthogonal directions and the presence of four construction joints in the E-W direction, may have resulted in the development of orthotropic properties in the flat slab. As a consequence the floor's bending stiffness in the N-S direction is estimated to be slightly lower (13%) than in the E-W direction.

6.5.2 Structure D: Harmonic Analysis

Figure 6.47 shows two FRF point mobilities corresponding to the antinode of the first analytical mode correlated with the experiments (mode 1 at 8.51 Hz, Figure 6.46) calculated by using the mode superposition technique. The first FRF (black line) is calculated superimposing the first 20 modes, whilst the blue line denotes an FRF generated using only mode 1. Similarly, Figure 6.48 shows a pair of point mobilities corresponding to the antinode of the second correlated mode (mode 3 at 8.93 Hz, Figure 6.46). Again, the black line presents the results of superimposing the first 20 modes, whereas the blue line represents the

frequency response of mode 3 only. In these calculations the values of modal damping corresponding to the four correlated modes were taken from experimental measurements, whilst the modal damping in other 16 uncorrelated modes was assumed to be 1%, which is reasonable considering the measured damping values (Table 5.21).

As the antinode points for modes 1 and 3 are very close, the two 20-mode point mobilities look practically identical. These two antinodes are very close to TP1, where the acceleration measurements were made, so the analytical and experimental results are comparable.

The plots of the four FRFs quite clearly demonstrate the superimposing effect of the closely spaced modes, as opposed to SDOF models where this effect does not exist. This is quantified in Table 6.22, which presents the summary of the pertinent FRF peaks. It is obvious that the SDOF models underestimate the response, but it is also clear that the maximum responses for individual modes do not simply add up as there is a phase lag between them.

Table 6.22: Structure D - A summary of FRF peak values corresponding to single- and multi-mode FRF calculations.

Test	Accel. @	Natural frequency excited [Hz]	Number of modes used in the FRF calculation	FRF peak [m/s^2]
1.1	Mode 1 antinode	8.51	20	0.000812
1.1	Mode 1 antinode	8.51	1	0.000521 (underestimation: 36%)
2.1	Mode 3 antinode	8.93	20	0.000691
2.1	Mode 3 antinode	8.93	1	0.000519 (underestimation: 21%)

Of the three walking excitation models, only WM2 is applicable to Structure D, as WM1 does not provide information about the 4th harmonic excitation, and WM3 is valid only up to 7.2 Hz which is well below the frequency of the two modes excited. Table 6.23 presents the simulated acceleration responses in terms of (10 s) gRMS values obtained after scaling the FRF peaks.

Table 6.23: Structure D - A comparison of experimentally measured and analytically calculated maximum responses for the excitation by WM2, assumed to be stationary.

Test	Excitation harmonic	Natural frequency excited [Hz]	Harmonic force [N]	Number of modes used in the FRF calculation	Measured [% gRMS]	WM2 simulation [% gRMS] (Error)
1.1	4th	8.51	30	20	0.1579	0.174 (10%)
1.1	4th	8.51	30	1	0.1579	0.112 (-29%)
2.1	4th	8.93	28	20	0.2200	0.142 (-36%)
2.1	4th	8.93	28	1	0.2200	0.106 (-52%)

A number of reasons could have contributed to the underestimation of measured gRMS values in three out of four calculated responses using harmonic response analysis.

Firstly, as Structure D was in open-space, the measurements consisted not only of responses to the 4th harmonic of walking, but also of responses to unmeasured ambient excitation. As Figure 5.103 illustrates,

this unmeasured part of the excitation could have produced a quarter (or even more) of the total RMS response. This indicates limitations of using open space structures for these exercises.

Secondly, it is possible that the actual participating modal mass of the floor was lower than predicted by the FE model if parts of this large structure, away from the walking paths, were not contributing to the responses.

Thirdly, the assumption of pure resonance conditions made in the harmonic analyses leads to responses which are very sensitive to the assumed value of damping. However, damping is traditionally an unreliable modal parameter and large errors in its estimation generate similarly large errors in the response calculations when resonance is assumed.

Finally, it is possible that WM2, simulating the 4^{th} harmonic excitation, is not accurate in this frequency range.

The above given reasons probably all contribute to the analytical underestimation of the measured responses. Nevertheless, the results provide some insight into the confidence margins of the results obtained.

6.5.3 Structure D: Transient Analysis under Moving Excitation

Figure 6.42 shows two walking paths used for the simulation of moving walking excitation, similarly as for Structures A, B and C. Only responses to the moving WM2 excitation have been calculated as WM1 and WM3 are not applicable for the same reason as given in the previously described harmonic analysis. As the pacing frequencies required were greater than 2 Hz (4^{th} harmonic greater than 8 Hz), the pace length assumed in these analyses was 0.9 m. Limitations in the computing power governed the decision to simulate only 30 s of acceleration responses which was sufficient to describe at least a single pass along WPs 1 and 2.

Tests 1.1 and 2.1 were simulated and responses calculated at the antinodes of the analytical modes 1 and 3. However, as the number of modes in the mode superposition harmonic analysis seemed to be important, a similar parametric study with both single and 20 modes was performed here as well. The results of this parametric study are shown in Table 6.24.

Table 6.24: Structure D - A comparison of analytically calculated and experimentally measured maximum responses for the excitation by WM2, assumed to be moving.

Test	Excitation harmonic	Natural frequency excited [Hz]	Number of modes used in the response calculation	Measured [% gRMS]	WM2 simulation [% gRMS] (Error)
1.1	4^{th}	8.51	20	0.1579	0.0445 (-72%)
1.1	4^{th}	8.51	1	0.1579	0.0372 (-76%)
2.1	4^{th}	8.93	20	0.2200	0.0417 (-81%)
2.1	4^{th}	8.93	1	0.2200	0.0374 (-83%)

As for the steady state harmonic analysis, ambient excitation, a limited floor vibration participating area, inaccurate damping and poor modelling of the excitation could all have contributed to the underestimation of responses. As expected, the amount of underestimation is, nevertheless, greater than in the non-moving case. This is because the moving excitation generally produces lower responses than the relevant stationary excitation for the same amplitudes of forces. Finally, it is interesting to note the differences between the single- and multi-mode response analyses (Table 6.24, and Figures 6.48 and 6.49).

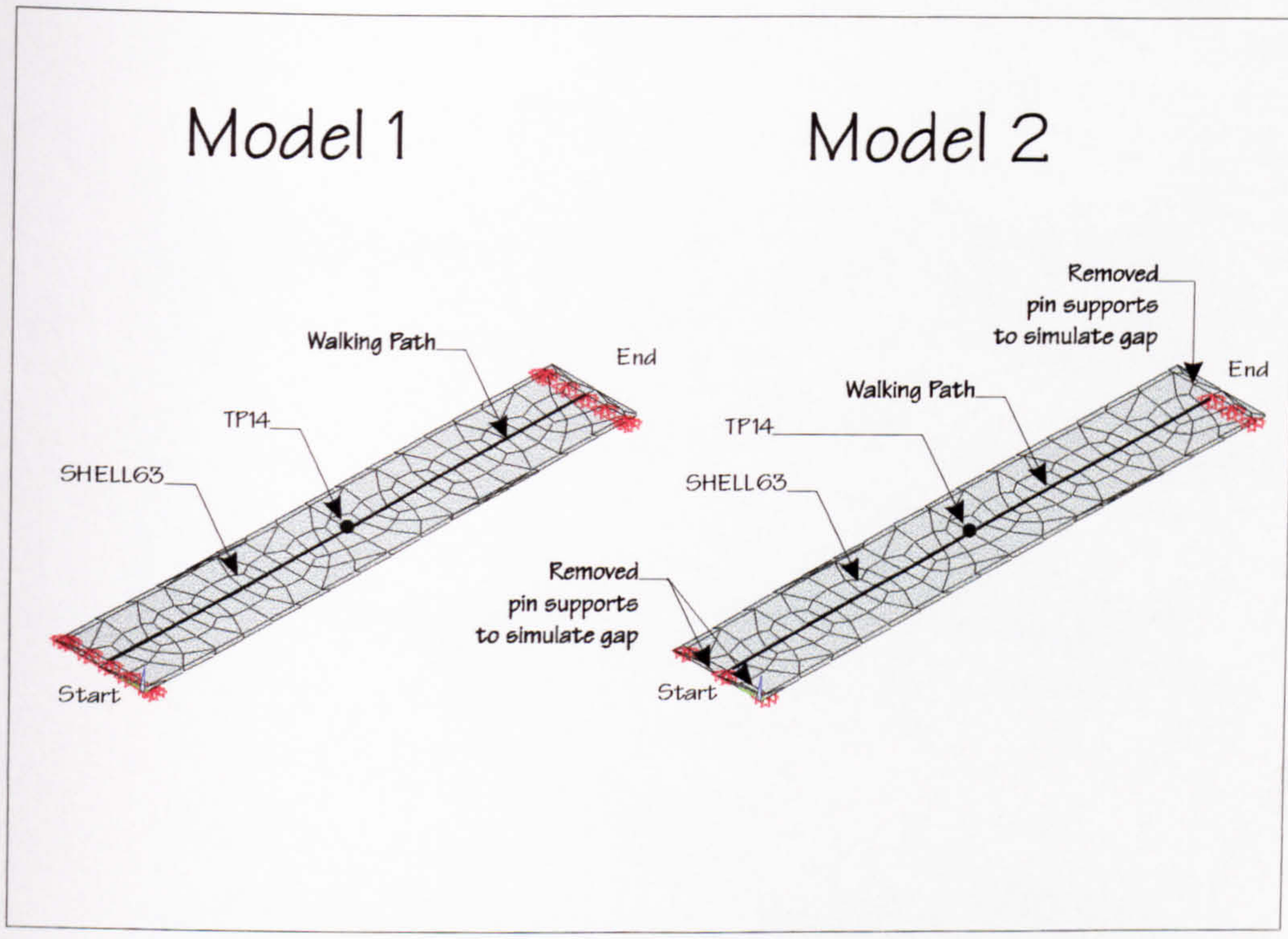

Figure 6.1: Structure A - FE Models 1 and 2 used in the correlation and updating.

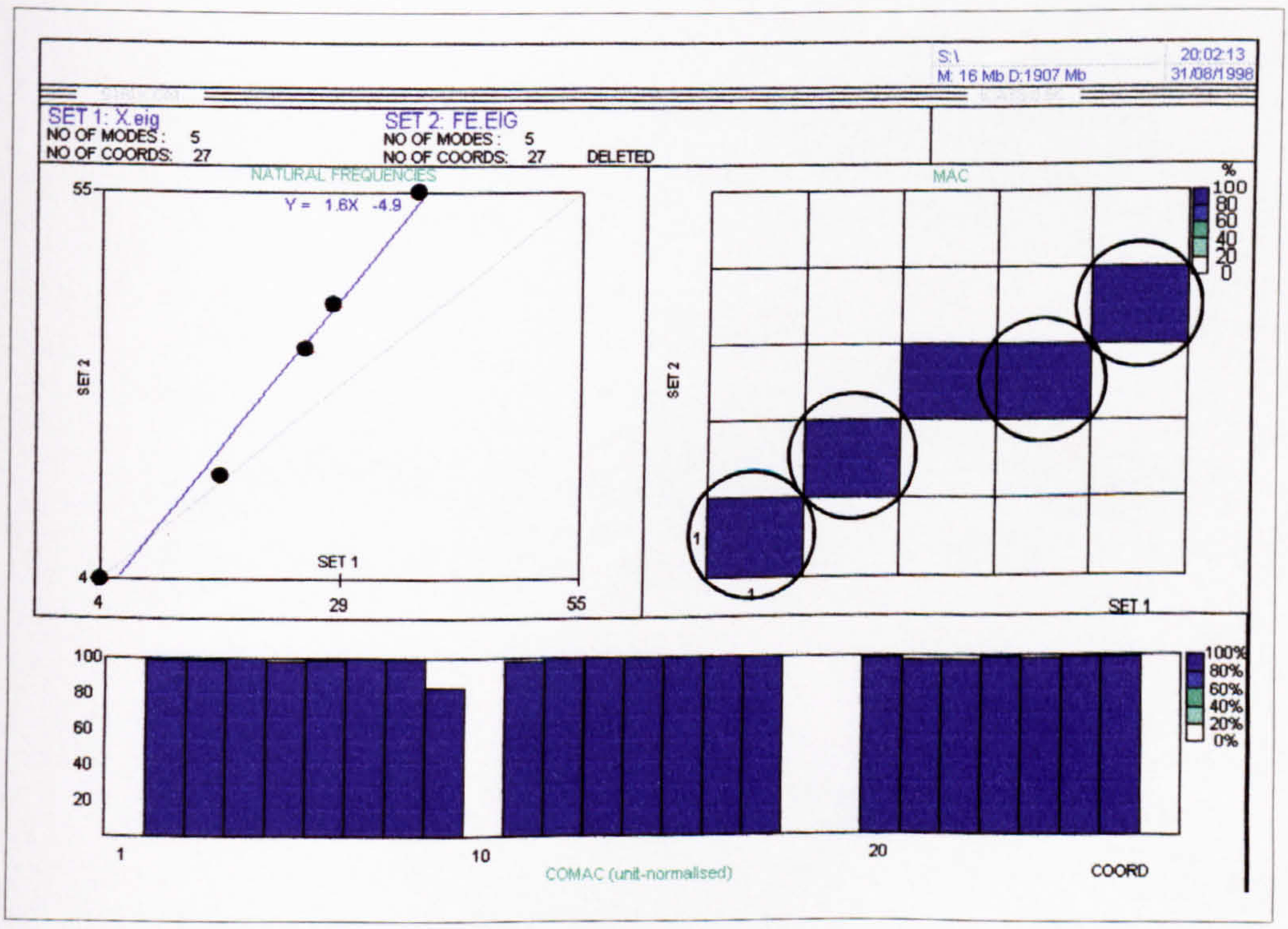

Figure 6.2: Structure A - Experimental (Set 1) vs analytical (Set 2) data. Comparison of natural frequencies (top left), mode shapes (middle), MAC (top right) and COMAC (bottom). Circled in the MAC matrix are the correlated mode pairs.

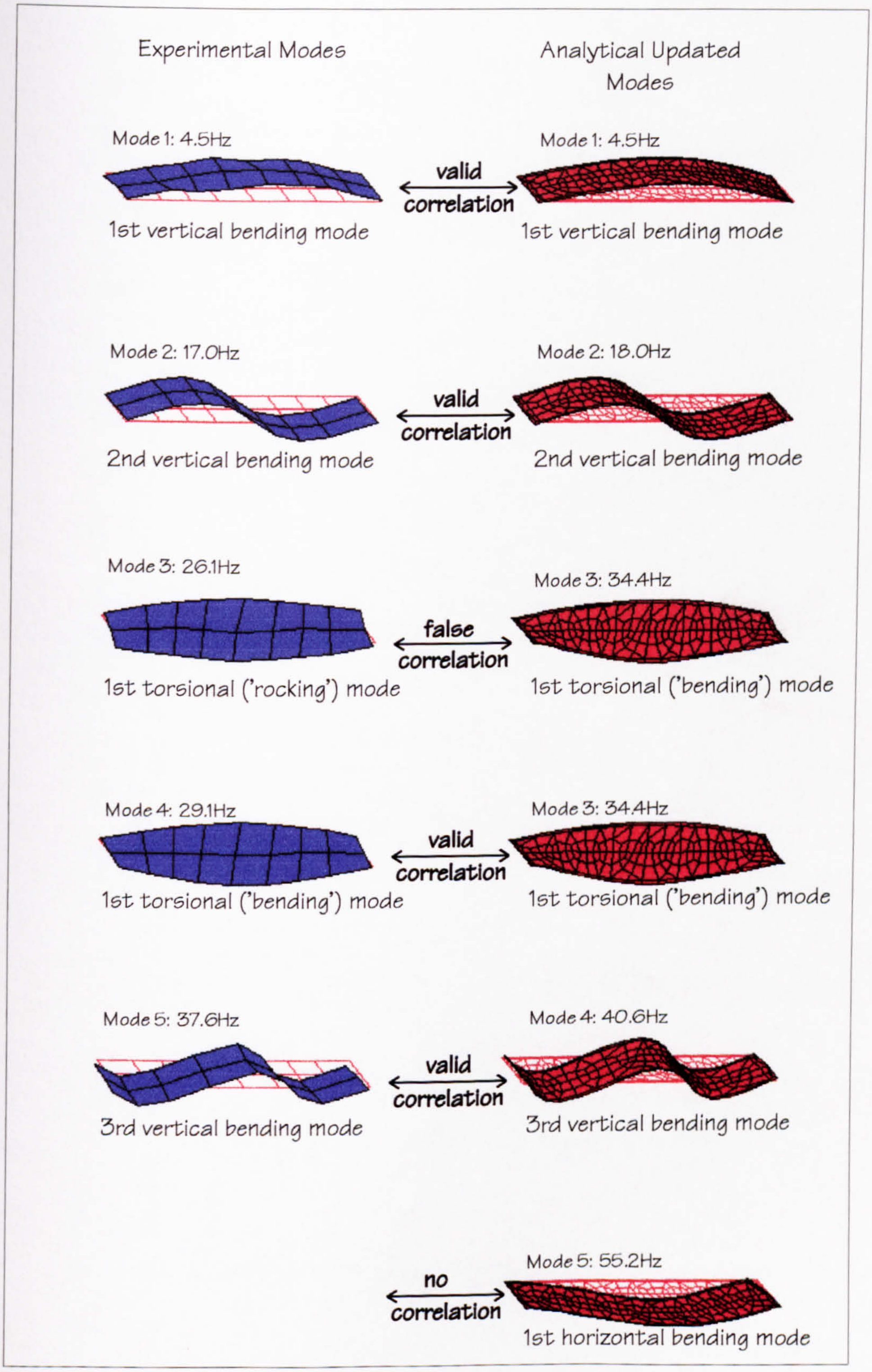

Figure 6.3: Structure A - Visual correlation between experimental modes and their analytical counterparts.

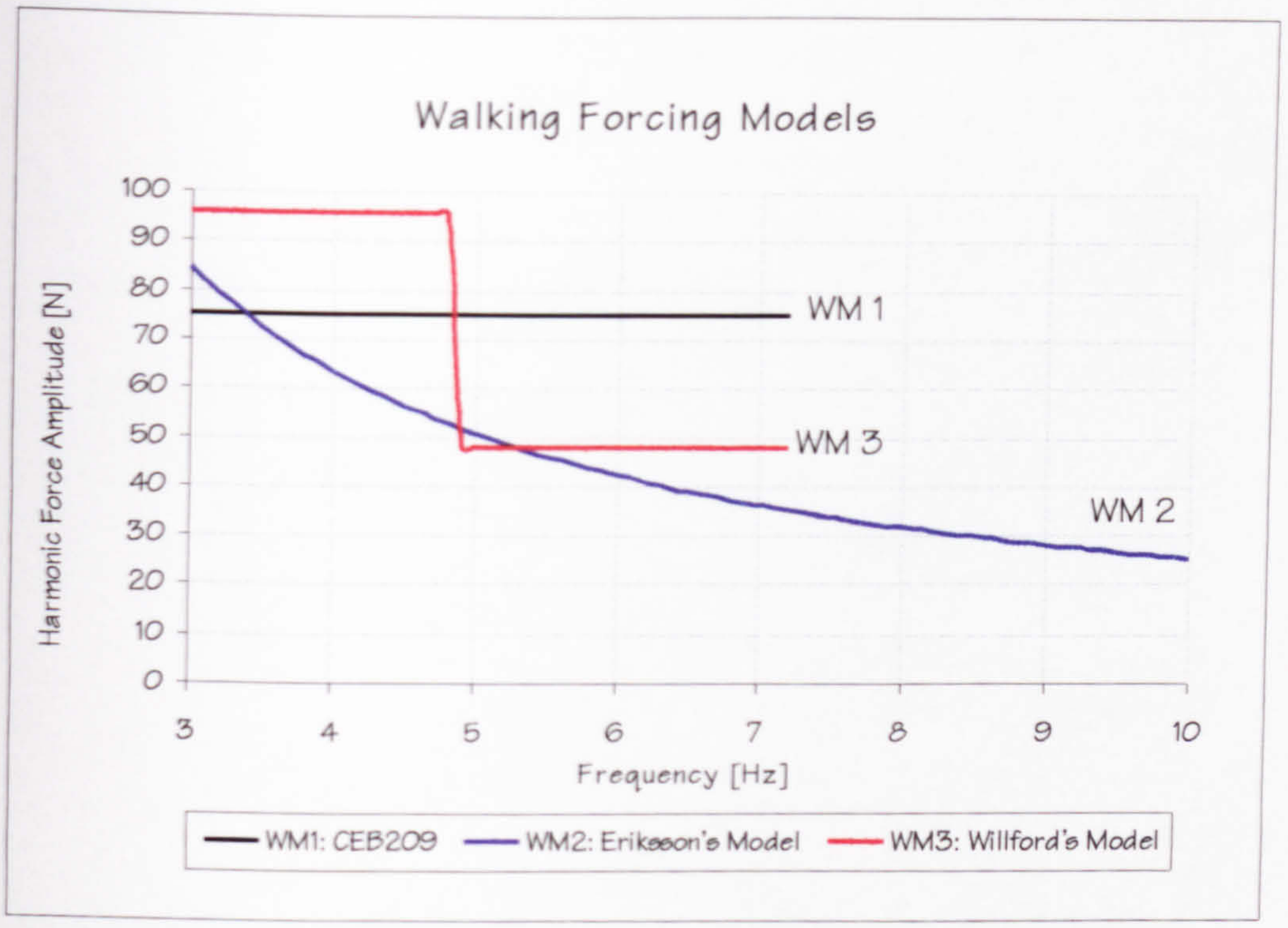

Figure 6.4: Harmonic amplitudes of the three walking excitation models investigated.

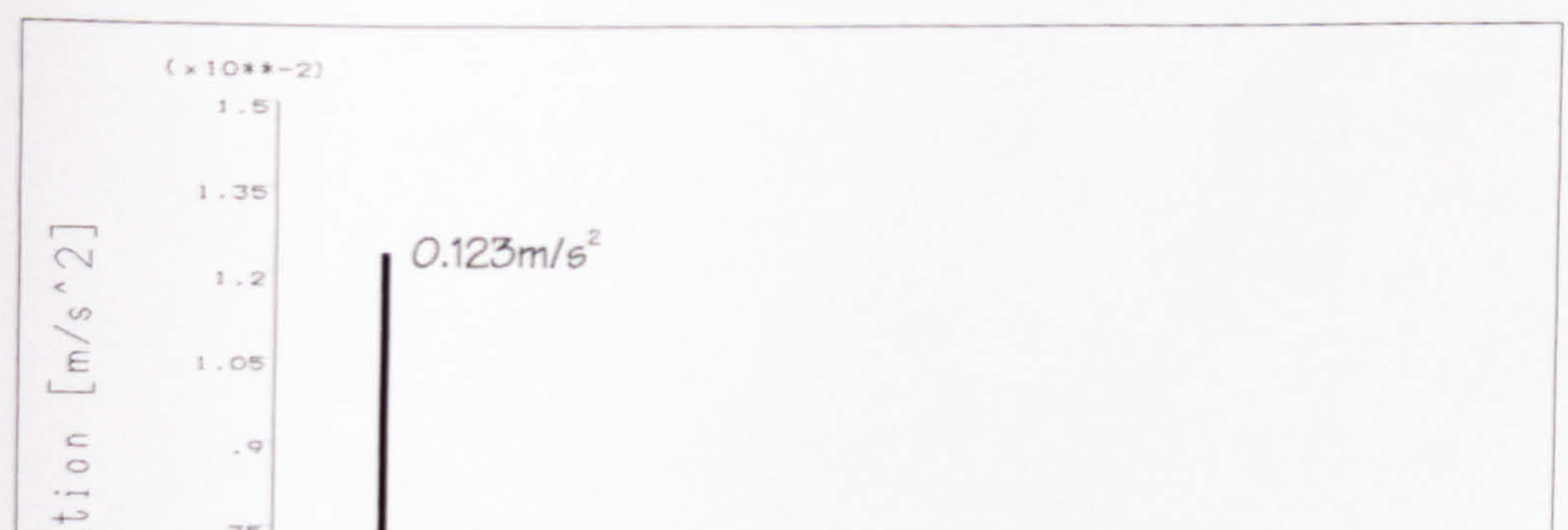

Figure 6.5: Structure A - Analytically calculated point mobility FRF corresponding to the antinode of the fundamental mode of vibration.

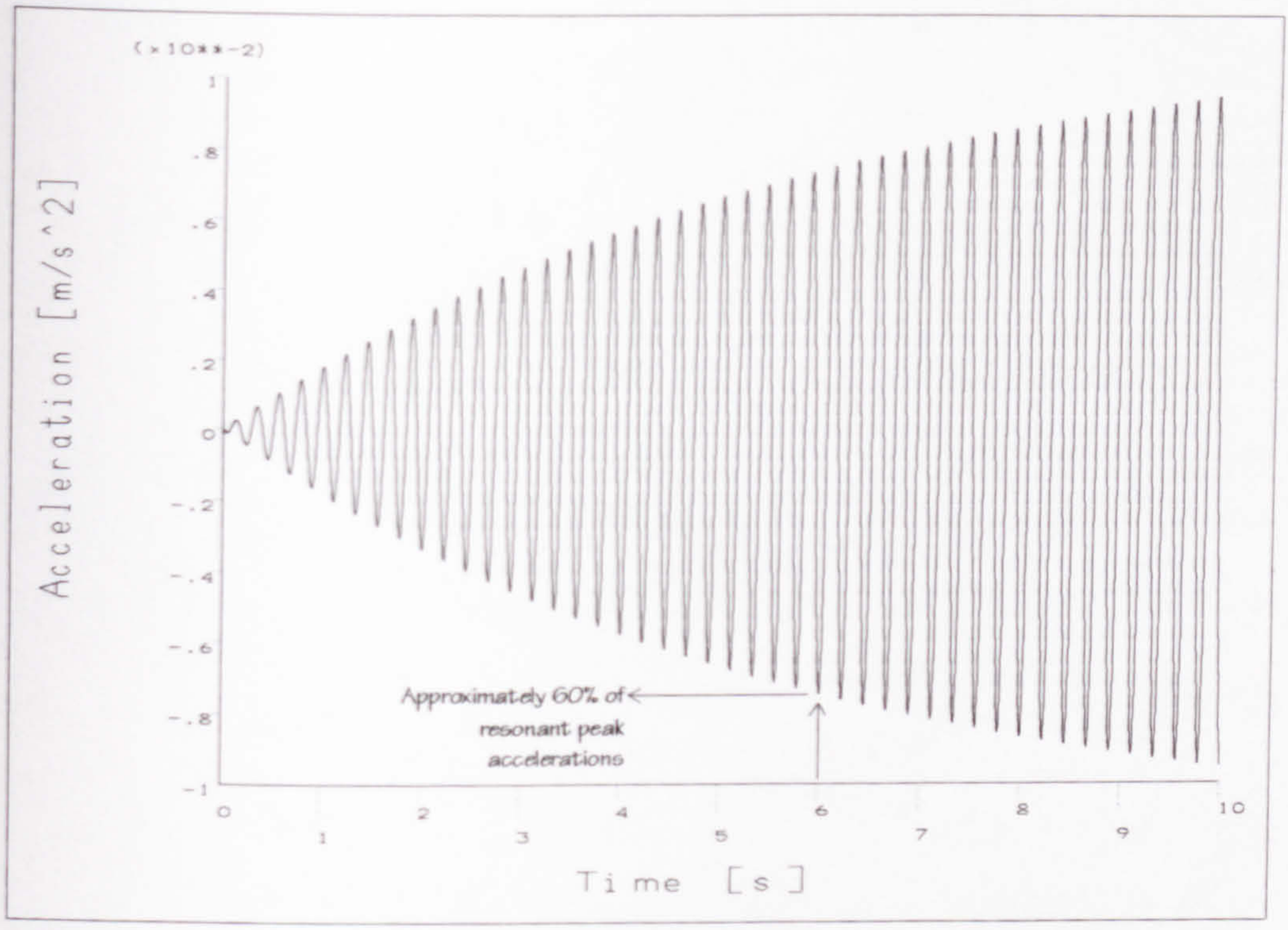

Figure 6.6: Structure A - Transient acceleration response at the mid point of the slab excited at the same place by a resonant sinusoid having 1.0N amplitude.

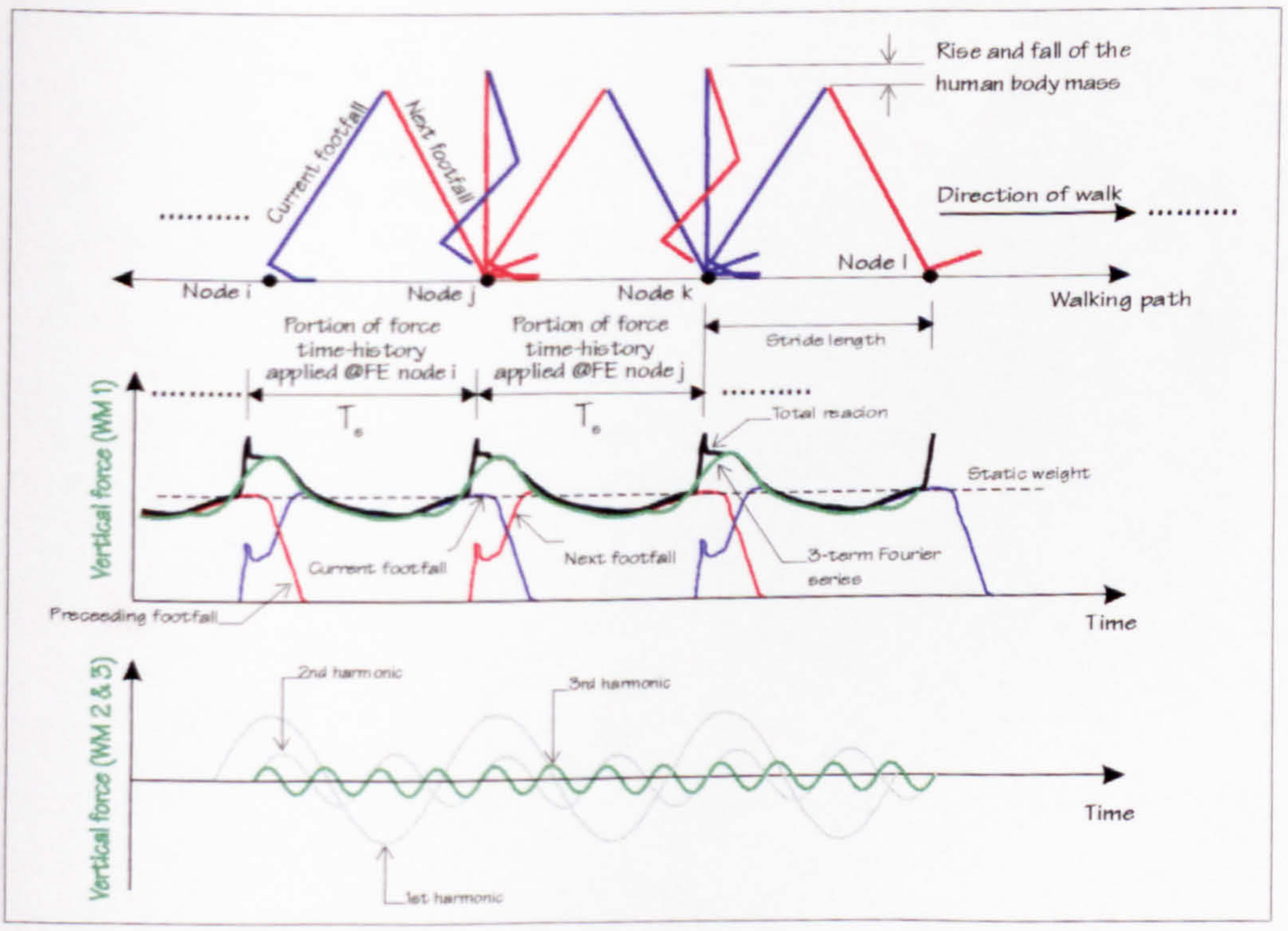

Figure 6.7: FE simulation of walking - Forces applied at node 'j'. The green lines represent qualitatively the time variation of the three walking forcing functions.

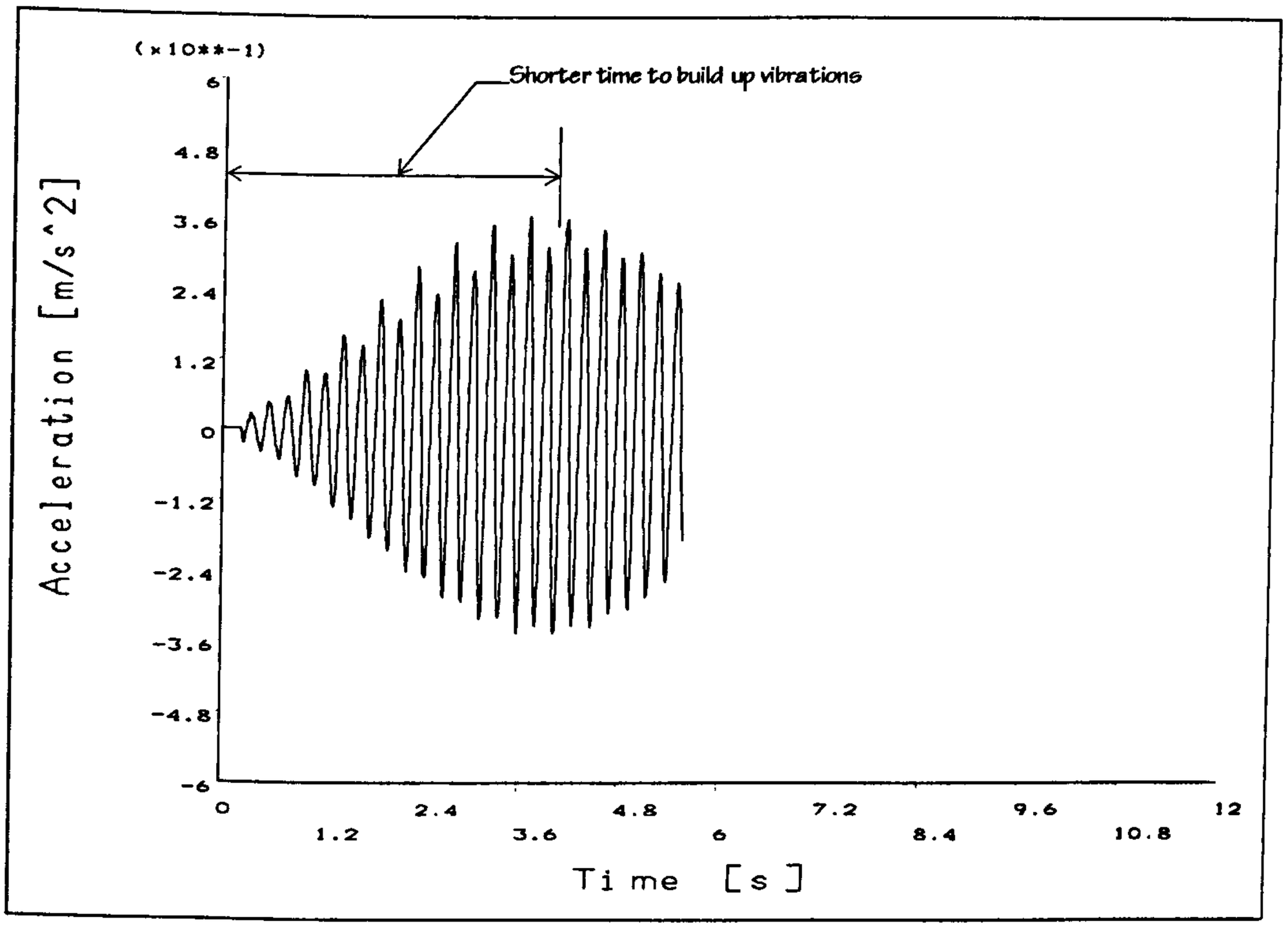

Figure 6.8: Structure A - Acceleration response at the slab strip mid-point to the walking excitation based on WM1. The assumed stride length is 0.9m at the pacing rate set to 2.25Hz. Single pass simulated.

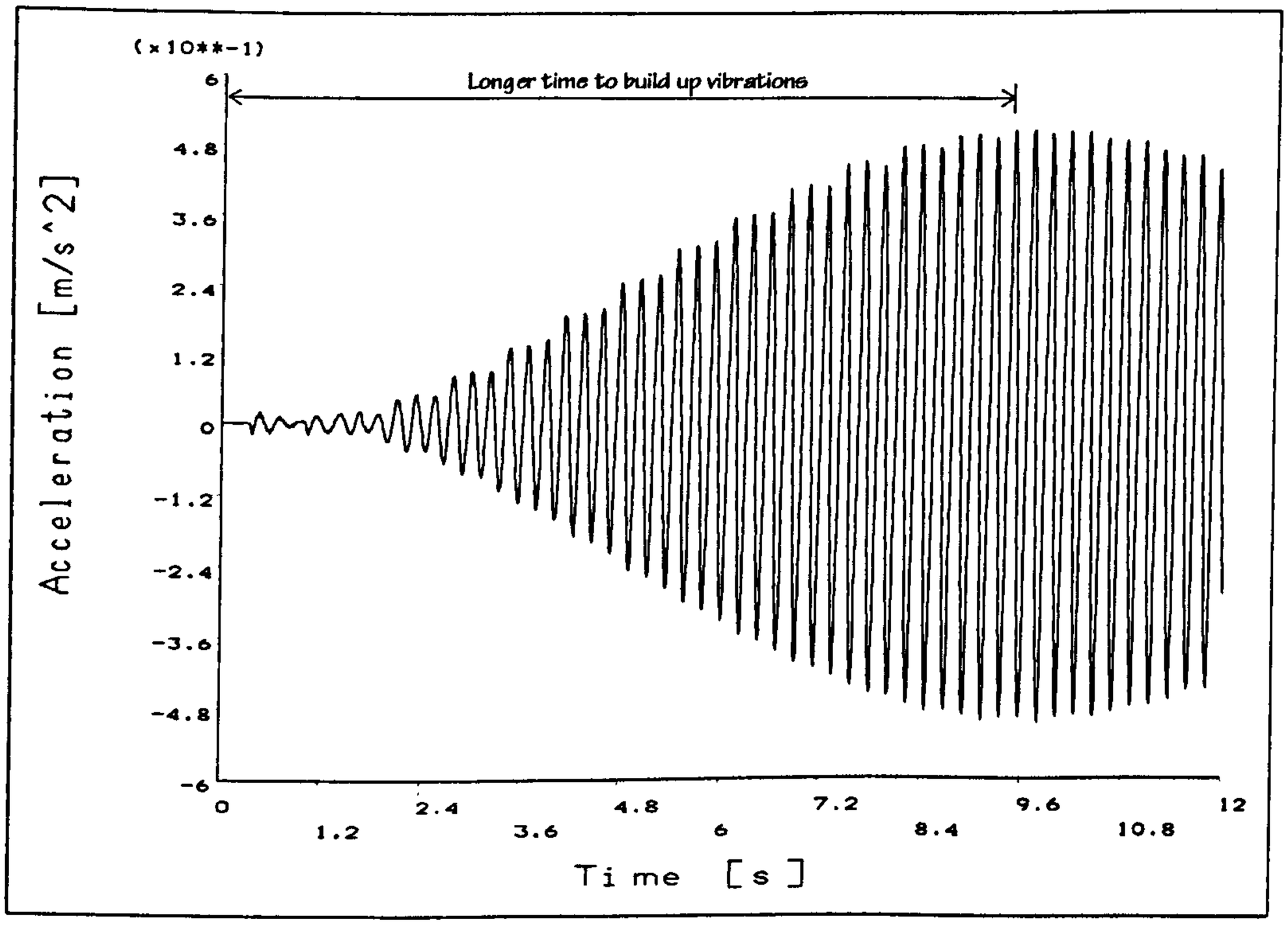

Figure 6.9: Structure A - Acceleration response at the slab strip mid-point to the walking excitation based on WM1. The assumed stride length is 0.6m at the pacing rate set to 1.50Hz. Single pass simulated.

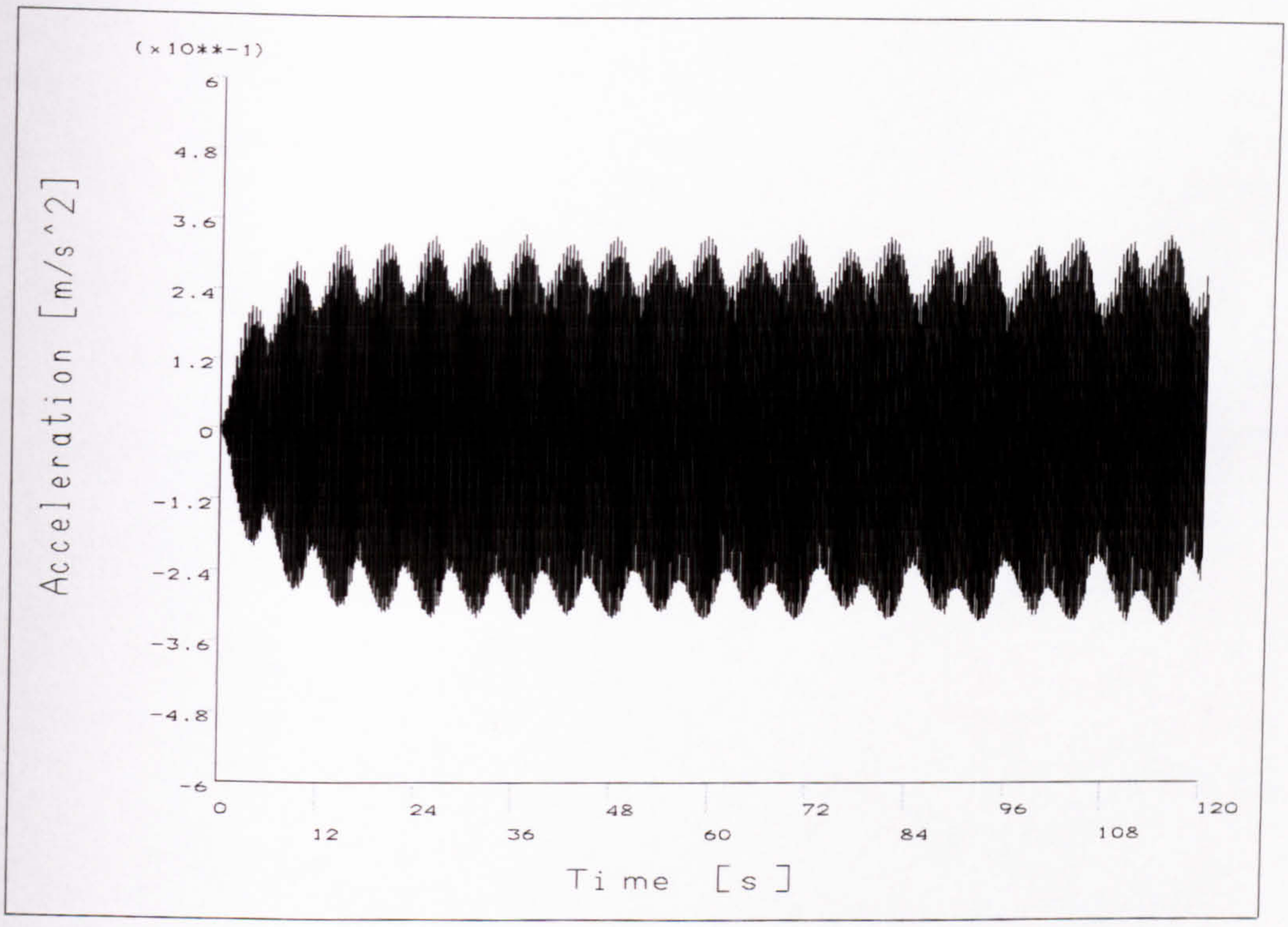

Figure 6.10: Structure A - Acceleration response at the slab strip mid-point to the walking excitation based on WM1. The assumed stride length is 0.9m at the pacing rate set to 2.25Hz. Multiple passes lasting 120s simulated.

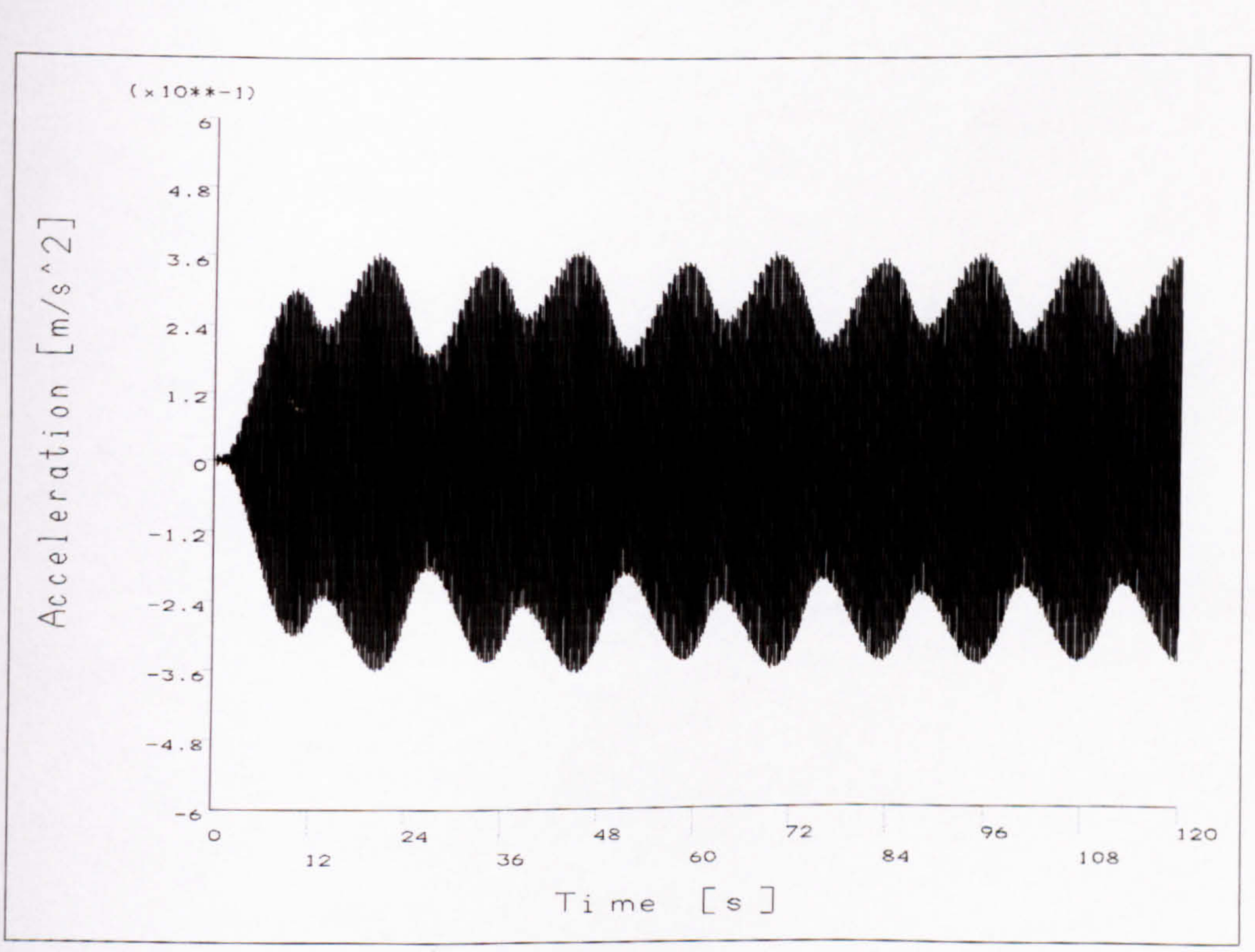

Figure 6.11: Structure A - Acceleration response at the slab strip mid-point to the walking excitation based on WM1. The assumed stride length is 0.6m at the pacing rate set to 1.50Hz. Multiple passes lasting 120s simulated.

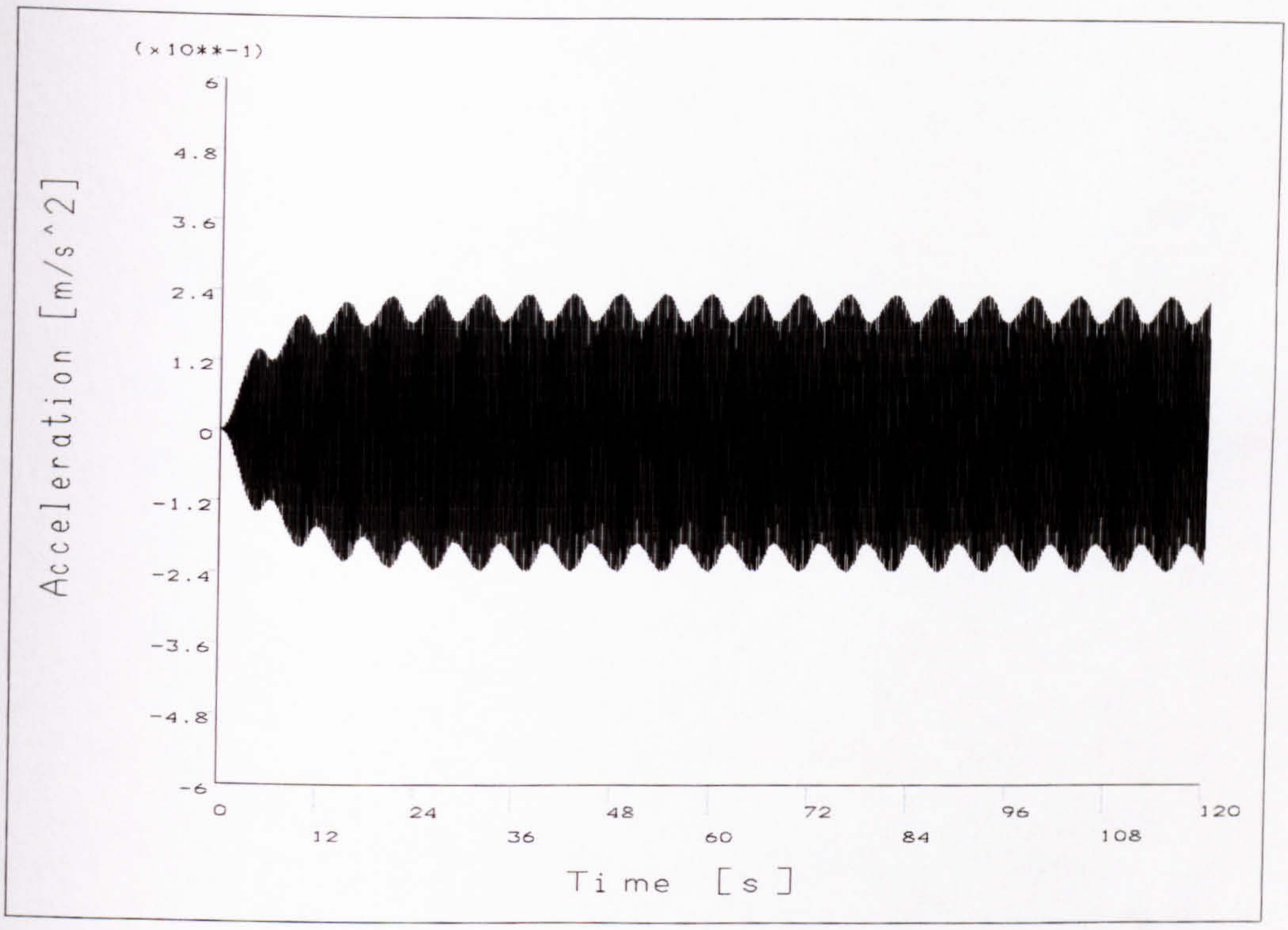

Figure 6.12: Structure A - Acceleration response at the slab strip mid-point to the walking excitation based on WM2. The assumed stride length is 0.9m at the pacing rate set to 2.25Hz. Multiple passes lasting 120s simulated.

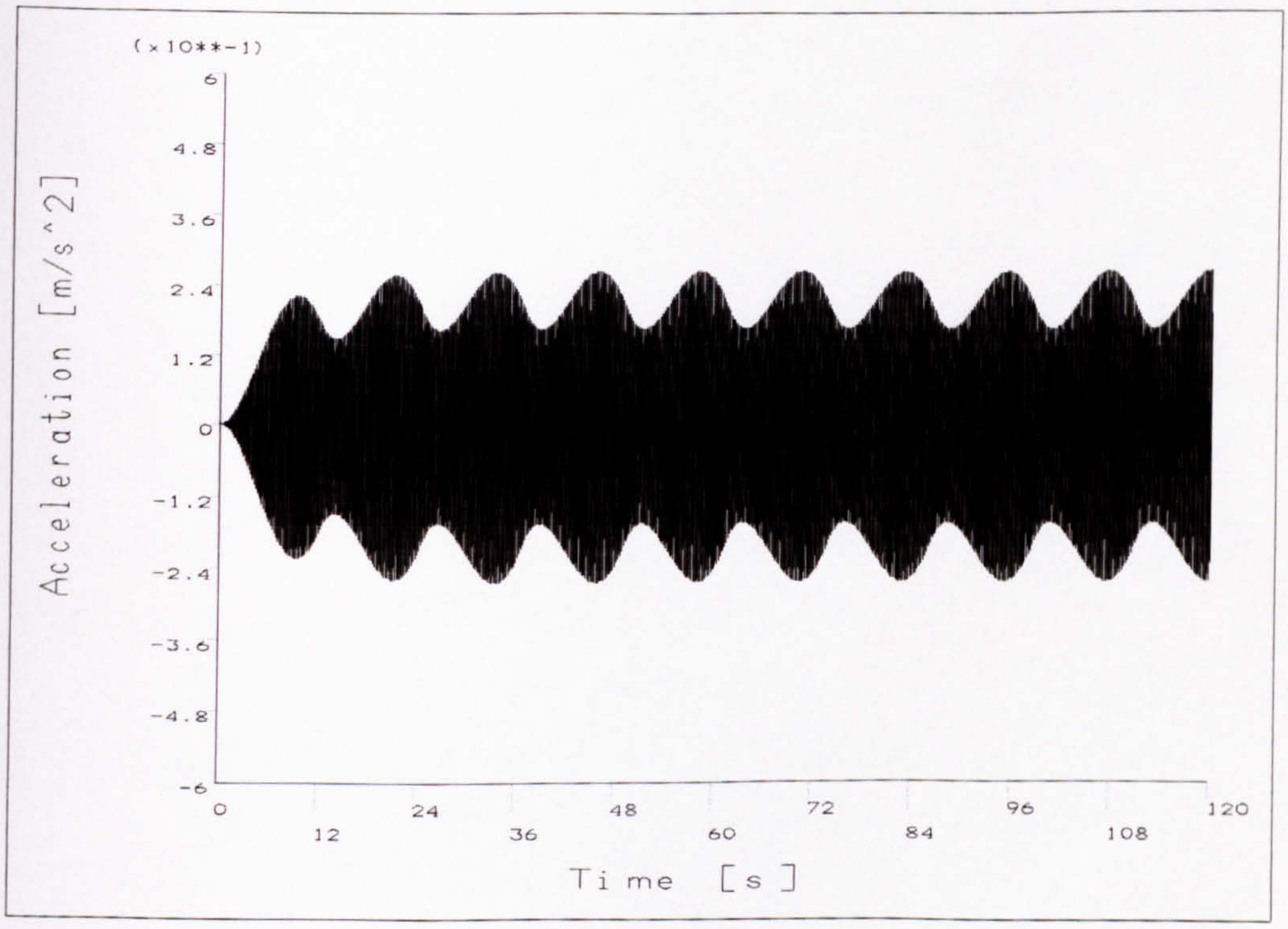

Figure 6.13: Structure A - Acceleration response at the slab strip mid-point to the walking excitation based on WM2. The assumed stride length is 0.6m at the pacing rate set to 1.50Hz. Multiple passes lasting 120s simulated.

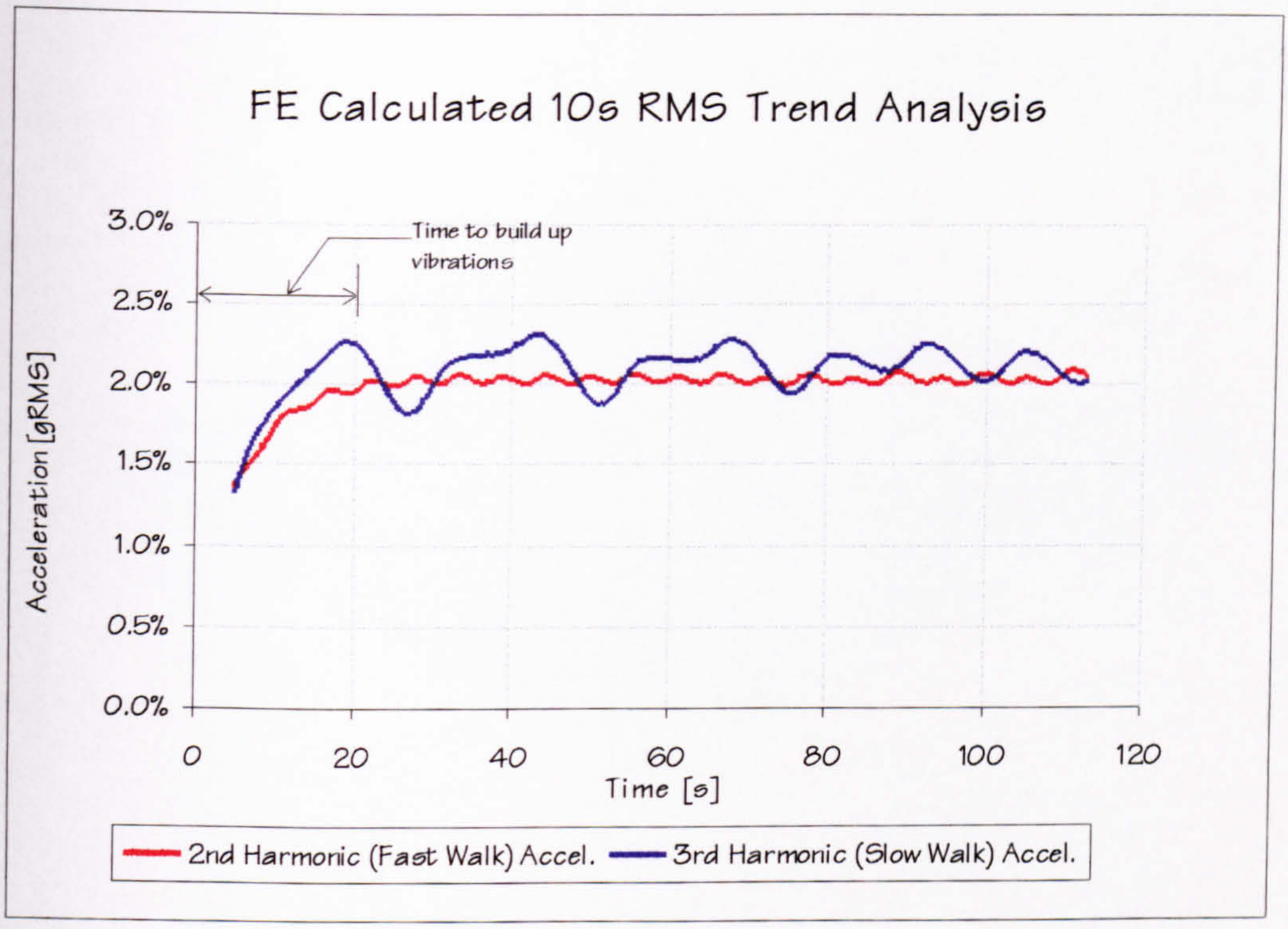

Figure 6.14: Structure A - 10s gRMS values corresponding to accelerations analytically calculated for WM1.

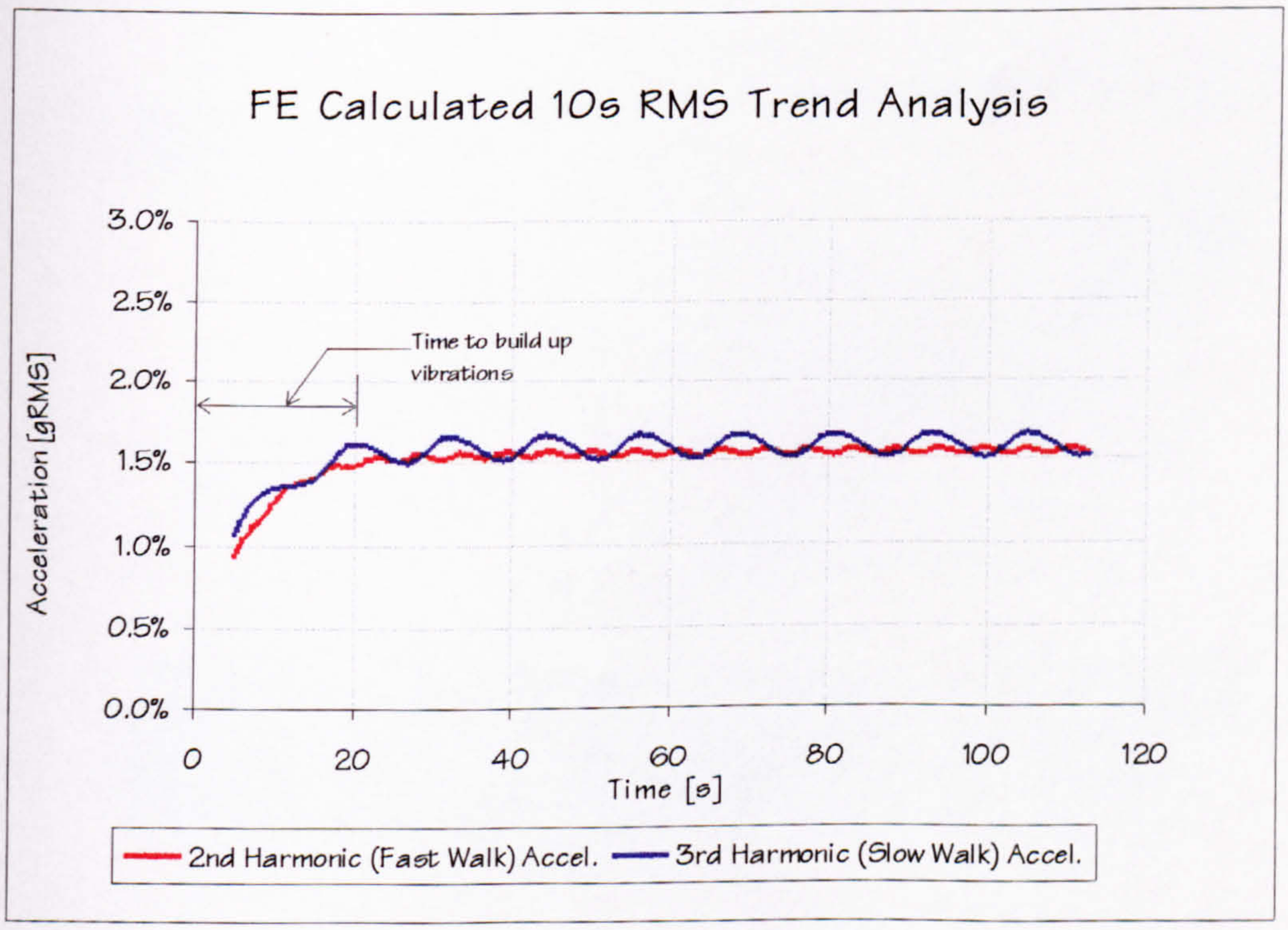

Figure 6.15: Structure A - 10s gRMS values corresponding to accelerations analytically calculated for WM2.

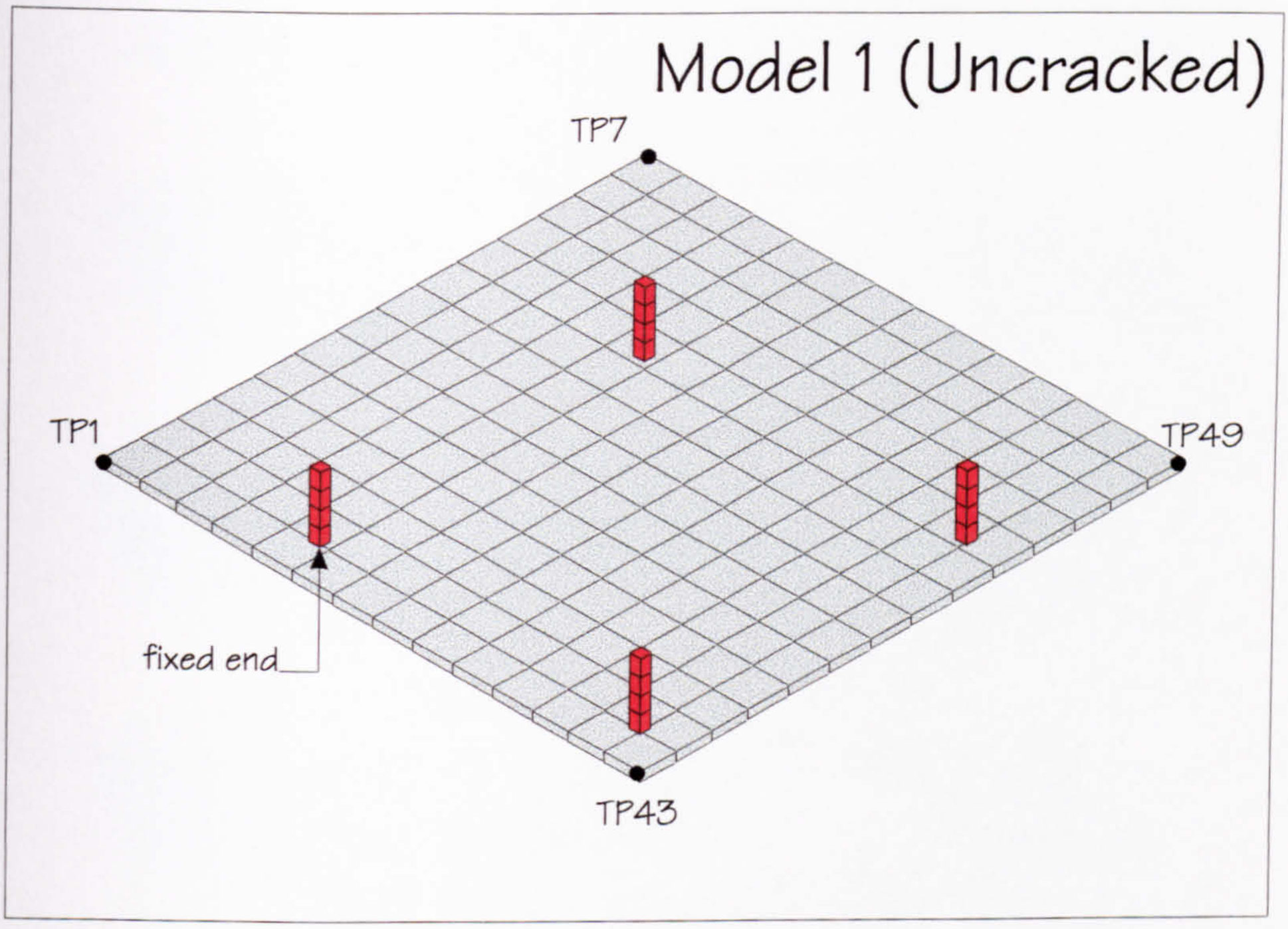

Figure 6.16: Structure B (Uncracked) - FE model using regular mesh.

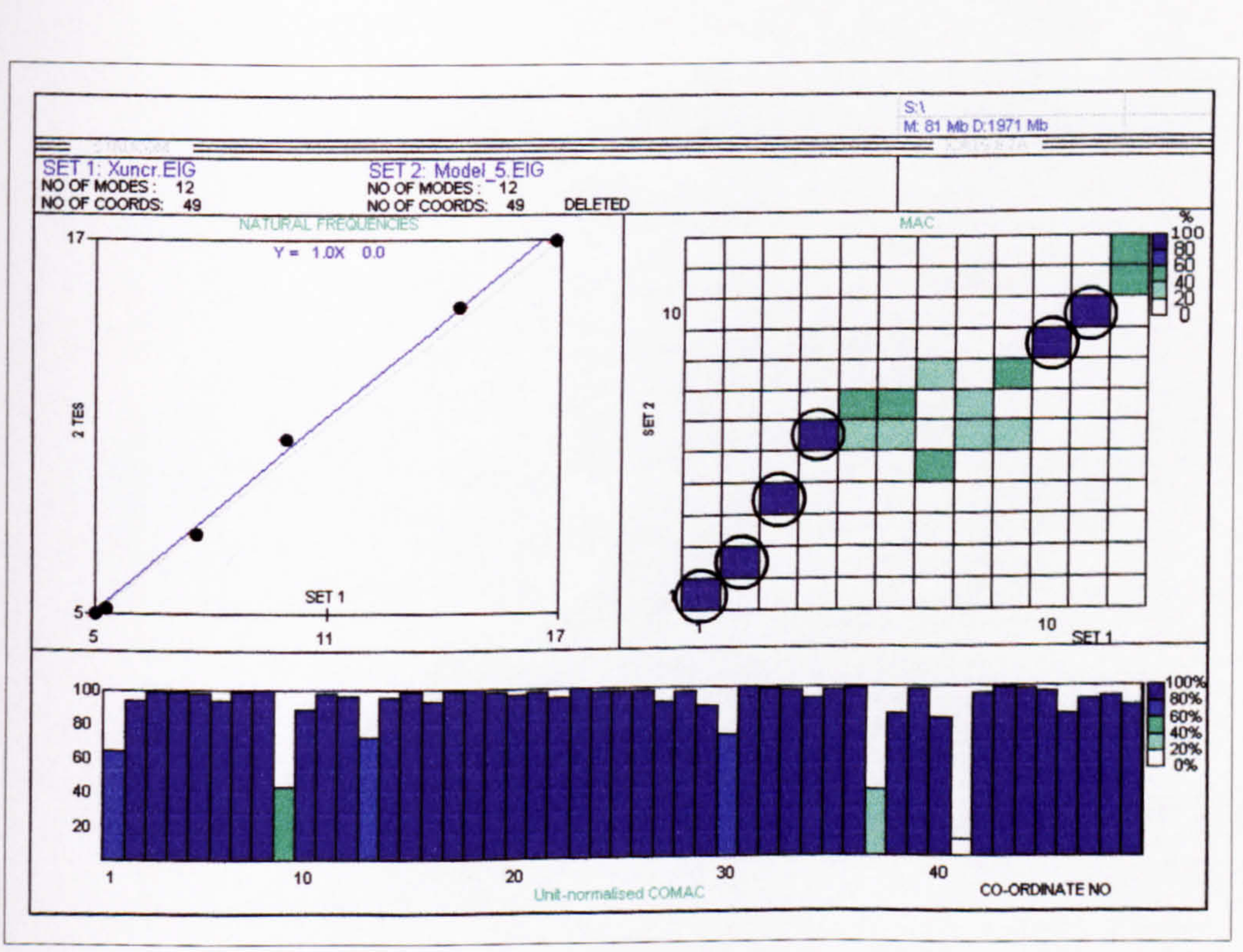

Figure 6.17: Structure B (Uncracked) - Comparison of natural frequencies, MAC and COMAC.

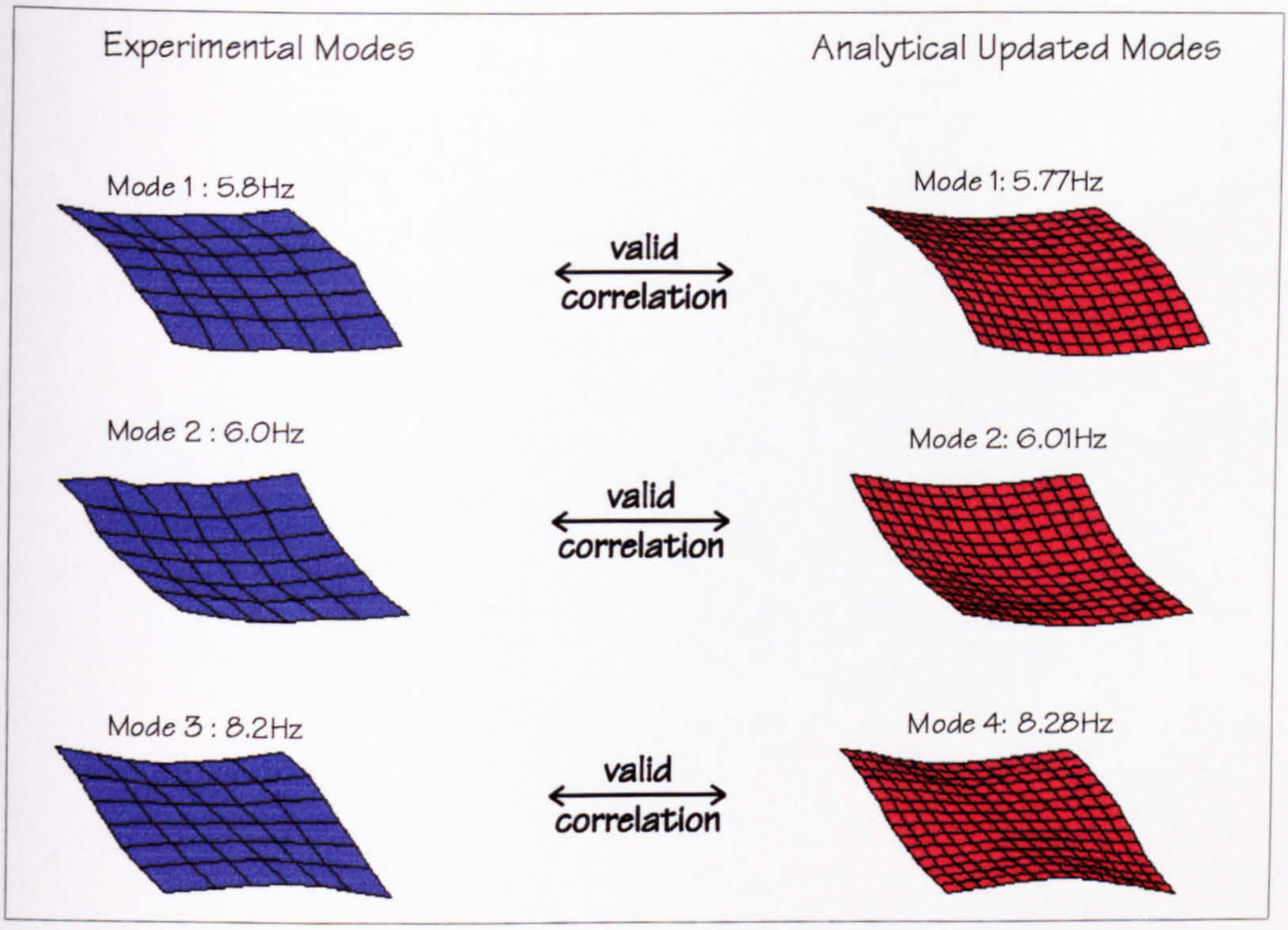

Figure 6.18: Structure B (Uncracked) - Visual inspection of the first three pairs of correlated mode shapes.

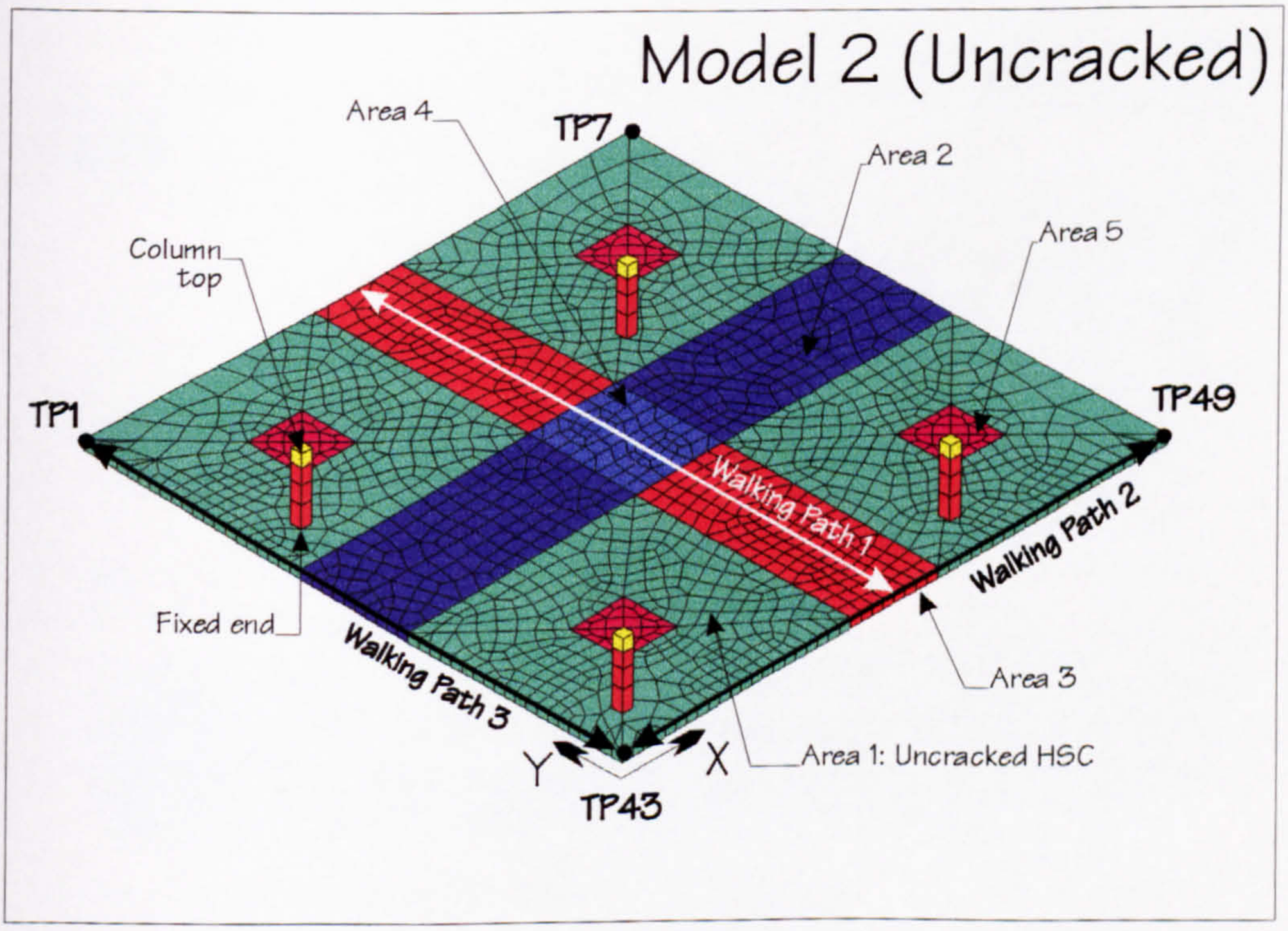

Figure 6.19: Structure B (Uncracked) - FE model used in parametric studies.

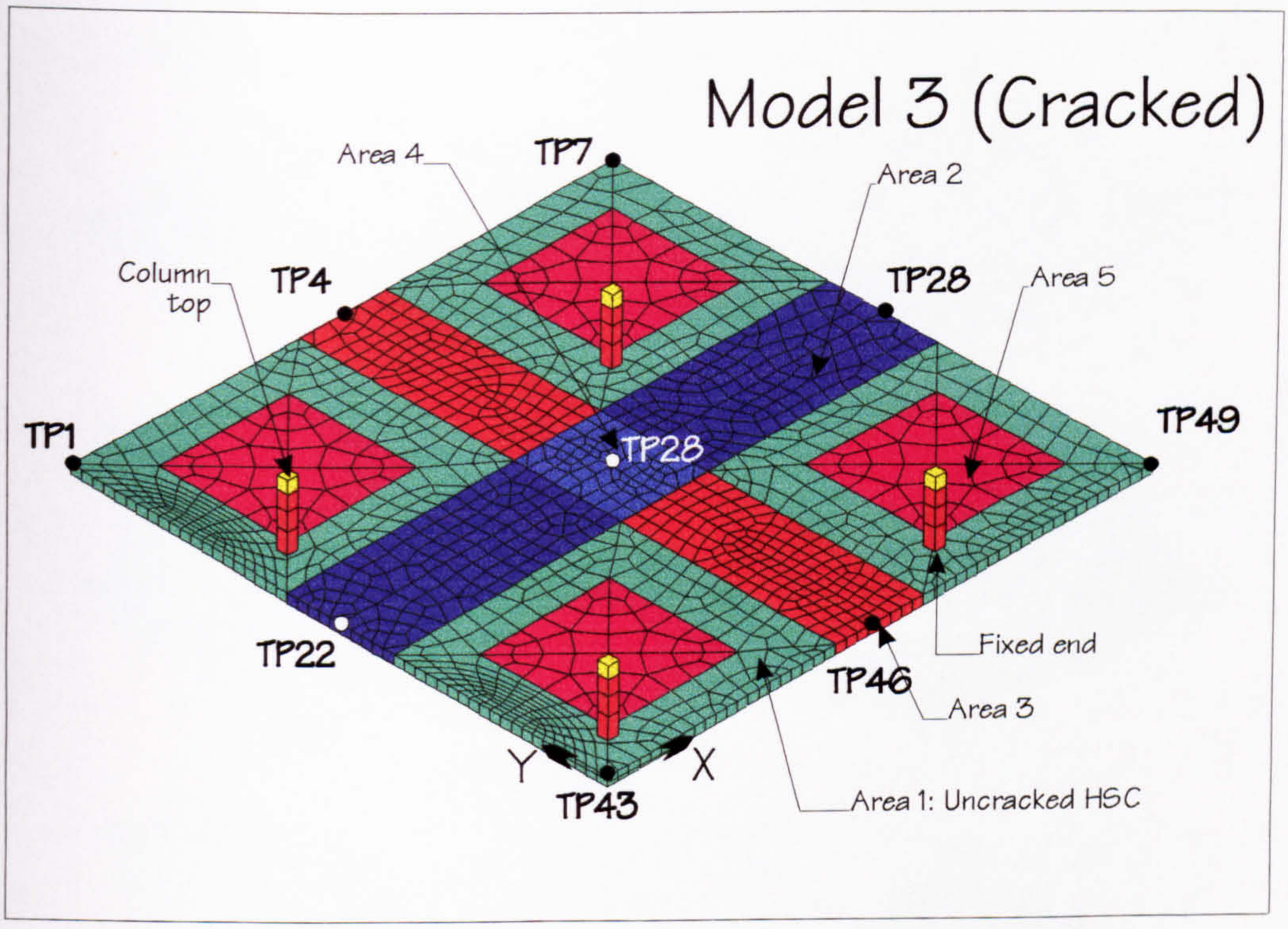

Figure 6.20: Structure B (Cracked) - Updated FE model.

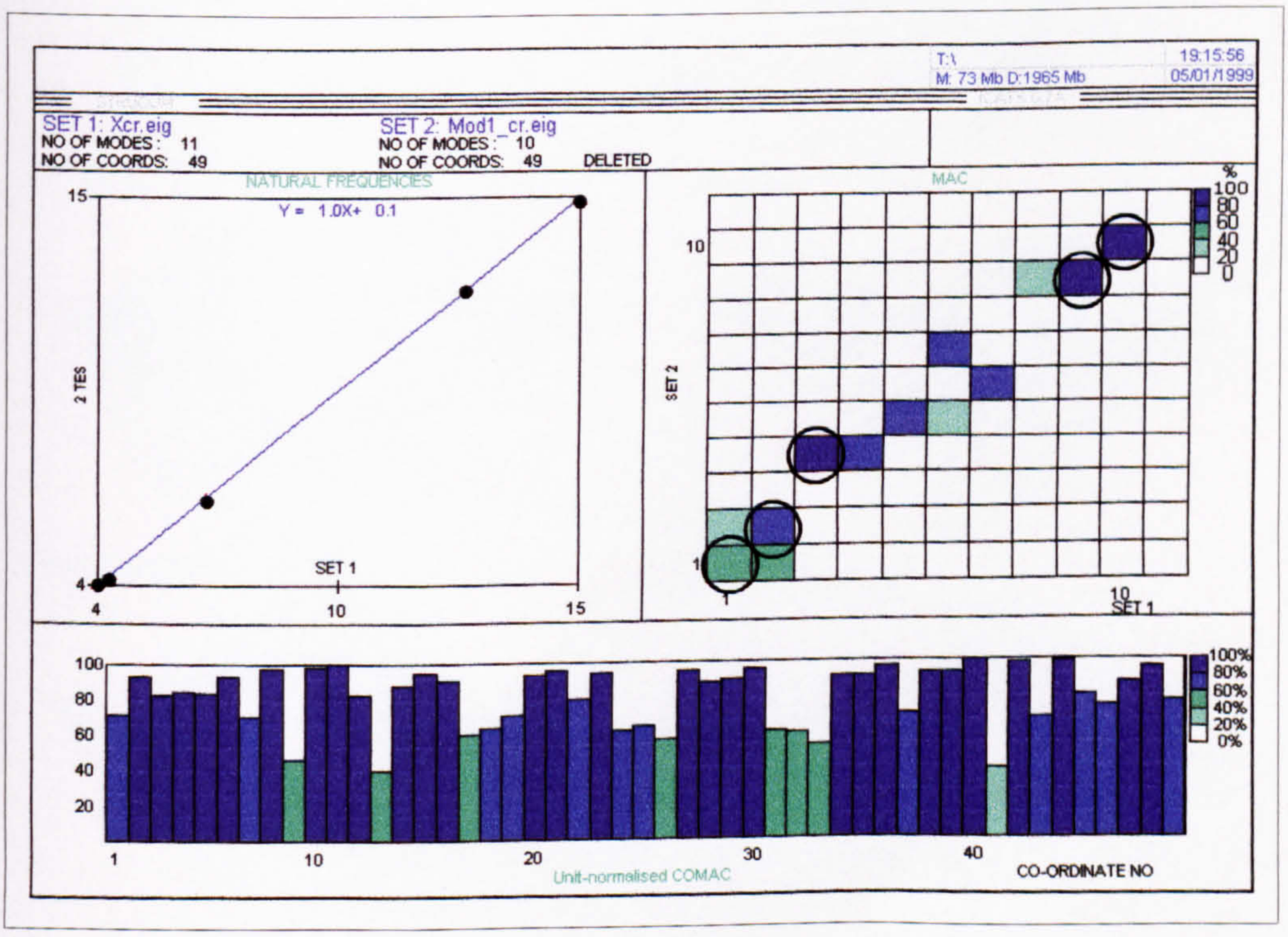

Figure 6.21: Structure B (Cracked) - Comparison of natural frequencies, MAC and COMAC.

Figure 6.22: Structure B (Cracked) - The analytically calculated mode shapes and natural frequencies.

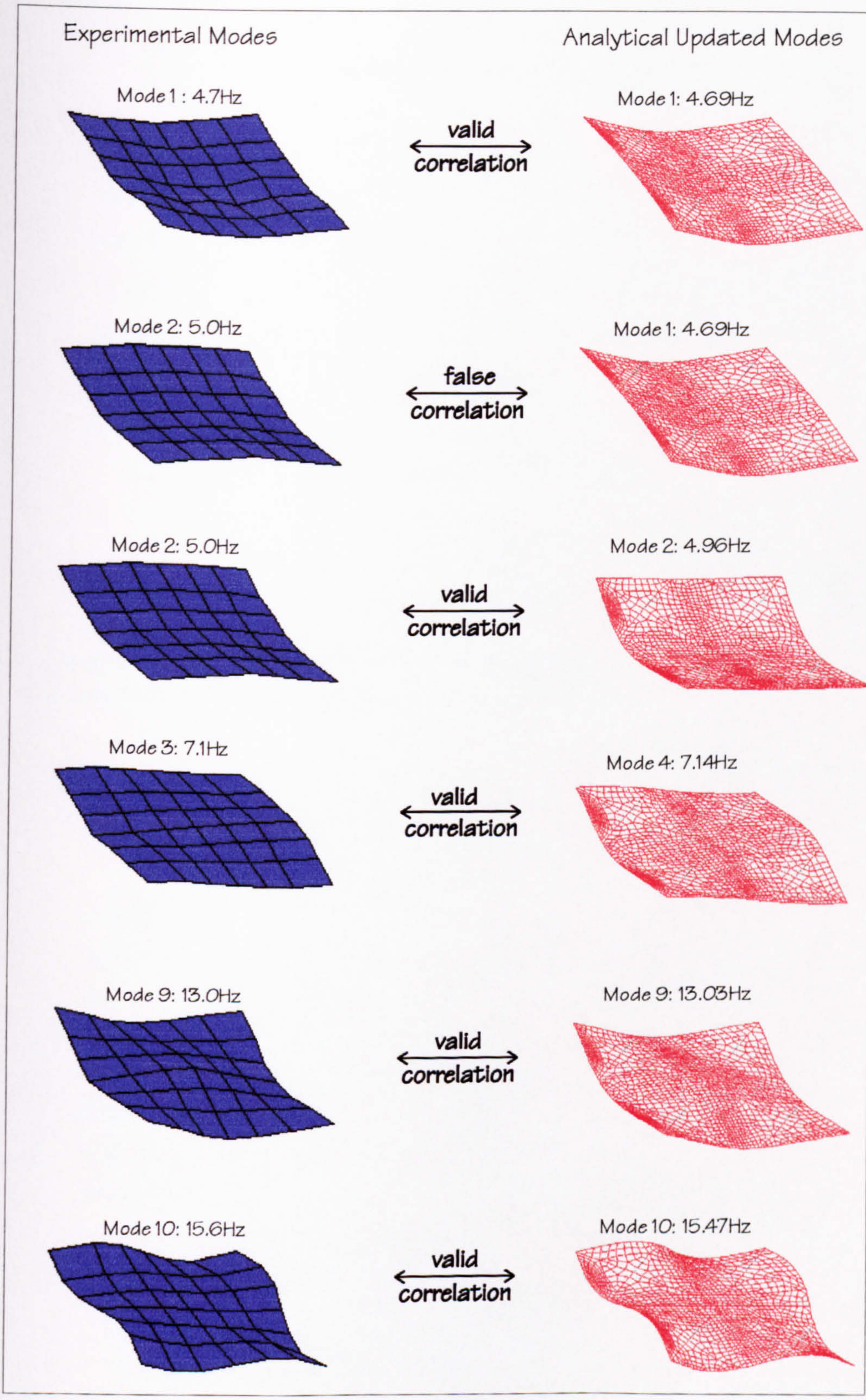

Figure 6.23: Structure B (Cracked) - The MAC correlated experimental and analytical mode shapes.

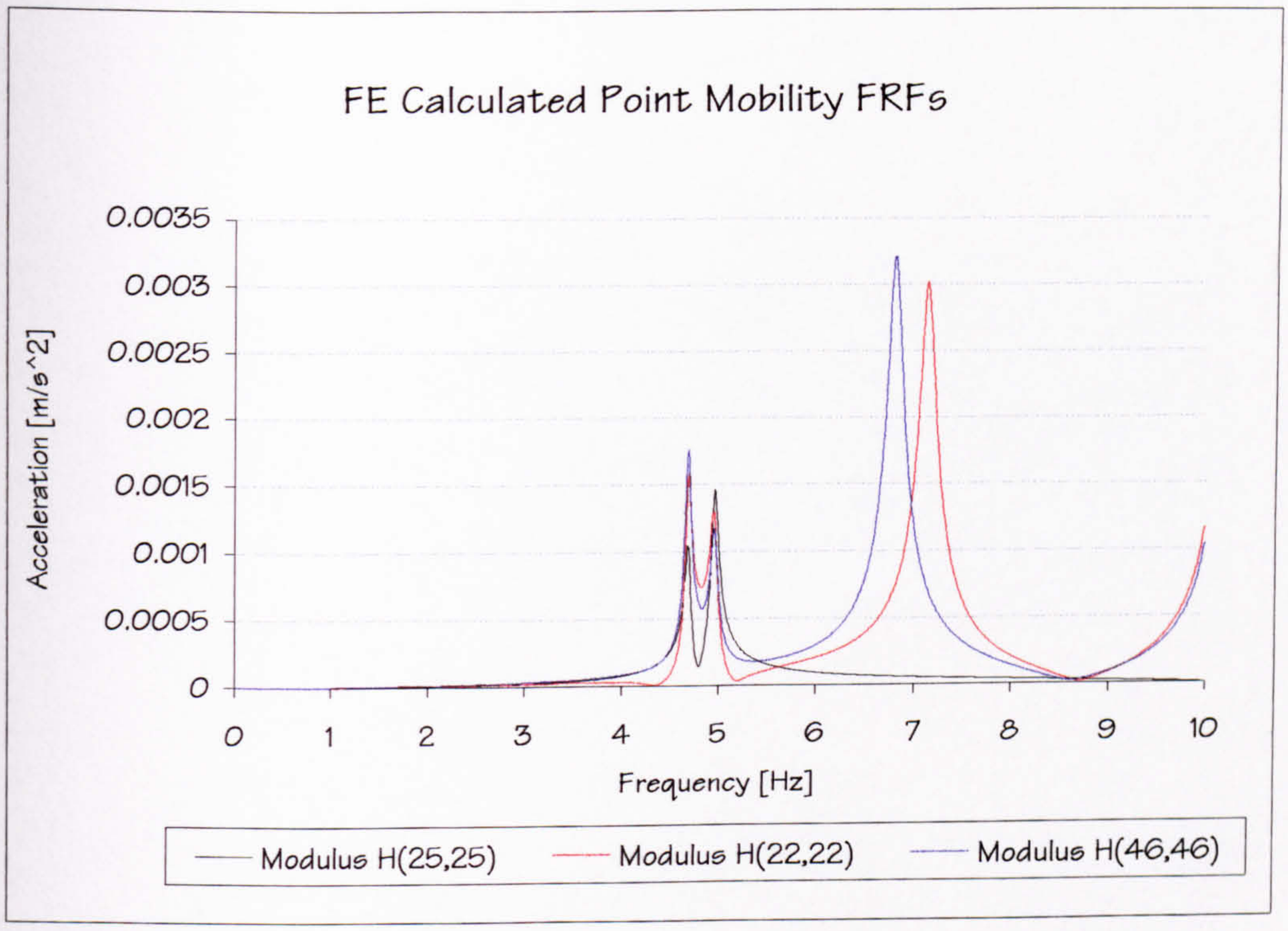

Figure 6.24: Structure B (Cracked) - Point mobilities corresponding to maximum mode shape amplitudes for analytical modes 1, 4 and 2, respectively.

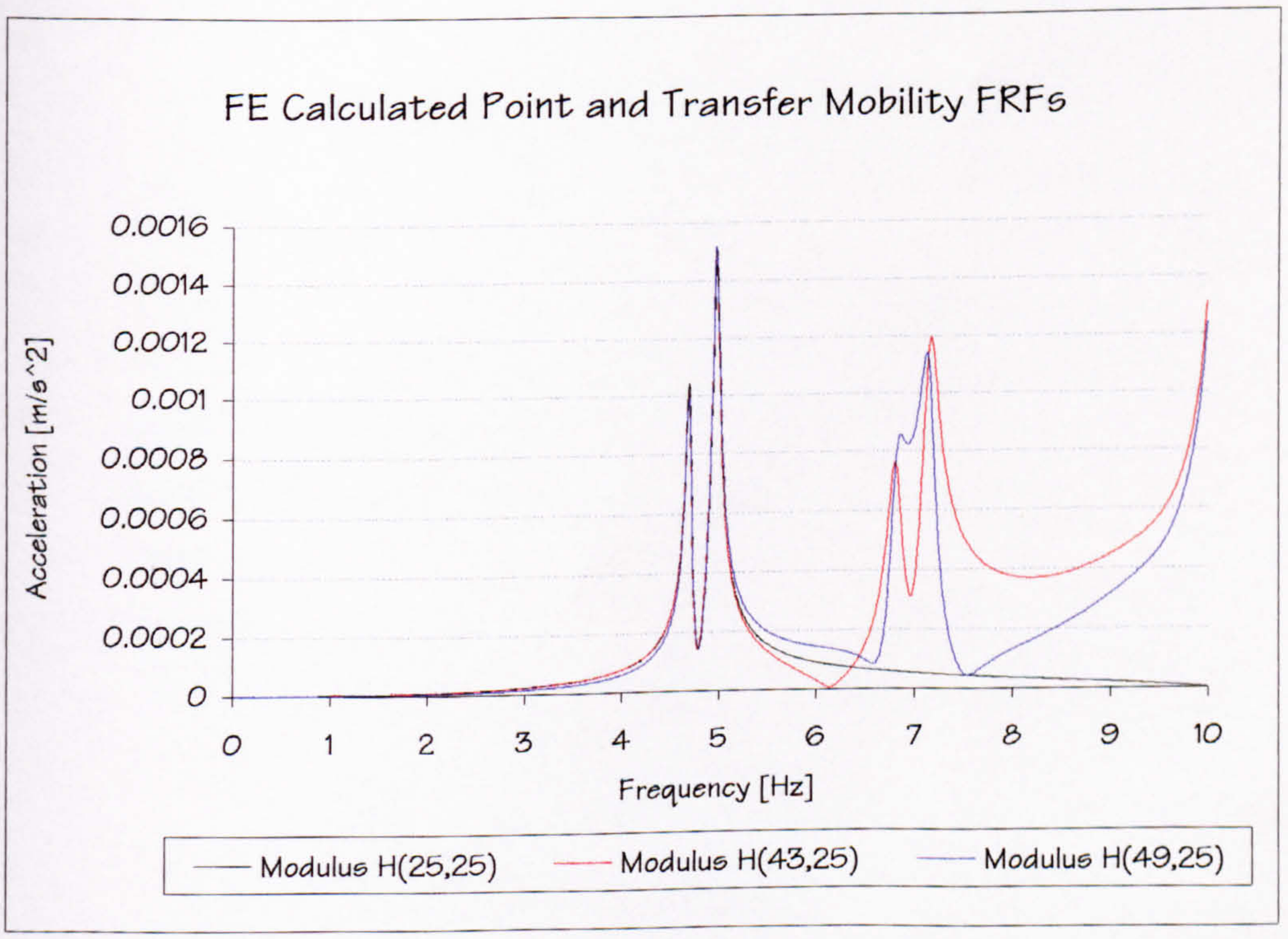

Figure 6.25: Structure B (Cracked) - Point and transfer mobilities corresponding to walking along WP1.

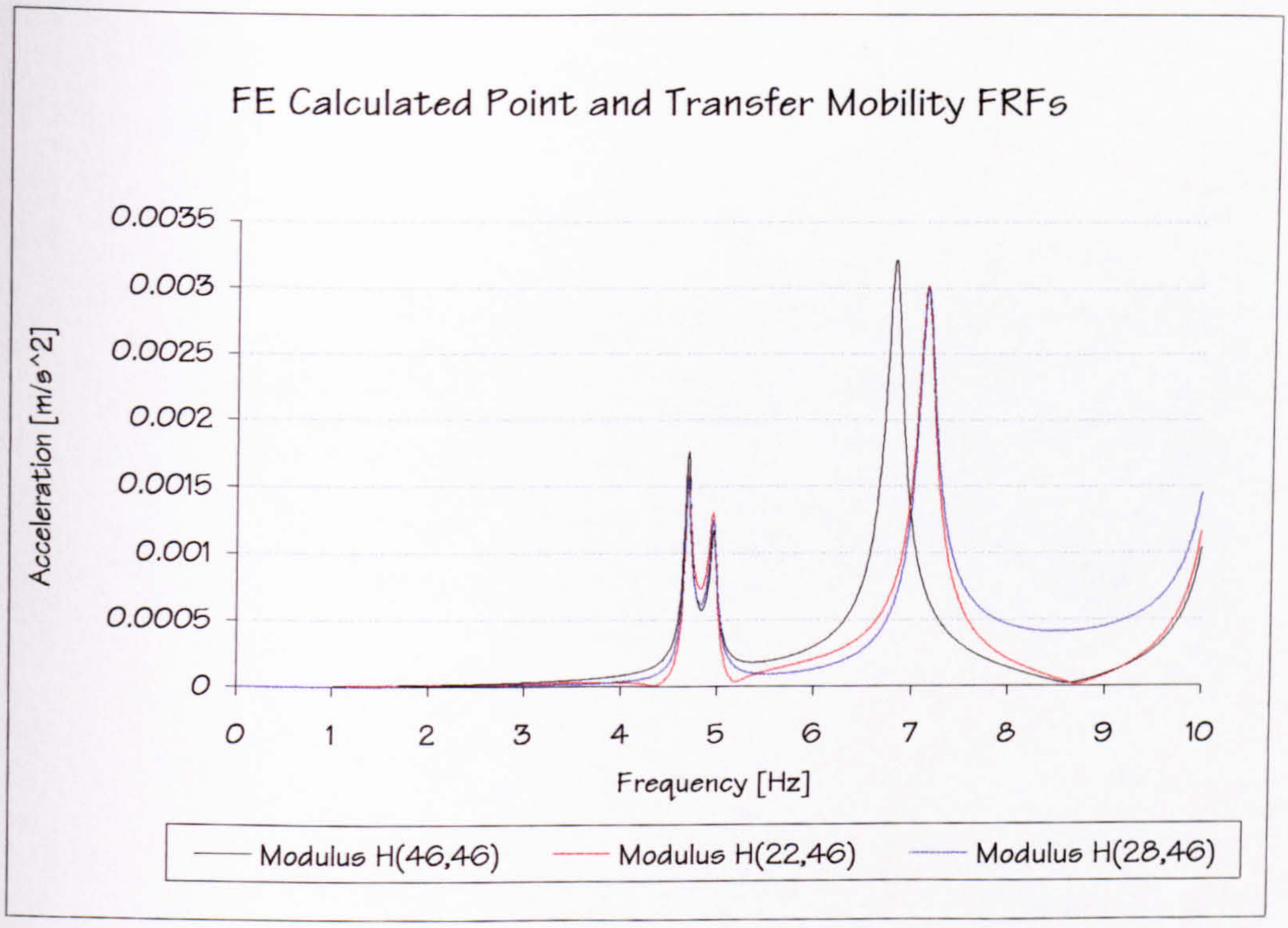

Figure 6.26: Structure B (Cracked) - Point and transfer mobilities corresponding to walking along WP2.

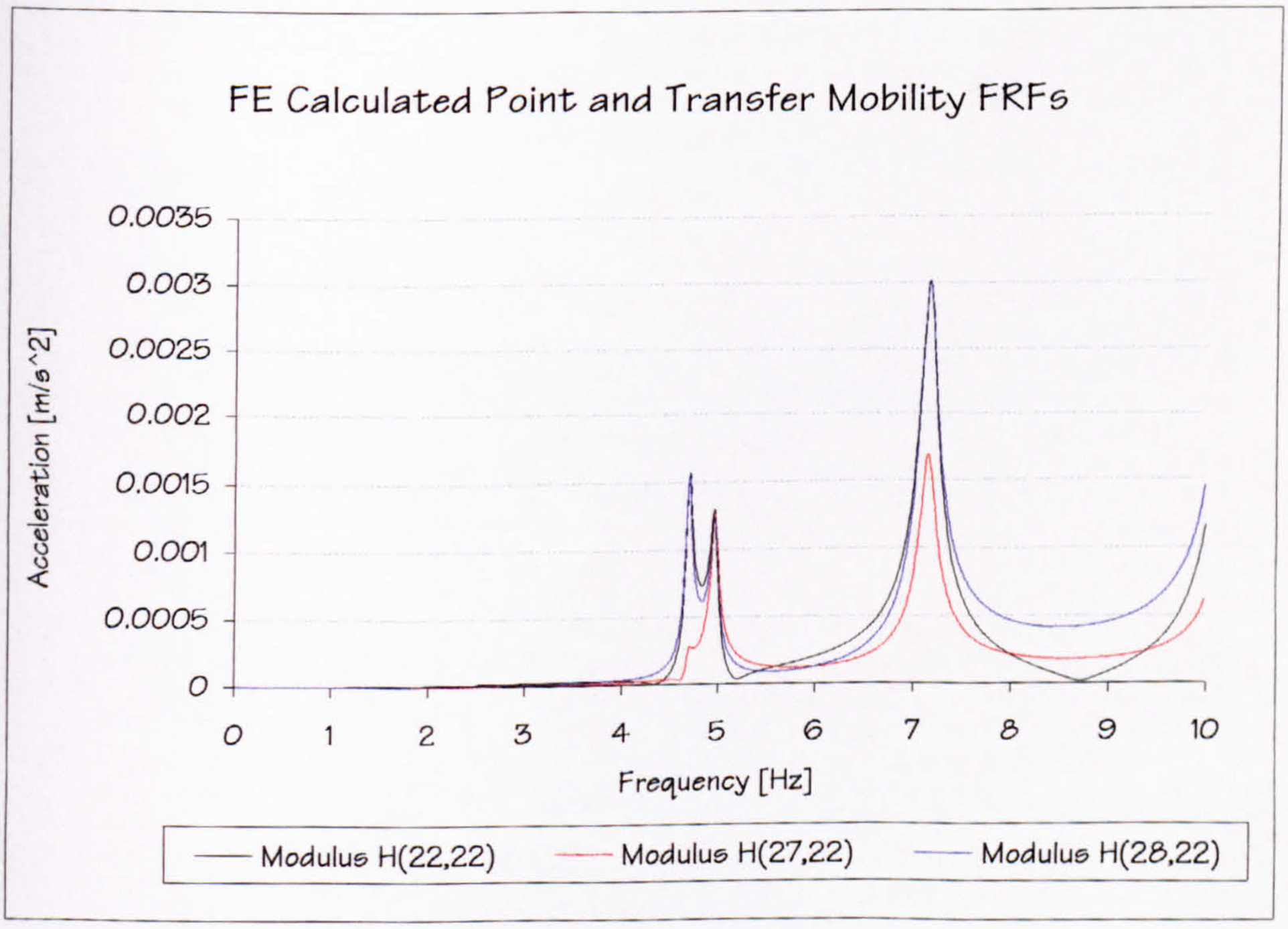

Figure 6.27: Structure B (Cracked) - Point and transfer mobilities corresponding to the excitation corresponding to walking along WP3.

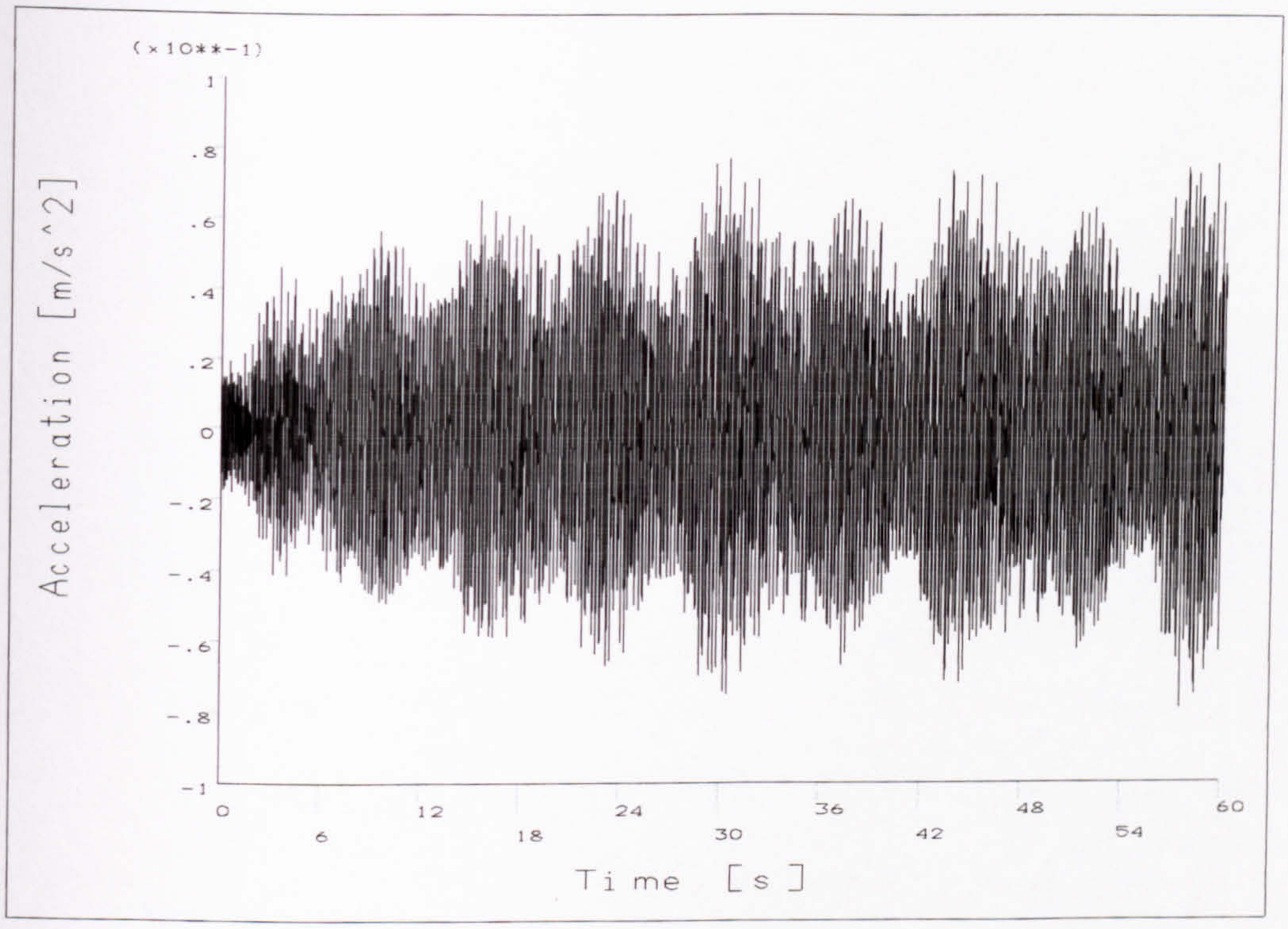

Figure 6.28: Structure B (Cracked) - FE simulated acceleration response @TP25 corresponding to Test 1.1a using the moving WM1.

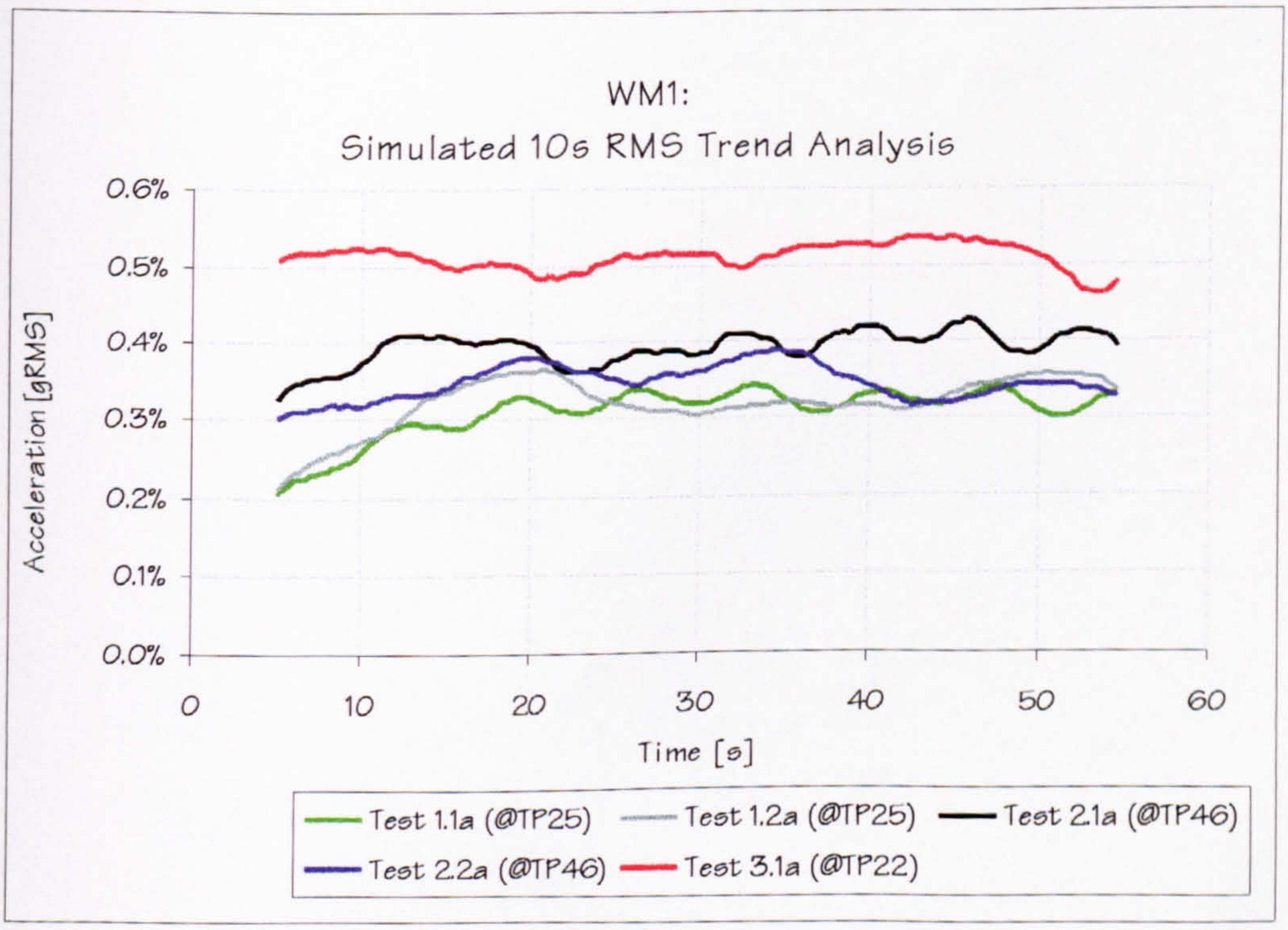

Figure 6.29: Structure B (Cracked) - 10s RMS acceleration trend analyses corresponding to all FE simulations using the moving WM1.

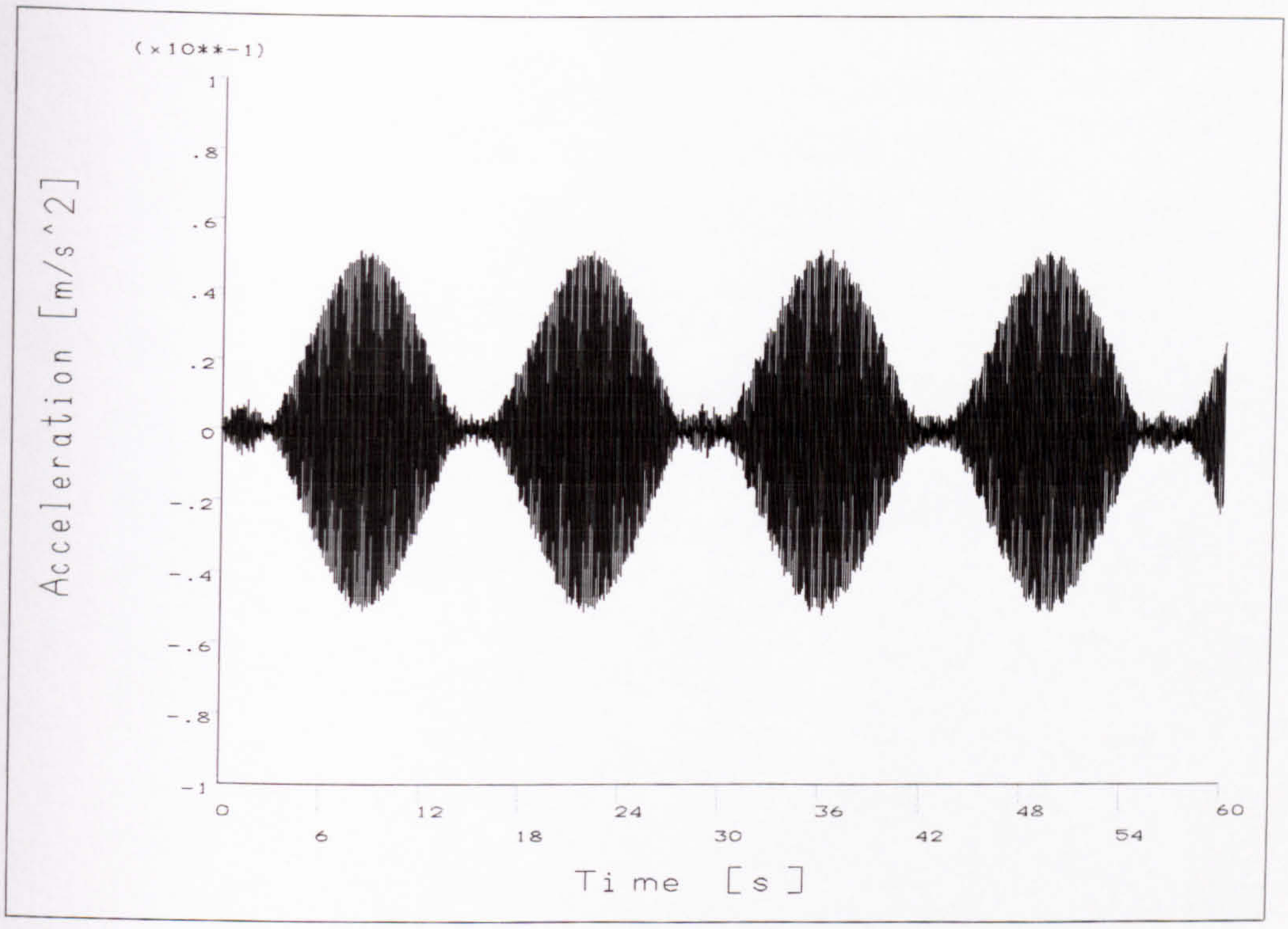

Figure 6.30: Structure B (Cracked) - FE simulated acceleration response corresponding to Test 3.1a @TP22 using WM2.

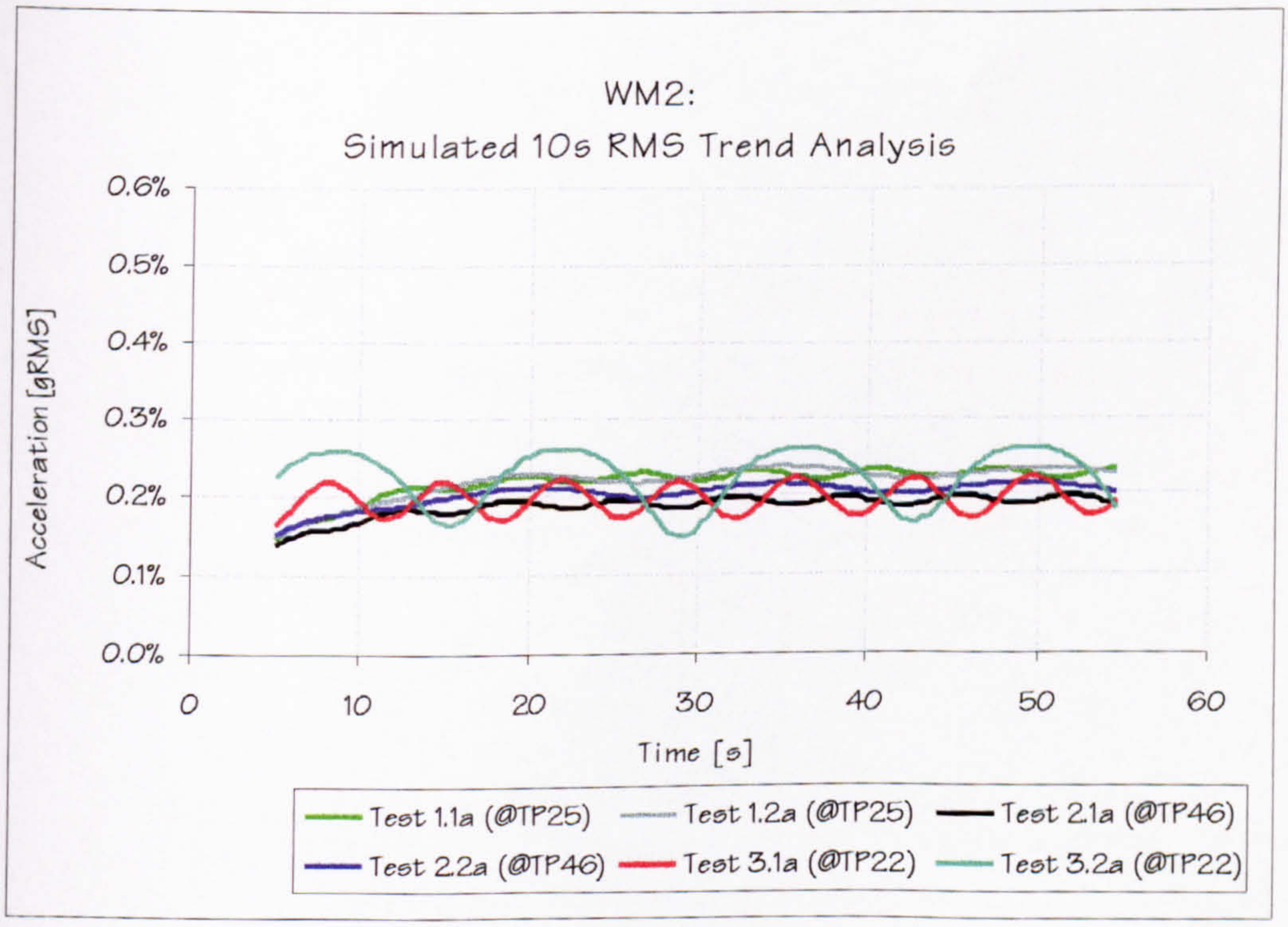

Figure 6.31: Structure B (Cracked) - 10s RMS trend analyses corresponding to simulations using WM2.

Figure 6.32: Structure B (Cracked) - Comparison of measured and FE simulated 10s RMS trend analyses corresponding to the 3rd harmonic excitation at 94spm.

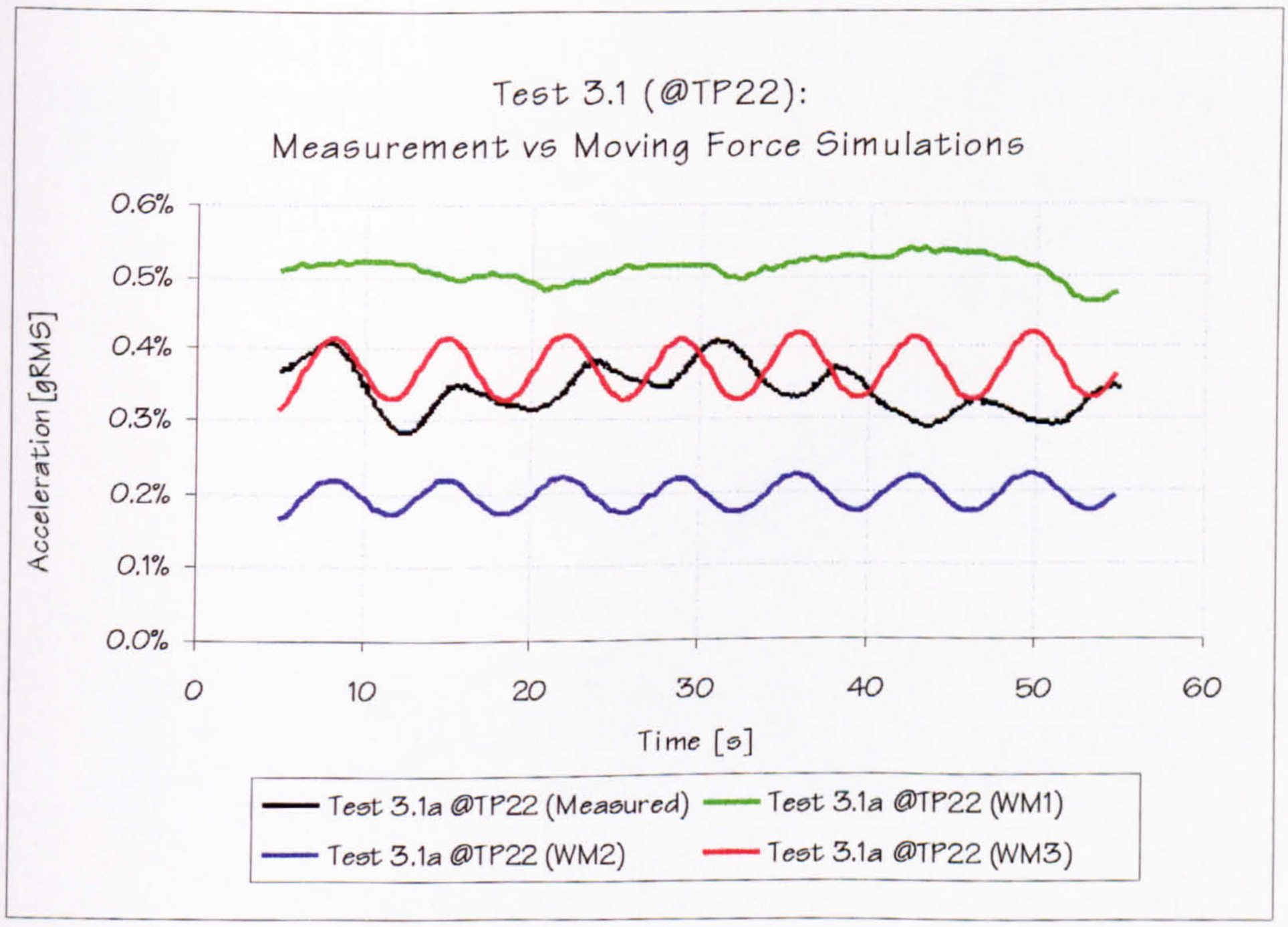

Figure 6.33: Structure B (Cracked) - Comparison of measured and FE simulated 10s RMS trend analyses corresponding to the 3rd harmonic excitation at 142spm.

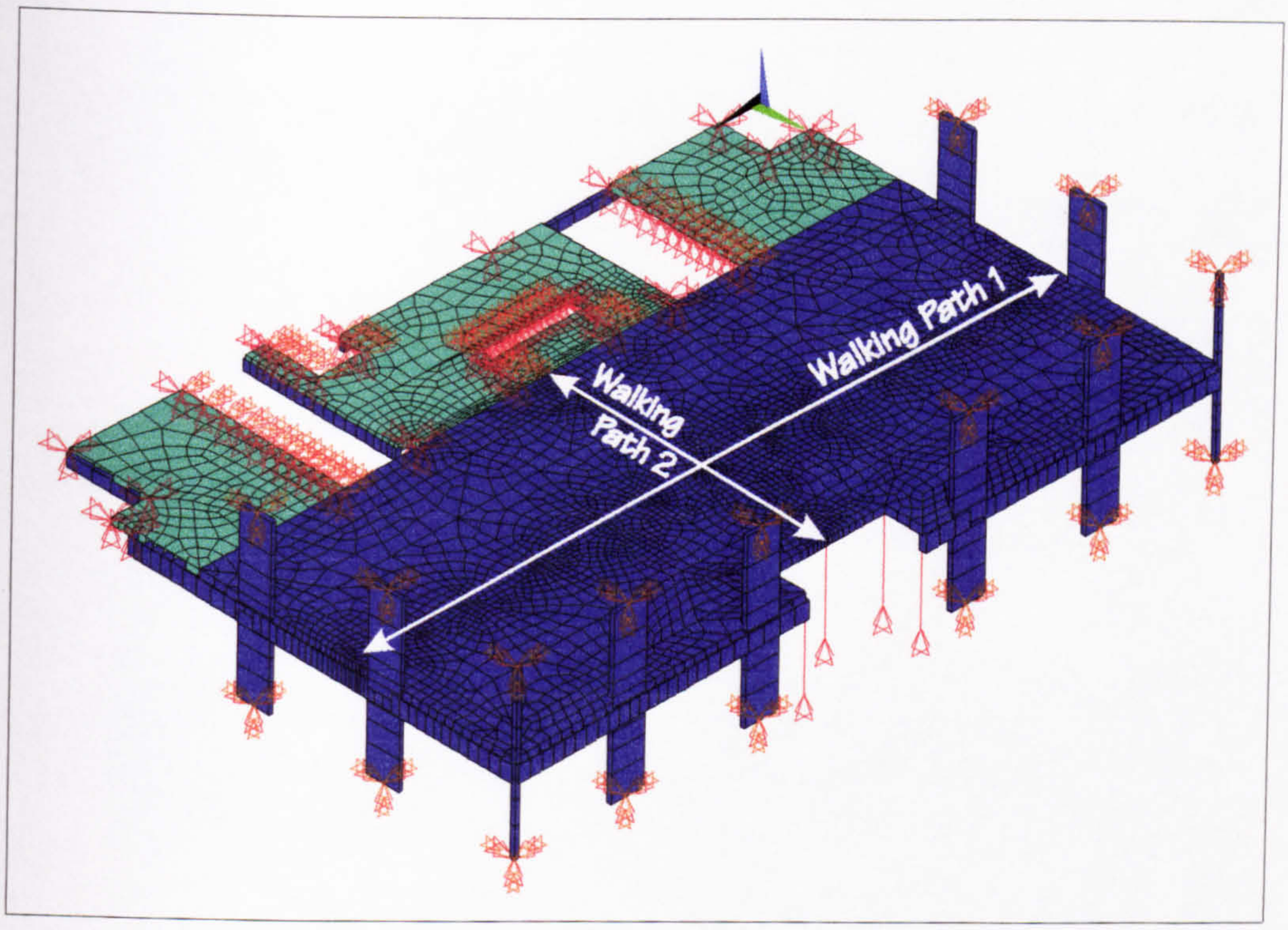

Figure 6.34: Structure C (Unclad) - Updated FE model.

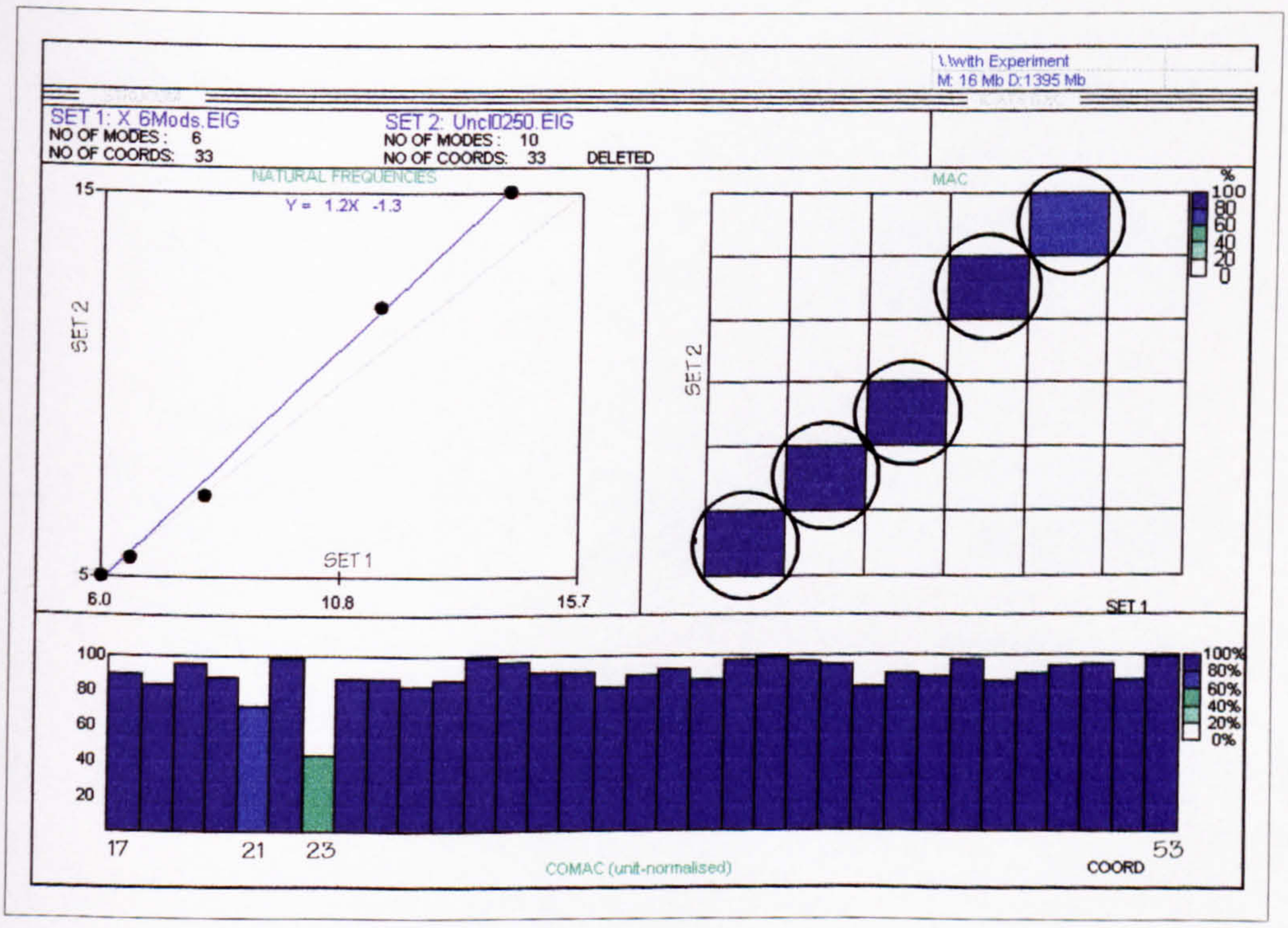

Figure 6.35: Structure C (Unclad) - Comparison of natural frequencies, MAC and COMAC using experimental and analytical updated modes.

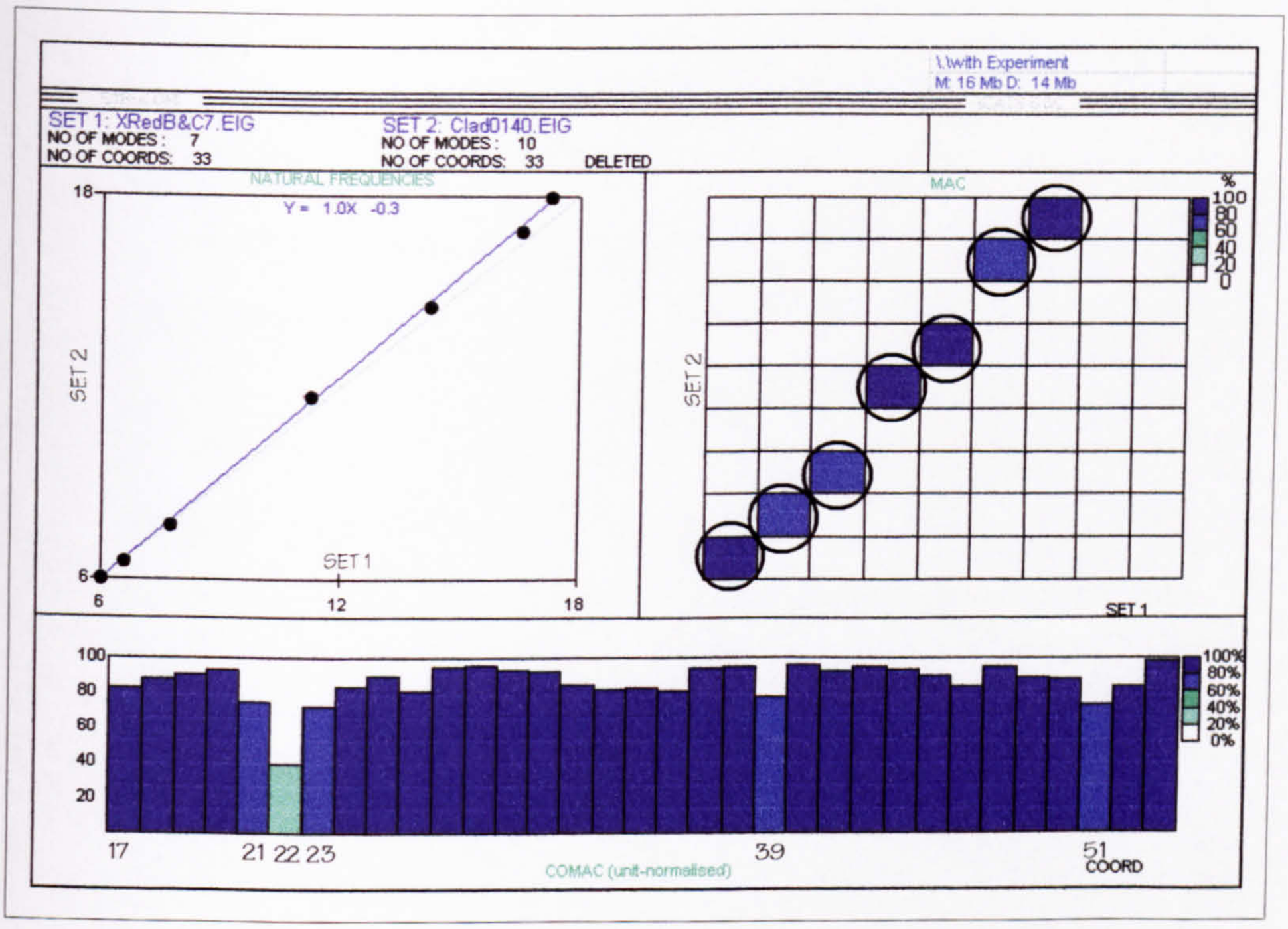

Figure 6.36: Structure C (Clad) - Comparison of natural frequencies, MAC and COMAC using experimental and analytical updated modes.

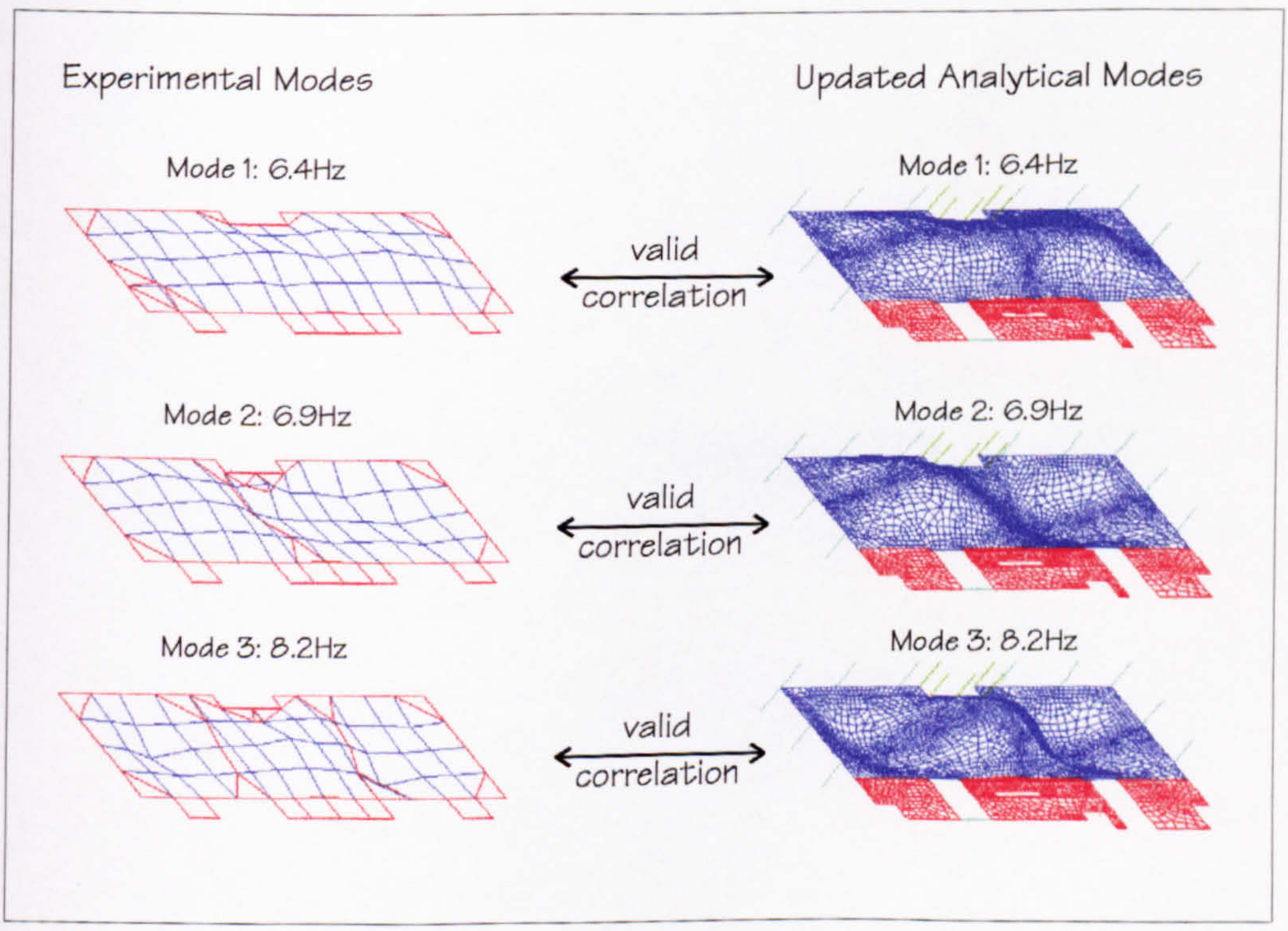

Figure 6.37: Structure C (Clad) - The first three MAC correlated experimental and analytical mode shapes.

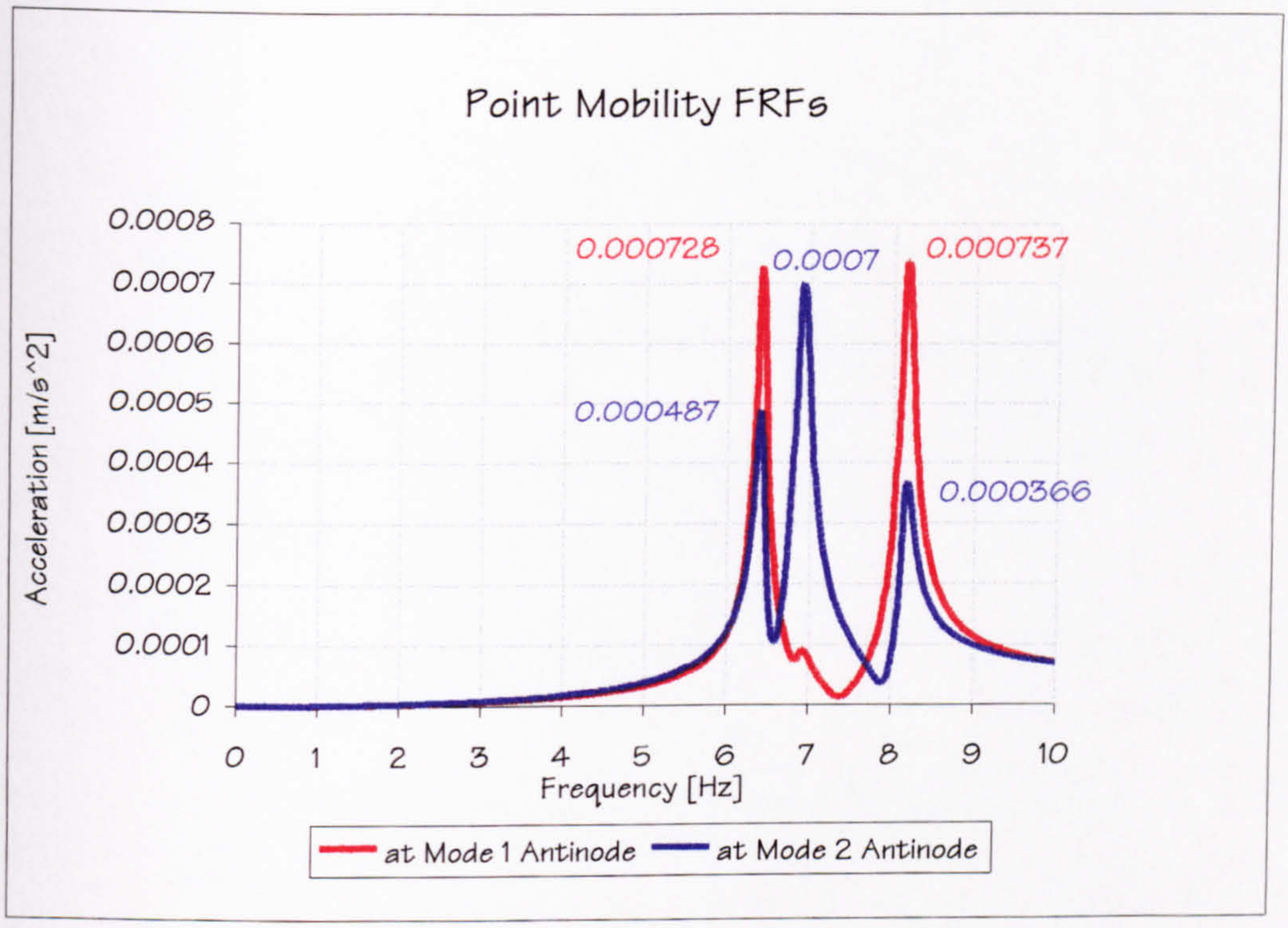

Figure 6.38: Structure C (Clad) - Two FRF point mobilities calculated using the updated FE model and corresponding to the antinodes of modes 1 and 2.

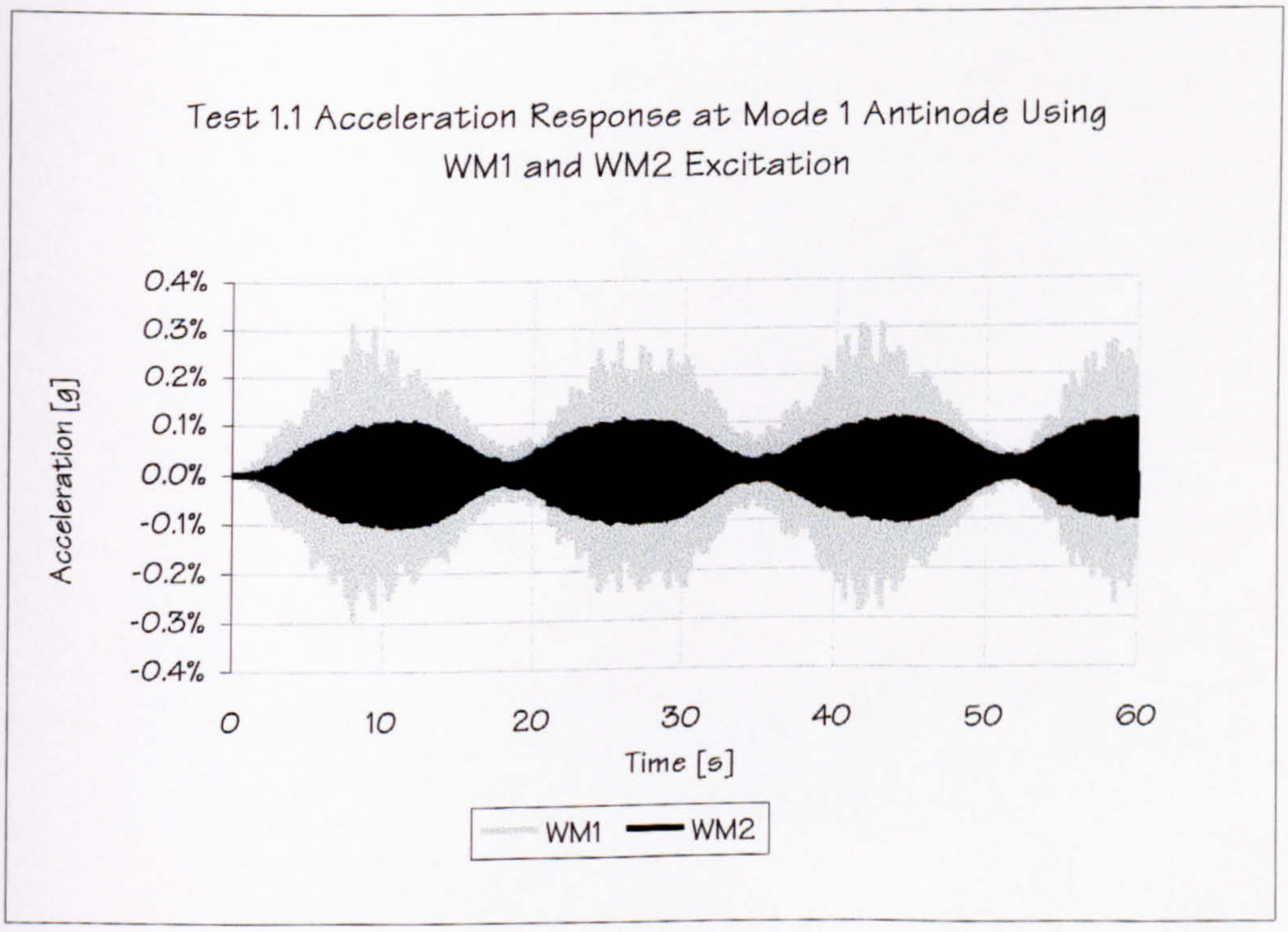

Figure 6.39: Structure C (Clad) - Comparison of 60s of simulated acceleration responses corresponding to Test 1.1 using WM1 and WM2 which move along WP1. Assumed pacing frequency is 2.13Hz with a step length of 0.9m.

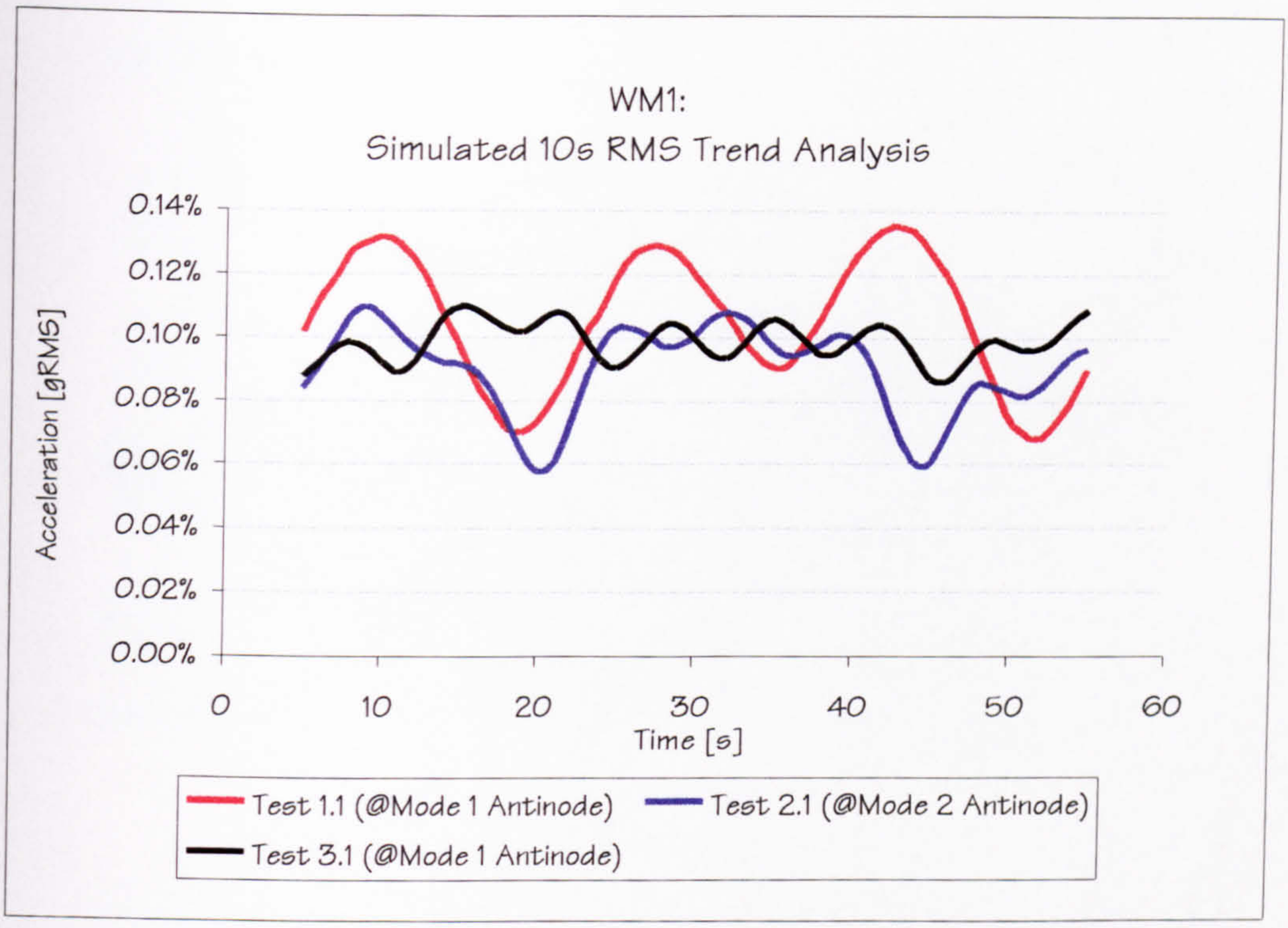

Figure 6.40: Structure C (Clad) - 10s gRMS values corresponding to accelerations analytically calculated for WM1.

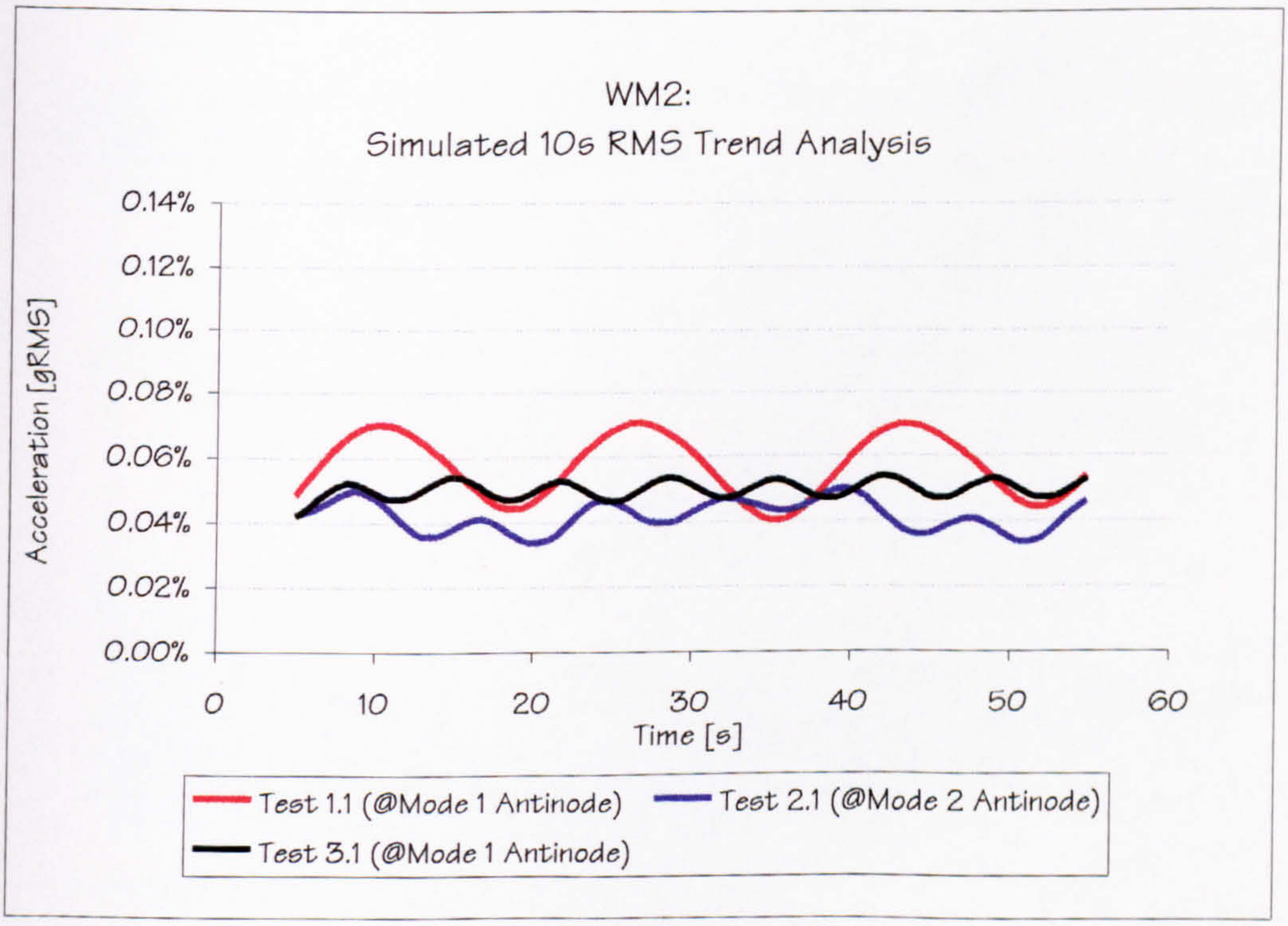

Figure 6.41: Structure C (Clad) - 10s gRMS values corresponding to accelerations analytically calculated for WM2.

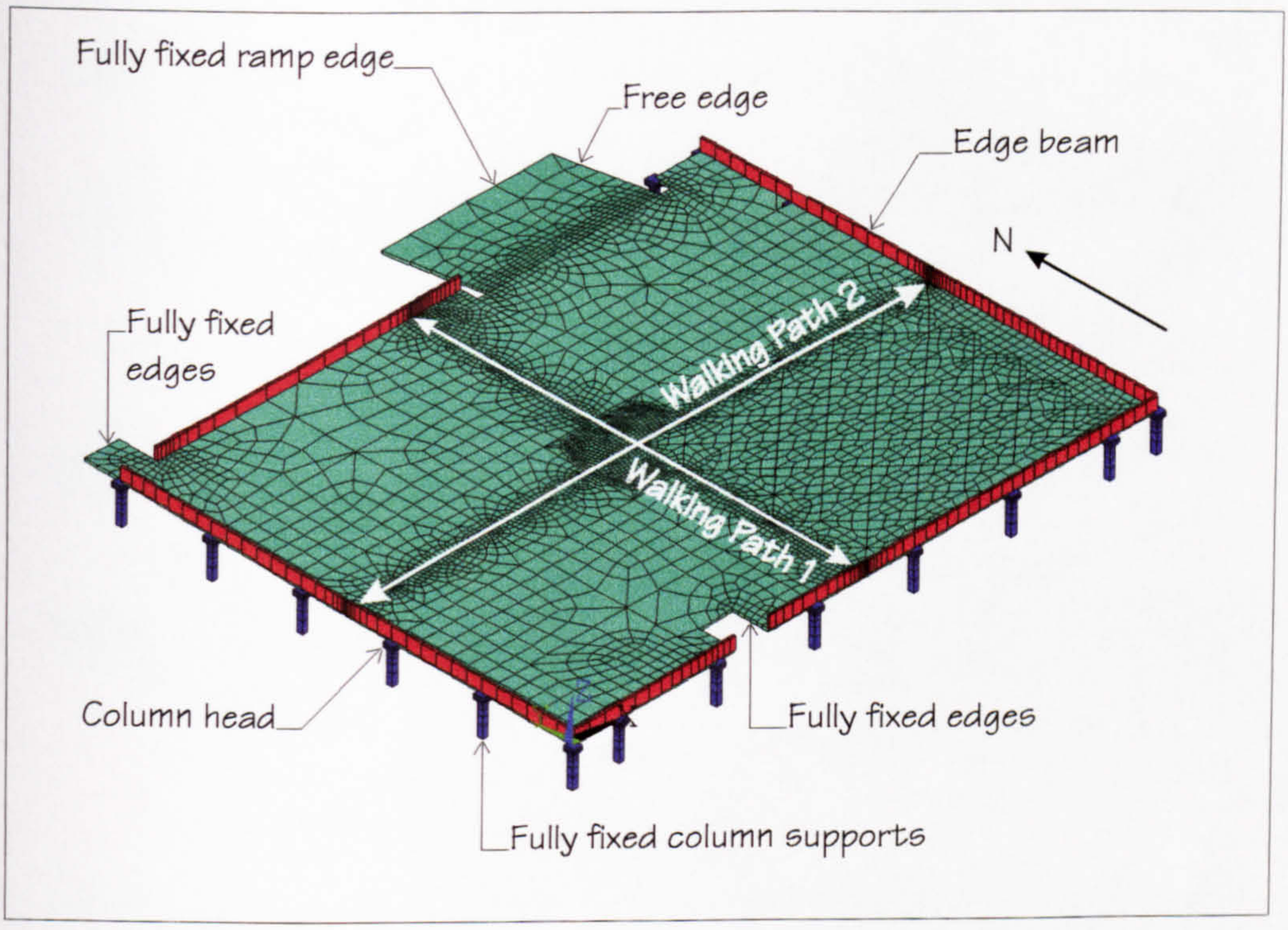

Figure 6.42: Structure D - Updated FE model.

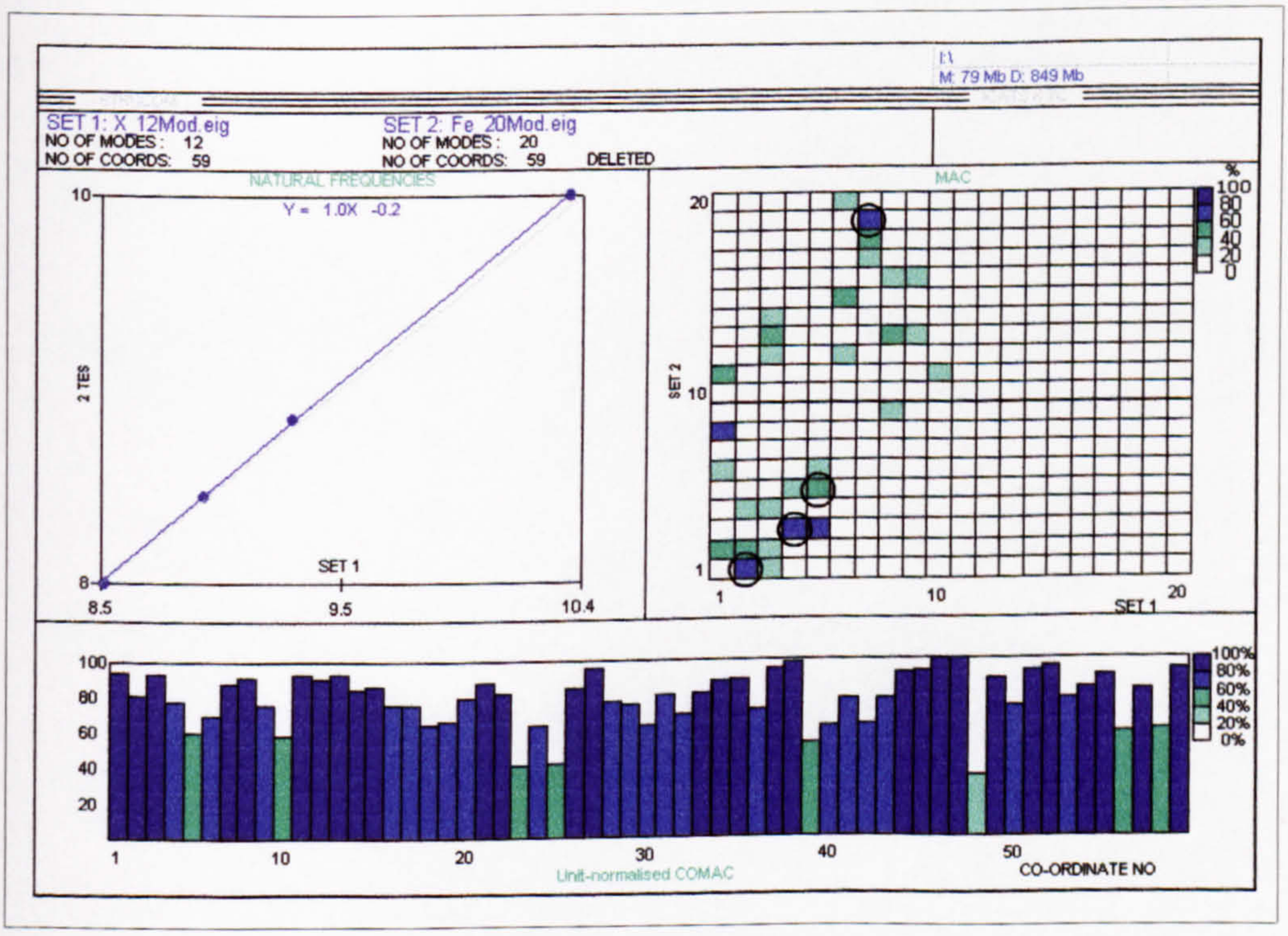

Figure 6.43: Structure D - Comparison of the natural frequencies, and MAC and COMAC calculations for the four correlated mode pairs (circled in the MAC matrix).

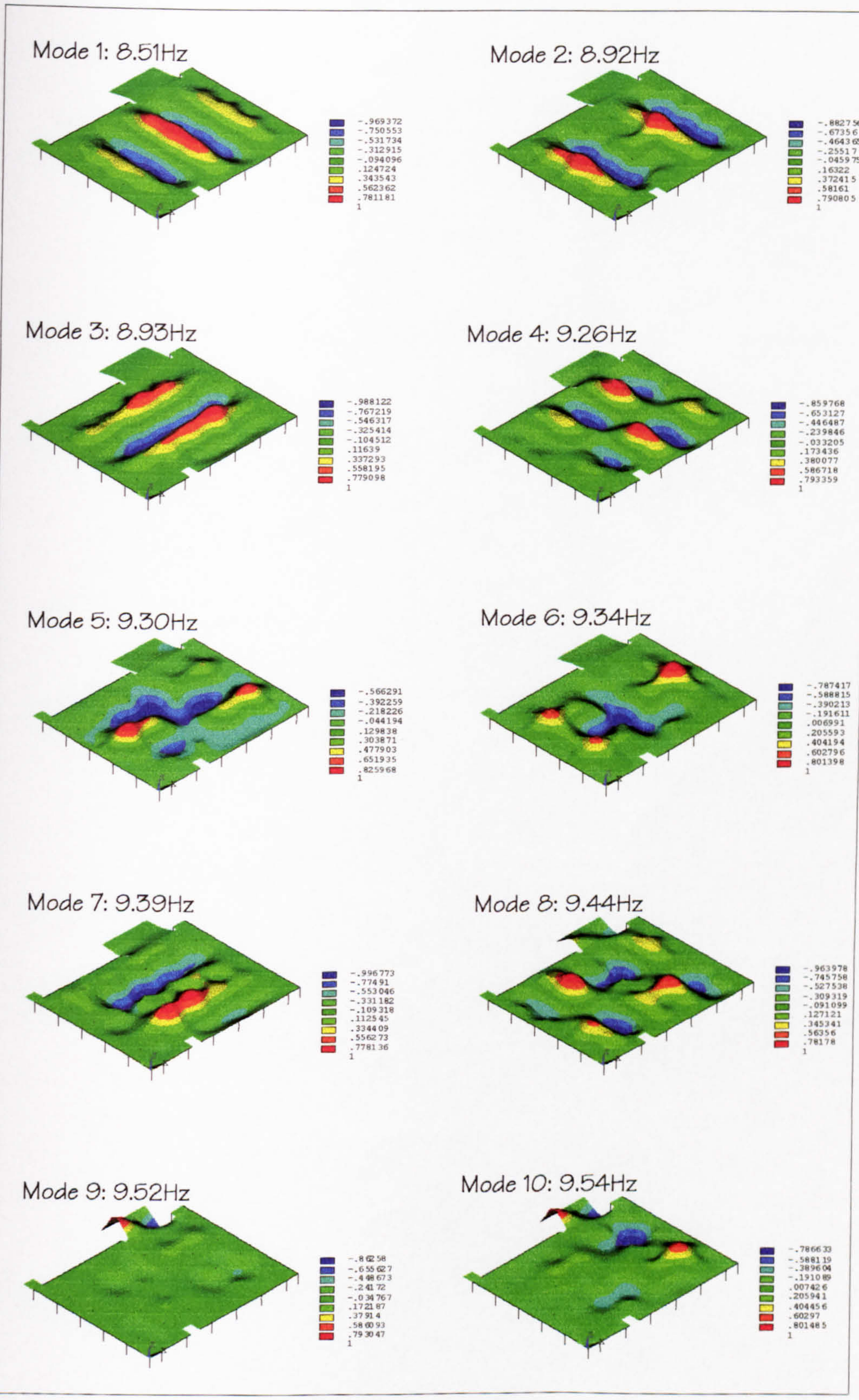

Figure 6.44: Structure D - The lowest 10 modes calculated using the updated FE model.

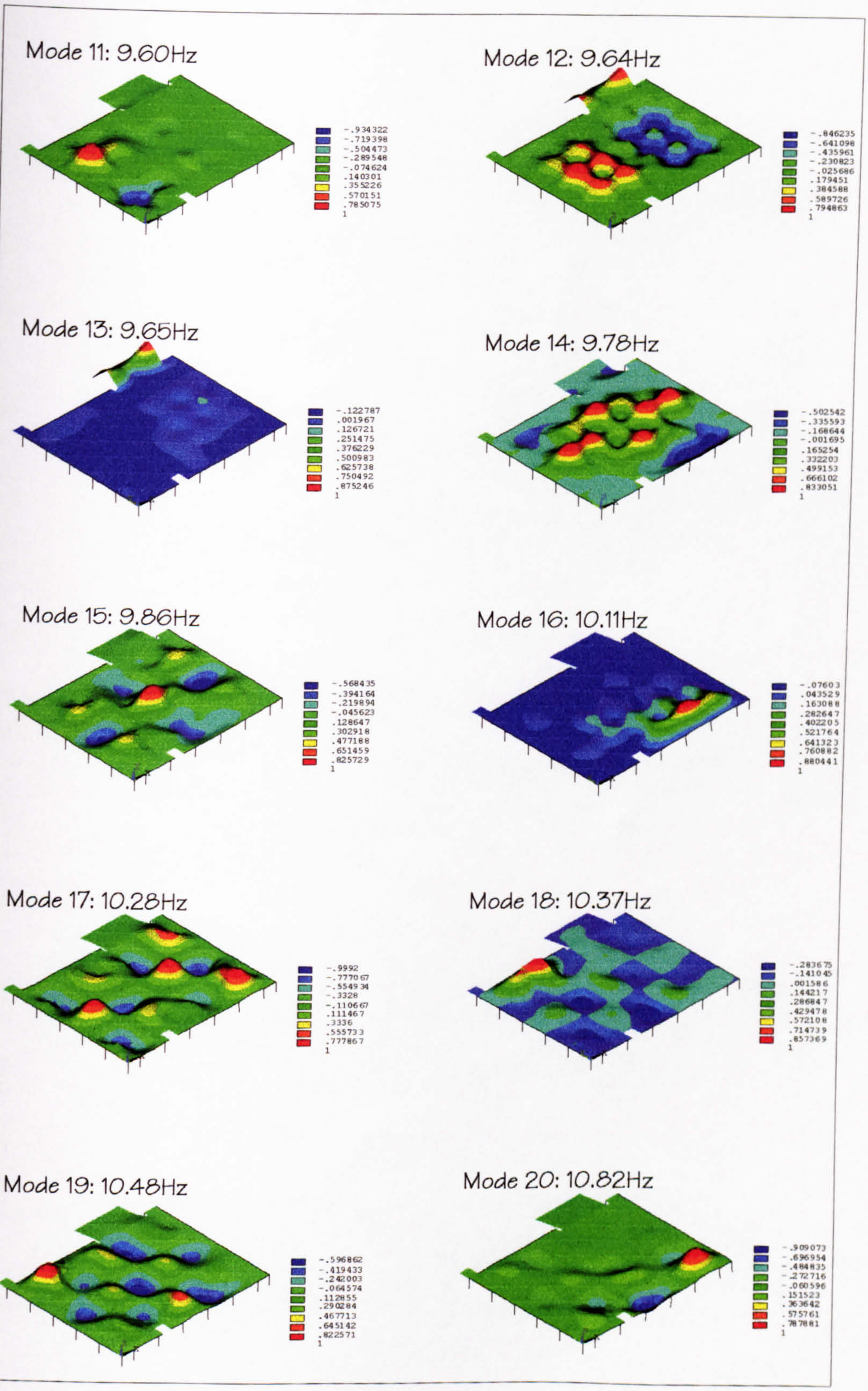

Figure 6.45: Structure D - Modes 11-20 calculated using the updated FE model.

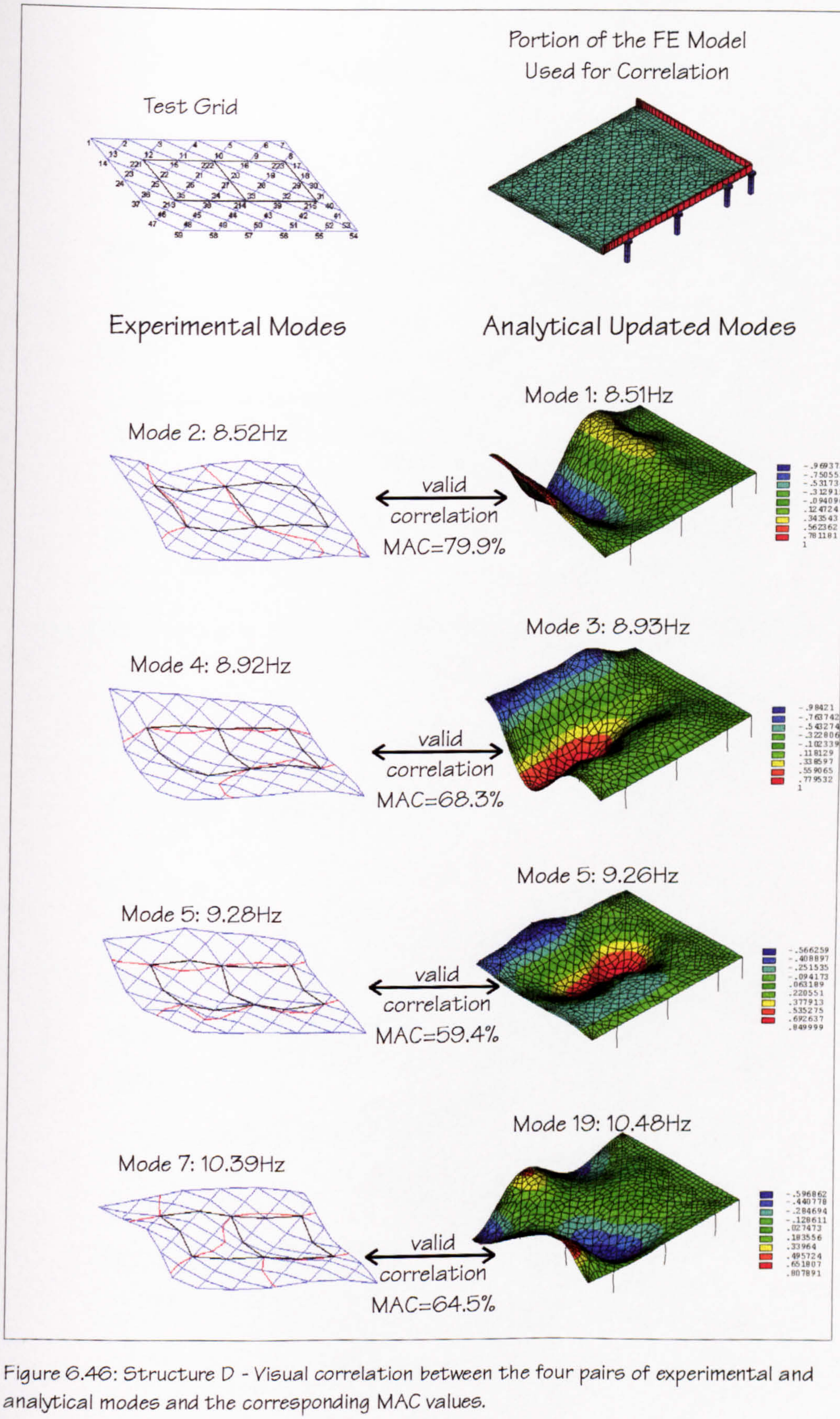

Figure 6.46: Structure D - Visual correlation between the four pairs of experimental and analytical modes and the corresponding MAC values.

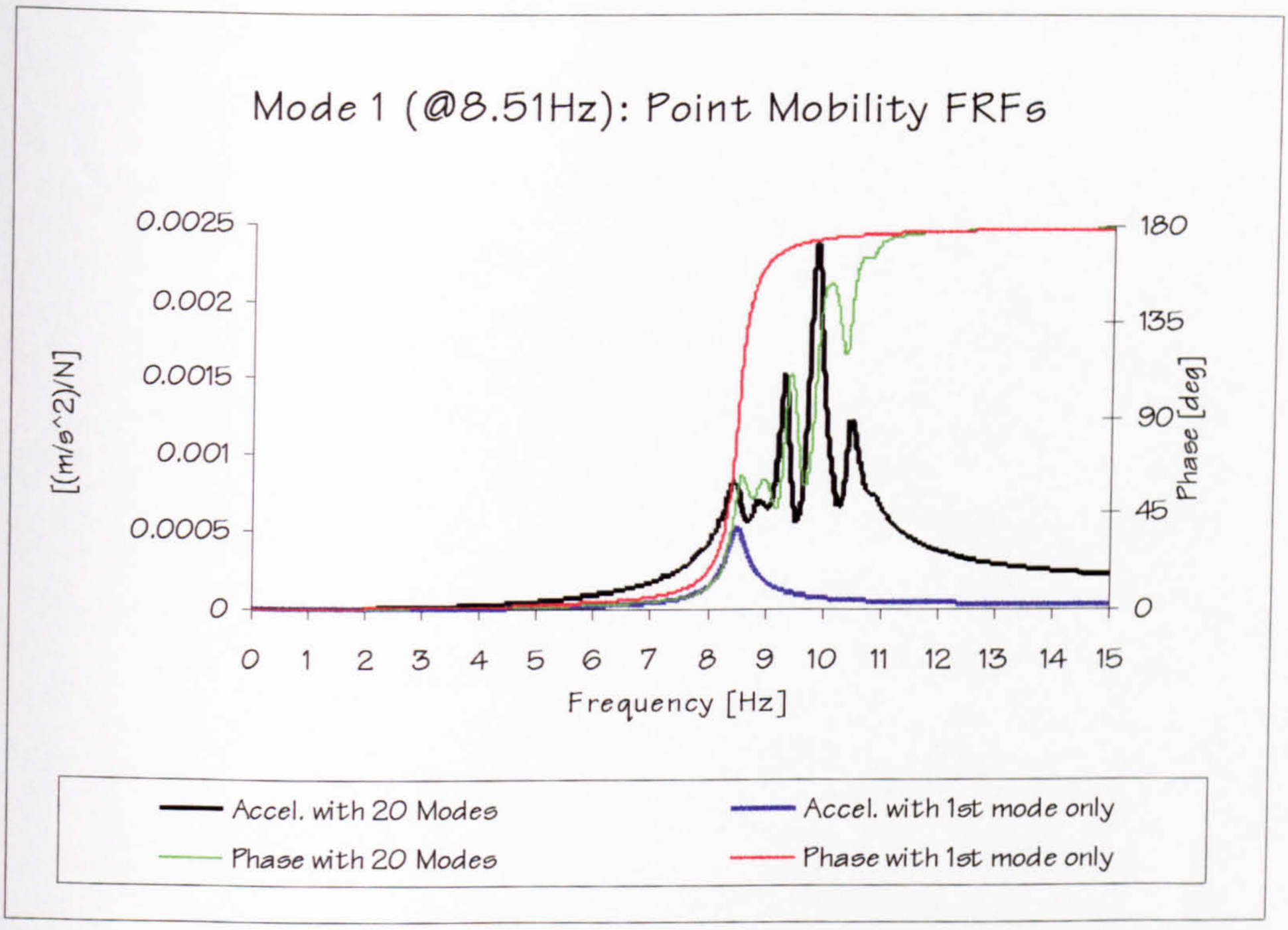

Figure 6.47: Structure D - Point mobility FRFs pertinent to the walking excitation along WP1.

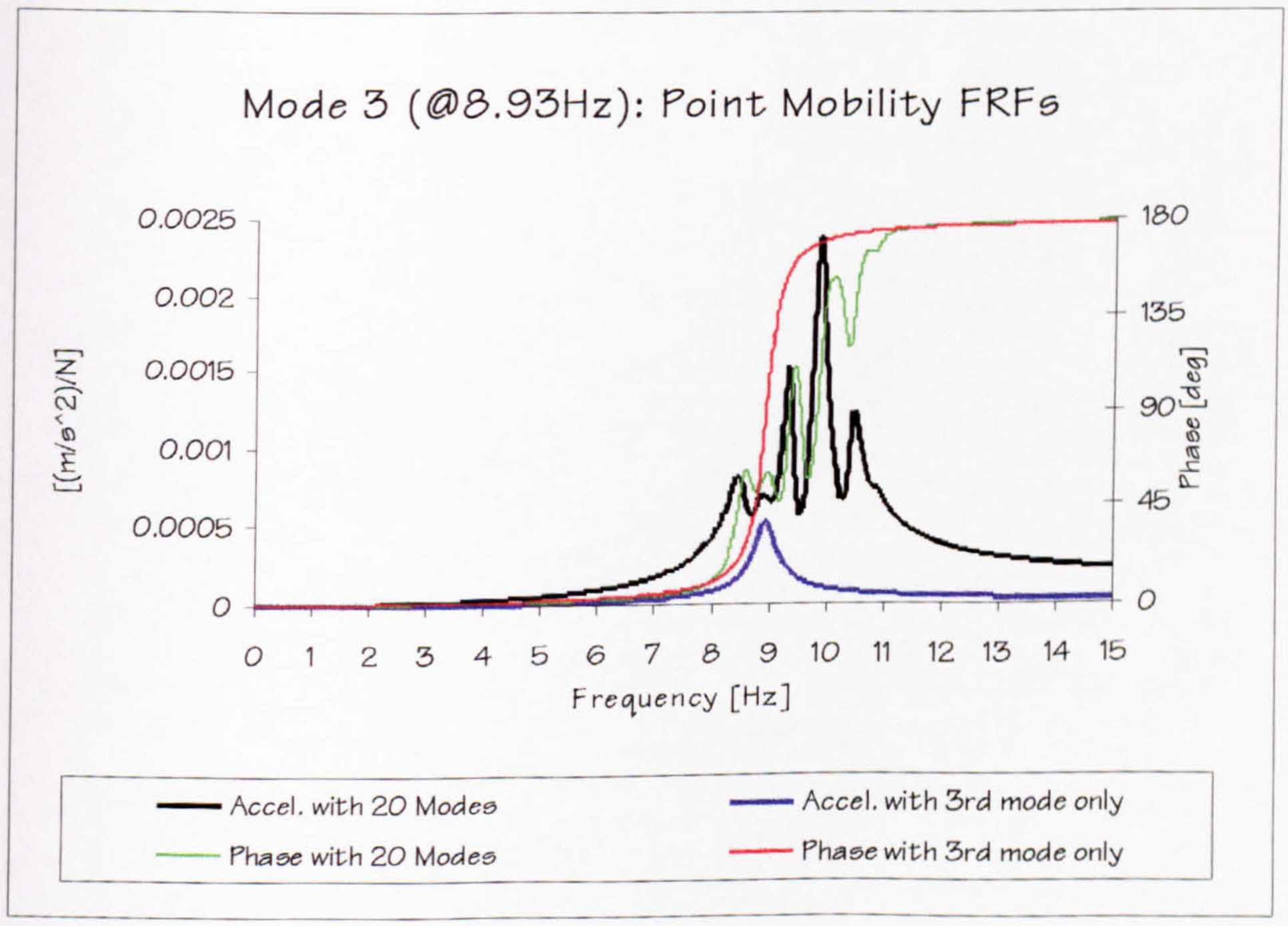

Figure 6.48: Structure D - Point mobility FRFs pertinent to the walking excitation along WP2.

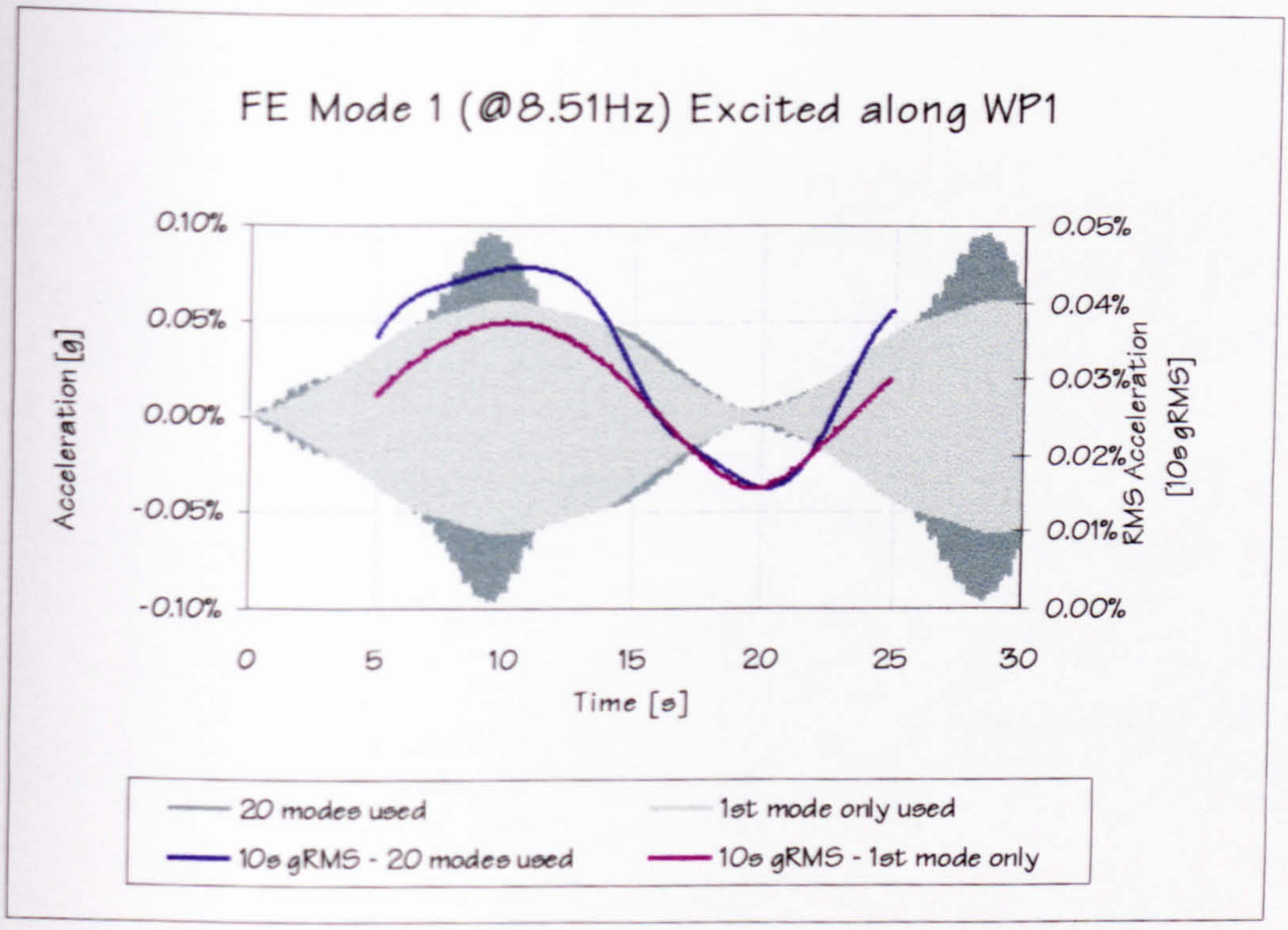

Figure 6.49: Structure D - Simulated acceleration responses to WM2 excitation moving along WP1.

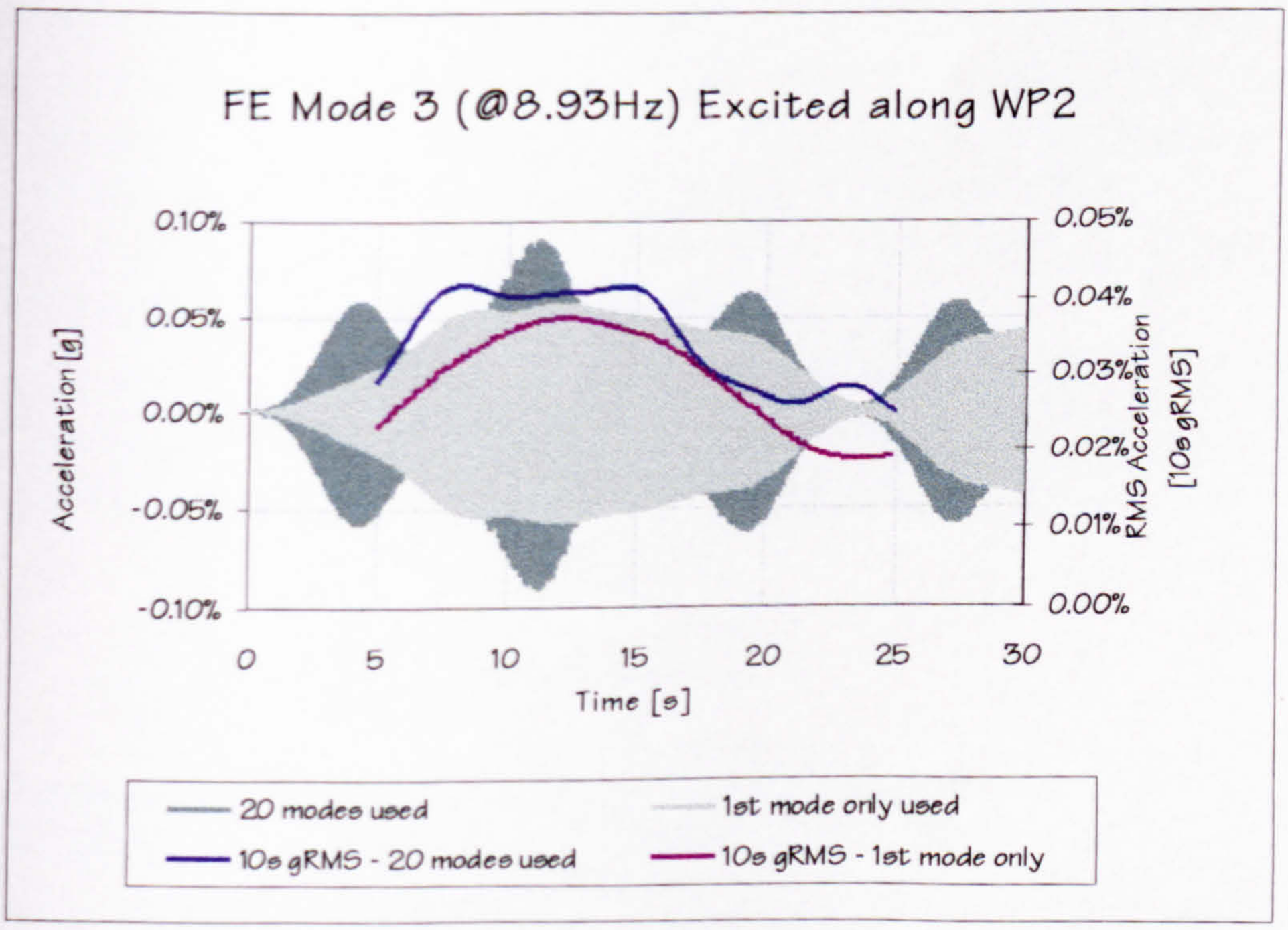

Figure 6.50: Structure D - Simulated acceleration responses to WM2 excitation moving along WP2.

7 Discussion

The modal testing and FE model updating exercises, described in Chapters 5 and 6, required simultaneous consideration of experimental and analytical results. This interdependency between the experiments and analysis also existed in other parametric studies related to the structural dynamic responses due to walking. Therefore, a considerable detailed discussion of the results of this research has already been presented in the previous two chapters.

This chapter presents an overview of the most important results which will serve as the basis for conclusions and recommendations for future work. The discussion firstly addresses the findings related to: (1) the modelling of walking (vibration source), (2) the boundary conditions, and mass, stiffness and damping properties of the floors investigated (vibration path), and (3) the assessment of the measured and calculated vibration levels (vibration rating). In light of these, an overview of the underpinning assumptions and a critical assessment of the CSTR43 vibration serviceability provision is given at the end of this chapter.

7.1 Vibration Source Considerations

Excitation caused by a single person walking as the main source of office floor vibration was modelled using three pre-selected walking models: WM1, WM2 and WM3. As explained in Chapter 6, these three models vary considerably although they represent the same thing – a single average person walking. Each of the four structures tested had at least one natural frequency which could be excited by the 2^{nd}, 3^{rd} or 4^{th} harmonic of the walking forcing function. However, the response measurements performed on Structure D were discarded from this exercise due to unreliable experimental data.

Two principal methods of analytically applying each of the three forcing functions were considered: when the force is stationary, as recommended in practically all current design guidelines, and when it is moving. Only responses to prolonged continuous excitations were considered in the following comparisons.

7.1.1 Assessment of WM1 Performance

Figure 7.1 presents a comparison of the maximum experimental and analytical responses to the 2^{nd} harmonic walking excitation, where WM1 was used in the analysis. Only Structures A and B had natural frequencies sufficiently low that they could be excitable by this harmonic. Whilst the stationary WM1 overestimated responses of Structure A considerably, it performed much better in the case of Structure B. The assumption of the moving WM1, when its 2^{nd} harmonic excites the resonance, underestimated the responses for both structures.

Figure 7.2 presents similar results, but for WM1 3rd harmonic excitation. Six natural frequencies on three structures were excitable. It is clear that the stationary WM1 exciting pure resonance overestimated all the measured results considerably. Depending on the natural frequency of the system, this overestimation may be up to 617%, as shown in Figure 7.7.

Probably the main reason for this is that the same dynamic loading factor of 0.1 is assumed for both the 2nd and 3rd harmonics of walking (CEB, 1991). It is likely that the dynamic loading factor for the latter harmonic would require reduction. However, when assumed to be moving, the 3rd harmonic excitation of WM1 performed much better as it was still conservative, but to a much lesser extent (Figure 7.7).

7.1.2 Assessment of WM2 Performance

Figure 7.3 shows that WM2, even when assumed to be stationary, may underestimate slightly the responses produced by the relatively brisk walking which 2nd harmonic excites the resonance.

However, Figure 7.4 shows that the simulations of the 3rd harmonic walking excitation by the stationary WM2 overestimated all responses, but to a lesser extent than the WM1 simulations.

The moving WM2, nevertheless, underestimated a considerable number of measured responses for both the 2nd and 3rd harmonic excitations. This was to be expected considering that the development of the stationary WM2 model actually took into account the fact that the force moves (Eriksson, 1994).

7.1.3 Assessment of WM3 Performance

Figure 7.5 indicates that the halving of the WM3 harmonic excitation amplitude of 96 N to 48 N at 4.8 Hz may be unrealistic in the case of the 2nd harmonic excitation. It can be seen that a stationary WM3 at 4.7 Hz overestimates the measured response by 72% and then at 5.0 Hz underestimates it by 21%. A smoother change of the excitation amplitude at 4.8 Hz may be more realistic.

Regarding the 3rd harmonic excitation, the stationary WM3 overestimated all responses in a manner which produces overconservative results for frequencies lower than 4.8 Hz, when the greater 96 N harmonic force is applied. For frequencies above 4.8 Hz when the excitation amplitude is halved, the stationary WM3 overestimated results less than WM1, but more than WM2.

The moving WM3 may underestimate the responses above 4.8 Hz.

7.1.4 Additional Observations

7.1.4.1 Summary of 3rd Harmonic Modelling Errors

As the 3rd harmonic excitation is particularly important when checking vibration serviceability of low-frequency floors in office buildings (Wyatt, 1989), Figure 7.7 presents errors made when calculating the maximum 10 s RMS acceleration responses to this excitation. A cursory inspection of this figure indicates that the following two walking forcing models performed best regarding the 3rd harmonic excitation:

- WM1, provided that it is modelled as a moving force, which is not how the CEB (1991) intended it to be applied (the moving force is expensive to analyse in the time domain, but it overestimates the results least), and
- WM2, provided that it is modelled as the stationary force (which is less expensive than the moving WM1 to analyse, but over-estimates the results more than the moving WM1).

7.1.4.2 4th Harmonic Excitation

Test 3.2 performed on Structure B clearly showed that the 4th harmonic excitation may be an issue in the case of a higher mode of vibration which has sufficiently low natural frequency and modal mass. Whereas WM1 does not have any provision for this harmonic, Figure 7.8 shows the results of the relevant WM2 and WM3 simulations.

The importance of the 4th harmonic walking excitation has been proven to some extent by the discarded response tests on Structure D. The two modes at 8.52 Hz and 8.92 Hz were clearly excited by the 4th harmonic of walking (Figures 5.102 and 5.103, respectively), though in a manner difficult to quantify due to extraneous excitation. In addition, the updated FE model of Structure D indicated a possibility for a number of additional local and closely spaced modes of vibration excitable by the 4th harmonic of vibration to occur. Having much lower modal mass than the modes at 8.52 Hz and 8.92 Hz (see Table 6.20), these local modes could have developed substantial responses to the 4th harmonic excitation. This hypothesis, however, has not been experimentally confirmed.

7.1.4.3 Transient vs. Continuous Excitations

Tests on Structure A indicated that a single pass across a floor may lead to lower responses compared to prolonged excitation. However, other tests, where the excitation duration for a single pass was prolonged due to longer walking paths, did not corroborate this observation.

Indeed, response tests performed on Structures C and D demonstrated that in the case of walking along continuous in-situ cast concrete floor surfaces, vibrations are not confined to a local area of the floor which is excited. Vibrations in the panel where the measurements were made can build up as the walker approaches it

traversing the floor area several panels away, as qualitatively shown in the response measurements on Structure D (Figures 5.102 and 5.103).

Also, experimental measurements and response calculations showed that in virtually all four test cases a certain time was required to build up the vibrations (approximately 10-20 s, depending on the length of the walking path and speed of walking). The peak level of RMS acceleration was not constant and it fluctuated as the walker was approaching and moving away from the point where the responses were measured/calculated (typically an antinode of the mode of vibration excited). This showed that the steady-state resonance conditions with a constant level of response had never been reached in any of the tests.

7.1.4.4 STOMPING IN PLACE

'Resonant' stomping in place at the antinode of Structure A's fundamental mode of vibration produced lower responses than the 'resonant' walking along the structure, where the force was applied over a range of lower amplitudes of the fundamental mode shape. This was somewhat surprising, but may be explained by:

1. the dampening effects of the human body positioned at the antinode while stomping, and
2. lower excitation levels, as the manner in which a human body moves when walking is different to the one when stomping in place.

7.2 Vibration Path Considerations: Floor Boundary Conditions, Mass, Stiffness and Damping

Modal testing of prototype floors and FE model updating exercises indirectly provided a unique insight into the boundary conditions, mass, stiffness and damping properties of the structures tested.

7.2.1 The Effects of Columns

FE model updating of the three concrete slabs (B, C and D) supported by in-situ concrete columns, undoubtedly proved that the bending stiffness of the columns was a major source of the floors' overall bending stiffness. Modelling of columns as vertical pin-supports allowing free rotation was shown not to be warranted. Although based on a limited sample, the consistency of this observation resolves the problem of conflicting information about the effects of in-situ columns identified in the published literature, as described in Chapter 2.

Also, the updating of Structure D demonstrated that in the case of directly supported flat slabs, the column heads require careful consideration as natural frequencies may be sensitive to their bending stiffness.

7.2.2 Stiffness of Band Beams

The investigation of Structure C demonstrated that the width of wide and shallow band beams, which are very common in ribbed PT floor design, contribute considerably to the lateral bending stiffness of the floor. A standard orthotropic shell element, such as the ANSYS SHELL63 element, having 'smeared' density and stiffness properties proved to be suitable for modelling this effect. Proper modelling of the increased lateral stiffness due to the effects of the width of the band beams is important as it enables a larger area of the floor to be engaged in vibration. This means that the r^{th} mode which is excited will have greater modal mass m_r and, therefore, lower acceleration response (Equations 3.15-3.17).

For example, the modal mass of mode 1 was 78 tonnes assuming that the lateral stiffness of unclad Structure C is 25% of the longitudinal stiffness (Figure 7.9), as established by model updating. However, its fundamental mode counterpart was reduced to 54 tonnes when calculated assuming that the floor lateral stiffness was only due to the 110 mm think concrete slab (4.3% of the longitudinal stiffness). Unity scaled mode shapes were used in both calculations. This behaviour is observable in Figure 7.9 where areas of the floor further away from the antinode of mode 1 participate less in the case of the lower lateral stiffness. The case of the lower lateral stiffness, therefore, engages less of the total floor mass in the fundamental mode of vibration. As a consequence, the acceleration levels in this mode would be 45% greater if the lateral stiffness of the band beams was neglected, as the modal response is inversely proportional to the modal mass.

7.2.3 Non-structural Components

Tests on unclad and clad Structure C, separated by 6 months, indicated that cladding and services underneath the floor may have notably changed its bending stiffness in both orthogonal directions. However, additional factors which could have affected this apparent change in stiffness were: the ageing of concrete, temperature effects and micro-cracking due to creep and shrinkage in the direction which was not prestressed. The exact contribution of these factors was not determined in this research.

7.2.4 Extensive Concrete Cracking

Extensive cracking of the long-span non-prestressed HSC floor Structure B caused a significant reduction in its natural frequencies. Modelling of this effect proved to be quite difficult, but a linear elastic approach based on 'smeared stiffness' produced some relatively reasonable results.

In the case of prestressed PT floors, however, such extensive cracking is not expected. Linear elastic modelling assuming gross sectional properties proved to be realistic considering the measured vibration behaviour of PT floors.

7.2.5 Dynamic Modulus of Elasticity

A value of dynamic modulus of elasticity of 38 GPa, as recommended by Wyatt (1989), was confirmed to be reasonable, although it could have been increased to 40 GPa or more for higher strength concretes.

7.2.6 Modal Properties

Floor modal properties, such as natural frequencies, and modal mass and stiffness, are governed by the spatial distribution of the floor mass and stiffness. Specific features related to these, which were encountered in this research, were:

1. closely spaced modes of vibration,
2. local low-frequency modes, and
3. low modal mass.

7.2.6.1 Closely Spaced Modes of Vibration

Structures B, C and, in particular, D all had closely spaced modes of vibration to a varying degree. In all three cases, experimental response measurements showed that it was not the fundamental, but rather the higher and relatively close modes that were producing maximum responses to walking excitation. Clearly, this provides overwhelming evidence that the use of simplified dynamic analysis of fundamental floor modes only may not be sufficient when performing vibration serviceability checks.

In addition, it is interesting to note that, in the case of the band-beam ribbed Structure C, the separation of modes was a function of the floor's lateral stiffness. The lower the lateral bending stiffness (relative to the main bending stiffness in the ribbed direction), the smaller the separation.

Finally, numerical investigations performed using the updated FE model of Structure D showed that neglecting higher modes of vibration in mode superposition, when a global mode is the principal mode excited, was underestimating the calculated response.

7.2.6.2 Modal Mass

A related issue to the closely spaced modes of vibration is their modal mass. Tables 6.8, 6.15 and 6.20 show modal masses for Structures B, C and D, respectively, calculated using their updated FE models and unity-scaled mode shapes. It is clear that a considerable variation in the modal masses exists. For these three structures, the modal masses of the modes of vibration excitable by normal walking were often significantly lower than one-quarter of the total floor mass. Consequently, the key assumption of the 'rectangular plate method' (Willford, 1997) appears not to be conservative. This is important as the Concrete Society (1994)

guidelines for checking the vibration serviceability of PT concrete floors, which are presented in detail later in this chapter, are based on the 'rectangular plate method'.

7.2.6.3 LOCAL MODES

A comparison of the results given for Structure B in Table 6.8 and Figure 6.22, and for Structure D in Table 6.20 and Figure 6.44, shows that the lowest modal masses were associated with modes which engage a relatively small area of the floor. These modes have a strong potential of producing the largest responses and should be considered in design. However, local modes are difficult to predict using simplified methods suitable for hand calculations. Currently, the only practical way to establish the likelihood of having local modes of which the writer is aware is to perform accurate numerical FE modelling of the floor.

7.2.6.4 MODAL DAMPING

Of all measured modal parameters, modal damping ratios were probably the least reliable. This might have been expected from the hammer testing of large structures when the hammer operator is present on the floor under test. For the four bare floor structures tested, such measured modal damping ratios were in the range between 0.59% (Structure A) to 2.32% (clad Structure C) with a relatively large scatter of results for each structure tested.

It is important to note here that, if pure steady-state resonance conditions are assumed, the responses are dominated by the resonant mode excited (Equations 4.3-4.7). The responses are then, more or less (depending on the separation between the modes), inversely proportional to the modal damping ratio assumed for the resonating mode. This means that this type of steady-state analysis is particularly sensitive to the modal damping ratio assumed, which is not a particularly reliable modelling parameter. Nevertheless, resonant conditions are frequently assumed in floor vibration serviceability calculations, mainly due to their analytical simplicity.

In any case, a modal damping value of about 1% seems to be a reasonable assumption for bare floor structures.

7.3 Assessment of Vibration Responses of Test Structure C

An assessment of floor vibration performance under walking excitation can be based either on experimental measurements or on analytical calculations. The experience gained in this research is that the response build-up time, its fluctuating nature, as well as the effects of extraneous noise existing during the measurements should all be carefully considered.

7.3.1 Vibration Serviceability Assessment to BS6472:1992

BS6472:1992 (BSI, 1992) is a revision of BS6472:1984 (BSI, 1984) which has been withdrawn. The main differences between the withdrawn standard and its revision are in the treatment of various types of vibration and the VDV. Vibration due to walking in the current BS6472 should be considered as continuous, and not as intermittent, as in BS6472:1984. However, by allowing vibrations to be assessed by the VDV, the new standard allows intermittency of walking vibration to be taken into account by considering the number of occurrences per day.

Regarding walking excitation, there is very little published information on the frequency of trafficking of office floors. However, as reported in Chapter 2, Eriksson (1994) suggested that a repeat time for a single person traversing an office floor can be assumed to be between 60 s (once every minute) and 3600 s (once every hour).

If vertical RMS accelerations are used to assess office floor vibrations, then the maximum allowable weighted RMS accelerations are 0.02 m/s^2 for continuous daytime exposure lasting 16 hours between 7am and 11pm. This formulation of the vibration limit typically assumes that vibrations are non-stop continuous and does not allow the intermittent nature of the walking vibration to be considered.

However, the VDV formulation (Equation 2.4) allows for the exposure time $T = t_2 - t_1$ to be considered. BS6472:1992 defines the various levels of adverse comment depending on the actual VDV calculated from the weighted acceleration time history $a_w(t)$. These are given in Table 7.1 (Table 7 in BS6472:1992).

Table 7.1: Vibration dose values (VDV in $m/s^{1.75}$) above which various levels of adverse comment may be expected in residential buildings.

Place	Level 1: Low probability of adverse comment	Level 2: Adverse comment possible	Level 3: Adverse comment probable
Residential buildings 16h day exposure	0.2 to 0.4	0.4 to 0.8	0.8 to 1.6
Residential buildings 8h night exposure	0.13	0.26	0.51

Although BS6472:1992 does not provide any information as to the rating of VDV values applicable to office buildings, considering that residential buildings generally have more stringent vibration serviceability criteria, the values in Table 7.1 corresponding to daytime usage seem to be on the conservative side and are appropriate for assessing the effects of vibrations in office buildings.

Another useful feature in BS6472:1992 is the conversion procedure between the RMS accelerations and VDV. This is done by calculating the so called 'estimated VDV' denoted as 'eVDV' which is given as:

$$eVDV = 1.4 a_{RMS} t^{0.25} \qquad \text{Equation 7.1}$$

where: a_{RMS} [m/s^2] is the weighted RMS acceleration calculated using Equation 2.3 and averaged over a limited time $T = t_2 - t_1$, and t [s] is the total exposure time which may be longer than the averaging time

T. It should be mentioned that if, for example, the maximum 10 s RMS acceleration $a_{RMS,10w}$ is used to represent a_{RMS}, the eVDV can be calculated as:

$$eVDV = 1.4 a_{RMS,10w} (n \cdot 10s)^{0.25} \qquad \text{Equation 7.2}$$

where n is the number of floor crossings each of which is assumed to last 10 s. The application of the VDV and eVDV will be demonstrated using the following example.

Let us assume conservatively that single pedestrians appear on the floor surface in a perfectly periodic and continuous manner every 10 s (therefore, return time is 10 s). Assuming that the maximum 10 s RMS acceleration $a_{RMS,10w}$ for such an excitation is, say, 0.04 m/s^2, the 16h exposure to this vibration gives:

$$eVDV = 1.4 \cdot 0.04 \cdot (5760 \cdot 10)^{0.25} = 0.868 m/s^{1.75} \qquad \text{Equation 7.3}$$

as there are 5760 occurrences lasting 10 s each. A floor having this response, when assessed against the criteria given in Table 7.1, may be characterised as "adverse comment probable", which is likely not to be satisfactory for an office floor. However, if, say, a more realistic 5 minute (300 s) pedestrian return time is assumed (Eriksson, 1994), then there are in total 192 occurrences during 16h of exposure. In this case the eVDV is:

$$eVDV = 1.4 \cdot 0.04 \cdot (192 \cdot 10)^{0.25} = 0.371 m/s^{1.75} \qquad \text{Equation 7.4}$$

The same floor has now improved its assessment and there is only a "low probability of adverse comment", which is more desirable for an office floor.

This example shows clear benefits of applying the 1992 revision of BS6472, as its 1984 counterpart did not have the facility for considering the beneficial 'intermittence' of the walking vibration. Furthermore, the example illustrates how the information on the frequency of floor trafficking is becoming of key importance for floor vibration serviceability design. This information depends on the required function of the floor and should, ideally, become a part of the client's floor design brief. Finally and most importantly, it has also been demonstrated that unrealistic and unduly conservative assumptions may easily condemn a floor structure from the vibration serviceability point of view.

7.3.2 Structure C (Clad): Assessment of Vibration Serviceability

Of the four structures tested, only measurements from the clad Structure C provided acceleration responses due to walking on a realistic office floor structure which merited assessment in accordance with BS6472:1992. This is also the most interesting structure, because it failed the CSTR43 vibration serviceability check, as reported in Chapter 5.

7.3.2.1 ASSESSMENT BASED ON MAXIMUM RMS ACCELERATION

Figure 7.10 shows the levels of maximum measured (Table 5.18) and calculated (Sections 6.4.3 and 6.4.4) 10 s RMS accelerations for modes 1 and 2 at 6.4 Hz and 6.9 Hz, respectively. These are plotted against BS6472:1992 baseline curve (R=1), and curves 4 (R=4) and 8 (R=8). According to CSTR43, response factor R=4 corresponds to maximum RMS levels appropriate for a 'special office' whereas R=8 is suitable for a 'general office'. The response factor R is a number describing how many times the calculated RMS acceleration response is greater than 0.005 m/s^2 RMS acceleration which corresponds to the baseline curve.

Figure 7.10 clearly shows that the large differences between the actual and predicted behaviour may again easily condemn a sound floor structure from the vibration serviceability point of view. For example, it can be seen that whilst the 'worst-case' experiments indicate that the floor actually satisfies 'special office' requirements, some response calculation models, such as the stationary WM1 and WM3, condemn it. Responses to stationary WM1 are actually so large that the floor becomes a borderline case even as a 'general office'. This is a powerful illustration of the possible consequences of large overestimation errors between the measured and calculated responses to the 3rd harmonic of walking which were observed in this research and are illustrated in Figure 7.7.

7.3.2.2 ASSESSMENT BASED ON ESTIMATED VDV

Using Equation 7.1 VDV were estimated by utilising as a_{RMS} the maximum 10 s RMS accelerations given in Figure 7.10. Considering the ratings given in Table 7.1 as well as further explanations given in BS6472:1992, the writer interpreted VDV values lower than 0.4 $m/s^{1.75}$ as satisfactory for 'special offices' (Level 1). Similarly, VDV between 0.4 and 0.8 $m/s^{1.75}$ should be satisfactory for 'general offices' (Level 2).

Three scenarios were investigated: (1) continuous vibration for 16 hours, (2) intermittent vibration lasting 10 s every minute, and (3) intermittent vibration lasting 10 s every hour. A conservative assumption was made that the RMS acceleration peaks (Figure 7.10) were achieved and maintained during each 10 s of intermittent vibration. Figure 7.11 shows the performance of the clad Structure C gauged in terms of eVDV using various methods for obtaining the response to single person walking.

Similarly as for RMS accelerations, measured responses indicated that the floor would have a satisfactory performance if used as a 'special office'. However, the stationary WM1 produces eVDV leading to "adverse comment probable" rating for non-stop excitation. This is not satisfactory even for a 'general office'. The possible beneficial effects of intermittency of walking when calculating the VDV are also illustrated in Figure 7.11. It is shown that even the stationary WM1 produces satisfactory responses for a 'special office' for 10 s of walking occurring every hour.

7.4 Description of CSTR43 Provision and Assessment of its Performance

Appendix G of CSTR43 proposes a method for calculating the dynamic response of PT floors of various structural configurations. As one of the aims of this project is to investigate the performance of this method and propose improvements, the writer considered it necessary to become as familiar as possible with the background of the method. Based only on information given in Appendix G of CSTR43 this background is not clear. Therefore close links were established with the authors of CSTR43 (Feltham, 1995; 1997) who willingly provided all necessary information related to the development of the vibration serviceability guidelines.

7.4.1 Modelling of Excitation in CSTR43

The walking force M2 determined by Ohlsson (1982) is assumed to be the only excitation of the floor. The force shape is very similar to the one shown in Figure 2.16a and is assumed to be perfectly periodic. As such, the force is presented in terms of Fourier components given in Table 7.2.

The M2 walking forcing function corresponds to the pacing frequency of 1.57 Hz (i.e. 1.57 steps per second or 94 steps per minute). The data in Table 7.2 show that the higher harmonics have comparatively lower amplitudes, so only the first 13 harmonics were considered as important. Having only this excitation available, and in order to excite at least one floor resonance, another assumption made was that one of the first 13 harmonics always excites the floor's 'fundamental mode(s)'. Therefore, it was necessary to calculate all possible modes of vibration of the floor between 1.57 Hz and 20.4 Hz. This led to another series of assumptions related to the mathematical modelling and analysis of the floor.

Table 7.2: Fourier components of M2 walking (static weight=687N)

Harmonic No.	Frequency f_h [Hz]	Amplitude P_h [N]	Phase φ_h [degrees]	Dynamic loading factor
1	1.57	124	16.4	124/687=0.180
2	2·1.57=3.14	93	199.0	93/687=0.135
3	3·1.57=4.71	38	63.3	38/687=0.055
4	4·1.57=6.27	27	63.2	27/687=0.039
5	5·1.57=7.84	13	350.9	13/687=0.019
6	6·1.57=9.41	10	17.8	10/687=0.015
7	7·1.57=10.98	12	3.15	12/687=0.017
8	8·1.57=12.55	11	340.6	11/687=0.016
9	9·1.57=14.12	8	318.6	8/687=0.012
10	10·1.57=15.69	4	329.8	4/687=0.006
11	11·1.57=17.25	5	324.5	5/687=0.007
12	12·1.57=18.82	4	306.6	4/687=0.006
13	13·1.57=20.40	4	284.3	4/687=0.006
14	14·1.57=21.96	4	257.3	4/687=0.006

Harmonic No.	Frequency f_h [Hz]	Amplitude P_h [N]	Phase φ_h [degrees]	Dynamic loading factor
15	15·1.57=23.53	5	234.4	5/687=0.007

7.4.2 Modelling of the Floor Structure and Response Calculations

The calculation of natural frequencies and dynamic response in CSTR43 is based on a simplified 'rectangular plate method' coupled with a somewhat streamlined mode superposition method.

CALCULATION OF NATURAL FREQUENCIES AND MODE SHAPES

The 'rectangular plate method' can be used for calculation of dynamic responses of floors with a regular rectangular grid (Figure 7.13a). The method considers separately two typical bays running in both orthogonal directions (shaded areas in Figure 7.13a). It assumes that each bay can be considered as a rectangular plate simply supported along its edges. If the bending stiffness in two orthogonal directions is different then each of the plates should be considered as orthotropic.

The modes of vibration of such plates are assumed to be the same as the modes of vibration of the whole floor. As the analysis is concerned only with the lowest modes of vibration, the ordinates of the global mode shape of the floor considered must alternate between adjacent bays (i.e. rectangular plates) in both orthogonal directions. This is how two families (x and y) of mode shapes are created (Figure 7.13c).

If, say, the x-direction bay is considered (Figure 7.13b), then the mode shapes and frequencies of the simplified rectangular plate are described by the numbers of half-waves in each of the two directions. In this case the natural frequency corresponding to such an assumed mode shape pattern is calculated as (Szilard, 1974):

$$f = \frac{\pi}{2}\sqrt{\frac{n_a^4}{(n_x \cdot l_x)^4} E \cdot I_x + \frac{n_b^4}{(n_y \cdot l_y)^4} E \cdot I_y} \cdot \sqrt{\frac{1}{m}} \qquad \text{Equation 7.5}$$

where: n_a is the number of half-waves in the x-direction, n_b is the number of half-waves in the y-direction, $E \cdot I_x$ and $E \cdot I_y$ are the bending stiffnesses per unit width in the x and y directions, respectively, and m is the slab's mass per unit area.

CSTR43 assumes that m is uniformly distributed and consists of the self weight of all permanent structural and non-structural elements and installations plus 10% of the live gravity load. Also, if the floor is ribbed i.e. orthotropic, then another assumption is that beams are narrow so that only the slab's thickness contributes to the lateral stiffness of the plate in the direction where there are no ribs. It should be mentioned that this may cause large differences between $E \cdot I_x$ and $E \cdot I_y$ leading to numerous and closely spaced natural frequencies

when n_b (or n_a), is kept constant whilst n_a (or n_b), is changed (depending on which direction is analysed).

As the CSTR43 method is concerned only with the low-frequency modes, only one half-wave is considered in the stiffer span direction of the bay analysed. For example, in the case shown in Figure 7.13b, and considering Equation 7.5, the shorter span is considered to be stiffer, so $n_a = 3$ and $n_b = 1$. CSTR43 considers modes with two half-waves in the stiffer direction as generally much higher and not excitable by walking.

7.4.2.1 CALCULATION OF ACCELERATION RESPONSE

For the given floor configuration simplified by the equivalent rectangular plates, Equation 7.5 typically produces a number of frequencies between 1.57Hz and 20.4Hz excitable by M2 walking. By using a mode superposition technique, the total floor response to all 13 walking harmonics is calculated as a linear superposition of individual responses of each mode to the 13 harmonics of excitation. Therefore, the problem has been reduced to the analysis of individual modes each of which is possible to be analysed as an individual mass-spring-damper SDOF system (Clough & Penzien, 1993).

The acceleration response of a SDOF system having mass m_n to each of the 13 sinusoidal harmonics given in Table 7.2 is calculated using the well known formula (Clough & Penzien, 1993):

$$\ddot{x}_h(t) = \frac{-\frac{P_h}{m_n}\left(\frac{f_h}{f_n}\right)}{\sqrt{\left(1-\left(\frac{f_h}{f_n}\right)^2\right)^2 + \left(2\varsigma_n\left(\frac{f_h}{f_n}\right)\right)^2}} \sin\left(2\pi f_h t - \varphi_h\right) \qquad \text{Equation 7.6}$$

where: P_h, f_h and φ_h are the amplitude, frequency, and phase angle of the h^{th} excitation harmonic, as given in Table 7.2, and m_n, f_n and ς_n are the SDOF mass, natural frequency and damping ratio.

The total SDOF response to all 13 harmonics is given in terms of RMS accelerations, and, as such, has been calculated by summing individual sinusoidal peak acceleration responses $\ddot{x}_{h,peak}$ to all 13 harmonics (each calculated using Equation 7.6) as follows:

$$\ddot{x}_{RMS} = \sqrt{\frac{\sum_h \left(\ddot{x}_{h,peak}\right)^2}{2}} \qquad \text{Equation 7.7}$$

These analyses were repeated for a range of SDOF systems having constant mass m_n of 1000 kg when the natural frequency f_n of the SDOF system was parametrically increased from 1 Hz to 20 Hz. The RMS response was calculated in terms of response factor R. An example of such a calculation is shown in Figure 7.12 for a series of SDOF systems when a 2% damping ratio is assumed for all of them. Similar analyses

were repeated for four additional series of SDOF systems having 3%, 4%, 6% and 8% critical damping. Naturally, the series of 1000kg SDOF systems with the smallest damping ratio of 2% had the greatest responses which were amplified at frequencies corresponding to the M2 walking harmonics (1.57 Hz, 3.14 Hz, etc.), as shown in Figure 7.12.

These responses served to formulate an 'envelope' of maximum response factors R for a SDOF system having 1000 kg mass and varying natural frequencies. These maximum response factors are given as a function of frequency in five frequency regions, as presented in Table 7.3.

Table 7.3: Maximum response factors R for a 1000 kg SDOF system.

Ranges of SDOF natural frequencies	Maximum response factor R
$f_r \leq 3Hz$	$\frac{61.2}{f_r^2 \varsigma}$
$3Hz \leq f_r \leq 4Hz$	$\frac{6.8}{\varsigma}$
$4Hz \leq f_r \leq 5Hz$	$\frac{20.8 - 3.5f_r}{\varsigma}$
$5Hz \leq f_r \leq 20Hz$	$\left[\frac{0.22 \cdot (20 - f_r)}{\varsigma} + 0.5(f_r - 5)\right]$
$20Hz \leq f_r$	7.5

Using the one-line formulas given in Table 7.3 is conservative and provides an upper bound RMS acceleration response which is higher than the real response of a SDOF system in resonance (Figure 7.12).

Another key feature in the development of the CSTR43 vibration serviceability guidelines is the assumption that the modal mass of each floor mode excited is exactly 25% of the total floor mass which is vibrating. This assumption stems directly from the dynamic modelling of the floor bays using simply supported ('knife edge') rectangular plates. All modes of such plates have identical modal mass which is exactly one-quarter of the plate's mass, when unity scaled mode shapes are used in the calculation of modal masses (Smith, 1989). This is a well known feature of rectangular plates and one of the key reasons why such plates have to be used when simplifying the calculation of the floor's dynamic response.

Therefore, CSTR43 proposes the response factor of the whole floor under a single pedestrian excitation, considering only modes in the r-direction (r is x or y) to be calculated as:

$$R_r = \frac{R \cdot N_r}{\left(\frac{mn_x n_y l_x}{4}\right)} = \frac{C_r N_r}{mn_x n_y l_x l_y} \qquad \text{Equation 7.8}$$

where: $mn_x n_y l_x l_y$ is the mass of the whole floor and $C_r = 4R$ (Table 7.4), where R is the maximum response corresponding to a 1-tonne SDOF system (Table 7.3). As Equation 7.6 suggests, the acceleration steady state response of each SDOF system (i.e. mode) is inversely proportional to its mass. Therefore, the 1-tonne maximum response factor R is divided in Equation 7.8 by the floor's modal mass expressed in tonnes, which is one-quarter of the total floor mass, to obtain a realistic response of each floor mode excited by walking.

Table 7.4: Maximum response factors C_r the whole floor, as published in CSTR43.

Ranges of floor fundamental frequencies	Maximum response factor C_r
$f_r \le 3Hz$	$4 \cdot \frac{61.2}{f_r^2 \varsigma} = \frac{244.8}{f_r^2 \varsigma}$
$3Hz \le f_r \le 4Hz$	$4 \cdot \frac{6.8}{\varsigma} = \frac{27.2}{\varsigma}$
$4Hz \le f_r \le 5Hz$	$4 \cdot \frac{20.8 - 3.5 f_r}{\varsigma} = \frac{83.2 - 14 f_r}{\varsigma}$
$5Hz \le f_r \le 20Hz$	$4 \cdot \left[\frac{0.22 \cdot (20 - f_r)}{\varsigma} + 0.5(f_r - 5) \right] = \frac{0.88 \cdot (20 - f_r)}{\varsigma} + 2 \cdot (f_r - 5)$
$20Hz \le f_r$	30

It is important to note here that CSTR43 offers a set of formulas for determining the fundamental frequencies of the floor f_r for both orthogonal directions depending on whether the floor is a solid or coffered slab, or ribbed. Such calculated frequencies should be used in conjunction with the formulas given Table 7.4.

Finally, the factor N_r in Equation 7.8 is empirically developed and it presents a number of floor modes excited by M2 walking. It is given as:

$$N_r = 1 + (0.5 + 0.1 \ln \varsigma) \cdot \lambda_r \text{ for solid or coffered slabs,} \qquad \text{Equation 7.9}$$

or

$$N_r = 1 + (0.65 + 0.1 \ln \varsigma) \cdot \lambda_r \text{ for ribbed slabs} \qquad \text{Equation 7.10}$$

where λ_r is termed "effective aspect ratio" in CSTR43. This ratio is defined for both orthogonal directions as:

$$\lambda_x = \frac{n_x l_x}{l_y} \sqrt[4]{\frac{EI_y}{EI_x}}, \text{ for bays in the x - direction,} \qquad \text{Equation 7.11}$$

and

$$\lambda_y = \frac{n_y l_y}{l_x} \sqrt[4]{\frac{EI_x}{EI_y}}, \text{ for bays in the y - direction.} \qquad \text{Equation 7.12}$$

The factor N_r is generally greater for ribbed slabs, and it increases as the damping and effective aspect ratios increase. This parameter is therefore greater for floors with a strong orthotropy and close modes leading to an increased number of modes in the frequency range of interest between 1.57 Hz and 20.4 Hz.

However, it must be stressed here that factor N_r in fact does not take into account the possibility that a mode closely spaced to the fundamental mode may occur and be excited in resonance. This is because the underlying assumption made while developing simplified formulas for N_r has been that only the fundamental mode of vibration is excited in resonance by one of the walking harmonics. The higher harmonics of the M2 walking model can only by chance excite some of the higher modes and those are not closely spaced to the fundamental mode as the frequency separation is at least 1.57 Hz. This separation is considerable for low frequency floors having fundamental modes between, say, 4 Hz and 7 Hz. Therefore, if the second floor mode, even when predicted by the simplified rectangular plate model, is close to the fundamental, it will not be excited in the CSTR43 method as it does not allow the effects of interaction of two or more of the closely spaced lowest modes of vibration to be evaluated. In essence, the CSTR43 method is an enhanced SDOF method, where the bulk of the floor response is practically controlled only by the response of its fundamental mode.

Another underlying assumption in the development of the CSTR43 guidelines is that the excitation force is always applied and the response evaluated at the antinode point (unity displacement amplitude) of the mode considered. This means that the worst case scenario is assumed as the walking force is treated as a stationary dynamic force exciting the floor at its 'weakest' point whereas the response is evaluated at the maximum response point.

The last assumption made in the CSTR43 response calculations is that the total floor response factor is the sum of response factors corresponding to two orthogonal directions (Figure 7.13c):

$$R_{total} = R_x + R_y \qquad \text{Equation 7.13}$$

Floor response factors R_x and R_y are determined by repeating virtually the same rectangular plate analysis twice for representative floor stiffnesses and spans in the x and y directions.

7.4.3 Structure C (Clad): Vibration Serviceability Check in Accordance with CSTR43

Although published in 1994, the vibration response rating in CSTR43 is adopted from the SCI guide (Wyatt, 1989) which is based on the provision of BS6472:1984 and not of its successor BS6472 published in 1992. Being based on the 1984 version of BS6472, the CSTR43 guidelines do not make any attempt to utilise the VDV or eVDV (when RMS accelerations are known or estimated) as the floor vibration response rating parameter.

In order to obtain a completely unbiased assessment of results produced in accordance with the CSTR43 provision, the writer asked the authors of the CSTR43 method, described in the private notes of Feltham (1995), to perform the necessary hand calculations. They kindly accepted the challenge and were supplied with all the data about geometric and material properties of Structure C in the form of a full set of construction drawings. In addition, they were not made aware of the results of experimental measurements. This was done following Severn's (1997) recommendation as to how to enhance a simulation of a real life design situation when evaluating structural dynamic performance.

The authors of CSTR43 modelled Structure C (Figure 5.66) as a single ribbed panel ($n_x = n_y = 1$) having spans $l_x = 14.86\text{m}$ and $l_y = 31.37\text{m}$. To be as close as possible to the measured situation, no live load was taken into account. The assumed dynamic modulus of elasticity was 40 GPa. Without going into further details of the 3-page calculations, made by Feltham (1997), the most important results of the hand calculations are that the frequency of the 'fundamental modes' in both orthogonal directions was 2.71 Hz ($f_r = f_x = f_y = 2.71\text{Hz}$), and that R=12.4 when only one direction was taken into account (no double counting). This response factor leads to RMS accelerations of:

$$12.4 \cdot 0.005\text{m/s}^2 = 0.062\text{m/s}^2 \qquad \text{Equation 7.14}$$

meaning that the floor is likely to be unacceptable for a 'general office' (Figures 7.10 and 7.11). The CSTR43 estimated response levels to the 3rd harmonic of excitation are almost an order of magnitude greater than those measured. This was the main reason why Structure C failed comprehensively the initial vibration serviceability check performed in accordance with CSTR43, as mentioned in Chapter 5.

This exercise, together with other results of this research, identified a number of possibly serious shortcomings in the CSTR43 guidelines for checking the vibration serviceability of in-situ cast PT floors. These are outlined in the following sub-section.

7.4.4 Identified CSTR43 Shortcomings

Problems were identified in each of the three key aspects of the floor vibration serviceability assessment: (1) in the modelling of the walking excitation, (2) in the modelling of the floor structure, and (3) in the rating of vibration responses.

7.4.4.1 Problems in the Modelling of the Vibration Source

The M2 pedestrian forcing function proposed by Ohlsson (1982), and used in CSTR43, corresponds to a relatively slow pacing rate of only 1.57 steps per second. No allowance was made to incorporate different amplitudes of the fundamental and higher harmonics if the pacing frequency is increased up to 2 Hz or more. Also, when applying this forcing function, an assumption has been made that only the fundamental mode is

excited in resonance by one of the harmonics between 1.57 Hz and 20.4 Hz. Therefore, close modes of vibration higher than the fundamental are assumed not to be excitable in resonance. This assumption may not be valid as demonstrated by response measurements on Structures B, C and D where the excitation of the higher modes produced maximum responses.

7.4.4.2 PROBLEMS IN THE MODELLING OF COLUMNS

One of the main reasons for the poor performance of CSTR43 in the case of the real-life Structure C is the estimate of the floor's fundamental frequency at 2.71 Hz, compared with the measured 6.41 Hz. This exposed the floor to much larger amplitudes of walking excitation. The main reason for such a large underestimation of the Structure C's fundamental frequency was the general inability of the CSTR43 guidelines to model the stiffening effects of the floor columns and the 'core' area (Figure 5.66).

7.4.4.3 PROBLEMS IN THE MODELLING OF COLUMN LINES

The 'rectangular plate method', which served as the basis for the development of the guidelines in CSTR43, inherently assumes that nodal lines exist along the column lines no matter which floor configuration is in question (beamless or not). As the pin-support assumption unduly reduces the floor stiffness and natural frequencies, so the assumption about the nodal lines along the column lines stiffens the floor and increases the natural frequency. Therefore, the two simplifications tend to cancel, but in a rather arbitrary and unpredictable way.

7.4.4.4 PROBLEMS IN THE MODELLING OF MODAL MASS

Modelling of floor bays with identical simply supported rectangular plates simplifies the calculation of modal mass which must always be one-quarter of the total floor mass. Updated FE models developed for Structures B, C and D undoubtedly showed that modal masses of real-life floors may easily be considerably less than 25% of the total floor mass.

7.4.4.5 PROBLEMS IN MODELLING THE EFFECTS OF THE HIGHER MODES OF VIBRATION

The concept of two families of mode shapes in two orthogonal directions which superimpose has very little physical meaning. Although CSTR43 acknowledges that this assumption is conservative, it may easily become overconservative due to double-counting of the same modes in the x and y directions.

7.4.4.6 PROBLEMS WITH LIMITED APPLICATION

The application of CSTR43 is limited to floors having a regular grid and geometry with perfect simply supported edge conditions, which do not exist in real-life situations. Further unwarranted approximations and considerable engineering judgement are required if the CSTR43 provision is to be applied to floors with a more or less irregular layout. This was the case with Structure C and, clearly, one can have little confidence in response calculations from such 'extrapolations'.

7.4.4.7 PROBLEMS WITH THE RATING OF THE VIBRATION RESPONSE

The vibration rating in the CSTR43 guidelines is based on the provision given in the old version of BS6472 (BSI, 1984) which was already superseded by BS6472:1992 at the time of the CSTR43 publication in 1994. The CSTR43 guidelines are, therefore, not based on the provision of the relevant British code of practice. Consequently, the CSTR43 vibration response rating is based on the RMS accelerations only as the VDV concept was not adopted in BS6472:1984. Thus, the VDV and the possible beneficial effects of intermittency of the walking excitation are not considered when performing the vibration rating.

7.4.5 Conclusions About CSTR43 Performance

Overall, the current CSTR43 provision for checking the vibration serviceability of PT floors is a diligent attempt to produce a method where all calculations required can be made by hand. This underlying principle required a significant number of simplifications which were made both on the conservative and non-conservative side. The consequences of these simplifications are that the final hand-calculated responses appear to be unreliable and estimated in a more or less arbitrary way. Such response calculations are of little value despite the fact that they can be made by hand. Even if it is assumed that CSTR43 can provide a good 'order of magnitude' check, the differences between the different vibration limits proposed in BS6472:1992 are small (factor of 2) meaning that such crude checks are usually meaningless.

To conclude, the principal failure of the CSTR43 vibration serviceability guidelines is that they over-simplify a very complex engineering problem, the solution of which is very sensitive to unwarranted assumptions.

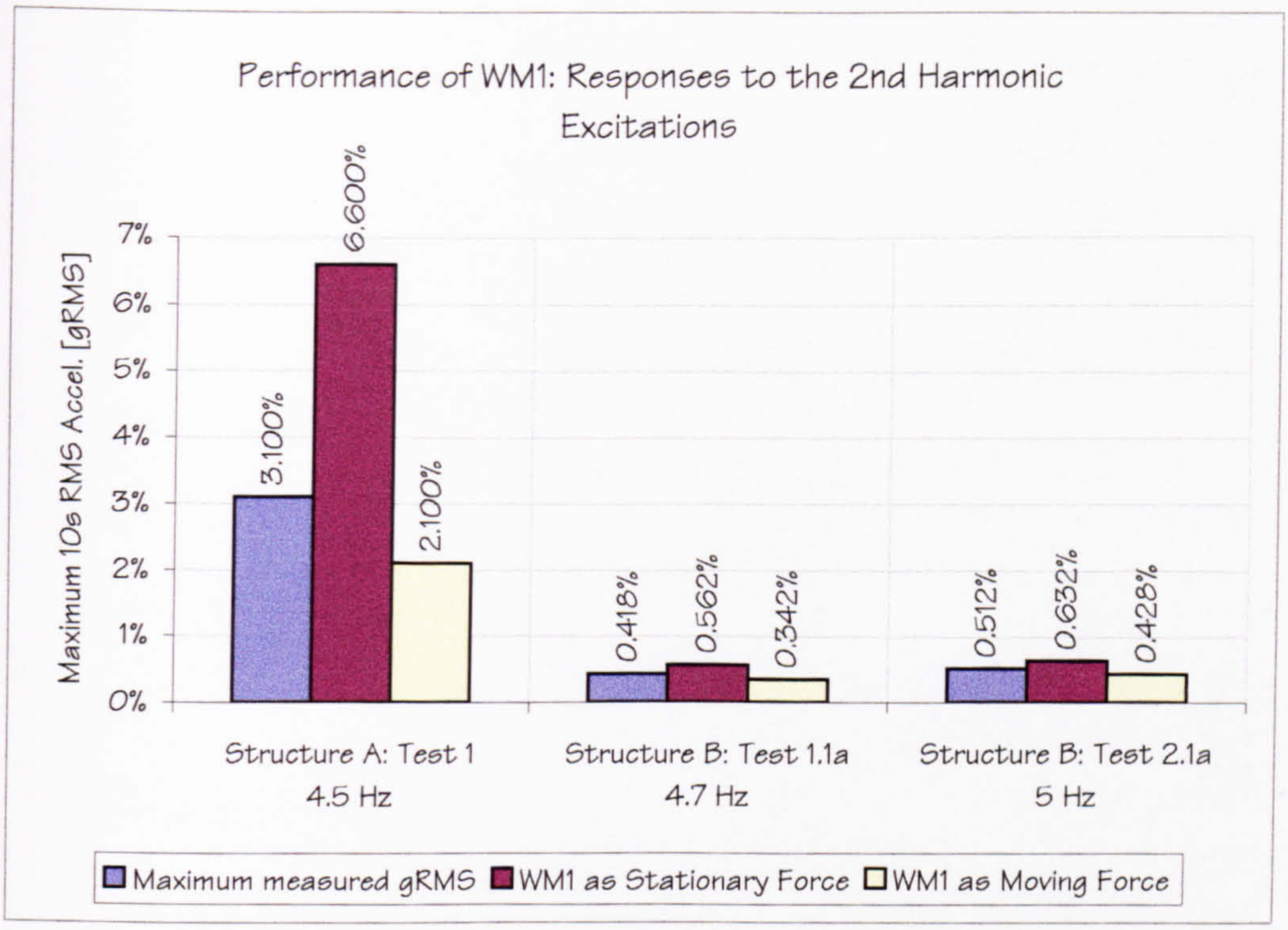

Figure 7.1: Walking Model 1 - Comparison of maximum measured and calculated responses for excitations by the 2nd harmonic of walking.

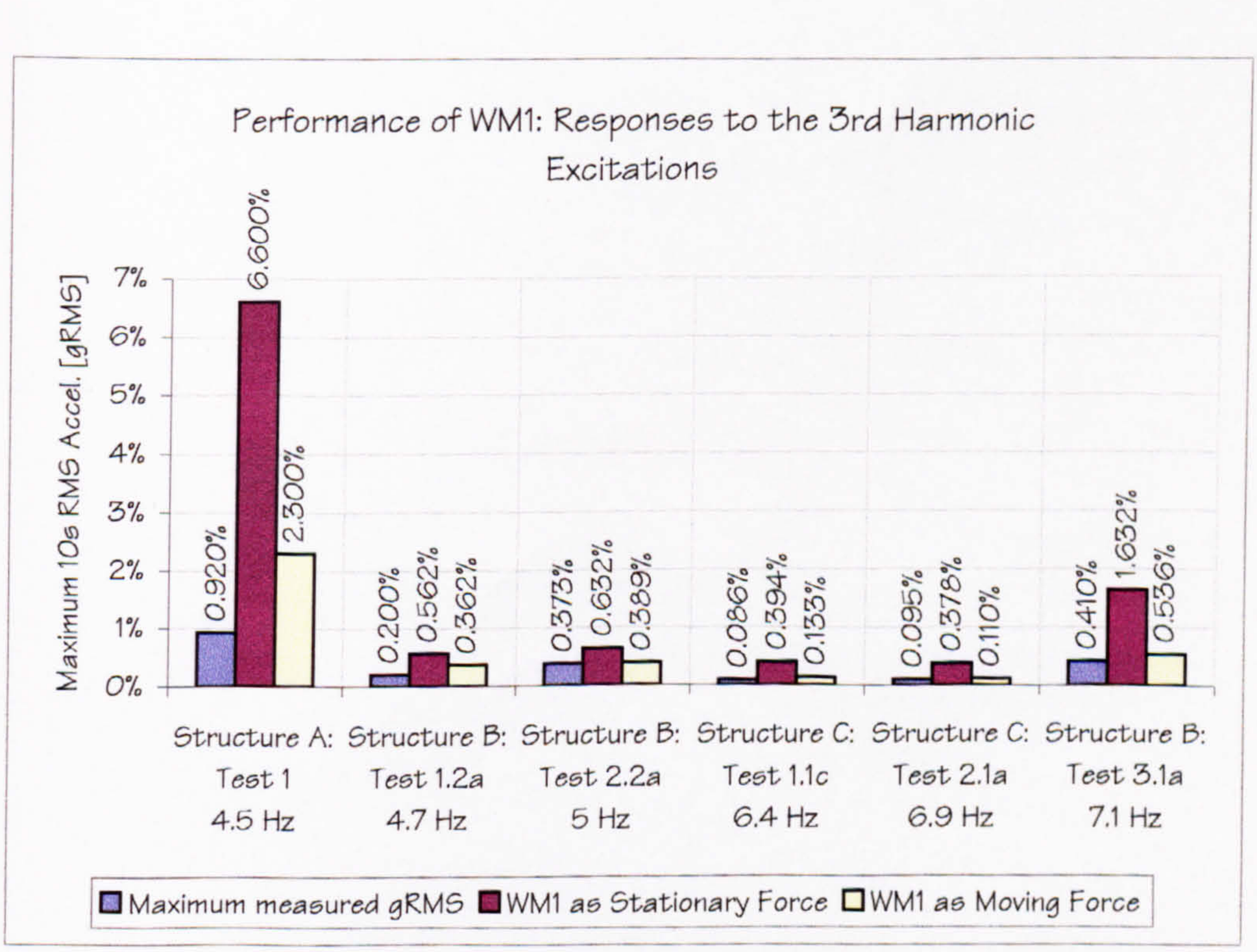

Figure 7.2: Walking Model 1 - Comparison of maximum measured and calculated responses for excitations by the 3rd harmonic of walking.

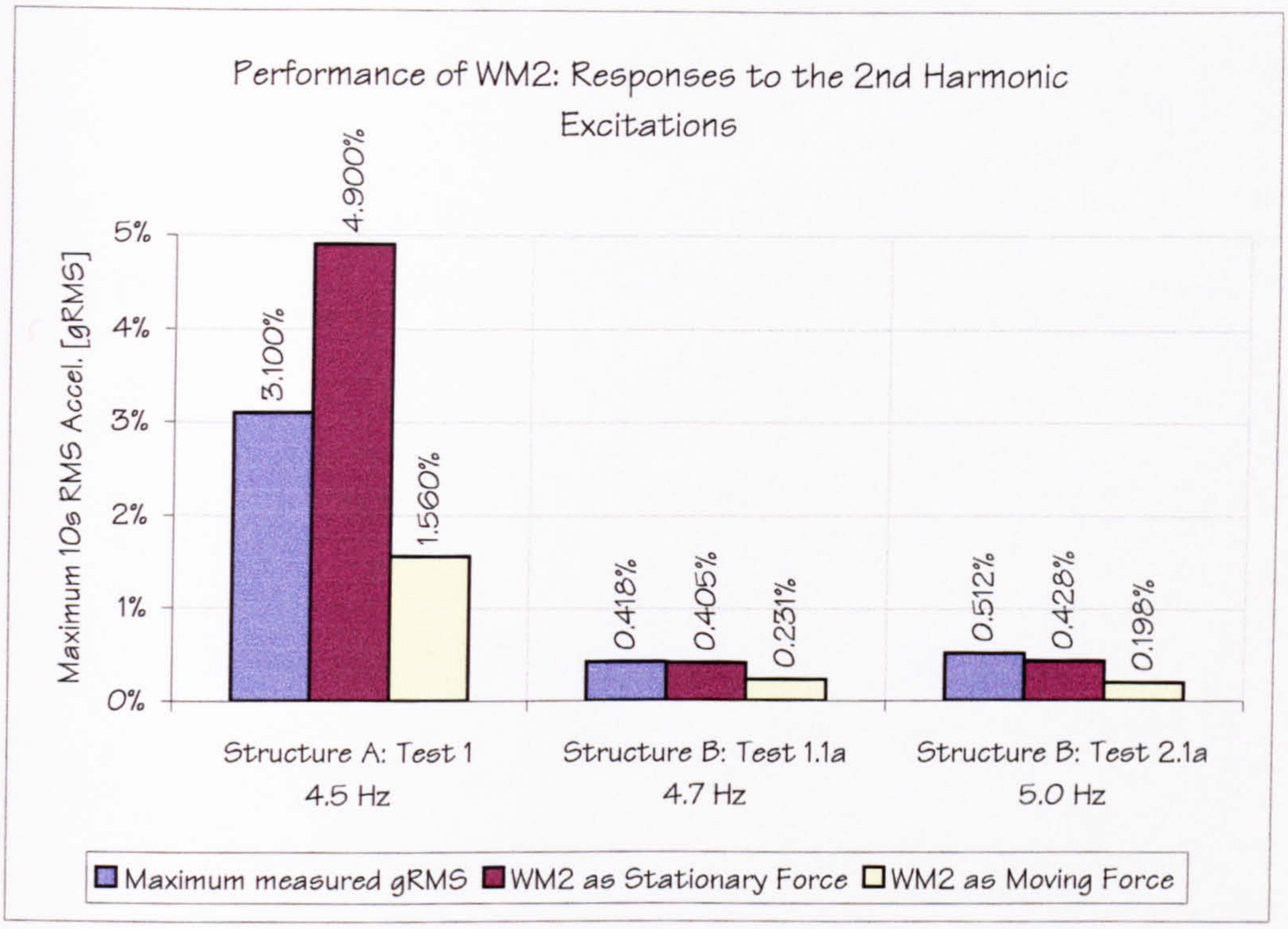

Figure 7.3: Walking Model 2 - Comparison of maximum measured and calculated responses for excitations by the 2nd harmonic of walking.

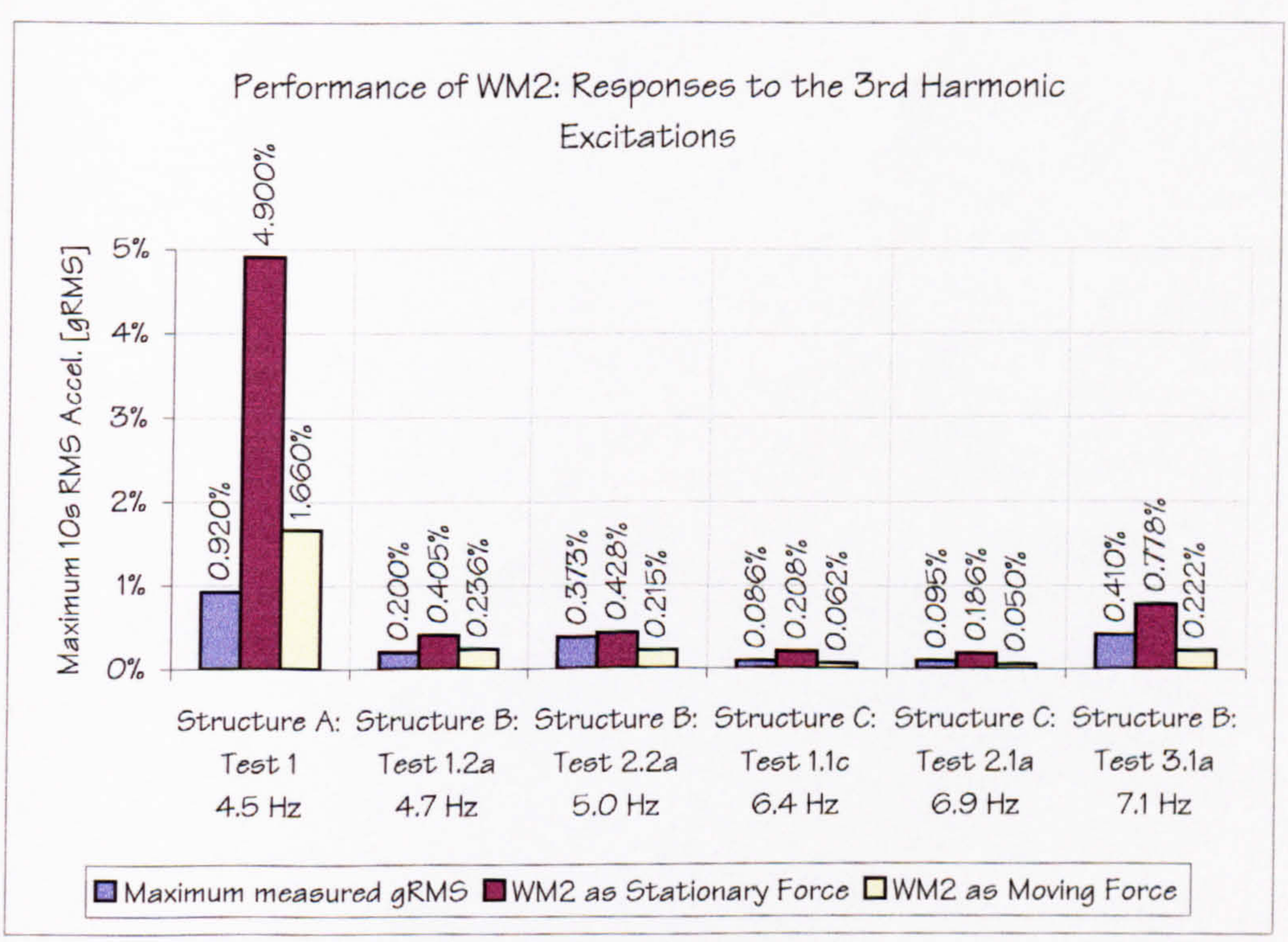

Figure 7.4: Walking Model 2 - Comparison of maximum measured and calculated responses for excitations by the 3rd harmonic of walking.

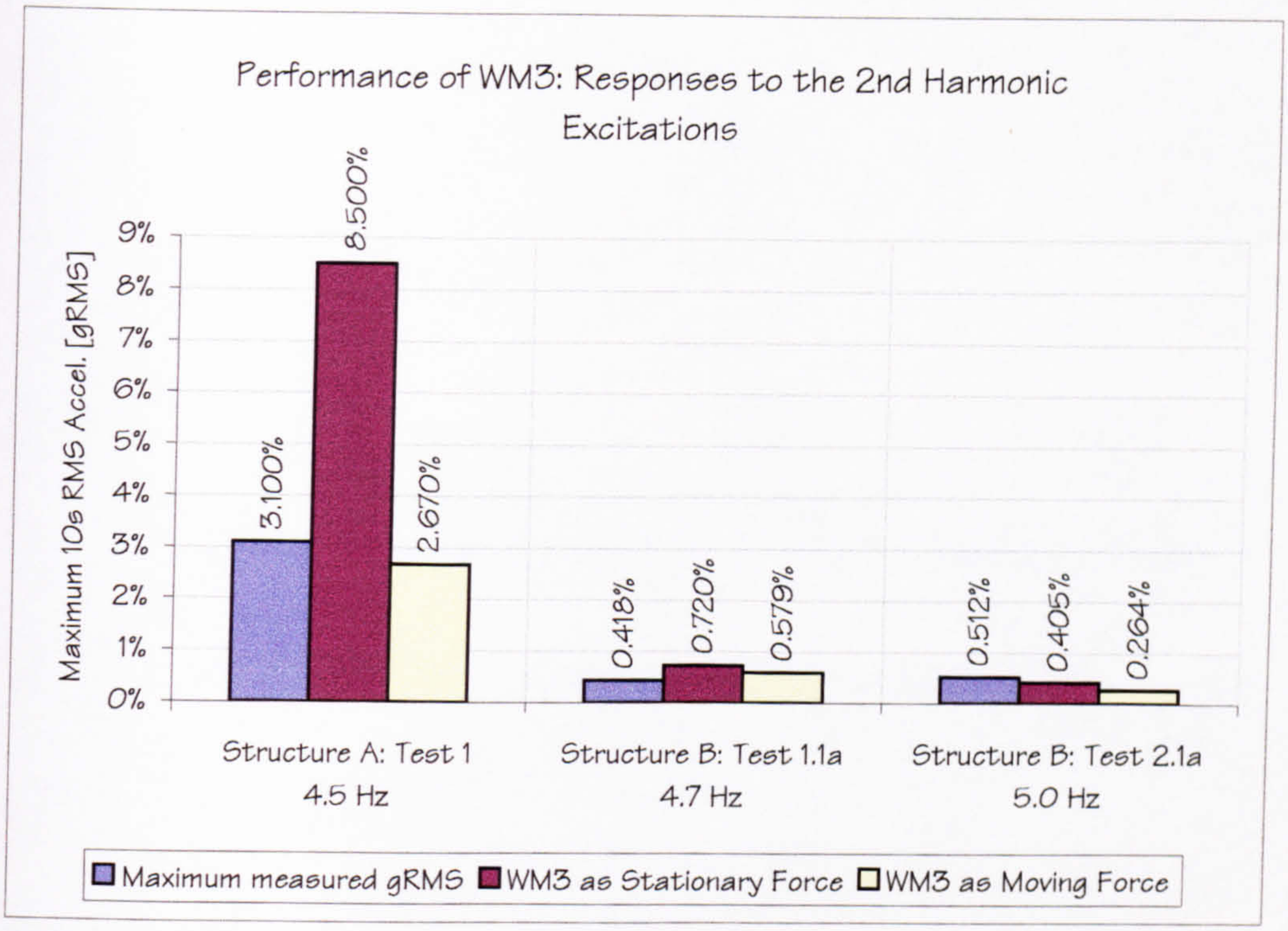

Figure 7.5: Walking Model 3 - Comparison of maximum measured and calculated responses for excitations by the 2nd harmonic of walking.

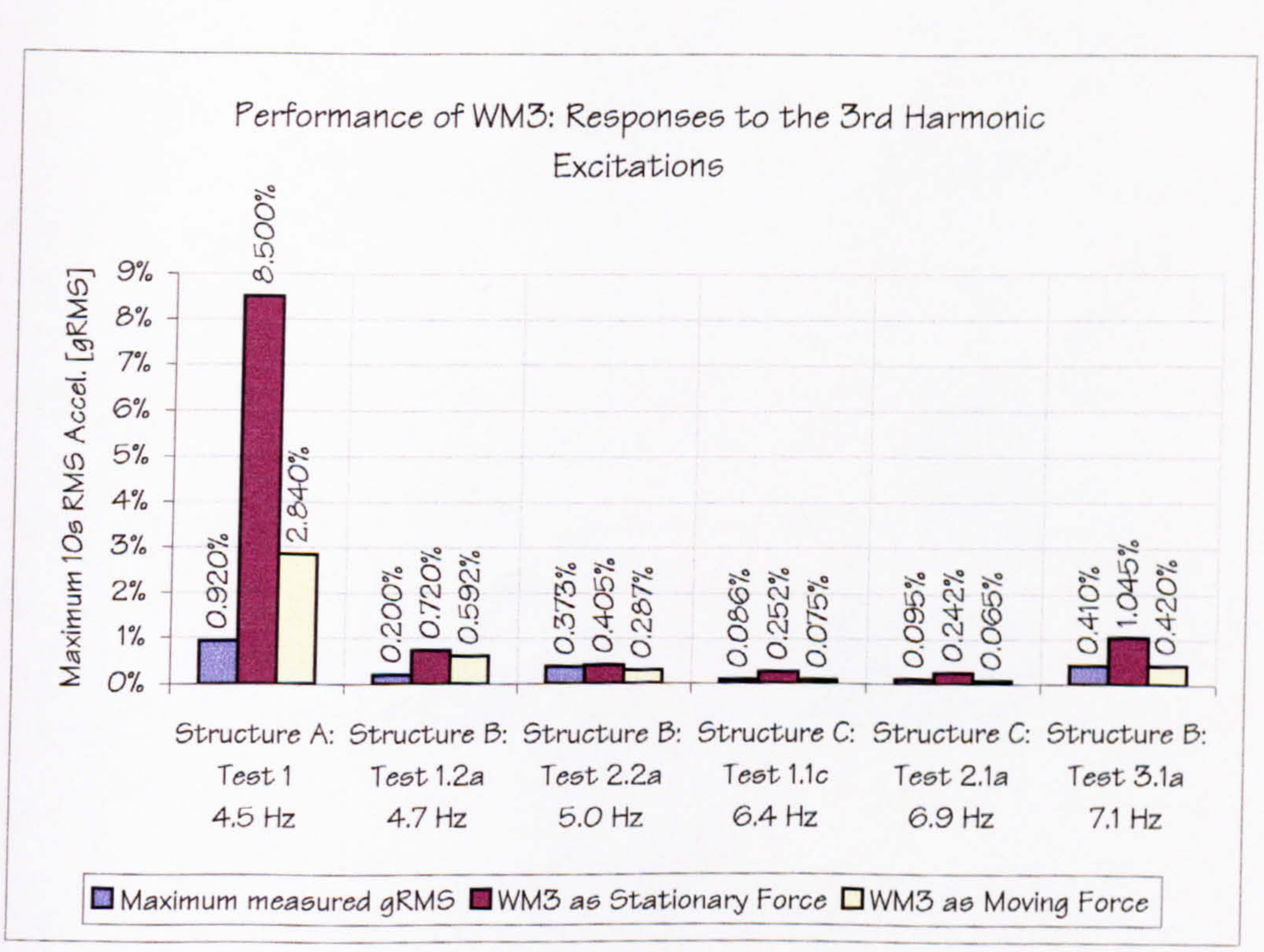

Figure 7.6: Walking Model 3 - Comparison of maximum measured and calculated responses for excitations by the 3rd harmonic of walking.

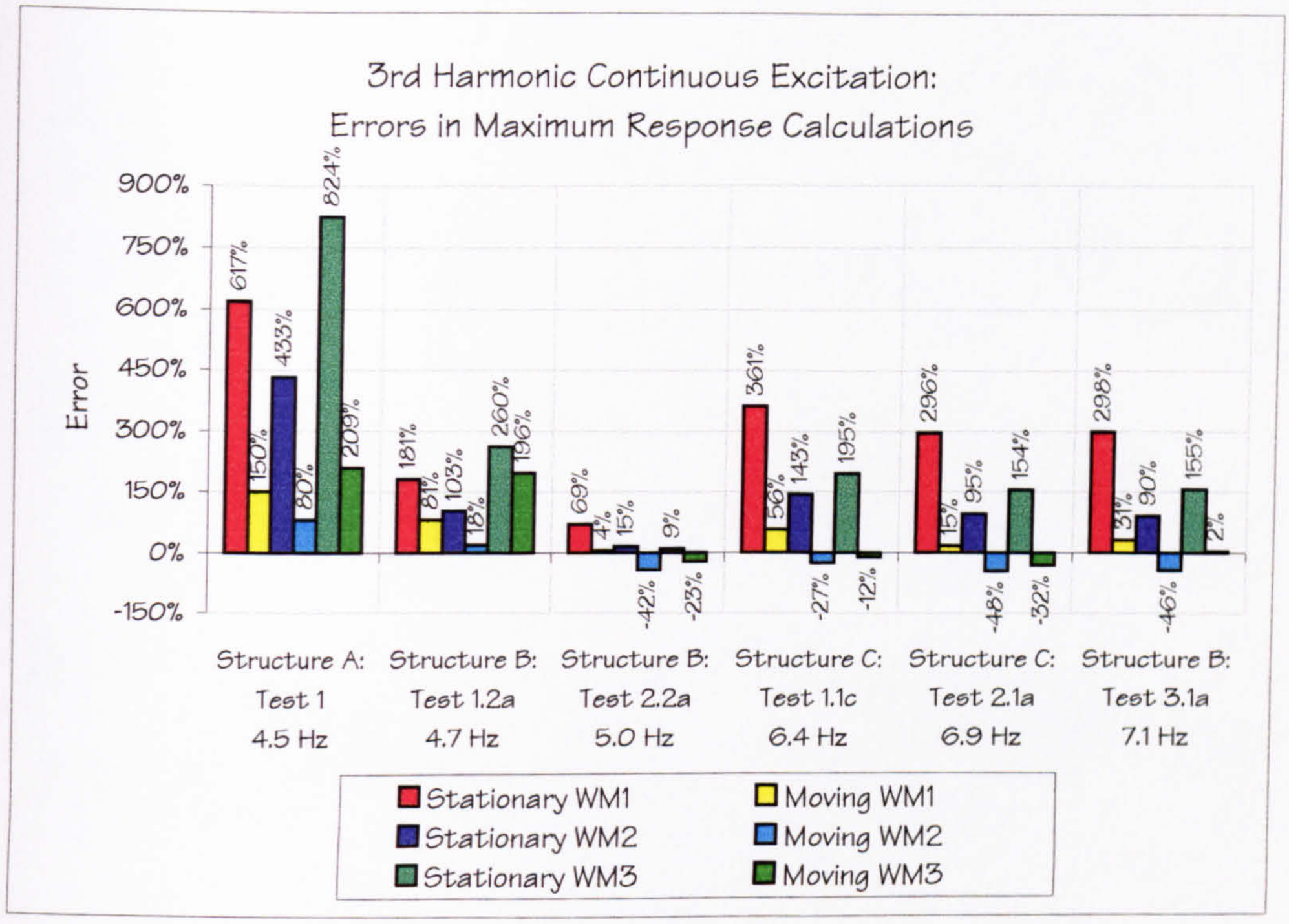

Figure 7.7: Comparison of errors made by applying WM1, WM2 and WM3 when simulating maximum responses to the continuous 3rd harmonic excitation for a range of natural frequencies excited.

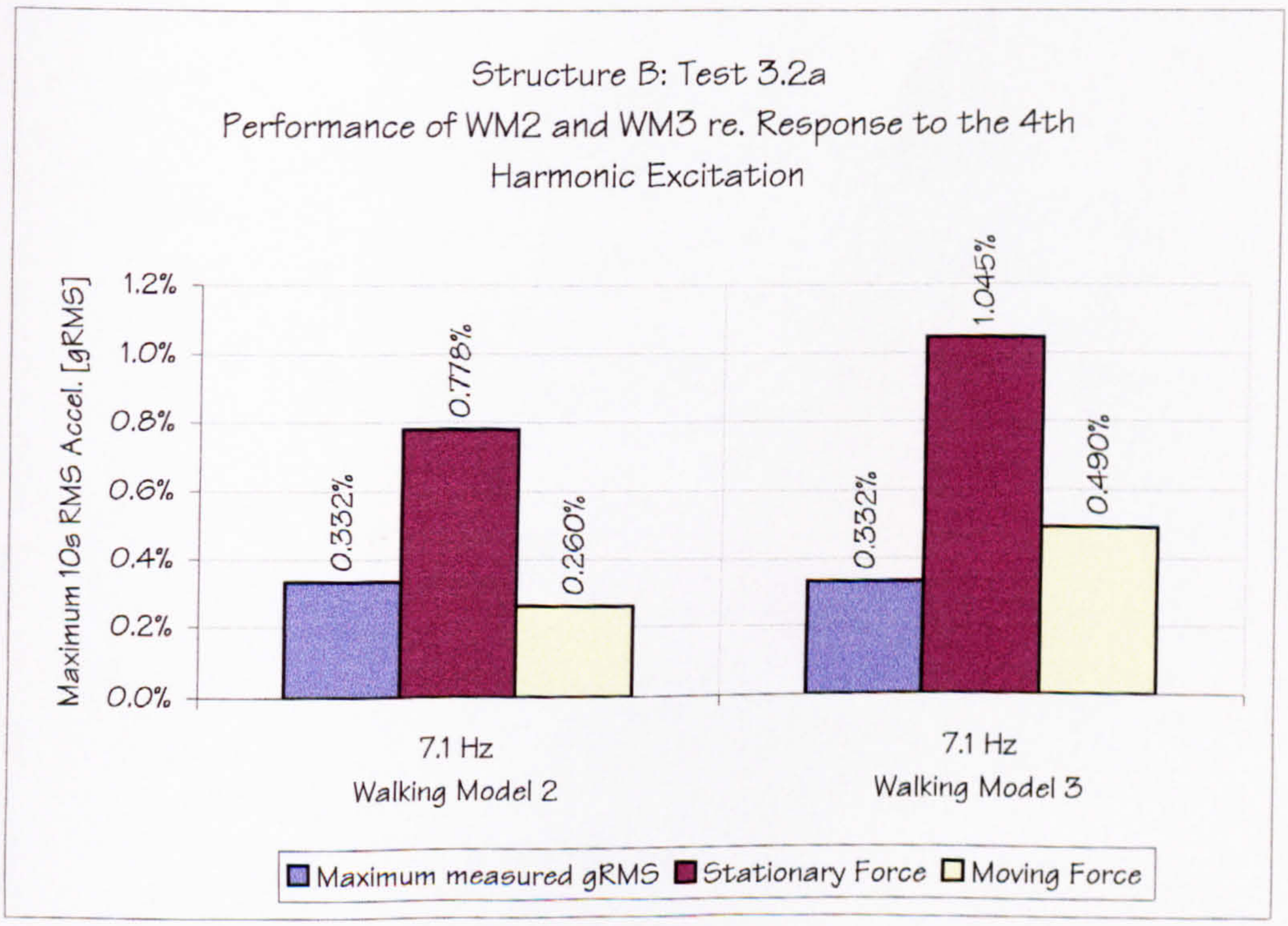

Figure 7.8: Structure B excited by the 4th harmonic of walking - Maximum measured responses vs. WM2 and WM3 simulations.

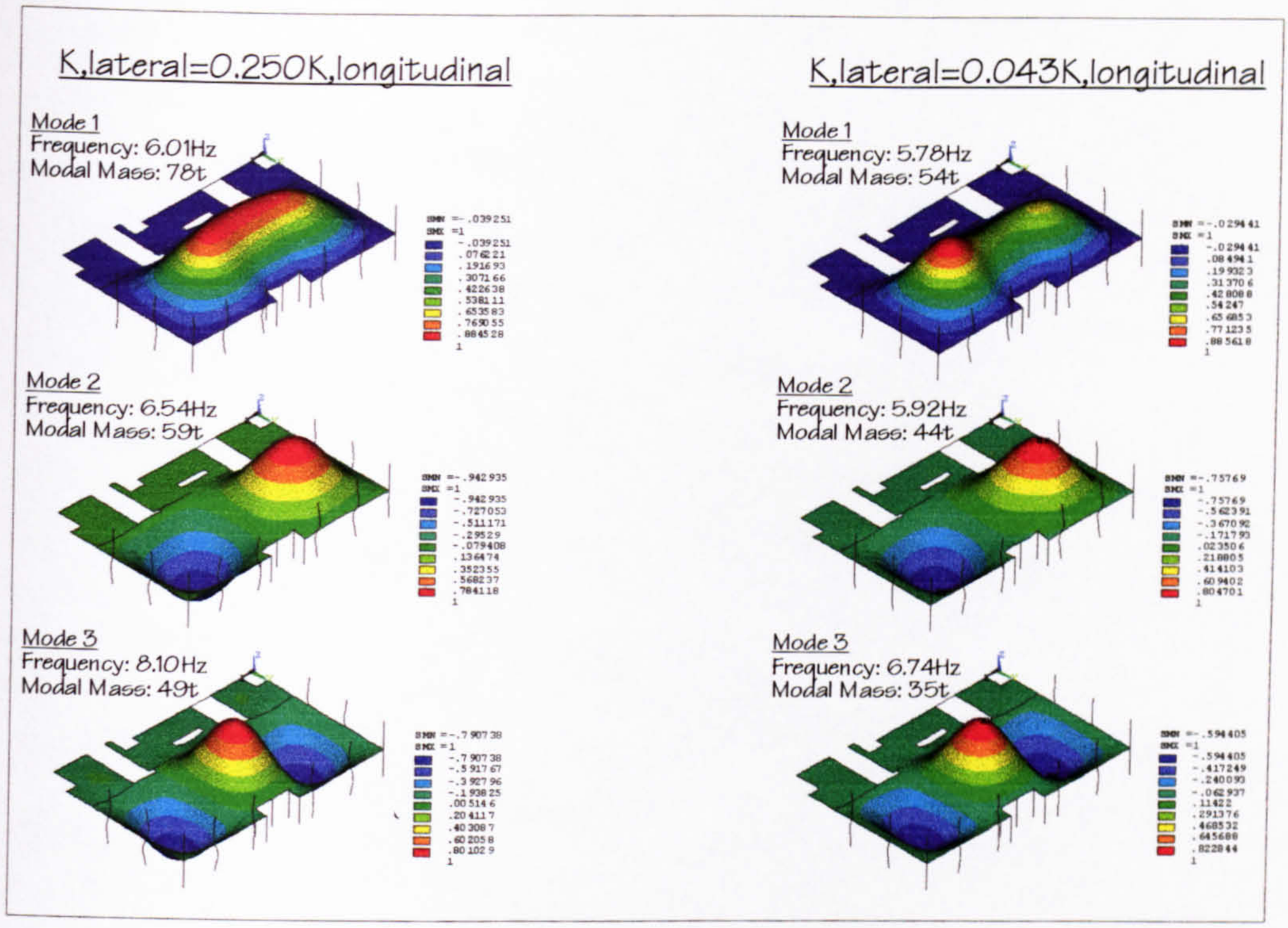

Figure 7.9: Structure C (Unclad) - Parametric study of the effect of lateral stiffness on modal mass of the first three modes of vibration.

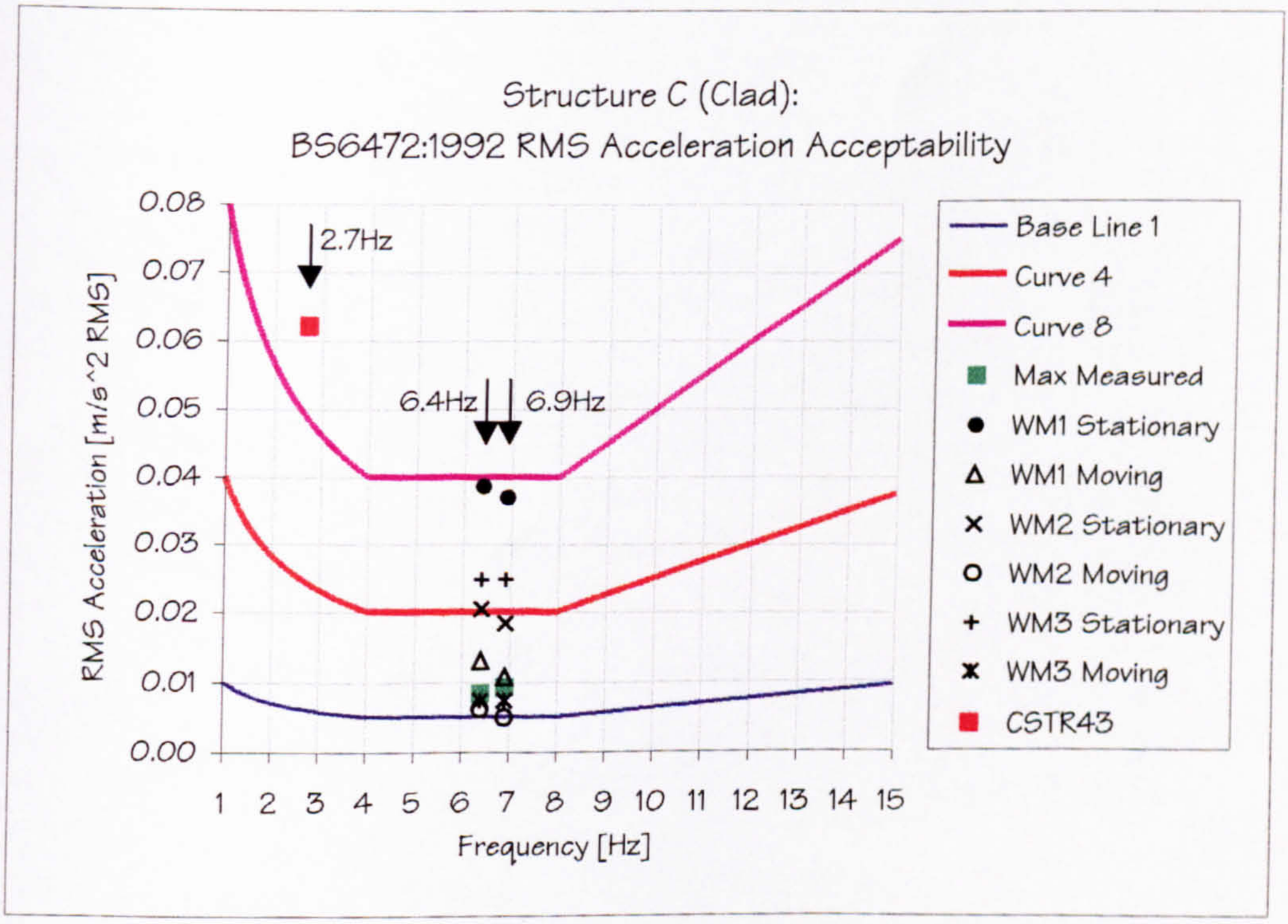

Figure 7.10: Structure C (Clad) - Vibration serviceability assessment based on maximum 10s RMS acceleration.

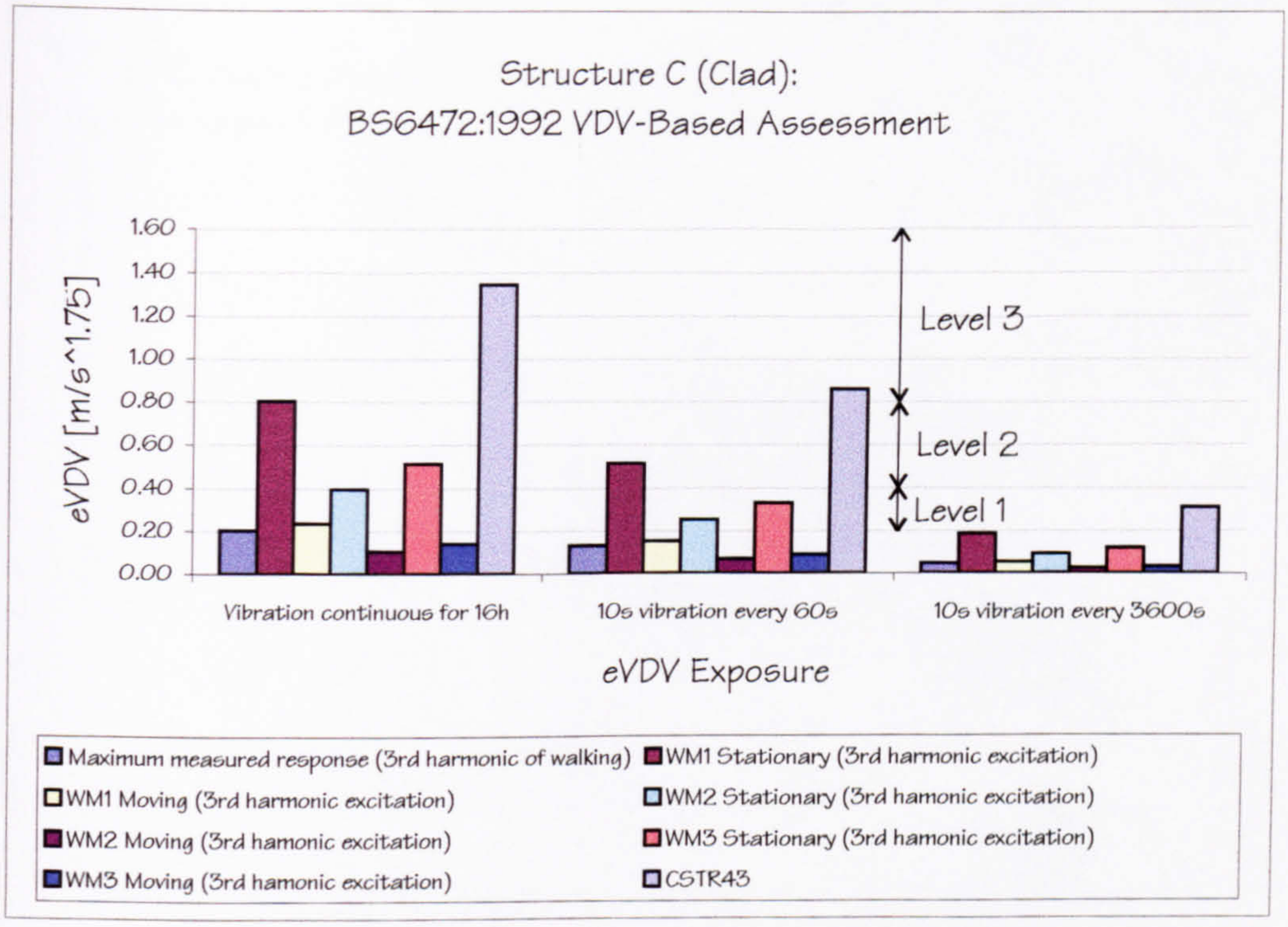

Figure 7.11: Structure C (Unclad) - Vibration serviceability assessment based on eVDV for varying duration of exposure.

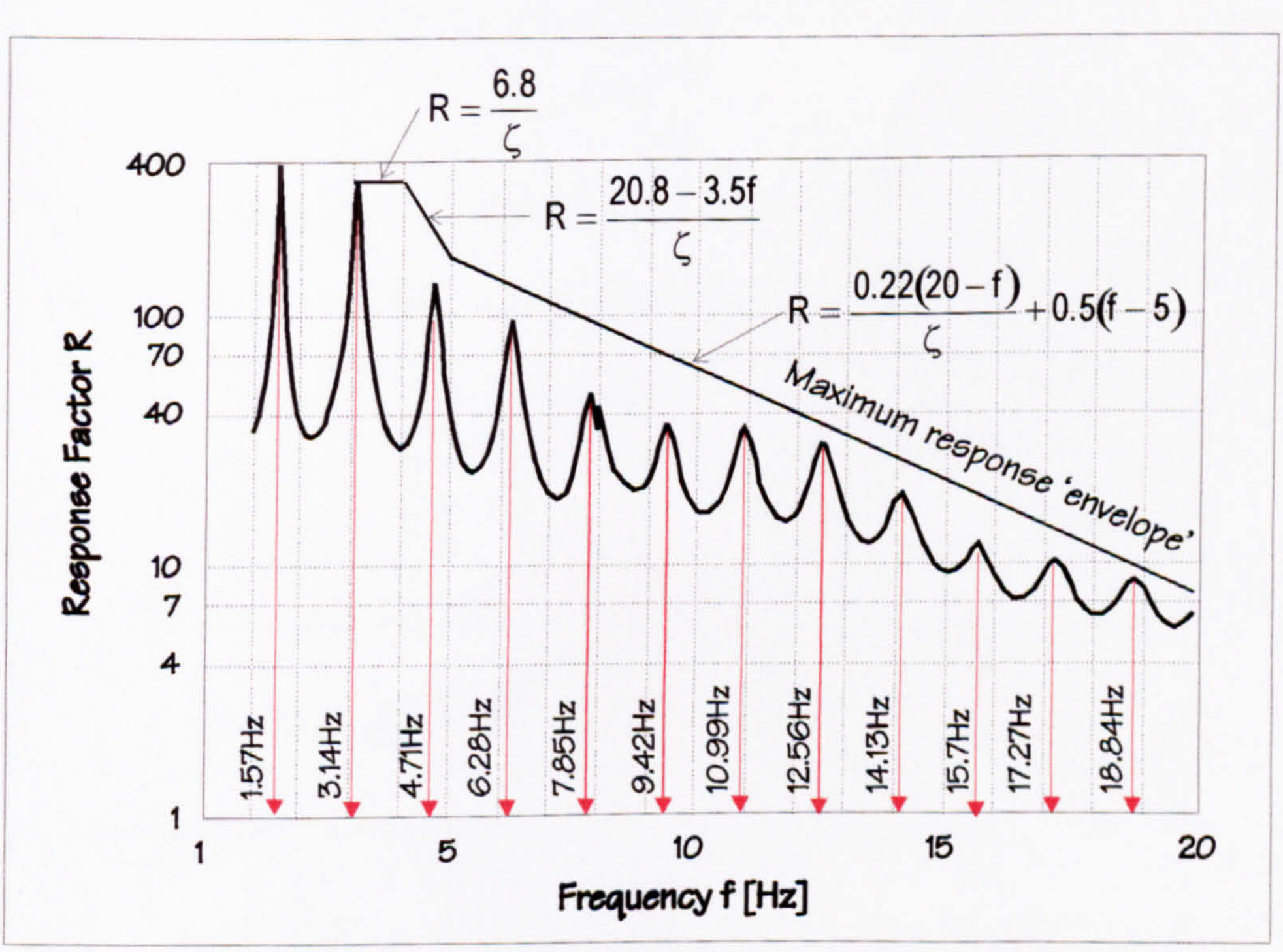

Figure 7.12: CSTR43 - Response of a SDOF system having mass of 1000kg to 13 harmonics of walking, when the natural frequency of the system is parametrically changed from 1Hz to 20Hz.

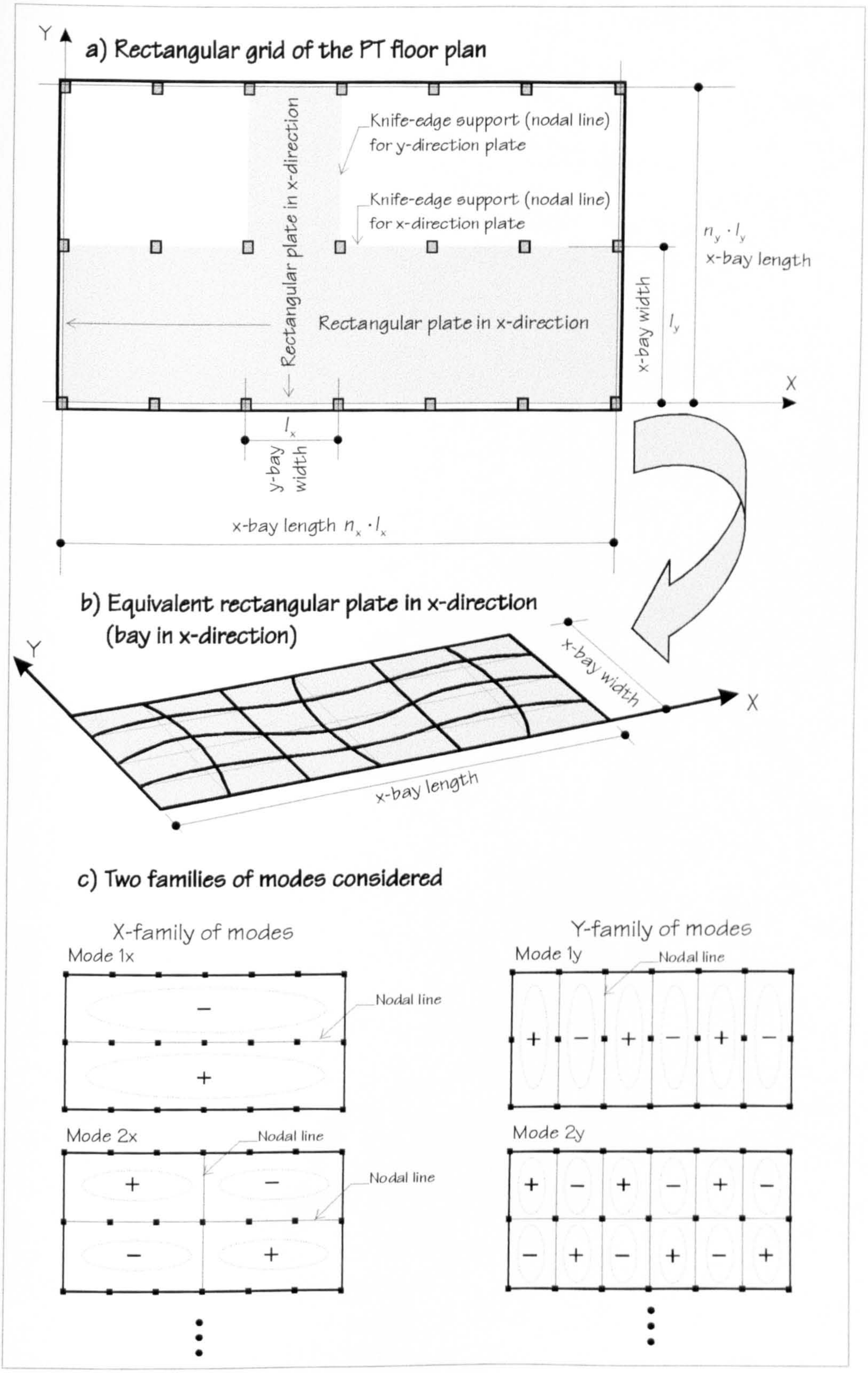

Figure 7.13: CSTR43 - Rectangular plate method.

8 Conclusions and Recommendations for Future Work

8.1 Conclusions

1. Modal testing and FE model updating of three full-scale in-situ cast concrete floor structures proved that the bending stiffness of the supporting in-situ cast concrete columns made a considerable contribution to the overall floor bending stiffness. As such, and contrary to widespread practice, columns should not be modelled as pin-supports when calculating floor modal properties for the purpose of vibration serviceability checks. Linear elastic FE models, where columns were modelled using bar elements rigidly connected to the floor and having their remote ends fully fixed, proved to be a fairly reliable means of calculating modal properties of in-situ floors. Apart from the columns, accurate modelling of the geometry and other boundary conditions of in-situ concrete floors was shown to be of crucial importance when estimating their modal properties. In testing a floor of an office building, stiffening effects of edge beams and non-structural elements, such as façade walls and services underneath the floor, were confirmed to exist and were quantified.

2. Lateral bending stiffness of band-beams in post-tensioned ribbed floors should be taken into account as it may increase the lateral floor stiffness by several orders of magnitude, depending on the exact floor layout. This may be beneficial as to the floor's vibration performance. FE model updating exercises demonstrated that modelling of this feature using orthotropic shell finite elements with 'smeared' mass and stiffness properties is reasonable.

3. When vibrating, in-situ cast concrete floors tend to act as continuous structures. This means that the modelling of such floors as isolated beams or floor panels, which may be suitable for static strength calculations, is not warranted for vibration serviceability checks. Such floor dynamic modelling, often seen in the literature, excludes the possibly beneficial effects of the increased modal mass and stiffness which exist.

4. Extensive cracking of a high-strength concrete floor cast in situ reduced its natural frequencies considerably, compared with the uncracked condition. However, only a slight increase in the modal damping of the structure was observed as a result of cracking. Generally speaking, a modal damping ratio of about 1% for all modes excitable by normal walking seems to be a reasonable value for all four bare and in-situ cast concrete floors tested, notwithstanding the relatively large scatter in the experimental data.

5. FE model updating exercises confirmed that a value of dynamic modulus for in-situ concrete floors of between 38 and 40 GPa was a reasonable assumption in the case of normal strength concretes. The high-strength concrete floor tested, however, required a significantly increased dynamic modulus of elasticity of about 47 GPa.

6. A detailed verification of three widely used walking excitation models, recommended by the CEB (1991), Eriksson (1994) and Willford (1997), revealed that:

   - The CEB model, recommended for checking vibration serviceability of concrete floors, overestimated considerably responses due to the 3rd harmonic of walking in all tests performed. The level of overestimation was such that the application of this walking model may condemn otherwise sound floor structures. The main reason for this is likely to be an excessively large dynamic loading factor of 0.1 for the 3rd harmonic of walking. This factor is the same as for the 2nd harmonic of walking in this model, which is somewhat surprising and clearly needs amending. When assumed to be moving (which is not how the CEB advocates its application), the performance of this excitation model simulating the 3rd harmonic of walking improved considerably. Finally, the CEB model does not have any provision for the 4th harmonic excitation which was shown to be capable of exciting higher, closely spaced floor modes having lower modal mass and stiffness.

   - Eriksson's model performed the best of all three models as its overestimation of the actual measured responses to the 3rd harmonic of walking was least conservative.

   - Willford's model generally proved to be the least reliable of the three walking excitation models investigated.

7. The above conclusions helped to pinpoint a number of serious shortcomings found in the new vibration serviceability guidelines recommended for post-tensioned floors in the Concrete Society Technical Report 43 (CSTR43) published in 1994. These shortcomings are:

   - An inappropriate walking forcing function corresponding only to 94 steps per minute, which does not consider variability of pacing rates and the corresponding variation in the levels of excitation.

   - Assumptions that in-situ cast columns supporting in-situ floors act as pin supports and floor edges always permit free rotation. These two assumptions may unduly underestimate floor natural frequencies. As shown in the case of an actual office floor (Structure C) this may lead to the unwarranted dismissal of a sound floor structure during design.

   - An assumption that column lines act as 'knife-edge' supports. This assumption stiffens the floor and counteracts the assumption of columns acting as pin supports in a rather unpredictable way.

   - The beneficial effects of the increased lateral stiffness of post-tensioned floors utilising band beams are not taken into account.

- An assumption that only the floor's fundamental mode is excited in resonance by walking. This assumption neglects the possibility that higher, but closely spaced, modes with lower modal mass may actually produce higher responses due to walking. This was corroborated by practical response measurements performed in this research where the excitation of higher modes actually produced maximum responses.

- An assumption that modal mass of all relevant modes of floor vibration is always 25% of the total floor mass. Updated FE models developed in this project showed that this assumption is not warranted and that modal masses of modes excitable by normal walking can actually be several times lower.

- The response analysis is based on the assumption that two families of floor modes exist in two orthogonal directions. This assumption has little physical meaning and may lead to overconservative responses due to double-counting of modal contributions.

- Assessment of vibration levels in CSTR43 is based on outdated BS6472:1984 guidelines which were replaced by BS6472:1992 two years before CSTR43 was published. As a consequence, the vibration dose value (VDV) and considerations of intermittency of walking vibrations do not feature in CSTR43.

8. Advanced modal testing and 'manual' FE model correlation and updating technologies have been successfully transferred from the mechanical and aerospace engineering industries. The testing, correlation and updating procedures adopted and, in particular, the utilisation of MAC and COMAC proved to be invaluable in this research. It was demonstrated that the development of a relatively crude FE model prior to modal testing may be an important means of ensuring better quality of the experimental data. This is particularly so when the testing is performed under severe time constraints, as is likely to be the case for modal testing of large prototype civil engineering structures. In addition, quiet conditions were shown to be essential for obtaining good quality results using instrumented hammer testing. However, when modal testing was performed using a hammer operator physically present on the floor, measured modes of vibration seemingly developed complexities indicating the presence of non-proportional damping.

8.2 Recommendations for Further Work

1. This research has explicitly identified a number of serious weaknesses in the methodology for vibration serviceability checks adopted currently by the Concrete Society (1994). Clearly, Appendix G of CSTR43 dealing with vibration serviceability of PT floors requires urgent attention. As it is unlikely that simple hand calculations would be able to deal with a problem as complex as vibration serviceability of post-

tensioned office floors, the best way forward, in principle, is linear dynamic computer analysis. Therefore, a substantial part of the current vibration serviceability provision in CSTR43 would require replacement with a set new of guidelines. These should be aimed primarily at specifying the best practice for numerical modelling of human-induced excitation as well as mass, stiffness and damping properties of post-tensioned floors when checking their vibration serviceability.

2. Due to the small number of tests of full-scale floor structures performed in this research project and worldwide in general, there is a serious lack of reliable data related to the actual as-built vibration performance of long-span in-situ concrete floors. Such experimental data are invaluable, particularly when coupled with FE model correlation and updating. Therefore, there is a clear need for more testing, analysis, correlation and updating exercises on long-span concrete floors which would provide greater insight into the vibration behaviour of a wider range of in-situ concrete floor configurations.

3. Single-person walking excitation, by its very nature, moves and is not perfectly periodic or predictable. However, the available models tend to treat it as a perfectly predictable, periodic/harmonic force which does not move and is capable of exciting pure resonance. Such models are much easier to formulate and apply, but their ability to represent reality is questionable. Although this research has found that Eriksson's (1994) walking model performs best of the three models investigated, relatively large overestimation errors still remained in the majority of the response tests corresponding to the 3rd harmonic excitation due to walking. This indicates that there is clear scope for further development of walking excitation models by:

- Introducing elements of uncertainty into them (e.g. in amplitudes, phase, pacing rates, etc.)
- Enhancing their statistical reliability by performing more measurements on different groups of people in different circumstances;
- Considering them as moving as opposed to stationary loads in a more sophisticated way;
- Considering that they may be used in different applications (e.g. office floors, footbridges, etc.) where the feeling of the motion ('motion feedback') and rate of occurrence may be important;
- Incorporating them as add-on modules into existing FE packages which would make their application as easy as hand calculations provided that engineers who use them have sufficient training and computer modelling skills.

4. More information about the usage of office floors and frequency of floor crossings by its occupants is required in order to improve the current provision of BS6472:1992 aimed at assessing the levels of vibrations in buildings.

5. There is a lack of information about the damping levels of floors supporting fully furnished offices occupied by people. For these floors, excitation-response measurements rendering FRFs which can be used to perform MDOF parameter estimation is the recommended way forward to estimate damping.

With regard to this, it is important to stress that good quality FRF measurements on prototype floor structures in operation, which weigh hundreds if not thousands of tonnes, are difficult to make and are expensive. Facilities to perform such measurements in the UK are limited. Therefore, there is a need to set up a national facility, possibly based on synchronised multi-shaker excitation, which would be able to perform this task.

6. 'Manually' updated FE models, developed along the lines demonstrated in this research, may further benefit from automatic FE model updating performed by some commercially available software, such as FEMtools (FEMtools, 1994). It is likely that the time consuming 'manual' fine tuning, after the key updating parameters in the FE model have been identified, would be much faster if performed automatically. However, the usefulness of the whole exercise, aimed at improving FE modelling for the purpose of vibration serviceability checks, remains to be determined.

7. In the case of very large continuous floor areas it remains unclear how far from the excitation point vibrations actually propagate. This is likely to affect the area of a large floor which actually participates in the vibrations. Also, this is related to the actual level of excitation and to the issue of 'dispersive damping' (as opposed to 'dissipation damping').

8. Further quantification is required of the effects of non-structural elements, such as façade, services underneath the floor, partitioning walls and, in particular, false floors on the floor's vibration performance under human-induced loading.

9. When checking vibration serviceability of in-situ floors which are not prestressed and are expected to crack, better and more reliable modelling of the cracking is required. Post-cracking linear elastic behaviour under low-level human induced excitation remains one of the areas which require further research work.

10. When vibration serviceability is thought to be an issue and in order to gain a better understanding of the dynamic performance of slender floors in buildings, there is a need to perform and publish high quality modal and dynamic response measurements on as-built floors after their construction.

9 References

Abe, T., Hashimoto, Y. and Hiromatsu T. (1994). Vibration-Proof Designing for Machine Support Systems - Study on Floor Vibration Interaction and Force Identification. In: Proceedings of the 12th IMAC. Vol. 2. (pp. 1778-1784). Honolulu, USA. January 31 - February 3.

Abe, T., Hiromatsu, T. and Kushida, H. (1990). Study on Estimation Methods for Floor Structure Vibration - Vibrational Characteristics of Orthogonal Anisotropic Floor Structures. In: Proceedings of the 8th IMAC. (pp. 645-651). Orlando, USA. January 29 - February 1.

Agardh, L. (1991). Modal Analyses of Two Concrete Bridges in Sweden. Structural Engineering International. 4/91. 35-39.

Agardh, L. (1994). Impact Excitation of Concrete Highway Bridges. In: Proceedings of the 12th IMAC. Vol. 2. (pp. 1329-1334). Honolulu, USA. January 31 - February 3.

Allemang, R. J. and Brown, D. L. (1993). Experimental Modal Analysis. In: A. S. Kobyashi (Ed.) Handbook on Experimental Mechanics (2nd Edition). (pp. 635-750). Bethel, USA: SEM.

Allen, D. E. (1990a). Building Vibrations from Human Activities. Concrete International. Vol. 12, No. 6. 66-73.

Allen, D. E. (1990b). Floor Vibrations From Aerobics. Canadian Journal of Civil Engineering. Vol. 17, No. 5. 771-779.

Allen, D. E. and Murray, T. M. (1993). Design Criterion for Vibrations Due to Walking. AISC Engineering Journal. Vol. 40, Part 4. 117-129.

Allen, D. E. and Pernica, G. (1984). A Simple Absorber for Walking Vibrations. Canadian Journal of Civil Engineering. Vol. 11. 112-117.

Allen, D. E. and Rainer, J. H. (1975). Floor Vibration. Canadian Building Digest. (September. pp. 173.1-173.4). Ottawa, Canada: Division of Building Research, NRCC.

Allen, D. E. and Rainer, J. H. (1976). Vibration Criteria for Long-Span Floors. Canadian Journal of Civil Engineering. Vol. 3, No. 2. 165-173.

Allen, D. E., Rainer, J. H. and Pernica, G. (1979). Vibration Criteria for Long-Span Concrete Floors. In: ACI Publication SP-60, Proceedings of the Symposium on Vibrations of Concrete Structures, 1977 Fall Convention of the ACI. (pp.67-78). New Orleans, USA. October 20.

Allen, D. E., Rainer, J. H. and Pernica, G. (1985). Vibration Criteria for Assembly Occupancies. Canadian Journal of Civil Engineering. Vol. 12, No. 3. 617-623.

Allen, D. L. (1974a). Vibrational Behaviour of Long-Span Floor Slabs. In: Proceedings of the Canadian Structural Engineering Conference. (pp. 1-19). Ontario, Canada.

Allen, D. L. (1974b). Vibrational Behaviour of Long-Span Floor Slabs. Canadian Journal of Civil Engineering. Vol. 1, No. 1. 108-115.

Allen, D. L. and Swallow, J. C. (1975). Annoying Floor Vibrations - Diagnosis and Therapy. Sound and Vibration. No. 3. 12-17.

Ammann, W. and Nussbaumer, H. (1991). Behaviour of Concrete and Steel under Dynamic Actions. In: Vibration Problems in Structures: Practical Guidelines Appendix F. CEB Bulletin D'Information No. 209. Lausanne, Switzerland: CEB.

ANSYS. (1995a). ANSYS User's Manual, Revision 5.2: Procedures (Volume I). Houston, USA: ANSYS, Inc.

ANSYS. (1995b). ANSYS User's Manual, Revision 5.2: Commands (Volume II). Houston, USA: ANSYS, Inc.

ANSYS. (1995c). ANSYS User's Manual, Revision 5.2: Elements (Volume III). Houston, USA: ANSYS, Inc.

ANSYS. (1995d). ANSYS User's Manual, Revision 5.2: Theory (Volume IV). Houston, USA: ANSYS, Inc.

APS Dynamics. (1996a). Instruction Manual ELECTRO-SEIS Model 113 Shaker. Carlsbad, USA: Author.

APS Dynamics. (1996b). Instruction Manual DUAL-MODE Model 114-EP Amplifier. Carlsbad, USA: Author.

ASCE. (1995). Minimum Design Loads for Building and Other Structures. ASCE 7-95 Standard (Revision of ANSI/ASCE 7-93.). Author.

Aswad, A. and Chen, Y. (1993). Vibration Properties of Precast Building Floors. Final Report. PCI: January.

Atherton, G. H., Polensek, A. and Corder, S. E. (1976). Human Response to Walking and Impact Vibration of Wood Floors. Forest Product Journal. Vol. 26, No.10. 40-47.

Bachmann, H. (1984). Vibrations of Building Structures Caused by Human Activities: Case Study of a Gymnasium. Canadian Institute for Scientific and Technical Information, Technical Translation NRC/CNR TT-2077. Ottawa, Canada: NRCC.

Bachmann, H. (1988). Practical Cases of Structures with Man-Induced Vibrations. In: Proceedings of the Symposium/Workshop on Serviceability of Buildings (Movements, Deformations, Vibrations). Vol. 1. (pp. 419-434). Ottawa, Canada. May16-18.

Bachmann, H. (1992). Vibration Upgrading of Gymnasia, Dance Halls and Footbridges. Structural Engineering International. Vol. 2, No. 2. 118-124.

Bachmann, H. and Ammann, W. (1987). Vibrations in Structures Induced by Man and Machines. Zurich, Switzerland: IABSE

Bachmann, H., Pretlove, A. J. and Rainer, H. (1991a). Vibrations Induced by People. In: Vibration Problems in Structures - Practical Guidelines. CEB Bulletin D'Information No. 209. Lausanne, Switzerland: CEB.

Bachmann, H., Pretlove, A. J. and Rainer, H. (1991b). Dynamic Forces from Rhythmical Human Body Motions. In: Vibration Problems in Structures - Practical Guidelines. Appendix G. CEB Bulletin D'Information No. 209. Lausanne, Switzerland: CEB.

Bachmann, H., Pretlove, A. J. and Rainer, H. (1995a). Vibrations Induced by People. In: Vibration Problems in Structures - Practical Guidelines. Basel, Switzerland: Birkhäuser Verlag.

Bachmann, H., Pretlove, A. J. and Rainer, H. (1995b). Dynamic Forces from Rhythmical Human Body Motions. In: Vibration Problems in Structures - Practical Guidelines. Appendix G. Basel, Switzerland: Birkhäuser Verlag.

Bainbridge, R. J. and Mettem, C. J. (1997). Serviceability Performance of Timber Floors. The Structural Engineer. Vol. 75, No. 16. 269-274.

Bathe, K-J. (1996). Finite Element Procedures. New Jersey, USA: Prentice Hall.

Becker, R. (1980). Simplified Investigation of Floors Under Foot Traffic. Journal of the Structural Division ASCE, ST11. Vol. 106. 2221-2234.

Beckwith, T. G., Marangoni, R. D. and Leinhard, J. H. (1995). Mechanical Measurements. Reading, Massachusetts, USA: Addison-Wesley Publishing Company.

Bennett, K. J. (1995). Private communication with K. J. Bennett, Technical Manager, PSC Freyssinet Ltd. (UK). Bracknell, UK.

Bennett, K. J. (1997). Private communication with K. J. Bennett, Technical Manager, PSC Freyssinet Ltd. (UK). Bracknell, UK.

Bishop, N. W. M., Willford, M. and Pumphrey, R. (1995). Human Induced Loading of Flexible Staircases. Safety Science. Vol. 18. 261-276.

Blanchard, J., Davies, B. L. and Smith, J. W. (1977). Design Criteria and Analysis for Dynamic Loading of Footbridges. In: Proceedings of the DOE and DOT TRRL Symposium on Dynamic Behaviour of Bridges. (pp. 90-106). Crowthorne, UK. May 19.

Bolton, A. (1994). Structural Dynamics in Practice - A Guide for Professional Engineers. London, UK: McGraw-Hill Book Company.

Bono, R. W., Hunt, V. J., Brown, D. L., Lally, M. J. and Aktan, A. E. (1996). Portable, Controllable Impact Excitation for Civil Infrastructure. In: Proceedings of the 14th IMAC. Vol. 2. (pp. 1185-1190). Dearborne, USA. February 12-15.

BRE. (1983). Vibrations: Building and Human Response. Building Research Establishment Digest. Watford, UK: Author.

Brigham, E. O. (1974). The Fast Fourier Transform. New Jersey, USA: Prentice-Hall.

Broch, J. T. (1984). Mechanical Vibration and Shock Measurements. Naerum, Denmark: Bruel and Kjaer.

Brown, D., Carbon, G. and Ramsey, K. (1977). Survey of Excitation Techniques Applicable to the Testing of Automotive Structures. In: Proceedings of the Society of Automotive Engineers International Automotive Engineering Congress and Exposition. (pp. 1-15). SAE Paper No. 770029. Detroit, USA. February 28 - March 4.

Brownjohn, J. M. W. (1988). Assessment of Structural Integrity by Dynamic Measurements. PhD Thesis. University of Bristol, UK.

BRS. (1955). Vibrations in Buildings (Building Research Station Digest No. 78). London, UK: HMSO.

BSI. (1978). Steel, Concrete and Composite Bridges, Part 2: Specification for Loads; Appendix C: Vibration Serviceability Requirements for Foot and Cycle Track Bridges. BS 5400. London, UK: Author.

BSI. (1984). Guide to the Evaluation of Human Exposure to Vibration in Buildings (1 Hz to 80 Hz). BS 6472. Hemel Hempstead, UK: Author.

BSI. (1985). Structural Use of Concrete. BS 8110. Milton Keynes, UK: Author.

BSI. (1987a). Measurement and Evaluation of Human Exposure to Whole-Body Mechanical Vibration and Repeated Shock. BS 6841. Milton Keynes, UK: Author.

BSI. (1987b). Experimental Determination of Mechanical Mobility, Part 1: Specifications for Transducers. BS 6897-1. Milton Keynes, UK: Author.

BSI. (1989). Mechanical Mounting of Accelerometers for Measuring Vibration and Shock. BS 7129. Milton Keynes, UK: Author.

BSI. (1990). Experimental Determination of Mechanical Mobility, Part 2: Measurements Using Single-Point Translation Excitation with an Attached Vibration Exciter. BS 6897-Part 2. Milton Keynes, UK: Author.

BSI. (1991). Glossary of Terms Relating to Mechanical Vibration and Shock. BS 3015. Milton Keynes, UK: Author.

BSI. (1992). Evaluation of Human Exposure to Vibration in Buildings (1Hz to 80Hz). BS 6472. Milton Keynes, UK: Author.

Burkhardt, L. R. (1961). Vibration Analysis for Structural Floor Systems. Journal of Structural Division ASCE, ST7. Vol. 87, Part 1. 97-106.

Buzdugan, G., Mihailescu, E. and Rades, M. (1987). Vibration Measurement. Dordrecht, Netherlands: Martinus Nijhoff Publishers.

Caetano, E. and Cunha, A. (1993). Experimental Identification of Modal Parameters on a Full Scale Structure. In: C. A. Brebbia and G. M. Carlomagno (Eds.) Proceedings of the 6th International Conference on Computational Methods and Experimental Measurements. Vol. 2: Stress Analysis. (pp. 321-335). University of Siena, Italy. May.

Campbell, T. I., Csagoly, P. F. and Agarwal, A. C. (1979). Frequency Matching in Continuous Post-Tensioned Concrete Highway Bridges. In: ACI Publication SP-60, Proceedings of the Symposium on Vibrations of Concrete, 1977 Fall Convention of the ACI. (pp. 139-154). New Orleans, USA. October 20.

Cantieni, R. (1988). Floor Vibrations - Two Case Studies. In: Proceedings of the Symposium/Workshop on Serviceability of Buildings (Movements, Deformations, Vibrations). Vol. 2. (pp. 497-511). Ottawa, Canada. May 16-18.

Cantieni, R. (1996). Updating of Analytical Models of Existing Large Structures Based on Modal Testing. In: Proceedings of the Workshop: US-Europe on Bridge engineering - Evaluation, Management and Repair. Barcelona, Spain. July 15-17.

Cantieni, R. and Pretlove, A. J. (1986a). Statics, Dynamics and Time. In: G. P. Tilly (Ed.) Dynamic Behaviour of Concrete Structures , Report of the RILEM 65 MDB Committee, Developments in Civil Engineering. Vol. 13. (pp. 3-6). Amsterdam, The Netherlands: Elsevier

Cantieni, R. and Pretlove, A. J. (1986b). Effects of Dynamics Loads. In: G. P. Tilly (Ed.) Dynamic Behaviour of Concrete Structures , Report of the RILEM 65 MDB Committee, Developments in Civil Engineering. Vol. 13. (pp. 6-8). Amsterdam, The Netherlands: Elsevier

Caverson, R. G. (1992). Vibration Characteristics of Suspended Concrete Slabs. MSc Thesis. University of Bristol, UK.

Caverson, R. G., Waldron P. and Williams, M. S. (1994). Review of Vibration Guidelines for Suspended Concrete Slabs. Canadian Journal of Civil Engineering. Vol. 6, No. 21. 931-939.

CEB. (1991). Vibration Problems in Structures - Practical Guidelines. Bulletin D'Information No. 209. Lausanne, Switzerland: Author.

CEB. (1993). CEB-FIP Model Code 1990. London, UK: Thomas Telford.

Chadha, J. and Allen, D. L. (1972). Natural Frequency Determination of Long-Span Floor Slabs. Transactions of the ASME Journal of Engineering for Industry. Vol. 94, No. 2. 660-664.

Change, N. D. (1995). Technical Articles. In: Piezoelectric Sensors For Dynamic Measurements: Force, Pressure, Vibration, Shock - Dytran General Catalog and Instrumentation Handbook (1995 Edition). Chatsworth, California, USA: Dytran Instruments.

Charlier, H. (1986). Human Discomfort. In: G. P. Tilly (Ed.) Dynamic Behaviour of Concrete Structures , Report of the RILEM 65 MDB Committee, Developments in Civil Engineering. Vol. 13. (pp. 137-144). Amsterdam, The Netherlands: Elsevier

Chen, Y and Aswad, A. (1994). Vibration Characteristics of Double Tee Building Floors. PCI Journal, Vol. 39, No. 1. 84-95.

Chien, E. Y. L. and Ritchie, J. K. (1984). Floor Vibration - Composite Construction. In: Composite Floor Systems. Markham, Canada: Canadian Institute of Steel Construction.

Chu, A. S., Eller, E. E. and Whittier, R. M. (1996). Vibration Transducers. In: C. M. Harris (Ed.) Shock and Vibration Handbook. (pp.12.1-12.39). New York, USA: McGraw-Hill.

Chui, Y. H. and Smith, I. (1988). A Serviceability Criterion to Avoid Human Discomfort for Light-Weight Wooden Floors. In: Proceedings of the Symposium/Workshop on Serviceability of Buildings (Movements, Deformations, Vibrations). Vol. 1. (pp. 512-525). Ottawa, Canada. May 16-18.

Clough, R. W. and Penzien, J. (1993). Dynamics of Structures. International Edition. New York, USA: McGraw-Hill.

Concrete Society. (1979). Flat Slabs in Post-Tensioned Concrete with Particular Regard to the Use of Unbonded Tendons - Design Recommendations. Technical Report 17. Slough, UK: Author.

Concrete Society. (1984). Post-Tensioned Flat-Slab Design Handbook. Technical Report 25. Slough, UK: Author.

Concrete Society. (1994). Post-Tensioned Concrete Floors Design Handbook. Technical Report 43. Slough, UK: Author.

Cook, R. D., Malkus, D. S. and Plesha, M. E. (1989). Concepts and Applications of Finite Element Analysis (3rd Edition). New York, USA: John Wiley and Sons, Inc.

Cowley, D. M. (1976). International Standards in the Vibration Field. In: Infrasound and Low Frequency Vibration. London, UK: Academic Press.

Craig, R. R. (1981). Structural Dynamics: An Introduction to Computer Methods. New York, USA: John Wiley and Sons.

CSA. (1989). Limit states Design of Steel Structures - A National Standard of Canada (Appendix G: Guide for Floor Vibrations). CSA Standard CAN 3-S16.1-M89. (pp. 127-134). Toronto, Canada: Author.

Dahlsjö, H. and Ohlsson, S. (1993). Vibration and Serviceability in Post Terminal Buildings. In: Proceedings of the IABSE International Colloquium on Structural Serviceability of Buildings. (pp. 327-332). Gothenburg, Sweden. June 9-11.

Dally, J. W., Riley, W. F. and McConnell, K. G. (1993). Instrumentation for Engineering Measurements. New York, USA: John Wiley and Sons, Inc.

DATS. (1995). DATS for Windows User Guide (for v4.2 and above). Fareham, UK: Prosig Limited.

Deak, G. and Holicky, M. (1993). Serviceability Requirements. In: Proceedings of the IABSE International Colloquium on Structural Serviceability of Buildings. (pp. 25-31). Gothenburg, Sweden. June 9-11.

Department of Transport. (1988). Design Criteria for Footbridges. Department of Transport, Highways and Traffic. Departmental Standard BD 29/87. London, UK: HMSO.

DI-2200 Real Time FFT Analyser/DSO Operating Manual. (undated). West Lothian, UK: Diagnostic Instruments Ltd.

Dieckmann, D. (1958). A Study of the Influence of Vibration on Man. Ergonomics. Vol. 1, No. 4. 347-355.

Dossing, O. (1988a). Structural Testing: Part 1 - Mechanical Mobility Measurements. Naerum, Denmark: Bruel and Kjaer.

Dossing, O. (1988b). Structural Testing: Part 2 - Modal Analysis and Simulation. Naerum, Denmark: Bruel and Kjaer.

DSP Technology. (1995). Biasing Internally Amplified Accelerometers. Application Note 3.0. Fremont, California, USA: Author.

DTA. (1993a). Handbook on Guidelines to Best Practice, Volume 1 - Instrumentation. Cranfield, UK: Author.

DTA. (1993b). Handbook on Guidelines to Best Practice, Volume 3 - Modal Testing. Cranfield, UK: Author.

DTA. (1993c). Modal Testing Primer on Best Practice in Dynamic Testing. Cranfield, UK: Author.

DTA. (1996). Handbook on Guidelines to Best Practice, Volume 0 - An Introduction to the DTA Its Products and Services. London, UK: Author.

Dupius, H. and Zerlett, G. (1986). The Effects of Whole-Body Vibration. Berlin, Germany: Springer-Verlag.

Dytran. (1992). Piezoelectric Sensors For Dynamic Measurements: Acceleration, Pressure, Force - General Catalog and Instrumentation Handbook No. 1192. Chatsworth, California, USA: Author.

Dytran. (1995). Piezoelectric Sensors For Dynamic Measurements: Force, Pressure, Vibration, Shock - Dytran General Catalog and Instrumentation Handbook (1995 Edition). Chatsworth, California, USA: Author.

Ebrahimpour, A. and Fitts, L. L. (1996). Measuring Coherency of Human-Induced Rhythmic Loads Using Flat Force Plates. Journal of Structural Engineering. Vol. 122, No. 7. 829 - 831.

Ebrahimpour, A. and Sack, R. L. (1988). Crowd Induced Dynamic Loads. In: Proceedings of the Symposium/Workshop on Serviceability of Buildings (Movements, Deformations, Vibrations). Vol. 1. (pp. 451-463). Ottawa, Canada. May 16-18.

Ebrahimpour, A. and Sack, R. L. (1996). Design Live Loads for Crowds in Motion. In: S. K. Ghosh and J. Mohammadi (Eds.) Proceedings of the 14th Structures Congress "Building an International Community of Structural Engineers". Vol. 1. (pp. 420-427). Chicago, USA. April 15-16.

Ebrahimpour, A., Hamam, A., Sack, R. L. and Patten, W. N. (1996). Measuring and Modelling Dynamic Loads Imposed by Moving Crowds. Journal of Structural Engineering. Vol. 122, No. 12. 1468-1474.

Ellingwood, B. (1989). Serviceability Guidelines for Steel Structures AISCE. Engineering Journal. Vol. 28, No. 1. 1-8.

Ellingwood, B. (1996). Structural Serviceability Review and Standard Implementation. In: Proceedings of International Conference on Building an International Community of Structural Engineers. Vol. 1. (pp. 436-443). Chicago, USA. April 15-18.

Ellingwood, B. and Tallin, A. (1984). Structural Serviceability: Floor Vibrations. Journal of Structural Engineering. Vol. 110, No. 2. 401-418.

Ellingwood, B., Allen, D. E., Elnimeiri, M., Galambos, T. V., Iyengar, H., Robertson, L. E., Stockbridge, J. and Turkstra, C. J. (1986). Structural Serviceability: A Critical Appraisal and Research Needs (By the Ad Hoc Committee on Serviceability Research, Committee on Research of the Structural Division). Journal of Structural Engineering. Vol. 112, No. 12. 2646-2664.

Ellis, B. R. (1980). An Assessment of the Accuracy of Predicting the Fundamental Natural Frequencies of Buildings and the Implications Concerning the Dynamic Analysis of Structures. In: Proceedings of the ICE. Vol. 69, Part 2. (pp. 763-776).

Ellis, B. R. (1992). Dynamic Testing. In: J. F. A. Moore (Ed.) Monitoring Building Structures. (pp. 68-92). Glasgow, UK: Blackie and Son Ltd.

Ellis, B. R. and Ji, T. (1994). Floor Vibration Induced by Dance-Type Loads: Verification. The Structural Engineer. Vol. 72, No. 3. 45-50.

Ellis, B. R. and Ji, T. (1997). Human-Structure Interaction in Vertical Vibrations. In: Proceedings of the ICE, Structures and Buildings. Vol. 122. 1-9.

Ellis, B. R., Kerridge, B. and Osborne, K. (1993). Vibration Characteristics of Shallow Floor Structures. In: Proceedings of the IABSE International Colloquium on Structural Serviceability of Buildings. (pp. 303-308). Gothenburg, Sweden: 9-11 June.

Endevco. (1979). Instruction Manual for Piezoelectric Accelerometers. Rancho Vejo, California, USA: Author.

Endevco. (1994). Instruction Manual: Model 102 ISOTRON Conditioner, Model 109 Power Supply. Rancho Vejo, California, USA: Author.

Eriksson, P-E. (1991). Modal Analysis of a Pre-Cast Concrete Floor Element. In: Proceedings of the 9th IMAC. Vol.1. Part 1. (pp. 430-434). Florence, Italy. April 15-18.

Eriksson, P-E. (1993). Low-Frequency Forces Caused by People: Design Force Models. In: Proceedings of the IABSE International Colloquium on Structural Serviceability of Buildings. (pp. 149-156). Gothenburg, Sweden: 9-11 June.

Eriksson, P-E. (1994). Vibration of Low-Frequency Floors - Dynamic Forces and Response Prediction. PhD Thesis (in English). Chalmers University of Technology, Goteborg, Sweden.

Eriksson, P-E. (1996) Dynamic Service Actions for Floor Systems - Human Activity. In: S. K. Ghosh and J. Mohammadi (Eds.) Proceedings of 14th Structures Congress "Building an International Community of Structural Engineers". Vol. 1. (pp. 413-419), Chicago, USA. April 15-16.

Eriksson, P-E. and Ohlsson, S. V. (1988). Dynamic Footfall Loading from Groups of Walking People. In: Proceedings of the Symposium/Workshop on Serviceability of Buildings (Movements, Deformations, Vibrations). Vol. 1. (pp. 497-511). Ottawa, Canada. May 16-18.

Ewins, D. J. (1975). Measurement and Application of Mechanical Impedance Data: Part 1 - Introduction and Ground Rules. Journal of the Society of Environmental Engineers. Vol. 14-4, No. 67. 3-12.

Ewins, D. J. (1976a). Measurement and Application of Mechanical Impedance Data: Part 2 - Measurement Techniques. Journal of the Society of Environmental Engineers. Vol. 15-1, No. 68. 23-30.

Ewins, D. J. (1976b). Measurement and Application of Mechanical Impedance Data: Part 1 - Interpretation and Application of Measured Data. Journal of the Society of Environmental Engineers. Vol. 15-2, No. 69. 7-17.

Ewins, D. J. (1979). Whys and Wherefores of Modal Testing. Journal of the Society of Environmental Engineers. Vol. 18, No. 3. 3-15.

Ewins, D. J. (1995). Modal Testing: Theory and Practice (Updated with New Notation). Taunton, UK: Research Studies Press Ltd. and John Wiley and Sons.

Fahy, F. J. and Westcott, M. E. (1978). Measurement of Floor Mobility at Low Frequencies in Some Buildings with Long Floor Spans. Journal of Sound and Vibration. Vol. 57, No. 1. 101-129.

Farah, A. (1979). Models of Human Response to Vibration for Assessing Structural Serviceability. In: Proceedings of the 7th Canadian Congress of Applied Mechanics. (pp. 833-834). Sherbrooke, Canada. May 27.

Farah, A. (1985). Structural Serviceability Under Dynamic Loading. In: ACI Publication SP-86, Deflections of Concrete Structures. (pp. 419-436).

Farrar, C. R., Baker W. E., Bell, T. M., Cone, K. M., Darling, T. W., Duffey, T. A., Eklund, A. and Migliori, A. (1994). Dynamic Characterisation and Damage Detection in the I-40 Bridge Over the Rio Grande. Report No. UC-906. Los Alamos, USA: Los Alamos National Laboratory.

Feltham, I. (1995). Private communication with I. Feltham, Associate Director, Ove Arup and Partners R and D, London, UK.

Feltham, I. (1997). Private communication with I. Feltham, Associate Director, Ove Arup and Partners R and D, London, UK.

FEMtools. (1994). FEMtools User's Manual. Version 1.3. Leuven, Belgium: DDS n. v.

Fintel, M. (Ed.). (1985). Handbook of Concrete Engineering (2nd Edition). New York, USA: Van Nostrand Reinhold.

Fintel, M. and Ghosh, S. K. (1982). Economics of Long-Span Concrete Slab Systems for Office Buildings - A Survey. Skokie, USA: Portland Cement Association.

FIP. (1980). Recommendations for the Design of Flat Slabs in Post-Tensioned Concrete (Using Unbonded and Bonded Tendons). Slough, UK: Cement and Concrete Association.

FIP. (1994). Planning and Design Handbook on Precast Building Structures. London, UK: Seto Ltd.

Foschi, R. O. and Gupta, A. (1987). Reliability of Floors Under Impact Vibrations. Canadian Journal of Civil Engineering. Vol. 14, No. 5. 683-689.

Freyssinet International. (1994). Northridge (Los Angeles) Earthquake. Freyssinet Magazine. October. 7-9.

Friswell, M. I. and Mottershead, J. E. (1995). Finite Element Model Updating in Structural Dynamics. Dordrecht, The Netherlands: Kluwer Academic Publishers.

Galambos, T. V. (1988). Vibration of Steel Joist concrete Slab Floor Systems, Technical Digest No. 5. Arlington VA, USA: SJI

Galambos, T. V., Gould, P. L., Ravindra, M. K. and Suryoutomo, H. (1973). Structural Deflections. A Literature and State-of-the-Art Survey. Building Science Series 47. Washington DC, USA: National Bureau of Standards, US Department of Commerce.

Galbraith, F. W. and Barton, M. V. (1970). Ground Loading from Footsteps. Journal of Acoustic Society of America. Vol. 48, No. 5. 1288-1292.

Gerber, G. (1991). Design and Construction of Concrete Floors. London, UK: Edward Arnold.

Gilbert, R. I. (1989). Determination of Slab Thickness in Suspended Post-Tensioned Floor Systems. ACI Structural Journal. Vol. 86, No. 5. 602-607.

Gilbert, R. I. and Mickleborough, N. C. (1990). Design of Prestressed Concrete. London, UK: Unwin Hyman.

Goodchild, C. H. (1995). Hybrid Concrete Construction. Crowthorne, UK: BCA.

Grace, N. F. and Kennedy, J. B. (1990). Dynamic Characteristics of Prestressed Waffle Slabs. Journal of Structural Engineering. Vol. 116, No. 6. 1547-1564.

Green, M. F. and Cebon, D. (1993). Modal Testing of Two Highway Bridges. In: Proceedings of the 11th IMAC. Vol. 2. (pp. 838-844). Kissmmee, USA. February 1-4.

Griffin, M. J. (1982). Human Response to Vibration. In: R. G. White. and J. G. Walker (Eds.) Noise and Vibration. (pp. 827-853). Chichester, UK: Ellis Horwood Ltd.

Griffin, M. J. (1996). Handbook of Human Vibration. London, UK: Academic Press.

Guignard, J. C. (1971). Human Sensitivity to Vibration. Journal of Sound and Vibration. Vol. 15, No.1. 11-16.

Guignard, J. C. and Irving, A. (1959). Effects of Low-Frequency Vibration on Man. Engineering. Vol. 159, No. 4925. 364-367.

Halvorsen, W. G. and Brown, D. L. (1977). Impulse Technique for Structural Frequency Response Testing. A reprint from Sound and Vibration, November 1977, pp. 8-21, by PSC Piezotronics, Inc., Buffalo, USA.

Hanagan, L. M. and Murray, T. M. (1997). Active Control Approach for Reducing Floor Vibrations. Journal of Structural Engineering. Vol. 123, No. 11. 1497-1505.

Hanagan, L. M., Rottmann, C. and Murray, T. M. (1996). Control of Floor Vibrations. In: S. K. Ghosh and J. Mohammadi (Eds.) Proceedings of the 14th Structures Congress Building an International Community of Structural Engineers. Vol. 1. (pp. 428-435). Chicago, USA. April. 15-16.

Harper, F. C. (1962). The Mechanics of Walking. Research Applied in Industry. Vol. 5, No. 1. 33-38.

Hartley, M. J. and Pavic, A. (1996). Risk Assessment Document and Code of Safe and Good Practice for Dynamic Field Testing of Large-Scale Civil Engineering Structures. Internal Report CCC/96/0053A. The Department of Civil and Structural Engineering, University of Sheffield, UK.

Hashimoto, Y., Abe, T. and Hiromatsu, T. (1994). Study on Estimation Methods of Floor Structure Vibration - Part II: Statistical Approach to Dynamic Characteristics of Floor Structures. In: Proceedings of the 12th IMAC. Vol. 2. (pp. 1785-1791). Honolulu, USA. January 31 - February 3.

Hatfield, F. J. (1992). Design Chart for Vibration of Office and Residential Floors. AISC Engineering Journal. Vol. 4, No. 29. 141-144.

Heins, C. P. and Yoo, C. H. (1975). Dynamic Response of a Building Floor System. Building Science. Vol. 10, 143-153.

Heylen, W., Lammens, S. and Sas, P. (1997). Modal Testing Theory and Testing. Leuven, Belgium: Katholieke Universiteit.

Hitchings, D. (undated). Structural Dynamics in Theory and Practice: A Companion to the NAFEMS Finite Element Dynamics Primer. London, UK: STRUCOM, Ltd.

Hudson, D. E. (1977). Dynamic Tests of Full-Scale Structures. ASCE Journal of Engineering Mechanics. Vol. 103, No. 6. 1141-1157.

Huggins, M. W and Barber, J. D. (1982). Building Deflections, Distortions and Vibrations - A Survey. Canadian Journal of Civil Engineering. Vol. 9, No. 1. 133-137.

Hughes, B. P. (1971). Limit State Theory for Reinforced Concrete (SI units). London, UK: Pitman Publishing.

Hurst, M. K. (1988). Prestressed Concrete Design. London, UK: Chapman and Hall.

Hveem, S. (1990). Vibration of Lightweight Floors. The Journal of CIB. Vol. 18, No. 1. 56-60.

Hyde, H. J and Lintern, H. R. (1929). The Vibrations of Roads and Structures, Proceedings of the ICE, Vol. 227. (pp. 187-242).

IABSE. (1993). Structural Serviceability of Buildings. Report Vol. 69. Proceedings of the Joint CIB/IABSE International Colloquium. Gothenburg, Sweden. 9-11 June.

ICATS. (1995). MODENT, MODESH, MODACQ, MESHGEN Reference Manual (Version 4). London, UK: Author.

ICATS. (1997). MODENT, MODESH, MODACQ, MESHGEN Reference Manual (Version 6). London, UK: Author.

Imregun, M. and Ewins, D. J. (1993). An Investigation into Mode Shape Expansion Techniques. In: Proceedings of the 11th IMAC. Vol. 1. (pp. 168-175). Orlando, USA. February 1-4.

Imregun, M. and Ewins, D. J. (1995). Complex Modes: Origins and Limits. In: Proceeding of the 13th IMAC. (pp. 496-506). Nashville, USA. February 13-16.

Irwin, A. W. (1978). Human Response to Dynamic Motion of Structures. The Structural Engineer. Vol. 56A, No. 9. 237-244.

ISO. (1985). Evaluation of Human Exposure to Whole-Body Vibration - Part 1: General Requirements. ISO 2631-1. Geneva, Switzerland. Author.

ISO. (1987). Mechanical Mounting of Accelerometers for Measuring Vibration and Shock. ISO 5348. Milton Keynes, UK: Author.

ISO. (1989). Evaluation of Human Exposure to Whole-Body Vibration - Part 2: Continuous and Shock-Induced Vibration in Buildings (1 to 80Hz). ISO 2631-2. Geneva, Switzerland. Author.

ISO. (1992). Bases for Design of Structures - Serviceability of Buildings Against Vibrations. ISO 10137. Geneva, Switzerland. Author.

ISO. (1994). Methods for the Experimental Determination of Mechanical Mobility, Part 5: Measurements Using Impact Excitation with an Exciter Which is not Attached to the Structure. ISO 7626-5. Geneva, Switzerland. Author.

ISO. (1997). Mechanical Vibration and Shock - Evaluation of Human Exposure to Whole-Body Vibration - Part 1: General Requirements. ISO 2631-1. Geneva, Switzerland: Author.

Janney, J. R. and Wiss, J. F. (1961). Load-Deflection and Vibration Characteristics of a Multi-Storey Precast Concrete Building. ACI Journal. Vol. 32, No. 10. 1323-1335.

Jeary, A. P. and Sparks, P. R. (1979). Some Observations on the Dynamic Sway Characteristics of Concrete Structures. In: ACI Publication SP-60, Proceedings of the Symposium on Vibrations of Concrete, 1977 Fall Convention of the ACI (pp. 155-180). New Orleans, USA. October 20.

Ji, T. and Ellis, B. R. (1993). Evaluation of Dynamic Crowd Effects for Dance Loads. In: Proceedings of the IABSE International Colloquium: Structural Serviceability of Buildings. Vol. 69. (pp. 165-172). Gothenburg, Sweden. June 9-11.

Ji, T. and Ellis, B. R. (1994). Floor Vibration Induced by Dance-Type Loads: Theory. The Structural Engineer. Vol. 72, No. 3. 37-44.

Ji, T. and Ellis, B. R. (1995). Human Actions on Structures, The SECED Newsletter. Autumn. 4-5.

Jones, A. J. and Saunders, D. J. (1972). Equal Comfort Contours for Whole Body Vertical Pulsed Sinusoidal Vibration. Journal of Sound and Vibration, Vol.1, No. 23. (pp. 1-14).

Keast, D. N. (1967). Measurements in Mechanical Dynamics. New York, USA: McGraw-Hill Book Company.

Khan, S. (1994). Private communication with S. Khan, Director, Bunyan Meyer and Partners, Epsom, UK.

Khan, S. and Williams, M. S. (1995). Post-Tensioned Concrete Floors. Oxford, UK: Butterworth-Heinemann Ltd.

Kong, F. K. and Evans, R. H. (1987). Reinforced and Prestressed Concrete (3rd Edition). Workingham, UK: Van Nostrand Reinhold (UK) Co. Ltd.

Kraus, C. A. and Murray, T. M. (1997). Vibration of Steel Framed Residential Floor Systems: Preliminary Guidelines. In: Leon Kempner, Jr. and Colin B. Brown (Eds.) Proceedings of Structures Congress XV: Building to Last. Vol. 1. (pp. 438-442). Portland, USA. April 13-16.

Lenzen, K. H. (1962). Vibration of Steel Joist-Concrete Slab Floor Systems. Studies in Engineering Mechanics Report No. 16, Lawrence: Center for Research in Engineering Sciences. The University of Kansas, USA.

Lenzen, K. H. (1966). Vibration of Steel Joist-Concrete Slab Floors. AISC Engineering Journal. Vol. 3. 133-136.

Lenzen, K. H. (1972). Vibration of Floor Systems of Tall Buildings. In: Proceedings of the ACSE-IABSE International Conference on Planning and Design of Tall Buildings. Vol. 11.17. (pp.667-673). Betlehem, USA. August.

Lenzen, K. H. and Murray, T. M. (1969). Vibration of Steel Beam Concrete Slab Floor Systems. Studies in Engineering Mechanics Report No. 29, Lawrence: Center for Research in Engineering Science. The University of Kansas, USA.

Lenzen, K. H., Dorsett, L. P. and Sokolowski, M. (1971). The Variation of the Vibrational Characteristics of Steel Joist-Concrete Slab Floor Systems with Changes in the Structural Parameters. Engineering Archives of the Polish Academy of Sciences. Vol. 17. 419-439.

Leonard, D. R. (1966). Human Tolerance Levels for Bridge Vibrations. Ministry of Transport RRL Report No. 34. Harmondsworth, UK: RRR.

Leonhardt, F. (1962). Spannbeton fur Die Praxis. Berlin, Germany: Verlag Von Wilhelm Ernst and Sohn (translation into Serbo-Croatian).

Libby, J. R. (1990). Modern Prestressed Concrete - Design Principles and Construction Methods (4th Edition). New York, USA: Van Nostrand Reinhold.

Licht, T. (1972). Measurement of Low Level Vibrations in Buildings. BandK Technical Review. (3-1972). 23-29.

Licht, T. R., Andersen, H. and Jensen, H. B. (1987). Recent Developments in Accelerometer Design. BandK Technical Review. (2-1987). 1-22.

Lin, T. Y. and Burns, N. H. (1982). Design of Prestressed Concrete Structures (3rd Edition). New York: John Wiley and Sons.

Long Stroke Shaker Model 113. (undated). Carlsbad, USA: APS Dynamics Inc.

Long Stroke Shaker Model 400. (undated). Carlsbad, USA: APS Dynamics Inc.

Long Time Record DI-Card Operating Manual, Revision 1.0. (undated). West Lothian, UK: Diagnostic Instruments Ltd.

Long Time Record DI-Card Operating Manual. (undated). Revision 1.0. West Lothian, UK: Diagnostic Instruments Ltd.

Low Impedance Voltage Mode (LIVM) Theory and Operation. (undated). Chatsworth, California, USA: Dytran Instruments.

Lyndon, F. D. and Iacovou, M. (1995). Some Factors Affecting the Dynamic Modulus of Elsticity of High Strength Concrete. Cement and Concrete Research. Vol. 25, No. 6. 1246-1256.

MacGregor, J. G. (1988). General Serviceability - Deflections, Differential Movement and Cracking. In: Proceedings of the Symposium/Workshop on Serviceability of Buildings (Movements, Deformations, Vibrations). Vol. 1. (pp.3-6). Ottawa, Canada. May 16-18.

Maguire, J. R. (1984). The Dynamic Characteristics of Elevated Piled Tanks and Other Selected Prototype Structures. PhD Thesis. University of Bristol, UK.

Maguire, J. R. (1995). Private communication with J. R. Maguire, Chief Engineer, Marine Division, (Lloyd's Register Guidance Note No. 9; Civil and Structural Engineering; Idelisation of Concrete Structures During Assessment).

Maguire, J. R. and Wyatt, T. A. (1999). ICE Design and Practice Guide: Dynamics – An Introduction for Civil and Structural Engineers. London, UK: Thomas Telford.

Maia, N. M. M., Silva, J. M. M., He, J., Lieven, N. A. J., Lin, R. M., Skingle, G. W., To, W-M and Urgueira, A. P. V. (1997). Theoretical and Experimental Modal Analysis. Taunton, UK: Research Studies Press Ltd. and John Wiley and Sons.

Matsumoto, Y., Nishioka, T., Shiojiri, H. and Matsuzaki, K. (1978). Dynamic Design of Footbridges. IABSE Proceedings P-17/78. 1-15.

Matthew, P. W. and Bennett, D. F. H. (1990). Economic Long-Span Concrete Floors. Crowthorne, UK: BCA.

Mays, G. C. (1979). A Review of the Development of the Current International Procedures for the Design and Construction of Prestressed Slabs in Buildings. In: Ravindra, K. D. and Munday, J. G (Eds.) Proceedings of the Conference on Advances in Concrete Slab Technology. (pp. 435-449). Dundee University, UK. April 3-6.

McConnell, K G. (1978). Notes on Vibration Frequency Analysis. Bethel, USA: SESA/SEM.

McConnell, K G. (1995). Vibration Testing Theory and Practice. New York, USA: John Wiley and Sons, Inc.

McConnell, K. G. and Riley, W. F. (1993). Force-Pressure-Motion Measuring Transducers. In: A. S. Kobayashi (Ed.) Handbook on Experimental Mechanics (2nd Edition). (pp. 119-163). Bethel, USA: SEM.

Meirovitch, L. (1980). Computational Methods in Structural Dynamics. Alpen aan den Rijn, The Netherlands: Sijthoff and Noordhoof.

Meirovitch, L. (1986). Elements of Vibration Analysis. New York, USA: McGraw-Hill.

Meyer, C. (1987). Introduction. In: C. Meyer (Ed.) Finite Element Idelaization for Linear Elastic Static and Dynamic Analysis of Structures in Engineering Practice. (pp. 1-16). New York, USA: ASCE.

Meyer, C. and Will, K. M. (1987). Models for Dynamic Analysis. In: C. Meyer (Ed.) Finite Element Idelaization for Linear Elastic Static and Dynamic Analysis of Structures in Engineering Practice. (pp. 273-301). New York, USA: ASCE.

Mickleborough, N. C and Gilbert, R. I. (1986). Control of Concrete Floor Slab Vibration by L/d Limits. In: Proceedings of the 10th Australian Conference on the Mechanics of Structures and Materials. (pp. 51-55). University of Adelaide, Australia.

Morley, L. J. and Murray, T. M. (1993). Predicting Floor Response Due to Human Activity. In: Proceedings of the IABSE International Colloquium on Structural Serviceability of Buildings. (pp. 297-302). Gothenburg, Sweden: 9-11 June.

Mouring , S. E. and Ellingwood, B. R. (1993). Minimising Floor Vibration Caused by Building Occupants. In: Proceedings of the IABSE International Colloquium on Structural Serviceability of Buildings. (pp. 125-132). Gothenburg, Sweden: 9-11 June.

Mouring , S. E. and Ellingwood, B. R. (1994). Guidelines to Minimise Floor Vibrations from Building Occupants. Journal of Structural Engineering. Vol. 120, No. 2. 507-526.

Mouring, S. E. and Ellingwood, B. R. (1996). Minimizing Floor Vibrations from Occupant Activities. In: S. K. Ghosh and J. Mohammadi (Eds.) Proceedings of ASCE Structures Congress XIV Building an International Community of Structural Engineers. (pp. 405-412). Chicago, Illinois: 15-16 April.

Murray, T. M. (1975). Design to Prevent Floor Vibrations. AISC Engineering Journal. Vol. 12, No. 3. 82-87.

Murray, T. M. (1981). Acceptability Criterion for Occupant-Induced Floor Vibrations. AISC Engineering Journal. Vol. 18, No. 2. 62-70.

Murray, T. M. (1985). Building Floor Vibrations. In: Proceedings of the 3rd Conference on Steel Developments. (pp. 145-149). Australian Institute of Steel Construction. Melbourne, Australia. May 20-22.

Murray, T. M. (1988). Practical Aspects of Floor Serviceability Design. In: Proceedings of the Symposium/Workshop on Serviceability of Buildings (Movements, Deformations, Vibrations). Vol. 1. (pp. 495-496). Ottawa, Canada. May16-18.

Murray, T. M. (1991). Building Floor Vibrations. AISC Engineering Journal. Vol. 28, No. 3. 102-109.

Murray, T. M. and Allen, D. E. (1993). Floor Vibrations: A New Design Approach. In: Proceedings of the IABSE International Colloquium on Structural Serviceability of Buildings. (pp. 119-124). Gothenburg, Sweden: 9-11 June.

NAFEMS (1992a). A Finite Element Primer. Glasgow, UK: Author.

NAFEMS (1992b). A Finite Element Dynamics Primer. Glasgow, UK: Author.

Nash, A. (1993). Transient Vibrations in Light Frame Floors. In: Proceedings of the IABSE International Colloquium on Structural Serviceability of Buildings. (pp. 231-236). Gothenburg, Sweden: 9-11 June.

Nawy, E. G. (1996). Fundamentals of High Strength High Performance Concrete. Harlow, UK: Longman.

Nelson, F. C. (1974). Subjective Rating of Building Floor Vibration. Sound and Vibration. Vol. 8. 34-37.

Neville, A. M. (1995). Properties of Concrete (4th Edition). Harlow, UK: Longman.

Newland, D. E. (1993). An introduction to Random Vibrations, Spectral and Wavelet Analysis (3rd Edition). Harlow, UK: Longman.

Nilson, A. H. (1987). Design of Prestressed Concrete (2nd Edition). New York, USA: John Wiley and Sons.

NRCC. (1985). Commentary A, Chapter 4, of the Supplement to the National Building Code of Canada. NRCC Associate Committee on the National Building Code. Ottawa, Canada: Author.

NRCC. (1988). Serviceability of Buildings (Movements, Deformations, Vibrations). Proceedings of the NRCC Symposium/Workshop. Ottawa, Canada. May 16-18.

Ohlsson, S. V. (1982). Floor Vibrations and Human Discomfort. PhD Thesis. Chalmers University of Technology, Gothenburg, Sweden: 9-11 June.

Ohlsson, S. V. (1988a). Springiness and Human-Induced Floor Vibrations: A Design Guide. Stockholm, Sweden: Swedish Council for Building Research.

Ohlsson, S. V. (1988b). Ten Years of Floor Vibration Research - A Review of Aspects and Some Results. In: Proceedings of the Symposium/Workshop on Serviceability of Buildings (Movements, Deformations, Vibrations). Vol. 1. (pp. 419-434). Ottawa, Canada. May 16-18.

Ohmart, R. D. and Lenzen, K. H. (1968). An Approximate Method for the Response of Stiffened Plates to Aperiodic Excitation. Studies in Engineering Mechanics Report No. 30, Lawrence: Center for Research in Engineering Studies. The University of Kansas, USA.

Olsen, N. (1984). Excitation Functions for Structural Frequency Response Measurements. In: Proceedings of the 2nd IMAC. Vol. 2. (pp. 894-902). Orlando, USA. February 6-9.

Onysko, D. M. (1988a). Performance Criteria for Residential Floors Based on Consumer Responses. In: R. Y. Itani (Ed.) Proceedings of the 1988 International Conference on Timber Engineering. (pp. 736-745). Seattle, USA. September 19-22.

Onysko, D. M. (1988b). Performance and Acceptability of Wood Floors - Forintek Studies. In: Proceedings of the Symposium/Workshop on Serviceability of Buildings (Movements, Deformations, Vibrations). Vol. 1. (pp. 477-494). Ottawa, Canada. May 16-18.

Operating Guide Model 3100B24 Ultra High Sensitivity LIVM Accelerometer Hermetically Sealed and Case Isolated. (undated). Chatsworth, California, USA: Dytran.

Operating Guide Model 4102B Battery Powered Unity Gain Current Source with BNC Sensor and Output Jacks for Powering LIVM Sensors. (undated). Chatsworth, California, USA: Dytran.

Operating Guide Model 5803A Instrumented Impulse Hammer Twelve Pound Sledge. (undated). Chatsworth, California, USA: Dytran.

Operating Instructions Model Series 5800A and 5801A LIVM Dynapulse Impulse Hammer. (undated). Chatsworth, California, USA: Dytran.

Operating Instructions Models 4105 and 4105B Battery Operated Current Source Power Units with Gains x1, x10 and x100. (undated). Chatsworth, California, USA: Dytran.

Osborne, K. P. and Ellis, B. R. (1990). Vibration Design and Testing of a Long-span Lightweight Floor. The Structural Engineer, Vol. 68, No. 10. 181-186.

Ouchiyama, M. and Yajima, R. (1993). Field Measurement and Experimental Study on Structural Behaviour of PPC Flat Slab with Unbonded Tendons. In: Proceedings of the FIP Symposium '93. (pp. 869-876). Kyoto, Japan. October 17-20.

Pandit, S. M. (1991). Modal and Spectrum Analysis: Data Dependent Systems in State Space. New Jersey, USA: John Wiley and Sons Inc.

Parsons, K. C. and Griffin, M. J. (1988). Whole Body Vibration Perception Thresholds. Journal of Sound and Vibration. Vol. 121, No.2. 237 - 258.

Pavic, A. (1993). Serviceability Limit States of Post-Tensioned Concrete Floors in Buildings. MSc Thesis (in Serbo-Croatian). University of Belgrade, Yugoslavia.

Pavic, A. and Reynolds, P. (1997). Investigation Into the Effects on Vibration Serviceability of Structural Modifications to the Inverted 'U' Beams Precast System Manufactured by SCC Ltd. Internal Report CCC/97/0064. The Department of Civil and Structural Engineering, University of Sheffield, UK.

Pavic, A. and Reynolds, P. (1999). ExCeL Exhibition Floor, London: Assessment of Vibration Serviceability. Final Report, Ref. RCU Quote 0931. The Department of Civil and Structural Engineering, University of Sheffield, UK.

Pavic, A. and Waldron, P. (1996a). Parameter Estimation and FE Model Correlation Using Modal Testing of an Experimental Full-Scale High Strength Concrete Floor. In: Proceedings of the International Conference on Identification in Engineering Systems. (pp. 668-677). University of Wales, Swansea, UK. March 27-29.

Pavic, A. and Waldron, P. (1996b). Guidelines on Modal Testing of Full-Scale Concrete Floors Using Instrumented Hammer Impact Excitation. In: Proceeding of Joint Institution of Structural Engineers/ City University International Seminar on Structural Assessment - The Role of Large and Full-scale Testing. (pp. 27.1-27-8). City University, London, UK. July 1-3.

Pavic, A., Crouch, R. S. and Waldron, P. (1995a). The Iterative Process of Linking the Experimental Modal Testing and FE Modelling of a Full-Scale Concrete Structure. NAFEMS Benchmark International Magazine for Engineering Designers and Analysts. September. 12-17.

Pavic, A., Crouch, R. S. and Waldron, P. (1995b). Experimental Validation of Finite Element Models for Vibrational Analysis of Thin Prestressed Concrete Slabs. In: Proceedings of the NAFEMS 5th International Conference on Reliability of Finite Element Methods for Engineering Applications. (pp. 319-330). Amsterdam, The Netherlands. May 10-12.

Pavic, A., Pimentel, R. L. and Waldron, P. (1998). Instrumented Sledge Hammer Impact Excitation: Worked examples. In: Proceedings of the 16th IMAC. (pp. 929-935). Santa Barbara, USA. February 2-5.

Pavic, A., Reynolds, P. and Waldron, P. (1997). Modal Testing of a Full-Scale Prestressed Concrete Floor: Testing Specifications and Quality Assurance Procedures. In: Proceedings of International Conference on Modern Practice in Stress and Vibration Analysis. University College, Dublin, Ireland. September 3-6.

Pavic, A., Williams, M. S., and Waldron, P. (1994). Dynamic FE Model for Post-Tensioned Concrete Floors Calibrated Against Field Test Results. In: Proceedings of the 2nd International Conference on Engineering Integrity Assessment. (pp. 357-366). Glasgow, Scotland. May 11-12.

Pearman, T. (1997). Private communication with T. Pearman, Consultant, Bunyan Meyer and Partners Ltd., Epsom, UK.

Pernica, G. (1987). Effect of Architectural Components on the Dynamic Properties of a Long-span Floor System. Canadian Journal of Civil Engineering. Vol. 14. 461-467.

Pernica, G. (1990). Dynamic Load Factors for Pedestrian Movements and Rhythmic Exercises. Canadian Acoustics. Vol. 18, No. 2. 3-18.

Pernica, G. and Allen, D. E. (1982). Floor Vibration Measurements in a Shopping Centre. Canadian Journal of Civil Engineering. Vol. 9, No. 2. 149-155.

Petkovski, M. (1999). Seismic Behaviour of Reinforced Concrete Frames with Energy Dissipation Elements. PhD Thesis. University of Sheffield, UK (to be submitted).

Petkovski, M., Reynolds, P., Pavic, A. and Waldron, P. (1997). SCC Precast Floors: Assessment of Vibration Serviceability of Union Arcade Car Park. Internal Report CCC/97/0058A. The Department of Civil and Structural Engineering, University of Sheffield, UK.

Petyt, M. (1990). Introduction to Finite Element Vibration Analysis. Cambridge, UK: Cabridge University Press.

Petyt, M. and Mirza, W. H. (1972). Vibration of Column-Supported Floor Slabs. Journal of Sound and Vibration. Vol. 21, No. 3. 355-364.

Pham, L. and Stark, G. (1993). Australian Performance Standard for Domestic Metal Framing. In: Proceedings of the IABSE International Colloquium on Structural Serviceability of Buildings. (pp. 99-104). Gothenburg, Sweden: 9-11 June.

Pham, L. and Yang, J. H. (1993). Dynamic Performance of Australian Domestic Floors. In: Proceedings of the IABSE International Colloquium on Structural Serviceability of Buildings. (pp. 237-242). Gothenburg, Sweden: 9-11 June.

Pietrzko, S., Cantieni, R. and Deger, Y. (1996). Forced Modal Test of the Vieux Emosson Gravity Dam, Reciprocity Based Experimental Determination of Dam-Foundation Interaction, FE-Modelling and Updating. In: A. Creechan (Ed.) NAFEMS/DTA/SECED, Proceedings of the 2nd International Conference on Structural Dynamics Modelling: Test, Analysis and Correlation. (pp. 413-424). Cumbria, UK. July 3-5.

Piezoelectric Accelerometers, Charge Amplifiers and Force Transducers. (undated). Naerum, Denmark: Bruel and Kjaer.

Pimentel, R. L. (1997). Vibrational Performance of Pedestrian Bridges Due to Human-Induced Loads. PhD Thesis. University of Sheffield, UK.

PL20 Series FFT Analyser/DSO Applications Manual. (undated). Revision 1.5. West Lothian, UK: Diagnostic Instruments Ltd.

PL202 Realtime FFT Analyser Getting Started Guide. (undated). Revision 2.2. West Lothian, UK: Diagnostic Instruments Ltd.

Polensek, A. (1970). Human Response to Vibration of Wood Joist Floors, Wood Science. Vol. 3. 111-119.

Postlethwaite, F. (1944). Human Susceptibility to Vibration. Engineering. Vol. 157, No. 4072. 61-63.

Post-Tensioned Slabs. (undated). Boulogne - Billancourt, France: Freyssinet International.

Pretlove, A. J. and Rainer, H. (1991). Human Response to Vibrations. In: Vibration Problems in Structures - Practical Guidelines. Appendix I. CEB Bulletin D'Information No. 209. Lausanne, Switzerland: CEB.

Pretlove, A. J. and Rainer, H. (1995). Human Response to Vibrations. In: Vibration Problems in Structures - Practical Guidelines. Basel, Switzerland: Birkhäuser Verlag.

Price, B. (1995). Private communication with Dr B. Price, Section Head, Taywood Engineering, London, UK.

Price, B. (1996). Stronger, Bigger, Better. Concrete. January/February. 28-29.

Product Data: Piezoelectric Accelerometers - DeltaShear and Uni-Gain-DeltaShear Types. (undated). Naerum, Denmark: Bruel and Kjaer.

PTI. (1977). Design of Post-Tensioned Slabs. Glenview, USA: Author.

PTI. (1990). Post-Tensioning Manual. Phoenix, USA: Author.

RACAL. (1979). RACAL Store 4DS Technical Manual. Southampton, UK: Author.

RACAL. (1993). RACAL Store Plus VL. Southampton, UK: Author.

Raghavendrachar, M. and Aktan, A. E. (1992). Flexibility by Multireference Impact Testing for Bridge Diagnostic. Journal of Structural Engineering. Vol. 118. 2186-2203.

Rainer, H., Bachmann, H. and Pretlove, A. J. (1995). Floors with Walking People. In: Vibration Problems in Structures - Practical Guidelines. (pp. 11-17). Basel, Switzerland: Birkhäuser Verlag.

Rainer, J. H. and Pernica, G. (1981). Damping of a Floor Sample. In: Proceedings of the 2nd Speciality Conference on Dynamic Response of Structures: Experimentation, Observation, Prediction and Control. (pp. 859-873). Atlanta, Georgia, USA. January 15-16.

Rainer, J. H. and Pernica, G. (1986). Vertical Dynamic Forces from Footsteps. Canadian Acoustics. Vol. 14, Part 2. 12-21.

Rainer, J. H. and Swallow, J. C. (1986). Dynamic Behaviour of a Gymnasium Floor. Canadian Journal of Civil Engineering. Vol. 13, No. 3. 270-277.

Rainer, J. H., Allen, D. E. and Pernica, G. (1988a). Dynamic Response of Floors Due to People in Motion. In: Proceedings of the Symposium/Workshop on Serviceability of Buildings (Movements, Deformations, Vibrations). Vol. 1. (pp. 465-476). Ottawa, Canada. May 16-18.

Rainer, J. H., Pernica, G. and Allen, D. E. (1988b). Dynamic Loading and Response of Footbridges. Canadian Journal of Civil Engineering. Vol. 15. 66-71.

Ramsey, K. A. (1975). Effective Measurements for Structural Dynamic Testing: Part 1, Sound and Vibration. Vol. 9, No. 11. 24-35.

Ramsey, K. A. (1976). Effective Measurements for Structural Dynamic Testing: Part 2, Sound and Vibration. Vol. 10, No. 4. 18-31.

Randall, R. B. (1987a). Frequency Analysis. Naerum, Denmark: Bruel and Kjaer.

Randall, R. B. (1987b). Vibration Measurement Equipment and Signal Analyzers. In: C. M. Harris (Ed.) Shock And Vibration Handbook (3rd Edition). (pp. 13.1-13.49). New York, USA: McGraw-Hill.

Randall, R. B. (1996). Vibration Measurement Instrumentation. In: C. M. Harris (Ed.) Shock and Vibration Handbook (4th Edition). (pp.13.1-13.17). New York, USA: McGraw-Hill.

Rasmunsen, G. (1982). Human Body Vibration Exposure and Its Measurements. Bruel and Kjaer Technical Review. No. 1. 3-31.

Reese, R. T. and Kawahara, W. A. (1993). Types of Structural Tests. In: R. T. Reese and Kawahara, W. A. (Eds.) Handbook of Structural Testing. (pp. 33-42). Bethel, USA: SEM.

Reid, W. M., Dickie, J. F. and Wright, J. (1997). Stadium Structures: Are They Excited. The Structural Engineer. Vol. 75, No. 22. 383-388.

Reynolds, P. (1999). The Effects of Raised Acces Floors on the Vibrational Performance of Long-Span Concrete Floors. PhD Thesis. University of Sheffield, UK (to be submitted).

Reynolds, P. and Pavic, A. (1996a). Excitation Signals for Shaker Testing. Internal Report No. CCC/97/0052A. The Centre for Cement and Concrete, University of Sheffield, UK.

Reynolds, P. and Pavic, A. (1996b). Documentation for In-House Software SG_CTRL. Technical Note No. CCC/97/0054A. The Centre for Cement and Concrete, University of Sheffield, UK.

Reynolds, P. and Pavic, A. (1996c). Documentation for In-House Software RANGEN. Technical Note No. CCC/97/0055A. The Centre for Cement and Concrete, University of Sheffield, UK.

Richardson, M. H. (1984). Global Frequency and Damping Estimates from Frequency Response Measurements. In: Proceeding of the 4th IMAC. (pp.465-470). Los Angeles, USA. February 3-6.

Ridlon, S. A. and Meyer, C. (1987). Dynamic Analysis – Modeling Guidelines. In: C. Meyer (Ed.) Finite Element Idelaization for Linear Elastic Static and Dynamic Analysis of Structures in Engineering Practice (pp. 397-441). New York, USA: ASCE.

Ritz, P., Matt, P., Tellenbach, C., Schlub, P. and Aeberhard, H. U. (1985). Post-Tensioned Concrete in Building Construction - Post-Tensioned Slabs. Bern, Switzerland: VSL International.

Rosenthal, I. and Itskovitch, M. (1988). Vibration Response of a Ribbed Slab Floor to Dancing. In: Proceedings of the Symposium/Workshop on Serviceability of Buildings (Movements, Deformations, Vibrations). Vol. 1. (pp. 526-532). Ottawa, Canada. May 16-18.

RS Components. (1997). The RS Catalogue on CD-ROM. Corby, UK: Author.

Sabins, G. M. (1979). Introduction and Background: Vibrations of Concrete Structures. In: ACI Publication SP-60, Proceedings of the Symposium on Vibrations of Concrete, 1977 Fall Convention of the ACI. (pp.1-12). New Orleans, USA. October 20.

Saul, W. and Tuan, C. Y. (1986). Review of Live Loads Due to Human Movements. Journal of Structural Engineering. Vol. 112, No. 5. 995-1004.

SEM. (1989). 1989 Buyers' Guide to Experimental Mechanics Equipment and Services. Experimental Techniques. July. 31-65. Bethel, USA: Author.

Serridge, M. and Licht, T. R. (1987). Piezoelectric Accelerometer and Vibration Preamplifier Handbook. Naerum, Denmark: Bruel and Kjaer.

Severn, R. T. (1997). The 6th Mallet-Milne Lecture: Structural Response Prediction Using Experimental Data. Rotterdam, The Netherlands: A. A. Balkema.

Severn, R. T., Brownjohn, J. M. W., Dumanoglu, A. A. and Taylor, C. A. (1988). A Review of Dynamic Testing Methods for Civil Engineering Structures, Keynote Paper 1 (with discussion). In: Proceedings of University of Bristol and SECED Conference: Civil Engineering Dynamics. (pp. 1-23). University of Bristol, UK. March 24-25.

Shioya, K. and Maebayashi, K. (1988). Micro-Vibration Control Procedure for High-Tech Facilities. In: Proceedings of the Symposium/Workshop on Serviceability of Buildings (Movements, Deformations, Vibrations). Vol. 1. (pp. 589-602). Ottawa, Canada. May 16-18.

Shock and Vibration Measurement Technology. (undated). An Application Oriented Short Course Notes P/N 29005. Rancho Vejo, USA: Endevco.

Smallwood, D. O. (1996). Vibration Testing Machines. In: C. M. Harris (Ed.) Shock and Vibration Handbook (4th Edition). (pp. 25.1-25.32). New York, USA: McGraw-Hill.

Smith, B. J., Peters, R. J. and Owen, S. (1996). Acoustics and Noise Measurements. Harlow, UK: Addison Wesley Longman Ltd.

Smith, I. and Chui, Y. H. (1988a). Design of Lightweight Wooden Floors to Avoid Human Discomfort. Canadian Journal of Civil Engineering. Vol. 15, No. 2. 254-262.

Smith, I. and Chui, Y. H. (1988b). Serviceability Calculations for Timber Building Components with Mechanical Connections. In: Proceedings of the Symposium/Workshop on Serviceability of Buildings (Movements, Deformations, Vibrations). Vol. 1. (pp. 465-476). Ottawa, Canada. May 16-18.

Smith, I. and Hu, L. J. (1993). Vibration Serviceability of Ribbed Plates by Modal Synthesis. In: Preoceedings of the IABSE International Colloquium on Structural Serviceability of Buildings. (pp. 243-250). Gothenburg, Sweden: 9-11 June.

Smith, J. D. (1989). Vibration Measurement and Analysis. London, UK: Butterworths.

Smith, J. W. (1969). The Vibration of Highway Bridges and the Effects on Human Comfort. PhD Thesis. University of Bristol, UK.

Smith, J. W. (1988). Vibration of Structures: Applications in Civil Engineering Design. London, UK: Chapman and Hall.

Spence, P. W., and Kenchington, C. J. (1993). The Role of Damping in Finite Element Analysis. Report R0021. Glasgow, UK: NAFEMS.

Steffens, R. J. (1952). The Assessment of Vibration Intensity and Its Application to the Study of Building Vibrations (National Building Studies Special Report No. 19). London, UK: HMSO.

Steffens, R. J. (1965). Some Aspects of Structural Vibration. In: Proceedings of the British National Section of the International Association for Earthquake Engineering Symposium "Vibration in Civil Engineering". (pp. 1-30). London, UK. April.

Steffens, R. J. (1974). Structural Vibration and Damage. London, UK: HMSO

Stevenson, A. M. (1994). Post-Tensioned Concrete Floors in Multi-Storey Buildings. Crowthorne, UK: BCA.

Stevenson, A. M. (1995). Private communication with M. Stevenson, Senior Partner, Gifford and Partners, York, UK.

Szilard R. (1974). Theory and Analysis of Plates. New Jersey, USA: Prentice-Hall.

Thomson, W. T. (1993). Theory of Vibration with Applications (4th Edition). London, UK: Chapman and Hall.

Tilly, G. P. (1986). Preface. In: G. P. Tilly (Ed.) Dynamic Behaviour of Concrete Structures , Report of the RILEM 65 MDB Committee, Developments in Civil Engineering. Vol. 13. (pp. v-vii). Amsterdam, The Netherlands: Elsevier.

Tilly, G. P., Cullington, D. W. and Eyre, R. (1984). Dynamic Behaviour of Footbridges. IABSE Surveys S-26/84. IABSE Periodica No. 2/84. 13-24.

Tolaymat, R. A. (1988a). A New Approach to Floor Vibration Analysis. AISCE Engineering Journal. Vol. 25, No. 4. 137-143.

Tolaymat, R. A. (1988b). An Automated Approach to Floor Vibration Analysis. In: Proceedings of the Symposium/Workshop on Serviceability of Buildings (Movements, Deformations, Vibrations). Vol. 1. (pp. 465-476). Ottawa, Canada. May16-18.

Trethewey, M. W. (1986). Truncation and Time Delay Bias Spectral Estimation Errors in Structural Testing. In: Proceedings of the 4th IMAC. Vol. 1. (pp. 123-129). Los Angeles, USA. February 3-6.

Tuan, C. Y. and Saul, W. E. (1985). Loads Due to Spectator Movements. Journal of Structural Engineering. Vol. 111, No. 2. 418-434.

Ungar, E. E. (1988). Damping of Panels. In: L. L. Beranek (Ed.) Noise and Vibration Control. (pp. 434-475). Washington DC, USA: Institute of Noise Control Engineering and McGraw Hill, Inc.

Ungar, E. E. and White, R. W. (1979). Footfall-Induced Vibrations of Floors Supporting Sensitive Equipment. Sound and Vibration, October 1979. (pp. 10-13).

Usher, M. J. and Keating, D. A. (1990). Sensors and Transducers: Characteristics, Applications, Instrumentation, Interfacing. London, UK: Macmillan.

Vibration-Testing Systems for Simulation and Analysis. (undated). Naerum, Denmark: Bruel and Kjaer.

Von Gierke, H E. and Brammer, A. J. (1996). Effects of Shock and Vibration on Humans. In: C. M. Harris (Ed.) Shock and Vibration Handbook (4th Edition). (pp. 44.1-44.67). New York, USA: McGraw-Hill.

VSL International. (1972). Post-Tensioned Flat Slabs - Explanation of Calculation Process. Bern, Switzerland: Author.

Waldron P., Pavic, A. and Reynolds, P. (1997). DOE Partners in Technology Research Project: Vibration of Post-Tensioned Concrete Floor Slabs. Progress Report 3, CCC/97/0055A. The Centre for Cement and Concrete, University of Sheffield, UK.

Waldron, P. and Pavic A. (1995). Parnell House Floor: Vibration Serviceability Assessment by Calculation. Internal Report CCC/95/0059. The Department of Civil and Structural Engineering, University of Sheffield, UK.

Waldron, P. and Williams, M. S. (1994). Evaluation of Methods for Predicting Occupant-Induced Vibrations in Concrete Floors. The Structural Engineer. Vol. 72, No. 20. 334-340.

Waldron, P., Caverson, R. G., Williams, M. S. and Zaman, A. (1993). Vibration Criteria for Unbonded Prestressed Concrete Floors. In: Proceedings of the FIP Symposium '93. (pp. 877-884). Kyoto, Japan. October 17-20.

Waller, R. A. (1969). Building on Springs. Oxford, UK: Pergamon Press.

Warwaruk, J. (1979). Deflection Requirements - History and Background Related to Vibrations. In: ACI Publication SP-60, Proceedings of the Symposium on Vibrations of Concrete, 1977 Fall Convention of the ACI. (pp.13-41). New Orleans, USA. October 20.

Wasserman, D. E. (1987). Human Aspects of Occupational Vibration. Amsterdam, The Netherlands: Elsevier.

Whale, L. (1983). Vibration of Timber Floors: A Literature Review. High Wycombe, UK: TRADA.

Wheeler, J. E. (1980). Pedestrian-Induced Vibrations in Footbridges. In: Proceedings of the 10th Australian Road Research Board (ARRB) Conference. Vol. 10, Part 3. (pp. 21-35). Sydney, Australia. August 27-29.

Wheeler, J. E. (1981). Crowd Loading on Footbridges. Technical Report No. 23. Australia: Main Roads Department Western Australia.

Wheeler, J. E. (1982). Prediction and Control of Pedestrian Induced Vibration in Footbridges. Journal of the Structural Division. Vol. 108. 2041-2065.

White, M. F. and Liasjø, K. H. (1982). Measurement of Mobility and Damping of Floors. Journal of Sound and Vibration. Vol. 81, No. 4. 535-547.

Wilcoxon Research. (1995). 1995 Industrial Vibration Sensors Product (Industrial Catalogue IND-95). Gaithersburg, USA: Author.

Wilcoxon Research. (1996). Test and Measurement Vibration Products 1996. Gaithersburg, USA: Author.

Willford, M. R. (1997). A Methodology for the Prediction of Floor Vibration to Walking. Revision 'B'. Internal Report. London, UK: Ove Arup and Partners.

Williams, M. S. (1997). Private communication with M. S. Williams, Lecturer, University of Oxford, UK.

Williams, M. S. and Waldron, P. (1994). Evaluation of Methods for Predicting Occupant-Induced Vibrations in Concrete Floors. The Structural Engineer. Vol. 72, No. 20. 334-340.

Williams, M. S., Zaman, A., Waldron, P. and Caverson, R. G. (1993). Comparison of Finite Element and Field Test Results for the Vibration of Concrete Floors. In: Proceedings of International Conference on Structural Dynamics Modelling, Test, Analysis and Correlation. (pp. 79-88). Milton Keynes, UK. July 7-9.

Wilson, J. and Heidebrecht A. (1976). Vibration Characteristics of Long-Span Floor Systems. A Report Prepared for the Canadian Steel Industries Construction Council. McMaster University. Toronto, Canada.

Wiss, J. F. and Parmelee, R. A. (1974). Human Perception of Transient Vibrations. Journal of Structural Division ASCE. Vol. 100, No. 4. 773-787.

Wright, D. T. and Green, R. (1959). Human Sensitivity to Vibration. Report No. 7. February. Queen's University, Kingston, Ontario, Canada.

Wyatt, T. A. (1985). Floor Excitation by Rhythmic Vertical Jumping. Engineering Structures. Vol. 7. 208-210.

Wyatt, T. A. (1989). Design Guide on the Vibration of Floors (SCI Publication 076). Ascot, UK: SCI.

Wyatt, T. A. (1997). Private communication with T. A. Wyatt, Wind Engineering Society, UK.

Wyatt, T. A. and Dier, A. F. (1989). Floor Serviceability under Dynamic Loading. In: Proceedings of the International Symposium "Building in Steel - The Way Ahead", (pp. 20.1-20.22). ECCS Publication No. 57, Stratford on Avon, UK. September 19-20.

Yolles M. S., Bergmann R, and Robbie, R. G. (1968). Systems Buildings. In: Proceedings of the Canadian Structural Engineering Conference. (pp.208-218). Toronto, Canada.

Zahn, F. A. and Ganz, H. R. (1992). Post-Tensioning in Buildings. Bern, Switzerland: VSL International.

Zaman, A. and Boswell, L. F. (1995). Using FEM to Predict Floor Vibration Response. In: Proceedings of the 5th International Conference on Reliability of Finite Element Method for Engineering Applications. (pp. 307-318). Amsterdam, The Netherlands. May 10-12.

Zaman, A. and Boswell, L. F. (1996a). Frequency Estimation of Long-Span Floors. In: Proceedings of the 2nd International Conference on Structural Dynamics Modelling: Test, Analysis and Correlation. (pp. 129-139). Cumbria, UK. July 3-5.

Zaman, A. and Boswell, L. F. (1996b). Vibration Response of Post-Tensioned Concrete Floors to an Impact. In: Proceedings of the FIP Symposium on Post-Tensioned Concrete Structures 1996. (pp. 538-549). London, UK. September 24-27.

Zaman, A. and Boswell, L. F. (1996c). Dynamic Response Testing and Finite Element Modelling of the LBTF Steel-Framed Building Floors. In: Proceedings of the Second Cardington Conference on Fire, Static and Dynamic Testing of Building Structures. (pp. 269-283). Cardington, UK. March 12-14

Zaman, A. and Boswell, L. F. (1996d). Review of Acceptability Criteria for the Vibration of Composite Floors. In: Proceedings of the Joint IStructE/City University International Seminar on Structural Assessment "The Role of Large and Full Scale Testing". (pp. 48.1-48.8). City University, London, UK. July 1-3.